WILEY-VCH

Edited by
Esther Alza

Flow and Microreactor Technology in Medicinal Chemistry

Volume 81
Series Editors:
R. Mannhold,
H. Buschmann, J. Holenz

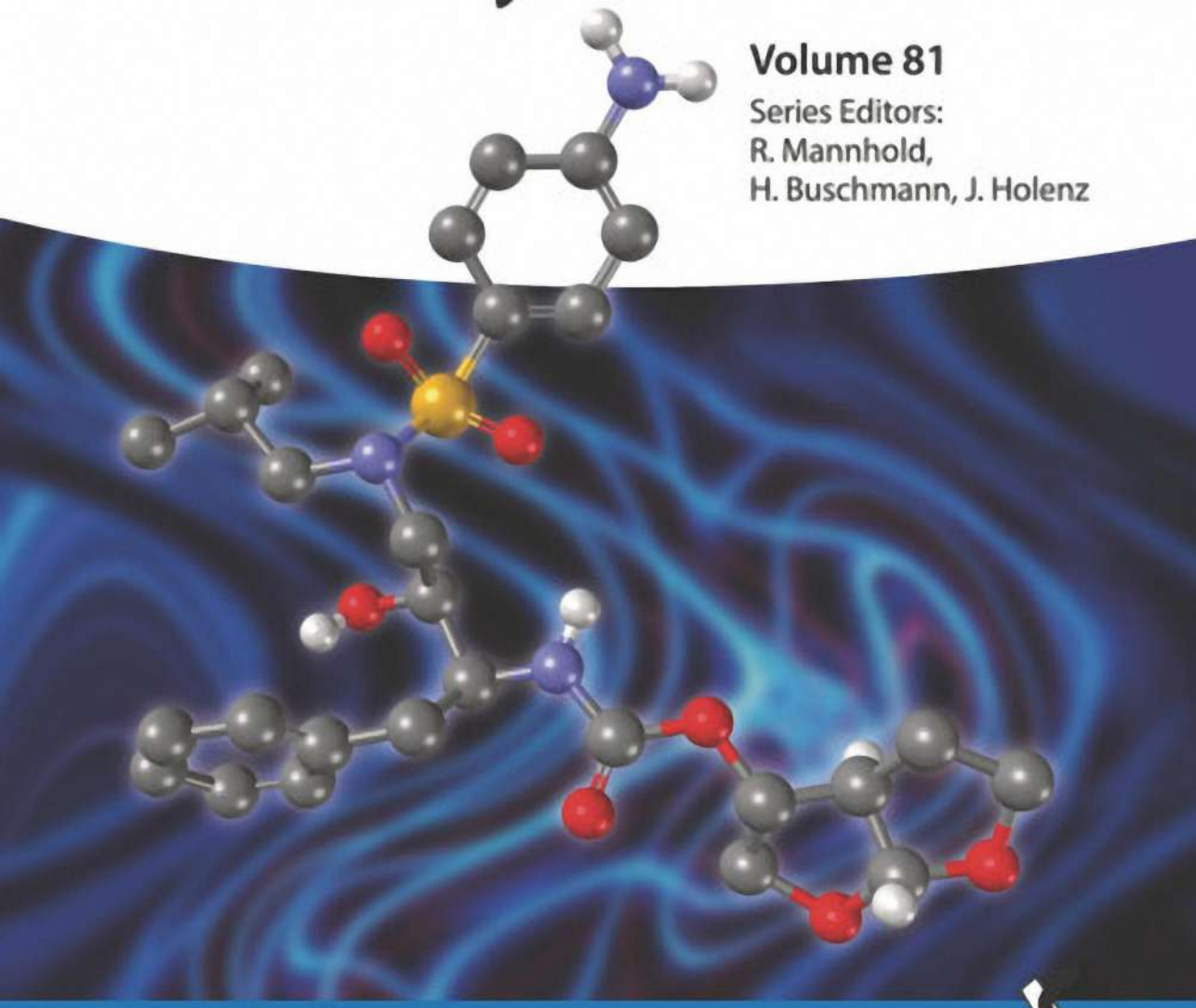

Methods and Principles in Medicinal Chemistry

Flow and Microreactor Technology in Medicinal Chemistry

https://www.twirpx.org & http://chemistry-chemists.com

Methods and Principles in Medicinal Chemistry

Edited by
R. Mannhold, H. Buschmann, J. Holenz

Editorial Board
G. Folkers, H. Kubinyi, H. Timmermann, H. van de Waterbeemd, J. Bondo Hansen

Previous Volumes of the Series

Bachhav, Y. (Ed.)

Innovative Dosage Forms

Design and Development at Early Stage

2022
ISBN: 978-3-527-34396-6
Vol. 81

Bachhav, Y. (Ed.)

Innovative Dosage Forms Design and Development at Early Stage

2019
ISBN: 978-3-527-34396-6
Vol. 76

Rübsamen-Schaeff, H., and Buschmann, H. (Eds.)

New Drug Development for Known and Emerging Viruses

2022
ISBN: 978-3-527-34337-9
Vol. 80

Gervasio, F. L., Spiwok, V. (Eds.)

Biomolecular Simulations in Structure-based Drug Discovery

2018
ISBN: 978-3-527-34265-5
Vol. 75

Gruss, M. (Ed.)

Solid State Development and Processing of Pharmaceutical Molecules

Salts, Cocrystals, and Polymorphism

2021
ISBN: 978-3-527-34635-6
Vol. 79

Sippl, W., Jung, M. (Eds.)

Epigenetic Drug Discovery

2018
ISBN: 978-3-527-34314-0
Vol. 74

Giordanetto, F. (Ed.)

Early Drug Development

2018
ISBN: 978-3-527-34149-8
Vol. 73

Plowright, A.T. (Ed.)

Target Discovery and Validation Methods and Strategies for Drug Discovery

2020
ISBN: 978-3-527-34529-8
Vol. 78

Handler, N., Buschmann, H. (Eds.)

Drug Selectivity

2017
ISBN: 978-3-527-33538-1
Vol. 72

Swinney, D., Pollastri, M. (Eds.)

Neglected Tropical Diseases Drug Discovery and Development

2019
ISBN: 978-3-527-34304-1
Vol. 77

https://www.twirpx.org & http://chemistry-chemists.com

Flow and Microreactor Technology in Medicinal Chemistry

Edited by

Esther Alza

WILEY-VCH

https://www.twirpx.org & http://chemistry-chemists.com

Volume Editor

Dr. Esther Alza
Alza & Associates S.L. Sustainable Chemistry Consulting
Rnda del Canigó, Agr 7, 10
08950 Esplugues de Llobregat
Spain

Series Editors

Prof. Dr. Raimund Mannhold
Rosenweg 7
40489 Düsseldorf
Germany

Dr. Helmut Buschmann
Sperberweg 15
52076 Aachen
Germany

Dr. Jörg Holenz
BIAL – PORTELA & CA., S.A.
São Mamede Coronado
Portugal

Cover
Background illustration: Pexels/Merlin

All books published by **WILEY-VCH** are carefully produced. Nevertheless, authors, editors, and publisher do not warrant the information contained in these books, including this book, to be free of errors. Readers are advised to keep in mind that statements, data, illustrations, procedural details or other items may inadvertently be inaccurate.

Library of Congress Card No.: applied for

British Library Cataloguing-in-Publication Data
A catalogue record for this book is available from the British Library.

Bibliographic information published by the Deutsche Nationalbibliothek
The Deutsche Nationalbibliothek lists this publication in the Deutsche Nationalbibliografie; detailed bibliographic data are available on the Internet at <http://dnb.d-nb.de>.

© 2022 WILEY-VCH GmbH, Boschstr. 12, 69469 Weinheim, Germany

All rights reserved (including those of translation into other languages). No part of this book may be reproduced in any form – by photoprinting, microfilm, or any other means – nor transmitted or translated into a machine language without written permission from the publishers. Registered names, trademarks, etc. used in this book, even when not specifically marked as such, are not to be considered unprotected by law.

Print ISBN: 978-3-527-34689-9
ePDF ISBN: 978-3-527-82460-1
ePub ISBN: 978-3-527-82461-8
oBook ISBN: 978-3-527-82459-5

Cover Design SCHULZ Grafik-Design, Fußgönheim, Germany
Typesetting Straive, Chennai, India

https://www.twirpx.org & http://chemistry-chemists.com

Contents

https://www.twirpx.org & http://chemistry-chemists.com

https://www.twirpx.org & http://chemistry-chemists.com

https://www.twirpx.org & http://chemistry-chemists.com

https://www.twirpx.org & http://chemistry-chemists.com

https://www.twirpx.org & http://chemistry-chemists.com

https://www.twirpx.org & http://chemistry-chemists.com

Series Editors Preface

Recently, application of the flow technologies for the preparation of fine chemicals, such as natural products or active pharmaceutical ingredients (APIs), has become very popular, especially in academia. Although pharma industry still relies on multipurpose batch or semi-batch reactors, it is evident that interest is arising toward continuous-flow manufacturing of organic molecules, including highly functionalized and chiral compounds. Therefore, it could be safely assumed that computer-controlled chemical synthesis using flow chemistry is becoming the key enabling technology for the chemistry laboratory of the future. Up to now these technologies were mainly being utilized in pharmaceutical industry in the field of the chemistry, manufacture, and control (CMC) by taking advantage of easy scale-up reactions. However, in the recent years many interesting articles by medicinal chemists have been reported, for example, the application of library synthesis in the hit and lead optimization field.

The book titled "Flow and Microreactor Technology in Medicinal Chemistry – An Emerging Technology Concept from Drug discovery to Process Development" describes current and future uses in medicinal chemistry of this ground-breaking technology. Beside general chapters describing concepts of lab automation, several case studies explain the broad field of current and future applications of flow technology in the different phases of drug discovery and development from early hit and lead optimization to process development of multi-step reactions. The contributing authors, all very well known as experts in this field, create a deep overview of the current status in the field and provide a solid ground that the reader will be inspired for future application. The following chapters give insight into this emerging technology:

- Chemistry at the Extremes: Turning Complex Reactions into Scalable Processes
- Automated Flow Chemistry Platforms
- Flow Chemistry Opportunities for Drug Discovery
- Flow Chemistry in Medicinal Chemistry – Applications to Bcr-Abl Kinase Inhibitors
- Integrated Systems for Continuous Synthesis and Biological Screenings
- Application of Continuous-Flow Processing in Multistep API and Drug Syntheses
- Continuous-Flow Multistep Synthesis of Active Pharmaceutical Ingredients

https://www.twirpx.org & http://chemistry-chemists.com

- Enantioselective (Bio)Catalysis in Continuous Flow as Efficient Tool for the Synthesis of Advanced Intermediates and Active Pharmaceutical Ingredients
- Innovative Process Development of Pharmaceutical Intermediates Under Continuous-Flow System

The book editor Esther Alza was for many years the Manager of ERTFLOW at the Institute of Chemical Research of Catalonia (ICIQ), in Tarragona, Spain. Having obtained her PhD from ICIQ working on asymmetric catalysis and flow chemistry, she moved to the University of Cambridge as a Wellcome Trust Postdoctoral Fellow to work on medicinal chemistry. After this, she returned to ICIQ to lead the establishment of ERTFLOW as technology development unit. In 2020 she founded a spin-off that creates advanced technological tools for scientific research in the field of photochemistry, and recently she has also founded a company to develop further applications of flow microreactor technology in medicinal chemistry, process development, and novel technologies to offer this experience to pharmaceutical and fine chemistry companies.

In the recent review of Antimo Gioiello "The Medicinal Chemistry in the Era of Machines and Automation: Recent Advances in Continuous Flow Technology" [1] the role of medicinal chemistry and the impact of emerging technologies is very well summarized as follows: "*Medicinal chemistry plays a fundamental and underlying role in chemical biology, pharmacology, and medicine to discover safe and efficacious drugs. Small molecule medicinal chemistry relies on iterative learning cycles composed of compound design, synthesis, testing, and data analysis to provide new chemical probes and lead compounds for novel and druggable targets. Using traditional approaches, the time from hypothesis to obtaining the results can be protracted, thus limiting the number of compounds that can be advanced into clinical studies. This challenge can be tackled with the recourse of enabling technologies that are showing great potential in improving the drug discovery process*."

There is no doubt that automated flow chemistry will significantly empower the medicinal chemistry in many areas. Automation in synthesis and related technologies have already gained a central role in lead and drug discovery as they may offer solutions to overcome current limitations with respect to throughput, synthesis time, and novel reaction pathways to increase the chemical universe of druggable structures.

Currently the revolution has started slowly; technical equipment and artificial intelligence will speed up the implementation of flow technology in medicinal chemistry dramatically. The book edited by Esther Alza will contribute to catalyze this process.

We, as series editors, would like to thank Esther to put the brilliant contributions of the authors together, all authors for their brilliant contributions, and Frank Weinreich, Stefanie Volk, and their co-workers for their great support to make this book possible.

Boston, Aachen, Porto and Frankfurt
May 2022

Helmut Buschmann
Jörg Holenz
Raimund Mannhold

https://www.twirpx.org & http://chemistry-chemists.com

Reference

1 Gioiello, A., Piccinno, A., Lozza, A.M., and Cerra, B. (2020). The medicinal chemistry in the era of machines and automation: recent advances in continuous flow technology. *J. Med. Chem.* 63: 6624–6647. https://doi.org/10.1021/acs.jmedchem.9b01956.

https://www.twirpx.org & http://chemistry-chemists.com

Volume Editor's Preface

The efficient production of new drugs represents a challenge for society. We face problems such as rapidly spreading pandemic disease outbreaks, as we have been suffering during the last two years, emerging drug resistance to antibiotics and antivirals, along with a myriad of other unmet medical needs. The translation to patients requires faster responses in the immediate term. Drug development research, however, is currently a slow and costly process and is not well suited to the need. At the same time, development is shifting from blockbusters toward niche products. This context creates a pressing need for disruptive and innovative methods and processes for efficient design and synthesis of compounds.

The aim of this book is to give an in-depth look of the advantages offered by continuous-flow chemistry and microreactors technology in medicinal chemistry to inspire chemists to boost new research lines for the synthesis of new complex molecules and active pharmaceutical ingredients (APIs) as an alternative of current processes. It is known that continuous-flow chemistry offers several advantages over conventional synthesis techniques – greater flexibility and modularity, increased productivity, shorter reaction times, lower waste volumes, higher pressures and temperatures, and lower overall production costs. But in addition, highly automated and machine-assisted flow chemistry processes have also increased the range of chemistries suitable for automation. The book describes current applications of flow chemistry from drug discovery to process development to show the powerful use of this technology without ignoring the limitations and challenges associated to this field from the perspective and broad knowledge of leading experts from both academia and industry.

The book starts introducing the reader to an overview of flow chemistry processes used by pharmaceutical industry, reviewing examples where flow chemistry shows advantages over batch techniques. Practical considerations that need to be addressed before setting up a reaction in continuous flow are included with special attention to scalability and novelty.

To move toward the lab of the future and eventually to an industry 4.0, global automation strategies of several steps of the discovery and development process as reaction scouting or library synthesis, for instance, are increasing their implementation in research labs. In this sense, the combination of flow chemistry advantages with those from automation will drive these enabling technologies into

https://www.twirpx.org & http://chemistry-chemists.com

faster producing, reducing repetitive work and more efficient and high-quality synthetic processes with the incorporation of artificial intelligence decisions. These concepts are presented in the following chapters, where the recent progress in automated-flow chemistry platforms with direct application to Medicinal Chemistry is presented. Intelligent algorithms to build autonomous high-throughput screening and modular platforms enabling self-optimized processes with the incorporation of process analytical technologies (PAT) are also discussed as well as the integration of flow chemistry in automated platforms to enhance productivity and reduce cycle times in drug discovery. How flow chemistry can be incorporated in the drug discovery process to access novel chemical space and the combination of flow chemistry with emerging technologies as photochemistry or electrochemistry is also highlighted. Additionally, representative examples that showcase the combination of continuous-flow synthesis with downstream operations and bioassays are also included in a chapter, including the latest developments in end-to-end machinery platforms as a whole discovery process. This strategy shows the impact of such integration of the available technology on lead identification and optimization.

Multiple examples of the use of flow chemistry in the synthesis of active pharmaceutical intermediates are presented in the current book. One chapter showcases several case studies focused on the application of flow chemistry technologies to the synthesis and discovery of inhibitors of Bcr–Abl kinase as a thread to show the solutions and strategies to overcome several challenges presented during the application of continuous-flow chemistry for these synthesis processes. These could include the use of heterogeneous reactions as well as the application of high prevalent reactions in drug discovery as, for instance, Pd-mediated cross-couplings. Other two chapters include most recent routes toward the continuous-flow synthesis of APIs, most of them being essential medicines. The potential of continuous-flow methodology as a viable technology for the efficient and sustainable discovery and manufacture of APIs including efficient multistep flow synthetic processes is highlighted. The interesting approach to how this technology can increase the capacity of production of such essential medicines in developing economies is also pointed out.

The last two chapters are focused, one on the application of enantioselective catalysis in continuous flow for the synthesis of important chiral building blocks and advanced intermediates of APIs. Enantioselective catalysis, including metal, organo-, and biocatalysis, is a methodology commonly used in pharma and fine chemicals industries and represents one of the main greener protocols for the synthesis of chiral molecules. In combination with the advantages of flow chemistry, this strategy provides a very efficient pathway for the synthesis of chiral APIs in comparison with classical batch reactions. Examples of homogeneous and heterogeneous catalysis are included as well as in applications of multistep total synthesis. And the other in the application of continuous flow to manufacturing processes for the synthesis of various pharmaceutical intermediates at large-scale productions using facilities under GMP condition. Handling hazardous reagents at large scale or the engineering challenges when scaled up are showcased, highlighting the safety, productivity, and scalability of such processes.

https://www.twirpx.org & http://chemistry-chemists.com

As editor of the book my goal was to provide a versatile overview on the applications of flow and microreactor technology in medicinal chemistry, not only from the cutting-edge and innovative point of view of academia, but also including the pragmatic, efficient, and objective-focused perspective of pharmaceutical industry. I would like to express my deepest gratitude to all the authors who have contributed with their excellent work to make this book a reality, as well as to *Methods and Principles in Medicinal Chemistry* series editors Helmut Buschmann, Raimund Mannhold, and Jörg Holenz, together with Frank Weinreich and co-workers from Wiley-VCH GmbH for their inestimable support.

I hope that reading this book will provide, from students to experienced chemistry scientists working in industry and academia, a greater knowledge of this technology and encourage them to open up new application possibilities in Medicinal Chemistry.

May 2022
Barcelona

Esther Alza

https://www.twirpx.org & http://chemistry-chemists.com

1

Flow Chemistry at the Extremes: Turning Complex Reactions into Scalable Processes

Andrew R. Bogdan

AbbVie, Inc., Drug Discovery Science and Technology, 1 North Waukegan Rd, North Chicago, IL 60064, USA

1.1 Introduction

The use of flow chemistry within the pharmaceutical industry is often used to facilitate the discovery of an active pharmaceutical ingredient (API) or to make its manufacturing route more efficient. Through the combined efforts of academia and industry, significant advances have been made in the field of flow chemistry, which in turn has led to a prevalence of this technology in high-impact settings. The benefits of running reactions in flow are well documented in a number of comprehensive reviews [1–17]. With these reviews, how flow setups can range drastically in their complexity has become obvious. Flow systems in early-stage pharmaceutical settings tend to be automation-intensive platforms, focused on reaction scouting, automated optimization, or library synthesis. For later-stage programs, however, the focus becomes designing highly efficient routes to synthesizing intermediates or final APIs. Depending on the setting, however, the same practical considerations need to be addressed before setting up a reaction in flow. Do reactions need to be run at very low or very high temperatures? Would improved heat transfer and mixing optimize yields and selectivity? If the synthetic route involves the use of a hazardous species, can flow be used to generate this material *in situ*? Is an alternate energy source such as light or current required? If the answer to any of these questions is yes, flow chemistry should be explored. If reactions are heterogeneous or sluggish, however, conventional batch reactors may still be preferred (Table 1.1). In this chapter, a number of examples from the pharmaceutical industry will be discussed where flow chemistry shows obvious advantages over batch techniques. These examples can likely be used as a basis for running future reactions in flow before running reactions in batch. Over time, a number of trends have emerged, and more and more often, specific types of chemistry are preferentially being run in flow on a large scale (Figure 1.1).

Flow and Microreactor Technology in Medicinal Chemistry, First Edition. Edited by Esther Alza.
© 2022 WILEY-VCH GmbH. Published 2022 by WILEY-VCH GmbH.

https://www.twirpx.org & http://chemistry-chemists.com

Table 1.1 Examples of when and when not to use flow chemistry in the pharmaceutical industry.

When TO use flow	When NOT TO use flow
High-/low-temperature applications	Heterogeneous/slurries
In situ use of hazardous intermediates	Slow reaction rates
Reactions mediated by alternative energy sources (photochemistry)	

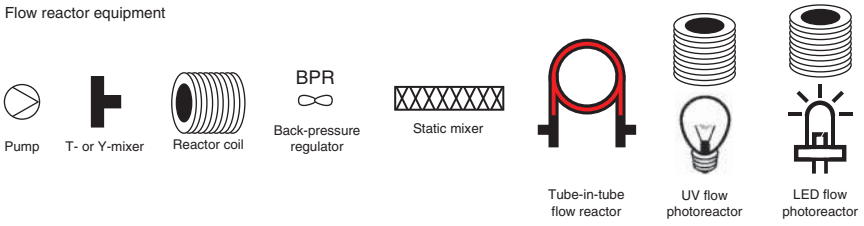

Figure 1.1 Legend for flow reactor equipment.

1.2 Temperature Extremes

Flow chemistry has remained a tried and true method for running low- and high-temperature reactions ever since the field started taking off in the early 2000s. Due to the high surface-area-to-volume ratios, flow reactors have unmatched heat transfer, often times leading to high yields and clean reaction profiles. For cryogenic reactions, flow reactors are readily able to dissipate any exotherms that may be generated. As a result, reactions that run at cryogenic temperatures in batch can frequently be run at higher temperatures in flow. Flow reactors can also reach temperatures that may otherwise be unattainable in batch, thus accelerating reaction rates and resulting in chemistry that is not feasible in batch. High-temperature reactions can also be run much safer in flow as active reactor volumes are lower in comparison to batch systems. In this section, a number of examples of flow chemistry at these two temperature extremes will be discussed in the context of the pharmaceutical industry.

1.2.1 Cryogenic Flow Chemistry

To grasp the differences in cooling a batch reactor versus a flow reactor, it is easiest to first envision cooling a large round-bottom flask. The heat transfer in this instance mainly occurs at the walls of the flask, meaning that as a flask size increases, the effective cooling of the reaction changes and temperature gradients are likely being formed across the reactor. In order to ensure proper reaction control, it is necessary to have excellent mixing and to add reagents in a dropwise manner to keep temperatures from fluctuating. Flow reactors, however, have dimensions on the order

https://www.twirpx.org & http://chemistry-chemists.com

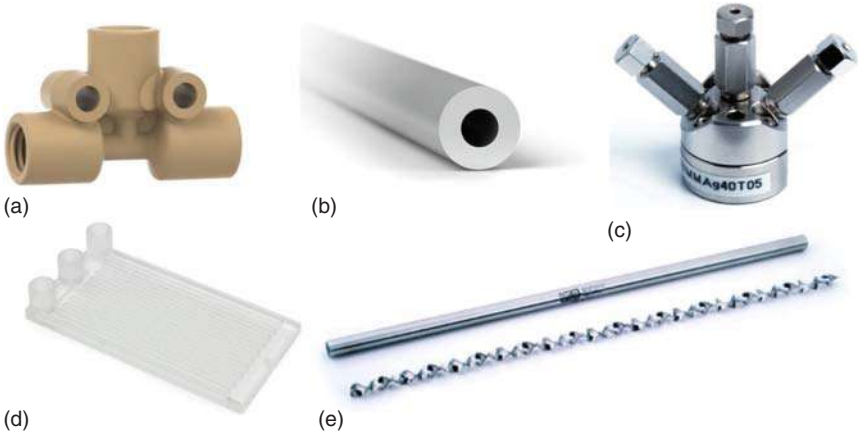

Figure 1.2 Examples of mixers for use in flow chemistry. (a) Standard T-mixer, (b) narrow-bore tubing, (c) IMM static mixer, (d) microchip mixer, or (e) Koflo static mixer.

of millimeters, which result in efficient cooling and limited hotspots. Being able to rapidly dissipate exotherms results in reactions that can be run much more cleanly and at potentially higher temperatures. It is also worth noting that while a 500 ml reaction in batch would likely require at least a 1 l reactor, the same-sized reaction in flow would require a far smaller reactor volume (potentially even a few milliliters). As opposed to a stir bar or impeller, flow reactors can be mixed using a number of options that vary depending on scale (Figure 1.2).

1.2.1.1 Organolithium Chemistry in Flow

Perhaps one of the most prevalent types of flow chemistry involves the use of organolithium species such as *n*-butyllithium or lithium diisopropylamide [18]. While in batch, these reactions are predominately run at −78 °C or lower, for safety and selectivity reasons. For these reason, running these reactions on large scale in batch can be somewhat limiting if these concerns are not mitigated. As a result, more and more examples of organolithium-mediated flow chemistry are being described within the literature. Frequently, these examples can be classified as "flash chemistry," a term coined by the Yoshida group, where reactions take place on the order of milliseconds to seconds [19].

1.2.1.1.1 Boronate Synthesis

Flow examples using organolithiums commonly involve a rapid deprotonation/transmetalation followed by a quench with some sort of electrophile such as a boronate (Scheme 1.1). These flow processes are completed typically by the use of some form of aqueous quench in batch, leading to the isolation of the desired product. A number of examples have been described to generate aryl boronates from both academic and industry laboratories. Ley's group has used the commercially available Polar Bear reactor to prepare gram quantities of (4-chloro-2-fluoro-3-methoxyphenyl)boronic acid [20, 21]. In this instance, the

https://www.twirpx.org & http://chemistry-chemists.com

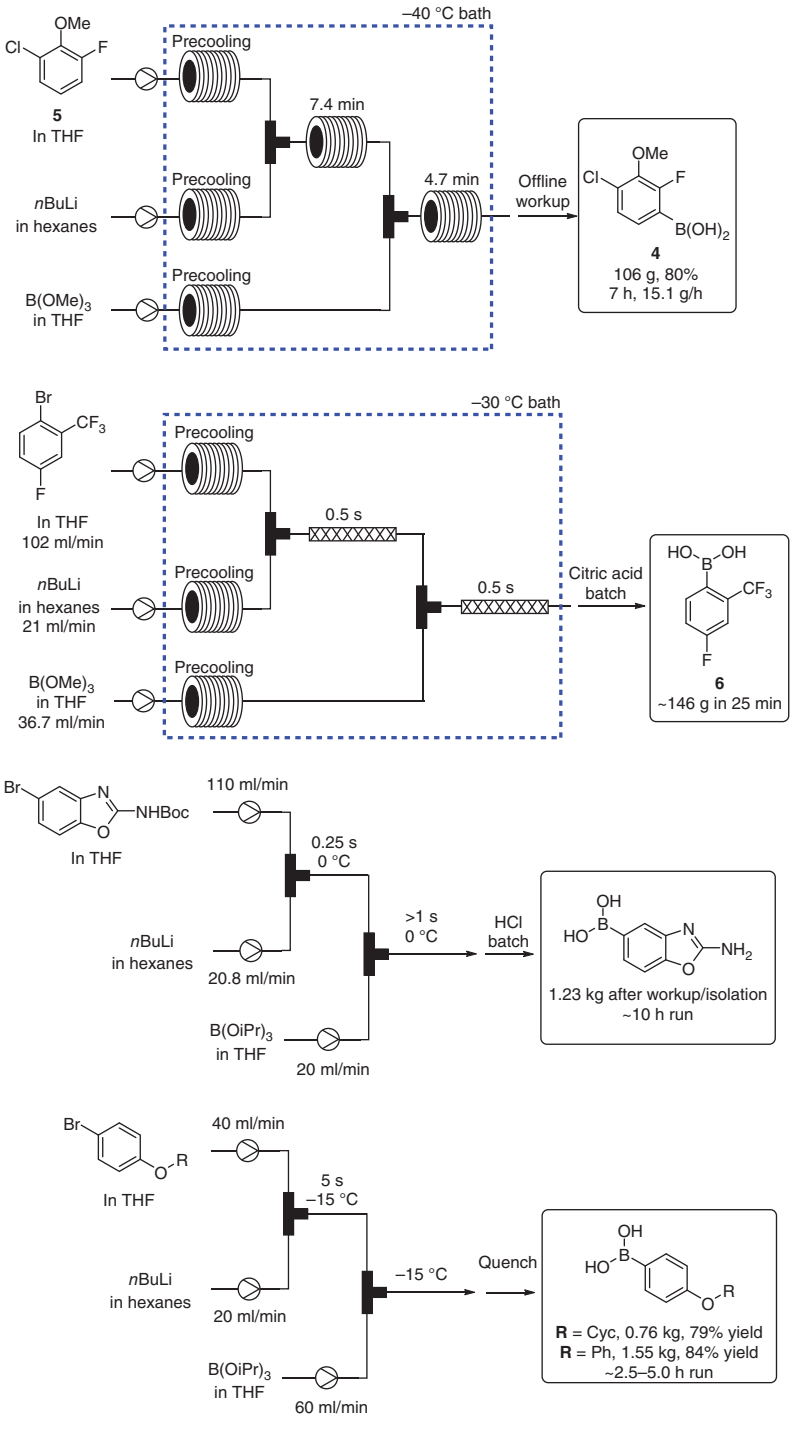

Scheme 1.1 Continuous flow boronate synthesis.

https://www.twirpx.org & http://chemistry-chemists.com

o-lithiation/quench occurred at −50 °C and was capable of preparing >100 g of product within seven hours.

Similarly, Novartis has reported a flow borylation based upon the transmetalation strategy [22]. Both the metalation and boronate quench occur at −30 °C, with a total residence time in the reactor of just one second. When used in scale-up mode, this process proves to be of incredibly high throughput, generating 146 g of product in just 25 minutes. The process operates at incredibly high flow rates, which coupled with the short reaction times allows kilos of this material to be generated in short order if needed. Takeda has exemplified two lithiation–borylation sequences that are used to generate kilogram quantities of various boronates [23, 24]. As with the work by Novartis, these examples could be characterized as "flash" chemistry, as their combined residence times are on the order of seconds. In the first reported example, a Boc-protected aminobenzoxazole is borylated at 0 °C. When run ~10 hours, 1.23 kg of the final boronate is isolated. Similarly, Takeda later reported their efforts to synthesize two aryl ether boronates on a large scale using a very similar procedure. Again, the use of flow chemistry permitted these reactions to occur at −15 °C, much higher than the norm for these types of reactions, allowing 0.75–1.55 kg of final material to be prepared in less than 5 hours. In all the cases described earlier, the use of flow has shown to be beneficial over traditional batch reactions. All processes are rapidly scaled and can operate effectively at temperatures >−78 °C. Not only does this increase in temperature provide some increase in kinetics, but also in many cases the warmer temperature can boost solubility, making the reactors far more stable for long-term operation.

1.2.1.1.2 Formylation

Similar to the boronate synthesis, aldehydes are frequently synthesized via a two-step flow process using organolithium species (Scheme 1.2). Again, a lithium–halogen exchange is carried out at low temperature in flow, followed by a rapid quench with *N*,*N*-dimethylformamide to afford the final product. Large-scale flow runs using this chemistry have been described by chemists at both Merck and Takeda. At Merck, a route to synthesize kilograms of a formylated intermediate was developed [25]. In this case, a lithium salt was used as a starting material in order to avoid competing deprotonation and transmetalation during and after treatment with the organolithium species. This lithium salt was mixed with *n*BuLi, and the resultant dianion was treated with a solution of dimethylformamide (DMF) in tetrahydrofuran (THF), to afford the formylated product. At Takeda, a similar formylation was carried on a substrate containing both an isopropoxycarboxylate and a cyano group [26]. These two functional groups led to rapid decomposition and by-product formation. Reaction times in this instance were on the order of milliseconds. While the flow process was initially screened at −50 °C, exotherms in the cooling bath were observed, as was an increase in reaction pressure. As both of these observations would hinder scale-up efforts, the temperature was dropped to −60 °C without having a deleterious effect on the reaction outcome. Although not high yielding (237 g of final product represents ~40% isolated yield), the product was otherwise unattainable in batch. Flow chemistry however makes this route

https://www.twirpx.org & http://chemistry-chemists.com

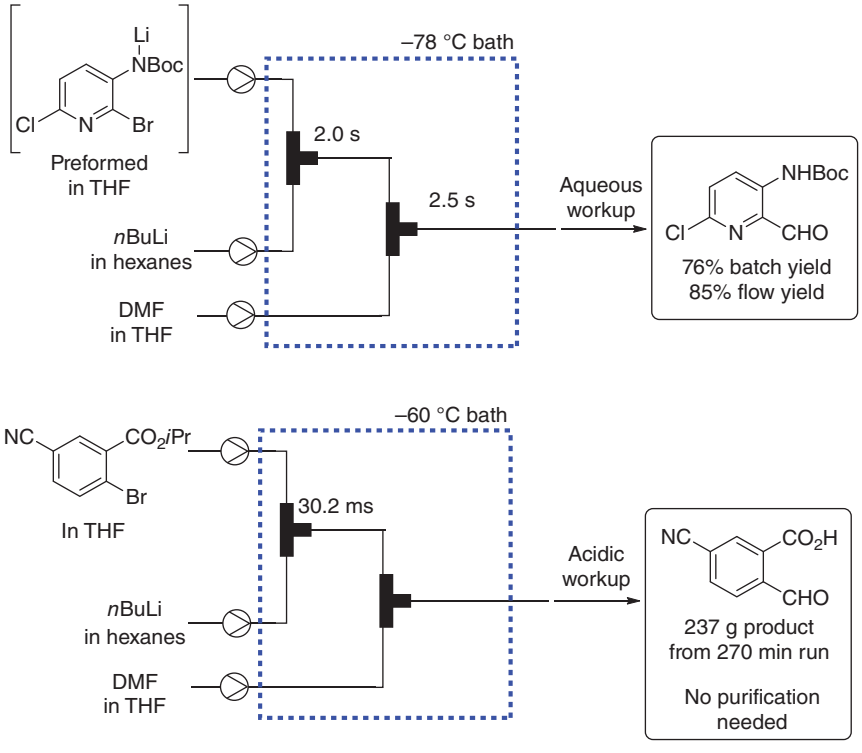

Scheme 1.2 Examples of continuous flow formylations.

tractable, benefitting from the rapid heat transfer and the rapid quench of the lithiated species. Another key to the success of these processes is their simplified batch workups. In both cases, substrates were subjected to an acidic workup followed by extraction. Final products were obtained following concentration, and further purification was deemed unnecessary.

1.2.1.1.3 Carboxylation

A flow carboxylation route was described by SARcode in the synthesis of Lifitegrast (Scheme 1.3) [27, 28]. After noting issues with the batch carboxylation process, an alternative, high-yielding flow method was developed. A feedstock of tetramethylethylenediamine (TMEDA) mixed with the dichloride intermediate was treated with a solution of *n*BuLi at −78 °C in flow, generating an anion species that was mixed with CO_2 gas. The output of the reactor was again subjected to an aqueous workup in batch to yield the desired product. The flow process described earlier was utilized to prepare >22 kg of the carboxylic acid material, typically in 4–5 kg, run with isolated yields consistently between 88% and 91%. This carboxylation process is complimentary to the borylation and formylation procedures described earlier as it highlights how a gas can be used to quench the lithiated species to generate high-value compounds.

https://www.twirpx.org & http://chemistry-chemists.com

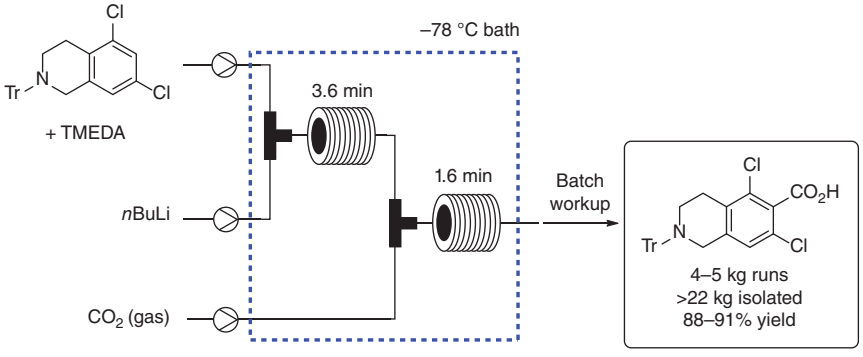

Scheme 1.3 Cryogenic flow carbonylation by SARcode. Source: Based on Refs. [27, 28].

1.2.1.1.4 Nucleophilic Addition

In their synthetic campaign toward eribulin mesylate, flow chemistry was utilized in two separate processes by Eisai (Scheme 1.4) [29]. Following a cryogenic flow reduction of an ester using DIBAL-H, *n*BuLi was used in flow to couple an advance sulfone intermediate to an aldehyde. In their work, a process was developed that takes <5 seconds to complete. While the process was previously run in batch at −70 °C, the flow process was capable of being run at 10 °C in flow due to the enhanced heat transfer exhibited with this type of reactor.

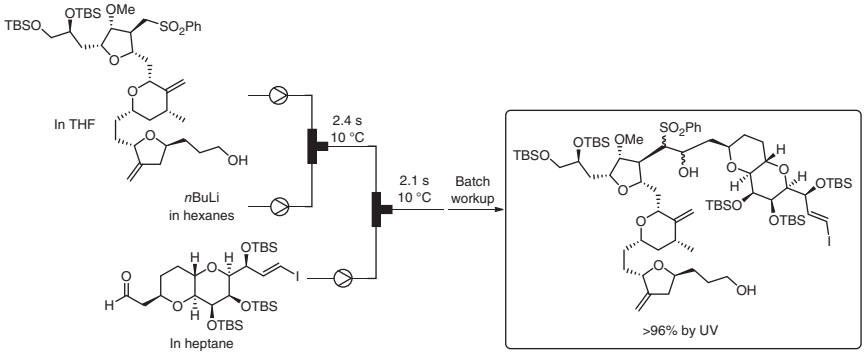

Scheme 1.4 Flow-enabled syntheses of eribulin mesylate intermediates. Source: Fukuyama et al. [29] / American Chemical Society.

1.2.1.1.5 Halomethyllithium Species

Both dichloromethyllithium and bromomethyllithium have proven to be versatile building blocks in organic synthesis; however their utility is somewhat limited due to their unstable nature, even at very low temperatures. To circumvent issues with these reagents, members of pharma and academia have resorted to flow chemistry in order to facilitate their use. At Novartis, it was discovered that dichloromethyllithium could be formed from dichloromethane and *n*BuLi at −30 °C (Scheme 1.5) [30]. In their setup, the deprotonation and quenching steps both took place in

https://www.twirpx.org & http://chemistry-chemists.com

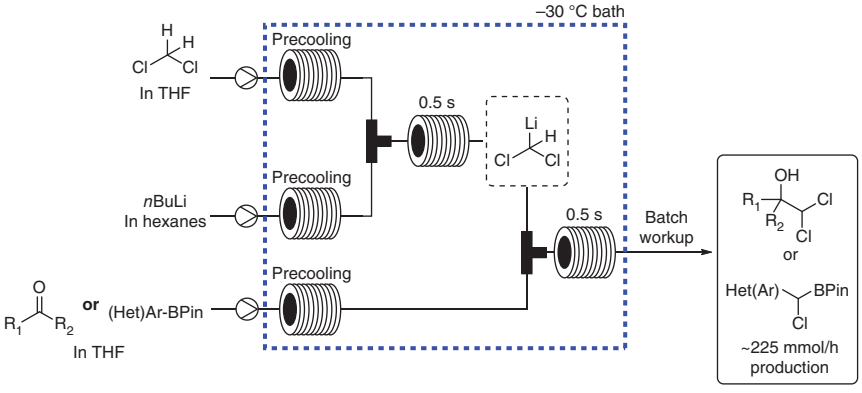

Scheme 1.5 Dichloromethyllithium generation in flow. Source: Hafner et al. [30] / American Chemical Society.

0.5 seconds. The dichloromethyllithium intermediate has a very short lifetime and is consumed almost immediately after it is generated. A series of carbonyl species are dichloromethylated, which provides an intermediate that is amenable to heterocycle synthesis. Furthermore, a series of boronates could be homologated by switching the reactor input to an aryl boronic ester. While the manuscript describes gram scale productions within five minutes, the process is capable of generating ~225 mmol/h of product.

A similar continuous flow boronate homologation has been reported, resulting in a process used to generate hundreds of kilograms of material in a good manufacturing practice (GMP) setting (Scheme 1.6) [31, 32]. Similar to the example highlighted by Novartis, dichloromethyllithium is prepared in flow by mixing *n*BuLi and dichloromethane. This reagent stream is subsequently mixed with a solution of the boronate and collected in a batch reactor containing $ZnCl_2$ in THF to facilitate the rearrangement to the desired product. After two additional steps, the final product vaborbactam could be completed.

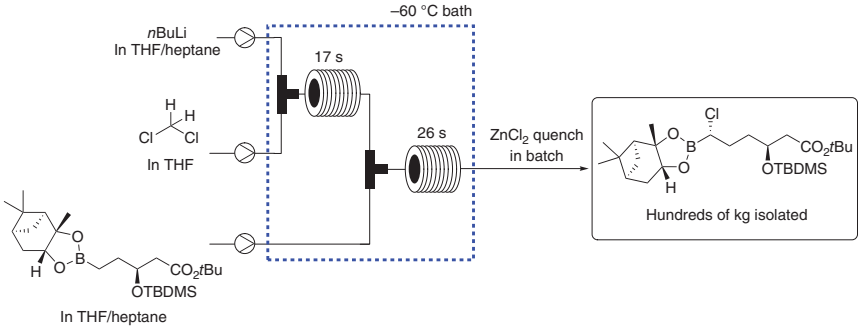

Scheme 1.6 Kilogram-scale flow homologation using dichloromethyllithium. Source: Based on Stueckler et al. [31].

https://www.twirpx.org & http://chemistry-chemists.com

Kappe and coworkers have demonstrated the utility of bromomethyllithium in flow. Similar to dichloromethyllithium, bromomethyllithium has extreme temperature sensitivity and, as a result, frequently needs to be used at around −120 °C. In flow, however, it has been observed to be stable between −80 and −20 °C. Upon treatment of a series of ketones with bromomethyllithium, a bromomethyl alkoxy intermediate forms, which cyclizes to a terminal epoxide upon warming to ambient temperature. A series of epoxides are prepared using this route in high yield, as is a complex chloromethyl epoxide that is an important building block in the synthesis of the drug fluconazole (Scheme 1.7).

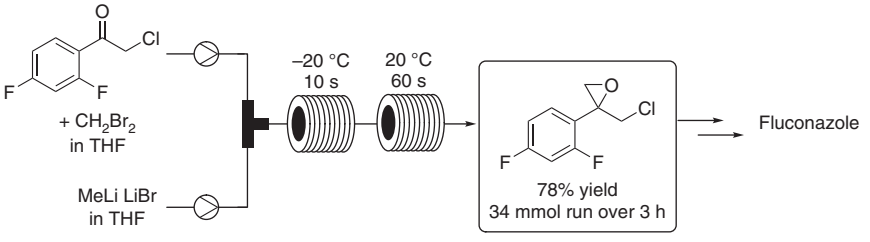

Scheme 1.7 The use of bromomethyllithium in the synthesis of fluconazole.

1.2.1.1.6 Mannich-Type Additions

A series of Mannich-type additions to sulfinyl imines has been reported by Merck and Eli Lilly, both generating >100 kg of material in continuous flow (Scheme 1.8). At Merck, a continuous flow route was explored in the synthesis of the verubecestat intermediate [33, 34]. Similar to the continuous flow formylation previously described by Merck, it was determined that it was optimal to preform the lithiated starting material in batch. This reagent stream was mixed with the aryl sulfinyl imine through a static mixer at high flow rates to afford the desired intermediate. In total, >100 kg of the intermediate was generated using this route, corresponding to an 88% yield. As there were concerns about the temperature stability of the lithiated starting material, the flow route was utilized due to its ability to better control exotherms caused when mixing the two reagent streams.

Similarly, chemists at Eli Lilly used flow chemistry to produce 185 kg of an isoquinoline intermediate of LY3154207, a dopamine D1 receptor-positive allosteric modulator [35]. In this process, a dibromo intermediate undergoes a lithium–halogen exchange at −70 °C and is treated with a chiral sulfinyl imine to generate an intermediate that, upon treatment with HCl, is converted to a chiral primary amine. The final tetrahydroisoquinoline intermediate was isolated after two subsequent batch steps (cyclization then deprotection). Overall, flow chemistry was beneficial in this instance for two reasons. First, the ability to telescope reactions reduced the total number of isolations that were required in the scale-up run. Second, the use of flow once again aided in the control of exotherms caused by the use of an organolithium. As a result, the scaling of this chemistry proved only to be successful in flow, and the batch route was abandoned. Also included in

https://www.twirpx.org & http://chemistry-chemists.com

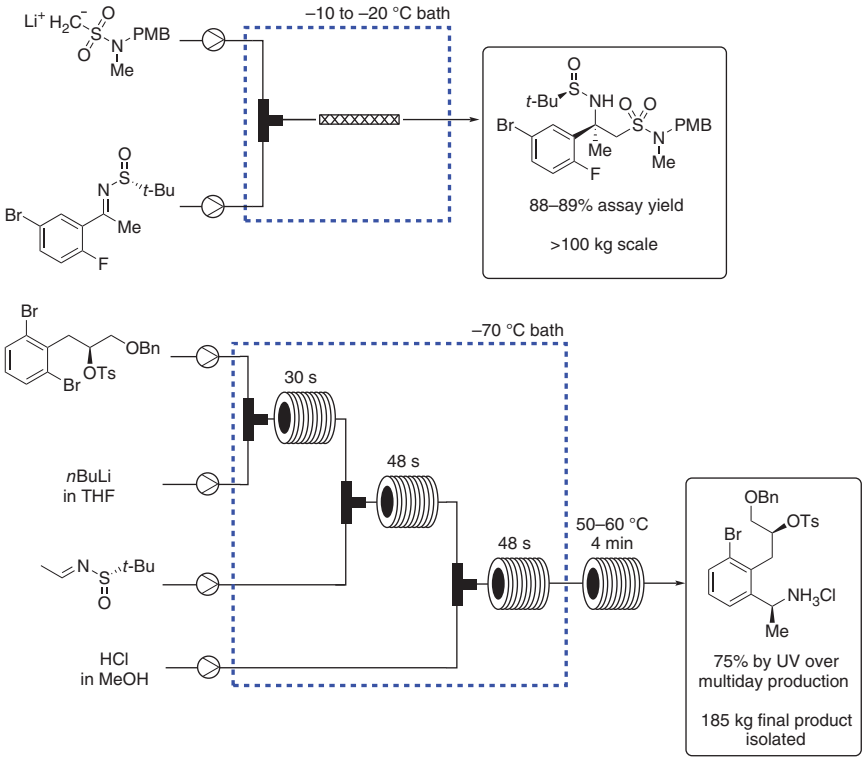

Scheme 1.8 Continuous flow Mannich-type syntheses from Merck and Eli Lilly.

the manuscript is an honest discussion about the trials and tribulations of running such a process on a scale >100 kg, as well as potential solutions to the problems highlighted.

1.2.1.2 Cyanation

Scientists at Gilead have performed a cryogenic flow cyanation on plant scale in the synthesis of an intermediate of remdesivir (Scheme 1.9) [36]. In order to achieve high levels of selectivity in this transformation, temperatures between −30 and −40 °C are preferred. While a batch process was used for early deliveries, much larger batches of material were processed using a flow setup, proving to have high selectivity as well as better control over reaction conditions. The manuscript highlights the optimization of the flow process from early-stage work, where a commercial Vapourtec reactor was used to prepare 9 g product per hour of material to the late-stage work where a custom-built plant-scale reactor was capable of generating nearly 2 kg of product per hour.

1.2.2 High-Temperature Flow Chemistry

Flow reactors have the ability to be run at elevated temperatures due to their ability to be pressurized. In doing so, traditional reaction solvents such as THF and EtOH can

https://www.twirpx.org & http://chemistry-chemists.com

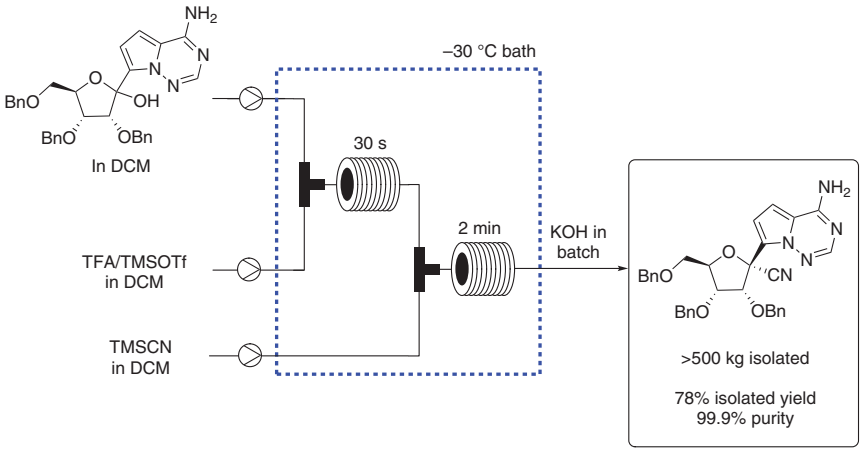

Scheme 1.9 Continuous flow cyanation work from Gilead. Source: Vieira et al. [36] / American Chemical Society.

be used at temperatures well above their boiling point, and the need for high-boiling, less favorable solvents can be mitigated. A number of smaller-scale operations have been reported by Roche, where a series of annulated pyridines were synthesized using a flow reactor coupled with a gas chromatograph oven [37, 38]. A commercial flow reactor capable of reaching 450 °C, the Phoenix from Thales Nano, has been used for parallel library synthesis of aminated heterocycles [39], as well as cyclization reactions such as the Gould–Jacobs [40–42] and Diels–Alder [43]. In all cases, solvents such as toluene, THF, and ethanol were used at temperatures between 230 and 390 °C (Scheme 1.10). Additionally, a series of substrates are synthesized in all cases, and reactions are generally proceeded in modest to high yield.

A high-temperature, additive-free *N*-Boc deprotection using the Phoenix has also been described (Scheme 1.11) [44]. Instead of treating substrate with acid, it was discovered that heating substrates to 300 °C for two minutes afforded quantitative yield to a wide variety of substrates. Furthermore, two multistep syntheses using a Boc deprotection are highlighted in which nearly 200 mg of material can be generated in under 10 minutes. Both processes also avoid any intermediate purification steps.

While the preceding examples were not carried out on particularly large scale, more examples are being reported where high-temperature flow chemistry can be carried out on scale. A flow-based Hemetsberger–Knittel indole formation has been reported by O'Brien et al. where an acrylazide is cyclized at temperatures between160 and 220 °C [45]. This process has inherent safety benefits as low volumes of azide are superheated at any given moment. In AbbVie discovery chemistry, this methodology was applied to the synthesis of various indoles and azaindoles on multigram scale (Scheme 1.12) (Bogdan, A. R., AbbVie Inc, North Chicago IL, Unpublished results).

Much larger-scale, high-temperature applications have been reported by Actelion Pharmaceuticals and Eli Lilly (Scheme 1.13). A flow-mediated Overman rearrangement at 220 °C was used to synthesize an intermediate for an API, capable of being

https://www.twirpx.org & http://chemistry-chemists.com

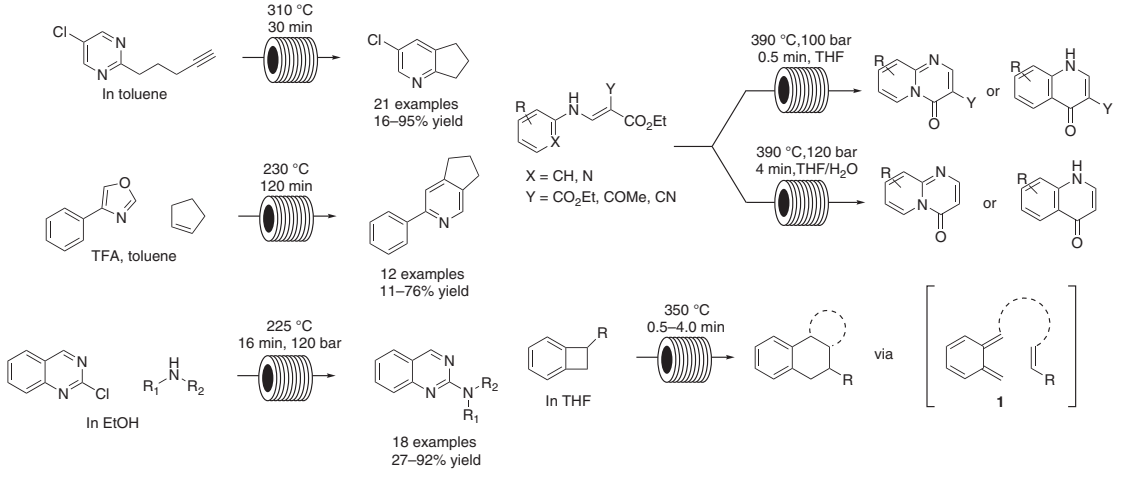

Scheme 1.10 Examples of high-temperature flow chemistry using standard solvents at elevated temperatures.

https://www.twirpx.org & http://chemistry-chemists.com

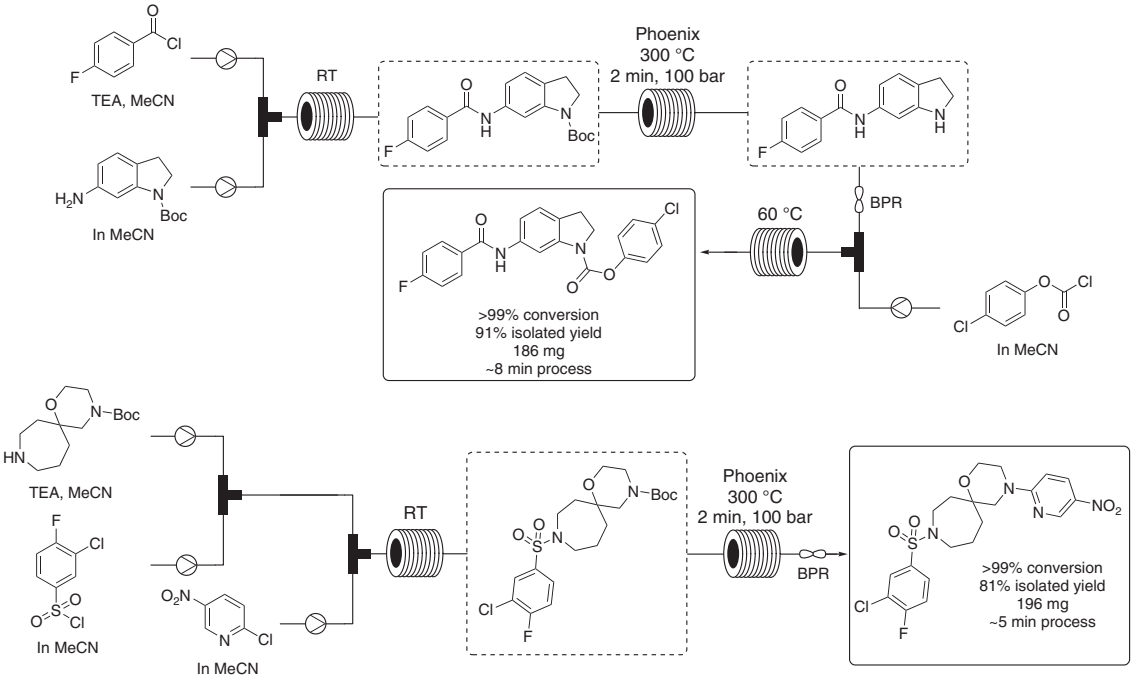

Scheme 1.11 Multistep syntheses carried out using high-temperature Boc deprotection. Source: Bogdan et al. [44] / American Chemical Society.

https://www.twirpx.org & http://chemistry-chemists.com

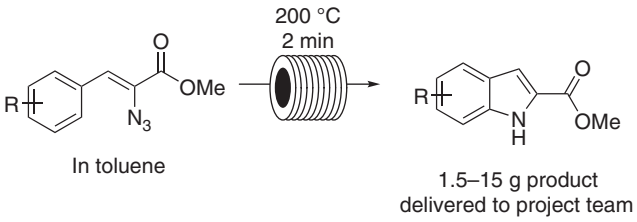

Scheme 1.12 Scale-up of indole using high-temperature-mediated indole formation in flow. Source: Bogdan, A. R., AbbVie Inc, North Chicago IL, Unpublished results.

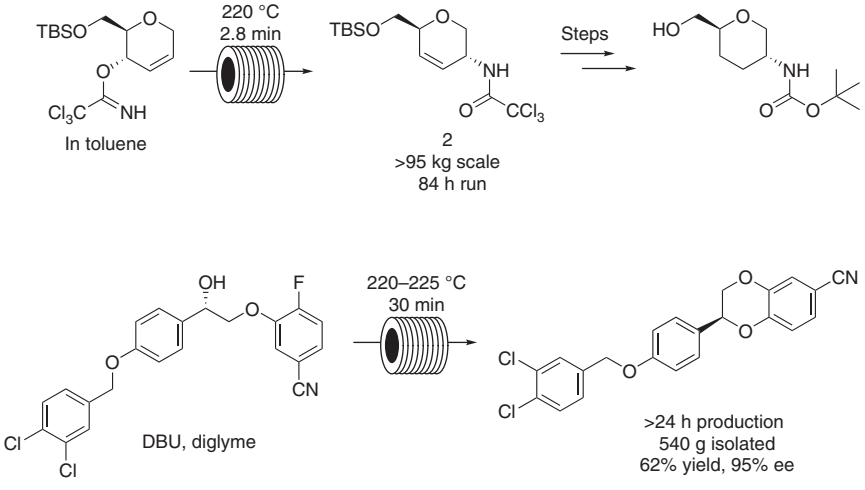

Scheme 1.13 High-temperature flow chemistry on large scale.

carried out on >95 kg scale over the course of 84 hours. The process benefited by high levels of heat transfer, enabling a quantitative yield of the desired compound. Eli Lilly has demonstrated a high-temperature ring cyclization in flow to enable the delivery of >500 g of material in support of early phase development [46]. Specifically, an intramolecular SnAr was developed where the combination of high heat, an organic base, and a less polar solvent led to high yields and enantioselectivity. Using more traditional SnAr conditions in batch resulted in higher impurity formation.

1.3 *In Situ* Use of Hazardous Reagents

A key benefit of flow chemistry is its ability to generate reactive or unstable intermediates and use them immediately in subsequent reaction steps. This has been highlighted previously in a number of cryogenic reactions. In addition, it can be applied at higher temperatures and can be used quite effectively on a large scale. Species such as these can also be prepared at ambient temperatures. By preparation of these species *in situ*, storage issues are mitigated, as are various other safety concerns.

https://www.twirpx.org & http://chemistry-chemists.com

1.3.1 Vilsmeier Reagent

The Vilsmeier reagent is a versatile formylating agent, typically prepared by the treatment of DMF and phosphorus oxychloride ($POCl_3$). However, thermal stability issues with this reagent can cause concern when being used on a large scale (specifically in exothermic processes). For this reason, a number of examples highlight preparing the Vilsmeier reagent in flow and using it directly in subsequent reaction steps (Scheme 1.14). In one such example, a series of pyrroles are formylated using a multistep flow process [47]. First, the DMF and $POCl_3$ are mixed at ambient temperature for 90 seconds, generating small quantities of the Vilsmeier reagent, which is subsequently mixed with the heterocycles being formylated. Output on this system can be in the grams per hour range. The process was later applied on an industrial scale, in flow in the synthesis of Vildagliptin [48]. Similar to the prior example, the Vilsmeier reagent is prepared at ambient temperature but is now reacted with an advanced intermediate to generate a cyanopyrrolidine at a rate of 5.8 kg/h/l.

Alternative Vilsmeier chemistry has been employed using diethylformamide (DEF) or *N*-formylmorpholine (NFM) as opposed to DMF (Scheme 1.15) [49]. Upon treatment of cyclohexanone with the Vilsmeier reagent and the subsequent reaction

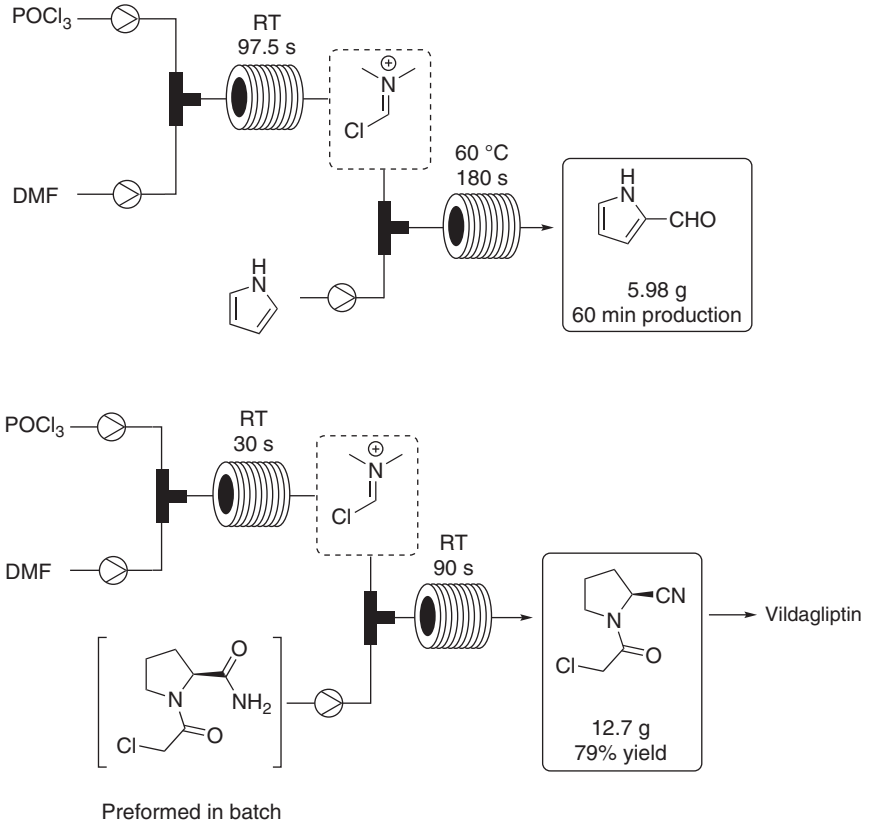

Scheme 1.14 Applications of *in situ* generated Vilsmeier reagent.

https://www.twirpx.org & http://chemistry-chemists.com

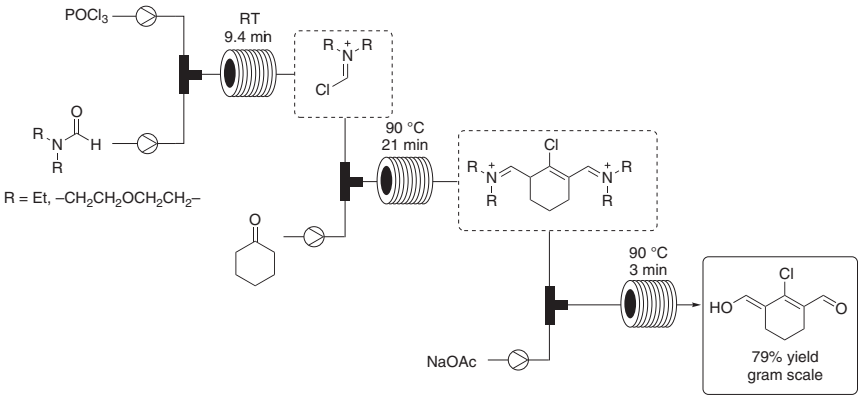

Scheme 1.15 Alternative Vilsmeier reagent use in flow. Source: Carrera et al. [49] / American Chemical Society.

with sodium acetate, 2-chloro-1-formyl-3-(hydroxymethylene)cyclohex-1-ene can be obtained in high yield. The described process not only benefits from not isolating the Vilsmeier reagents in large quantities but also relies on more environmentally friendly formamides than previously reported examples.

1.3.2 Phosgene

Phosgene is another versatile chemical in organic synthesis; however, its hazards are well known, and large-scale use is avoided if possible. Flow chemistry again can be used to generate this hazardous reagent on the fly. In this work, a solution of phosgene in toluene is prepared by mixing triphosgene and tributylamine in flow for five seconds and immediately reacted with a tetrahydroisoquinoline [50]. The developed process has the potential to result in vast amounts of material, given that 64 g of material was isolated in under five minutes (Scheme 1.16).

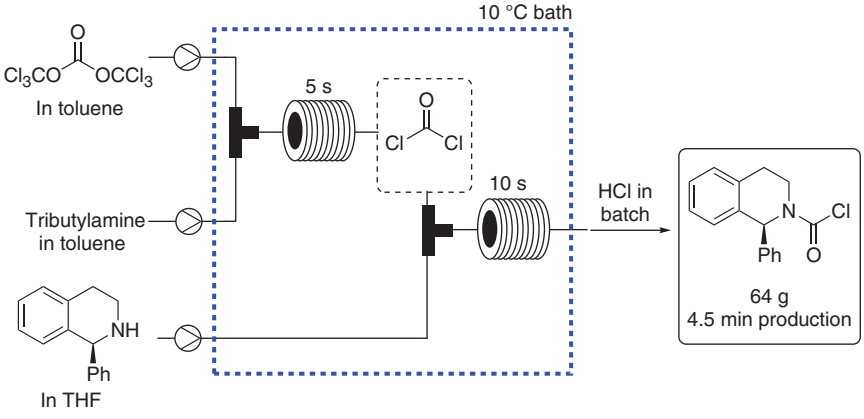

Scheme 1.16 Synthesis and reaction of phosgene **31** in flow.

https://www.twirpx.org & http://chemistry-chemists.com

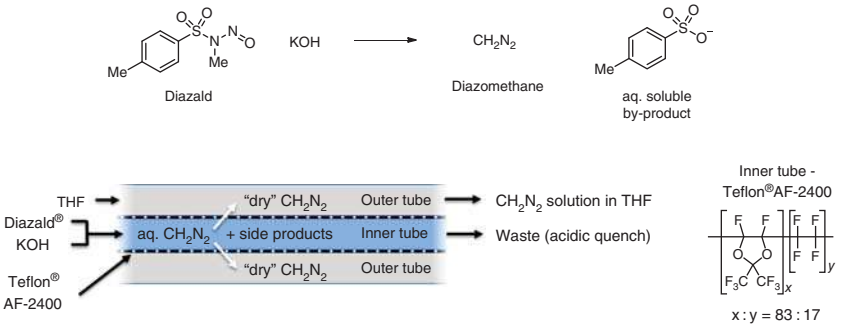

Figure 1.3 Schematic of a tube-in-tube reactor and the structure of Teflon AF-2400.

1.3.3 Diazomethane

Diazomethane (CH_2N_2) is a versatile reagent in organic synthesis; however, its use is limited due to the safety concerns associated with its use [51]. This reagent, however, is gaining broader utility due to recent advances in flow chemistry technology, specifically with the development of tube-in-tube reactors or other gas-permeable membranes. With a tube-in-tube reactor, an inner gas-permeable tube (commonly made of Teflon AF-2400) is housed within a larger, standard piece of tubing. Gases permeate through the Teflon AF-2400 into the outer stream, where reactions can take place (Figure 1.3). For the examples to be highlighted, Diazald and potassium hydroxide are mixed within the inner tube of the tube-in-tube reactor and the generated gas permeates out into a reaction or solvent stream.

The Kappe group has pioneered the generation of diazomethane using tube-in-tube reactors [52]. In this case, a series of reactions are carried out to synthesize cyclopropanes, methyl esters, and α-diazocarbonyls (Figure 1.4). A stream of reactant is passed through the outer tube of the tube-in-tube reactor to generate a product. A multistep process was later developed where the α-diazocarbonyls was treated with HCl to generate α-chloromethyl ketones on gram scale, in excellent yield [53]. Similarly, by treating the α-diazocarbonyl species with water, followed by irradiation with ultraviolet (UV) light, a series of homologated amino acids could be prepared in a multistep continuous flow process (Scheme 1.17) [54].

Scientists at AbbVie have developed the diazomethane reactor in flow technology (DRIFT) platform to automate diazomethane production, in both library and scale-up format [55]. A key difference between the DRIFT platform and the examples highlighted earlier is that DRIFT prepares an anhydrous solution of diazomethane in THF in the outer tube of the tube-in-tube reactor, which is used in downstream reactions (Figure 1.5). During development, it was noted that when running reactions in the outer tube of the tube-in-tube reactor, results were inconsistent and long-term use was not feasible. On the DRIFT platform, a small library of cyclopropyl boronates was synthesized in modest yield with an output of up to 190 mg/h (Scheme 1.18). The DRIFT platform continues to be applied to various projects in support of discovery chemistry programs.

https://www.twirpx.org & http://chemistry-chemists.com

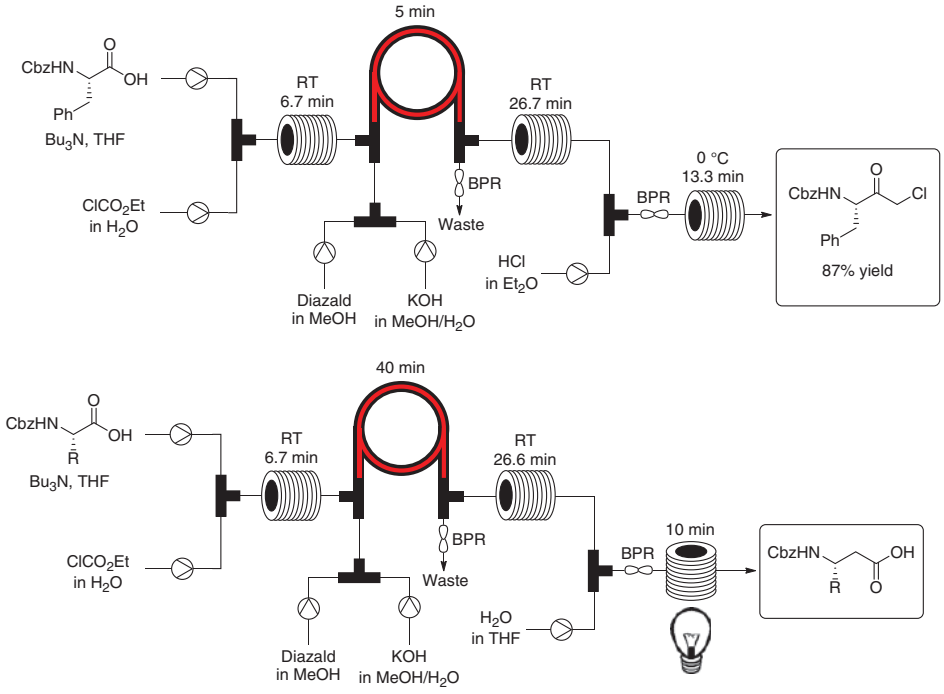

Scheme 1.17 Multistep continuous flow diazomethane chemistry. Source: Based on Pinho et al. [54].

https://www.twirpx.org & http://chemistry-chemists.com

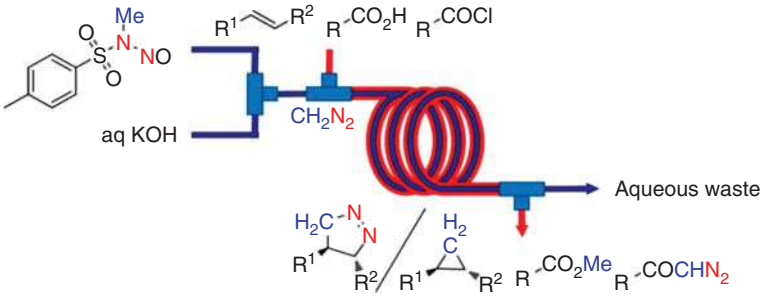

Figure 1.4 Tube-in-tube reactor using diazomethane technology.

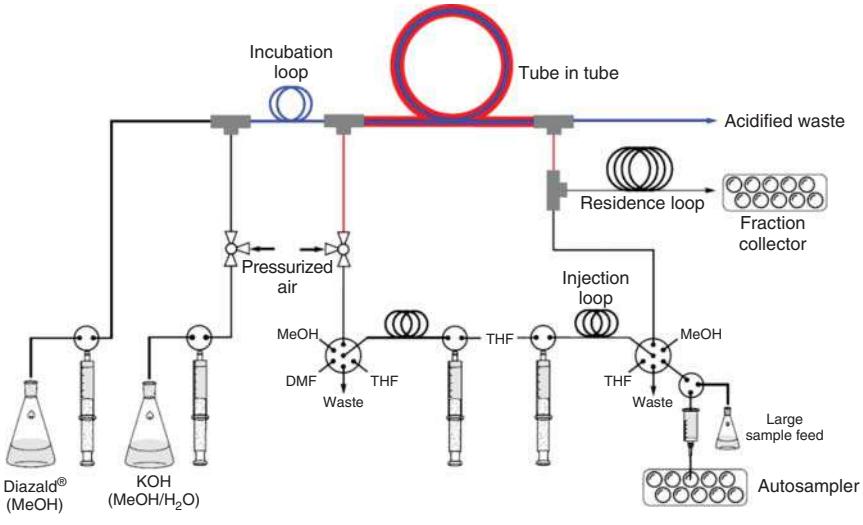

Figure 1.5 Schematic of the DRIFT flow reactor.

While many of the aforementioned diazomethane reactions are high yielding, they are limited by their output. To address this, the Kappe group has developed hybrid batch/flow procedure for facile scaling of diazomethane reactions [56]. A coil of AF-2400 tubing is submerged within a batch reaction vessel, and substrates are added. Diazomethane is generated by mixing Diazald and KOH in flow, and diazomethane permeates out of the AF-2400 tubing, converting starting materials to product (Figure 1.6). Larger scales can be achieved by adding additional coils of the AF-2400 tubing. This process was reported to synthesize >40 g of methyl benzoate during an eight hour run.

More recent examples of diazomethane chemistry have emerged in flow chemistry, where the diazomethane gas is extracted by way of a gas-permeable membrane (Figure 1.7) [57]. In this case, substrates are treated with a gaseous stream of diazomethane in a nitrogen carrier gas, as opposed to an organic solvent. Examples highlighted using this approach include methyl ester formation, as well as the cyclopropanation of styrene. In both instances, multigram per hour outputs were noted,

https://www.twirpx.org & http://chemistry-chemists.com

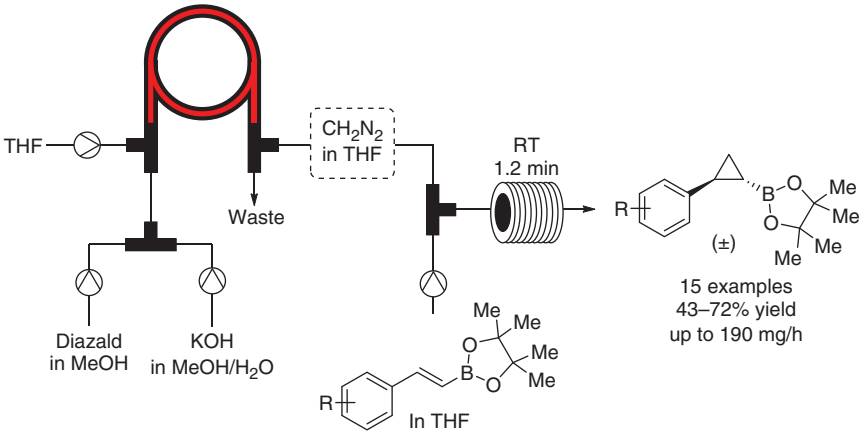

Scheme 1.18 Library production using tube-in-tube diazomethane reactor.

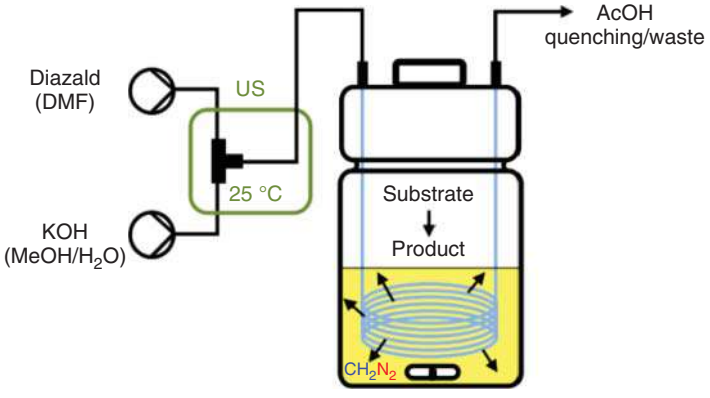

Figure 1.6 New approach for running tube-in-tube reactions with diazomethane in batch using Teflon AF-2400 coil.

where a relatively small amount of diazomethane was present at a given time. As such, this route is proposed as a method to be used in small-scale manufacturing in the event that diazomethane is required for synthesis.

1.4 Photochemistry on Scale

Photochemistry on scale has gained far more attention over the past decade, thanks to a variety of simple flow reactors [58–63]. In many cases, the systems can rapidly be prepared using traditional photoreactor equipment, coupled with a pump and some tubing (Figure 1.8). Many of the benefits of running a flow photochemical reaction are the result of short path lengths (i.e. tubing diameter). For this reason, there have been a number of gram- to kilogram-scale processes developed using flow chemistry, using either UV or visible light sources. (In Chapter 3 the reader could

https://www.twirpx.org & http://chemistry-chemists.com

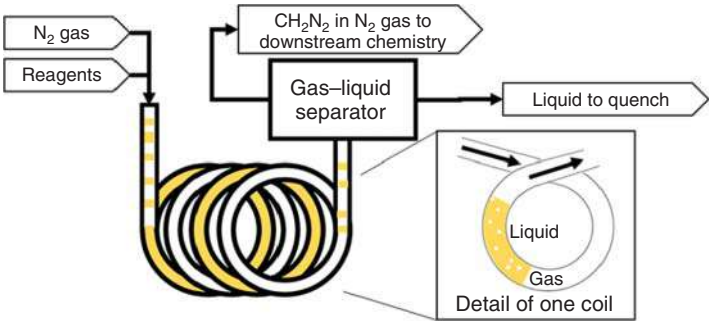

Figure 1.7 Diazomethane generation using gas–liquid separator. Source: Sheeran et al. [57] / American Chemical Society.

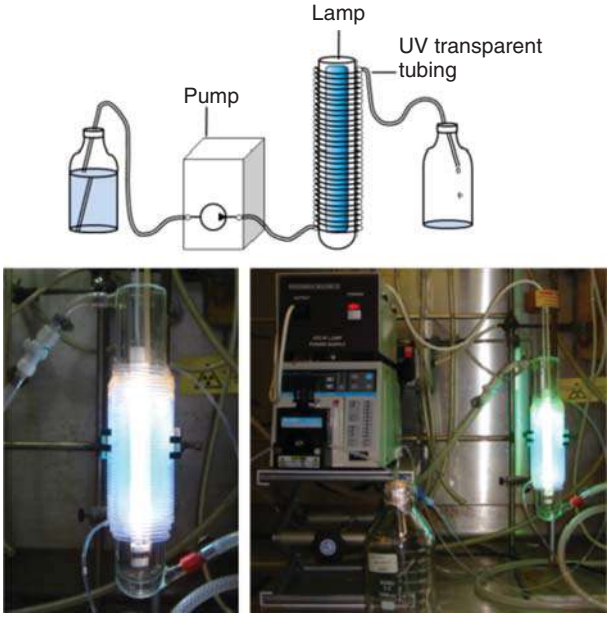

Figure 1.8 Example of flow photochemical reactor.

also find several examples of photochemical transformation in continuous flow at smaller scale, useful for medicinal chemistry).

Flow photochemical reactors can be readily prepared to accommodate various scales of chemistry. While a number of microscale photoreactors are available, larger-scale operations can be achieved by wrapping tubing around an immersion well or a glass/quartz sleeve. A standard setup has been highlighted by the Booker-Milburn group [64], which has subsequently been utilized in various industrial and academic applications.

Scientists at Vertex have utilized flow photochemistry to generate lactams on multigram scale via a light-catalyzed rearrangement of spiro-oxaziridines

https://www.twirpx.org & http://chemistry-chemists.com

(Scheme 1.19) [65]. Examples highlighted within the manuscript are high yielding and often have shorter reaction times than corresponding batch reactions. Similarly, the Booker-Milburn used a photochemical Paternò–Büchi reaction to reach a key intermediate in the synthesis (+)-goniofufurone (Scheme 1.19) [66]. After 83 hours of continuous processing, 42 g of intermediate (2 : 1 mixture of regioisomers) was obtained in a 97% isolated yield.

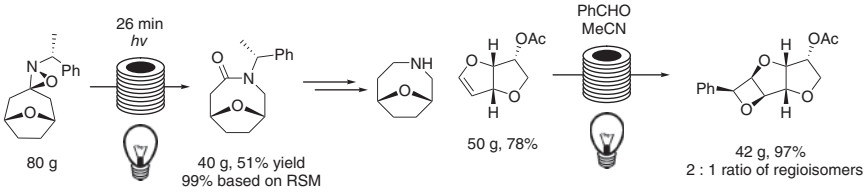

Scheme 1.19 Flow photochemistry-enabled rearrangements. Source: Cochran and Waal [65] / American Chemical Society.

Flow photochemistry is not just limited to traditional UV light sources. Recently, a number of examples have been exemplified using longer wavelength light sources such as LEDs. Enamine, for example, has expanded the scope of scalable flow processes by generating 1 kg of a high-value 2,4-methanopyrrolidine intermediate (Scheme 1.20) [67]. The process was carried out using a 366 nm light source and run continuously for one day. The resulting compound was subsequently converted to dozens of methanopyrrolidine substrates.

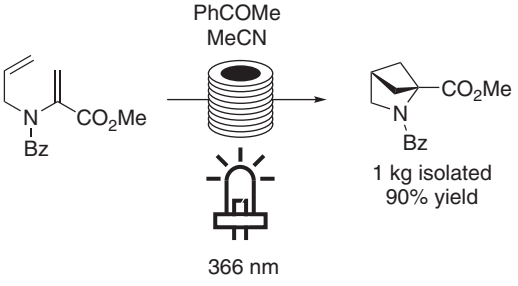

Scheme 1.20 Flow preparation of 2,4-methanopyrrolidine intermediate. Source: Levterov et al. [67] / American Chemical Society.

A fair amount of research has additionally been undertaken to synthesize the highly strained 1,4-cubanedicarboxylate (Scheme 1.21). Early examples of photochemistry to synthesize this compound were run on pilot scale, isolating nearly 3 kg of material over the course of 173 hours (~1 week) [68]. The apparatus described within uses a 6.4 l quartz flow cell, used in conjunction with a 2 kW medium-pressure mercury lamp. While this represents an impressive example of flow photochemistry on scale, the process uses highly specialized equipment and required further optimization of the light sources. Linclau and coworkers have since reported a simplified, laboratory-scale flow photochemical reactor capable of

https://www.twirpx.org & http://chemistry-chemists.com

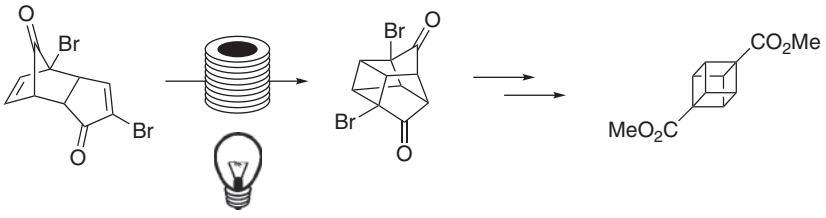

Scheme 1.21 Flow-mediated synthesis of 1,4-cubanedicarboxylate.

generating ~40 g material per day [69]. In this example, cheap 310 nm UV lamps are used and provide clean conversion. In developing a simplified, yet scalable synthesis, the process could be further adapted to synthesize additional sp^3-rich building blocks such as this.

A series of simplified trifluoromethylation papers were published by Stephenson's group, where trifluoroacetic anhydride was used as the trifluoromethylating agent [70, 71]. Early examples were reported to be scalable up to 100 g in flow (Scheme 1.22). The process was further explored to trifluoromethylate, an additional pyrrole on roughly 1 kg scale in 24 hours. In the large-scale reactor, PFA tubing was wrapped around three blue LED lamps and submerged in a garbage bin to provide cooling (Figure 1.9).

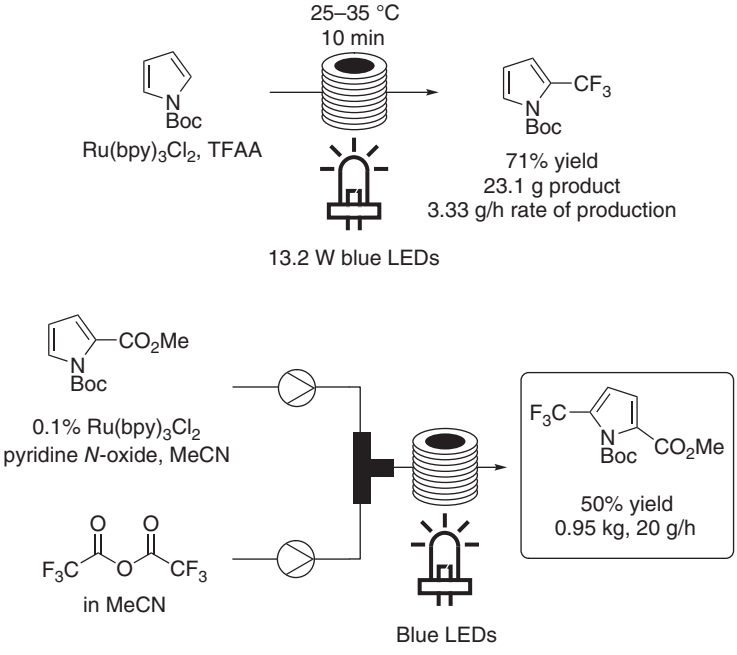

Scheme 1.22 Trifluoromethylation in flow using trifluoroacetic anhydride.

Scientists at Merck have reported the use of a flow photochemical reactor to synthesize bicyclo[1.1.1]pentane (BCP) trifluoroborate salts (Scheme 1.23) [72]. Up to

https://www.twirpx.org & http://chemistry-chemists.com

Figure 1.9 Scale-up of flow trifluoromethylation.

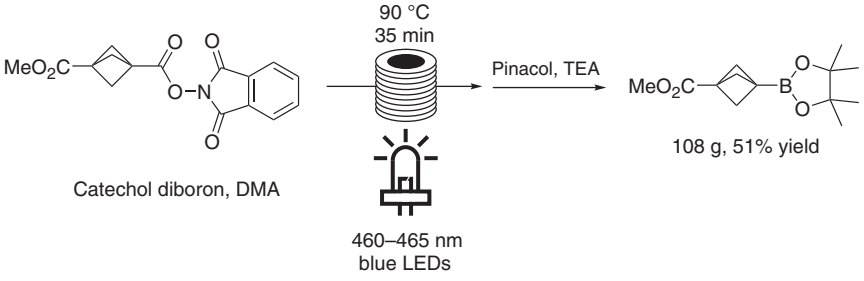

Scheme 1.23 Flow synthesis of bicyclo[1.1.1]pentane (BCP) trifluoroborate salts. Source: VanHeyst et al. [72] / American Chemical Society.

100 g of BCP pinacol esters are synthesized in flow, before being converted to the corresponding trifluoroborate salt in batch. In doing so, a jacketed photoreactor was prepared capable of heating/cooling reactions while being irradiated with 465 nm blue LEDs.

A number of manuscripts highlight efforts to push flow photochemistry to a large scale (Figure 1.10). A photoreactor capable of kilograms per day output has been reported by Merck [73]. The reactor overall has a small footprint (fitting within a standard fume hood) and can be built from a number of readily available pieces. The light source on this reactor consists of a series of high-power LED connected to a heat sink to assist with dissipating temperature. Amgen, in collaboration with Asymchem, has developed a production-scale photoreactor that was demonstrated to prepare >50 kg of a [2+2] cycloaddition product from a single run [74]. In their setup, a series of high watt 365 nm LED panels were used to irradiate a 29 l reactor coil. These examples highlight how there are relatively few limitations on the scale that can be achieved using photochemistry. A lot of this technology is facilitated by the development of new LED light sources of varying power and wavelength. Coupled with the narrow path lengths of flow chemistry, photochemistry is no longer a thing of the past and will continue to gain more utility across the chemical industry.

https://www.twirpx.org & http://chemistry-chemists.com

Figure 1.10 Examples of large-scale photoreactors built by Merck (left) and Amgen (right).

1.5 Conclusion and Outlook

In conclusion, there exists a litany of examples where flow chemistry has obvious advantages over traditional batchwise processes. By this point, most major pharmaceutical companies have developed large-scale flow operations that can deliver hundreds of grams, if not hundreds of kilograms, of material in relatively short order.

Reactions being run at high- and low-temperature extremes are no longer novel, small-scale processes. Cryogenic "flash" reactions have shown great promise. Coupled with proper pumps and mixing, incredibly high-throughput processes can be developed to synthesize valuable building blocks in API development. At the other end of the spectrum, reactions that were found to behave well under high-heat have been readily scaled up in flow. Issues of superheating large reactor volumes are mitigated using a flow process, and temperatures well above solvent boiling points can be used. In both the low- and high-temperature examples, flow has inherent safety advantages as well as superb control over reaction parameters. Looking forward, it is anticipated that the volume of examples highlighting these temperature extremes will continue to increase.

Flow chemistry also offers the ability to generate hazardous reagents *in situ*, eliminating the hazards associated with working with these materials on larger scale. Reagents such as the Vilsmeier reagent and phosgene can be used on large scale, without even having to isolate or store these materials prior to their use. Other reagents such as diazomethane are also gaining more traction in synthetic chemistry due to newer, safer methods of use.

A final area seeing continuous growth is the area of photochemistry. Thanks to new, improved light sources, as well as a rapid expansion of photoredox reactions, more and more examples of flow photochemistry are being highlighted to enhance scalability. Both simplified and complex systems have been developed to address concerns of scalability in photochemistry. Now, an area that was once viewed as limited by scale can be used to prepare tens of kilograms of material. This area, too, will likely continue to grow, specifically as more cross-coupling reactions are developed and run on larger scale.

https://www.twirpx.org & http://chemistry-chemists.com

The lowest hanging fruit in the flow chemistry realm is likely the expansion of scalable flow electrochemistry. This is viewed almost as a complementary tool as photoredox chemistry, where an alternative energy source is used to facilitate a reaction. A few examples exist already, highlighting the scalability of these processes, which shows great promise in the future of the field (some of them are presented in Chapter 3) [75, 76]. Initial reports demonstrate how >100 g of material can be prepared via electrochemistry in flow, and its growth within pharma will likely increase over time.

While the initial uptake of flow chemistry in the pharmaceutical industry was slow, we have reached a point where these processes are safely and effectively being applied on scale. Companies have either implemented their own infrastructure or are working with contract manufacturing organizations (CMOs)/contract research organizations (CROs) to enable this technology. Very large deliveries of compound are now being handled exclusively in flow, whereas a similar process would not have been considered a few years ago. As time goes by, new applications of flow will continue to emerge, and the barriers to apply this technology will continue to fade. And while not all reactions benefit from being run in flow, there are a number of applications where flow chemistry should potentially be explored as a first pass.

Notes

The authors declare no competing financial interest.

References

1 Ahmed-Omer, B., Brandt, J.C., and Wirth, T. (2007). Advanced organic synthesis using microreactor technology. *Org. Biomol. Chem.* 5: 733–740.

2 Deal, M. (2012). Continuous flow chemistry in medicinal chemistry, Chapter 5. In: *New Synthetic Technologies in Medicinal Chemistry* (ed. E. Farrant), 90–125. The Royal Society of Chemistry.

3 Gutmann, B., Cantillo, D., and Kappe, C.O. (2015). Continuous-flow technology-a tool for the safe manufacturing of active pharmaceutical ingredients. *Angew. Chem. Int. Ed. Engl.* 54: 6688–6728.

4 Hartman, R.L., McMullen, J.P., and Jensen, K.F. (2011). Deciding whether to go with the flow: evaluating the merits of flow reactors for synthesis. *Angew. Chem. Int. Ed. Engl.* 50: 7502–7519.

5 Hughes, D.L. (2018). Applications of flow chemistry in drug development: highlights of recent patent literature. *Org. Process Res. Dev.* 22: 13–20.

6 Malet-Sanz, L. and Susanne, F. (2012). Continuous flow synthesis. A pharma perspective. *J. Med. Chem.* 55: 4062–4098.

7 Mason, B.P., Price, K.E., Steinbacher, J.L. et al. (2007). Greener approaches to organic synthesis using microreactor technology. *Chem. Rev.* 107: 2300–2318.

8 McQuade, D.T. and Seeberger, P.H. (2013). Applying flow chemistry: methods, materials, and multistep synthesis. *J. Org. Chem.* 78: 6384–6389.

https://www.twirpx.org & http://chemistry-chemists.com

9 Pastre, J.C., Browne, D.L., and Ley, S.V. (2013). Flow chemistry syntheses of natural products. *Chem. Soc. Rev.* 42: 8849–8869.

10 Plutschack, M.B., Pieber, B., Gilmore, K., and Seeberger, P.H. (2017). The hitchhiker's guide to flow chemistry. *Chem. Rev.* 117: 11796–11893.

11 Poechlauer, P., Colberg, J., Fisher, E. et al. (2013). Pharmaceutical roundtable study demonstrates the value of continuous manufacturing in the design of greener processes. *Org. Process Res. Dev.* 17: 1472–1478.

12 Porta, R., Benaglia, M., and Puglisi, A. (2015). Flow chemistry: recent developments in the synthesis of pharmaceutical products. *Org. Process Res. Dev.* 20: 2–25.

13 Wegner, J., Ceylan, S., and Kirschning, A. (2011). Ten key issues in modern flow chemistry. *Chem. Commun. (Camb)* 47: 4583–4592.

14 Baumann, M., Moody, T.S., Smyth, M., and Wharry, S. (2020). A perspective on continuous flow chemistry in the pharmaceutical industry. *Org. Process Res. Dev.* 24 (10): 1802–1813.

15 Bogdan, A.R. and Dombrowski, A.W. (2019). Emerging trends in Flow Chemistry and applications to the pharmaceutical industry. *J. Med. Chem.* 62: 6422–6468.

16 Gioiello, A., Piccinno, A., Lozza, A.M., and Cerra, B. (2020). The medicinal chemistry in the era of machines and automation: recent advances in continuous flow technology. *J. Med. Chem.*

17 Guidi, M., Seeberger, P.H., and Gilmore, K. (2020). How to approach flow chemistry. *Chem. Soc. Rev.* 49: 8910–8932.

18 Power, M., Alcock, E., and McGlacken, G.P. (2020). Organolithium bases in flow chemistry: a review. *Org. Process Res. Dev.* 24 (10): 1814–1838.

19 Yoshida, J., Takahashi, Y., and Nagaki, A. (2013). Flash chemistry: flow chemistry that cannot be done in batch. *Chem. Commun. (Camb)* 49: 9896–9904.

20 Newby, J.A., Blaylock, D.W., Witt, P.M. et al. (2014). Design and application of a low-temperature continuous flow chemistry platform. *Org. Process Res. Dev.* 18: 1211–1220.

21 Newby, J.A., Blaylock, D.W., Witt, P.M. et al. (2014). Reconfiguration of a continuous flow platform for extended operation: application to a cryogenic fluorine-directed ortho-lithiation reaction. *Org. Process Res. Dev.* 18: 1221–1228.

22 Hafner, A., Filipponi, P., Piccioni, L. et al. (2016). A simple scale-up strategy for organolithium chemistry in flow mode: from feasibility to kilogram quantities. *Org. Process Res. Dev.* 20: 1833–1837.

23 Usutani, H., Nihei, T., Papageorgiou, C.D., and Cork, D.G. (2017). Development and scale-up of a flow chemistry lithiation–borylation route to a key boronic acid starting material. *Org. Process Res. Dev.* 21: 669–673.

24 Usutani, H. and Cork, D.G. (2018). Effective utilization of flow chemistry: use of unstable intermediates, inhibition of side reactions, and scale-up for boronic acid synthesis. *Org. Process Res. Dev.* 22: 741–746.

25 Grongsaard, P., Bulger, P.G., Wallace, D.J. et al. (2012). Convergent, kilogram scale synthesis of an Akt kinase inhibitor. *Org. Process Res. Dev.* 16: 1069–1081.

https://www.twirpx.org & http://chemistry-chemists.com

26 Seto, M., Masada, S., Usutani, H. et al. (2019). Application of continuous flow-flash chemistry to scale-up synthesis of 5-cyano-2-formylbenzoic acid. *Org. Process Res. Dev.* 23: 1420–1428.

27 Tweedie, S., Venkatraman, S., Liu, S. et al. (2016). Continuous flow carboxylation reaction. US 2016/0090361 A1.

28 Tweedie, S., Venkatraman, S., Zeller, J. (2017). Continuous flow carboxylation reaction. US 9,725,413 B2.

29 Fukuyama, T., Chiba, H., Kuroda, H. et al. (2015). Application of continuous flow for DIBAL-H reduction and n-BuLi mediated coupling reaction in the synthesis of eribulin mesylate. *Org. Process Res. Dev.* 20: 503–509.

30 Hafner, A., Mancino, V., Meisenbach, M. et al. (2017). Dichloromethyllithium: synthesis and application in continuous flow mode. *Org. Lett.* 19: 786–789.

31 Stueckler, C., Hermsen, P., Ritzen, B. et al. (2019). Development of a continuous flow process for a Matteson reaction: from lab scale to full-scale production of a pharmaceutical intermediate. *Org. Process Res. Dev.* 23: 1069–1077.

32 Felfer, U., Stueckler, C., Steinhofer, S. et al. (2016). Apparatus and continuous flow process for production of boronic acid derivatives. WO 2016/100043.

33 Thaisrivongs, D.A., Naber, J.R., Rogus, N.J., and Spencer, G. (2018). Development of an organometallic flow chemistry reaction at pilot-plant scale for the manufacture of verubecestat. *Org. Process Res. Dev.* 22: 403–408.

34 Thaisrivongs, D.A., Naber, J.R., and McMullen, J.P. (2016). Using flow to outpace fast proton transfer in an organometallic reaction for the manufacture of verubecestat (MK-8931). *Org. Process Res. Dev.* 20: 1997–2004.

35 Cole, K.P., Argentine, M.D., Conder, E.W. et al. (2020). Development and Production of an Enantioselective Tetrahydroisoquinoline Synthesis Enabled by Continuous Cryogenic Lithium–Halogen Exchange. *Org. Process Res. Dev.* 24: 2043–2054.

36 Vieira, T., Stevens, A.C., Chtchemelinine, A. et al. (2020). Development of a large-scale cyanation process using continuous flow chemistry en route to the synthesis of Remdesivir. *Org. Process Res. Dev.* 24: 2113–2121.

37 Martin, R.E., Morawitz, F., Kuratli, C. et al. (2012). Synthesis of annulated pyridines by intramolecular inverse-electron-demand hetero-Diels–Alder reaction under superheated continuous flow conditions. *Eur. J. Org. Chem.* 2012: 47–52.

38 Lehmann, J., Alzieu, T., Martin, R.E., and Britton, R. (2013). The Kondrat'eva reaction in flow: direct access to annulated pyridines. *Org. Lett.* 15: 3550–3553.

39 Charaschanya, M., Bogdan, A.R., Wang, Y., and Djuric, S.W. (2016). Nucleophilic aromatic substitution of heterocycles using a high-temperature and high-pressure flow reactor. *Tetrahedron Lett.* 57: 1035–1039.

40 Lengyel, L.C., Sipos, G., Sipőcz, T. et al. (2015). Synthesis of condensed heterocycles by the Gould–Jacobs reaction in a novel three-mode pyrolysis reactor. *Org. Process Res. Dev.* 19: 399–409.

41 Lengyel, L., Nagy, T.Z., Sipos, G. et al. (2012). Highly efficient thermal cyclization reactions of alkylidene esters in continuous flow to give aromatic/heteroaromatic derivatives. *Tetrahedron Lett.* 53: 738–743.

https://www.twirpx.org & http://chemistry-chemists.com

42 Tsoung, J., Bogdan, A.R., Kantor, S. et al. (2017). Synthesis of fused pyrimidinone and quinolone derivatives in an automated high-temperature and high-pressure flow reactor. *J. Org. Chem.* 82: 1073–1084.

43 Tsoung, J., Wang, Y., and Djuric, S.W. (2017). Expedient Diels–Alder cycloadditions with ortho-quinodimethanes in a high temperature/pressure flow reactor. *React. Chem. Eng.* 2: 458–461.

44 Bogdan, A.R., Charaschanya, M., Dombrowski, A.W. et al. (2016). High-temperature boc deprotection in flow and its application in multistep reaction sequences. *Org. Lett.* 18: 1732–1735.

45 O'Brien, A.G., Levesque, F., and Seeberger, P.H. (2011). Continuous flow thermolysis of azidoacrylates for the synthesis of heterocycles and pharmaceutical intermediates. *Chem. Commun. (Camb)* 47: 2688–2690.

46 Li, P., Yang, S., Zhu, R. et al. (2020). Continuous flow conditions for high temperature formation of a benzodioxan pharmaceutical intermediate: rapid scaleup for early phase material delivery. *Org. Process Res. Dev.* 24: 1938–1947.

47 van den Broek, S.A.M.W., Leliveld, J.R., Becker, R. et al. (2012). Continuous flow production of thermally unstable intermediates in a microreactor with inline IR-analysis: controlled Vilsmeier–Haack formylation of electron-rich arenes. *Org. Process Res. Dev.* 16: 934–938.

48 Pellegatti, L. and Sedelmeier, J. (2015). Synthesis of vildagliptin utilizing continuous flow and batch technologies. *Org. Process Res. Dev.* 19: 551–554.

49 Carrera, M., De Coen, L., Coppens, M. et al. (2020). A Vilsmeier Chloroformylation by Continuous Flow Chemistry. *Org. Process Res. Dev.* 24: 2260–2265.

50 Yasukouchi, H., Nishiyama, A., and Mitsuda, M. (2018). Safe and efficient phosgenation reactions in a continuous flow reactor. *Org. Process Res. Dev.* 22: 247–251.

51 Yang, H., Martin, B., and Schenkel, B. (2018). On-demand generation and consumption of diazomethane in multistep continuous flow systems. *Org. Process Res. Dev.* 22: 446–456.

52 Mastronardi, F., Gutmann, B., and Kappe, C.O. (2013). Continuous flow generation and reactions of anhydrous diazomethane using a teflon AF-2400 tube-in-tube reactor. *Org. Lett.* 15: 5590–5593.

53 Pinho, V.D., Gutmann, B., Miranda, L.S. et al. (2014). Continuous flow synthesis of alpha-halo ketones: essential building blocks of antiretroviral agents. *J. Org. Chem.* 79: 1555–1562.

54 Pinho, V.D., Gutmann, B., and Kappe, C.O. (2014). Continuous flow synthesis of β-amino acids from α-amino acids via Arndt–Eistert homologation. *RSC Adv.* 4: 37419–37422.

55 Koolman, H.F., Kantor, S., Bogdan, A.R. et al. (2016). Automated library synthesis of cyclopropyl boronic esters employing diazomethane in a tube-in-tube flow reactor. *Org. Biomol. Chem.* 14: 6591–6595.

56 Dallinger, D. and Kappe, C.O. (2017). Lab-scale production of anhydrous diazomethane using membrane separation technology. *Nat. Protoc.* 12: 2138–2147.

https://www.twirpx.org & http://chemistry-chemists.com

57 Sheeran, J.W., Campbell, K., Breen, C.P. et al. (2021). Scalable on-demand production of purified diazomethane suitable for sensitive catalytic reactions. *Org. Process Res. Dev.* 25: 522–528.

58 Ciriminna, R., Delisi, R., Xu, Y.-J., and Pagliaro, M. (2016). Toward the waste-free synthesis of fine chemicals with visible light. *Org. Process Res. Dev.* 20: 403–408.

59 Su, Y., Straathof, N.J., Hessel, V., and Noel, T. (2014). Photochemical transformations accelerated in continuous-flow reactors: basic concepts and applications. *Chemistry* 20: 10562–10589.

60 Cambie, D., Bottecchia, C., Straathof, N.J. et al. (2016). Applications of continuous-flow photochemistry in organic synthesis, material science, and water treatment. *Chem. Rev.* 116: 10276–10341.

61 Tucker, J.W., Zhang, Y., Jamison, T.F., and Stephenson, C.R. (2012). Visible-light photoredox catalysis in flow. *Angew. Chem. Int. Ed. Engl.* 51: 4144–4147.

62 Knowles, J.P., Elliott, L.D., and Booker-Milburn, K.I. (2012). Flow photochemistry: old light through new windows. *Beilstein J. Org. Chem.* 8: 2025–2052.

63 Politano, F. and Oksdath-Mansilla, G. (2018). Light on the horizon: current research and future perspectives in flow photochemistry. *Org. Process Res. Dev.* 22: 1045–1062.

64 Hook, B.D.A., Dohle, W., Hirst, P.R. et al. (2005). A practical flow reactor for continuous organic photochemistry. *J. Org. Chem.* 70: 7558–7564.

65 Cochran, J.E. and Waal, N. (2016). Photochemical rearrangement of chiral oxaziridines in continuous flow: application toward the scale-up of a chiral bicyclic lactam. *Org. Process Res. Dev.* 20: 1533–1539.

66 Ralph, M., Ng, S., and Booker-Milburn, K.I. (2016). Short flow-photochemistry enabled synthesis of the cytotoxic lactone (+)-goniofufurone. *Org. Lett.* 18: 968–971.

67 Levterov, V.V., Michurin, O., Borysko, P.O. et al. (2018). Photochemical in-flow synthesis of 2,4-methanopyrrolidines: pyrrolidine analogues with improved water solubility and reduced lipophilicity. *J. Org. Chem.* 83: 14350–14361.

68 Falkiner, M.J., Littler, S.W., McRae, K.J. et al. (2013). Pilot-scale production of dimethyl 1,4-cubanedicarboxylate. *Org. Process Res. Dev.* 17: 1503–1509.

69 Collin, D.E., Jackman, E.H., Jouandon, N. et al. (2021). Decagram synthesis of dimethyl 1,4-cubanedicarboxylate using continuous-flow photochemistry. *Synthesis* 53: 1307–1314.

70 Beatty, J.W., Douglas, J.J., Cole, K.P., and Stephenson, C.R. (2015). A scalable and operationally simple radical trifluoromethylation. *Nat. Commun.* 6: 7919.

71 Beatty, J.W., Douglas, J.J., Miller, R. et al. (2016). Photochemical perfluoroalkylation with pyridine N-oxides: mechanistic insights and performance on a kilogram scale. *Chem* 1: 456–472.

72 VanHeyst, M.D., Qi, J., Roecker, A.J. et al. (2020). Continuous flow-enabled synthesis of bench-stable bicyclo[1.1.1]pentane trifluoroborate salts and their utilization in metallaphotoredox cross-couplings. *Org. Lett.* 22: 1648–1654.

73 Lévesque, F., Di Maso, M.J., Narsimhan, K. et al. (2020). Design of a kilogram scale, plug flow photoreactor enabled by high power LEDs. *Org. Process Res. Dev.* 24: 2935–2940.

https://www.twirpx.org & http://chemistry-chemists.com

74 Beaver, M.G., Zhang, E.-x., Liu, Z.-q. et al. (2020). Development and execution of a production-scale continuous [2+2] photocycloaddition. *Org. Process Res. Dev.* 24: 2139–2146.

75 Li, H., Breen, C.P., Seo, H. et al. (2018). Ni-catalyzed electrochemical decarboxylative C-C couplings in batch and continuous flow. *Org. Lett.* 20: 1338–1341.

76 Peters, B.K., Rodriguez, K.X., Reisberg, S.H. et al. (2019). Scalable and safe synthetic organic electroreduction inspired by Li-ion battery chemistry. *Science* 363: 838.

https://www.twirpx.org & http://chemistry-chemists.com

https://www.twirpx.org & http://chemistry-chemists.com

2

Automated Flow Chemistry Platforms

Juan A. Rincón, María José Nieves-Remacha, and Carlos Mateos

Centro de Investigación Lilly S.A.U., Avda. de la Industria, 30, Alcobendas-Madrid, Spain

2.1 Introduction

Medicinal chemists are relentlessly looking for new ways of improving productivity. The pharmaceutical industry, like any other sector, has been revolutionized by the advent of Industry 3.0 and the computerization and simple process automation advantages. In the case of medicinal chemistry, high-throughput and high-performance solutions that automate several aspects of the discovery and development process in areas like compound library synthesis, sample preparation for analysis and/or biological testing, reaction screening, route scouting, or drug formulation screening have been developed with success.

Industry 4.0 [1] is a term that originated from a technological high-level strategy of the German government and was adopted ultimately across the world. This new paradigm involves the integration of all parameters with increased digitalization, smart automation, and real-time process monitoring. Basically, a smart factory would be constituted by cyber-physical modules that would communicate with each other and with humans in real time. Inside the pharmaceutical sector, the industry is entering a new stage with Chemistry 4.0 [2], in which digitalization and sustainability play key roles. In this regard, flow chemistry and continuous processing [3], in general, provide a much better parameter control, new possibilities for process development, and easier real-time analysis and process monitoring [4]. All these advantages together are the main drivers and foundation for the development of automated flow chemistry platforms.

2.2 Analytical Techniques

The development of analytical techniques for monitoring chemical processes or purity determination, also known as process analytical technology (PAT), is key for the success of automated platforms whether in batch or flow [5]. Different classifications can be done for analytical techniques. If we consider the position

Flow and Microreactor Technology in Medicinal Chemistry, First Edition. Edited by Esther Alza.
© 2022 WILEY-VCH GmbH. Published 2022 by WILEY-VCH GmbH.

https://www.twirpx.org & http://chemistry-chemists.com

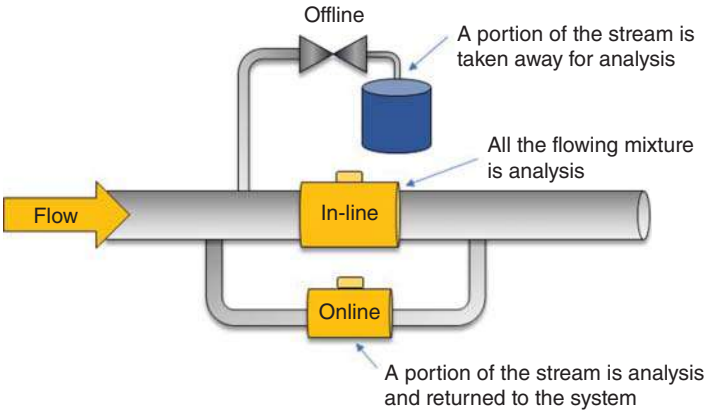

Figure 2.1 In-line, online, and offline analytical techniques.

of the analytical sensor, we can differentiate between in-line, online, and offline analysis (Figure 2.1).

For *in-line* analysis, the sensor can be placed in the stream of flowing material to conduct the analysis (e.g. in-line nuclear magnetic resonance [NMR] monitoring, in-line infrared [IR] analysis, UV spectroscopy monitoring). The real-time acquisition of analytical data allows fast and efficient screening of the reaction mixture composition for the monitoring of reactive intermediates and offers the possibility of changing the reaction parameters "on the fly." For *online* analysis, analyzers are connected to the process usually through a bypass line in order to discriminate the process from the analysis stream, avoiding technical challenges such as blockages or product loss during the analysis and allowing isolation of the analytical system to perform routine or maintenance activities, including equilibration, flushing, cleaning, calibration, or software updates (e.g. online HPLC, online GC). In contrast to the previous types, *offline* analysis consists on samples being taken away from the reaction stream or from the reactor outlet and performing the analysis (any standard technique) in a separate equipment.

In an ideal situation, the availability of multiple monitoring techniques in a bespoke platform would allow for choosing the best option for every case. This is exactly what Kappe and coworkers have recently described for the optimization of a multistep organolithium transformation, developing a platform that couples real-time monitoring by in-line IR and NMR, in addition to online ultra-performance liquid chromatography (UPLC) [6] (Figure 2.2).

However, other more common classification can be done based on the analytical technique itself, and a brief description of the most used techniques is discussed in the following text.

2.2.1 In-line NMR Monitoring

NMR is probably the most powerful and sophisticated spectroscopic technique available to synthetic chemists, but its integration in flow chemistry setups is complicated by the cost and the size of standard high-field NMR spectrometers. Although flow

https://www.twirpx.org & http://chemistry-chemists.com

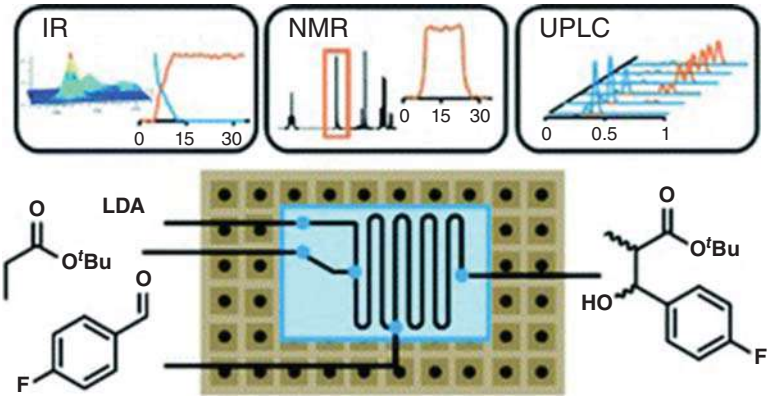

Figure 2.2 Multiple integrated PAT tools for multistep reactions. Source: Sagmeister et al. [6]/Royal Society of Chemistry/CC BY.

cells that permit the monitoring of reactions exist for some decades [7], high-field systems need specific locations for its efficient use due to their size and need of cryogenic liquids and therefore are usually far from the fume hoods where the chemical reactions take place. Moreover, the acquisition and maintenance costs and the intrinsic sophistication of these systems have hampered the implementation as a routine monitoring technique. However, the technique has grown to a great extent in the recent years, thanks to the development of low-field (or benchtop) NMR spectrometers [8]. These pieces of kit, in contrast to the high-field instruments, have a much smaller footprint, as a result of not requiring cryogenic liquid so they can be placed inside of the hoods next to the flow reactors. They are equipped with a permanent magnet and offer reasonable resolution at fields of 1–2 T (40–80 MHz) with the present state of the art, and most of them have a built-in flow cell [9]. Given all the advantages depicted earlier, these equipment have been used, apart from monitoring chemical processes, in a variety of biochemical applications such as food and agricultural analyses, structural and forensic chemistry, and potential biofluid screening and metabolomics studies for disease monitoring [10]. Additionally, the affordability, low maintenance, and easy-to-use characteristics of these devices make them ideal for academic teaching [11].

2.2.2 In-line Infrared Spectroscopy (IR)

it is a very powerful technique as it allows the identification of structural elements in quasi real time [12]. One of the limitations is that the analysis is often complicated by overlapping signals; thus, careful choice of the structural motif band to focus in must be done. There are a small number of relevant examples utilizing this technique in the context of automated flow platforms [13, 14].

2.2.3 Online HPLC and GC Sampling

Online HPLC and GC sampling remain the most versatile techniques and are the workhorse tools of pharmaceutical analytical chemistry mainly due to its

https://www.twirpx.org & http://chemistry-chemists.com

capability of qualitatively and quantitatively separating mixtures, without the interfering problems with solvents or reagents that other techniques have. These chromatographic methods are probably the most frequently used in batch chemistry monitoring, as offline analyzers, and therefore they are ubiquitous in research and development labs. Thus, their implementation in automated flow chemistry platforms is very wide [15–17]. The main limitation though are the long cycle times that limit the optimization speed. In this direction, recent developments toward UPLC (three to five minutes run times) and multiple injections in a single experimental run (MISER)-based approaches aim to reduce the analysis time [18].

On the other hand, they are mainly online analyzers as the flow stream is bypassed, and samples are injected into the column after sometimes dilution, derivatization, or pre-purification to remove interfering components and increase the measurement sensitivity [19].

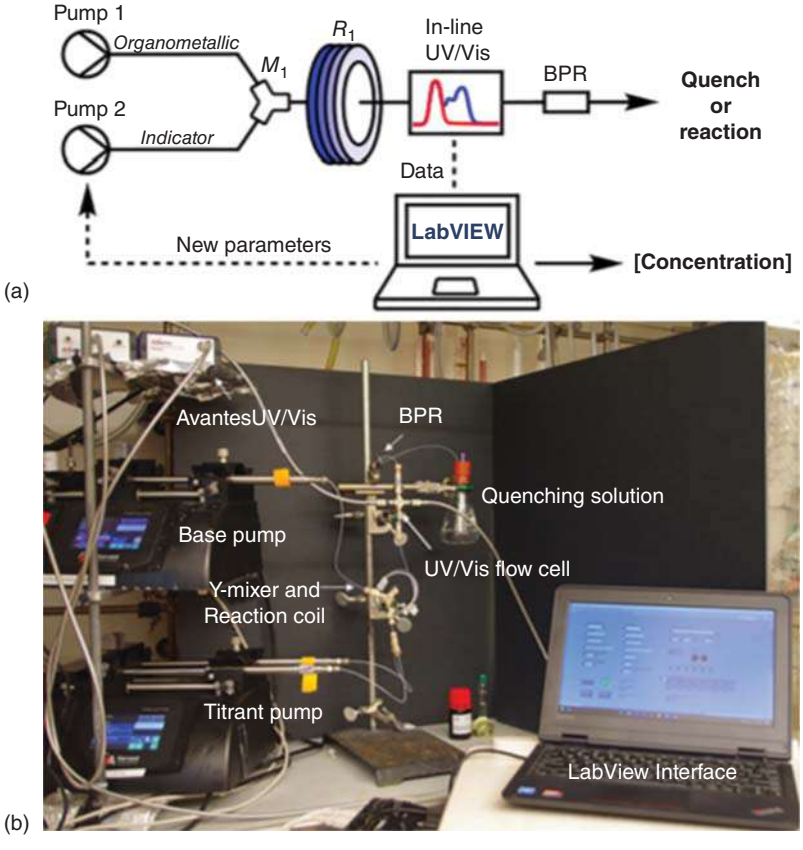

Figure 2.3 (a) General schematic for flow titrations. BRP = back pressure regulator. (b) Photograph of the automated titration system. Source: Bedermann et al. [20] / with permission from the American Chemical Society.

https://www.twirpx.org & http://chemistry-chemists.com

2.2.4 UV/Vis Spectroscopy

Little structural information can be obtained from UV/Vis spectroscopy, hence only a few examples of its use are described in the field. However, the technique is very powerful and sensitive. This has been utilized by Jamison et al. to discern subtle changes in color based on small shifts in the spectra, for the development of an automated flow chemistry platform to titrate organometallics (Figure 2.3) [20].

2.2.5 Other Analytical Techniques

2.2.5.1 Online Mass Spectroscopy

Online MS has been used to overcome the issues of the long duration analyses of other techniques. It enables rapid quantification (<1 minute analysis) and can monitor continuous reactors for the identification of compounds and intermediates or analysis of relative composition. MS can provide structural information and product composition, all in real time due to its short method times. Therefore, it could be the ideal analytical technique for optimizing an automated flow reactor as it can determine steady state and then calculate a product yield with minimal data manipulation. In a recent example, Bourne and coworkers exploited these features to enable rapid optimization of an ester **1** amidation with methylamine using an automated flow reactor (Figure 2.4) [21].

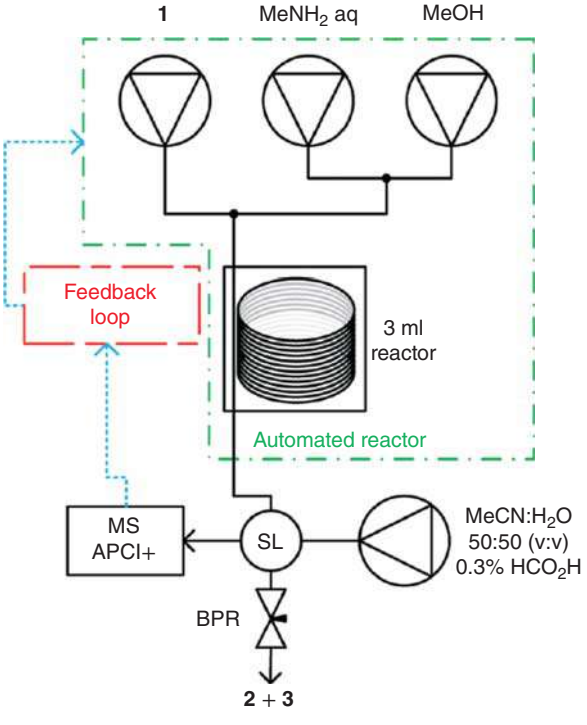

Figure 2.4 Rapid optimization of an amidation process monitoring by MS. Source: Reproduced from Holmes et al. [21] with permission from The Royal Society of Chemistry.

https://www.twirpx.org & http://chemistry-chemists.com

2.2.5.2 In-line Raman Spectroscopy

It shares many characteristics with near or mid-IR spectroscopy but has some advantages, like the weak Raman signal of water that makes it more convenient to analyze aqueous mixtures. However, it is not as straightforward to implement as IR as high concentrations and high-power lasers are needed, which limits its use [22].

2.2.6 Future Opportunities

PAT in the context of continuous-flow chemistry is an area of remarkable activity, and end users, instrument, and data analysis vendors are collaboratively trying to design effective solutions for the challenges that the pharmaceutical industry are facing for the safe and sustainable manufacturing of active ingredients [23].

2.3 Automation

2.3.1 High-Throughput Screening Platforms

High-throughput experimentation (HTE) has proved to be a very powerful tool to optimize chemical reactions and has traditionally helped to the discovery of new lead compounds in medicinal chemistry. The development of different instrumentation and technology, capable to work at nanoliter scale, has permitted to validate the chemistry until a level that minimize the amount of material required for biological assays. This miniaturization of the chemistry has been enabled by the implementation of elegant engineering solutions applied to nanomole-scale screening, allowing the synthesis of complex molecules [24].

Moreover, the integration of nanomole-scale HTE with flow chemistry platforms permits to expand the scope of the possible reactions to be made by circumventing the issues found with chemistry in plates associated with solvent volatility and limits of reaction temperature and pressure. In this regard, researchers at Pfizer have developed a fully automated system that integrates HTE with flow chemistry technology and in-line high-resolution LC–MS analysis for real-time reaction monitoring [25]. This platform was successfully applied to a Suzuki–Miyaura reaction and was able to perform up to 1500 reactions in 24 hours. Due to the potential air sensitivity of the chemicals and catalysts used in this reaction, the flow chemistry platform was placed in a glove box to ensure the maximum probability of technical success. The flow setup essentially consisted of three synergic, dynamic components working with aim of getting maximum throughput: two UPLC–MS that alternated analysis and waiting time and the reaction segment preparation unit (Figure 2.5).

Thus, each different reaction segment was elaborated in a preparation unit where the chemical stock solutions were injected using a precise nanoliter handler. The residence time of each segment was controlled by the pump flow rate, and the temperature was set in a controlled reactor coil. It was critical that each reaction segment was analyzed as it came out from the reactor so two UPLC–MS systems were put in place alternating analysis and waiting time.

https://www.twirpx.org & http://chemistry-chemists.com

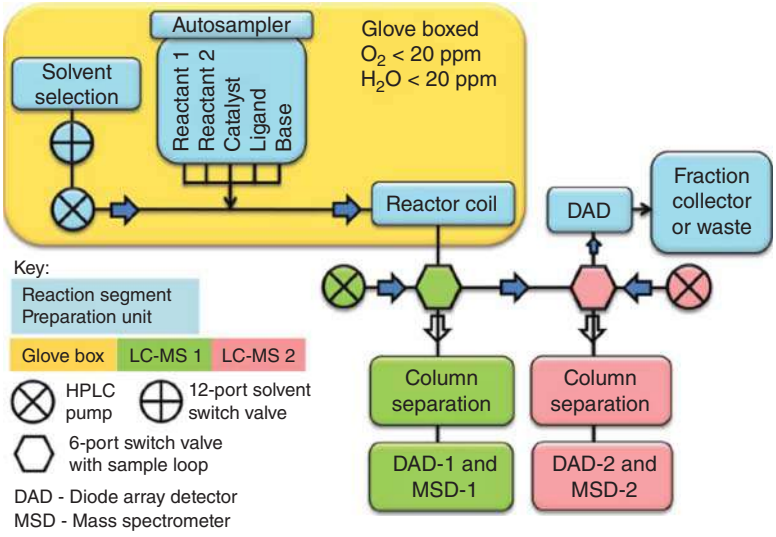

Figure 2.5 Flow system setup and segment preparation. Schematic depiction of the flow system. Source: Reproduced from Perera et al. [25] with permission from American Association for the Advancement of Science.

The reaction segments preparation was validated first by mixing four internal standards in increasing volume and methanol as carrier solvent and allowed to diffuse together. The offline analysis of each segment, split in 40 µl fractions, showed that the ration of each internal standard was equivalent through the segments and demonstrated homogeneous diffusion of the components in the carrier solvents and that the stoichiometries of the components were consistent with the ones intended for the real reaction (Figure 2.6). The platform was used to screen the Suzuki–Miyaura cross-coupling between different quinoline and indazole coupling partners using 12 ligands (including blank one), eight bases (including the blank one), and four aqueous-based solvents to avoid precipitation of inorganic salts. These appropriate combinations made up 5760 different reactions evaluated, which pushed the boundaries of the high-throughput experimentation using a flow chemistry approach.

2.3.2 Integrated Chemistry and Bioactivity Screening Platforms

The integration of microfluidic systems with biological platforms is gaining a lot of interest due to the ability of the flow chemistry technology to simplify the process of interacting potential protein binders and further analysis putting in place PATs. Chapter 5 of the present book is focused in this subject. In a recent work, Guo and coworkers [26] have devised a microscale and screening platform for the development of protein-directed dynamic combinatorial chemistry (DCC) for the rapid identification of bioactive molecules using a microflow system (Figure 2.7). They used a size-exclusion chromatography (SEC)–mass spectrometry (MS) analysis technique, which isolates highly sensitive binders from a dynamic combinatorial

https://www.twirpx.org & http://chemistry-chemists.com

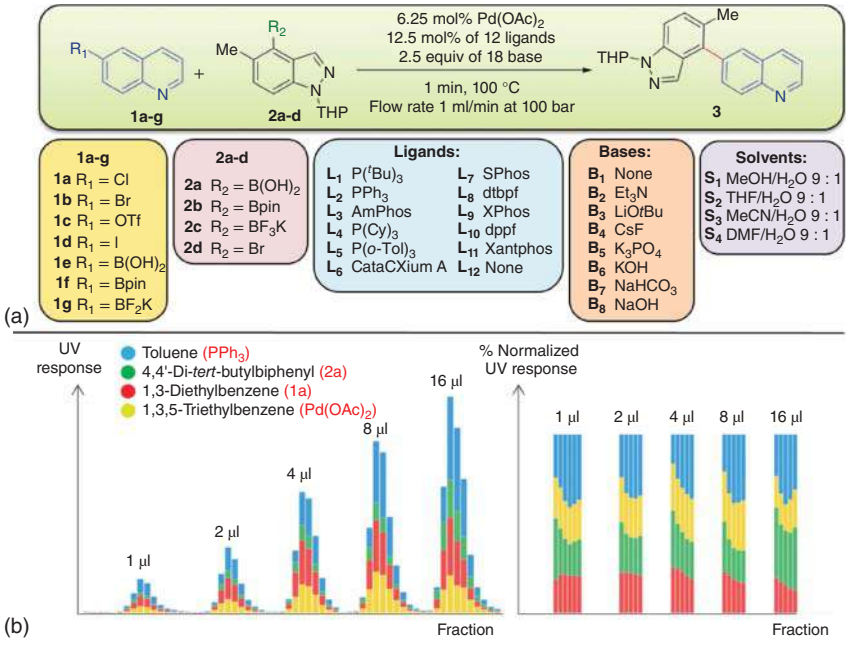

Figure 2.6 Model Suzuki–Miyaura cross-coupling. (a) Coupling evaluates electrophiles 1a–1d/2d, with 2a–2c/1e–1 g evaluated across a matrix of 11 ligands (plus one blank) × 7 bases (plus one blank) × 4 solvents. (b) UV analysis of internal standards (see legend) in the fractionated reaction segment derived from increasing volumes of components confirming adequate mixing. Source: Reproduced from Perera et al. [25] with permission from American Association for the Advancement of Science.

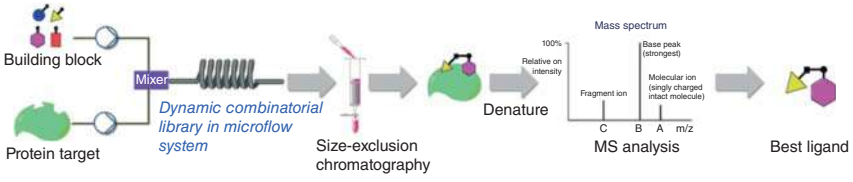

Figure 2.7 The general protocol for protein-directed DCC in the microflow system with SEC-MS as an analytical method. Source: Reproduced from Qiu et al. [26] with permission of The Royal Society of Chemistry.

library (DCL) and then exclusively identifies the best binders by MS analysis. The use of a microflow system turned out to be beneficial since it provided better mixing and mass transfer to enhance the contact between compounds and the protein of interest, and the short equilibration times avoided hydrolysis or decomposition of the potential inhibitors.

Very recently, Felpin and coworkers [27] have designed a reconfigurable flow platform for automated reagent screening to optimize an oxidative dimerization using different Co^{II}(salen) complexes as catalysts and oxidants (Figure 2.8) for natural product synthesis. This platform sought to be particularly attractive in terms of flexibility since it was used to first identify the best pair of oxidant and catalyst

https://www.twirpx.org & http://chemistry-chemists.com

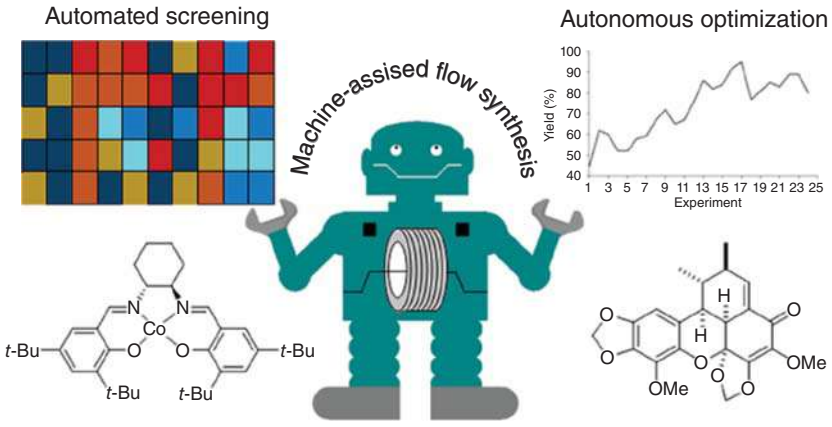

Figure 2.8 Reconfigurable flow platform for automated reagent screening and autonomous optimization. Source: Reproduced from Figure 2.3: Schematic drawing of the reconfigurable platform used for the reaction screening and automated self-optimizing platform. Reproduced from Aka et al. [27] with permission from the American Chemical Society.

and then used to self-optimize the reaction of interest, by simply integrating an additional optimization algorithm to the process control software.

The yield of the reaction was optimized in a four-dimension space using the residence time, temperature, equivalent of the ^{t}BuOOH, and loading of the [Co] catalyst as input variables. A very satisfactory optimum was located after only 16 experiments, and the system reached a stopping criterion after only 24 experiments (Figure 2.9).

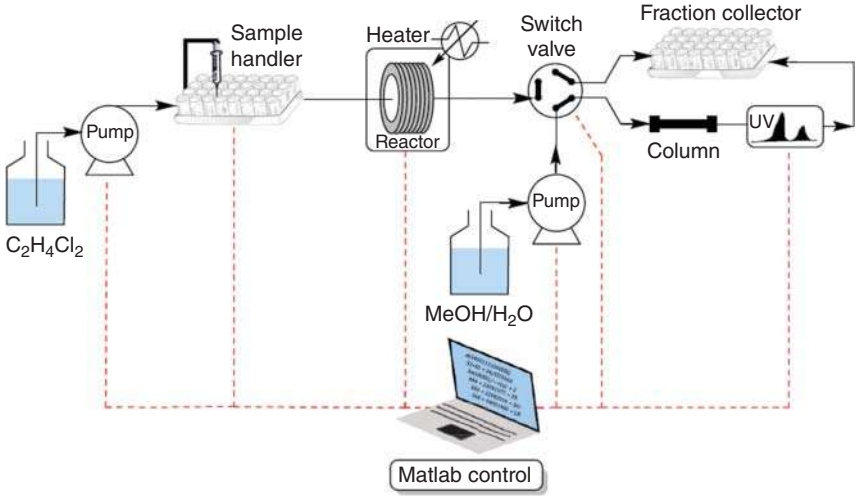

Figure 2.9 Schematic drawing of the reconfigurable platform used for the reaction screening and automated self-optimizing platform. Source: Reproduced from Aka et al. [27] with permission from the American Chemical Society.

https://www.twirpx.org & http://chemistry-chemists.com

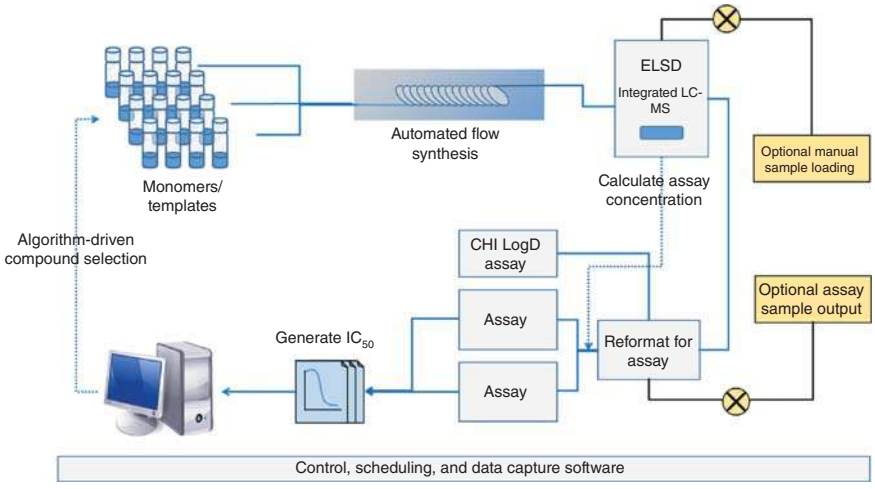

Figure 2.10 Schematic of the CyclOps platform indicating the key components, fluidic path, and the optional functionality (yellow boxes) to omit either or both of synthesis and assay. Source: Reproduced from Parry et al. [17] with permission of the American Chemical Society.

Probably, one of the most ambitious approaches to integrate the synthesis of new compounds and their testing in biological assays by means of intelligent, microfluidic platforms was done by Cyclofluidic Ltd [17]. The Cyclofluidic Optimisation Platform (CyclOps™) was born with the aim of shortening the lead discovery design–synthesis–test cycle from weeks to minutes and connected flow chemistry, purification, screening, and drug design in a closed loop mode (Figure 2.10). All these elements were combined with a machine learning algorithm that used the structure–activity relationship data generation from every iteration into the algorithm for the selection of the next compound to make.

Different pharmaceutical companies took advantage of this platform to rapidly generate SAR for drug discovery. Interestingly, Sanofi-Aventis applied this technology to the integrated synthesis and testing of substituted xanthine-based DPP4 inhibitors [28]. To validate this platform, Sanofi-Aventis provided a series of compounds with known inhibitory activity against DPP4 in a blinded experiment. First, the reproducibility of the process was confirmed by synthesizing and screening a single compound 10 times on the integrated platform. The consistency between cycles was achieved within normal error and the IC_{50} agreed with a discrete sample determined manually. Once the reproducibility of the platform was confirmed, a series of different diamines and amino alcohols were synthesized in two flow steps: one step involving the displacement of the 8-bromosubstiuted xanthine and the second one with the deprotection of the Boc-protected intermediate (Figure 2.11). Thus, the product obtained at the maximum concentration was injected via loop into LC–MS purification system. The middle of the HPLC peak, the so-called heart cut, provided the desired compound at the highest purity and concentration. This was enough for testing, even for low-yielding reactions, due to low material requirements for the biological assay. The total cycle time per compound for

https://www.twirpx.org & http://chemistry-chemists.com

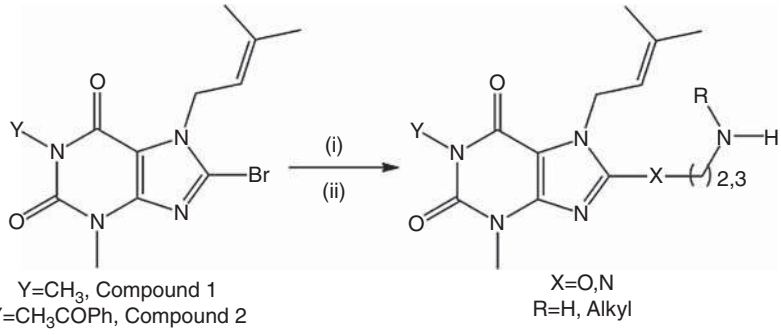

Figure 2.11 General synthesis of the DPP4 inhibitors. Source: Reproduced from Czechtizky et al. [28] with permission of the American Chemical Society.

synthesis, purification, and testing was around 120 minutes, and the data generated with this platform agreed with the previously reported values by Sanofi-Aventis.

Going beyond the validation and proving the correlation with the traditional medicinal chemistry approach, Cyclofluidic Ltd. also implemented a self-optimizing activity model to identify a novel and potent series of Abelson tyrosine kinase inhibitors (Abl), which will be presented in depth in Chapter 4 [29]. This was achieved by using the microfluidic synthesis and screening of compounds, from a virtual chemical space, coupled with an activity mapping algorithm that used the random forest activity prediction under two design strategies: "chase potency" and "most active under sampled." This approach created a bioactivity prediction model that was automatically updated after every single screening result.

2.3.3 Flexible and Modular Automated Platforms

Automating flow platforms require using different types of equipment for hardware control and monitoring of process variables and species. Due to the different requirements of the chemistries of interest, it is very frequent that the individual equipment components are changed in order to meet the specific needs. Thus, automating the entire process requires software solutions that integrate all individual systems into a master control unit to execute the scheduled events. Moreover, the level of autonomy is increased by integrating automated systems with monitoring techniques and feedback loops (also called "closed loops") that enable the machines to take decisions in real time based on instant process behaviors. The challenge is that each equipment unit comes from a different vendor, having different communication protocols and commands.

Today, there is a trend toward developing automated flexible, modular platforms from the software and hardware standpoints and with the aim of extending the usability of the platforms to nonexperts in automation, reducing time-consuming development of application-specific control programs. In a general framework, it is worth mentioning the global initiative to standardize software interfaces in research instrumentation for laboratory automation, known as SiLA [30]. In the world of continuous-flow chemistry, there are different solutions that have been adopted. The

https://www.twirpx.org & http://chemistry-chemists.com

commercial solutions most broadly used are LabVIEW™ [31], MATLAB® [32], and LabManager® and LabVision® from HiTec Zang [33], as shown by different publications. However, there is a continuous effort to develop open-source alternatives that drive efficient and accessible solutions to the community. Richard Ingham developed an open-source platform named *Octopus* [34] using Python [35] as programming language for controlling flow chemistry systems, with a similar structure to that of *Clarity* [36] written in C# programming language developed at Harvard University. Although this approach involves developing drivers and control tools using a programming language and, thus, increased implementation efforts at first, it has the potential to provide a fully customized software to specific needs. In addition, it can benefit from already developed solutions that are freely shared and available on the Internet in platforms such as GitHub [37].

In this section we describe in detail examples of automated flow platforms with modularity and flexibility from the point of view of hardware and software. Some of these also include artificial intelligence (AI) to drive the synthesis of compounds or self-optimization algorithms to obtain the best operating conditions for a predefined chemistry and objective function.

2.3.3.1 Robotic Platform for Synthesis in Flow Informed by AI Planning

Jensen and coworkers developed a system in 2019 [38] that used AI for planning the synthesis of compounds and a robotic platform to execute the synthesis in flow. The developed software, open source, was trained on millions of reactions from the Reaxys database and the US Patent and Trademark Office. The recipes were generated through the web-based graphical interface called ASKCOS [39] for each small molecule to synthesize, which suggests batch reaction conditions that are manually screened in order to find proper concentrations and residence times for implementation in flow.

The robotic arm is able to (i) find the selected process units according to the recipe, (ii) place them into the process stack, and (iii) perform the appropriate fluidic connections of reagents. The system has available different process modules to choose from: (i) laminar flow reactors (100 µl to 3 ml); (ii) packed-bed reactors (1–3 ml), with maximum temperatures of 200 °C and pressures of 250 psig; and (iii) liquid–liquid membrane separator.

The robotic platform was demonstrated with several medicinally relevant small molecules: aspirin, secnidazole, lidocaine, diazepam, (S)-warfarin, and safinamide. In addition, the system included two 24-way selector valves that enabled selection of many different feeds. This feature enabled synthesizing a library of five angiotensin-converting-enzyme (ACE) inhibitors based around quinapril and derivatives and a two-dimensional compound library of nonsteroidal anti-inflammatory drugs (NSAIDs) based around celecoxib (Figure 2.12).

2.3.3.2 Reconfigurable System for Automated Optimization of Diverse Chemical Reactions

It is noteworthy to mention the automated continuous-flow system developed by Jamison and coworkers [16] in 2018, which was built to integrate hardware,

https://www.twirpx.org & http://chemistry-chemists.com

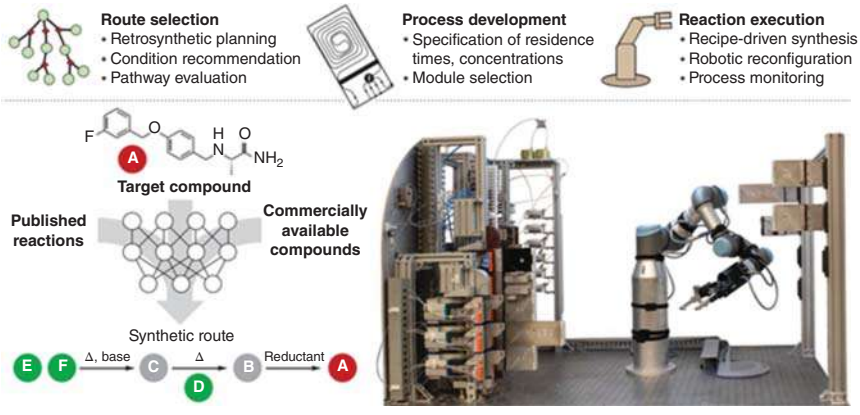

Figure 2.12 Planning and execution. A robotically reconfigurable flow chemistry platform performs multistep chemical syntheses planned in part by AI. Source: Reproduced from Coley et al. [38] / with permission of American Association for the Advancement of Science.

software, and analytics inspired by gas chromatography and high-performance liquid chromatography systems. This platform is plug and play, reconfigurable for diverse chemical reactions, and with the possibility to perform (i) automated self-optimization of a specific reaction or sequence of reactions, (ii) synthesis of different substrates under user-selected conditions, and (iii) scale-up of selected synthesis under the optimal conditions obtained.

From the hardware viewpoint, the platform was designed to be reconfigurable in terms of reactor modules and separators, while the pumps, tubes, valves, and other flow components were fixed, allowing a maximum of six different reagents and/or solvents to be delivered. To achieve hardware modularity, a standardized and flexible interface with five bays accepting six different modules was built: (i) heated reactor (to 120 °C), (ii) cooled reactor (to −20 °C), (iii) light-emitting diode (LED)-based photochemistry reactor, (iv) packed-bed reactor, (v) membrane liquid–liquid separator, and (vi) bypass for minimal volume reagent addition, mixing or unused bay. The reactor volumes range from 215 to 860 µl and the entire platform occupies a total of 0.22 m^3 (Figure 2.13).

The software was developed in LabVIEW, providing a user-friendly and intuitive interface to facilitate its use requiring only minimal expertise. MATLAB was used to implement the "black-box" global optimization algorithm Stable Noisy Optimization by Branch and Fit (SNOBFIT), which does not require previous knowledge of the system to perform optimization and ensures a global optimum is found. Monitoring of the process and species was achieved by integration of a variety of sensors and analytical equipment, which enabled performing closed-loop optimizations. The process was monitored by two pressure sensors, two flow meters, one phase sensor, five IR-based temperature sensors, and two cameras for web-based remote monitoring. Regarding the analytical techniques to monitor species, HPLC, IR, MS, and Raman were available. The platform was demonstrated to be portable in terms of software and physical system between two laboratories (Jensen and Jamison laboratories at Massachusetts Institute of Technology), each

https://www.twirpx.org & http://chemistry-chemists.com

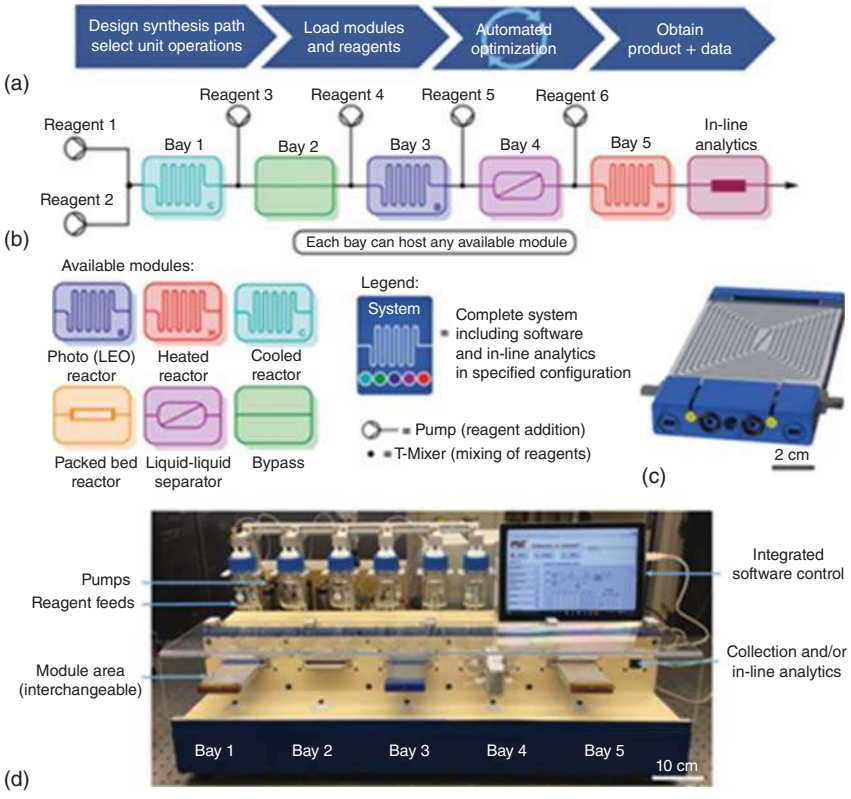

Figure 2.13 Plug-and-play, reconfigurable, continuous-flow chemical synthesis system. (a) General four-step protocol for using the system. (b) Representative configuration of the components in the system. (c) CAD (computer-aided design) representation of the LED reactor – shown as a view of the end that attaches to a universal bay on the system. (d) Schematic representation of the configuration shown in (b) and available modules. Source: Bédard et al. [16] / with permission of American Association for the Advancement of Science.

one using its own HPLC analytical equipment, for the optimization of a Paal–Knorr reaction.

In order to demonstrate the general applicability of this reactor system, the platform was used to optimize six different chemical transformations: (i) Buchwald–Hartwig (BH) amination, (ii) Horner–Wadsworth–Emmons (HWE) olefination, (iii) reductive amination, (iv) Suzuki–Miyaura cross-coupling, (v) nucleophilic aromatic substitution (SNAr), and (vi) visible-light photoredox reaction.

Table 2.1 includes the chemical transformations that were tested in the platform, with the number of variables optimized, the required number of experiments to reach the optimum conditions, and the total time required for the optimization of a model compound for each transformation. The optimal conditions were used to increase the scope of the transformation to different substrates, which is also shown in the summary table, together with the range of yields and productivity achieved.

https://www.twirpx.org & http://chemistry-chemists.com

Table 2.1 Summary of chemical transformations tested in reconfigurable platform.

Reaction	Chemical transformation	Modules	N	M	t_{opt} (h)	Optimal conditions	S_{scope}	Y (%)	P (mg/h)
Buchwald–Hartwig amination	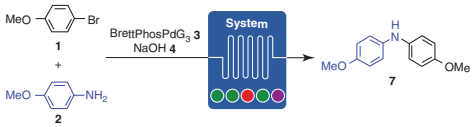	Heated reactor, liquid–liquid separator	5	32	21	1: 1.0 equiv, 2: 1.2 equiv BrettPhosPdG$_3$: 1.4 mol% NaOH: 1.5 equiv T: 100 °C t_R: 1.80 min	9	72–99	436–816
HWE olefination	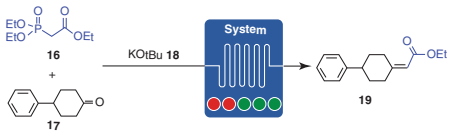	Two heated reactors	5	33	10	16: 1.0 equiv, 17: 1.5 equiv KOtBu: 1.6 equiv T: 40 °C, 66 °C t_R: 2.61 min	10	73–96	696–3083
Reductive amination	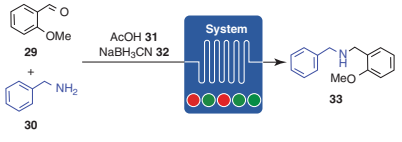	Two heated reactors	5	33	14	29: 1.0 equiv, 30: 1.2 equiv AcOH: 4.0 equiv $NaBH_3CN$: 1.9 equiv T: 100 °C, 100 °C t_R: 2.05 min	9	73–97	173–338
Suzuki–Miyaura	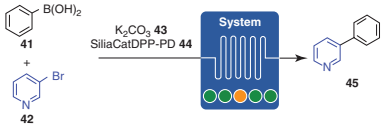	Packed-bed reactor	4	30	8	41: 1.0 equiv, 42: 1.0 equiv K_2CO_3: 4.0 equiv T: 43 °C t_R: 2.54 min	10	84–98	630–1652

(*continued*)

https://www.twirpx.org & http://chemistry-chemists.com

Table 2.1 (Continued)

Reaction	Chemical transformation	Modules	N	M	t_{opt} (h)	Optimal conditions	S_{scope}	*Y* (%)	*P* (mg/h)
S_NAr	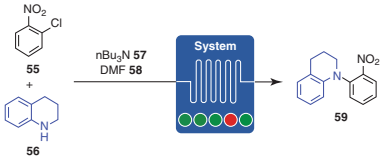	Heated reactor	4	34	12	55: 1.0 equiv, 56: 1.0 equiv nBu_3N: 10 equiv *T*: 100 °C t_R: 1.82 min	10	88–99	253–496
Photoredox	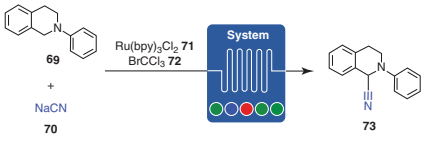	LED-photoreactor with active cooling	3	33	7	69: 1.0 equiv, NaCN: 1.0 equiv $Ru(bpy)_3Cl_2$: 2.6 mol% $BrCCl_3$: 4.2 equiv *T*: 5 °C, 25 °C t_R: 4.28 min	5	73–93	223–283
Multistep ketene generation and cyclo-addition	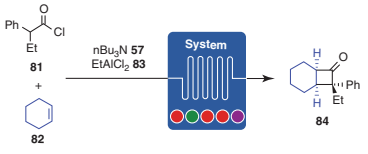	Heated reactors, quench, separator	5	45	34	81: 1.0 equiv, 82: 1.2 equiv nBu_3N: 1.0 equiv $EtAlCl_2$: 6.7 equiv *T*: 25 °C, 25 °C, 78 °C t_R: 11.3 min	5	47–90	201–353

N: number of variables optimized; *M*: number of experiments; t_{opt}: total optimization time (h), S_{scope}: substrate scope, in number of chemical compounds tested; *Y*: yield of all products (%); *P*: productivity of all products (mg/h).
Source: Chemistry excerpts reproduced from Bédard et al. [16] with permission of American Association for the Advancement of Science.

https://www.twirpx.org & http://chemistry-chemists.com

2.3.3.3 OpenFlowChem as a Flexible Software Platform

In 2018, Cherkasov et al. [40] developed a flexible automation platform from the software viewpoint with integrated self-optimization of flow chemistry. This platform, open access, is based on LabVIEW and is cloud based for data transfer interacting with MATLAB. This platform incorporates, in addition to a stepwise operation and self-optimization, a proportional integral derivative (PID) control.

The software platform was developed inspired by the necessity of accommodating to changes ensuring quick deployment and minimal effort, based on the following requirements: (i) operational safety, (ii) robustness, (iii) automated and manual control, (iv) quick extendibility, (v) low entry level for system alteration, (vi) built-in data logging, (vii) visual interface, (viii) remote control and operation. To achieve this goal, the OpenFlowChem platform contains three main layers: (i) device monitors (self-sufficient), (ii) module to integrate individual components and enable interaction among them, and (iii) optional external safety devices. In this way, the software allows the design of complex control systems by plugging the instrument-specific programming elements through the integration module, so that a flow chemist can create a control system within hours.

The platform was demonstrated with three examples of hydrogenation reactions in flow using catalyst-coated tubular reactors:

- First, the authors studied the reversibility of the catalyst (5 wt% Pd/SiO_2) poisoning by quinoline through automatic stepwise predefined operations in a spreadsheet file (Figure 2.14). In this experiment, the safety layer included sensors for the detection of hydrogen that would shut down the pumps, mass flow controllers, and oven. With this system that took approximately 20 hours to automate, the authors were able to demonstrate catalyst recovery to the initial performance prior to addition of quinoline with varying recovery times, ranging from 2 to 20 minutes, depending on quinoline concentration.
- The second experiment aimed to maximize the throughput of a heterogeneously catalyzed hydrogenation of nitrobenzene by adjusting the operating conditions using a PID controller that monitored hydrogen consumption. Arduino relays

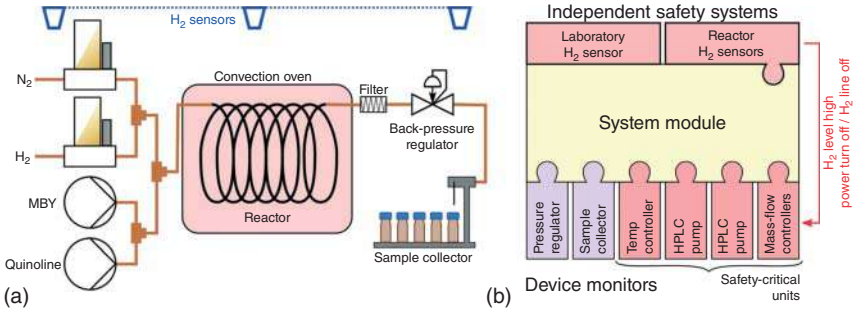

Figure 2.14 (a) Scheme of the reactor used in the automated stepwise study of the quinoline poisoning reversibility in 2-methyl-3-butyn-2-ol (MBY) semihydrogenation. (b) Scheme of the OpenFlowChem automation system with the jigsaw joints showing digital communication. Source: Reproduced from Cherkasov et al. [40] with permission of The Royal Society of Chemistry.

https://www.twirpx.org & http://chemistry-chemists.com

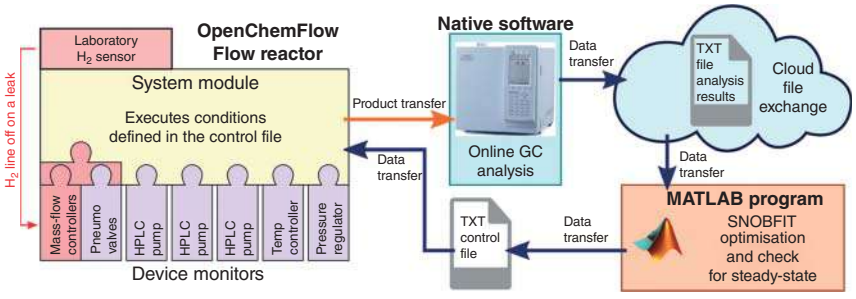

Figure 2.15 Scheme of the OpenFlowChem self-optimization reactor containing a flow reactor, a MATLAB program calculating the next set of experimental conditions, and an online GC with the native software for the analysis of the reaction products with the data transferred to the main computer via the cloud. Source: Reproduced from Cherkasov et al. [40] with permission of The Royal Society of Chemistry.

were used to control pneumatic valves to prevent from gas leaks after the mass flow controllers. The reactor outlet passed through an in-line liquid sensor and was analyzed by an online GC for reaction validation. In this example, the automation involves two horizontal systems: (i) OpenFlowChem *reactor*, of a similar function as in the first example, and (ii) OpenFlowChem *control system*, for the Arduino microcontroller that was connected to the liquid sensor. The system adjusted the nitrobenzene flow rate to ensure full conversion, maintaining the product liquid holdup at 95%. Both automated systems established a connection and interaction through text files: the *control* system updated a text file every two minutes with new set of parameters, and the *reactor* system sent the new set points to the equipment for operation. The creation of this software took about five hours.

– The third example involved a three-dimensional (3D) self-optimization of the hydrogenation of 2-methyl-3-butyn-2-ol (MBY), with the following variables to optimize: substrate flow rate, catalyst poison, and IPA solvent. The communication between the reactor system and the GC was performed through text files generated by its native software that were stored in the cloud. These were read from a different computer by a MATLAB program that suggested the next operating conditions given by the SNOBFIT algorithm and wrote them into text files read by the reactor system (Figure 2.15). Minimization of the objective function – which considered MBY flow rate, MBE selectivity, and MBY conversion – yielded an optimum yield of 96.5% MBE, MBY conversion of 98.6%, and MBE selectivity of 97.9% for substrate flow rate of 100 µl/min, quinoline flow of 165 µl/min, and solvent flow rate of 200 µl/min.

2.3.3.4 Internet-Based Software Platform

Other software platforms have been developed within the context of the *Internet of Things* and *Industry 4.0* in chemistry research, such as the Internet-based solution published by Steven Ley and coworkers in 2016 [41], called *LeyLab*. This platform facilitates the laboratory control by researchers without requiring advanced

https://www.twirpx.org & http://chemistry-chemists.com

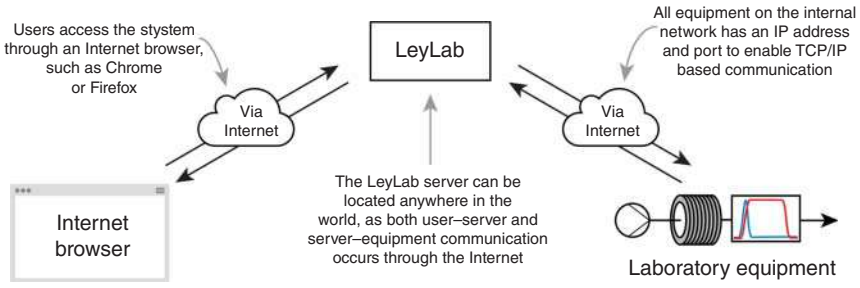

Figure 2.16 LeyLab communicates with both users and equipment through the Internet (TCP/IP), rendering it a fully cloud-based system. Source: Reproduced from Fitzpatrick et al. [41] with permission of the American Chemical Society.

programming skills. It is based on Internet protocols (TCP/IP) for user–server and server–equipment communication, using serial-to-Ethernet adapters for the equipment that communicates via RS232 and can be accessed through any Internet browser in the world (Figure 2.16). This software has four main components: (i) a graphical interface, (i) database (for experiment, equipment, and user information), (iii) equipment communication module, and (iv) equipment command module. The implementation of new modules to integrate new pieces of equipment would take about 30 minutes.

Implemented within the software is a modified version of the Simplex algorithm (called *Complex*), which allows to perform self-optimization of reaction conditions, where relative performance is used for iteration ranking. The self-optimizing platform was tested with two different examples [40].

In another publication [13], Ley et al. demonstrated the use of their web-based platform across different countries with servers located in Tokyo (Japan), the laboratories in Cambridge (UK), and the researcher in Los Angeles (USA) for the self-optimization of the synthesis of tramadol, lidocaine, and bupropion.

2.3.3.5 Other Platforms

Recent efforts have been directed toward developing modular software packages, although not specific to flow chemistry. *ChemOS* was developed by Aspuru-Guzik and coworkers [42] and includes different structured layers enabling autonomous lab operation: interaction with researchers, databases, robots, characterization, analysis, and artificial intelligence-based learning procedures. Another example is the *Chemputer* platform from Steiner et al. [43] who developed a chemical programming language that standardizes chemical synthesis and unit operations protocols through different integrated robotic modules within a backbone of series of pumps and valves. This system was validated for the synthesis of three pharmaceutical compounds: Nytol, rufinamide, and sildenafil.

It is also worth mentioning the current trends toward using low-cost open-source hardware. For instance, O'Brien et al. [44] implemented an automated computer-vision controlled liquid–liquid extraction step using a Raspberry Pi® [45] single-board computer to interface with the motors and valves. Ingham

https://www.twirpx.org & http://chemistry-chemists.com

et al. [46] describe the use of the same microcomputer to control multiple flow chemistry devices through Ethernet connections for remote control and equipment communication and apply it to the multistep synthesis of pyrazine-2-carboxamide and piperazine-2-carboxamide. Open-source microcontrollers, such the Arduino board, have been often used to control syringe pumps [47, 48] or peristaltic pumps [49].

2.3.4 Self-Optimization Algorithms

A common objective in today's automated optimization platforms is to work in an autonomous manner through experimentation guided by an algorithm reducing human bias and following the most efficient path to the optimum. An N-dimensional optimization problem involves the modification of N variables (i.e. reagent flow rates, reactor temperature, reagent concentration, equivalents, and residence time, among others) until (i) a target value for an objective function is reached, (ii) the difference between two consecutive evaluation functions is smaller than a specified tolerance, or (iii) the maximum number of iterations has been reached. For an automated platform to behave autonomously with minimal human intervention, sensors and process analytical technologies are required to analyze the output of a reaction, a computer to process the data, and algorithms to decide what is the set of parameters to test in the next iteration step (Scheme 2.1). The self-optimization of a chemical reaction in continuous flow is thus at the interface of chemistry, engineering, and computer science.

There are recent reviews on self-optimizing platforms and algorithms [5, 50, 51] related to flow chemistry. In this section we cover the basics of the most used algorithms and discuss a few application examples.

The decision on the next values for the input variables depends on the algorithm used. It is important to note that not all algorithms perform in the same way, and not all of them guarantee finding a global optimum. A *local optimum* is a solution that is better than the neighboring solutions but may not be the best within the design space. A *global optimum* is the best solution within the design space, with a value of the objective function that is better than any other feasible solutions. The optimization algorithms can also be classified as *gradient-based* or *gradient-free*, depending on whether they require first- and/or second-order derivatives for the objective function and/or constraints. The advantage of gradient-based methods is their rapid convergence. However, their derivatives are not always available or are unknown.

Another aspect to consider is the applicability of the algorithm to the specific problem to solve with respect to the modified variables and the response(s) or objective function to optimize. While numerous publications consider self-optimizing *continuous* variables (such as flow rates, temperature, residence time), very few include the optimization of *discrete* variables (i.e. solvents, ligands, or bases). Frequently, the response to optimize is strongly dependent on other responses that are also important. Although most self-optimizing platforms target a *single-objective* function, *multi-objective* optimization has recently gained more attention.

https://www.twirpx.org & http://chemistry-chemists.com

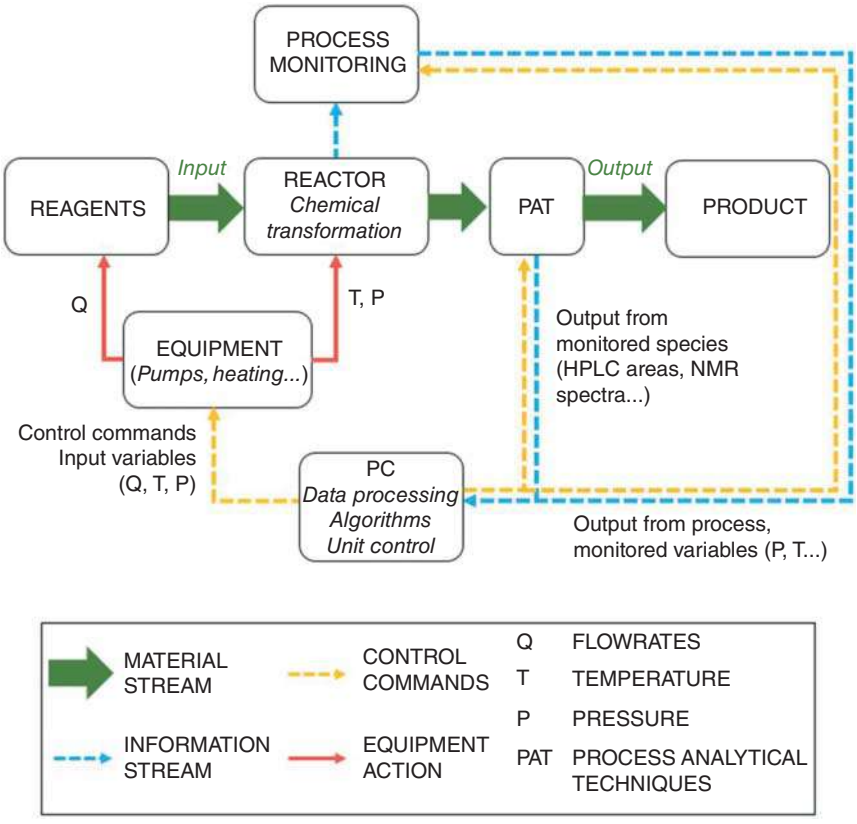

Scheme 2.1 Typical elements of a closed-loop reaction optimization platform. A material stream with reagents and solvents pumped into the reactor, where a chemical transformation occurs. The output of the reactor is a crude reaction mixture stream that is analyzed by a process analytical technique (PAT). Sensors attached to the reactor and PAT generate data that is stored and processed by a computer, which also sends commands to the equipment according to the self-optimization algorithm output that selects the next operating conditions. Source: Reproduced from Mateos et al. [5] with permission of The Royal Society of Chemistry.

The most frequently used algorithms for single-objective optimization problems include model-based design of experiments (MBDoE), Nelder–Mead Simplex algorithm with its variations, and SNOBFIT.

Among the model-based examples, the work by Reizman and Jensen, who created a droplet-based microfluidic automated system (Figure 2.17) that optimized Pd-catalyzed Suzuki–Miyaura cross-coupling reactions [52] based on a DoE strategy that was able to optimize both discrete (palladacycle and ligand) and continuous variables (temperature, time, loading) within 96 experiments, is worth mentioning. Variables were randomized through fractional factorial DoEs, and discrete variables were treated as yes/no decisions. Response surface models for each precatalyst consider linear, interactions, and quadratic effects, as well as independent temperature

https://www.twirpx.org & http://chemistry-chemists.com

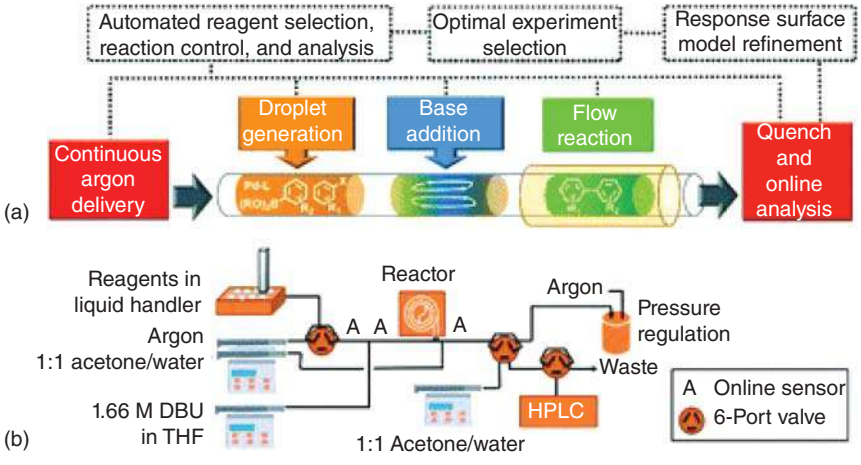

Figure 2.17 (a) Concept and (b) flow diagram for automated Suzuki–Miyaura cross-coupling optimization. Source: Reproduced from Reizman et al. [52] under the Creative Commons Attribution License [53].

and pre-exponential offsets for each discrete variable set, to iteratively predict reaction performance.

Another example from Reizman and Jensen is the optimization of the alkylation of 1,2-diaminocyclohexane in 16 µl droplets, for discrete (solvents, catalysts, ligands) and continuous (reaction time, temperature, equivalents) variables [54]. They used fractional factorial DoEs and additional feedback to refine response surface models and remove poor-performing discrete variables. They identified DMSO out of 10 solvents as the most favorable one and used a gradient-based search to reach the optimum.

In 2017, Lapkin and coworkers optimized a Pd-catalyzed C—H activation process to synthesize aziridines [55]. They demonstrated that MBDoE generates rapidly process models to enable *in silico* training of optimization surrogate models. The Latin hypercube sampling (LHS) was used to discretize the experimental space and the multi-objective active learning (MOAL) algorithm to perform self-optimization. They demonstrated that this algorithm was suited for multimodality, enabling the detection of multiple possible solutions.

More recently, Gavriilidis and coworkers [56] designed an autonomous platform for improved kinetic parameter estimation and model discrimination for a liquid–solid heterogeneous catalytic reaction, namely, the esterification of benzoic acid with ethanol using Amberlyst-15. The platform was automated with LabVIEW and integrated with Python for the online MBDoE, and parameter estimation was achieved using the Nelder–Mead Simplex algorithm, with 1000 restarts to prevent the algorithm from converging to a local solution.

The **Nelder–Mead Simplex algorithm** is a derivative-free, black-box local optimization algorithm designed to optimize single-objective functions with fewer than 10 variablses and was developed first by Nelder and Mead (Figure 2.18) [57].

https://www.twirpx.org & http://chemistry-chemists.com

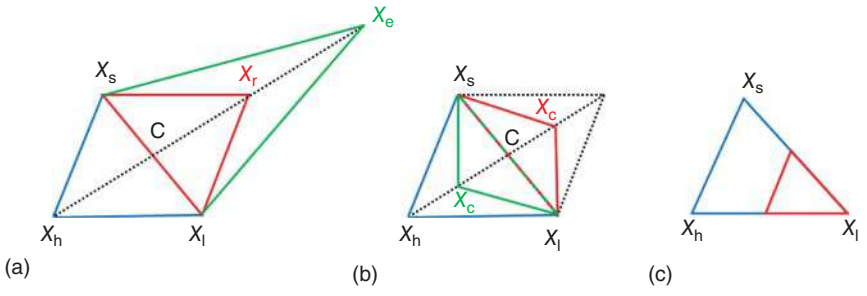

Figure 2.18 Graphical representation of the Simplex algorithm. It forms a Simplex with $n+1$ vertices, reshaping at each iteration depending on the new evaluation function value after reordering the vertices: (a) reflection (red) and expansion (green), (b) outside contraction (red) and inside contraction (green), (c) shrinking (red). The blue line represents the original Simplex. Nomenclature of vertices: x_h, worst; x_l, best; x_s, second best; x_r, reflected; x_c, contracted; x_e, expanded; c, centroid [57].

Perhaps it is the first, with its derived algorithms, used in self-optimization platforms for chemical synthesis in flow. One of the earliest examples of its application is the self-optimization of a Heck reaction using an automated microreactor platform, by McMullen et al. in 2010 [58]. They optimized the reaction yield in 19 iterations by adjusting equivalents of alkene reagent and residence time. Ley and coworkers applied a modified version of the Simplex algorithm (called Complex) to several optimization examples [41]. (i) First is the 3D optimization of the heterogeneous hydration of 3-cyanopyridine to its amide over manganese dioxide, using an Advion miniature MS. Residence time, temperature, and concentration were optimized within 12 experiments and 17 hours, based on the ratio between the product and starting material MS as objective function. (ii) Second is the five-dimensional optimization of an Appel reaction, using an in-line IR for species monitoring (Figure 2.19). Within 30 iterations, 92% yield was reached at 111 °C reactor temperature, residence time of 4.3 minutes, and overall concentration of 0.3 M with 0.87 and 1.72 equivalents (to the alcohol) of CBr_4 and PPh_3, respectively. For this optimization, an evaluation function that accounted for contributions of conversion, throughput, and material consumption was defined. However, instabilities in the performance of the algorithm were observed depending on the weighting factors and form of the different terms in the evaluation function.

In 2011, Poliakoff and coworkers [59] applied the super-modified Simplex algorithm to self-optimize continuous reactions in supercritical carbon dioxide. Optimizations were completed in 35 hours, and an efficient and cost-effective exploration of parameter space (temperature, flow rates, and pressures) was achieved. Felpin and coworkers demonstrated the use of this algorithm for constrained optimizations using different objective functions, requiring 14 experiments to maximize yield, 13 to maximize throughput, and 18 to minimize production cost [60]. In another publication of the same group, they combined the Simplex algorithm with a golden search method to optimize a four-step synthesis to maximize yield in 66 experiments (Figure 2.20) [61].

https://www.twirpx.org & http://chemistry-chemists.com

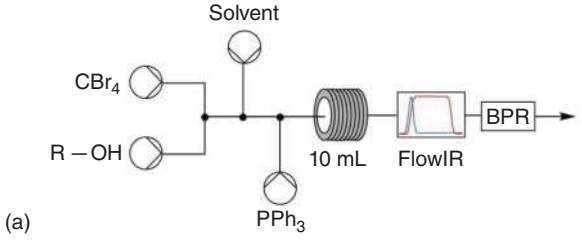

(a)

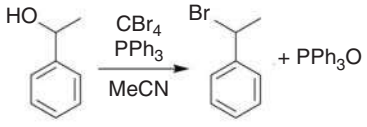

(b)

(c)

Temperature
Residence time
Equiv. CBr_4
Equiv. PPh_3
Overall conc.

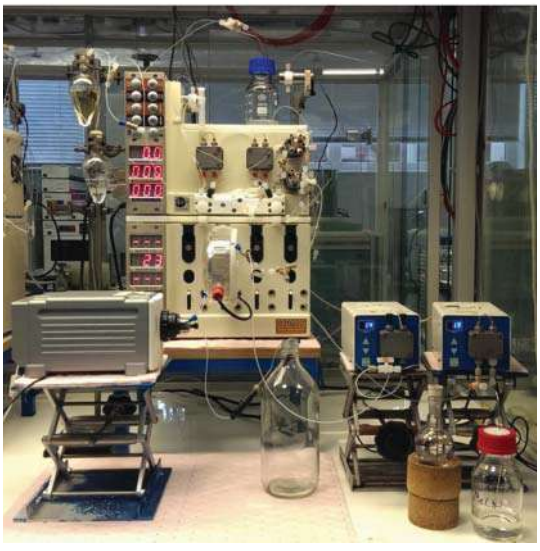

(d)

Figure 2.19 (a) Equipment configuration for the five-dimensional optimization of the Appel optimization: four pumps and in-line infrared detector for composition monitoring; (b) the optimized Appel reaction; (c) five variables optimized; (d) picture of the experimental setup in the laboratory for this experiment. Source: Reproduced from Fitzpatrick et al. [41] with permission of the American Chemical Society.

Rueping and coworkers recently demonstrated an adaptive and automated system optimization for heterogeneous flow-hydrogenation reactions of carbonyl compounds to alcohols using solid Pd/C catalyst and N-heterocycles using solid Ir@CNT catalyst to amines [62]. They used FT-IR, and after 12 iterations a broad parameter space was screened to deliver conversions greater than 18%. In this work and in an earlier one where a photochemical Paternò–Büchi reaction was optimized in 25 iterations [63], they demonstrated the robustness and ability of the Simplex algorithm to reject experimental errors or adaptively regulate fluctuations such as changes in stock concentration.

The **SNOBFIT algorithm** is a derivative-free global optimization algorithm for continuous variables, developed by Huyer and Neumeier [64]. The algorithm combines global and local search by branching and local fits. It uses a combination of stochastic linear and quadratic surrogate models to map the process inputs to an

https://www.twirpx.org & http://chemistry-chemists.com

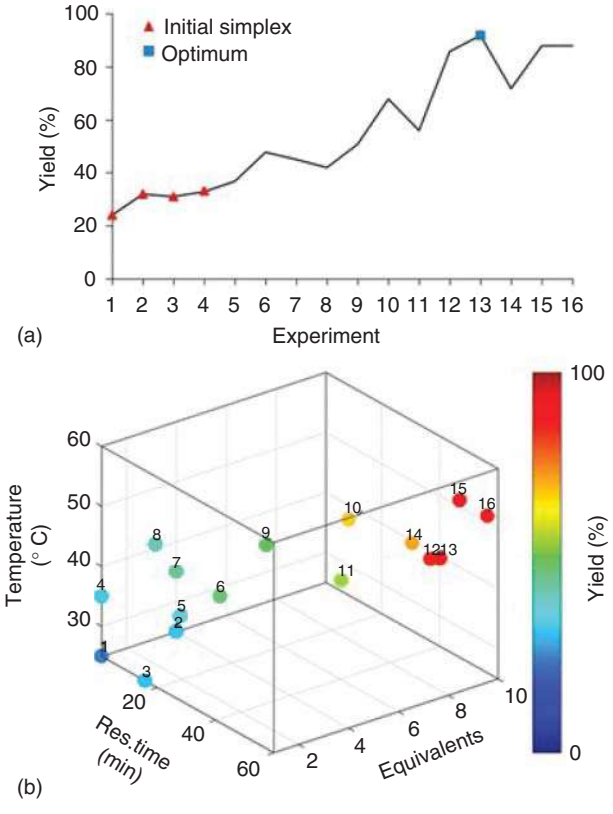

Figure 2.20 Example of Simplex optimization: (a) evolution of the yield of carpanone with iteration number, (b) representation of the three-dimensional experimental conditions for the maximization of the yield of the last reaction step for carpanone synthesis. Source: Reproduced from Cortés-Borda et al. [61] with permission of the American Chemical Society.

objective function, and it generates points that are widely distributed across the design space to increase the chances of finding a global optimum.

The SNOBFIT algorithm was already applied in 2007 by Krishnadasan et al. to the synthesis of CdSe nanoparticles, maximizing the intensity for a chosen emission wavelength by modifying injection rates and temperature [65]. Bourne et al. [66] used an automated flow reactor to self-optimize the final two steps (amide coupling followed by an elimination reaction) in the synthesis of EGFR kinase inhibitor AZD9291, using an at-line HPLC (Figure 2.21). Four parameters (temperature and three flow rates) were optimized in 42 experiments and 26 hours, achieving yields of 89%, calculated as the ratio of percent area of product to percent area of an internal standard. In another publication Bourne and coworkers [21] performed a central composite face-centered (CCF) DoE to account for curvature, fitted the data to surface response models, and compared the optimum conditions obtained with self-optimization strategy, for the amidation of methyl nicotinate with aqueous $MeNH_2$, obtaining >93% yield.

https://www.twirpx.org & http://chemistry-chemists.com

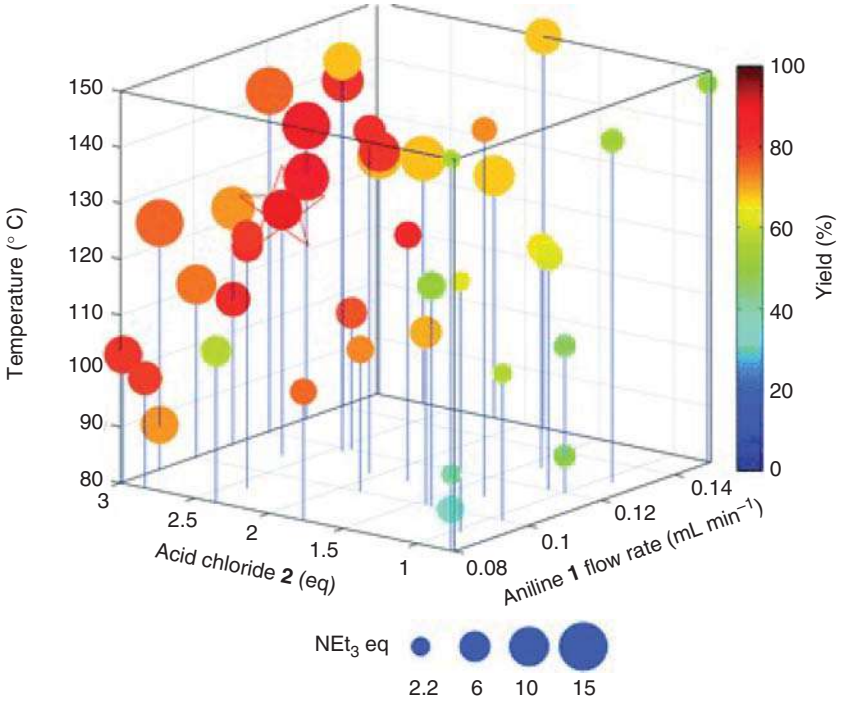

Figure 2.21 Multidimensional plot of the optimization of acrylamide. The three-axis flow rate shows the aniline **1** flow rate (*x*-axis), acid chloride equiv (*y*-axis), and temperature (*z*-axis). The size of the point corresponds to the molar equiv of NEt_3; the color is the yield. Optimum conditions: 9.36 minutes, 123.9 °C, 10.5 equiv NEt_3, 2.7 equiv are highlighted by the star. Source: Reproduced from Holmes et al. [66] / Royal Society of Chemistry / CC BY-3.0.

Jensen and coworkers [16] selected the SNOBFIT algorithm to perform the self-optimization of several reaction chemistries in their reconfigurable flow platform: C—C and C—N cross-couplings, olefination, reductive amination, nucleophilic aromatic substitutions, photoredox catalysis, and multistep sequence. A total of 30–45 experiments were required to optimize 3–5 parameters to maximize yield with a total experiment time range of 7–14 hours, depending on the reaction to optimize.

Cherkasov et al. [40] performed a 3D self-optimization of alkyne semihydrogenation with substrate, catalyst poison, and solvent flow rates as process parameters to maximize alkene yield in a tubular reactor coated with 5 wt% Pd/SiO_2 catalyst. The objective function incorporated the squared product yield calculated through selectivity to product and substrate conversion, reaching convergence in 61 experiments for an alkene yield of 96.5%.

Simultaneous optimization of various responses has been frequently approached in the past by the definition of the objective function as a weighted average of single responses and addition of penalty terms to account for multiple performance criteria. However, this approach has several disadvantages: (i) it does not account for

https://www.twirpx.org & http://chemistry-chemists.com

trade-offs between opposing performance variables, (ii) finding appropriate values for the weights may require additional experimentation, and (iii) instabilities on the performance may be found. Algorithms that target multi-objective optimization problems include the multi-objective active learning algorithm (MOAL) and Thomson-sampling efficient multi-objective optimization (TSEMO).

The **multi-objective active learning algorithm** (MOAL) [67] is a black-box sequential optimization algorithm that combines Gaussian processes (GPs), mutual information, and genetic algorithms for multitarget optimization of expensive-to-evaluate functions. Lapkin and coworkers demonstrated its use for the optimization of a C—H activation reaction in flow, with cost and yield as evaluation functions. The process required 11 iterations, 5 of which were used in the training set [54].

The **Thompson sampling efficient multi-objective optimization** (TSEMO) algorithm is used for expensive-to-evaluating black-box multi-objective optimization problems. It uses a Bayesian methodology with GPs surrogate models, coupled with acquisition functions to be optimized, random sampling to determine the next point of evaluation, and the elitist genetic algorithm to propose a set of candidate points. Its use was demonstrated by Lapkin and coworkers in 2018 to obtain a Pareto front for productivity environmental competing objectives with fewer iterations than genetic algorithms [4], and solvent selection for optimal reactivity and selectivity, finding solvent descriptors that were incorporated to create predictive surrogate models [68]. Lapkin and coworkers recently published an automated self-optimization of a multistep reaction and separation using this algorithm [69]. They demonstrated that using batches of four experiments increased the optimization speed. They optimized a Sonogashira reaction in 13 hours and obtained a Pareto front for the trade-off between conversion and productivity, using 20 initialized LHS experiments and 60 subsequent experiments as designed by the TSEMO algorithm. The challenge of determining the termination criterion was

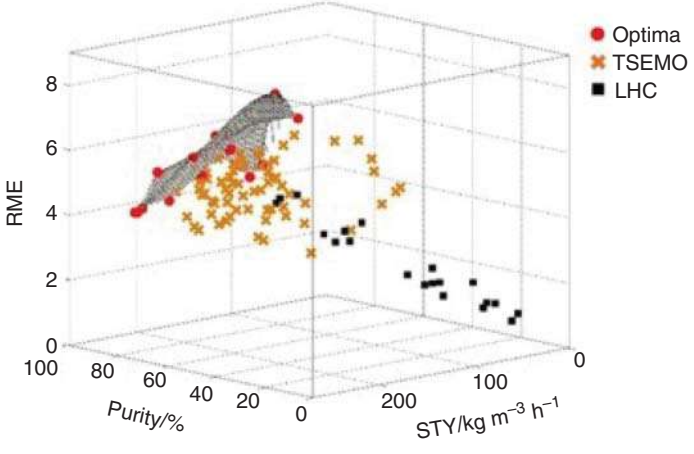

Figure 2.22 Results for the multi-objective self-optimization of the Claisen–Schmidt condensation reaction. Source: Reproduced from Clayton et al. [69] / ELSEVIER / CC BY-4.0.

https://www.twirpx.org & http://chemistry-chemists.com

overcome by monitoring visually the Pareto front, observing no significant changes to the GP surrogate models between experiments 60 and 80. A second example demonstrated the optimization of a Claisen–Schmidt condensation reaction and work-up simultaneously. Four variables (residence time, acetone/sodium hydroxide equivalent ratio, solvent ratio, and temperature) were optimized to maximize three objective functions: purity, space–time yield, and reaction mass efficiency (Figure 2.22). The optimization started with 20 LHC experiments followed by 89 experiments designed by the TSEMO algorithm, requiring 65 hours to complete, being more efficient than other optimization strategies; for example, the SNOBIFT would require 252–420 experiments and does not provide a Pareto front for the trade-off of objectives.

2.4 Summary and Future Perspective

As described earlier, the significance of the automated flow chemistry platforms has been demonstrated in many cases and exemplified in very different types of chemistry. The implementation of flow chemistry processes in the pharmaceutical industry, either in drug discovery or manufacturing phases, has become very mature and is very often integrated with automated tasks, such as PAT control, extraction and/or purification, and biological testing, giving systems with higher performance that simplify routine operations and can make a very large number of experiments for synthesis of libraries and reaction optimization. The flexible and modular design also permits different configurations capable to adapt to different chemistries, and the use of intelligent algorithms increases the level of autonomy of the machines that learn, make decisions, and take actions depending of the different scenarios that arise with minimal human intervention. The integration of the synthetic and biological capabilities in microfluidic platforms turned out to be a powerful tool for the identification of active scaffolds and lead compounds in terms of productivity and shortening the cycle times. Although the combination of artificial intelligent algorithms that learn from past data and guide the experimentation facilitates to drive the SAR, this is still far to be used as the default strategy in early drug discovery programs. However, we expect to see the use of deep learning algorithms increasing soon and the industries adapting these methodologies driven by market demand, innovation speed, and cost reduction.

References

1 Kirschneck, D. (2016). End-to-end continuous manufacturing: chemical synthesis, workup and liquid formulation. *Speciality Chemicals Magazine* 36: 36.
2 Alcacer, V. and Cruz-Machado, V. (2019). Scanning the industry 4.0: a literature review on technologies for manufacturing systems. *Eng. Sci. Technol. Int. J.* 22: 899–919.

https://www.twirpx.org & http://chemistry-chemists.com

3 Bogdan, A.R. and Dombrowski, A.W. (2019). Emerging trends in flow chemistry and applications to the pharmaceutical industry. *J. Med. Chem.* 62: 6422–6468.

4 Schweidtmann, A.M., Clayton, A.D., Holmes, N. et al. (2018). Machine learning meets continuous flow chemistry: automated optimization towards the pareto front of multiple objectives. *Chem. Eng. J.* 352: 277–282.

5 Mateos, C., Nieves-Remacha, M.J., and Rincón, J.A. (2019). Automated platforms for reaction self-optimization in flow. *React. Chem. Eng.* 4: 1536–1544. and references therein.

6 Sagmeister, P., Williams, J.D., Hone, C.A., and Kappe, C.O. (2019). Laboratory of the future: a modular flow platform with multiple integrated PAT tools for multistep reactions. *React. Chem. Eng.* 4: 1571–1578.

7 Haner, R.L. and Keifer, P.A. (2009). Flow probes for NMR spectroscopy. In: *Encyclopedia of Magnetic Resonance*, 1–11. Wiley.

8 (a) Giraudeau, P. and Felpin, F.-X. (2018). Flow reactors integrated with in-line monitoring using benchtop NMR spectroscopy. *React. Chem. Eng.* 3: 399–413. (b) Gomez, M.V. and de la Hoz, A. (2017). NMR reaction monitoring in flow synthesis. *Beilstein J. Org. Chem.* 13: 285–300.

9 Vendors offering benchtop NMR spectrometers: (a) www.magritek.com. (b) www.nanalysis.com. (c) www.thermofisher.com. (d) Oxford instruments: www.oxinst.com. (e) www.bruker.com

10 Grootveld, M., Percival, B., Gibson, M. et al. (2019). Progress in low-field benchtop NMR spectroscopy in chemical and biochemical analysis. *Anal. Chim. Acta* 1067: 11–30.

11 Riegel, S.D. and Leskowitz, G.M. (2016). Benchtop NMR spectrometers in academic teaching. *Trends Anal. Chem.* 83 (Part A): 27–38.

12 Perro, A., Lebourdon, G., Henry, S. et al. (2016). Combining microfluidics and FT-IR spectroscopy: towards spatially resolved information on chemical processes. *React. Chem. Eng.* 1: 577–594.

13 Fitzpatrick, D.E., Maujean, T., Evans, A.C., and Ley, S.V. (2018). Across-the-world automated optimization and continuous-flow synthesis of pharmaceutical agents operating through a cloud-based server. *Angew. Chem.* 57: 15128–15132.

14 Keles, H., Susanne, F., Livingstone, H. et al. (2017). Development of a robust and reusable microreactor employing laser based mid-IR chemical imaging for the automated quantification of reaction kinetics. *Org. Process Res. Dev.* 21: 1761–1768.

15 Escribà-Gelonch, M., Shahbazali, E., Honing, M., and Hessel, V. (2018). Quality-in (process) line (QuIProLi) process intensification for a micro-flow UV-photo synthesis enabled by online UHPLC analysis. *Tetrahedron* 74: 3143–3151.

16 Bédard, A.-C., Adamo, A., Aroh, K.C. et al. (2018). Reconfigurable system for automated optimization of diverse chemical reactions. *Science* 361: 1220–1225.

17 Parry, D.M. (2019). Closing the loop: developing an integrated design, make, and test platform for discovery. *ACS Med. Chem. Lett.* 10: 848–856.

https://www.twirpx.org & http://chemistry-chemists.com

18 Equitz, T.R. and Rodriguez-Cruz, S.E. (2017). High-throughput analysis of controlled substances: combining multiple injections in a single experimental run (MISER) and liquid chromatography–mass spectrometry (LC-MS). *Foren. Chem.* 5: 8–15.

19 Patel, D.C., Lyu, Y., Gandarilla, J., and Doherty, S. (2019). Unattended reaction monitoring using an automated microfluidic sampler and on-line liquid chromatography. *Anal. Chim. Acta* 1004: 32–39.

20 Bedermann, A.A., McTeague, A., and Jamison, T.F. (2019). Automated on-demand titration of organometallic reagents in continuous flow. *Org. Process Res. Dev.* 23: 278–282.

21 Holmes, N., Akien, G.R., Savage, R.J.D. et al. (2016). Online quantitative mass spectrometry for the rapid adaptive optimisation of automated flow reactors. *React. Chem. Eng.* 1: 96–100.

22 Schwolow, S., Braun, F., Raedle, M. et al. (2015). Fast and efficient acquisition of kinetic data in micro-reactors using in-line Raman analysis. *Org. Process Res. Dev.* 19: 1286–1292.

23 Challener, C.A. (2017). *PAT for Continuous Manufacturing Progresses*, 23. Pharmaceutical Technology. April.

24 Buitrago Santanilla, A., Regalado, E.L., Pereira, T. et al. (2015). Nanomole-scale high-throughput chemistry for the synthesis of complex molecules. *Science* 347: 49–53.

25 Perera, D., Tucker, J.W., Brahmbhatt, S. et al. (2018). A platform for automated nanomolescale reaction screening and micromole-scale synthesis in flow. *Science* 359: 429–434.

26 Qiu, C., Fang, Z., Zhao, L. et al. (2019). Microflow-based dynamic combinatorial chemistry: a microscale synthesis and screening platform for the rapid and accurate identification of bioactive molecules. *React. Chem. Eng.* 4: 658–662.

27 Aka, E.C., Wimmer, E., Barré, E. et al. (2019). Reconfigurable flow platform for automated reagent screening and autonomous optimization for bioinspired lignans synthesis. *J. Organomet. Chem.* 84 (21): 14101–14112.

28 Czechtizky, W., Dedio, J., Desai, B. et al. (2013). Integrated synthesis and testing of substituted xanthine based DPP4 inhibitors: application to drug discovery. *ACS Med. Chem. Lett.* 4: 768–772.

29 Desai, B., Dixon, K., Farrant, E. et al. (2013). Rapid discovery of a novel series of Abl kinase inhibitors by application of an integrated microfluidic synthesis and screening platform. *J. Med. Chem.* 56 (7): 3033–3047.

30 SiLA is a consortium for Standarization in Lab Automation. https://sila-standard.com (accessed 26 October 2019).

31 (a) LabVIEW (Laboratory Virtual Instrument Engineering Workbench) is a graphical programming language from National Instruments for automation control and data acquisition: www.ni.com (accessed on 26 October 2019);
(b) Elliott, C., Vijayakumar, V., Zink, W., and Hansen, R. (2007). National Instruments LabVIEW: a programming environment for laboratory automation and measurement. *JALA* 12 (1): 17–24.

https://www.twirpx.org & http://chemistry-chemists.com

32 MATLAB® https://www.mathworks.com/products/matlab.html (Accessed on 22 February 2019).

33 HiTec Zang: Laboratory Reactor Systems and Automation. https://www.hitec-zang.de/en (accessed 26 October 2019).

34 Ingham, R. (2014). *Control Tools for Flow Chemistry Processing and their Application to the Synthesis of Bromodomain Inhibitors* PhD Thesis. Cambridge, UK: Ley Group, Department of Chemistry https://doi.org/10.17863/CAM.16300.

35 Python is a programming language first released in 1991 with a philosophy of code readability, friendly and easy-to-learn. It is developed under an OSI-approved open source license, making it freely usable and distributable, even for commercial use. https://www.python.org (accessed on 26 October 2019).

36 Delaney, N.F., Rojas Echenique, J.I., and Marx, C.J. (2013). Clarity: an open-source manager for laboratory automation. *J. Lab. Autom.* 18 (2): 171–177.

37 GitHub is a code development platform used by developers to build, share and maintain open-source software: https://github.com (accessed on 22 February 2019).

38 Coley, C.W., Thomas, D.A. III, Lummis, J.A.M. et al. (2019). A robotic platform for flow synthesis of organic compounds informed by AI planning. *Science* 365 (6453): 1–9.

39 ASKCOS: Automated System for Knowledge-based Continuous Organic Synthesis. http://askcos.mit.edu (accessed on 11 April 2019).

40 Cherkasov, N., Bai, Y., Expósito, A.J., and Rebrov, E.V. (2018). Open-FlowChem – a platform for quick, robust and flexible automation and self-optimization of flow chemistry. *React. Chem. Eng.* 3: 769–780.

41 Fitzpatrick, D.E., Battilocchio, C., and Ley, S.V. (2016). A novel internet-based reaction monitoring, control and autonomous self-optimization platform for chemical synthesis. *Org. Process Res. Dev.* 20: 386–394. https://pubs.acs.org/doi/10.1021/acs.oprd.5b00313 (further permissions related to the material excerpted should be directed to the ACS).

42 Roch, L.M., Häse, F., Kreisbeck, C. et al. (2018). *ChemOS: An Orchestration Software to Democratize Autonomous Discovery*. ChemRxiv. Preprint.

43 Steiner, S., Wolf, J., Glatzel, S. et al. (2019). Organic synthesis in a modular robotic system driven by a chemical programming language. *Science* 363 (6423): 1–8.

44 O'Brien, M., Konings, L., Martin, M., and Heap, J. (2017). Harnessing open-source technology for low-cost automation in synthesis: flow chemical deprotection of silyl ethers using a homemade autosampling system. *Tetrahedron Lett.* 58 (25): 2409–2413.

45 Raspberry Pi® is a credit card-sized computer. https://www.raspberrypi.org (accessed on 11 April 2019).

46 Ingham, R.J., Battilocchio, C., Hawkins, J.M., and Ley, S.V. (2014). Integration of enabling methods for the automated flow preparation of piperazine-2-carboxamide. *Beilstein J. Org. Chem.* 10: 641–652.

https://www.twirpx.org & http://chemistry-chemists.com

47 Neumaier, J.M., Madani, A., Klein, T., and Ziegler, T. (2019). Low-budget 3D-printed equipment for continuous flow reactions. *Beilstein J. Org. Chem.* 15: 558–566.

48 LeSuer, R.J., Osgood, K.L., Stelnicki, K.E., and Mendez, J.L. (2018). OMIS: the open millifluidic inquiry system for small scale chemical synthesis and analysis. *HardwareX* 4: 1–14.

49 Fitzpatrick, D.E. and Ley, S.V. (2016). Engineering chemistry: integrating batch and flow reactions on a single, automated reactor platform. *React. Chem. Eng.* 1: 629–635.

50 Clayton, A.D., Manson, J.A., Taylor, C.J. et al. (2019). Algorithms for the self-optimisation of chemical reactions. *React. Chem. Eng.* 4: 1545–1554.

51 Fabry, D.C., Sugiono, E., and Rueping, M. (2014). Self-optimizing reactor systems: algorithms, on-line analytics, setups, and strategies for accelerating continuous flow process optimization. *Isr. J. Chem.* 54 (4): 341–350.

52 Reizman, B.J., Wang, Y.M., Buchwald, S.L., and Jensen, J.F. (2016). Suzuki-Miyaura cross-coupling optimization enabled by automated feedback. *React. Chem. Eng.* 1: 658–666.

53 Creative Commons Attribution License website, https://creativecommons.org/licenses/by-nc/3.0 (accessed on 12 November 2019).

54 Reizman, B.J. and Jensen, K.F. (2015). Simultaneous solvent screening and reaction optimization in microliter slugs. *Chem. Commun.* 51: 13290–13293.

55 Echtermeyer, A., Amar, Y., Zakrzewski, J., and Lapkin, A. (2017). Self-optimisation and model-based design of experiments for developing a C–H activation flow process. *Beilstein J. Org. Chem.* 13: 150–163.

56 Waldron, C., Pankajakshan, A., Quaglio, M. et al. (2019). Closed-loop model-based design of experiments for kinetic model discrimination and parameter estimation: benzoic acid esterification on a heterogeneous catalyst. *Ind. Eng. Chem. Res.* 58 (49): 22165–22177.

57 (a) Nelder, J.A. and Mead, R. (1965). *Comput. J.* 7: 308–313. (b) Lagarias, J.C., Reeds, J.A., Wright, M.H., and Wright, P.E. (1998). *SIAM J. Control Optim.* 9 (1): 112–147. (c) Singer, S. and Nelder, J. (2009). *Scholarpedia* 4 (7): 2928. http://www.scholarpedia.org/article/Nelder-Mead_algorithm (accessed 12 January 2019).

58 McMullen, J.P., Stone, M.T., Buchwald, S.L., and Jensen, K.F. (2010). An integrated microreactor system for self-optimization of a heck reaction: from micro- to mesoscale flow system. *Angew. Chem. Int. Ed.* 49 (39): 7076–7080.

59 Parrott, A.J., Bourne, R.A., Akien, G.R. et al. (2011). Self-optimizing continuous reactions in supercritical carbon dioxide. *Angew. Chem. Int. Ed.* 50 (16): 3788–3792.

60 Cortés-Borda, D., Kutonova, K.V., Jamet, C. et al. (2016). Optimizing the heck–Matsuda reaction in flow with a constraint-adapted direct search algorithm. *Org. Process Res. Dev.* 20: 1979–1987.

61 Cortés-Borda, D., Wimmer, E., Gouilleux, B. et al. (2018). An autonomous self-optimizing flow reactor for the synthesis of natural product carpanone. *J. Organomet. Chem.* 83 (23): 14286–14299. https://pubs.acs.org/doi/10.1021/acs

https://www.twirpx.org & http://chemistry-chemists.com

.joc.8b01821 (further permissions related to the material excerpted should be directed to the ACS).

62 Fabry, D.C., Heddrich, S., Sugiono, E. et al. (2019). Adaptive and automated system-optimization for heterogeneous flow-hydrogenation reactions. *React. Chem. Eng.* 4: 1486–1491.

63 Poscharny, K., Fabry, D.C., Heddrich, S. et al. (2018). Machine assisted reaction optimization: a self-optimizing reactor system for continuous-flow photochemical reactions. *Tetrahedron* 74: 3171–3175.

64 Huyer, W. and Neumaier, A. (2008). SNOBFIT – stable Noisy optimization by branch and fit. *ACM Trans. On Math. Software* 35 (2): 1–25.

65 Krishnadasan, S., Brown, R.J.C., DeMello, A.J., and DeMello, J.C. (2007). Intelligent routes to the controlled synthesis of nanoparticles. *Lab Chip* 7: 1434–1441.

66 Holmes, N., Akien, G.R., Blacker, A.J. et al. (2016). Self-optimisation of the final stage in the synthesis of EGFR kinase inhibitor AZD9291 using an automated flow reactor. *React. Chem. Eng.* 1: 366–371.

67 Peremezhney, N., Hines, E., Lapkin, A., and Connaughton, C. (2014). Combining gaussian processes, mutual information and a genetic algorithm for multi-target optimization of expensive-to-evaluate functions. *Eng. Optim.* 46 (11): 1593–1607.

68 Amar, Y., Schweidtmann, A.M., Deutsch, P. et al. (2019). Machine learning and molecular descriptors enable rational solvent selection in asymmetric catalysis. *Chem. Sci.* 10: 6697–6706.

69 Clayton, A.D., Schweidtmann, A.M., Clemens, G. et al. (2019). Automated self-optimisation of multi-step reaction and separation processes using machine learning. *Chem. Eng. J.* 384: 123340.

https://www.twirpx.org & http://chemistry-chemists.com

https://www.twirpx.org & http://chemistry-chemists.com

3

Flow Chemistry Opportunities for Drug Discovery

María Lourdes Linares[1], Enol López[2], Eduardo Palao[1], and Jesús Alcázar[1]

[1] *Janssen Research and Development, Janssen-Cilag, S.A., Discovery Chemistry, C/ Jarama, 75, 45007 Toledo, Spain*
[2] *Universidad de Castilla-La Mancha, Facultad de Ciencias y Tecnologías Químicas, Av. Camilo José Cela, 14, 13005 Ciudad Real, Spain*

3.1 Introduction

3.1.1 Drug Discovery

The development of new drugs is a very costly, long, and tedious process. It is established that the average time of a new drug to be found, developed, and approved by FDA is more than 12 years with an associate cost of more than 1000 million euros [1]. One of the limiting steps in this process is the large number of molecules generated that fail at different stages of the drug discovery path [2].

The drug discovery process is considerably complex and starts with the identification of a certain protein target linked to a certain disease. However, the same illness can have several pathways, and this situation is where a large number of companies compete to have their own active pharmaceutical ingredients (APIs) in the market [3]. These reasons are really key for medicinal chemists to access the widest possible chemical space.

Once the protein target has been identified and validated, the process of discovering a new drug can be divided into several stages, hit identification (Hit I.d.), hit to lead (HtL), lead optimization (LO), and late lead optimization (LLO):

– Hit Identification. At this stage the first binders for the selected protein target are identified. Herein, an appropriate profiling of the molecules found is key to avoid failures down in the process due to unexpected toxicities or lack of activity. Among all the strategies to discover good hits, the most used ones within pharma companies is high-throughput screening (HTS), in which a large number of compounds are tested in each campaign [4]; chemical genomics, study of genomic responses to chemical compounds [5]; virtual screening, computational *in silico* filtering to select candidates; [6] and fragment-based screening, alternative or additional to HTS that involves the study of interactions between small fragments and the protein by spectroscopic techniques, such as nuclear magnetic resonance

Flow and Microreactor Technology in Medicinal Chemistry, First Edition. Edited by Esther Alza.
© 2022 WILEY-VCH GmbH. Published 2022 by WILEY-VCH GmbH.

https://www.twirpx.org & http://chemistry-chemists.com

or X-ray diffraction [7]. All these approaches need to be combined with the most applicable and precise assays to identify the best molecules to start [8].

- Hit to Lead. Once a limited number of active molecules in a micromolar range have been identified (Hits), medicinal chemists begin to modify such molecules to establish structure–activity relationships (SARs) and structure–property relationships (SPR) [9]. These studies help them to rank the series of compounds into clusters and select the most suitable ones for further exploration [4]. The final goal at this stage is having compounds in the nanomolar range with suitable selectivity and pharmacokinetics (PK) properties to test them in available *in vivo* models.
- Lead Optimization. Compounds that have shown activity *in vivo* at the HtL phase are further modified at this phase to optimize their absorption, distribution, metabolism, excretion, and toxicity (ADMET) properties in order to establish their (PK/pharmacodynamic (PD)) relationship. Only compounds with enough difference between these parameters (therapeutic window) are selected as potential compounds to be tested in humans.
- Late Lead Optimization. All the information collected in the previous step will allow the selection of one or two candidates that will be further studied in this phase. The selected compounds are prepared in a multigram scale in order to carry out preclinical studies that optimize the target product profile to be presented to the regulatory authorities.

Each phase of the drug development process is reviewed to make "go-no-go" decisions to continue to the next level. The chemistry during these stages moves from the synthesis of a large number of compounds at milligram scale during HtL studies to the 50-g scale required for the selected candidates at the end of the process.

3.1.2 Flow Chemistry

There is a growing interest in expanding the medicinal chemistry toolbox by introducing new synthetic technologies to reach what is nowadays considered as inaccessible chemical space [10, 11]. In this regard, continuous-flow chemistry has appeared as a real alternative for the preparation of organic molecules to get novel drug-like compounds in a more efficient and sustainable manner. This chapter will disclose the important benefits of using this technology as well as recent advances for drug discovery [12–16].

The advantages of continuous chemistry compared with conventional batch processes are well established [17–19]. Very likely, one of the main concerns in the pharmaceutical environment is related to safety. For this reason, the small reactor size used in flow chemistry is ideal, specially, when hazardous reagents or unstable intermediates are involved. In addition, chemical reactions requiring gaseous reagents, such as hydrogenations or carbonylations, are also included due to the little space of vapor pressure of the reactor that minimizes the risk of an explosion and toxicity.

Likewise, higher temperatures and pressures can also be achieved in continuous flow, resulting in an acceleration of the reaction times. The improved mixture and heat transfer processes, as a result of a high surface area-to-volume ratio, allow simple scale-up of exothermic reactions, which can be problematic otherwise. Moreover,

https://www.twirpx.org & http://chemistry-chemists.com

the accurate control of the reaction parameters such as temperature, concentration, or residence times is also related with more selective transformations. Consequently, improved purity and better yields are normally obtained, with a smaller footprint than batch processes.

This technique is also versatile in terms of setup size because it can be adapted depending on the requirements of the reaction. Thus, several pieces of equipment (pumps, mixers, reactors) can be installed to increase the productivity of the transformation as well as *in situ* analysis of the reaction with different analytical techniques (Fourier transform-infrared spectrometry (FT–IR), nuclear magnetic resonance (NMR) spectroscopy, mass spectrometry (MS)) and/or subsequent purification procedures. The facility of combining flow methodologies with novel synthetic approaches such as photochemistry, electrochemistry, or biocatalysis supports their acceptance by medicinal chemist. On top of that, continuous-flow protocols allow the realization of fully integrated automated systems, which clearly increases sustainability and reduces cost and time of the process.

The chance to make organic transformations safer, cleaner, faster, and with shorter reaction times is always desirable from a pharmaceutical perspective. So in the last few decades, many companies such as Eli Lilly, Novartis, GSK, Pfizer, or Janssen have made important investments in the field. Although this technology has been mostly implemented in process scale, the benefits for drug discovery have already been introduced, but not significantly used so far.

3.1.3 Merging Flow Chemistry and Drug Discovery

Drug discovery programs require a rapid investigation of the chemical space. In consequence, the development of new methodologies, which can provide a wide variety of new entities in short time frames, is highly desirable. Typically, a few milligrams of a compound are usually enough to carry out *in vitro* assays. For that reason, the use of microreactors, the so-called lab-on-a-chip, offers the opportunity to optimize the reaction by sequentially conducting a series of experiments to synthetize a family of analogs. This parallelization and miniaturization of the reactions reduce the cost and time required to achieve the desired compounds.

In order to identify new drug candidates that can interact with the protein, a wide variety of chemical analogs must be produced. First, parallel synthesis speeds up the preparation of chemical libraries, which are subsequently screened with biological targets; for that reason, automation fits perfectly in this goal. A diverse number of reagents are loaded into the system, and the different corresponding products are collected individually. In this regard, segmented flow is a very suitable strategy because separated reaction droplets are flowing continuously between an inert solvent. Subsequent analysis and separation of the different microreactions are carried out automatically at the end of the system, giving rise to a diverse set of products.

Furthermore, the small size of these reactors allows the installation of novel techniques such as photochemistry or electrochemistry, which have gained attention during the last years. The chance to carry out these technologies under continuous

https://www.twirpx.org & http://chemistry-chemists.com

flow not only increases the selectivity of the transformation but also overcomes some limitations found in batch, facilitating undoable reactions [20].

Diversity-oriented synthesis (DOS) is also a very convenient approach. The simplicity of preparing reactive intermediates in flow allows the combination of simple starting materials with different substrates, which cover the maximum of the chemical space.

3.2 Current Drug Discovery Toolkit

Several publications have reported the most used reactions carried out in pharma companies in the last 20 years. The commercial availability of the starting reagents, high chemoselectivity, and the sense of urgency to deliver have been identified as the main reasons for the lack of novelty observed. For instance, Roughley and Jordan [21] described the reactions that medicinal chemists at GSK, AstraZeneca, and Pfizer had used most frequently in this period. The conclusion of this analysis is that the reactions of formation of C-heteroatom bonds were the most numerous followed by those of amide bond formation. Subsequently, Boström, Brown, and coworkers [11, 22] have shown that since that publication, some of the most popular reactions have changed, although, some remain part of the top five (Figure 3.1). Therefore, for example, the reactions of amide bond formation are still the most numerous (divided in peptide synthesis and other amide bond formation), followed by Suzuki–Miyaura cross-coupling reactions, S_NAr (aromatic nucleophilic substitution), reductive amination reactions, and protection/deprotection of amines with Boc.

As mentioned in a previous section, flow chemistry sometimes represents an advantage over traditional or batch chemistry that is why an increment of publications that involve flow and pharma companies has been observed. For instance, most of the reaction in Figure 3.1 have been reported in flow.

3.2.1 Reactions for C-Heteroatom Bond Formation

As has been highlighted before, amide bond formation is a very common transformation in medicinal chemistry that usually consists of three stages: hydrolysis, acid activation, and treatment with the amine. To avoid these three steps, it is very common to use trimethylaluminum ($AlMe_3$), which is a pyrophoric reagent difficult to handle on a large scale. Therefore, Seeberger et al. described the synthesis of trimethylaluminum-mediated amide bonds in continuous flow using a microreactor [23]. They use this methodology as a key step for the synthesis of rimonabant (anti-obesity drug) and efaproxiral (enhancement of radiation therapy). The use of microreactors makes the synthesis of amides with $AlMe_3$ safer, controlling the exotherm of the reactions and shortening reaction times.

Another example of a synthesis of amides in flow is described by Janssen's researchers in collaboration with the University of Castilla La Mancha [24], where they carry out the Bodroux reaction as a safer alternative for the preparation of amides in a single step. Starting from different esters and amines and using a

https://www.twirpx.org & http://chemistry-chemists.com

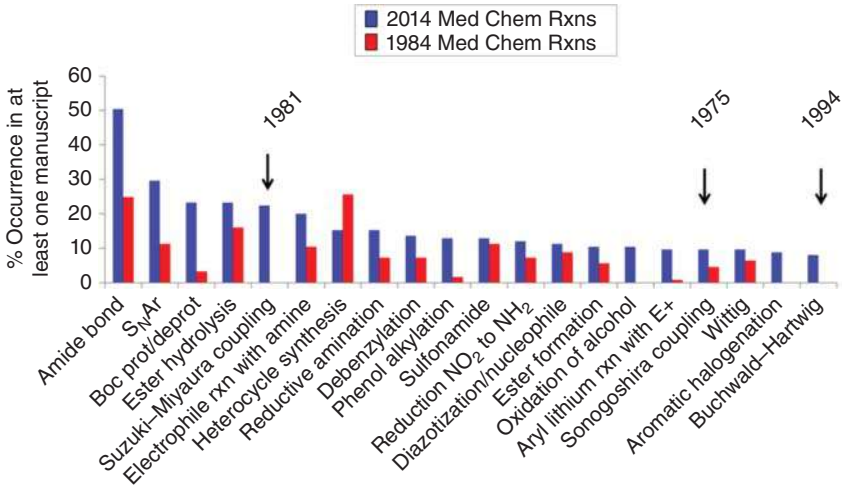

Figure 3.1 Evolution of reaction types used in pharma. Source: Reprinted with permission from Brown and Boström [22]. © 2016 American Chemical Society.

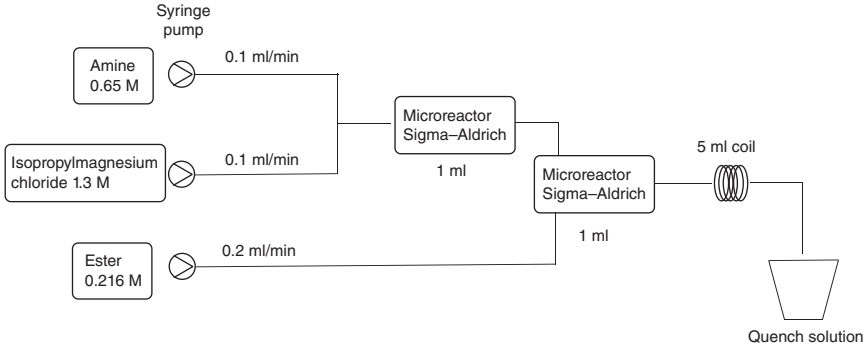

Scheme 3.1 Preparation of amides by Bodroux reaction in flow.

simple Sigma-Aldrich microreactor, a coil, and isopropylmagnesium chloride in tetrahydrofurane (THF) as base, the corresponding amides were obtained at room temperature with very good yields and with a broad scope of esters and amines (Scheme 3.1). This straightforward and simple methodology could be considered a greener alternative to others described in literature.

In a follow-up article, the same group in collaboration with the University of Leuven, described the synthesis of amides using lithium bis(trimethylsilyl)amide (LiHMDS **3**) from esters **1** and low nucleophilic heterocyclic amines **2** [25]. This procedure, in turn, is an alternative of the Bodroux reaction because the solubility of many of these heterocyclic amines is very poor in the aprotic solvents used. LiHMDS was selected due to its high basicity and low nucleophilicity, thereby resulting in a large functional group tolerance compared to what was described previously with other organometallic reagents (Scheme 3.2).

https://www.twirpx.org & http://chemistry-chemists.com

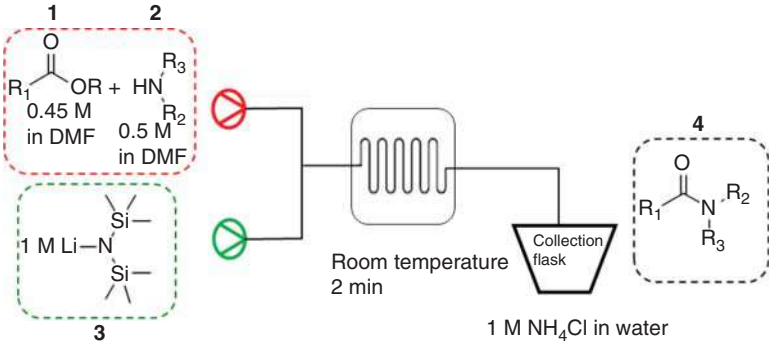

Scheme 3.2 Preparation of amides with LiHMDS in flow.

Peptide synthesis is another chemistry that contributes to the large use of the amide formation reaction in Pharma. There are several methods described in flow; for instance, Tanaka et al. [26] carried out the synthesis of biologically active oligopeptides in a linear manner that allows the coupling of several amino acids quickly and with the minimum protection of the terminal carboxyl group, minimizing the formation of undesirable diketopiperazines.

Another example of the peptide flow synthesis was reported by Pentelute et al. who described an automated flow approach of the solid phase peptide synthesis, carrying out the formation of the amide bond in a very short period of time (seven seconds) and with a total synthesis time of 40 seconds for each amino acid residue [27]. The yields obtained are comparable to those described for solid phase synthesis of peptides in batch, allowing the synthesis of a large number of peptides in a very short period of time.

Nevertheless, other alternative reaction to form an amide bond was described by James and Lange [28]. They obtained a library of aminoindazolines in only 17 minutes using the Conjure™ flow reactor [29] in a three-step process that involved amide formation, Sonogashira coupling, and subsequent ring closure reaction (Scheme 3.3).

Reductive amination is one of the most used reactions in pharma. One of the first examples was described by Seeberger, McQuade, and coworkers [30]. They carry

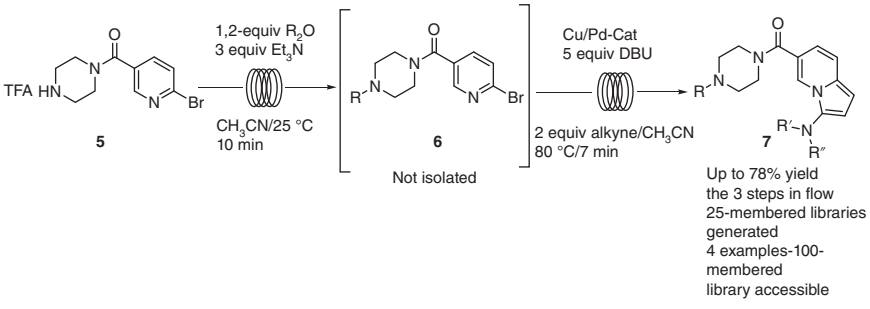

Scheme 3.3 Library synthesis of aminoindazolines in flow.

https://www.twirpx.org & http://chemistry-chemists.com

out a method for reductive amination in flow using solid sodium borohydride. In this protocol, they flowed a mixture of the carbonyl compound with the corresponding amine through a column prepared with the borohydride, Celite®, and LiCl in a Vapourtec reactor. With this system they can perform the reductive amination in good yields and in a safer and greener manner because the residual active material is destroyed with methanol and disposed of as a solid waste (Scheme 3.4).

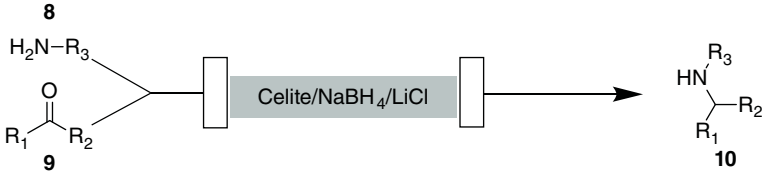

Scheme 3.4 Reductive amination using supported sodium borohydride.

Another method to carry out reductive amination reactions in flow is by using hydrogen as a reducing agent. Kobayashi et al. described the continuous-flow reductive amination of aromatic and aliphatic aldehydes and ketones with primary and secondary amines using a cartridge of Pt/C and a source of H_2 regulated by a mass flow controller. With this method they can prepare a great variety of secondary and tertiary amines with an excellent functional group tolerance, with good yields, and in a procedure that is both safe and without production of any hazardous chemical waste (Scheme 3.5) [31].

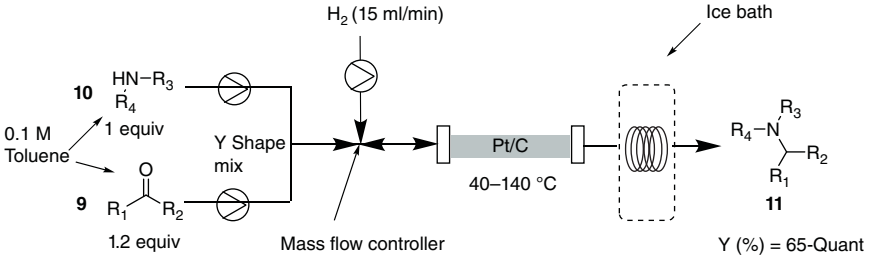

Scheme 3.5 Reductive amination by catalytic hydrogenation. Source: Laroche et al. [31]/John Wiley & Sons.

Examples reporting flow reductive aminations for the synthesis of APIs can also be found in literature. For instance, the one described by Matsuo et al. where they combined flow reductive amination with an Ullmann reaction in batch with aqueous ammonia to prepare abemaciclib, a selective ATP-competitive inhibitor of cyclin-dependent kinases CDK4 and CDK6 for the treatment of multiple types of cancer [32].

Nucleophilic aromatic substitution (S_NAr) has been widely used in medicinal chemistry as shown in Figure 3.1 and recently transferred to flow. For example, Djuric et al. used this reaction to prepare a library of 2-aminoquinazolines

https://www.twirpx.org & http://chemistry-chemists.com

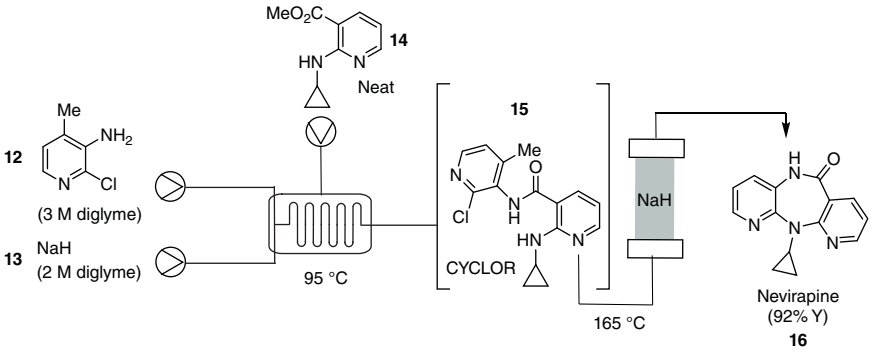

Scheme 3.6 Preparation of nevirapine in flow.

by reaction of 2-chloroquinazoline with different amines in ethanol at high temperatures and pressures (225 °C, 120 bar) with moderate to good yields [33].

It is common to find the S_NAr reaction as a key step for the preparation of APIs, such as the one described by Gupton and coworkers for the continuous synthesis of nevirapine **16** (non-nucleoside reverse transcriptase inhibitor for the treatment of HIV-1) [34]. They reported the synthesis of a key intermediate, which they called CYCLOR **15**, used to prepare **16** by intramolecular nucleophilic substitution through a column filled with sodium hydride at 165 °C (Scheme 3.6). This API was obtained in 92% yield, decreasing drastically its cost when compared with the procedure previously described in batch.

Although C—O bond formation is less numerous than C—N, authors like Varghese and coworkers developed a novel and efficient procedure, by coupling heteroaryl chlorides **17** with primary aliphatic alcohols and phenols **18** under mild conditions to form pyrimidines **19** and pyridines [35]. Reactions are carried out in a continuous-flow microfluidic reactor, which leads to a clean and high-yielding process, which does not require the use of transition metal catalysts (Scheme 3.7). By this method, intermediates of industrial importance (requiring the formation of a C—O bond) can be prepared in a safer manner.

Buchwald–Hartwig amination reaction has become a popular alternative method to build C—N bonds within the medicinal chemistry community [36]. This is

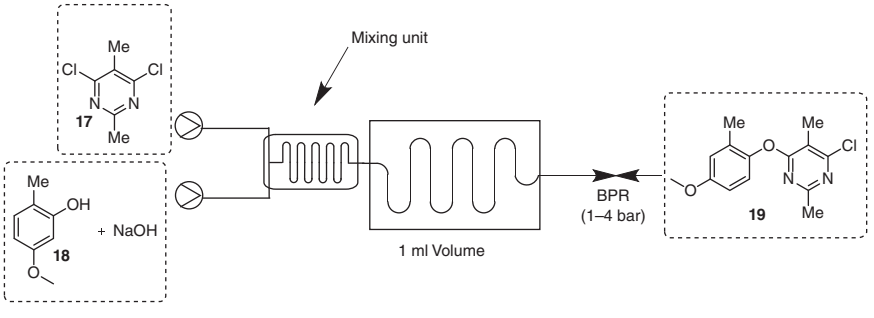

Scheme 3.7 Preparation of aryl ethers in flow.

https://www.twirpx.org & http://chemistry-chemists.com

shown in the increasing number of publications in the literature applying the Buchwald–Hartwig coupling reaction to prepare biologically active aryl amines and amides. This fact has caught the attention of flow chemists who have explored the use of this technology for the reactions and its possible application in drug discovery [37, 38]. Most of these examples have to deal with the use of inorganic strong bases, such as potassium *tert*-butoxide, which have limited solubility in the organic solvents usually used. Different strategies have been developed to overcome this limitation such as the one described by Buchwald et al. that combined a new reactor design with the use of acoustic irradiation [39].

As an improvement to these methods, Buchwald and Jensen described an alternative method to carry out the C—N coupling reactions catalyzed by palladium using a wide range of organic bases such as triethylamine (TEA) or 1,8-diazabicyclo[5.4.0]undec-7-ene (DBU) [40]. The advantage of this method is that all the bases are soluble and their different pKa's allowed a broad functional group tolerance (Scheme 3.8).

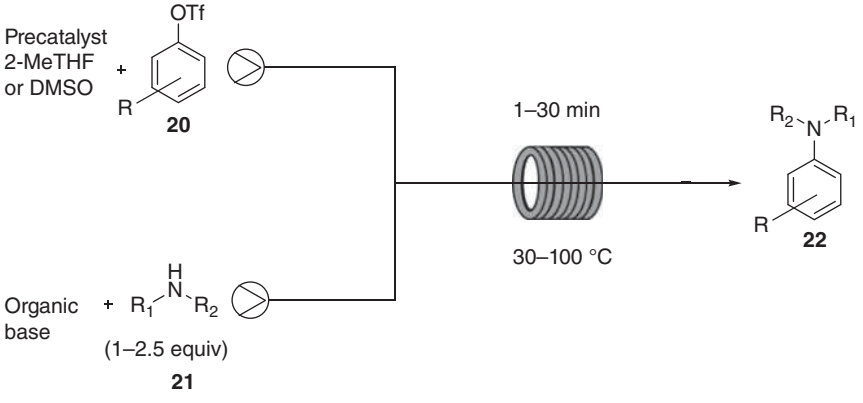

Scheme 3.8 Buchwald–Hartwig amination in flow using organic bases.

3.2.2 Reactions for C—C Bond Formation

One of the most popular reactions for medicinal chemists is the Suzuki–Miyaura cross-coupling. This is the most used reaction for building C—C bonds (Figure 3.1). Therefore, the implementation of the Suzuki–Miyaura coupling under flow conditions is highly desirable to allow its use in continuous production of the desired APIs. A representative example of this approach is the one described by Janssen's researchers in collaboration with the University of Castilla La Mancha [41]. The supported palladium catalyst allows a broad reaction scope for both aryl halides and boronic acids in less than five minutes (Scheme 3.9). The silica support offers a better thermal stability than polymeric supports, and it is also compatible with a numerous type of solvents due to its lack of swelling. This was proved by reusing the catalyst up to 30 times without decreasing its catalytic activity, having clean reaction crudes and free from phosphine ligands that prevent subsequent purification by column chromatography.

https://www.twirpx.org & http://chemistry-chemists.com

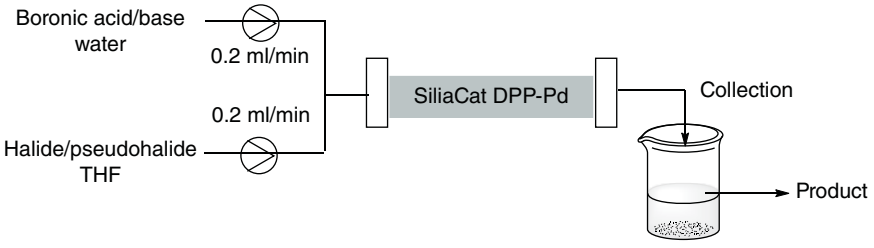

Scheme 3.9 Suzuki–Miyaura coupling using silica supported catalyst.

Another application of this type of C—C bonds formation was described by Martin-Matute et al. in collaboration with the University of Stockholm [42]. In this case, researchers packed the catalyst (Pd@MIL-101-NH_2) in a microflow reactor, describing the first example of nanoparticle supported on mesoporous MOF as catalyst in a flow environment. The reactions were carried out either with boronic acids, boronates, and *N*-methyliminodiacetic acid ester (MIDA), having very good yields with a great variety of aryl halides, and the protocol used was susceptible to automation. The products were absent of metal contamination, but after 12 reactions the supported catalyst became unproductive.

More recently, Senayake and coworkers reported the preparation of (BIDIME)Pd **26**, a third generation palladacycle commonly used in Buchwald coupling reactions in batch [43]. The reaction was carried out in flow with only 0.5% catalyst and at 80–120 °C to get the coupling products **25** in very good yields (Scheme 3.10).

The Sonogashira reaction is another common procedure used by medicinal chemists that requires a palladium catalyst and copper cocatalyst to form a C—C bond between a terminal alkyne and an aryl or vinyl halide [44]. The use of the copper cocatalyst allows the reaction to be carried out under mild conditions and, therefore, increasing its compatibility with a higher number of functional groups and attracting the interest of the pharmaceutical industry. Those facts make this reaction very attractive to transfer to flow [45–47]. Variants of the Sonogashira reaction have been developed such as the copper-free cross-coupling in which the absence of Cu as cocatalyst allows for the carrying out of the reaction under air, thereby avoiding the unwanted homocoupling products. One example was described by Routier and coworkers where they used continuous chemistry to prepare 7-azainoles (presented in many products with biological activity) by copper-free Sonogashira coupling using a recyclable palladium catalyst [48].

3.2.3 Heterocyclic Synthesis

Heterocyclic synthesis has been an important part of drug discovery throughout the years (Figure 3.1). Heterocycles present the capacity to interact with the target proteins through the different heteroatoms present in the ring. Flow chemistry has been also used for the synthesis of heterocycles [49]. As the topic is very broad, this chapter will only cover some representative examples.

https://www.twirpx.org & http://chemistry-chemists.com

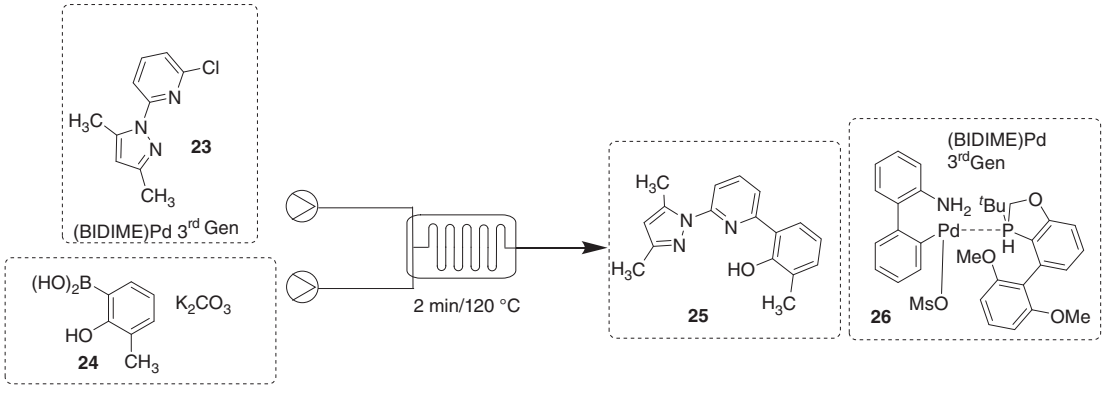

Scheme 3.10 Suzuki–Miyaura coupling with (BIDIME)Pd catalyst.

https://www.twirpx.org & http://chemistry-chemists.com

Click chemistry is a chemical reaction that joins two small units through a 1,2,3-triazole core. It was introduced by Sharpless and coworkers in 2001, and they were inspired by the fact that nature also generates substances by combining small modular units [50]. These reactions are known for being modular, high yielding, wide ranging, stereospecific, and physiologically stable and having a large thermodynamic force and a high atom economy. In addition, these reactions are usually simple, using available starting reagents and benign solvents and with an effortlessly isolation of the products. All of that makes this methodology extremely interesting for the pharmaceutical industry to generate large libraries of compounds to screen in discovery research and also very attractive for its development in flow.

The first example in a continuous reactor was described by Bogdan and Sach [51]. They prepared a library of triazoles using a copper tube reactor generating the compounds in a fast manner (residence times of five minutes), without loss in catalytic activity of copper after hundreds of reactions, with a completely safe handling of organic azide intermediates and where the copper reactor is also useful for other types of copper-mediated couplings such as Sonogashira and Ullman couplings [52].

Since then, many publications have appeared in literature, such as the one described by Vögtle and Leforestier in which they show a procedure for the preparation of chlorine azide as intermediate to prepare triazoles in a safe manner [53]. Once the chlorine azide specie (ClN_3) is generated, by the reaction between NaN_3 and NaOCl in toluene in the presence of acetic acid, it is trapped with olefins **27** in a 1,2-addition. Afterward, these intermediates **28** react with alkynes **29** in a copper-catalyzed click reaction to give the corresponding triazoles **30** with good yields (Scheme 3.11).

One year later, in 2017, Raić-Malić et al. presented a series of click reactions of an azido compound derivative of L-ascorbic acid as a precursor for Cu(I)-catalyzed 1,3-dipolar cycloaddition with alkynes [54]. These reactions were carried out either in batch or flow at the same time to compare both methodologies. To successfully transfer the batch conditions, ultrasound irradiation and flow microreactors were employed, and reaction times were decreased from hours to only minutes, improving significantly the yields. This methodology (explained more in detail in Chapter 5) was described as an important method to prepare novel molecular entities that can exhibit biological properties, in which flow chemistry shows a great advantage versus batch.

In 2018, Lin et al. described a 1,3-dipolar cycloaddition between azides **32** and terminal alkynes **31** catalyzed by copper (I) (CuAAC) in flow conditions at low pressures to generate a library of triazoles **33** with biological interest [55]. The use of an AuCu nanopore membrane as catalyst allows the click reaction to be carried out in a completely homogeneous medium, avoiding the difficulties of separating the catalyst in comparison with other heterogeneous methods (Scheme 3.12) [56–58]. The authors also showed the reusability of this membrane, reusing the same membrane up to five times without decreasing its catalytic activity. They highlight the importance of this method to prepare several important pharmaceutical drugs, for example, α-glucosidase inhibitors and the possibility to prepare these products on gram scale.

https://www.twirpx.org & http://chemistry-chemists.com

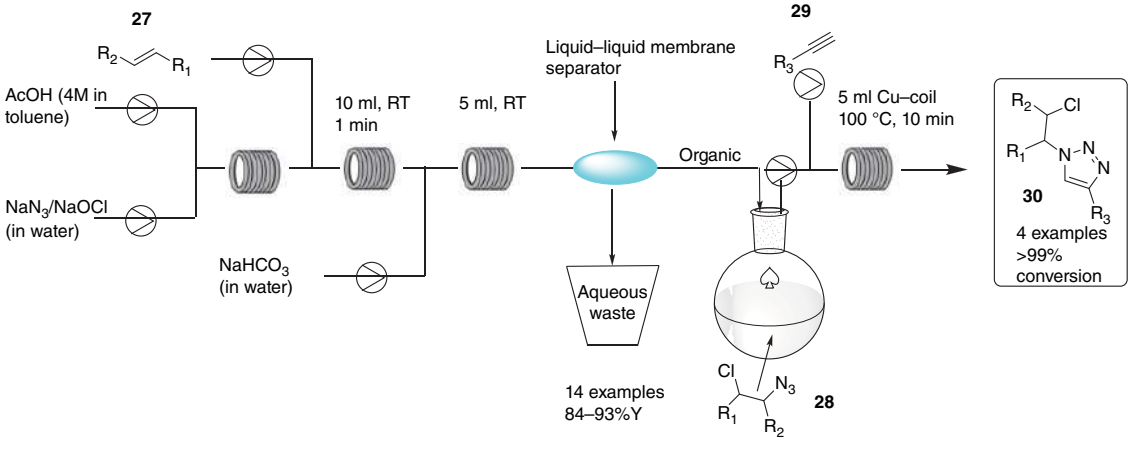

Scheme 3.11 Telescoped procedure for triazole synthesis in flow.

https://www.twirpx.org & http://chemistry-chemists.com

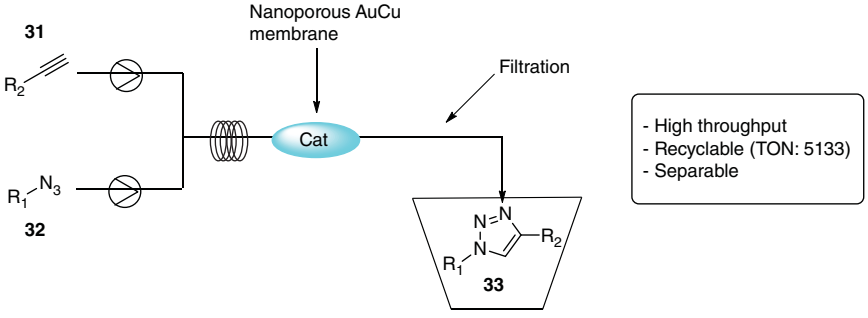

Scheme 3.12 Click reaction using an AuCu nanopore membrane. Source: Based on Refs. [56–58].

Buchwald and Chen published an example of synthesis of benzotriazoles **36** in continuous flow, which is interesting from the point of view of medical chemistry since benzotriazoles are key structures that are present in antibacterial, antifungal, or antimalarial compounds as well as in kinase inhibitors or potassium channel activators [59]. They described two different approaches for the synthesis of benzotriazoles **36**, depending on the electronic of the chloronitrobenzene **34**, used as a starting material. One was an S_NAr or by Pd-catalyzed C—N cross-coupling reaction, followed by hydrogenation and diazotization/cyclization (Scheme 3.13).

They rationalize the big advantages that this method presents versus batch such as safer diazotization, less time-consuming, and labor intensive. They also mention that this process is efficient and regiospecific.

3.3 Expanding Drug Discovery Toolkit Through Flow Chemistry

In the previous section, the use of flow chemistry to improve the most used processes in drug discovery has been overviewed. However, flow chemistry cannot be limited to improve what is usually used, but to expand the toolkit bringing back to the bench uncommon chemistries, reactions that are usually disregarded due to the presence of chemical species that are difficult or dangerous to handle. The capability of flow to keep under control these kind of reagents, which are used as they are made, opens up new avenues to medicinal chemists to access a chemical space, which was not considered before. Moreover, flow can be easily combined with other technologies, such as photochemistry or electrochemistry, to enable novel reactions.

3.3.1 Handling Hazardous and Unstable Reagents

A very useful advantage that flow chemistry provides is the *in situ* generation of reactive intermediates, which can be used in the same reaction media. For example, diazo and diazonium derivatives are versatile intermediates in medicinal chemistry; however, these highly energetic compounds have inherent risks associated because they are potentially explosive and toxic agents as has been discussed in Chapter 1

https://www.twirpx.org & http://chemistry-chemists.com

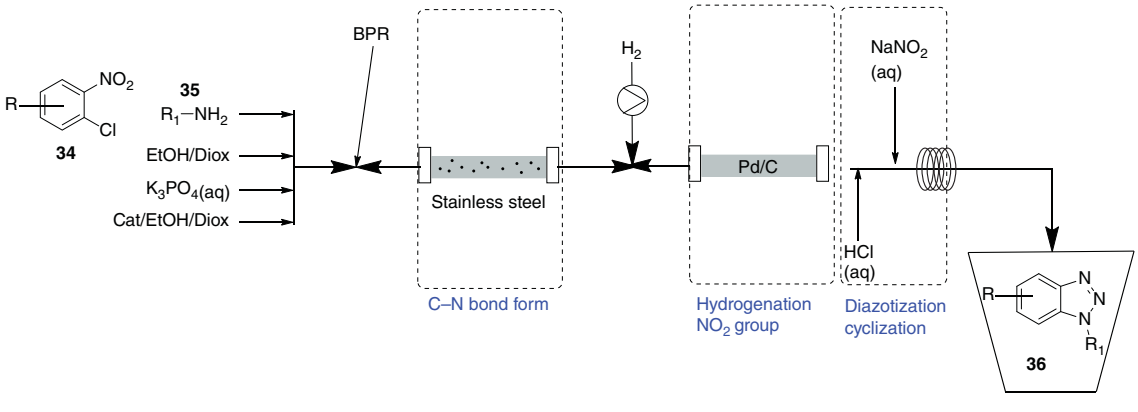

Scheme 3.13 Sequential preparation of benzotriazoles in flow.

https://www.twirpx.org & http://chemistry-chemists.com

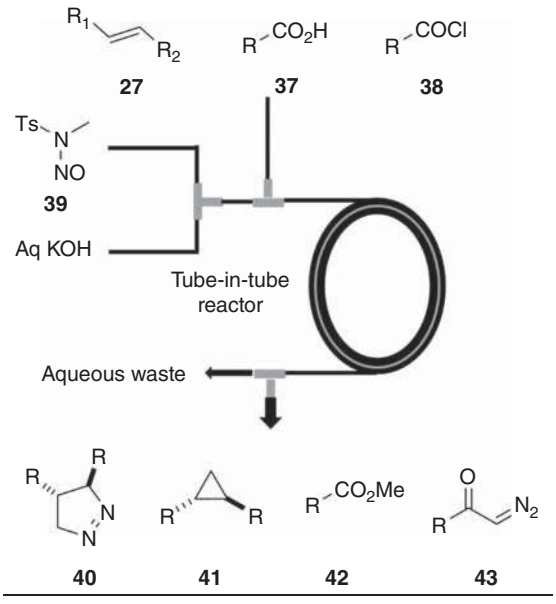

Scheme 3.14 Handling diazomethane in a tube-in-tube reactor.

[60]. The generation in flow from readily available starting materials eliminates the need of isolation, therefore, improving safety.

Kappe et al. reported the *in situ* preparation of diazomethane in the inner-tube of a tube-in-tube reactor. In this manner, diazomethane passes through a gas permeable membrane, and it is mixed with the coupling partner (Scheme 3.14). Thus, several interesting transformations such as cyclopropanations, 1,3-dipolar cycloadditions, or methylation of acids were successfully achieved [61].

In recent years, DOS has appeared as an interesting tool for the rapid access to a broad chemical space from simple starting materials [62]. The high reactivity of hazardous and unstable reagents can be controlled in flow and used to get a different compound. One illustrative example was reported by Janssen and University of Castilla-La Mancha researchers through the Reformatsky and Blaise reactions in flow [63]. Collection of the intermediates obtained over different electrophiles and nucleophiles allowed the access to different and important intermediates and heterocyclic cores **46**–**50** (Scheme 3.15).

In a follow-up article, the authors reported the preparation of Grignard reagents using a column filled with magnesium [64]. After the generation of the corresponding Grignard derivative, different electrophiles were reacted in either batch or flow, depending on their solubility. In this example, the same starting material gave rise to eight different products **9**, **54**–**57**, which demonstrates the value of the methodology for DOS purposes (Scheme 3.16).

Escaping flatland has been identified as a key feature to access a chemical space that is not covered currently [65–67]. Increasing C(sp^3) fraction in bioactive molecules has been linked to higher chances to get clinical candidates.

https://www.twirpx.org & http://chemistry-chemists.com

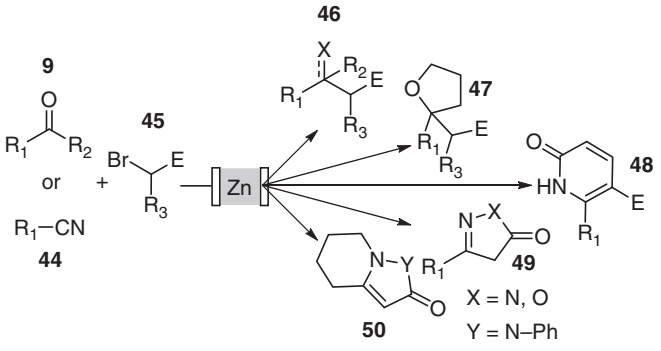

Scheme 3.15 Reformatsky and Blaise reaction in flow.

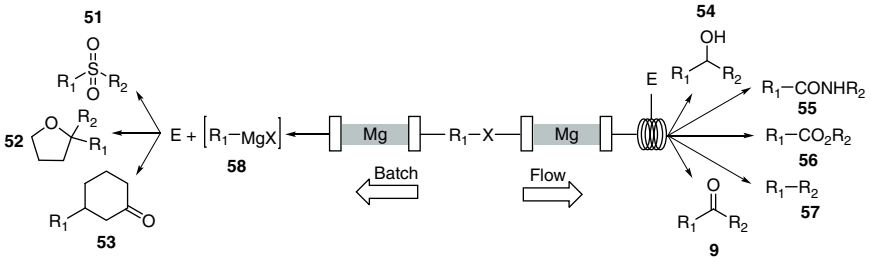

Scheme 3.16 Preparation of Grignard reagents in flow.

Researchers at Janssen and Florida State University demonstrated that alkyl organozinc reagents can be easily obtained in flow by passing the alkyl halide through a column filled with zinc [68, 69]. These unstable reagents can be directly used in a subsequent Negishi coupling as a way to introduce C(sp^3) motifs (Scheme 3.17) [70].

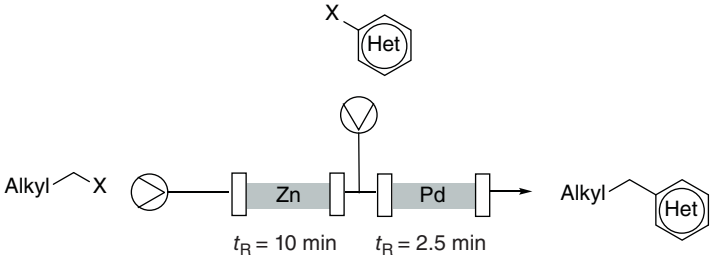

Scheme 3.17 Zinc insertion-Negishi coupling as a way to introduce C(sp^3) motifs. Source: Egle et al. [70] 3.21/ Springer Nature.

The generation of highly reactive intermediates has been also used to carry out fast reactions in a highly controllable manner. This concept named as "flash chemistry" gives access to new reactivities, not suitable in batch due to the short reaction times achieved [71]. In this context, Yoshida and coworkers described the

https://www.twirpx.org & http://chemistry-chemists.com

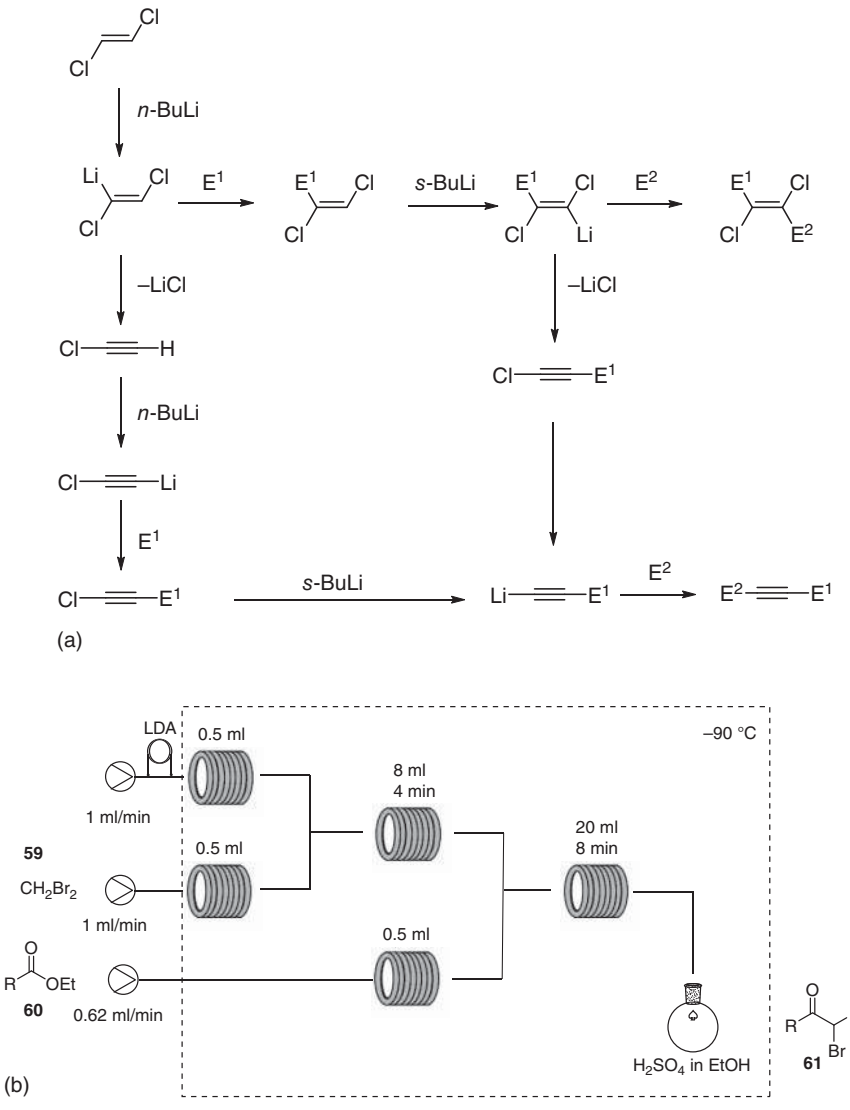

Scheme 3.18 Selective metalations of halogenated derivatives.

lithiation of 1,2-dichloroethene using flow microreactors [72]. The accurate control of the reaction conditions provided by continuous chemistry produces different vinylic or propargylic organic scaffolds, showing the versatility of the transformation (Scheme 3.18a). The lithiation of different halogenated starting materials has been also described by Ley's group [73]. The metalation of dibromomethane **59** and subsequent reaction with an ester **60** give rise to α-dibromoketones **61**, which are important building blocks for the synthesis of heterocycles in the pharmaceutical industry (Scheme 3.18b).

https://www.twirpx.org & http://chemistry-chemists.com

Another advantage of flash chemistry approach is the possibility to run reactions at higher temperatures than the corresponding batch process. Due to the continuous generation and reaction of the unstable intermediates, low temperatures are not required as reaction times are drastically reduced. For instance, Knochel and coworkers described the formation of organomagnesium heterocycles **64** and acrylates **65** using TMPMgCl·LiCl (TMP = 2,2,6,6-tetramethylpiperidyl) under continuous flow [74]. Despite the typical conditions found in batch, the reaction takes place at room temperature. Several transformations were achieved from the intermediates formed such as iodination, generation of the corresponding zincate and Negishi coupling (Scheme 3.19).

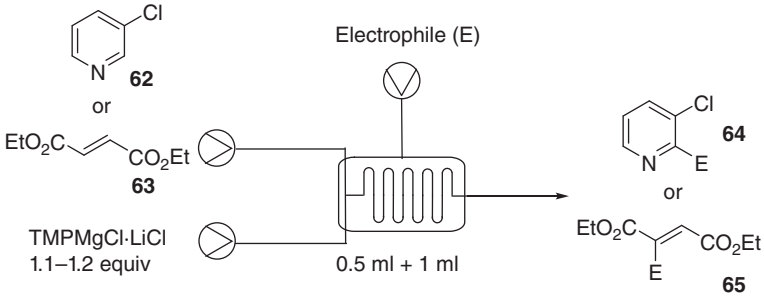

Scheme 3.19 Selective metalations of heterocyclic compounds.

3.3.2 Combining Flow with Emerging Technologies

The facility of combining flow technologies with novel synthetic methodologies opens the doors to preparing complex organic molecules, which are difficult to achieve by traditional approaches. In this regard, an increasing number of enzymatic, photo-, and electrochemical (EC) transformations have been reported in the last years.

The number of enzymatic reactions reported in medicinal chemistry is limited due to the low mass transfer between the organic substrate and the hydrophilic enzyme. Continuous-flow alternatives have overcome this problem. First, segmented flow enhances enzymatic transformations, reducing emulsion formation and providing a better separation [75]. Another convenient approach is flowing the organic substrate through an immobilized enzyme. In this case, better selectivity and less amount of the biological partner are regarded as important advantages. One such example was reported by Pentelute and coworkers. The researchers afforded a sortase-mediated ligation of peptides, which allows generating protein bioconjugates, nonaccessible by a solution phase in batch mode [76].

3.3.2.1 Photochemistry

Recent advances using photochemistry have been described using flow methodologies [77–79]. These photoflow reactions provide a more homogeneous and effective irradiation of the entire reaction mixture, shortening reaction times

https://www.twirpx.org & http://chemistry-chemists.com

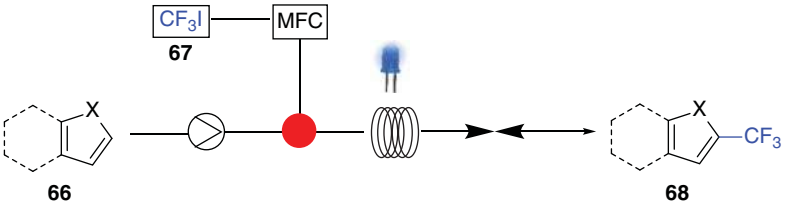

Scheme 3.20 Trifluoromethylation in flow with CF_3I.

and reducing the possibility of side reactions. Typically, these transformations involve the participation of excited species as key intermediates. In drug discovery programs, photochemistry has been used for the preparation of high value building blocks, opening new chemical space [80, 81].

Introduction of trifluoromethyl groups is important in medicinal chemistry as it can modulate different parameters in bioactive compounds, such as permeability or metabolic stability [82, 83]. Noël's group described the trifluoromethylation and perfluoroalkylation of five-membered ring heterocycles using $Ru(bpy)_3^{2+}$ as photocatalyst and TMEDA as base [84]. A variety of pyrroles and indoles **66** were perfluoroalkylated in continuous microflow, generating the products **68** in moderate to excellent yields. The gaseous reagent CF_3I **67** was introduced in a segmented gas–liquid flow system to perform the trifluoromethylation under light irradiation. The mixture with the corresponding heterocycle takes place before being irradiated (Scheme 3.20). Comparing with the analogous batch process, this continuous-flow protocol supposes a great reduction of the reaction time (from up to 72 hours in batch to less than 20 minutes in flow).

Another trifluoromethylation reaction of highly functionalized arenes and heteroarenes was reported by the same group in collaboration with Janssen researchers. In this work, the combination of the solid and air-stable trifluoromethylating agent CF_3SO_2Na with iridium catalysts provides trifluoromethylated heterocycles **71** and **72** in reasonable yields and after 30 minutes of residence time (Scheme 3.21) [85].

In the previous section the importance of the introduction of sp^3-carbon moieties into potential drug candidates has been highlighted. In this regard, photochemical transformations have gratifyingly contributed to achieve this goal.

For instance, Ley's group described a photoredox process combining iridium and nickel catalysts with Lewis bases to generate radical intermediates from boronated

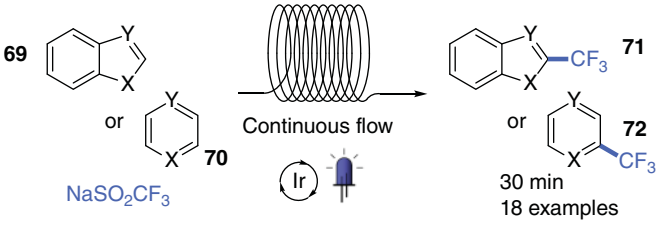

Scheme 3.21 Trifluoromethylation in flow with CF_3SO_2Na. Source: Abdia et al. [85] / Georg Thieme Verlag KG.

https://www.twirpx.org & http://chemistry-chemists.com

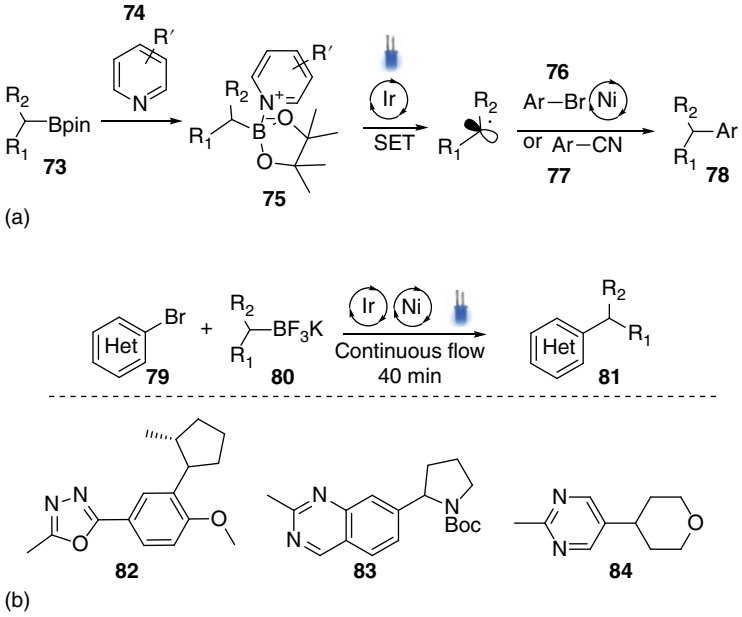

Scheme 3.22 Flow photoredox with organoboron compounds.

derivatives **73**. Once generated, radicals give rise to an sp^2–sp^3 cross-coupling reaction using cyanoheteroarenes **77** or bromoarenes **76** [86]. The use of boronic esters instead of trifluoroborate salts allows the synthesis under continuous flow due to solubility issues of the boronic scaffold (Scheme 3.22a). A soluble version for the continuous-flow cross-coupling of trifluoroborate salts with alkyl bromides **79** was reported by the Boyd group [87]. With this methodology, a small library of quinazolines **82**–**84** was prepared, and the procedure was also scalable (Scheme 3.22b).

Scientists from Janssen described a decarboxylative arylation of cyclic amines through a dual photoredox-nickel catalysis (Scheme 3.23). This transformation supposes an sp^2–sp^3 cross-coupling reaction, in which interesting heterocycles are functionalized with aryl groups [88]. This new protocol under continuous-flow conditions allows the preparation of typical drug-like scaffolds at a higher throughput than the previously reported batch process [89].

Different photosensitizers as iridium and ruthenium complexes have been widely used in photoredox catalysis. Despite the great number of reactions promoted by

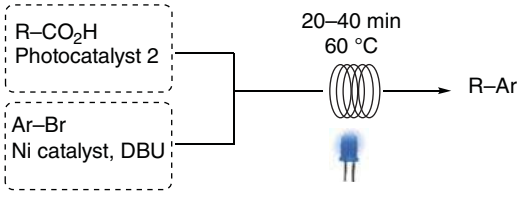

Scheme 3.23 Dual photoredox and nickel catalysis in flow.

https://www.twirpx.org & http://chemistry-chemists.com

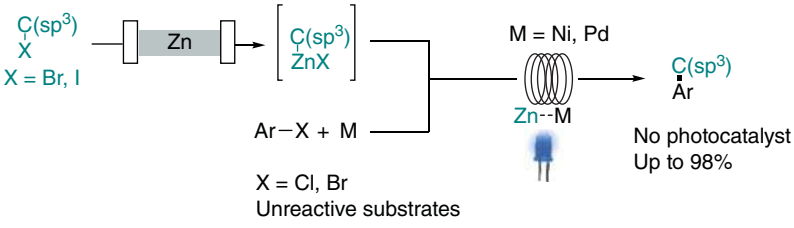

Scheme 3.24 Light-induced Negishi coupling in flow.

these complexes, their high cost, toxicity, and low abundancy make it necessary to look for greener alternatives. A collaboration between Janssen and University de Castilla-La Mancha researchers allowed the installation of $C(sp^3)$ moieties, from readily available alkyl halides into aromatics using nickel [90] or palladium [91] catalysts in the absence of a photosensitizer (Scheme 3.24). This methodology based on the Negishi cross-coupling expands the functional groups tolerated due to the acceleration of the key step in the catalytic cycle.

Another approach for the light-promoted formation of sp^2–sp^3 bonds under continuous flow has been recently reported using iron catalysis [92]. This continuous-flow version of the Kumada cross-coupling favors the reaction between aliphatic Grignard reagents **86** and a variety of aryl chlorides **85**, affording the products **87** in good to excellent yields in shorter times (Scheme 3.25).

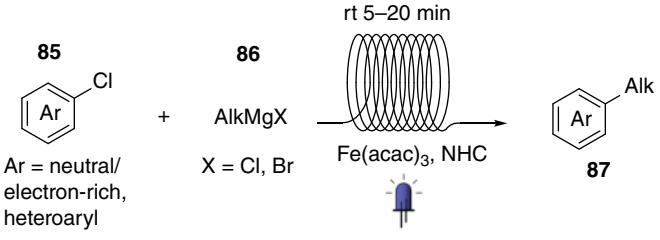

Scheme 3.25 Light-induced Kumada coupling in flow.

3.3.2.2 Electrochemistry

During the last decade, a renaissance in EC transformations for the creation of new organic molecules has been experienced [93, 94]. The chance of using electric current as a cheap reagent supposes a greener method in terms of sustainability. Strong oxidizing or reducing agents can be avoided, increasing safety and reducing waste generation. Moreover, the reactivity of the different functional groups can be controlled by simply adjusting the potential [95].

From a drug discovery perspective, an important application of flow electrochemistry is the generation of drug metabolites. Oxidative processes of drug candidates can give information of which positions of the molecule are more susceptible to suf-

https://www.twirpx.org & http://chemistry-chemists.com

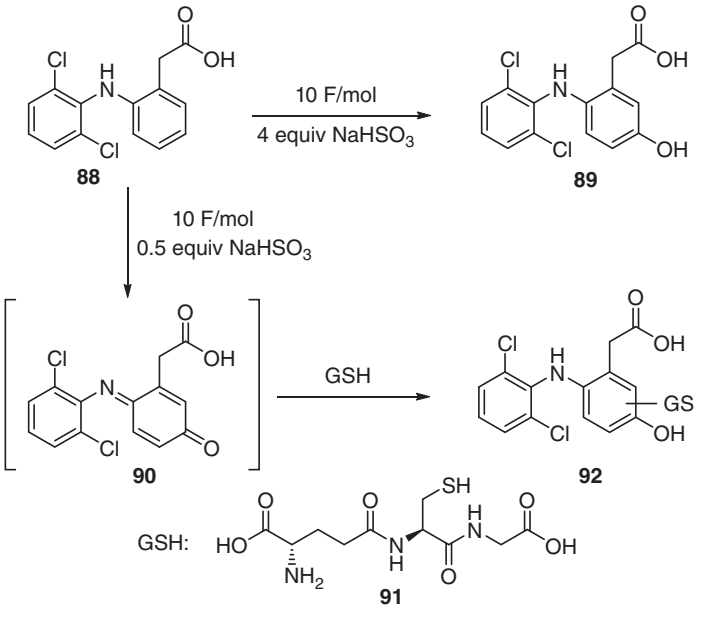

Scheme 3.26 Preparation of metabolites through electrochemistry in flow.

fer chemical transformations *in vivo*, simulating CYP450 oxidation. Considering the biological studies of the derivatives formed (e.g. pharmacological activity, toxicology screens), the direction of the medicinal chemistry program can be directed or reconducted in order to achieve a better drug candidate.

The EC oxidation of drug metabolites was described by Shono and coworkers in 1980s [96, 97]. The online detection of the biotransformation was achieved through an EC/mass spectroscopy system. However, this work was regarded as an analytical technique, and not as a synthetic method. One such example for the synthesis of metabolites was reported by Stalder and Roth using a new EC module [98]. Commercial drugs such as diclofenac, primidone, albendazole, tolbutamide, and chlorpromazine were subjected to EC oxidation (Scheme 3.26). Metabolites were obtained in a 10–100 mg scale, an amount great enough to carry out activity versus toxicity studies. Instead of carrying out a de novo synthesis for each of these new analogs, different derivatives were achieved in a single step by changing the reaction conditions. This approximation in the derivatization of late-state drug candidates will accelerate the discovery of improved chemical scaffolds in terms of PK and metabolic stability.

The EC synthesis of a small library of indole alkaloids **96** was reported by Ley and coworkers. In this transformation, α-methoxyamine derivatives **94** were initially generated in high yields from the Shono oxidation of cyclic amines **93**. A change in the solvent and filtration allows the outcome solution to react in a subsequent Pictet–Spengler reaction under microwave irradiation (Scheme 3.27) [99].

https://www.twirpx.org & http://chemistry-chemists.com

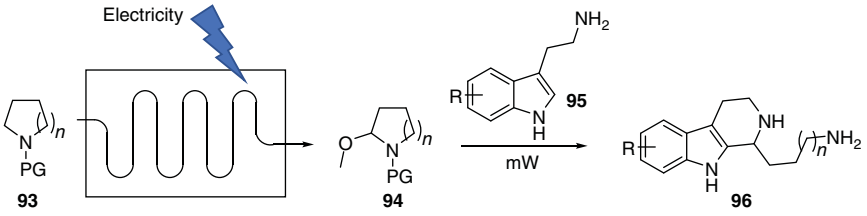

Scheme 3.27 Preparation of metabolites through electrochemistry in flow. Source: Kabeshov et al. [99] / Georg Thieme Verlag KG.

3.4 Automated Flow Synthesis

The pharmaceutical industry is constantly evolving, and for that reason it needs to be adapted to these changes. The pressure to have a new drug in the market on time is higher than ever before, which has led to changes in their research and development process. Therefore, innovative strategies have been developed to accelerate and improve drug discovery programs.

A new emerging approach for the preparation of series, which provide large amount of information in early stages of drug discovery programs, is the use of automated flow reactors as has been introduced in Chapter 2. These systems allow a fast reaction optimization in the early stages and rapid scalability.

There are several examples in literature of synthesis of drugs in continuous flow and fully automated. For example, James and Lange described a fully automated way for the synthesis of 3-aminoindolizine libraries **101**, important compounds for medicinal chemists, with three points of diversification [28]. The choice of the heterocycle, followed by a derivatization in the free amino group presented by the molecule and ending with a Sonogashira reaction with different propargylamines **100** followed by a cycloisomerization step, afforded the desired compounds **101** in good yields. They generate a matrix of four different heterocycles with four different derivatizations in the free amino groups plus five different propargylamines, giving rise to a total of 100 compounds that can be carried out employing the Conjure™ flow reactor system (Figure 3.2).

In 2019, Vilé et al. [100] described the synthesis in a continuous-flow reactor of *N*-fused-trifluoromethylated heterocycles **105** and **106**. These reactions were carried out in the Vapourtec R2S-series flow reactor by continuously mixing different amines **102** and **103** with trifluoroacetic anhydride (TFAA **104**) as a CF_3 source. Subsequent dehydration using TEA as base at 80 °C for 30 minutes afforded the corresponding compounds **105** and **106** in acceptable yields and with good productivity (Scheme 3.28). They also showed that the compounds can be scaled-up to gram quantities.

Pasau and coworkers described the synthesis of 1,3-disubstituted arylcyclobutanes **108** and **109** by reaction between halo-heteroaromatic compounds and different functionalized cyclobutylzinc reagents [101]. The authors showed two different protocols to prepare these analogs, a batch procedure using Zn Rieke as metal source and other flow-based procedure using a column containing activated

https://www.twirpx.org & http://chemistry-chemists.com

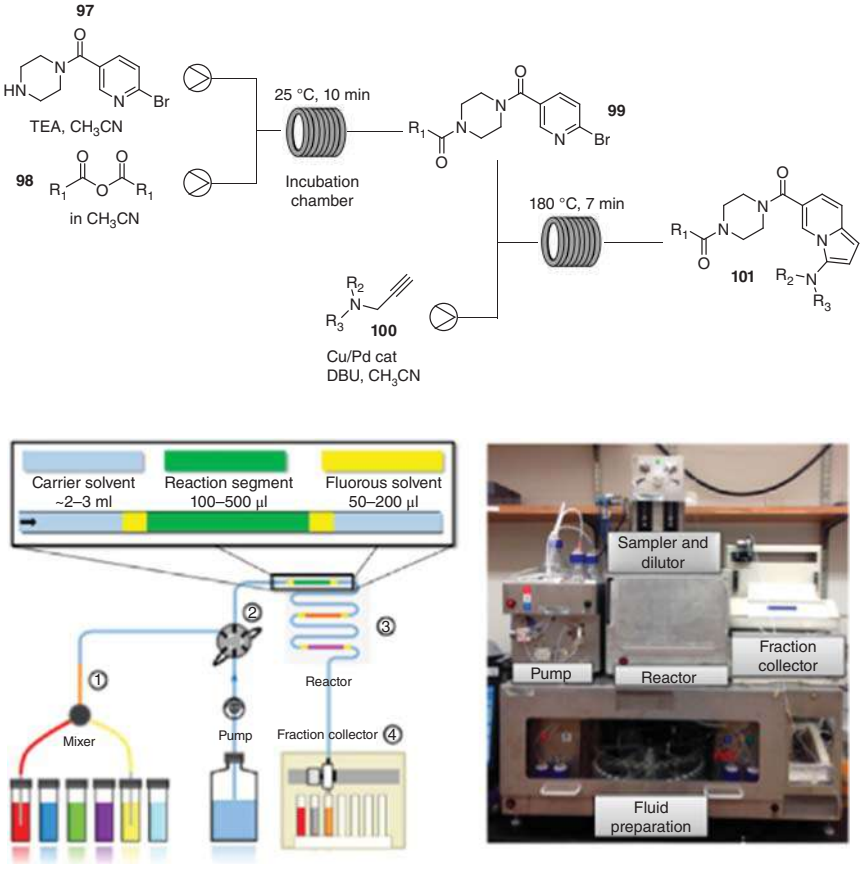

Figure 3.2 Automated synthesis of 3-aminoindolizine libraries. Source: Lange et al. [28] / with permission of American Chemical Society.

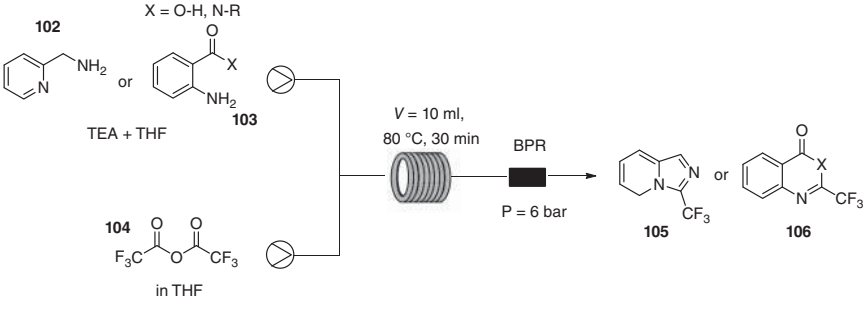

Scheme 3.28 Automated synthesis of trifuoromethylated heterocycles.

https://www.twirpx.org & http://chemistry-chemists.com

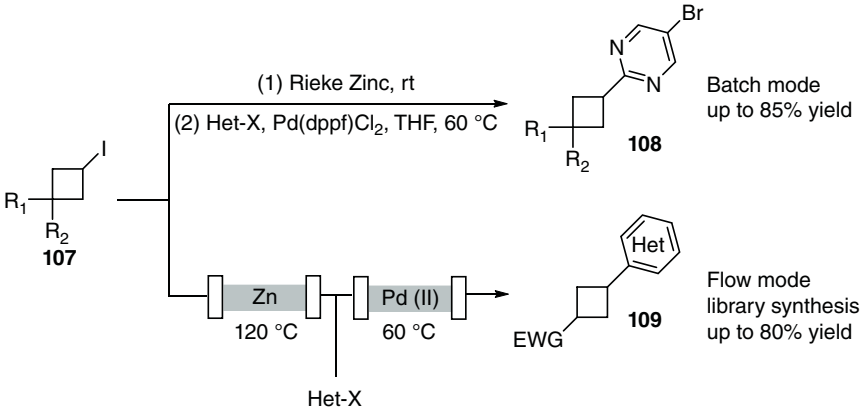

Scheme 3.29 Automated zinc insertion-Negishi coupling in flow.

Zn. They proved that the outcomes for both protocols are comparable. They also demonstrated that the flow process can be automated by integrating two autosamplers for reagents loading and a fraction collector for reaction compilation (Scheme 3.29). In this way, libraries of functionalized cyclobutane derivatives can be obtained from stable halogenated reagents **107**.

The combination of automated synthesis with design-of-experiments (DoE) has been regarded as an interesting alternative to reduce the optimization stage. Using this approach, reaction variables can be optimized using advanced algorithms [102]. Jensen and Jamison groups have developed a reconfigurable system, which optimize automatically a series of different transformations, with relevant application in the pharmaceutical industry (Buchwald–Hartwig amination, S_NAr, Suzuki–Miyaura coupling, and photoredox) [103]. Up to five variables can be optimized, and the data is obtained between 7 and 34 hours depending on the number of screening conditions carried out. Subsequent scale-up can also be performed in the same platform once the best parameters are found (Scheme 3.30).

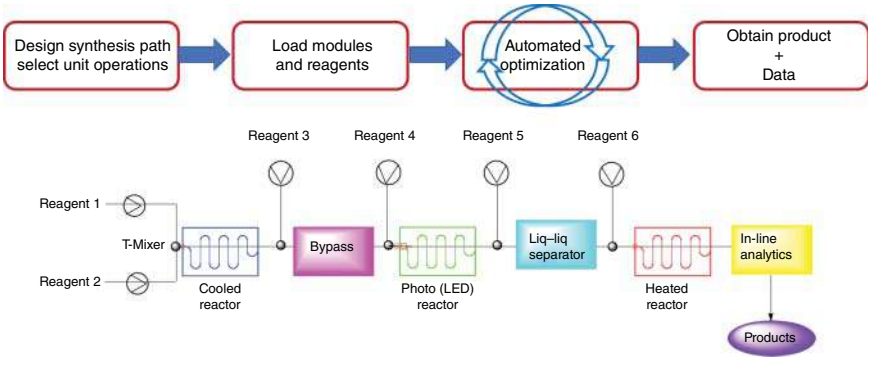

Scheme 3.30 Reconfigurable system for reaction optimization.

https://www.twirpx.org & http://chemistry-chemists.com

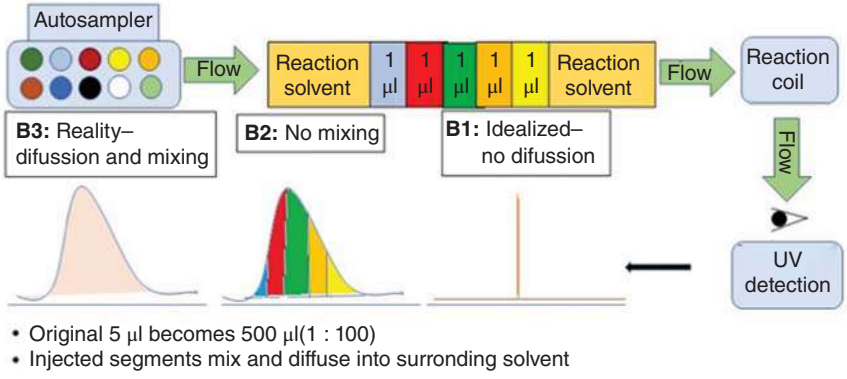

Figure 3.3 Flow platform for reaction optimization and library synthesis.

Attending to the high-throughput experimentation area (HTE), scientists from Pfizer developed an automated flow-based system for screening and synthesis on submilligram scales. This concept is also explained in Chapter 2 [104]. A set of reaction variables (temperatures, solvents, ligands, bases) were analyzed to validate the platform using the Suzuki–Miyaura coupling. As microliter volumes were used for each reagent, a great number of combinations were achieved obtaining a real-time analysis data in a fast manner. Thus, the system is able to run more than 1500 reactions in a 24-hour period, which can be translated to scale-up in both batch and flow (Figure 3.3).

Artificial intelligence (AI) has also been implemented as an outstanding alternative in continuous-flow integrated systems. Massachusetts Institute of Technology (MIT) researchers reported the automated synthesis of complex organic molecules combining AI and a robotic platform under continuous flow [105]. This autonomous platform analyzes scientific databases through an integrated software, which evaluates the best synthetic route (Scheme 3.31). Thus, while AI allows planning the synthesis, the execution of chemical libraries is done robotically. This combination supposes a reduction of time and cost in drug discovery, not only in HtL but also in LO.

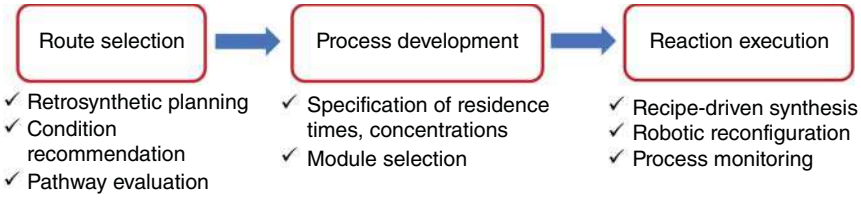

Scheme 3.31 Flow platform integrating automated synthesis, robotics, and AI.

3.5 Integrated Platforms

Automatic synthesis capabilities described earlier can be coupled with automated purification, biological screening, and algorithmic predictions for a full automation

https://www.twirpx.org & http://chemistry-chemists.com

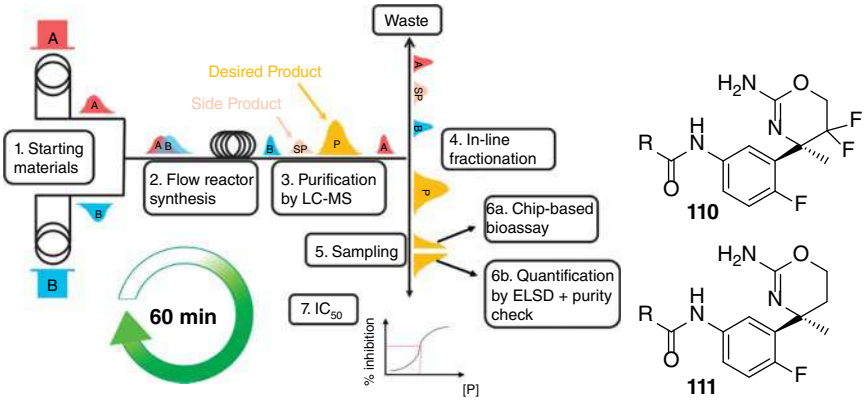

Figure 3.4 Hoffmann-La Roche platform for drug optimization.

of the design-make-test cycle. This will reduce the time required to optimize a drug candidate [106]. Compared with the parallel methodology, a more rational synthesis is achieved diminishing the number of compounds synthetized. Multiple research groups have investigated these integrated platforms [107–111].

For instance, scientists at Cyclofluidic developed a platform combining a reagent autosampler connected to a high-performance liquid chromatography (HPLC) mass spectrometer. The purification and characterization of the products is done through an integrated liquid chromatography mass spectrometry (LC–MS) attached. Subsequent concentration of the samples using an evaporative light-scattering detector (ELSD) can be followed by biological assays including SAR to discover new DPP4 [112] and Abl kinase inhibitors [113]. In this last example, the authors use the Random Forest Regression with sampling algorithms to explore the chemical space, which allows the setup of an activity model, which is refined after each repetition of synthesis and biological result. By this method and with only 21 compounds synthesized, they were able to identify a novel motif with $pIC_{50} > 8$ against Abl-Kinase. In comparison with the several days required for the preparation, purification, and transport of the compounds submitted to biological assays, this integrated system only takes two hours, considering all the steps. A more detailed explanation can be found in Chapter 2.

For instance, an approach comprising synthesis, purification, and quantification of the derivatives was developed by Hoffman-La Roche researchers. [114] The generation of SAR data for BACE1 inhibitors **110** and **111** was carried out using a chip-based assay generating the corresponding IC_{50} values. In this case, a cycle time of 60 minutes per compound was necessary for the synthesis, purification, and biological screening. This considerable reduction of time clearly showcases an efficient manner to accelerate drug discovery programs using integrated systems (Figure 3.4). This example, among many others, integrating systems for continuous synthesis and biological screenings is widely explained in Chapter 5.

https://www.twirpx.org & http://chemistry-chemists.com

3.6 Conclusions and Outlook

Flow chemistry has grown over the last decade to become a useful tool for drug discovery. Initially it had been used to improve problematic chemical processes but limited to reproduce the same reactions that has been applied in this field over the years. More recently, it has been used to bring back to bench reactions rarely used in a medicinal chemistry setting but very valuable in terms of exploring novel chemical space. Currently the use of automated flow platforms and the combination with underused technologies, such as electrochemistry and photochemistry, allows to access new chemical space in a more efficient manner, reducing cycle times in drug discovery.

This interesting present is opening a brilliant future where flow chemistry will be a central capability in the discovery of new drugs. Automated multistep reactions will be done in flow, allowing full structure chemical libraries to be synthesized and purified online, drastically reducing the time needed to move from hit to lead and from lead to clinical candidate when combined with in line biological screening and AI.

References

1 Edwards, L., Fox, A., and Stonier, P. (ed.) (2010). *Principles and Practice of Pharmaceutical Medicine*, 3e. Oxford: Wiley Blackwell.

2 Leeson, P.D. and Empfield, J.R. (2010). Reducing the risk of drug attrition associated with physicochemical properties. *Annu. Rep. Med. Chem.* 45: 393–407.

3 DiMasi, J.A. and Faden, L.B. (2011). Competitiveness in follow-on drug R&D: a race or imitation? *Nat. Rev. Drug Discov.* 10: 23–27.

4 Hughes, J.P., Rees, S., Kalindjian, S.B., and Philpott, K.L. (2011). Principles of early drug discovery. *Br. J. Pharmacol.* 162: 1239–1249.

5 Zanders, J.H., Bailey, D.S., and Dean, P.M. (2002). Probes for chemical genomics by design. *Drug Discov. Today.* 7: 711–718.

6 Lavecchia, A. and di Giovani, C. (2013). Virtual screening strategies in drug discovery: a critical review. *Curr. Med. Chem.* 20: 2839–2860.

7 Erlanson, D.A., McDowell, R.S., and O'Brien, T. (2004). Fragment-based drug discovery. *J. Med. Chem.* 47: 3463–3482.

8 Keseru, G.M. and Makara, G.M. (2006). Hit discovery and hit-to lead approaches. *Drug Discov. Today* 11: 741–748.

9 Lipinski, C.A., Lombardo, F., Dominy, B.W., and Feeney, P.J. (2001). Experimental and computational approaches to estimate solubility and permeability in drug discovery and development settings. *Adv. Drug. Deliv. Rev.* 46: 3–26.

10 Bogdan, A.R. and Dombrowski, A.W. (2019). Emerging trends in flow chemistry and applications to the pharmaceutical industry. *J. Med. Chem.* 62: 6422–6468.

11 Boström, J., Brown, D.G., Young, R.J., and Keserü, G.M. (2018). Expanding the medicinal chemistry synthetic toolbox. *Nat. Rev. Drug Discov.* 17: 709–727.

https://www.twirpx.org & http://chemistry-chemists.com

12 Urge, L., Alcázar, J., Huck, L., and Dorman, G. (2017). Recent advances of microfluidics technologies in the field of medicinal chemistry. *Annu. Rep. Med. Chem.* 50: 87–147.

13 Alcázar, J. (2017). Sustainable flow chemistry in drug discovery. In: *Sustainable Flow Chemistry* (ed. L. Vaccaro), 135–164. Weinheim: Wiley-VCH.

14 Bogdan, A.R. and Organ, M.G. (2018). Flow chemistry as a drug discovery tool: a medicinal chemistry perspective. In: *Flow Chemistry for the Synthesis of Heterocycles* (ed. U.K. Sharman and E.V. Van der Eycken), 319–341. Cham: Springer International Publishing AG.

15 Alcázar, J., de la Hoz, A., and Díaz-Ortiz, A. (2019). Flow chemistry in drug discovery. In: *Green Synthetic Processes and Procedures* (ed. R. Ballini), 53–78. Cambridge: RSC publishing.

16 Palao, E. and Alcázar, J. (2019). Organometallic chemistry in flow in the pharmaceutical industry. In: *Flow Chemistry: Integrated Approaches for Practical Applications* (ed. S.V. Luis and E. Garcia-Verdugo), 86–128. Cambridge: RSC publishing.

17 Souza, J.M., Galaverna, R., Souza, A.A.N. et al. (2018). Impact of continuous flow chemistry in the synthesis of natural products and active pharmaceutical ingredients. *An. Acad. Bras. Cienc.* 90: 1131–1174.

18 Bana, P., Orkenyi, R., Lovei, K.A. et al. (2017). The route from problem to solution in multistep continuous flow synthesis of pharmaceutical compounds. *Bioorg. Med. Chem.* 25: 6180–6189.

19 Cole, K.P. and Johnson, M.D. (2018). Continuous flow technology *vs* the batch-by-batch approach to produce pharmaceutical compounds. *Expert Rev. Clin. Pharmacol.* 11: 5–13.

20 Gerardy, R., Emmanuel, N., Toupy, T. et al. (2018). Continuous flow organic chemistry: successes and pitfalls at the interface with current societal challenges. *Eur. J. Org. Chem.* 2301–2351.

21 Roughley, S.D. and Jordan, A.M. (2011). The medicinal chemist's toolbox: an analysis of reactions used in the pursuit of drug candidates. *J. Med. Chem.* 54: 3451–3479.

22 Brown, G.D. and Boström, J. (2016). Analysis of past and present synthetic methodologies on medicinal chemistry: where have all the new reactions gone? *J. Med. Chem.* 59: 4443–4458. https://pubs.acs.org/doi/10.1021/acs.jmedchem.5b01409.

23 Gustafsson, T., Ponten, F., and Seeberger, P.H. (2008). Trimethylaluminium mediated amide bond formation in a continuous flow microreactor as key to the synthesis of rimonabant and efaproxiral. *Chem. Commun.* 1100–1102.

24 de M Muñoz, J., de la Hoz, A., Díaz-Ortiz, A. et al. (2012). Preparation of amides mediated by isopropylmagnesium chloride under continuous flow conditions. *Green Chem.* 14: 1335–1341.

25 Vrijdag, J.L., Delgado, F., Alonso, N. et al. *Chem. Commun.* 50: 15094–15097.

26 Fuse, S., Mifune, Y., Nakamura, H., and Tanaka, H. (2016). Total synthesis of feglymicin based on a linear/convergent hybrid approach using micro-flow amide bond formation. *Nat. Commun.* 7: 13491.

https://www.twirpx.org & http://chemistry-chemists.com

27 Mijalis, A.J., Dale, A.T., Simon, M.D. et al. (2017). A fully automated flow-based approach for accelerated peptide synthesis. *Nat. Chem. Biol.* 13: 464–468.

28 Lange, P.P. and James, K. (2012). Rapid access to compound libraries through flow technology: fully automated synthesis of a 3-aminoindolizine library via orthogonal diversification. *ACS Comb. Sci.* 14: 570–578.

29 Hawbaker, N., Wittgrove, E., Christensen, B. et al. (2016). Dispersion in compartmentalized flow systems: influence of flow patterns on reactivity. *Org. Process Res. Dev.* 20: 465–473.

30 Gilmore, K., Vukelic, S., McQuade, D.T. et al. (2014). Continuous reductions and reductive amination using solid $NaBH_4$. *Org. Process Res. Dev.* 18: 1771–1776.

31 Laroche, B., Ishitani, H., and Kobayashi, S. (2018). Direct reductive amination of carbonyl compounds with H_2 using heterogeneous catalysts in continuous flow as an alternative to N-alkylation with alkyl halides. *Adv. Synth. Catal.* 360: 4699–4704.

32 Frederick, M.O., Pietz, M.A., Kjell, D.P. et al. (2017). Development of a Leuckart-Wallach reaction in flow for the synthesis of Abemaciclib. *Org. Process Res. Dev.* 21: 1447–1451.

33 Charaschanya, M., Bogdan, A.R., Wang, Y., and Djuric, S.W. (2016). Nucleophilic aromatic substitution of heterocycles using a high-temperature and high-pressure flow reactor. *Tetrahedron Lett.* 57: 1035–1039.

34 Verghese, J., Caleb, J.K., Rivalti, D. et al. (2017). Increasing global access to the high-volume HIV drug nevirapine through process intensification. *Green Chem.* 19: 2986–2991.

35 Alam, M.P., Jagodzinska, B., Campagna, J. et al. (2016). C-O bond formation in a microfluidic reactor; high yield S_NAr substitution of heteroaryl chlorides. *Tetrahedron Lett.* 57: 2059–2062.

36 Ruíz-Castillo, P. and Buchwald, S.L. (2016). Applications of palladium-catalyzed C-N cross-coupling reactions. *Chem. Rev.* 116: 12564–12649.

37 Hartman, R.L., Naber, J.R., Zaborenko, N. et al. (2010). Overcoming the challenges of solid bridging and constriction during Pd-catalyzed C-N bond formation in microreactors. *Org. Process Res. Dev.* 14: 1347–1357.

38 Falb, S., Tomaiuolo, G., Perazzo, A. et al. (2016). A continuous process for Buchwald-Hartwig at micro-, lab-, and mesoscale using a novel reactor concept. *Org. Process Res. Dev.* 20: 558–567.

39 Noël, T., Naber, J.R., Hartman, R.L. et al. (2011). Palladium-catalyzed amination reactions in flow: overcoming the challenges of clogging via acoustic irradiation. *Chem. Sci.* 2: 287–290.

40 Baumgartner, L.M., Dennis, J.M., White, N.A. et al. (2019). Use of a droplet platform to optimize Pd-catalyzed C-N coupling reactions promoted by organic bases. *Org. Process Res. Dev.* 23: 1549–1601.

41 de Muñoz, J., M., Alcázar, J., de la Hoz, A., and Díaz-Ortíz, A. (2012). Cross-coupling in flow using supported catalysts: mild, clean, efficient and sustainable Suzuki-Miyaura coupling in a single pass. *Adv. Synth. Catal.* 354: 3456–3460.

https://www.twirpx.org & http://chemistry-chemists.com

42 Pascanu, V., Hansen, P.R., Bermejo Gómez, A. et al. (2015). Highly functionalized biaryls via Suzuki-Miyaura cross-couplings catalyzed by Pd@MOF under batch and continuous flow regimes. *ChemSusChem* 8: 123–130.

43 Sieber, J.D., Buono, F., Brusoe, A. et al. (2019). Application of a preformed Pd-BIDIME precatalyst to Suzuki-Miyaura cross-coupling reaction in flow. *J. Org. Chem.* 84: 4926–4931.

44 Sonogashira, K. (2002). Development of Pd-Cu catalyzed cross-coupling of terminal acetylenes with sp^2-carbon halides. *J. Organomet. Chem.* 653: 46–49.

45 Tan, L.-M., Sem, Z.-Y., Chong, W.-Y. et al. (2013). Continuous flow Sonogashira C-C coupling using a heterogeneous palladium-copper dual reactor. *Org. Lett.* 15: 65–67.

46 Placzek, M.S., Chmielecki, J.M., Houghton, C. et al. (2013). Fluoroalkunylations of aryl halides under continuous-flow homogeneous catalysis. *J. Flow. Chem.* 3: 46–50.

47 Znidar, D., Hone, C.A., Inglesby, P. et al. (2017). Development of a continuous-flow Sonogashira cross-coupling protocol using propyne gas under process intensified conditions. *Org. Process Res. Dev.* 21: 878–884.

48 D'Attoma, J., Cozien, G., Brun, P.L. et al. (2016). Fast functionalization of (7-aza)indoles using continuous flow processes. *ChemistrySelect* 3: 338–342.

49 Sharman, U.K. and der Eycken, E.V. (ed.) (2018). *Flow Chemistry for the Synthesis of Heterocycles*. Cham: Springer International Publishing AG.

50 Kolb, H.C., Finn, M.G., and Sharpless, K.B. (2001). Click chemistry: diverse chemical function from a few good reactions. *Angew. Chem. Inter. Ed.* 40: 2004–2021.

51 Bogdan, A.R. and Sach, N.W. (2009). The use of copper flow reactor technology for the continuous synthesis of 1,4-disubstituted 1,2,3-triazoles. *Adv. Synth. Catal.* 351: 849–854.

52 Zhang, Y., Jamison, F.T., Patel, S., and Mainolfi, N. (2011). Continuous flow coupling and decarboxylation reactions promoted by copper tubing. *Org. Lett.* 13: 280–283.

53 Leforestier, B. and Vögtle, M. (2016). Safe generation and direct use of chlorine azide in flow chemistry: 1,2-azidochlorination of olefins and access to triazoles. *Synlett* 27: 1957–1962.

54 Meščić, A., Šalić, A., Gregorić, T. et al. (2017). Continuous flow-ultrasonic synergy in click reactions for the synthesis of novel 1,2,3-triazolyl appended 4,5-unsaturated l-ascorbic acid derivatives. *RSC Adv.* 7: 791–800.

55 Wen, J., Wu, K., Yang, D. et al. (2018). Low-pressure flow chemistry of CuAAC click reaction catalyzed by nanoporous AuCu membrane. *ACS Appl. Mater. Interfaces* 10: 25930–25935.

56 Dervaux, B. and Du Prez, F.E. (2012). Heterogeneous azide-alkyne click chemistry: towards metal-free end products. *Chem. Sci.* 3: 959–966.

57 Wang, B., Durantini, J., Nie, J. et al. (2016). Heterogeneous photocatalytic click chemistry. *J. Am. Chem. Soc.* 138: 13127–13130.

https://www.twirpx.org & http://chemistry-chemists.com

58 Jin, T., Yan, M., and Yamamoto, Y. (2012). Click chemistry of alkyne-azide cycloaddition using nanostructured copper catalysts. *Chem. Cat. Chem.* 4: 1217–1229.

59 Chen, M. and Buchwald, S.L. (2013). Continuous-flow synthesis of 1-substituted benzotriazoles from chloronitrobenzenes and amines in a C-N bond formation/hydrogenation/diazotization/cyclization sequence. *Angew. Chem. Int. Ed.* 52: 4247–4250.

60 Deadman, B.J., Collins, S.G., and Maguire, A.R. (2015). Taming hazardous chemistry in flow: the continuous processing of diazo and diazonium compounds. *Chem. Eur. J.* 21: 2298–2308.

61 Mastronardi, F., Gutmann, B., and Kappe, C.O. (2013). Continuous flow generation and reactions of anhydrous diazomethane using a teflon AF-2400 tube-in-tube reactor. *Org. Lett.* 15: 5590–5593.

62 Schreiber, S.L. (2000). Target-oriented and diversity-oriented organic synthesis in drug discovery. *Science* 287: 1964–1969.

63 Huck, L., Berton, M., de la Hoz, A. et al. (2017). Reformatsky and Blaise reactions in flow as a tool for drug discovery. One pot diversity-oriented synthesis of valuable intermediates and heterocycles. *Green Chem.* 19: 1420–1424.

64 Huck, L., de la Hoz, A., Diaz-Ortiz, A., and Alcazar, J. (2017). Grignard reagents on a tab: direct magnesium insertion under flow conditions. *Org. Lett.* 19: 3747–3750.

65 Lovering, F., Bikker, J., and Humblet, C. (2009). Escape from flatland: increasing saturation as an approach to improving clinical success. *J. Med. Chem.* 52: 6752–6756.

66 Walters, W.P., Green, J., Weiss, J.R., and Murcko, M.A. What do medicinal chemists actually make? A 50-year retrospective. *J. Med. Chem.* 54: 6405–6416.

67 Tsukamoto, T. (2013). Tough times for medicinal chemists: are we to blame? *ACS Med. Chem. Lett.* 4: 369–370.

68 Alonso, N., Miller, L.Z., de M. Muñoz, J. et al. (2014). Continuous synthesis of organozinc halides coupled to Negishi reactions. *Adv. Synth. Catal.* 356: 3737–3741.

69 Berton, M., Huck, L., and Alcázar, J. (2018). On-demand synthesis of organozinc halides under continuous flow conditions. *Nat. Protoc.* 13: 324–334.

70 Egle, B., de M. Muñoz, J., Alonso, N. et al. (2014). First example of alkyl-aryl Negishi cross-coupling in flow: mild, efficient and clean introduction of functionalized alkyl groups. *J. Flow Chem.* 4: 22–25.

71 Yoshida, J.-I. (ed.) (2008). *Flash Chemistry: Fast Organic Synthesis in Microsystems*. Chichester: Wiley.

72 Nagaki, A., Matsuo, C., Kim, S. et al. (2012). Lithiation of 1,2-dichloroethene in flow microreactors: versatile synthesis of alkenes and alkynes by precise residence-time control. *Angew. Chem. Int. Ed.* 51: 3245–3248.

73 Hartwig, J., Metternich, J.B., Nikbin, N. et al. (2014). Continuous flow chemistry: a discovery tool for new chemical reactivity patterns. *Org. Biomol. Chem.* 12: 3611–3615.

https://www.twirpx.org & http://chemistry-chemists.com

74 Petersen, T.P., Becker, M.R., and Knochel, P. (2014). Continuous flow magnesiation of functionalized heterocycles and acrylates with TMPMgCl·LiCl. *Angew. Chem. Int. Ed.* 53: 7933–7937.

75 Karande, R., Schmid, A., and Buehlera, K. (2011). Miniaturizing biocatalysis: enzyme-catalyzed reactions in an aqueous/organic segmented flow capillary microreactor. *Adv. Synth. Catal.* 353: 2511–2521.

76 Policarpo, R.L., Kang, H., Liao, X. et al. (2014). Flow-based enzymatic ligation by sortase A. *Angew. Chem. Int. Ed.* 53: 9203–9208.

77 Beeler, A.B. and Corning, S.R. (2016). Photochemistry in flow. In: *Photochemistry* (ed. A. Albini and E. Fasani), 173–190. Cambridge: RSC Publishing.

78 Cambié, D., Bottecchia, C., Straathof, N.J.W. et al. (2016). Applications of continuous-flow photochemistry in organic synthesis, material science and water treatment. *Chem. Rev.* 116: 10276–10341.

79 Politano, F. and Oksdath-Mansilla, G. (2018). Light on the horizon: current research and future perspectives in flow photochemistry. *Org. Process Res. Dev.* 22: 1045–1062.

80 Fang, Y. and Tranmer, G.K. (2016). Continuous flow photochemistry as an enabling synthetic technology: synthesis of substituted-6(5*H*)-phenanthridinones for use as poly(ADP-ribose) polymerase inhibitors. *Med. Chem. Commun.* 7: 720–724.

81 Di Filippo, M., Bracken, C., and Baumann, M. (2020). Continuous flow photochemistry for the preparation of bioactive molecules. *Molecules* https://doi.org/10.3390/molecules25020356.

82 Tseng, C.-C., Baillie, G., Donvito, G. et al. (2019). The trifluoromethyl group as a bioisosteric replacement of the aliphatic nitro group in CB_1 receptor positive allosteric modulators. *J. Med. Chem.* 62: 5049–5062.

83 Gillis, E.P., Eastman, K.J., Hill, M.D. et al. (2015). Applications of fluorine in medicinal chemistry. *J. Med. Chem.* 58: 8315–8359.

84 Straathof, N.J.W., Gemoets, H.P.L., Wang, X. et al. (2014). Rapid trifluoromethylation and perfluoroalkylation of five-membered heterocycles by photoredox catalysis in continuous flow. *ChemSusChem* 7: 1612–1617.

85 Abdiaj, I., Bottecchia, C., Alcázar, J., and Noël, T. (2017). Visible-light-induced trifluoromethylation of highly functionalized arenes and heteroarenes in continuous flow. *Synthesis* 49: 4978–4985.

86 Lima, F., Kabeshov, M.A., Tran, D.N. et al. (2016). Visible light activation of boronic esters enables efficient photoredox $C(sp^2)$-$C(sp^3)$ cross-couplings in flow. *Angew. Chem. Int. Ed.* 55: 14085–14089.

87 DeLano, T.J., Bandarage, U.K., Palaychuk, N. et al. (2016). Application of the photoredox coupling of trifluoroborates and aryl bromides to analog generation using continuous flow. *J. Org. Chem.* 81: 12525–12531.

88 Abdiaj, I. and Alcazar, J. (2017). Improving the throughput of batch photochemical reactions using flow: dual photoredox and nickel catalysis in flow for $C(sp^2)$-$C(sp^3)$ cross-coupling. *Biorg. Med. Chem.* 25: 6190–6196.

https://www.twirpx.org & http://chemistry-chemists.com

89 Zuo, Z., Ahneman, D.T., Chu, L. et al. (2014). Dual catalysis. Merging photoredox with nickel catalysis: coupling of α-carboxyl sp^3-carbons with aryl halides. *Science* 345: 437–440.

90 Abdiaj, I., Fontana, A., Gomez, M.V. et al. (2018). Visible-light-induced nickel-catalyzed Negishi cross-couplings by exogenous-photosensitizer-free photocatalysis. *Angew. Chem. Int. Ed.* 57: 8473–8477.

91 Abdiaj, I., Huck, L., Mateo, J.M. et al. (2018). Photoinduced palladium-catalyzed Negishi cross-couplings enabled by the visible-light absorption of palladium-zinc complexes. *Angew. Chem. Int. Ed.* 57: 13231–13236.

92 Wei, X.-J., Abdiaj, I., Sambiagio, C. et al. (2019). Visible-light-promoted iron-catalyzed $C(sp^2)$-$C(sp^3)$ Kumada cross-coupling in flow. *Angew. Chem. Int. Ed.* 58: 13030–13034.

93 Wiebe, A., Gieshoff, T., Möhle, S. et al. (2018). Electrifying organic synthesis. *Angew. Chem. Int. Ed.* 57: 5594–5619.

94 Noël, T., Cao, Y., and Laudadio, G. (2019). The fundamentals behind the use of flow reactors in electrochemistry. *Acc. Chem. Res.* 52: 2858–2869.

95 Atobe, M., Tateno, H., and Matsumura, Y. (2018). Applications of flow microreactors in electrosynthetic processes. *Chem. Rev.* 118: 4541–4572.

96 Shono, T., Toda, T., and Oshino, N. (1981). Preparation of N-dealkylated drug metabolites by electrochemical simulation of biotransformation. *Drug. Metab. Dispos.* 9: 481–482.

97 Shono, T., Toda, T., and Oshino, N. (1982). Electron transfer from nitrogen in microsomal oxidation of amine and amide. Simulation of microsomal oxidation by anodic oxidation. *J. Am. Chem. Soc.* 104: 2639–2641.

98 Stalder, R. and Roth, G.P. (2013). Preparative microfluidic electrosynthesis of drug metabolites. *ACS Med. Chem. Lett.* 4: 1119–1123.

99 Kabeshov, M.A., Musio, B., Murray, P.R. et al. (2014). Expedient preparation of nazlinine and a small library of indole alkaloids using flow electrochemistry as an enabling technology. *Org. Lett.* 16: 4618–4621.

100 Amini-Rentsch, L., Vanoli, E., Richard-Bildstein, S. et al. (2019). Novel and efficient continuous-flow route to prepare trifluoromethylated N-fused heterocycles for drug discovery and pharmaceutical manufacturing. *Ind. Eng. Chem. Res.* 58: 10164–10171.

101 Tissot, M., Body, N., Petit, S. et al. (2018). Synthesis of electron-deficient heteroaromatic 1,3-substituted cyclobutyls via zinc insertion/Negishi coupling sequence under batch and automated flow conditions. *Org. Lett.* 20: 8022–8025.

102 Moore, J.S. and Jensen, K.F. (2013). Automation in microreactor systems. In: *Microreactors in Organic Chemistry and Catalysis* (ed. T. Wirth), 81–100. Weinheim: Wiley-VCH.

103 Bédard, A.-C., Adamo, A., Aroh, K.C. et al. (2018). Reconfigurable system for automated optimization of diverse chemical reactions. *Science* 361: 1220–1225.

104 Perera, P., Tucker, J.W., Brahmbhatt, S. et al. (2018). A platform for automated nanomole-scale reaction screening and micromole-scale synthesis in flow. *Science* 359: 429–438.

https://www.twirpx.org & http://chemistry-chemists.com

105 Coley, C.W., Thomas, D.A. III, Lummiss, J.A.M. et al. (2019). A robotic platform for flow synthesis of organic compounds informed by AI planning. *Science* 365: https://doi.org/10.1126/science.aax1566.

106 Rodrigues, T., Schneider, P., and Schneider, G. (2014). Accessing new chemical entities through microfluidic systems. *Angew. Chem. Int. Ed.* 53: 5750–5758.

107 Hawkes, S.Y.F.W., Chapela, M.J.V., and Montembault, M. (2005). Leveraging the advantages offered by microfluidics to enhance the drug discovery process. *QSAR Comb. Sci.* 24: 712–721.

108 Wang, J., Sui, G., Mocharla, V.P. et al. (2006). Integrated microfluidics for parallel screening of an in situ click chemistry library. *Angew. Chem. Int. Ed.* 45: 5276–5281.

109 Wang, Y., Lin, W.Y., Liu, K. et al. (2009). An integrated microfluidic device for large-scale in situ click chemistry screening. *Lab Chip* 9: 2281–2285.

110 Petersen, T.P., Mirsharghi, S., Rummel, P.C. et al. (2013). Multistep continuous-flow synthesis in medicinal chemistry: discovery and preliminary structure-activity relationships of CCR8 ligands. *Chem. Eur. J.* 19: 9343–9350.

111 Guetzoyan, L., Nikbin, N., Baxendale, I.R., and Ley, S.V. (2013). Flow chemistry synthesis of zolpidem, alpidem and other GABAA agonists and their biological evaluation through the use of in-line frontal affinity chromatography. *Chem. Sci.* 4: 764–769.

112 Czechtizky, W., Dedio, J., Desai, B. et al. (2013). Integrated synthesis and testing of substituted xanthine based DPP4 inhibitors: application to drug discovery. *ACS Med. Chem. Lett.* 4: 768–772.

113 Desai, B., Dixon, K., Farrant, E. et al. (2013). Rapid discovery of a novel series of Abl kinase inhibitors by application of an integrated microfluidic synthesis and screening platform. *J. Med. Chem.* 56: 3033–3047.

114 Werner, M., Kuratli, C., Martin, R.E. et al. (2014). Seamless integration of dose-response screening and flow chemistry: efficient generation of structure-activity relationship data of β-secretase (BACE1) inhibitors. *Angew. Chem. Int. Ed.* 53: 1704–1708.

https://www.twirpx.org & http://chemistry-chemists.com

4

Flow Chemistry in Medicinal Chemistry: Applications to Bcr-Abl Kinase Inhibitors

Paul Richardson

Pfizer-La Jolla, Medicine Design, 10770 Science Center Drive, La Jolla, CA 92121, USA

4.1 Introduction

There are numerous recent reviews highlighting the advantages of flow chemistry with several specifically focused on the potential benefits to be realized within drug discovery [1]. While core benefits of the technology are well recognized (for example, automation, speed, reproducibility, enhanced safety, smaller footprint) [2], it can sometimes be challenging to see how these can be an immediate advantage to a conventional medicinal chemist [3]. While, there are multiple impressive flow chemistry-based technology platforms in current use to facilitate medicinal chemistry programs (for example, library synthesis, reaction screening), it is important to bear in mind that the development (conceive/build/test) of these requires a relatively significant investment in terms of cost/resource and time with the realization that the payback for this will be provided through their continued utility (naturally with minor tweaks in terms of enhancements), typically by dedicated specialist users over time on multiple medicinal chemistry programs [4]. However, in the regular classical discovery research laboratory, it appears that except for several specific applications (for example, flow-based hydrogenation) [5], the uptake of flow chemistry on a routine day-to-day basis has been somewhat limited.

At the outset, it is instructive to consider the reasons behind this trend with several possible causes. The first to consider is somewhat counterintuitive particularly considering that it is often cited as one of the main drivers for incorporation of flow within early-stage medicinal chemistry programs, and that is increased speed and efficiency. As has been well documented, in a conventional setting, drug discovery programs operate with a "design–make–test–analyze" based cycle, with the speed at which a team can move through each iterative sequence often being defined as a quantitative measure of project progress (Figure 4.1) [6]. Whereas, clearly, the situation is not as straightforward as this, one can distill out the baseline fact that the "faster one can synthesize-relevant drug-like compounds" is likely to determine a go/no-go decision for a specific project. With this statement, it is important to also highlight the importance of a team reaching a "no-go" decision. While clearly not

Flow and Microreactor Technology in Medicinal Chemistry, First Edition. Edited by Esther Alza.
© 2022 WILEY-VCH GmbH. Published 2022 by WILEY-VCH GmbH.

https://www.twirpx.org & http://chemistry-chemists.com

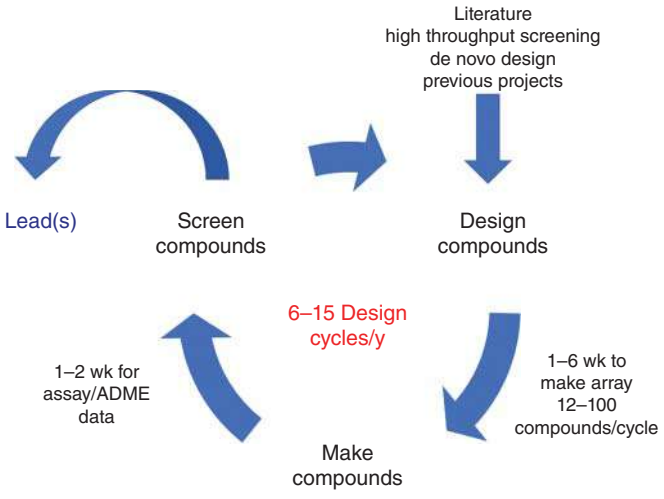

Figure 4.1 Conventional "design–make–test–analyze" drug discovery cycle. Source: Based on Ref. [6].

the optimal outcome, given the established high costs associated with drug discovery in general, being able to rapidly reach a judicious decision regarding a program long-term feasibility for success prior to it progressing to development (or the clinic) represents an opportunity to dedicate resources (time/cost) elsewhere.

The intention of the current review is to take a slightly different perspective on the application of flow chemistry technologies within medicinal chemistry and place a more narrow focus on how solutions have been developed in this space toward a specific problem, namely, the synthesis of imatinib and related Bcr-Abl inhibitors. Hopefully from the work described, the reader will note that there is not only an array of flow-based techniques to evaluate and solve a problem but also that a significant amount of development/optimization work often has to be invested to identify a successful path forward. It is the latter point that perhaps presents the greatest barrier to wider uptake of flow within medicinal chemistry. Several different approaches to the synthesis of imatinib are presented, namely, those from the laboratories of Ley, Buchwald, and Jamison. One thing to note here is that all feature a critical dependence on Pd-mediated couplings to assemble the target molecule and highlight the challenges inherent in executing this chemistry in a continuous manner. It is instructive to see how each of the case studies provides a different approach to overcoming this, and these can provide guidance for future practitioners in developing strategies to carry out these highly prevalent Pd-mediated (and related) couplings in their own laboratories. The "hybrid" flow/batch approach to imatinib shifts focus to another common problem encountered when investigating synthetic routes to pharmaceutically relevant molecules in flow specifically the insolubility of many of the intermediates encountered [7]. Finally, a more aspirational approach to drug discovery is describe notably a "closed-loop" discovery platform followed by its application to the discovery of next-generation Bcr-Abl kinase inhibitors.

https://www.twirpx.org & http://chemistry-chemists.com

Despite the challenges, there is no doubt that there will continue to be an uptake of flow chemistry within medicinal chemistry laboratories most notably owing to the next generation of scientists emerging from academic laboratories having a greater appreciation for the concepts and skills required in this space [8]. In addition, while flow hydrogenation has enjoyed uptake based on the ability to safely execute this chemistry in a discovery setting, there is growing recognition that for methodologies growing in use such as photoredox transformations that flow may present the most viable method to successfully scale such chemistries [9]. It is hoped that the work presented herein will highlight both the creativity and flexibility in which solutions applicable to successfully carry out the desired chemistry can be implemented in a practical manner.

4.2 Discovery of Imatinib

When considering the utility of flow methods to access active pharmaceutical ingredients (APIs) and their analogs, it is of value to study the development of such syntheses and compare/contrast the advantages and disadvantages with the reported conventional batch-based approaches. In addition, herein looking at four flow-based approaches enables us to see how different solutions can be employed through rapid developments in this technology to overcome key issues presented by flow chemistry. These studies not only provide an insight into how to develop multistep flow syntheses and the planning behind them but also highlight how novel synthetic disconnections can be enabled that would be challenging to execute under batch conditions.

Imatinib is a Bcr-Abl tyrosine kinase inhibitor launched by Novartis in 2001 for the treatment of chronic myeloid leukemia (CML) and gastrointestinal stromal tumors (GIST) and is produced under the brand name Gleevec (USA) and Glivec (Europe, Australia, and Latin America) as the mesylate salt. Bcr-Abl kinase has been shown to induce leukemia in mice and is produced by a chromosomal translocation known as the Philadelphia chromosome. Being implicated as a cause of CML, the kinase is unable to self-regulate as a result of fusion of the Bcr domain to the protein, and as such the undesired signaling path is permanently turned "on," thus promoting progression of disease. Since its initial report, imatinib has represented a popular target for synthetic chemists, though herein we will consider only four reported flow-based approaches as well as the commercial route to the API [10].

Given the remarkable efficacy observed in clinical trials, the expeditious progression of imatinib through development led to an urgent need to generate a suitable process for the APIs commercial manufacture. This led to an overall 12-step synthesis featuring formation of the pyrimidine **5** through condensation of the appropriate guanidine **4** with the 3-dimethylaminoenone **2** as a key step. Nitro-group reduction and amide bond formation with the functionalized acid chloride followed by salt formation led to the desired mesylate salt as the required final form of imatinib **8** (Scheme 4.1). This commercial route is very similar to that initially reported by medicinal chemistry for imatinib with exploration of analogs

https://www.twirpx.org & http://chemistry-chemists.com

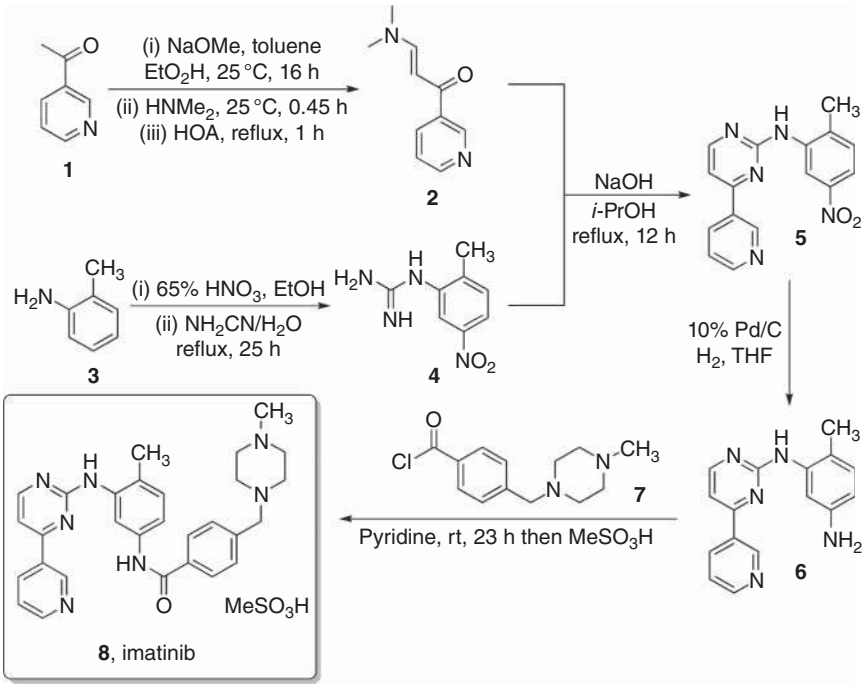

Scheme 4.1 Commercial synthesis of imatinib.

relaying on the availability (or ease of access) of the acetyl-substituted heterocycles and substituted phenylguanidine derivatives [11].

4.3 Ley Flow Synthesis of Imatinib

One of the major cited barriers for the implementation of flow chemistry is the inability to handle solids. Given the reported insolubility of both the nitro- and guanidine-substituted materials utilized in many syntheses (including the commercial route) of imatinib, Ley and coworkers proposed an alternative strategy to obtain the molecule of interest (Scheme 4.2) [12]. Notably, this approach effectively reverses the steps involved, avoiding a potentially hazardous nitration reaction (though this may be somewhat surprising given the advantages offered by flow in performing such chemistries) as well as opening up diversification studies for analog synthesis through alternative pools of building block starting materials (**9**, **11**, and **12**).

The strategy implemented in developing a multistep synthesis in flow here involved breaking the route down into its constituent steps and looking to optimize each of these (in some cases initially in batch) focusing on the key elements for reactivity as well as monitoring the nature (components, purity, and concentration) of the output stream. One hallmark of the reported approach developed by Ley and coworkers is the utilization of packed columns of reagents or scavenger resins in

https://www.twirpx.org & http://chemistry-chemists.com

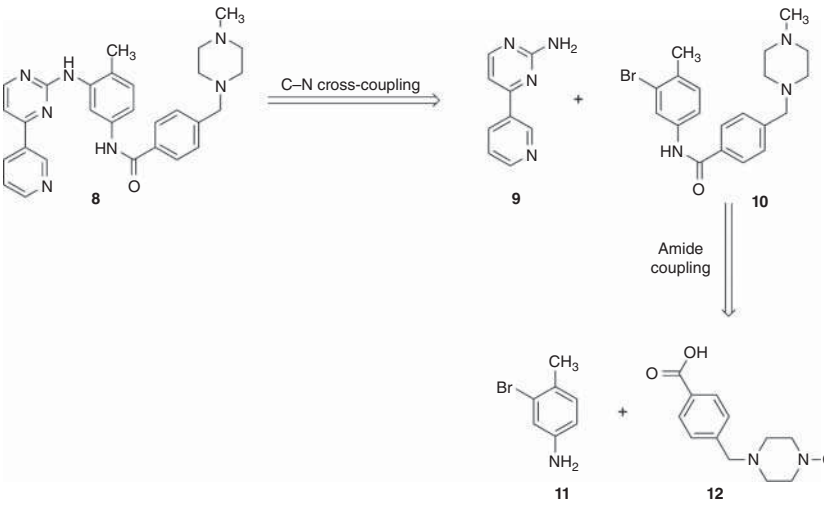

Scheme 4.2 Proposed initial disconnection for flow-based synthesis of imatinib. Source: Based on Ref. [12].

order to either mediate reactions and/or facilitate purification. Whereas this can become somewhat impractical on scale owing to the escalating costs and the need to replace (or regenerate) exhausted solid reagent cartridges, it can be an extremely useful methodology to employ on typical discovery chemistry scales. One reason that packed-bed columns are perhaps underutilized in flow in drug discovery laboratories could be the limited understanding of the flow dynamics/diffusion of reactants through the column, which is a topic that is addressed well in this imatinib work. However, this also highlights a broader barrier to wider implementation of flow by conventional chemists in a somewhat limited grounding in the principles of chemical engineering. Successful examples of use of continuous processing in the pharmaceutical industry have consistently demonstrated the critical synergy between chemists and engineers to generate innovative solutions to deliver an optimal solution.

The initial proposed step involves amide bond formation between the aniline **11** and the carboxylic acid **12** (formed from chloride displacement of 4-(chloromethyl)benzoic acid) with methyl-piperazine (Scheme 4.3). Previous work had demonstrated that amide bond formation could be achieved by initial activation of the acid by passing a *N*,*N*-dimethylformamide (DMF)-solution of this combined with PyBrOP and Hunig's base through a packed column of PS-HOBt (polymer-supported) resin [13]. Subsequent reaction of the generated supported active ester with the amine would then lead to the desired amide.

Implementation though of this protocol with the functionalized acid and 3-bromo-4-methyl-aniline **11** led to only ~5% conversion of the desired amide despite an excess of the acid being used to ensure saturation of the PS-HOBt column. Replacing the amine with allylamine (**14**) to probe whether poor nucleophilicity might be the reason for the low conversion only gave a minor

https://www.twirpx.org & http://chemistry-chemists.com

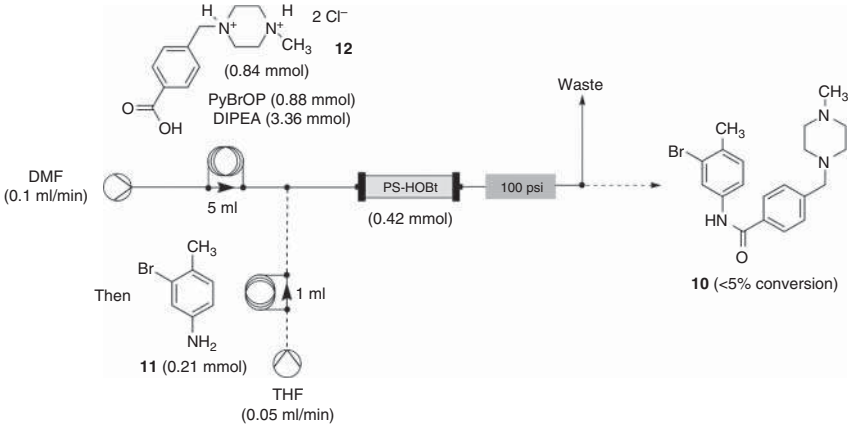

Scheme 4.3 Initial attempt at amide bond formation through acid activation.

improvement (~15%) to the reaction output, leading to the hypothesis that the basicity of the *N*-methylpiperazine might be the pivotal issue here. Coupling of the 4-(chloromethyl)benzoic acid **13** with allylamine **14** under these conditions led to a significantly improved 55% yield of the amide **15**, though reverting to the "real" aniline substrate only provided ~20% conversion, suggesting that relative nucleophilicity combined possibly with reduce reactivity of immobilized reagents – a key point that is often overlooked – was an issue (Scheme 4.4).

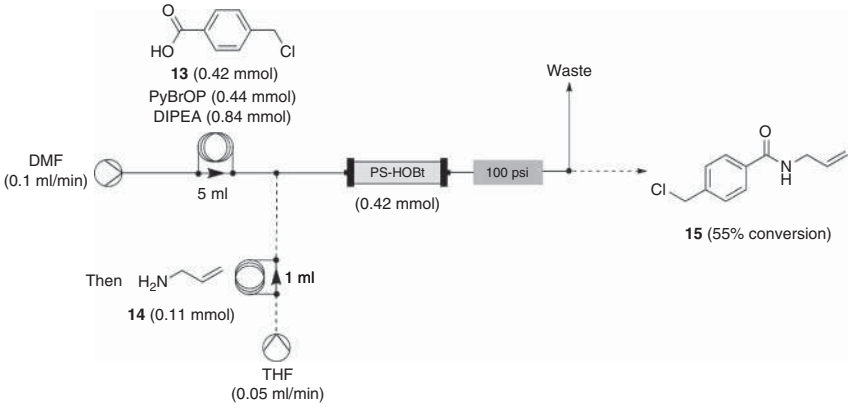

Scheme 4.4 Probing the effect of amine nucleophilicity on the amide bond formation.

An alternative approach was investigated based on coupling of the acid chloride with the aniline compound (Scheme 4.5). 4-(Chloromethyl)benzoyl chloride **16** is commercially available and presents a better solubility profile than the corresponding acid. Whereas acid chloride/amine coupling in batch is relatively straightforward, the corresponding reaction in flow presents challenges specifically with precipitation of *in situ* generated hydrochloride salts representing a concern.

https://www.twirpx.org & http://chemistry-chemists.com

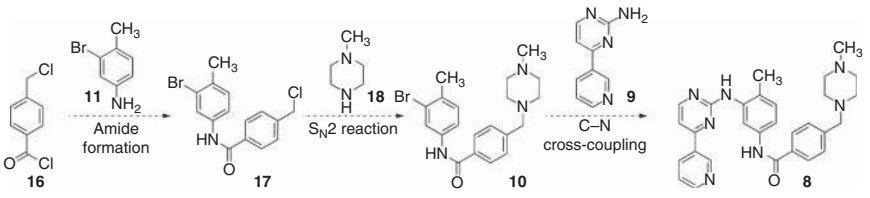

Scheme 4.5 Revised retrosynthesis with later introduction of the *N*-methylpiperazine fragment.

Screening of base/solvents in batch rapidly revealed that a soluble base was likely to be necessary, as without one, rapid precipitation of the aniline salt of **11** occurred, while the use of a solid-supported base (QP-DMA – polymer-supported dimethyl amine) led to formation of the DMF as a significant by-product. With soluble tertiary amine bases, solvent selection was also a key factor based now on the tendency of the amide product precipitating from solution. The use of *N*,*N*-diisopropylethylamine (DIPEA) in dichloromethane (methylene chloride) (DCM) proved to be a suitable combination for translation to flow with the reactor output monitored by both in-line UV and liquid chromatography (LC)–mass spectrometry (MS). Removal of the DIPEA hydrochloride by-product was achieved by passage through a single-scavenging column containing both PS-DMA (to trap HCl) and PS-SO_3H (to trap the free DIPEA). Evaluating the complete flow setup led to isolation of the amide **17** in 67% yield (>95% purity) (Scheme 4.6). Yield loss is caused by chromatographic effects of the immobilized reagents, while an elution time of 35 minutes (monitored by UV compared with the expected theoretical time of 25 minutes) is attributed to increased dispersion due to diffusion/mixing occurring to a larger extent as the reaction passes through a column of polymer-supported reagents.

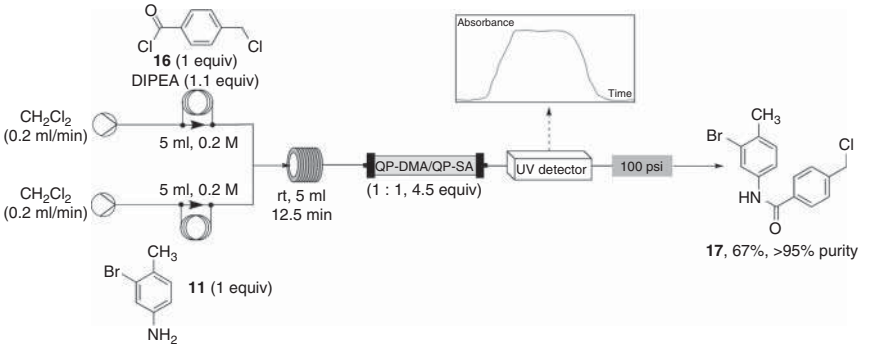

Scheme 4.6 Amide bond formation utilizing the acid chloride as starting material.

Ideally, the flow stream with DCM as the solvent would be taken directly into the next step, which is planned to be the displacement of the benzylic chloride with *N*-methylpiperazine (**18**), with the excess nucleophile then being trapped with a polymer-supported electrophile. Testing this reaction in batch demonstrated that

https://www.twirpx.org & http://chemistry-chemists.com

the desired product precipitated from DCM, thus leading to the investigation into identifying a suitable cosolvent. The utilization of DMF proved to be effective with control of the stoichiometry of the nucleophile important to ensure a reaction rate suitable for translation to flow and balancing this with the need to avoid a large excess in order to minimize the amount of scavenging resin required to treat the outlet stream (Scheme 4.7).

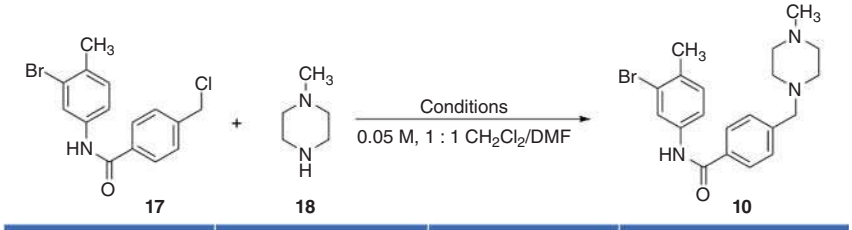

Amine equivalents	Temperature (°C)	Time (h)	Conversion (%)
1.5	100	1.5	70
2	120	0.5	80
3	120	0.5	95

Scheme 4.7 Batch optimization on *N*-methylpiperazine displacement reaction.

Translation to flow using 1 : 1 DMF/DCM as the solvent system not only provided guidance on the impact of concentration, temperature, and residence time on the conversion but also showed that protonation of both product **10** and *N*-methylpiperazine **18** by the HCl generated was inhibiting the overall reaction, suggesting that the use of a solid-supported base might be beneficial (Scheme 4.8). Challenges herein revealed with PS-carbonate leading to hydrolysis of the halide lead to the corresponding alcohol, though PS-TBD or PS-BEMP could be used with the former proving to be the reagent of choice (Scheme 4.9).

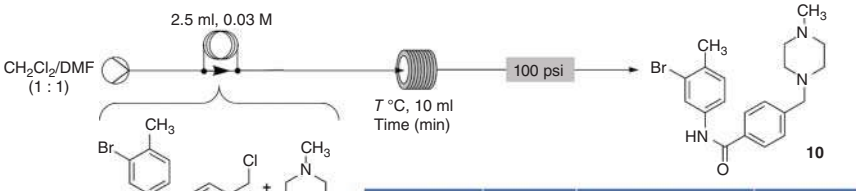

Flow (ml/min)	Temp (°C)	Residence time (min)	Conversion
0.3	120	33	62
0.3	130	33	61
0.15	120	67	68
0.15	130	67	71

Scheme 4.8 Translation of displacement reaction from batch to flow.

The excess *N*-methylpiperazine **18** was removed using the macroporous resin version of polymer-supported isocyanate with the desired product then "caught" on a QP-SA column. Elution with methanolic ammonia led to the desired product **10** in

https://www.twirpx.org & http://chemistry-chemists.com

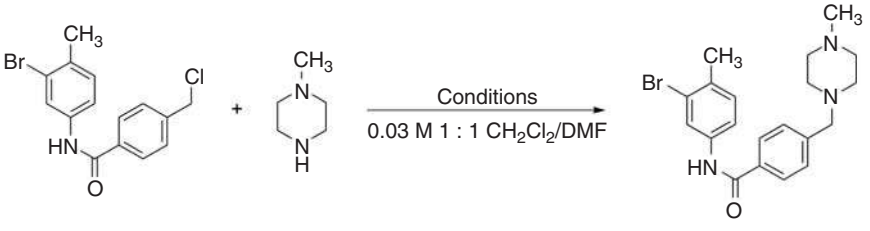

17 (1 equiv) **18** (2 equiv) **10**

Base	Equivalents	Temperature (°C)	Time (h)	Conversion (%)
PS-BEMP	2	100	0.5	SM + product
PS-CO_3	2	60	0.5	67 (13 alcohol)
PS-CO_3	2	60	1	76 (14 alcohol)
PS-TBD	1	60	0.5	68
PS-TBD	1	100	0.5	79
PS-TBD	2	60	0.5	88
PS-TBD	2	80	0.5	94
PS-TBD	2	80	1	97

Scheme 4.9 Base/condition screening for the displacement reaction.

56% yield (lower than expected due to incomplete elution of the resin) and >95% purity (Scheme 4.10). While PS-TBD represents a short-term solution, the resin is relatively expensive, and, thus, this was replaced with powdered K_2CO_3. This is only sparingly soluble in the reaction solvent system and being inexpensive can be used in large excess enabling an increased retention time to be employed to drive the reaction to completion (Scheme 4.11).

While both steps have been optimized in a discrete manner, combining them in a single flow process presents challenges most notably with how to introduce the *N*-methylpiperazine reagent **18** in a consistent manner while enabling an "in-line" solvent switch. An initial strategy to accomplish this was to UV-trigger collection of the product output from the amidation step into a DMF-solution of *N*-methylpiperazine (**18**) to provide a homogeneous solution of known concentration ready for injection into the next reactor. This approach was subsequently tested, though led variable conversions in the displacement reaction demonstrate a critical dependence of this step on the overall concentration (Scheme 4.12). A specific issue herein was believed to be the dispersion in the scavenging process after the amidation leading to a limitation in terms of the concentration of the output stream that can be achieved, thus impacting the subsequent step.

To mitigate this issue, an alternative method for the synthesis of the amide **17** was investigated, though initial loading of the acid chloride **16** onto PS-DMAP with elution of the desired product was achieved through reaction with the aniline **11** (Scheme 4.13). Control of the solution of the latter was critical with higher concentrations (0.5 M), leading to crystallization of the amide within the flow system. While lower concentrations of the aniline resulted in the desired amide formation, this was

https://www.twirpx.org & http://chemistry-chemists.com

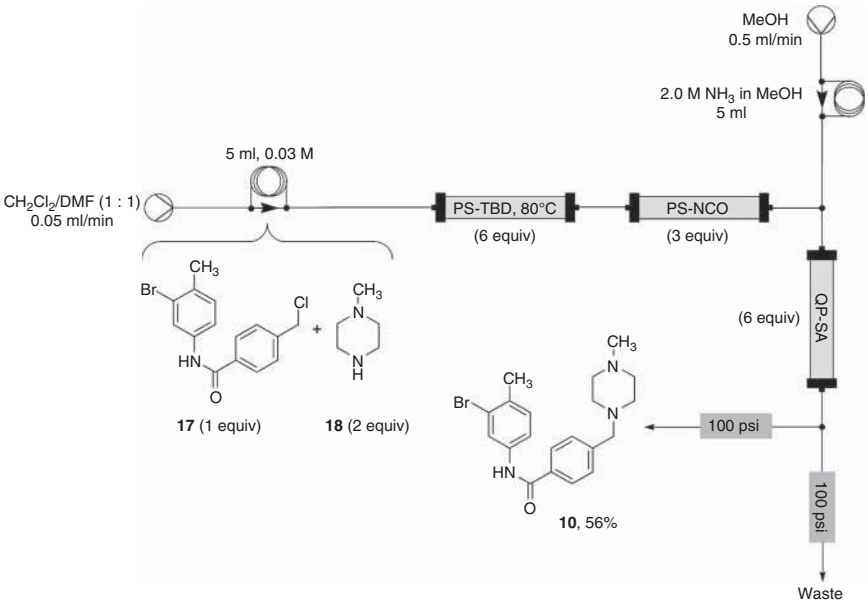

Scheme 4.10 Displacement reaction with integration of "catch–release" purification.

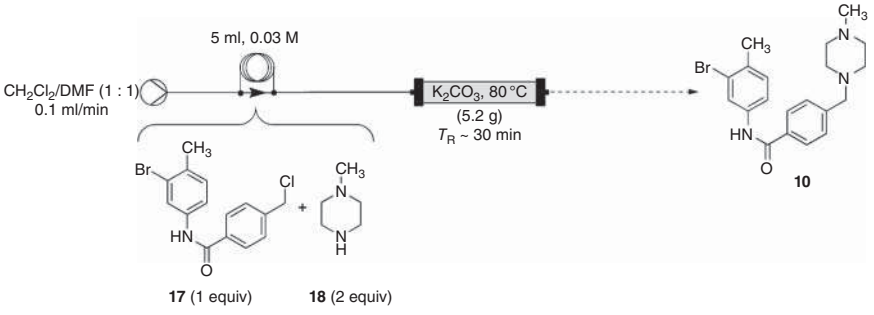

Scheme 4.11 Switching to K_2CO_3 as a cheaper, solid inorganic base for displacement chemistry.

contaminated by the corresponding carboxylic acid (from hydrolysis of the acid chloride presumably caused by residual water within the resin), though this could be efficiently scavenged using a cartridge filled with QP-DMA, leading to the amide **10** in 78% yield (~95% purity) after removal of the solvent. After elution from the reaction, the product monitored through UV was collected in a fraction collector prior to dilution with DMF. Addition of *N*-methylpiperazine **18** was then carried out with the reaction mixture and then passed through a column of K_2CO_3 at 80 °C. With a 2 : 1 mixture of DCM to DMF, a 62% conversion was recorded compared with 80% (1 : 1 DCM/DMF) and 95% in neat DMF, indicating that the presence of DCM was inhibiting the reaction. In addition, a co-eluting carbamate by-product was observed resulting from the K_2CO_3 acting as a CO_2 source.

https://www.twirpx.org & http://chemistry-chemists.com

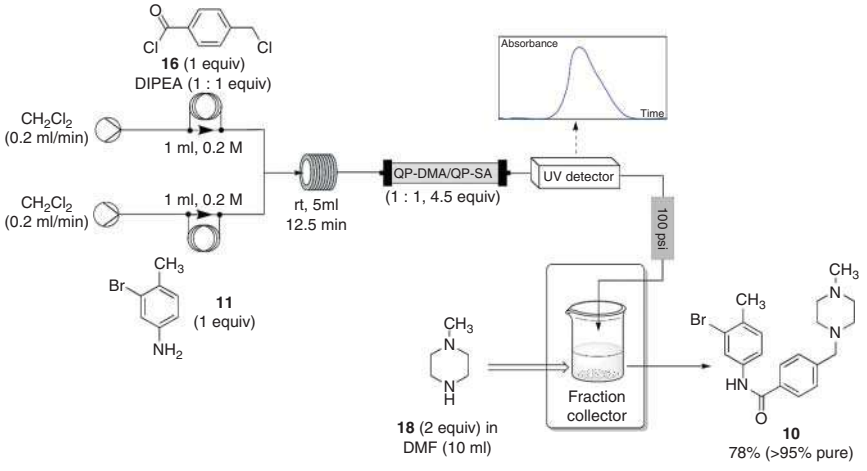

Scheme 4.12 Combination of amide bond formation/displacement in continuous flow.

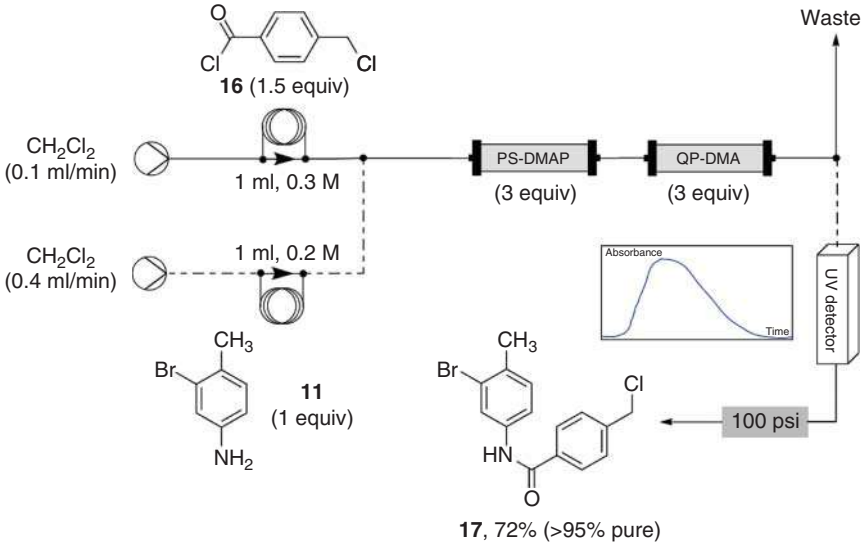

Scheme 4.13 Re-evaluation of amide bond formation to minimize issues with dispersion.

These pilot studies highlighted the need to identify an alternative suitable base to mediate the reaction while also implementing a complete solvent switch between reaction steps. For the former, $CaCO_3$ was tested based on the hypothesis that being less soluble in adventitious water, it would be less likely to liberate the CO_2 required for the carbamate formation. Testing the displacement led to a 95% conversion without any by-product formation.

A facile innovative solution was developed to carry out the solvent switch taking advantage of the fact that DCM is significantly more volatile than DMF. This entailed collection of the output stream from the amidation reaction into a vial,

https://www.twirpx.org & http://chemistry-chemists.com

which already contained a DMF-solution of *N*-methylpiperazine **18**, capped with a rubber septum and venting tube on a hot plate. Passing a stream of nitrogen through this vial expedited the evaporation of DCM, enabling the preparation of a solution ready for the displacement reaction. Another issue that was noted in the first-generation approach to this step was the "slow diffusion" of the product from the "catch and release" purification of the sulfonic acid-based resin. To address this, a switch was made to evaluate a similar purification strategy through using a sulfonic acid-functionalized silica, which features smaller particles with the acid moieties on the surface, thus presenting an enhanced surface area for faster scavenging and release with the desired outcome being a more concentrated "slug" of material being obtained for the next step (Scheme 4.14).

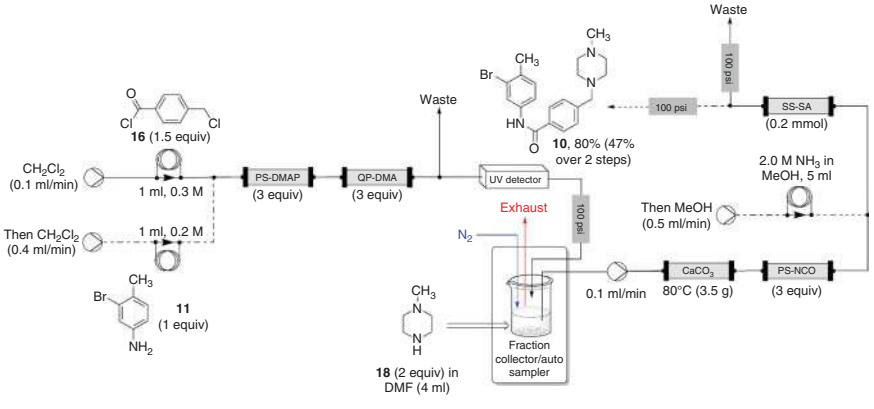

Scheme 4.14 Modified amide bond formation/displacement reaction in flow.

Optimization of the stoichiometries of both the *N*-methylpiperazine **18** and the PS-NCO scavenging resin was carried out utilizing the projected yield/output from the amidation step with the desired product **10** obtained in 47% yield (>95% purity) after the coupling of the two flow steps. This yield reflects an 80% yield for the displacement (cf. 56% using PS-TBD), while a visual change was noted with the silica-supported sulfonic acid column, allowing the progress of the reaction to be monitored.

The prevalence of Pd-mediated couplings within the pharmaceutical industry makes this a prominent research area for performing and optimizing such processes in a flow paradigm [14]. One of the chief challenges to enabling the Buchwald–Hartwig reaction under evaluation herein is that this Pd-mediated process is typically carried out in nonpolar solvents, leading to potential solubility concerns for cases involving pharmaceutically relevant substrates such as this. Inspired by the previous work on the synthesis of nilotinib (**20**), a solvent mixture of 1,4-dioxane/*t*-AmOH (2 : 1) was evaluated, while Xantphos was chosen as the ligand owing to its previous application in this synthesis (Scheme 4.15).

Selection of the base also proved to be critical for this transformation with optimization screening carried out in batch using microwave irradiation to balance reactivity with solubility concerns (Scheme 4.16). While both NaO*t*Bu and Cs_2CO_3 were

https://www.twirpx.org & http://chemistry-chemists.com

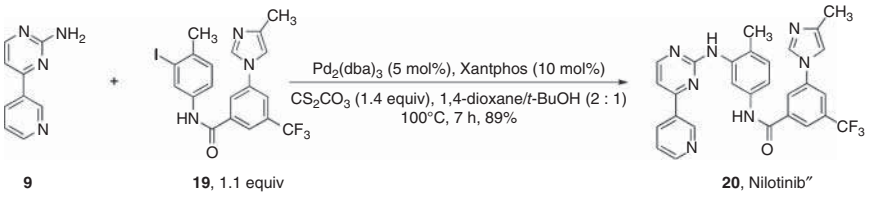

9 **19**, 1.1 equiv **20**, Nilotinib″

Scheme 4.15 Buchwald–Hartwig coupling in the synthesis of nilotinib.

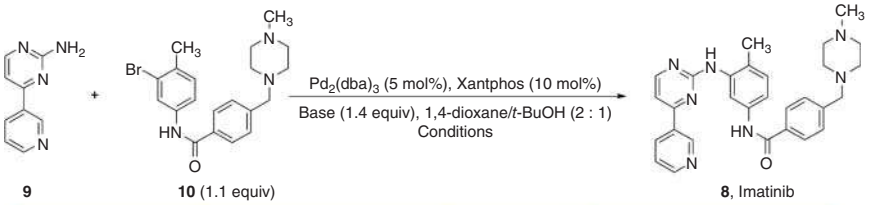

9 **10** (1.1 equiv) **8**, Imatinib

Base	Temperature (°C)	Time (h)	Conversion (%)
NaO*t*-Bu	100	1	40
NaO*t*-Bu	120	0.5	60
NaO*t*-Bu	150	0.5	100 (57 yield)
Na_2CO_3	100	1	0
K_2CO_3	100	1	0
NaO*t*-Bu	100	1	0
Cs_2CO_3	100	1	<10
Cs_2CO_3	120	1	<10
Cs_2CO_3	140	1	60
Cs_2CO_3	150	1	70
Cs_2CO_3	150	2	95
K_3PO_4	150	1	0

Scheme 4.16 Base/condition screening for Buchwald–Hartwig coupling.

shown to be effective, the former led to issues with precipitation of NaBr and the formation of Pd black as the reaction progressed. However, though effective, challenges remain in transitioning the use of Cs_2CO_3 to a flow paradigm for the reaction specifically with the goal of achieving a long enough residence time using a packed column of the base to ensure high conversion to the desired product **8**. While the use of the base with a Celite packing material to enable a larger column volume to be achieved coupled with a low flow rate of 0.05 ml/min led to a residence time of 30 minutes and a corresponding conversion of 60% (Scheme 4.17), these results were somewhat capricious, leading to an alternate solution being sought. Evaluating an excess of K_2CO_3 did lead to an increase in residence time though led only to the protodehalogenated material being obtained from the reaction.

https://www.twirpx.org & http://chemistry-chemists.com

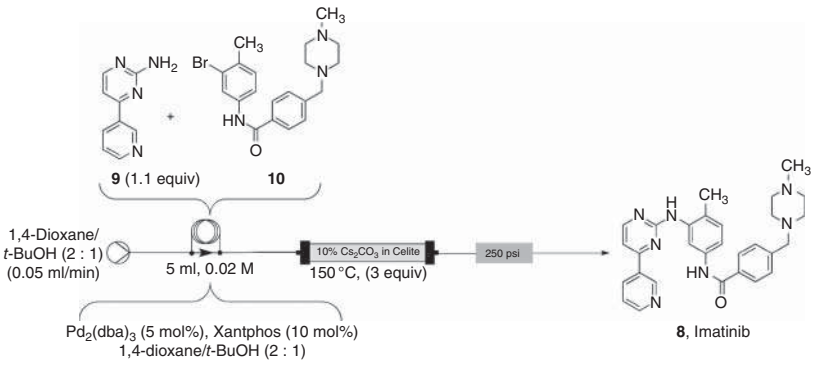

Scheme 4.17 Flow-based Buchwald–Hartwig coupling mediated by a solid base.

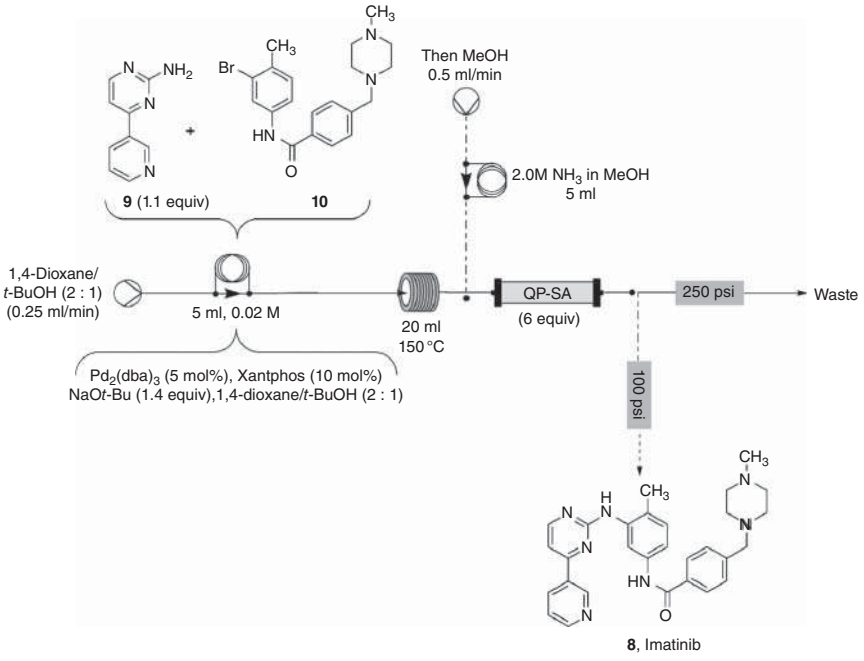

Scheme 4.18 Modified C—N coupling using a soluble base.

In light of these issues, the use of NaO*t*Bu as the base for the reaction was revisited with the initial studies focusing on lowering the reaction concentration to ensure solubility of the base with the formed product being envisioned to be trapped on an in-line PS sulfonic acid column after reaction for subsequent release (Scheme 4.18). On initial testing of this scenario, buildup of Pd black was observed, and although complete conversion could be achieved through increasing the amount of Pd catalysts (10–20%), this exacerbated the precipitation issue leading to eventual blockage of the flow reactor.

Given the propensity of reported Pd-ligand systems able to mediate Buchwald–Hartwig and related cross-couplings, an alternative strategy was adopted to prevent

https://www.twirpx.org & http://chemistry-chemists.com

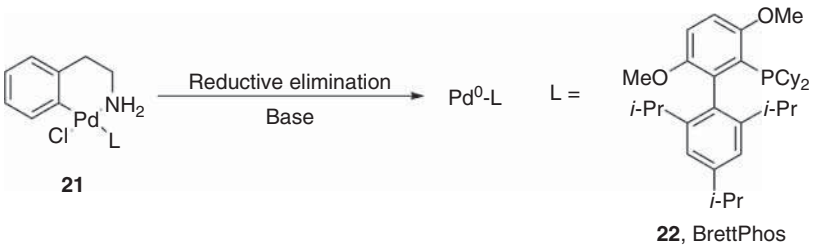

Scheme 4.19 Advantages of a Pd(II)-precatalyst complex.

Pd black formation from catalyst decomposition. To this end, the use of an air-stable Pd(II)-precatalyst complex was explored for *in situ* generation of an active Pd(0) species with minimal decomposition (Scheme 4.19). The precatalyst derived from BrettPhos **22** was employed in the reaction mixture, and although a totally homogeneous solution was not obtained, sonication fragmented the larger particles providing a mixture suitable for injection. While precipitation was observed rapidly within the reaction coil, this was still a relatively free-flowing suspension containing a "fine" colorless solid attributed to NaBr with dilution with an aqueous stream post-reactor employed to dissolve this, thus preventing buildup and blockage of the QP-SA (sulfonic acid) "catch and release" column. Analysis of the output after this "in-line purification" demonstrated that this was composed of both starting materials (**9** and **10**), imatinib (**8**), and the protodehalogenated side product with a 61% theoretical yield of desired being projected based on the mass of the output (Scheme 4.20).

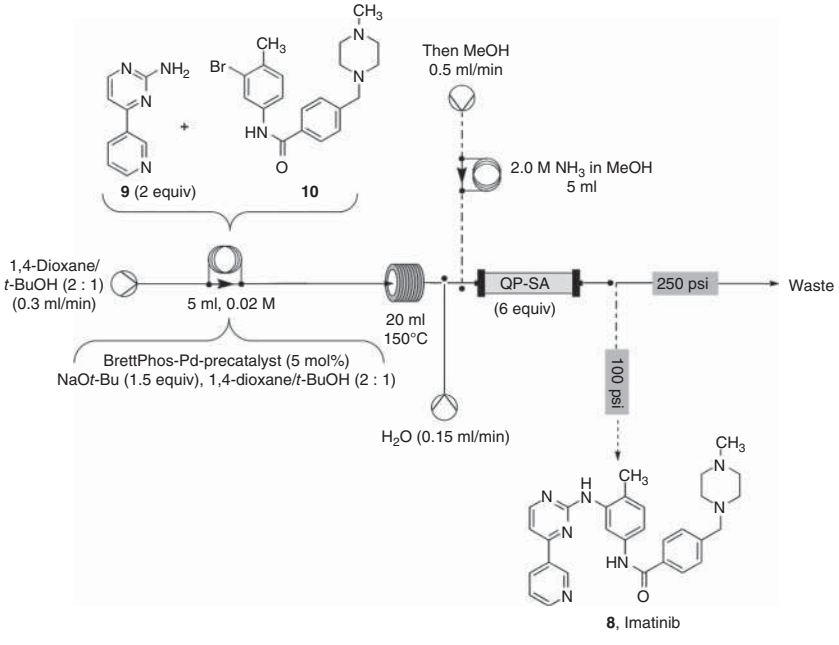

Scheme 4.20 Flow synthesis using a Pd(II)-precatalyst to mediate the reaction.

https://www.twirpx.org & http://chemistry-chemists.com

The purification of this mixture is exceptionally challenging using scavenger resins particularly given the chemical similarity of the starting halide **10**, the protodehalogenated material, and the desired imatinib **8**. It was thought that the primary amine based starting material **9** could be effectively scavenged using a supported electrophile, though issues were encountered either through lack of reactivity or the desired product also being sequestered onto the resin. A second approach was investigated to trap the basic components of the product stream on acidic resins and then modulate the basicity of the eluent stream to selectively release each component sequentially, though this proved to be unsuccessful leading to conventional chromatography being chosen as the preferred option for product purification.

The final challenge to achieve the flow synthesis of imatinib **8** was to couple the previously described amidation/displacement sequence with the Buchwald–Hartwig coupling. Optimally, the use of the NaO*t*Bu base required for the Pd-catalyzed coupling would be utilized to directly elute the intermediate **10** (from the initial two steps) off the acid resin using the desired 1,4-dioxane/*t*-BuOH (2 : 1) solvent system, though attempts to achieve this led to blockage of the column frits. To address this, 1,8-Diazabicyclo[5.4.0]undec-7-ene (DBU) was utilized as the base for the "catch and release" given that it is a stronger base than *N*-methylpiperazine **18** with a separate experiment conducted to demonstrate that incorporation of DBU had a negligible impact on the Buchwald–Hartwig reaction. The optimal way to achieve the coupling in flow consisted of releasing the intermediate with DBU into a stream containing the primary amine, Pd catalyst, and NaO*t*Bu with both mobile phases in 1,4-dioxane/*t*-BuOH combined before passing through a heated coil at 150 °C. DBU was demonstrated to quantitatively elute the intermediate **10** from the sulfonic acid column in a controlled manner, thus ensuring a consistent stoichiometry for the subsequent coupling reaction. Combination of reagents was achieved using a T-piece connector with dilution with water performed after reaction. Evaporation of the output led to a residue that after column chromatography led to imatinib **8** being isolated in 32% overall yield from the three-step process (Scheme 4.21).

While this yield is lower than that for the batch process, the ability to carry out the synthesis in a single-flow procedure with only one manual purification represents advantages in terms of resources and efficiency especially in order to access analogs. Within this study, 10 further compounds (of 11 attempted) were prepared using the flow protocol, highlighting the versatility of this methodology through variations of the aniline in the amide bond formation, the secondary amine in the displacement, and the primary amine using in the Buchwald–Hartwig reaction (Scheme 4.22). All the analogs were formed in a single procedure with purification achieved again through silica gel chromatography though after an aqueous workup to remove the salts in order to enable a more efficient separation. The stoichiometry of reagents for the benzylic chloride displacement were based on an 80% estimated yield for the amide bond formation with the only failed analog featuring imidazole as the amine component (**24**) in this reaction, which not only gave a poor conversion presumably due to the reduced nucleophilicity of the heterocycle but also was not effectively "trapped" on the acidic column. The amount of DBU was varied to

https://www.twirpx.org & http://chemistry-chemists.com

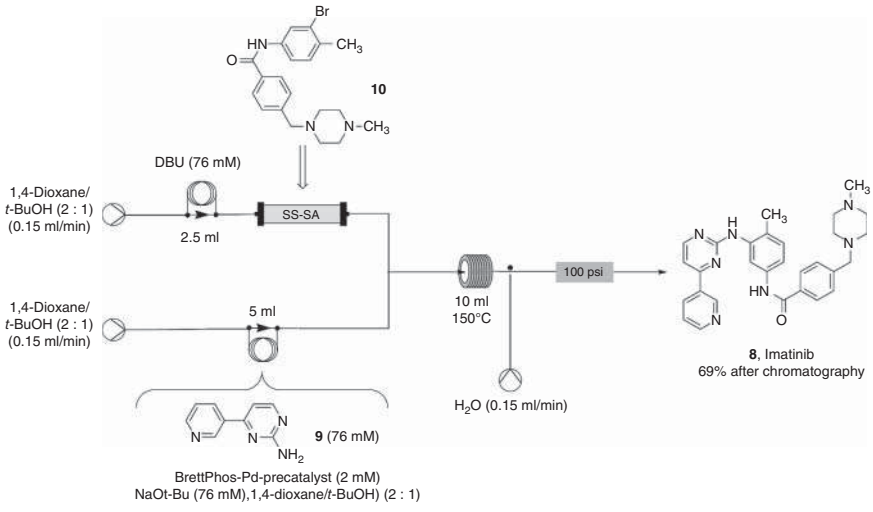

Scheme 4.21 Optimized C–N coupling for the synthesis of imatinib.

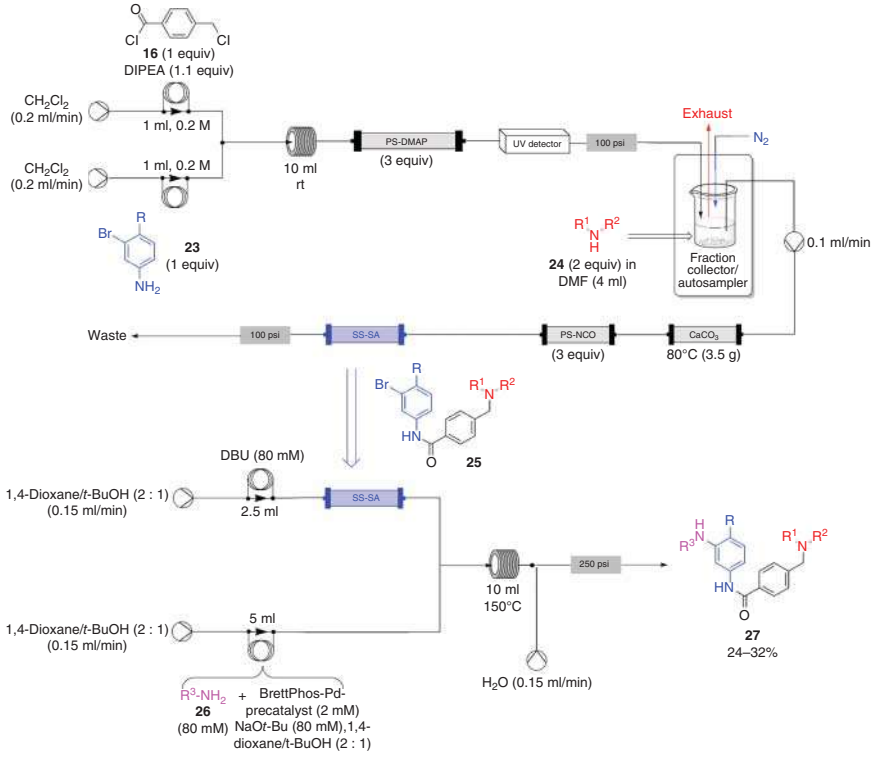

Scheme 4.22 Integrated flow synthesis of imatinib analogs.

https://www.twirpx.org & http://chemistry-chemists.com

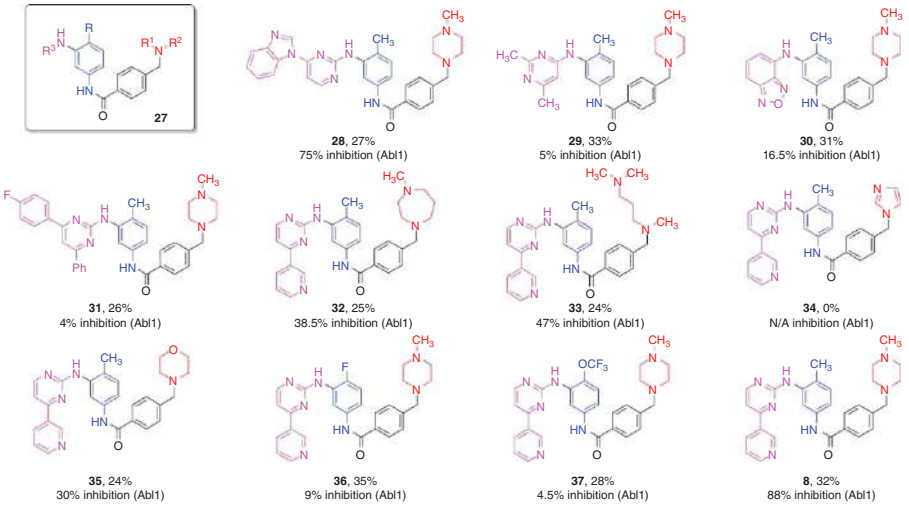

Figure 4.2 Structural variations of imatinib analogs synthesized in flow.

https://www.twirpx.org & http://chemistry-chemists.com

release the intermediates **25** depending on the loading of the silica-based sulfonic acid column, though the concentrations of the Buchwald–Hartwig coupling step remained the same.

The potency of all the new analogs (**28–37**) was evaluated in a "% inhibition" assay against Abl1 with these studies highlighting both how minor structural variations (removal of the *o*-methyl group, changes in the aminopyrimidine) lead to a dramatic loss of potency as well as the importance of the piperazine moiety for optimal receptor binding in addition to being a solubilizing group (Figure 4.2).

4.4 Buchwald Flow Synthesis of Imatinib

The Buchwald flow synthesis of imatinib follows an identical sequence in terms of bond disconnections to that reported by Ley and coworkers [12], though its origins arose from a program to develop general reaction conditions to enable efficient Pd-mediated C—N bond formations in flow [15]. Specifically herein, the work sought to address the challenges that such reactions cause in flow as noted by Ley with the formation and precipitation of intermediates and inorganic salts leads to reactor clogging, while the range of compatible solvents for such reactions generally leads to the requirement for downstream solvent switching to be carried out [16]. In addition, as we saw with the final step in the previous synthesis of imatinib, the C—N coupling leads to the formation of by-products, which in that case needed to be separated by conventional silica gel chromatography though can interfere with subsequent reactions when carried through multistep flow syntheses.

The use of amphiphilic solvents and surfactant additives in biphasic systems represents an established methodology to broker contact between organic/aqueous components of a reaction while maintaining a high local concentration of the reactants. In a similar manner to flow chemistry, this leads to more efficient mass transfer and faster reaction rates. Furthermore, such solvents are capable of enhancing the solubility of a wide range of organic compounds, thus preventing precipitation and potentially negating the need for downstream solvent switches in multistep sequences. While phase transfer catalysts have previously been evaluated and shown to significantly promote C–N cross-coupling reactions in a toluene/water-based system, the generality of this approach is still greatly limited particularly for translation to flow by substrate and product solubility (most notably for heteroaromatic systems). *N,N'*-Dimethyloctanamide **38** (DMO) has previously been used as a crystallization inhibitor as well as in crop protection formulations, and has similar Hansen solubility parameters to those reported for DCM. In addition, it is readily available as a high production volume chemical, has low solubility in water (4.3 g/l), and possesses a favorable toxicological profile comparable to many common laboratory solvents (Figure 4.3).

For the C–N coupling, model studies were carried out in flow on the reaction between aniline **39** and 4-chloroanisole **40**. Initial studies were carried out using DMO as a sole solvent to mediate the reaction using an XPhos-based precatalyst and aqueous KOH as the base. The nature of the reactor utilized was shown to be

https://www.twirpx.org & http://chemistry-chemists.com

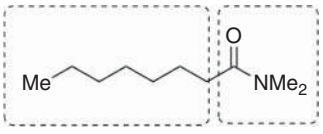

38, *N*,*N*′-dimethyloctanamide (DMO)

Figure 4.3 Structure/properties of DMO as an additive for biphasic flow reactions.

critical with only poor conversions observed when a perfluoroalkoxyalkane (PFA) tube reactor was employed, while a stainless steel packed-bed reactor apparatus was shown to lead to a significant improvement in yield (68% versus 7% at a residence time of 15 minutes), presumably due to more efficient mixing being achieved in the biphasic flow system [17]. Switching to a BrettPhos-based precatalyst led to a further improvement in yield (97%). Further optimization studies focused on employing a cosolvent with both toluene and 2-MeTHF evaluated for this purpose. These were both shown to be effective with DMO utilized as an additive (10%) with yields of >90% achieved with a residence time of 7.5 minutes while control experiments indicated the benefits of the additive with incomplete conversions being obtained in either 2-MeTHF (~80%) or toluene (~70%) after the same residence time with reactor clogging also being observed as an issue, owing to product precipitation with this exacerbated upon extending the residence time (Scheme 4.23).

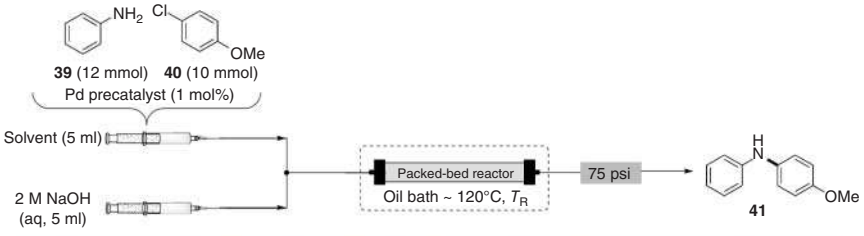

Solvent	Precatalyst	Yield (%)	Conversion (%)	T_R (min)	Notes
DMO	XPhos	7	11	15	PFA reactor
DMO	XPhos	68	74	15	
DMO	BrettPhos	97	>95	15	
Toluene/DMO (1 : 1)	BrettPhos	98	>95	7.5	
Toluene/DMO (9 : 1)	BrettPhos	95	>95	7.5	
2-MeTHF/DMO (9 : 1)	BrettPhos	93	>95	7.5	
Toluene	BrettPhos	70	71	7.5	Reactor clogging
2-MeTHF	BrettPhos	80	84	7.5	
2-(2-(Hexyloxy)ethyl)THF	BrettPhos	93	94	7.5	Reactor clogging

Scheme 4.23 Solvent/condition screening for C–N coupling using a packed-bed reactor.

Scope studies on the generality of the methodology were carried out using the toluene/DMO (10%) conditions with a range of aryl chlorides and bromides (**43**) featuring either electron-withdrawing or electron-donating substituents being effectively coupled with aniline partners (**42**) at temperatures between 100 and 120 °C and

https://www.twirpx.org & http://chemistry-chemists.com

residence times from 2 to 15 minutes. Ortho-substitution on either reaction partners was also well tolerated with primary alkyl amines also demonstrated to be suitable substrates for the reaction. With the precise control of reaction conditions, a range of base-sensitive functionalities (for example, methyl esters **45**) could also be accommodated with the scope of the electrophile component extended to aryl triflates (**49**) with only minimal hydrolysis being observed under the reaction conditions. Coupling of fenofibrate, which is used to reduce cholesterol levels, with 3-trifluoromethylaniline is provided (to give **51**) as an example to demonstrate the utility of the methodology for the late-stage functionalization of medicinally relevant compounds (Scheme 4.24).

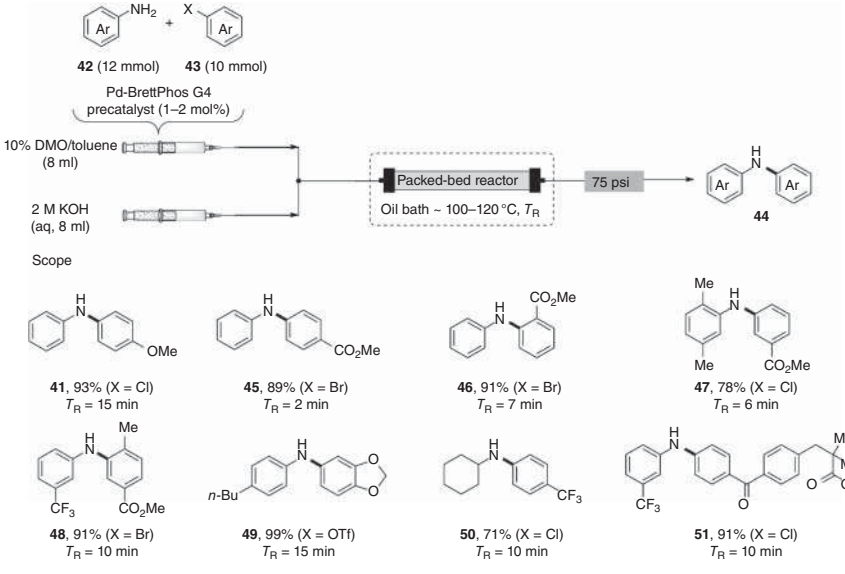

Scheme 4.24 Scope of C−N bond formation using DMO as an additive.

With the potential applicability to medicinal chemistry in mind, the scope of the methodology was extended to include heteroaromatic compounds with pyridines, thiophenes, benzothiazoles, quinolines, piperazines, and phenothiazines all being shown to smoothly couple with (hetero)aromatic or aliphatic amine partners (Scheme 4.25). Again base-sensitive groups were well tolerated under the flow conditions, with the coupling of the anti-psychotic drug chlorpromazine with 2-aminopyridine (**62**) demonstrated as proof of concept for applicability of the methodology to proven bioactive substrates.

The propensity of commercially available phenols leads to their activated derivatives such as the corresponding triflates being attractive substrates for such C–N coupling procedures, with the current protocol already being demonstrated to be effective for these compounds. However, the instability of the intermediate triflates plus the general need to prepare them prior to reaction (typically at low temperatures) make this a somewhat laborious endeavor. With this in mind, a two-step single-flow

https://www.twirpx.org & http://chemistry-chemists.com

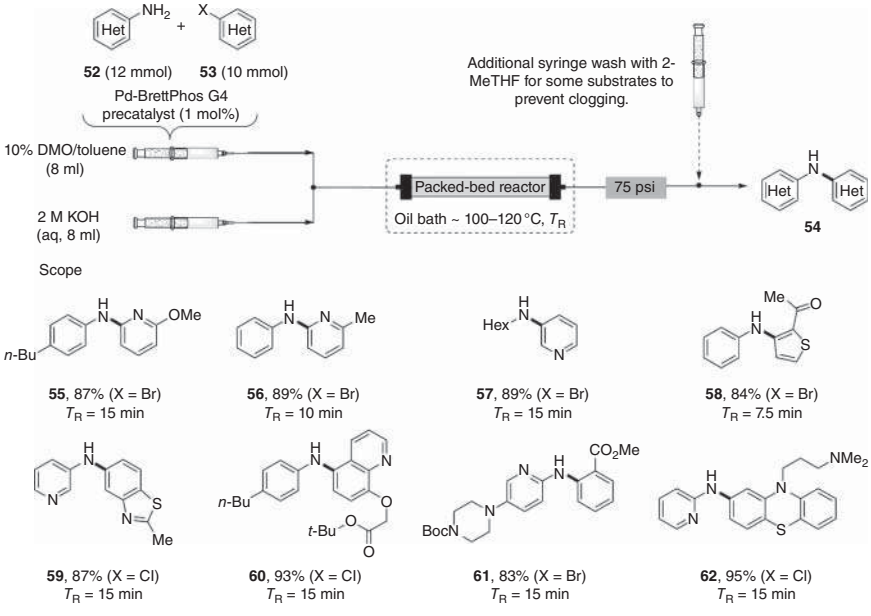

Scheme 4.25 Reaction scope utilizing heteroaromatic substrates.

sequence for the direct conversion of phenols into biarylamines was developed via the intermediacy of the aryl triflate, which is not isolated (Scheme 4.26). Similar methodology had previously been disclosed involving triflate formation followed by a Pd-catalyzed Heck reaction, though, in this case [18], an intermediate solvent switch was carried out with DCM from the triflate formation being removed by microfluidic distillation prior to being exchanged for DMF for the Heck coupling.

In the current study, the triflation was carried out in a packed-bed reactor in toluene using aqueous K_3PO_4 as the base with in contrast to the typical batch conditions no requirement for low temperatures to be employed nor a need for slow addition of the triflic anhydride to the system. For the subsequent C–N cross-coupling step, the emerging flow stream from the phenol activation was combined with solutions of the aniline/Pd precatalyst in 20% DMO/toluene and further aqueous K_3PO_4 prior to being passed through a second packed-bed reactor heated to 120 °C (Schemes 4.27 and 4.28). Excellent yields of the products were obtained over two steps with the protocol being further extended to a phenol tosylation/C–N cross-coupling sequence (Scheme 4.29).

As noted, it was then planned to incorporate this methodology into a continuous-flow synthesis of imatinib **8**. To achieve this, a similar series of bond disconnections were envisioned to those demonstrated by the Ley group though with subtle variations in the conditions utilized to obviate the need for packed solid columns either as reagents or for purification purposes. For the amidation step, 2-MeTHF solutions of the acid chloride **16** and aniline **11** were combined

https://www.twirpx.org & http://chemistry-chemists.com

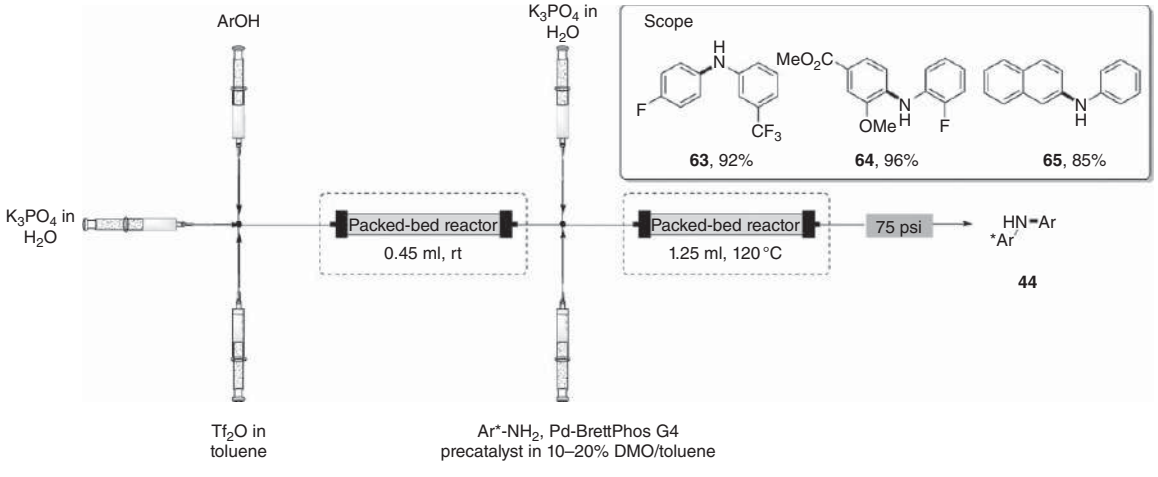

Scheme 4.26 *In situ* phenol activation for two-step flow-based C—N bond formation.

https://www.twirpx.org & http://chemistry-chemists.com

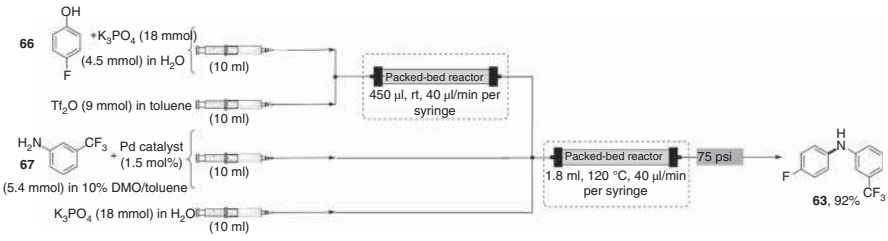

Scheme 4.27 Specific reaction configuration for the synthesis of **63**.

with aqueous KOH (excess as this will also serve as the base in subsequent steps) to give a biphasic mixture (Schotten–Baumann conditions) that was passed through a coil reactor at room temperature to give the desired amide **17** in 87% yield. For the nucleophilic substitution of the benzylic halide **17**, an aqueous solution of *N*-methylpiperazine **18** (3 equiv) was added to the system with the mixture then pumped through a packed-bed reactor at 120 °C for a residence time of ~15 minutes. For the final C–N coupling step, there are two important aspects of the flow reaction to note. The first is that the excess *N*-methylpiperazine **18** from the displacement reaction is not removed from the flow stream as it was in the Ley synthesis in which a polymer-supported isocyanate-based resin was used to achieve this. In Buchwald's approach, the high selectivity of BrettPhos (**22**) for the coupling of primary amines is exploited, thus enabling the *N*-methylpiperazine **18** to be present in the reaction mixture (Scheme 4.30).

The second issue to be addressed is the low solubility of the desired aniline coupling partner **9** in organic solvents, and in order to overcome this, the compound is introduced into the flow stream as an aqueous solution of its hydrochloride salt. To execute the coupling step, the output from the displacement reaction is injected both the BrettPhos precatalyst (5 mol% in 30% DMO/2-MeTHF) and the aqueous solution of the amine hydrochloride **9** (1 equiv) with the complete mixture then passed through a packed-bed reactor at 120 °C for a 15 minutes residence time. Workup of the output from the reaction consisted of acid/base extraction followed by trituration with acetonitrile to provide imatinib **8** in 56% overall yield (Scheme 4.31).

Although there are no syntheses of analogs of imatinib **8** reported, given that the disconnections and chemistry involved are identical to the route developed by Ley et al., it is not hard to envision that simple substitution of the various starting materials would enable the same series of compounds to be prepared particularly given the scope studies on the C–N coupling (Scheme 4.32). The second route is higher yielding and avoids intermediate purifications using supported resins, as well as in-line solvent switches. Key features to note in order to achieve this are the use of DMO (**38**) as an organic cosolvent to facilitate a biphasic reaction as well as the use of packed-bed reactors for optimal mixing efficiency. For the imatinib synthesis, the final workup and purification is also very efficient comprising of an extractive workup followed by precipitation to obtain the desired product, thus making this an attractive approach for potential scale-up.

https://www.twirpx.org & http://chemistry-chemists.com

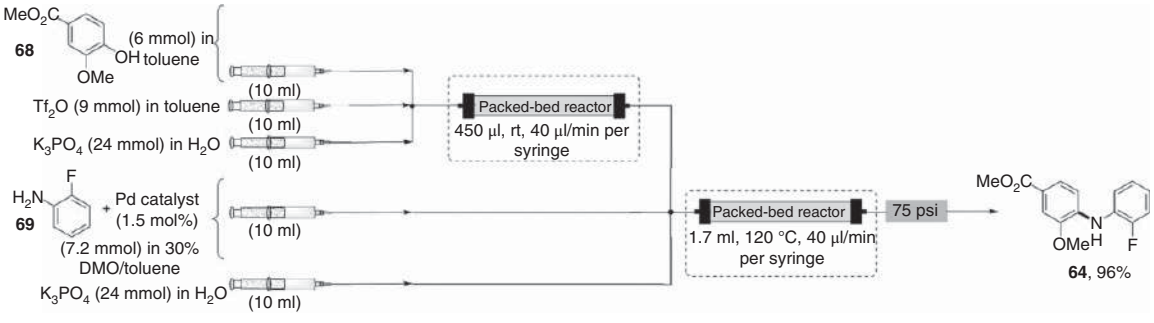

Scheme 4.28 Specific reaction configuration for the synthesis of **64**.

https://www.twirpx.org & http://chemistry-chemists.com

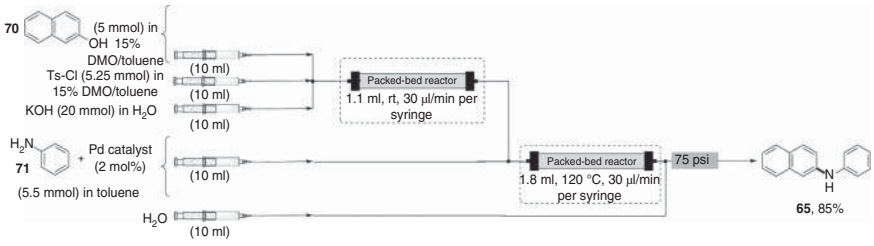

Scheme 4.29 Use of Ts-Cl for *in situ* activation of phenols in C—N bond formation.

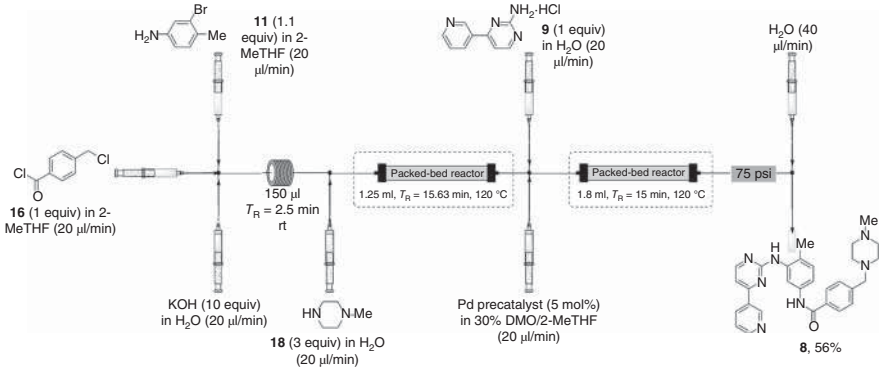

Scheme 4.30 Synthesis of imatinib in flow exploiting packed-bed reactors and DMO as an additive.

4.5 Jamison Flow Synthesis of Imatinib

Whereas the two previously reported approaches to imatinib have enabled access to the API and in the case of the Ley synthesis, a series of analogs, there still remains a potential issue with regard to a limited variation in terms of the substitution patterns available of the functionalized substrates used, thus restricting the structural diversity of related analogs that can be accessed. To alleviate this, Fu and Jamison developed an alternative retrosynthetic approach allowing the synthesis of imatinib and a series of structural analogs, though starting from differently functionalized building blocks of which a wide variety are reported to be available [19]. Specifically, the proposed synthesis involves initial hydration of an aryl nitrile **72** to form the intermediate primary amide **73**, which is proposed to undergo Pd-mediated selective C–N coupling with a dihalobenzene derivative **74**. This intermediate then undergoes a second Pd-mediated C–N coupling with an aminopyrimidine **9** to afford imatinib **8** (and its analogs). This approach taps into the pool of both aryl halides and nitriles as starting materials, which are inexpensive and broadly available, while avoiding issues with the handling of the moisture-sensitive acid chloride as well as the functionalized aniline through formation of the amide through an alternative reaction paradigm (Scheme 4.33).

https://www.twirpx.org & http://chemistry-chemists.com

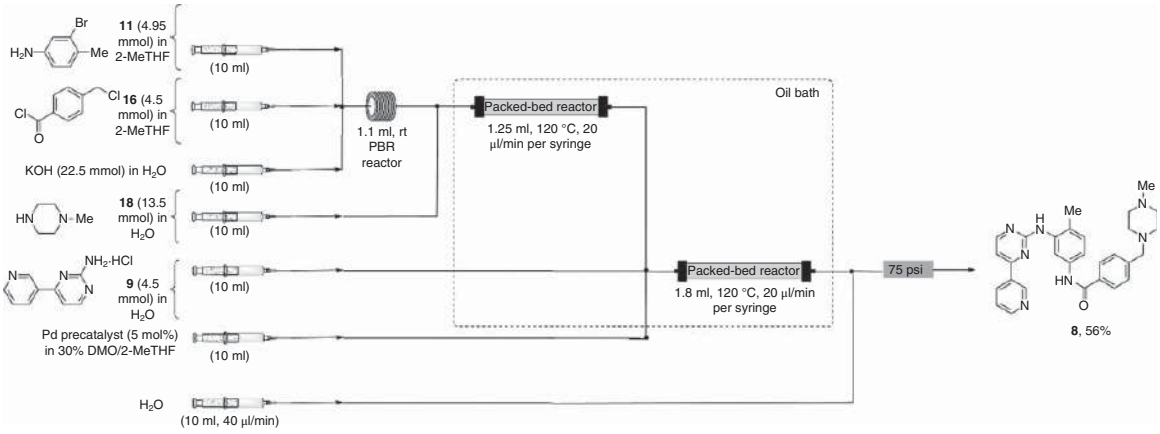

Scheme 4.31 Precise reaction configuration for the synthesis of imatinib in flow.

https://www.twirpx.org & http://chemistry-chemists.com

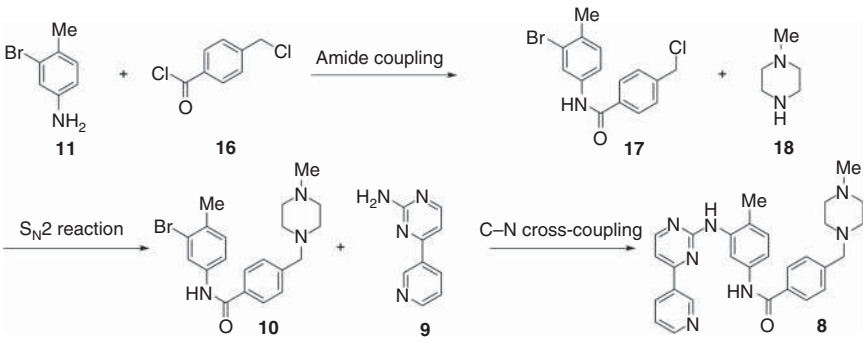

Scheme 4.32 Disconnections enable potential syntheses of imatinib analogs.

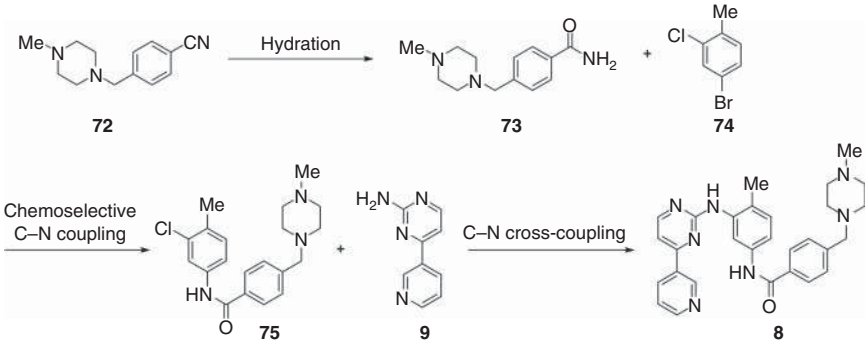

Scheme 4.33 Alternative disconnections to imatinib featuring two C—N bond formations.

While not only offering the opportunity to access novel chemical space, Fu and Jamison also sought an alternative solution to the challenges presented in running Pd-mediated C—N bond couplings in flow. Acoustic irradiation has been employed herein [16], and in the work of Buchwald, we saw how packed-bed reactors had been utilized to facilitate the mixing in such biphasic processes. However, in the latter case, the formation of Pd black was observed and as such running the reaction for a prolonged period can lead to accumulation and aggregation at the frits or within the packing materials leading to side reactions, pressure spikes, and eventual clogging of the equipment.

The initial reaction to be investigated within the sequence was the Pd-catalyzed amidation of a 2,4-dihalotoluene derivative. Screening the transformation in batch using benzamide as a model substrate demonstrated that while low yields and poor chemoselectivities were obtained using either dichloro- or dibromo-toluene derivatives, 4-bromo-2-chlorotoluene **74** provided favorable results using the BrettPhos Pd G4 precatalyst (Scheme 4.34). A biphasic mixture of 1,4-dioxane and water using K_3PO_4 as the base enabled the reaction mixture to remain homogeneous, while the enhanced solubility of the Pd catalyst in organic solvents was a promising attribute for the direct translation of this transformation to flow.

To translate the batch process into flow, it was envisioned that combining separate streams of catalyst, substrate, and base through a cross-mixer with a small

https://www.twirpx.org & http://chemistry-chemists.com

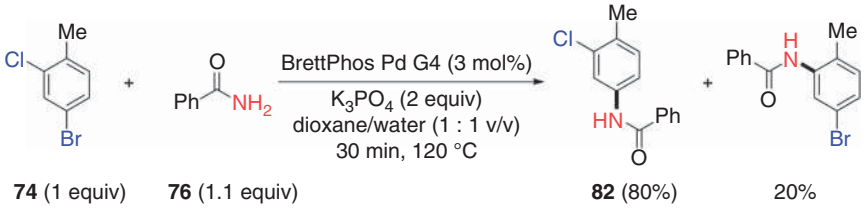

Scheme 4.34 Demonstration of chemoselective C—N bond formation using dihaloaromatic systems.

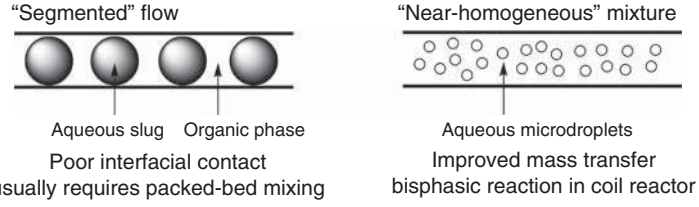

Figure 4.4 Biphasic reaction mixtures in flow highlighting mixing characteristics.

inner diameter would lead to a near-homogeneous stream containing small aqueous microdroplets, which would significantly increase the interfacial contact between the aqueous and organic phases in contrast to conventional segmented-flow systems (Figure 4.4). Using a stainless-steel reactor with a residence time of 15 minutes and temperature of 120 °C led to a 69% yield, while increasing the temperature to 150 °C (thus superheating the reaction mixture) provided 83% of the desired product **82**. Employing a sand packed-bed coil reactor for the analogous transformation led to clogging, owing to accumulation of Pd black at the output frit (Scheme 4.35).

With a view to develop the protocol for the synthesis of imatinib analogs, the scope of the chemoselective amidation was evaluated given that the dihaloarene forms the central core of the anticipated kinase inhibitor scaffold (Scheme 4.35). Both electron-rich and electron-deficient aryl dihalides reacted in a chemoselective fashion, while removal of the steric hindrance imparted by the methyl group in the model substrate had no effect on the reaction outcome. Heteroatoms were tolerated in either the dihalide or amide component, while for the nucleophile, lactams (**95**, **96**) and anilines (**97**, **98**) were also well tolerated. For poorly soluble (specifically polar amides), addition of 2–15% (v/v) methanol was employed to maintain homogeneity of the reaction system.

The chemoselective amidation represents the second step in the planned modular synthesis of imatinib **8** with the generation of the desired amide coupling partner in flow being designed as step 1. Nitriles are easily accessible and have wide commercial availability with simple hydration provided access to the primary amide for the Pd-mediated coupling. Previous reports have highlighted this transformation in flow using a MnO_2-packed reactor to mediate the transformation [20]. Application of this methodology to the precursor (**101**) required for the synthesis of imatinib was unsuccessful with only trace amounts of 4-formylbenzonitrile being isolated resulting from oxidative cleavage of the piperazine moiety.

https://www.twirpx.org & http://chemistry-chemists.com

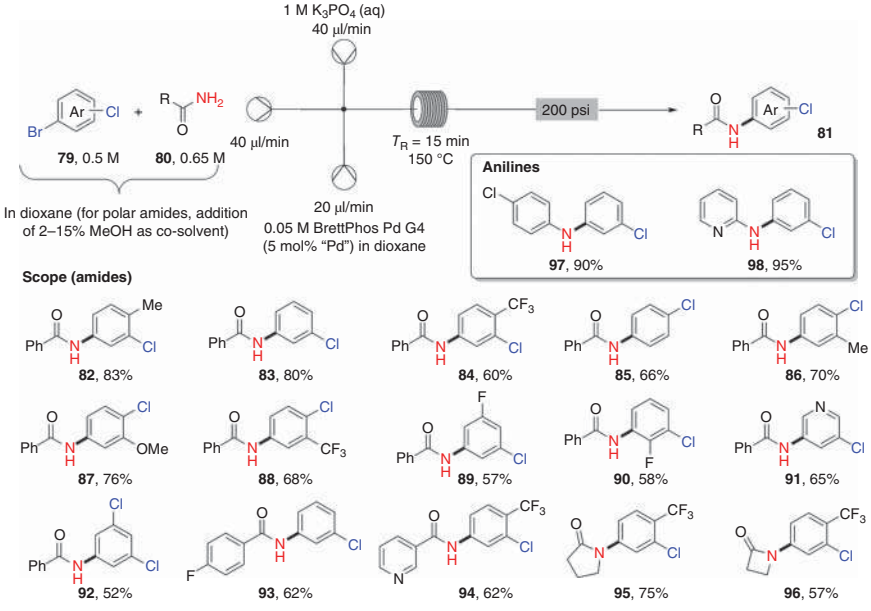

Scheme 4.35 Flow setup and substrate scope for chemoselective C—N bond formation with amides.

Numerous alternative approaches have been reported for the hydration of nitriles including treatment with stoichiometric quantities of a base such as K_2CO_3 under thermal conditions. Translation of this to flow conditions would enable the transformation to be carried out at elevated temperatures, thus potentially accelerating the reaction time. This was indeed shown to be the case with reaction in a stainless-steel coil reactor at 150 °C, providing a yield of 75% with a residence time of only five minutes (comparative yields in batch at reflux were shown to take c. three hours). Further studies on the reaction provided the optimal conditions using 10 mol% of Cs_2CO_3 to achieve complete conversion at 180 °C with a residence time of 15 minutes. The sequence of experiments were carried out using a solvent mixture of 1,4-dioxane/water (2 : 3 v/v) to obviate the need for a solvent switch before the Pd-catalyzed amidation. From a scope perspective a range of (hetero)aromatic (**109**, **110**) and aliphatic nitriles (**112**) was well tolerated with addition of an alcoholic cosolvent (*i*PrOH or *t*BuOH) used without impacting the reaction in cases in which substrate solubility in the reaction medium proved to be an issue (Scheme 4.36).

The final step of the sequence to assemble imatinib **8** (and analogs) constitutes the C—N bond formation between a 2-aminopyrimidine derivative **9** and a sterically encumbered aryl chloride. An initial obstacle here is the low solubility of the requisite amine coupling partner in organic solvents, though this was overcome through using the corresponding hydrochloride salt, which is readily soluble in water, and was combined with a solution of the Pd catalyst in dioxane to form one flow stream. Utilizing 2-chlorotoluene **113** as the substrate, a 1,4-dioxane solution of this was combined with aqueous K_3PO_4 to afford flow slugs to mimic the output

https://www.twirpx.org & http://chemistry-chemists.com

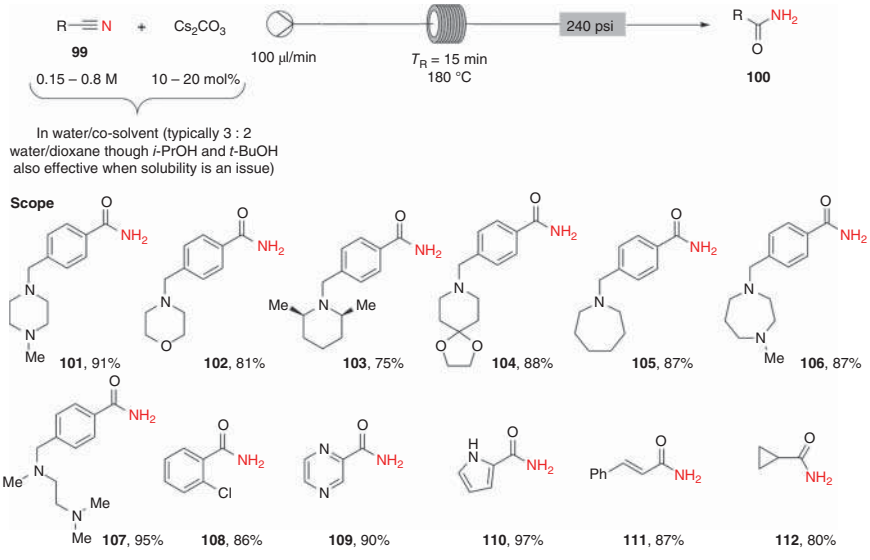

Scheme 4.36 Flow-based nitrile hydration to generate primary amides for displacement chemistry.

of the initial amidation reaction (step 2) to form the second flow stream. These two streams were combined through a Y-mixer to form a near-homogeneous mixture with the mild laminar mixing preventing precipitation and aggregation of the free base of the amine coupling partner formed upon contact with the K_3PO_4 base. For the model reaction performed at 150 °C in a stainless-steel coil, a 97% isolated yield of the coupled product **114** was obtained after a residence time of 15 minutes with this being the first time this biphasic reaction had been performed without using a packed-bed reactor (Scheme 4.37).

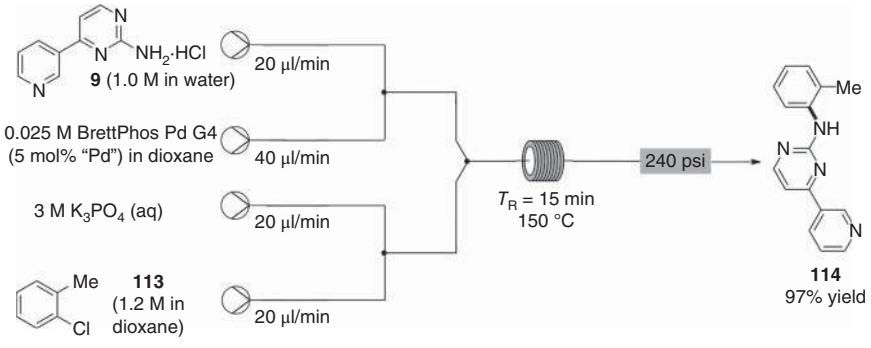

Scheme 4.37 Flow conditions for C—N bond formation under "near-homogeneous" conditions.

With the optimal conditions to execute each of the three steps in flow in a discrete manner, attention shifted to marrying the transformations together in a seamless manner to realize a flow synthesis of imatinib **8**. Here, important elements for

https://www.twirpx.org & http://chemistry-chemists.com

consideration include not only the concentrations of reagents/products involved but also the potential impact of by-products from previous steps on downstream reaction performance and whether these would necessitate in-line workups to be used. The output from the initial hydration process was telescoped directly into the Pd-mediated amidation process for which the aryl halide **74** and Pd precatalyst were pre-mixed and combined with separate streams of aqueous K_3PO_4 base and the newly formed primary amide intermediate. Utilization of a cross-mixer formed the reaction mixture to be passed through a stainless-steel reactor coil at 150 °C for 18 minutes. Control of the concentration (0.306 M) proved to be critical with decreases leading to a significant attrition in yield, while increases led to clogging owing to crystallization of the polar amide intermediate. The optimal process utilized an excess of the amide for the coupling (1.3 equiv), while addition of a stream of *i*-PrOH to the exiting reaction stream prevented precipitation and blocking of the back-pressure reactor. Over two steps, a 67% isolated yield of the intermediate **116** was obtained after 33 minutes (Scheme 4.38).

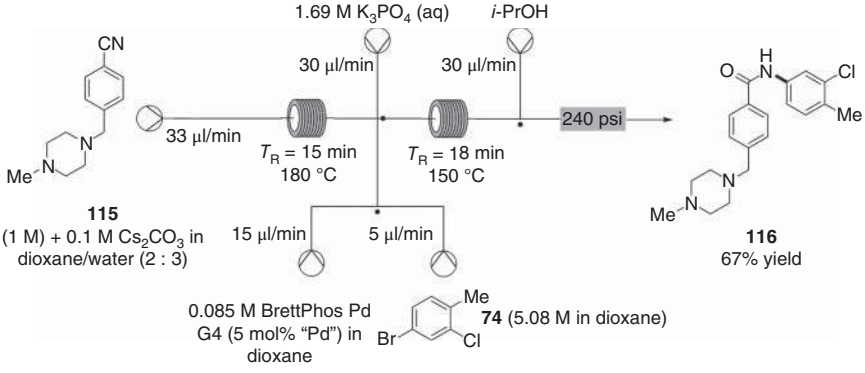

Scheme 4.38 Combination of nitrile hydration and initial C—N bond formation in flow.

Incorporation of the final C—N bond formation into the sequence highlights the need to make judicious modifications on the fly in order to telescope the reactions together. Herein, the solubility of the aminopyrimidine **9** continued to cause problems specifically with the neutralization of the hydrochloride salt on contact with the reaction stream leading to crystallization in the mixing unit. To overcome this, the base and Pd catalyst was combined with the reaction mixture directly from the previous two steps prior to joining a stream (50/50 dioxane/water to increase the overall organic content of the reaction) containing the hydrochloride salt of the aminopyrimidine **9**. This modification enabled a faster overall flow rate while decreasing the overall concentration by 25%, though despite these changes clogging was still observed at the Y-mixer shortly after equilibration of the system. To mitigate this issue, which was believed to arise from seeded crystallization due to solvent incompatibilities, an additional stream of *i*-PrOH was pumped through the operational hydration module for 30 minutes. Processing this through the subsequent reactors enabled unreacted materials to be dissolved by the alcoholic solvent leading to a

https://www.twirpx.org & http://chemistry-chemists.com

semi-homogeneous system and preventing solid buildup and subsequent blocking. Carrying out the final amination step in a stainless-steel coil allowed imatinib **8** to be isolated in 58% overall yield with residence time of 48 minutes and a production rate of 0.663 mol/h. This represents the highest production rate for the synthesis of imatinib in flow, while avoiding both in-line purification/solvent exchange between discrete steps and packed-bed apparatus. The challenge of the mass transfer in the biphasic C–N coupling steps is addressed through judicious selection of the solvent mixtures as well as careful mixing considerations in the flow setup (Scheme 4.39).

While the presented method offers differentiation with previous approaches and potential advantages for flow chemistry specifically in how Pd-mediated reactions are handled in flow, a further distinction from the flow syntheses of Ley and Buchwald is the strategic bond disconnections employed, thus offering from a medicinal chemistry perspective access to an orthogonal set of analogs based on the pools of starting material building blocks available. Herein, elements of the structural diversity that can be achieved through judicious selection of the aryl nitriles and halides are demonstrated through the flow syntheses of two analogs (**119**, **120**) in 57–66% yields with complete chemoselectivity. The broad scope demonstrated for the nitrile hydration and Pd-catalyzed amidation is suggestive that numerous other related compounds can be rapidly made. Utilizing 3,5-dichlorobromobenzene as a starting material allowed access to a novel analog (**121**) (Scheme 4.39) through two consecutive C—N bond-forming processes on the functionalized 3,5-dichlorobenzene derivative, demonstrating the ability of this approach to explore uncharted chemical space in an expeditious manner.

4.6 "Hybrid Approach" to Imatinib

With the syntheses of imatinib that we have considered, one of the main challenges encountered has been the insolubility of many of the intermediates. A possible approach to alleviate this is to carry out a "hybrid" approach in which a portion of the molecule is made taking advantage of flow technology with the final steps of the synthesis being carried out in a conventional batch-based fashion (Scheme 4.40).

Ley and coworkers have exploited such a strategy called "catch–react–release" methodology for the general synthesis of a range of 2-aminopyrimidines, which represents important components in a range of bioactive molecules in addition to being a pivotal kinase hinge binding fragment within imatinib **8** [21]. Typical approaches to this motif include metal-mediated cross-couplings (as we have already seen) or displacement of halogens or activated alkyl thiol derivatives. The latter method is particularly attractive given that the requisite pyrimidine precursors are generally easy to prepare, utilizing functionalized thioureas as starting materials, and are typically stable throughout a synthesis requiring oxidation (with a wide range of mild oxidants capable of achieving this transformation) to enable the subsequent nucleophilic displacement to occur. There are however disadvantages to this methodology, which detract from its widespread use, most notably the stench and toxicities associated with the sulfur-based by-products, as

https://www.twirpx.org & http://chemistry-chemists.com

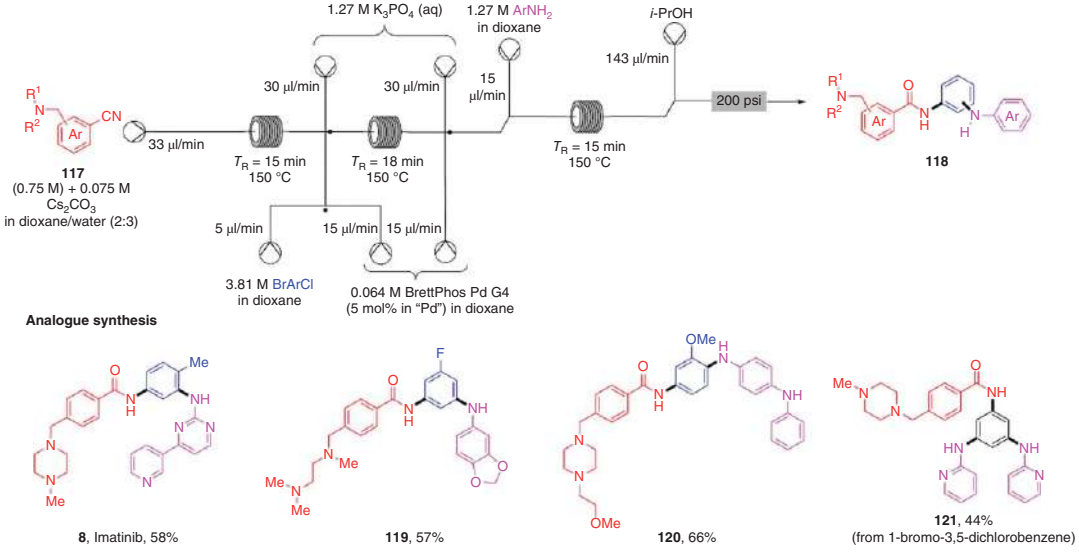

Scheme 4.39 Synthesis of imatinib and analogs in continuous flow.

https://www.twirpx.org & http://chemistry-chemists.com

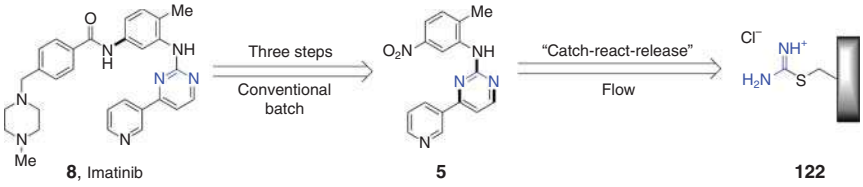

Scheme 4.40 Disconnections highlighting "hybrid" approach to imatinib.

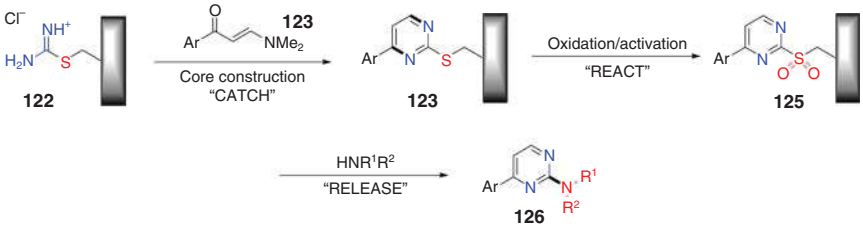

Scheme 4.41 Concept of "catch–react–release" for the synthesis of 2-aminopyrimidines.

well as their potential to contaminate the desired 2-aminopyrimidine products **126**. A possible way to alleviate this is through a "catch–react–release"-based method on which the thiopyrimidine derivative is prepared directly immobilized to a suitable solid support. Subsequent oxidation followed by reaction with an amine allows elution of the aminopyrimidine products **126** with the sulfur residues still retained on the heterogeneous support (Scheme 4.41).

While automation can enable such a protocol to be performed in a flow-based paradigm, the advantages of solid-phase synthesis can also be harnessed allowing super-stoichiometric amounts of reagents to be employed to push transformations to completion with the excess simply being washed away from the resin after reaction. In contrast, carrying out transformations using heterogeneously supported reactants in flow does present challenges with the judicious selection of the specific support critical for success. While conventional polymer beads can require specialized equipment for the preparation of functionalized variants, their effectiveness when used in flow is also suboptimal owing to solution channeling. From an ease of synthesis perspective, functionalized macroporous monoliths can be easily generated and possess a well-defined rigid cross-linked structure forcing the flow stream to pass through the column leading to optimal contact efficiencies (Figure 4.5) [22].

The initial challenge was the synthesis of a polymer-supported isothiouronium salt **122** with the emphasis on both developing a reproducible approach and ensuring high porosity and stability of the material to utilize in a flow-based system to avoid issues such as over-pressurization or diminished performance over time. The use of the isothiouronium salt herein would present a barrier to traditional polymerizations to form gel-phase beads owing to its aqueous solubility, prohibiting the use of the typical biphasic solvent systems employed therein. With regard to the formation of the monoliths, addition of water and 1-propanol was required to accommodate the different solubility profiles of the parent salt **127** and the divinylbenzene

https://www.twirpx.org & http://chemistry-chemists.com

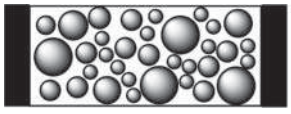

"Polystyrene-based resins"
Irregular solvent-dependent swelling characteristics. Flow stream seeks easy way through the reactor leading to pressure drops and poor reproducibility

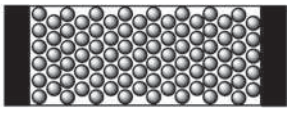

"Monolith-containing column"
Single continuous piece of porous material. Tailored morphologies with easy control of poor dimensions, etc. Rigidiy leads to a consistent flow-path and consistent reactions though pressure drops still observed

Figure 4.5 Flow characteristics of polystyrene resins and monolith-containing columns. Source: Based on Ref. [22].

cross-linker **128**. The preparation involved homogenization of the components at 50 °C prior to addition of the initiator 1,1′-azobis-(cyclohexane carbonitrile) (ACHC) followed by transfer of the mixture to a glass column, which was sealed and heated at 90 °C (using a Vapourtec system) for 20 hours. After cooling, the columns were washed with EtOH at 60 °C to remove the porogen and excess monomer to provide rigid, white monoliths **122**, which could be prepared and stored in a range of sizes (3–15 mm diameter) with elemental analysis indicating a reproducible loading of 2.4 mmol/g isothiouronium chloride (Scheme 4.42).

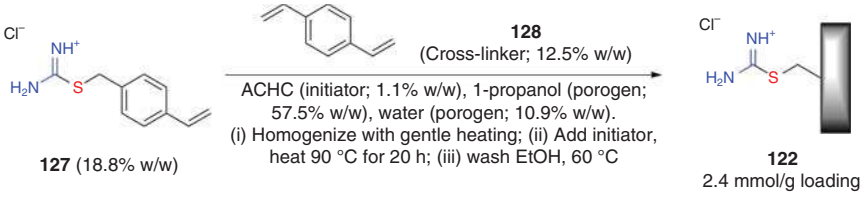

Scheme 4.42 Synthesis of functionalized monolith-containing columns.

For the "catch" step involving formation of the pyrimidine core on the solid-phase, solutions of an enaminone **123** and Hunig's base were passed through the monolith **122** at elevated temperature (Scheme 4.43). While excess reagents can be used to push the reaction to completion, it should be noted that the surplus enaminone **123** can be recovered from the output stream and recycled. The monoliths **124** were washed to remove the unbound reagent with elemental analysis of the polymer, indicating a reagent loading of 2 mmol/g, while ^{13}C nuclear magnetic resonance (NMR)/IR were employed to confirm conversion of the bound isothiouronium salt to the desired pyrimidine.

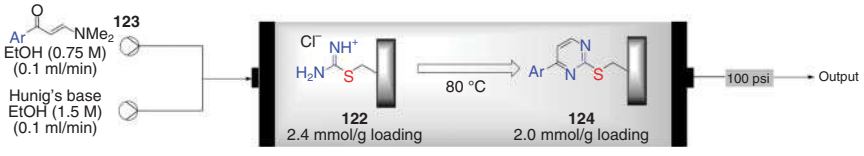

Scheme 4.43 Formation of the pyrimidine core on the solid support.

The next step for the sequence is the oxidation of the sulfur functionality to enable displacement upon reaction with an amine of the desired aminopyrimidine

https://www.twirpx.org & http://chemistry-chemists.com

from the solid phase. As noted, there are a variety of oxidants capable of achieving sulfur oxidation for use in a flow process; solubility of the chosen reagent becomes a key consideration. In addition, oxidation at sulfur can often lead to a mixture of the sulfoxide and the sulfone, and although using large excesses of oxidant can be a strategy employed to drive the reaction to the sulfone, it may not be necessary as reports indicate that the sulfoxide can also be a suitable substrate for the displacement and unreacted sulfur-based material in the final S_NAr reaction remains attached to the monolith. Excess meta-chloroperbenzoic acid (*m*-CPBA) was used to mediate the oxidation, utilizing a solution in DCM that is passed through the monolith **124** with elemental analysis, indicating that as assumed a mixture of the sulfoxide and sulfone **125** had been produced (Scheme 4.44).

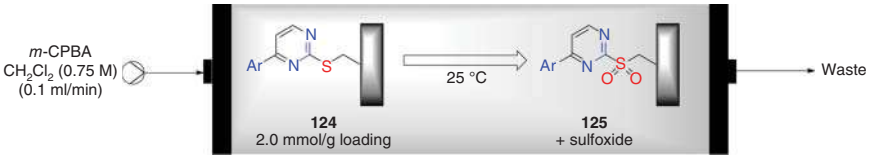

Scheme 4.44 Activation of the pyrimidine for displacement through oxidation.

For the displacement, one of the barriers often cited for the implementation of flow methodology is the reaction kinetics specifically in its application to slower reactions. This problem can be exacerbated when heterogeneous (or solid-supported) reagents are involved. While, here, reactions could be accelerated using an excess of amine in the displacement, a superior solution involved using a "stop-flow" reaction technique. Here, a flow stream of the amine for displacement and Hunig's base are introduced, allowing enough volume to fill the monolith **125** prior to stopping the pumps. The reaction mixture is then held and heated to facilitate the process over a specified time period. After this has elapsed, the desired pyrimidine product **126** and excess amine are eluted to be subjected to aqueous workup and purification (Scheme 4.45). Although somewhat counter to a conventional continuous process, this approach does enable advantages of flow to be exploited such as ease of purification and automation.

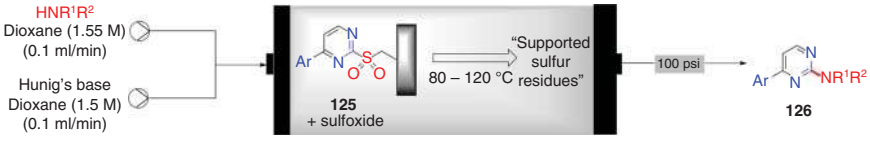

Scheme 4.45 "Release" – displacement with amines forms the desired product.

The reported approach offers two points of diversity for the assembly of the 2-aminopyrimidines, notably the nature of the aromatic enaminone (**123**) used in the condensation to form the pyrimidine and the amine used in the displacement. A selection of six enaminones were exemplified in the chemistry with five amines (both aliphatic and aromatic) used in the displacement with the products being

https://www.twirpx.org & http://chemistry-chemists.com

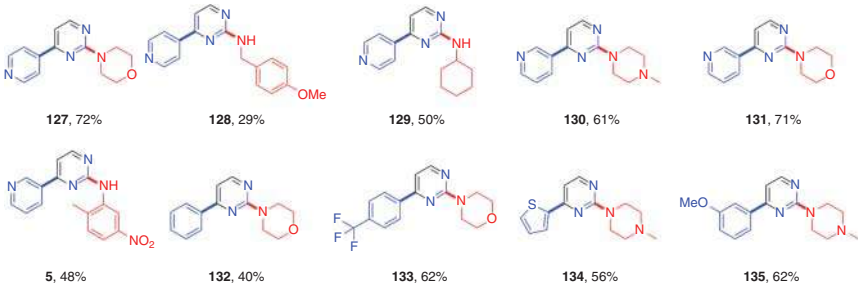

Figure 4.6 Scope of 2-aminopyrimidines formed using the "catch–react–release" protocol.

obtained in moderate to good yields after three steps with the overall success of the process shown to loosely correlate with the nucleophilicity of the amine (compare **127** and **128**) (Figure 4.6).

For the synthesis of imatinib **8**, the requisite aminopyrimidine **5** was obtained from the "catch–react–release" methodology in 48% yield. Hydrogenation of the nitro group, amide bond formation, and followed by displacement with 1-methylpiperazine **18** led to imatinib **8** in 40% overall yield (85% over the final three steps) with no issues encountered due to intermediate insolubility (Scheme 4.46).

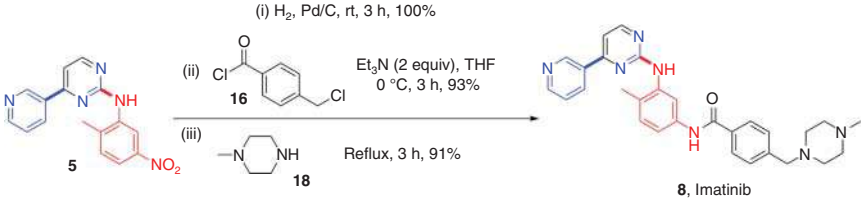

Scheme 4.46 Completion of imatinib synthesis under conventional batch conditions.

4.7 Closed-Loop Discovery

The case studies we have so far evaluated have focused very much on synthetic strategies to assemble a known inhibitor using a flow-based platform and then expanded upon the potential diversity of the accessible analogs through variation of the available monomers in a "plug and play"-based approach. This very much fits in with the classical drug discovery paradigm of iterative synthesis cycles followed by *in vitro* screening with the results informing the next series of molecular designs. However, it can be easily envisioned that exponential efficiencies can be realized if these two activities were combined on a single platform with an aspirational goal to incorporate a "closed-loop" algorithm in which the activity data resulting from a synthesized compound automatically "informs" the platform which analog should be synthesized next (Figure 4.7). On paper, this endeavor sounds relatively simplistic though in reality represents a significant challenge most notably based on differing scales for synthesis/biology as well as incorporating a purification module

https://www.twirpx.org & http://chemistry-chemists.com

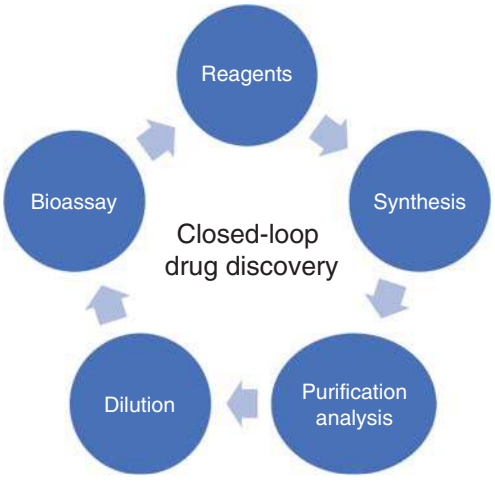

Figure 4.7 Integrated design–make–test cycle platform.

in series. The chronology and logistics behind the "closed-loop" platform developed by Cyclofluidics Ltd. have been disclosed while there continues to be a growth of interest in the integration of continuous-flow synthesis with in-line analysis and data generation [23]. Work at Cyclofluidics to develop a module featuring design, synthesis, and the assay or new molecular entities was initiated in 2008 based on work originating from GlaxoSmithKline Inc. (GSK) [24].

The success of this project requires a collaborative partnership between a range of disciplines. Firstly, the challenges presented to implement each of the challenges in a continuous-flow manner need to be highlighted with solutions, providing a suitable output for the next scientific operation in the chain. For chemistry, this, while making the compounds in flow, is clearly the most logistical choice; questions remain around delivery of reagents, suitable synthetic methods, and in-line purification/dilution to deliver a sample suitable to be directly introduced into a biological assay. Commercial Vapourtec flow apparatus was utilized given its ease of use and modular setup with compounds planned to be synthesized on microfluidic scale (<1 mm diameter tubing and μl volumes) to limit the use of precious building blocks/reagents. The initial system carried out the syntheses on a "glass-chip," while a 24-sample carousel was used for storage and dispensation of samples.

A standard high-performance liquid chromatography (HPLC) system was placed in-line to directly analyze/purify reactions directly off the reactor system with evaporative light scattering detection (ELSD) selected for quantification, owing to its applicability and consistent response to the majority of drug-like molecules. A sample of the desired product was isolated from the center of the corresponding HPLC peak (the so-called "heart cut") and diluted to a suitable concentration of the subsequent in-line biological assay. The initial prototype of the instrument profiled feasibility studies running biological assays in flow on custom glass chips featuring 80 μm channels, though these were quickly discarded and replaced with 75 μm ID capillary tubing owing to both costs and ease of replacement. Additional challenges that needed to be addressed were ensuring compound solubility specifically after

https://www.twirpx.org & http://chemistry-chemists.com

dilution with excess aqueous-based buffer as well as the need to accurately deliver assay reagents at low flow rates and high pressures over a defined gradient using a nano-HPLC pump to allow realistic determination/comparison of IC_{50} values of test compounds.

Though the initial setup enabled proof of concept to be achieved for the integrated "make–test" part of the cycle, it also served to highlight several severe shortcomings that would hinder expansion to a full-scale operational platform, while both integration of a feedback loop and automation and seamless software control of the various components have not yet been considered. For chemistry the use of the Vapourtec system allowed a facile switch to a tube-based reactor platform with two-step reaction sequences (with potentially a third deprotection step incorporated) considered to represent the "sweet-spot" for the platform's operation, provided that pre-evaluation of reagent compatibility and solubility were taken into account. Longer sequences were considered out of scope based on the likelihood that intermediate workup (an exception to this is in the case of metal-mediated transformations in which a silica plug was placed in line prior to HPLC purification to remove polar impurities and remove metal ions that could potentially adversely affect the biological assay) and possibly purification would have to be integrated thus complicating the configuration of the platform [25].

With regard to reagent storage/delivery, the overall intended capacity of the fully functional platform was taken into consideration, and, given this, it was felt that the initial 24-position carousel would not be sufficient to allow a wide degree of chemical space and diversity to be explored. There are numerous commercial options available to address this requirement, though it is important to consider not only an equipment's capacity but also its ease of operation, reliability, and ability to be integrated with the other components within the platform. With an aspirational target to evaluate, c. 1 million compounds within a project, this would require space for 300 reagents ($100 \times 100 \times 100$ for a two-step reaction sequence) and was considered more than sufficient in executing a lead optimization campaign.

The HPLC purification utilizing ELSD for quantification had proven to be highly successful even for the isolation of suitable amounts of test materials from low-yielding reactions, though key to the whole process was triggering the capture of the "heart cut" of the peak of interest as it emerged from the purification module. Given that the chemistry was carried out on a scale that led to millimolar amounts of material being isolated, a mass dilution was required to the low micromolar scale to allow use directly in biological assays. In developing the HPLC method, consideration was paid to the organic solvents utilized to avoid possible interference with the downstream biological analysis, while a dilution module was developed to allow a threefold dilution to be performed with a suitable assay buffer.

While running the biochemical assays in flow potentially provides a boost in efficiency in providing single-point data, complications arise particularly in ensuring consistent seamless performance of the assay. With the next-generation platform (Figure 4.8), a switch was made to utilize more conventional robust microtiter plate-based assays. While the synthesis/purification modules provide an assay-ready sample, numerous commercial vendors offer options for dispensing assay reagents

https://www.twirpx.org & http://chemistry-chemists.com

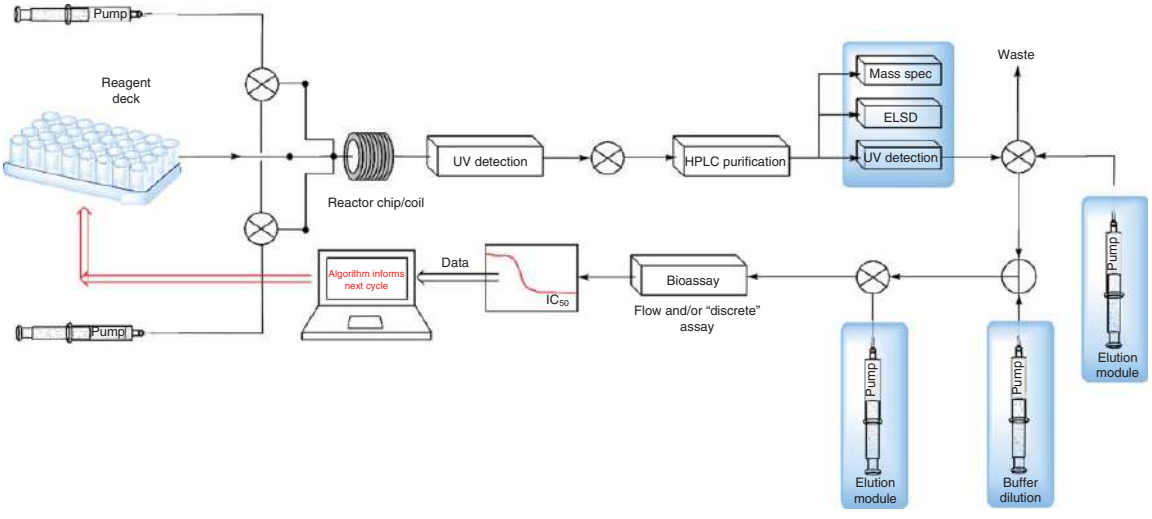

Figure 4.8 Schematic of Cyclofluidics optimization platform.

https://www.twirpx.org & http://chemistry-chemists.com

as well as reading 96/384 well plates leading to the development of a single probe liquid handling platform. The majority of assays employ fluorescence-based techniques with an optical cartridge plate reader used for detection, while assay standardization particularly concerning reagent stability is key to successful continuous operation. Switching to a plate-based approach also enabled parallel assays to be conducted on the synthesized compounds most notably through integration of a second HPLC system, allowing measurement of Log D, concentration, and QC purity.

While vendor software was typically employed to control the individual components of the platform, it was key to integrate these to enable seamless communication, data capture, and scheduling throughout the closed-loop environment. A proprietary control software was developed that allowed overall control through either application program interface or contact-closures triggering events between the system's hardware.

Despite the ability to robustly capture data and precisely control the experimental parameters, the greatest challenge of the whole endeavor was developing an algorithm to incorporate into the platform's software and informatics infrastructure to enable compound optimization in a serial fashion while minimizing the overall number of cycles/experiment time to reach an successful end point. Several methodologies could possibly be applied to this problem with a random forest approach selected and optimized utilizing a wide range of molecular descriptors to build a predictive model while being capable of carrying out a multiparameter optimization once the nature and weighting of the parameters had been determined. Implementation required a known area of chemical space to be defined for each structure activity relationship (SAR)-based exploration to facilitate the subsequent optimization. Two possible approaches exist to achieve this, either through a broad survey of activity data across the entire collection of compounds or through identification of the best molecule through a sequential compound-by-compound approach focusing on incremental increases in potency. While both have their merits, in practice, it is best to implement a hybrid approach with initial cycles focusing on broad structural requirements that enhance activity within the lead series with the following cycles drilling down to a specific compound with the optimal potency/properties within a subset of the overall chemical space under evaluation.

4.8 Identification of Novel Bcr-Abl Kinase Inhibitors Through Closed-Loop Discovery

To validate and confirm the potential of the platform for lead optimization purposes, a specific target-based project was undertaken [26]. As we have seen, Bcr-Abl (breakpoint cluster region Abelson tyrosine kinase) inhibitors initially through the discovery of imatinib (**8**) have established themselves as effective medications for the treatment of CML. Despite robust efficacy, some patients relapse due to the emergence of clinically relevant mutations (as exemplified by T315I – the gatekeeper mutation), and while second- and third-generation inhibitors have been reported (**20**, **136**, and **137**), which demonstrate enhanced efficacy against mutated

https://www.twirpx.org & http://chemistry-chemists.com

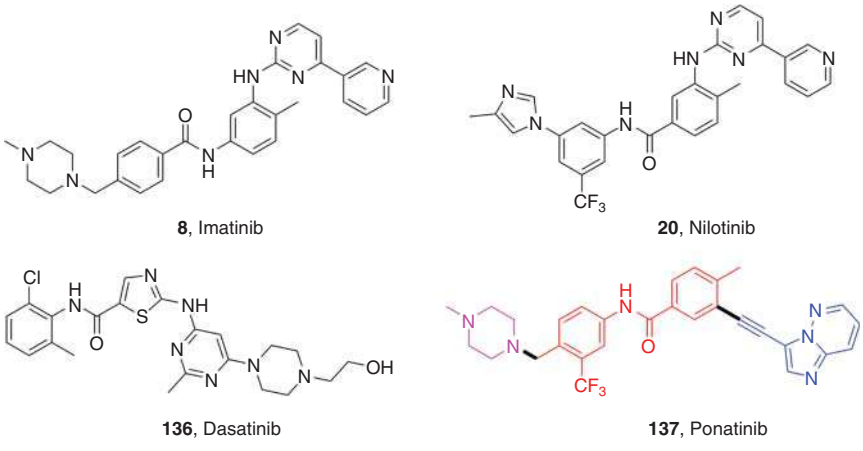

Figure 4.9 Reported inhibitors of Bcr-Abl kinase. Source: Based on Ref. [27].

versions of the kinase, the identification of new inhibitors of Bcr-Abl remains an attractive and valuable endeavor (Figure 4.9) [27]. Furthermore, Bcr-Abl is an established drug target with known validated assays as well as a range of data reported for previous inhibitors, while similar soluble protein targets (kinases) are amenable to structure-based drug design approaches and are commonly pursued within drug discovery.

To initiate the search for novel inhibitors of Bcr-Abl, it was important to not only define the chemical space for exploration but also identify a robust flow-based sequence in order to assemble the molecules of interest. Utilization of structural insight gained from binding mode exemplified by the third-generation alkyne-based inhibitor ponatinib (**137**) (that does show appreciable efficacy against the T315I mutant enzyme) enabled a generic model structure to be proposed, featuring a heterocyclic hinge-binding group (an imidazopyridine in ponatinib) linked through an alkyne to a structural motif (based on three specific templates) that binds to the "DFG-out" conformation of Abl and terminates with a basic amine (Figure 4.10) [28].

Planning for the assembly of the target molecules on the integrated platform, it was rationalized that a Sonogashira-type coupling between a (hetero)aryl alkyne (**151**) and the "DFG-templated" halide (**150**) would represent a robust, modular bond disconnection to the desired compounds as exemplified for ponatinib (**137**) (Scheme 4.47). This reaction is mediated using Pd/Cu catalysis with numerous examples of such Cu-mediated reactions being reported in flow with the necessary exposure to the catalyst provided through employing a copper reaction coil [29].

Further planning as to the chemical space to be investigated highlights one of the main barriers typically associated with drug discovery endeavors based around the synthesis of compound collections, namely, access to the desired building blocks required to assemble the molecules of interest. The importance of this aspect of planning cannot be overemphasized given the strong argument that the "drug-likeness" and "potential for success" are inherently based on the judicious

https://www.twirpx.org & http://chemistry-chemists.com

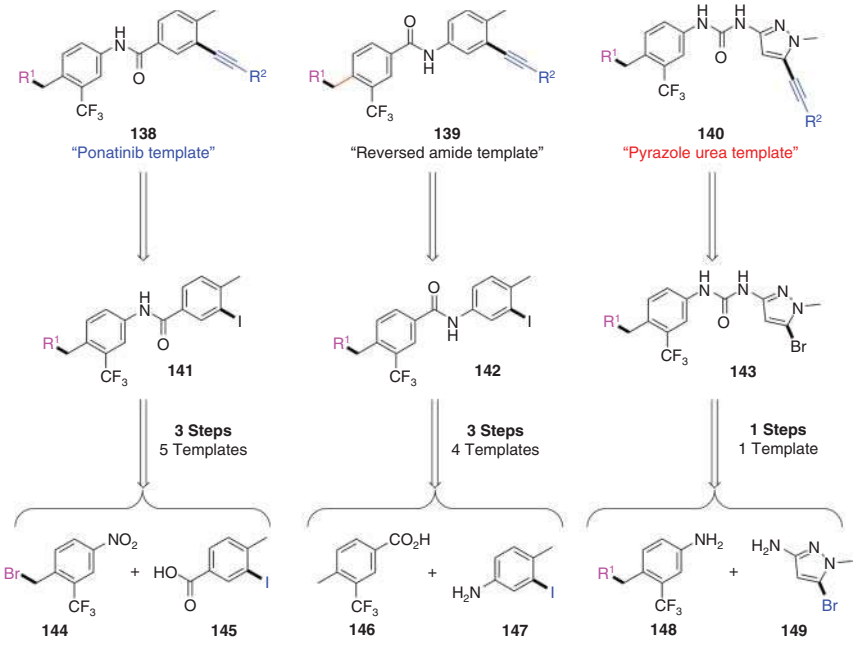

Figure 4.10 Proposed inhibitor templates featuring disconnections to DFG-binding moiety. Source: Deng et al. [28] / Elsevier.

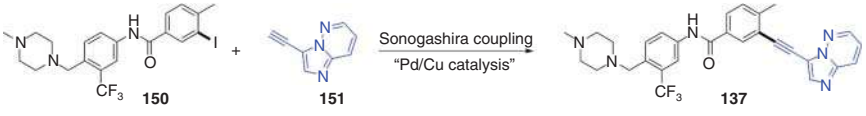

Scheme 4.47 Sonogashira coupling to form ponatinib **137**.

selection of these building blocks/monomers [30]. This is clearly evidenced by the exponential increase in both the sheer number of pharmacophoric monomers available as well as the commercial sources to access them from. Usually, such offerings are organized into specific collections based on the reactive functionalities present through which these can be further elaborated. However, there are still numerous structural classes of monomers, which are underrepresented in terms of commercial availability. This is exemplified in the example here with evaluation of a series of databases demonstrating that there are relatively few (hetero)aryl alkynes available. However, these can be accessed in a trivial fashion from the wide variety of either bromo- or iodo-based heterocycles that can be sourced; still this endeavor highlights an aspect of flow chemistry for library syntheses within medicinal chemistry that is often overlooked. While streamlined synthesis of libraries of drug-like compounds can be realized in flow, this exercise may rely on the need for the offline synthesis/storage of custom building blocks, thus entailing investments both in cost and time resource. It is interesting to note here that the key reaction required to synthesize these compounds is the classical Sonogashira coupling performed in batch,

https://www.twirpx.org & http://chemistry-chemists.com

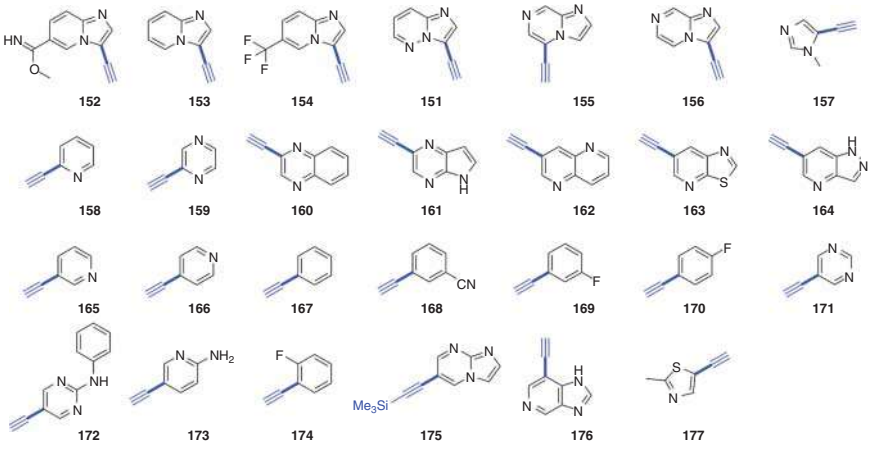

Figure 4.11 Monomers selected to probe hinge-binding motif.

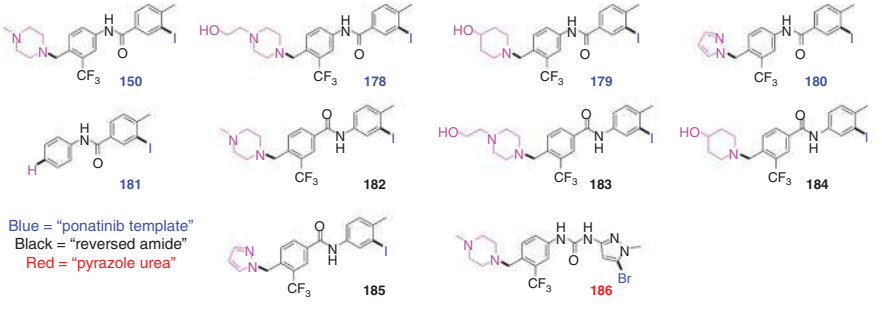

Figure 4.12 DFG-binding monomers synthesized for flow-synthesis evaluation.

which is also envisioned to be the pivotal bond-forming step for the assembly of lead molecules on the flow platform. Triage of the heterocycles was achieved through a combined analysis involving comparison with other hinge-binding motifs and overlay with the available ponatinib-Abl co-crystal structure, leading to 27 monomers being selected for purchase/synthesis (**151**–**177**, Figure 4.11).

Similarly, a degree of synthetic investment was required to assemble the DFG-binding templates (Figure 4.12). Key differentiators between the 10 selected motifs were the nature of both the connector (amide, reversed amide, urea – color coded in Figure 4.12) incorporated therein, the aryl moieties, and the basic-amine substituent. Only a small range of these were evaluated with the main vector of structural diversity of the 270 possible new compounds intended to be the hinge-binding heterocycle.

With the necessary monomers for the platform in hand, a key requirement became identifying robust flow-based conditions in flow for the Sonogashira coupling in order to access the compounds selected for synthesis by the design algorithm. To achieve this, a commercial Vapourtec R4 synthesizer was used as the flow instrument with 120 mM solutions of the two reactants in DMF combined and passed

https://www.twirpx.org & http://chemistry-chemists.com

through a 1 mm ID copper coil (capacity 2 ml) heated to 150 °C at a flow rate of 100 µl/min to provide a residence time of 20 minutes. The Pd catalyst was added to one of the reactant solutions with the removal of metal residues from the exiting stream achieved by passing the crude reaction through a plug of silica. Following this at maximum concentration, 10 µl was collected in an injection loop, which was switched automatically to load the sample onto an LC/MS for purification before reformatting for the subsequent bioassay (Scheme 4.48).

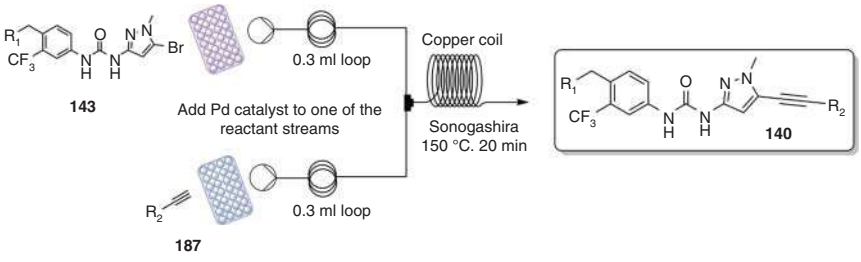

Scheme 4.48 Optimization of the key Sonogashira coupling on the flow platform.

While the synthetic chemistry carried out on the platform can be considered to be somewhat routine (a characteristic of library chemistries in general), the most significant differentiator of this approach above and beyond the integrated nature of the platform is the algorithm driving the design of the next compound from the available virtual chemical space based on the data as it is collected. This program utilizes random forest activities using as noted a blend of "chase potency" and "most active under-sampled" strategies. The key consideration for employment of an algorithm for a machine learning-based exercise is the ability to break down the compounds into a combination of numerical descriptors (MW, H-bond donors, topological polar surface area (TPSA), etc.) as well as a molecule fingerprint that captures the structure of the compound in a machine-readable form. The popularity of random forest-based optimizations within chemistry-based endeavors is due to its ability to perform non-linear regression while being resistant to over-fitting and requiring very few tuning parameters.

Regarding the design strategies used, "chase potency" simply sorts all the possible compounds based on predicted potency and then prioritizes the "best" compounds for synthesis. The "most active under-sampled" methodology is designed to ensure fuller coverage of the virtual chemical space under consideration. To accomplish this, the program considers how often each of the available reactants is utilized within a systematic series of designs and queues compounds for synthesis to sample all the reactants as equally as possible. Ideally, though in a lead discovery campaign, one wants to rapidly identify the optimal compound as quickly as possible while not missing something, and so to achieve this a combination of the two approaches is desirable, running sequential loops between scanning for pockets of activity and then drilling down to the most active compounds in each space.

Critical to the success of this endeavor as a whole is to be able to predict activity, and, in order to achieve this, a "training set" of compounds with known potency

https://www.twirpx.org & http://chemistry-chemists.com

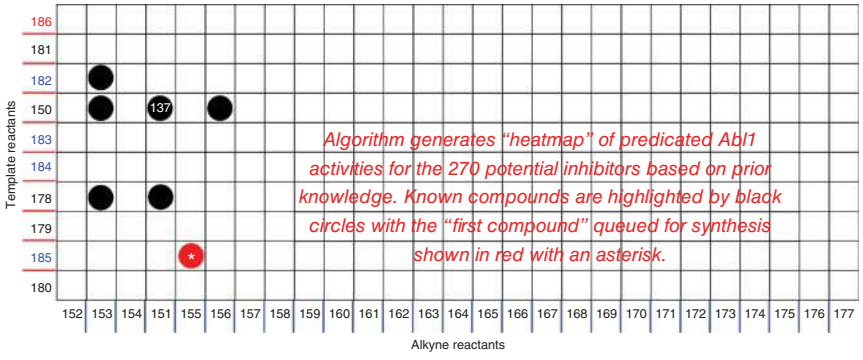

Figure 4.13 Initial heatmap featuring positions of known inhibitors and proposed first compound for synthesis. Template reactants are color-coded by series (Figure 4.12).

against the target has to be provided to the algorithm either from within the virtual chemical space or through closely related compounds. As noted Abl1 is a well-established target, and, given this, the data around ponatinib (**137**) and related analogies (36 compounds in all) were used to seed the design model leading to the output of predicted activity for the 270 proposed possible compounds for synthesis (note based on the monomer selection, ponatinib (**137**) itself is included within the virtual chemical space allowing data to be generated from a positive control). In order to validate the generation of IC_{50} data on the platform, the synthesis of imatinib (**8**) was carried out using Ley's flow-based approach, which we discussed previously [12]. Screening of the authentic sample both on the platform and in a conventional manual assay provided IC_{50} values that were consistent with those reported in the literature and allowed validation of the platform-based assay (Figure 4.13).

For the experimental strategy, three parts were devised in which the first one would evaluate "most active under-sampled" areas of the virtual space to ensure broad coverage while identifying areas of enhanced potency. In the second phase, drilling down into the design spaces featuring the more active compounds would be pursued through a "chase potency" approach, while a third cycle would combine the two strategies to identify and subsequently optimize additional activity "hot-spots."

This is best visualized in practice through surveying the data, with the first part of the SAR investigation consisting of 29 design–screen–synthesis cycles taking approximately 30 hours to complete. From the loops, 22 compounds (76% success rate) were assayed with six failing in the synthesis step with a further analog failing QC (Figure 4.14). Learnings from the initial round of syntheses highlighted the pyrazole urea-based template (**186**) featured in compounds with promising activity while several compounds featuring the ponatinib heterocyclic template also stood out. In the areas of weaker potency, gratifyingly compounds with a phenyl motif (**167**–**170** and **174**) as the proposed hinge-binding component were prominent and served as a negative control given that such compounds are unable to make the necessary hydrogen bond interactions in the pocket of the protein.

https://www.twirpx.org & http://chemistry-chemists.com

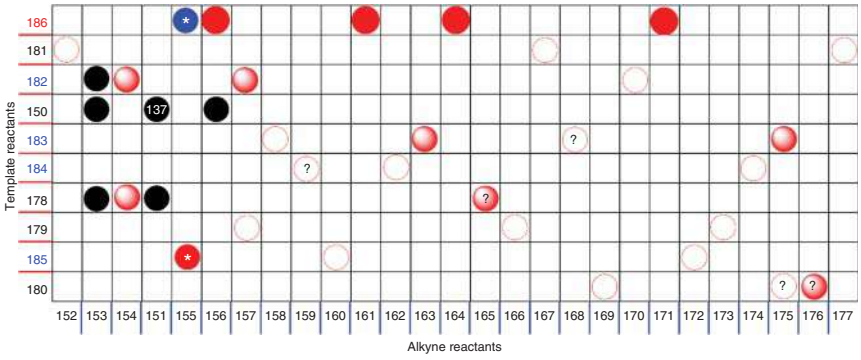

Figure 4.14 First cycle of synthesis using "most active under-sampled" strategy. Compounds made are red circles. Relative potency highlighted through shading (empty circles are less potent, while solids represent most potent). Question mark indicates compound failed synthesis/QC or bioassay.

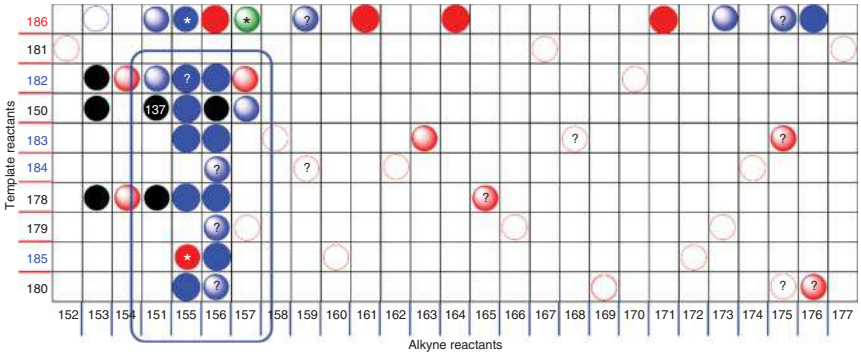

Figure 4.15 Blue circles highlight second round of synthesis cycles using "chase potency" strategy. Note clustering of compounds made in the blue box.

Part two enabled focus on areas identified with relatively potent compounds ("chase-potency"). A deeper evaluation around the SAR of a novel hinge-binding motif specifically investigates potency variations based on the nature of the connections in the DFG-binding templates (amide, reverse-amide, urea). Twenty design/synthesis loops were carried out with 14 compounds being successfully synthesized, enabling a refined heatmap of predicting activities (now incorporating the data from the 36 new compounds made into the model) to be generated for utilization in part three (Figure 4.15).

The final combined design approach utilized six alternating cycles of "most active under-sampled" and "chase potency" strategies (a total of 12 cycles). Through these, a further 41 loops were executed, leading to access to 28 more compounds (68% success rate) with the main outcomes of this cycle being a more thorough exploration of two novel hinge-binding motifs predicted to have good activity (Figure 4.16).

In summary, 90 design–synthesis loops were carried out leading to 64 new compounds (71% overall success rate) being assayed against Abl1/Abl2. Whereas from a conventional library success rate, the chemistry is pretty much comparable, what is

https://www.twirpx.org & http://chemistry-chemists.com

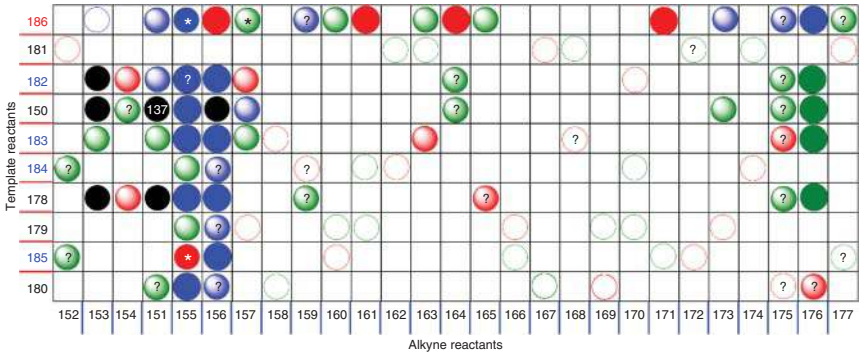

Figure 4.16 Green circles show third round of synthesis using combination of approaches. "Chase potency" filling out missed compounds around activity clusters, while "most active under-sampled" probes to ensure nothing has been missed.

notable here is the ability for the platform to purify enough material for testing from low-yielding (~5–10%) reactions.

At this juncture, it is instructive to benchmark this endeavor with a typical medicinal chemistry program in the hit identification space. One can hypothesize that the exercise would initially start with the goal to identify alternative lead matter to ponatinib. A similar library design could be envisioned based around the pivotal bond formation originating from a Sonogashira coupling. As noted previously, one of the key elements of the overall design is in the selection of suitable building blocks, and this is likely to follow the same process used in a conventional approach. This would lead to a 27×10 matrix compound library, which is certainly within scope for many parallel synthesis-based groups utilizing plate-based approaches, though the likelihood is that a bottleneck will occur during a downstream purification step. In addition, the success of this purification may depend not only obviously on the methodology (HPLC, supercritical fluid chromatography (SFC)) employed (with a common method being likely, which is analogous to the platform) but also potentially on a pre-purification QC that sets cutoffs on what level of desired product needs to be detected in a specific well for the reaction to be processed to the actual purification. In addition, further downstream processing, transfer, and reformatting will be required to prepare the samples for the relevant assays. However, once this is done, the biological assays are typically processed in a high-throughput plate-based fashion. Another interesting aspect of this comparison is in the downstream logistics and most notably in the amounts of compound made. In the conventional scenario, all the compound is purified with excess material retained after reconstitution of samples for absorption, distribution, metabolism and excretion (ADME)/biological studies, and while this might in some ways be seen to be wasteful, it does provide amounts of compound for further downstream assays, enable rigorous QC analysis of the compounds, and enable samples of novel chemical matter to be added to a larger collection of compounds for future high-throughput screening campaigns. One parameter, which we did not discuss in the conventional setting and which mitigates to a large extent the issue of waste, is the scale on which a library campaign is run. With advances in

https://www.twirpx.org & http://chemistry-chemists.com

liquid handling and purification capabilities, there is now a tendency to run such chemistries on an analytical scale yielding 1–3 mg of the compounds of interest. In contrast, whereas the platform operates on a relatively efficient scale, only a fraction of the output from the flow reaction is segmented from the major product peak and processed through purification, thus leading to the remainder being treated as waste. In this paradigm, sample transfers/logistics are effectively replaced after purification by dilution, this leaves residual organic solvents, which could in principle interfere with the assay. Finally, concentration is assayed by ELSD as opposed to arguably a more rigorous approach based on accurate weighing after a standard library prep. The biggest distinction though between the two approaches from a chemistry perspective is based on the number of and speed by which compounds get made. While with a conventional approach, the synthesis of all the compounds in the matrix will be attempted, and although ~25–30% will fail (given that the same chemistry is being employed, it is a somewhat safe assumption to say that the synthesis of the same compounds will fail in both paradigms), one is highly likely to identify the same activity trends as one would with the platform-based approach in which only a subset of compounds are synthesized (~24% in the Abl example) based on a predictive algorithm. In the latter case, these compounds in tandem with the up-front model data provided informs the heatmap for the remaining (i.e. those not synthesized) compounds potency data. One caveat to an assumption we have made herein is that the use of a flow-based method of synthesis may allow access to novel ("forbidden") compound space or enable compounds to be obtained (either through superior purifications of "low-yielding" reactions or through enhanced reactivity), which would be classed as "failed" under normal circumstances. Still though, to some degree, the questions around "gaps in data" from compounds that fail synthesis (or are not made) lead to frustrations of potential missed opportunities for practicing medicinal chemists.

To conclude the study on the identification of novel Abl inhibitors, four of the compounds (**188**–**191**) identified from the platform were resynthesized as solids for further profiling. Three of these featured the novel pyrazole urea (**186**), while one presented an amide-linker, all possessing novel heterocycles as the hinge-binding motif. In contrast, all the compounds possessed the same aryl moiety of the DFG-binding fragment found in ponatinib (**137**). For further validation of the data obtained from the platform a further, five mildly potent compounds were resynthesized for testing. In general, for all the compounds, the correlation between platform, retest on solid material, and predicted values (Abl1 only) for Abl1/Abl2 IC50 data was excellent (Figure 4.17).

The four lead compounds (**188**–**191**) showed excellent potency against all the clinically relevant Abl-mutants (including T315I) as well as good selectivity against closely related kinases. While the compounds had mediocre physicochemical properties (clearance, permeability), it is proposed that further loops of optimization could address this. The identification of the pyrazole urea DFG-out motif (**186**) as a replacement for the benzamide present in ponatinib (**137**) is cited as the highlight of the endeavor, though it is important to recognize that this decision was implicit in the compound design for the initial selection of the building blocks [31].

https://www.twirpx.org & http://chemistry-chemists.com

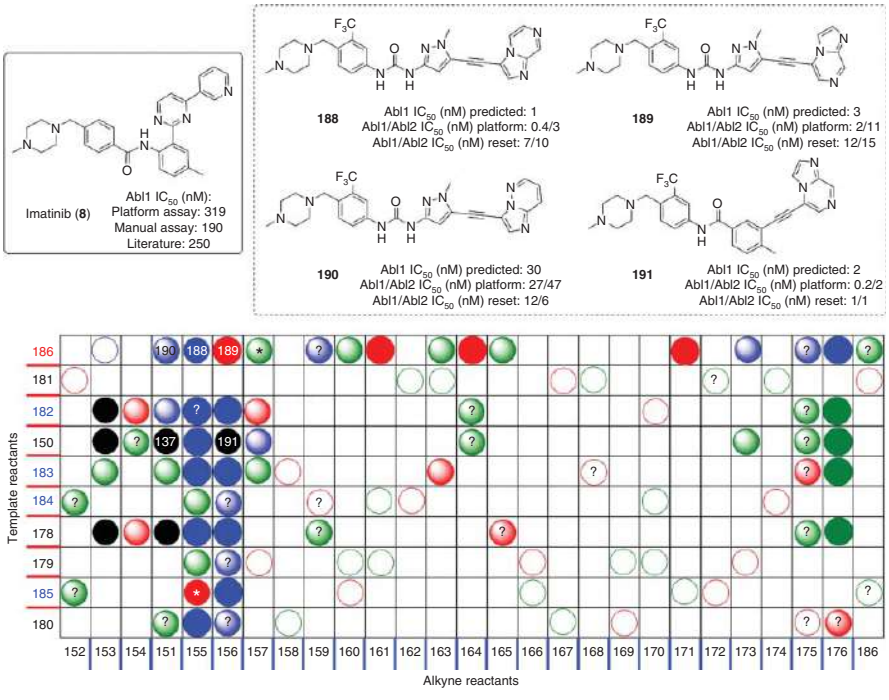

Figure 4.17 Lead analogs identified through the platform optimization process. Also shown highlighted on the heatmap demonstrating identification of "pyrazole urea" template as a novel motif for DFG binding.

https://www.twirpx.org & http://chemistry-chemists.com

4.9 Conclusion

The work described herein has aimed to present a somewhat different perspective on the utilization of flow chemistry with a view to its implementation in a medicinal chemistry setting with a specific focus on how it has been utilized in cases directed to one target (Bcr-Abl kinase). It is interesting to compare/contrast the various synthetic approaches described toward imatinib in a critical manner looking at not only their ability to rapidly make analogs of the lead compound but also in terms of their long-term sustainability in being directly employed to make multigram quantities of the compound of interest [32]. One common feature that emerges is that a fair amount of development/optimization is required to have the right conditions and reactor configuration to execute on the transformation of interest. This presents a barrier to uptake of flow chemistry in medicinal chemistry laboratories, and there has been a shift with literature reports providing more modular approaches to performing flow chemistry in a more seamless manner [33]. These will no doubt continue to emerge, though there remains a gap typically in industrial research laboratory flow, presenting a "go-to" solution for specific challenges such as hazardous [34] or photoredox-based chemistries for conventional chemists with dedicated technology specialists tasked with developing high-value sustainable flow-based platforms applicable to a wider portfolio of projects around areas such as high-throughput reaction optimization [35] and focused library syntheses [36].

References

1 See for example (a) Gioiello, A., Piccinno, A., Lozza, A.M., and Cerra, B. (2020). Medicinal chemistry in the era of machines and automation: recent advances in continuous flow technology. *J. Med. Chem.* 63: 6624–6647. (b) Baumann, M., Moody, T.S., Smyth, M., and Wharry, S. (2020). A perspective on continuous flow chemistry in the pharmaceutical industry. *Org. Process Res. Dev.* 24 (10): 1802–1813. (c) Porta, R., Benaglia, M., and Puglisi, A. (2016). Flow chemistry: recent developments in the synthesis of pharmaceutical products. *Org. Process Res. Dev.* 20 (1): 20–25. (d) Bogdan, A.R. and Dombrowski, A.W. (2019). Emerging trends in flow chemistry and applications to the pharmaceutical industry. *J. Med. Chem.* 62 (14): 6422–6468. (e) Bogdan, A.R. and Organ, M.G. (2018). Flow chemistry as a drug discovery tool: a medicinal chemistry perspective. *Top. Heterocycl. Chem.* 56: 319–342. (f) Browne, D.L., Howard, J.L., and Schotten, C. (2017). Continuous flow processing as a tool for medicinal chemical synthesis. *Compr. Med. Chem. III* 1: 135–185. (g) Fanelli, F., Parisi, G., Degenarro, L., and Luisi, R. (2017). Contribution of microreactor technology and flow chemistry to the development of green and sustainable synthesis. *Beilstein J. Org. Chem.* 13: 520–542. (h) Jensen, K.F. (2017). Flow chemistry-microreaction technology comes of age. *AlChE J.* 63 (3): 858–869. (i) Lummiss, J.A.M., Morse, P.D., Beingessner, R.L., and Jamison, T.F. (2017). Towards more efficient, greener syntheses through flow chemistry. *Chem. Rec.* 17 (7): 667–680. (j) Baumann, M. and Baxendale,

https://www.twirpx.org & http://chemistry-chemists.com

I.R. (2015). The syntheses of active pharmaceutical ingredients (APIs) using continuous flow chemistry. *Beilstein J. Org. Chem.* 11: 1194–1219.

2 Plutschack, M.B., Pieber, B., Gilmore, K., and Seeberger, P.H. (2017). The Hitchhiker's guide to flow chemistry. *Chem. Rev.* 117 (18): 11796–11893.

3 Farrant, E. (2020). Automation of synthesis in medicinal chemistry: progress and challenges. *ACS Med. Chem. Lett.* 11: 1506–1513.

4 See for example (a) Liu, C., Xie, J., Wu, W. et al. (2021). Automated synthesis of prexasertib and derivatives enabled by continuous-flow solid-phase synthesis. *Nat. Chem.* 13: 451–457. (b) Baranczak, A., Tu, N.P., Marjanovic, J. et al. (2017). Integrated platform for expedited synthesis-purification-testing of small molecule libraries. *ACS Med. Chem. Lett.* 8: 461–465. (c) Ahn, G.-N., Sharma, B.M., Lahore, S. et al. (2021). Flow parallel synthesizer for multiplex aryl diazonium libraries via efficient parameter screening. *Commun. Chem.* 4: 53. https://doi.org/10.1038/s42004-021-00490-6. (d) Perera, D., Tucker, J.W., Brahmbhatt, S. et al. (2018). A platform for automated nanomole-scale reaction screening and micromole-scale synthesis in flow. *Science* 359 (6374): 429–434. (e) Chatterjee, S., Guidi, M., Seeberger, P.H., and Gilmore, K. (2020). Automated radial synthesis of organic molecules. *Nature* 579: 379–384. (f) Hart, T., Schultz, V.L., Thomas, D. III, et al. (2020). Development of a versatile modular flow chemistry benchtop system. *Org. Process Res. Dev.* 24: 2105–2112.

5 (a) Cossar, P.J., Hizartzidis, L., Simone, M., I. et al. (2015). The expanding utility of continuous flow hydrogenation. *Org. Biomol. Chem.* 13: 7119–7130. (b) Bryan, M.C., Wernick, D., Hein, C.D. et al. (2011). Evaluation of a commercial packed bed flow hydrogenator for reaction screening, optimization, and synthesis. *Beilstein J. Org. Chem.* 7: 1141–1149.

6 See (a) Paul, S.M., Mytelka, D.S., Dunwiddie, C.T. et al. (2010). How to improve R&D productivity: the pharmaceutical industry's grand challenge. *Nat. Rev. Drug Discovery* 9: 203–241. (b) Plowright, T., Johnstone, C., Kihlberg, J. et al. (2012). Hypothesis driven drug design: improving quality and effectiveness of the design–make–test–analyse cycle. *Drug Discovery Today* 17: 56–62.

7 For commentaries on the challenges in flow chemistry, see (a) Wegner, J., Ceylan, S., and Kirschning, A. (2011). Ten key issues in modern flow chemistry. *Chem. Commun.* 47: 4583–4592. (b) Hartman, R.L., McMullen, J.P., and Jensen, K.F. (2011). Deciding whether to go with the flow: evaluating the merits of flow reactors for synthesis. *Angew. Chem. Int. Ed.* 50 (33): 7502–7519. (c) Sharma, M.K., Acharya, R.B., Shukla, C.A., and Kulkarni, A.A. (2018). Assessing the possibilities of designing a unified multistep continuous flow synthesis platform. *Beilstein J. Org. Chem.* 14: 1917–1936. (d) Rossetti, I. and Comppagnoni, M. (2016). Chemical reaction engineering, process design and scale-up issues at the frontier of synthesis: flow chemistry. *Chem. Eng. J.* 296: 56–70.

8 Guides to approaching the implementation of flow chemistry have appeared in the literature. See for example (a) Britton, J. and Jamison, T.F. (2017). The assembly and use of continuous flow systems for chemical synthesis. *Nat. Protoc.* 12: 2423–2446. (b) Guidi, M., Seeberger, P.H., and Gilmore, K. (2020). How to approach flow chemistry. *Chem. Soc. Rev.* 49: 8910–8932.

https://www.twirpx.org & http://chemistry-chemists.com

9 See for example (a) Politano, F. and Oksdath-Mansilla, G. (2018). Light on the horizon: current research and future perspectives in flow photochemistry. *Org. Process Res. Dev.* 22 (9): 1045–1062. (b) Harper, K.C., Moschetta, E.G., Bordawekar, S.V., and Wittenberger, S.J. (2019). A laser driven flow chemistry platform for scaling photochemical reactions with visible light. *ACS Cent. Sci.* 5 (1): 109–115. (c) Sambiagio, C. and Nöel, T. (2020). Flow photochemistry: shine some light on those tubes! *Trends Chem.* 2 (2): 92–106.

10 Deadman, B.J., Hopkin, M.D., Baxendale, I.R., and Ley, S.V. (2013). The synthesis of Bcr-Abl inhibiting anticancer pharmaceutical agents imatinib, nilotinib and dasatinib. *Org. Biomol. Chem.* 11: 1766–1800.

11 Zimmermann, J., Buchdunger, E., Mett, H. et al. (1997). Potent and selective inhibitors of the ABL-kinase: phenylaminopyrimidine (PAP) derivatives. *Bioorg. Med. Chem. Lett.* 7 (2): 187–192.

12 See (a) Hopkin, M.D., Baxendale, I.R., and Ley, S.V. (2013). An expeditious synthesis of imatinib and analogues utilising flow chemistry methods. *Org. Biomol. Chem.* 11: 1822–1839. (b) Hopkin, M.D., Baxendale, I.R., and Ley, S.V. (2010). A flow-based synthesis of imatinib: the API of Gleevec. *Chem. Commun.* 46: 2450–2452.

13 Baxendale, I.R., Griffiths-Jones, C.M., Ley, S.V., and Tranmer, G.K. (2006). Preparation of the neolignan natural product grossamide by a continuous-flow process. *Synlett* 2006: 427–430.

14 Noël, T. and Buchwald, S.L. (2011). Cross-coupling in flow. *Chem. Soc. Rev.* 40: 5010–5029.

15 Yang, J.C., Niu, D., Karsten, B.M. et al. (2016). Use of a "catalytic" cosolvent, *N,N*-dimethyl octanamide, allows the flow synthesis of imatinib with no solvent switch. *Angew. Chem. Int. Ed.* 55: 2531–2535.

16 Nöel, T., Naber, J.R., Hartman, R.L. et al. (2011). Palladium-catalyzed amination reactions in flow: overcoming the challenge of clogging via acoustic irradiation. *Chem. Sci.* 2: 287–290.

17 Naber, J.R. and Buchwald, S.L. (2010). Packed-bed reactors for continuous-flow C–N cross-couplings. *Angew. Chem. Int. Ed.* 49: 9469–9474.

18 Hartman, R.L., Naber, J.R., Buchwald, S.L., and Jensen, K.F. (2010). Multistep microchemical synthesis enabled by microfluidic distillation. *Angew. Chem. Int. Ed.* 49: 899–903.

19 Fu, W.C. and Jamison, T.F. (2019). Modular continuous flow synthesis of imatinib and analogues. *Org. Lett.* 21: 6112–6116.

20 Battilocchio, C., Hawkins, J.M., and Ley, S.V. (2014). Mild and selective heterogeneous catalytic hydration of nitriles to amides by flowing through manganese dioxide. *Org. Lett.* 16: 1060–1063.

21 Ingham, R.J., Riva, E., Nikbin, N. et al. (2012). A "catch–react–release" method for the flow synthesis of 2-aminopyrimidines and preparation of the imatinib base. *Org. Lett.* 14 (15): 3920–3923.

22 (a) Baumann, M., Baxendale, I.R., Ley, S.V. et al. (2008). Azide monoliths as convenient flow reactors for efficient Curtius rearrangement reactions. *Org. Biomol. Chem.* 6: 1587–1593. (b) Grace Russel, M., Veryser, C., Hunter, J.F. et al. (2020).

https://www.twirpx.org & http://chemistry-chemists.com

Monolithic silica support for immobilized catalysis in continuous flow. *Adv. Synth. Catal.* 362: 314–319.

23 Baumann, M. (2019). Integrating continuous flow synthesis with in-line analysis and data generation. *Org. Biomol. Chem.* 16: 5946–5954.

24 Parry, D.M. (2019). Closing the loop: developing an integrated design, make, and test platform for discovery. *ACS Med. Chem. Lett.* 10: 848–856.

25 For reviews on multistep syntheses in flow, see (a) Wegner, J., Ceylan, S., and Kirschning, A. (2012). Flow chemistry – a key enabling technology for (multistep) organic synthesis. *Adv. Synth. Catal.* 354 (1): 17–57. (b) Webb, D. and Jamison, T.F. (2010). Continuous flow multi-step organic synthesis. *Chem. Sci.* 1: 675–680. (c) Britton, J. and Raston, C.L. (2017). Multi-step continuous-flow synthesis. *Chem. Soc. Rev.* 46: 1250–1271.

26 Desai, B., Dixon, K., Farrant, E. et al. (2013). Rapid discovery of a novel series of Abl kinase inhibitors by application of an integrated microfluidic synthesis and screening platform. *J. Med. Chem.* 56: 3033–3047.

27 See for example (a) Talpaz, M., Shah, N.P., Kantarjian, H. et al. (2006). Dasatinib in imatinib-resistant Philadelphia-chromosome positive leukemias. *N. Engl. J. Med.* 354: 2531–2541. (b) Tanaka, R. and Kimura, S. (2008). Abl tyrosine kinase inhibitors for over-riding Bcr-Abl/T3151I: from the second to the third generation. *Expert Rev. Anticancer Ther.* 8: 1387–1398. (c) Huang, W.S., Metcalf, C.A., Sundaramoorthi, R. et al. (2010). Discovery of 3-[2-(imidazo[1,2-*b*]pyridazin-3-yl)ethynyl]-4-methyl-*N*-{4-[(4-methylpiperazin-1-yl) methyl]-3-(trifluoromethyl)phenyl}benzamide (AP24534), a potent, orally active pan-inhibitor of breakpoint cluster region-Abelson (BCR-ABL) kinase including the T315I gatekeeper mutant. *J. Med. Chem.* 53: 4701–4719. (d) Carlson, R.H. (2011). Ponatinib effective in heavily pretreated CML patients with T315I mutation. *Oncol. Times U.K.* 8 (3): 17–18. (e) Lu, X.Y., Cai, Q., and Ding, K. (2011). Recent developments in the third generation inhibitors of Bcr-Abl for overriding T315I mutation. *Curr. Med. Chem.* 18: 2146–2157. (f) Zhou, T., Commodore, L., Huang, W.-S. et al. (2011). Structural mechanism of the pan-BCR-ABL inhibitor ponatinib (AP24534): lessons for overcoming kinase inhibitor resistance. *Chem. Biol. Drug Des.* 77 (1): 1–11.

28 Deng, X., Lim, S.M., Zhang, J., and Gray, N.S. (2010). Broad spectrum alkynyl inhibitors of T315I Bcr-Abl. *Bioorg. Med. Chem. Lett.* 20: 4196–4200.

29 See for example (a) Zhang, Y., Jamison, T.F., Patel, S., and Mainolfi, N. (2011). Continuous flow coupling and decarboxylation reactions promoted by copper tubing. *Org. Lett.* 13 (2): 280–283. (b) Bogdan, A.R. and James, K.R. (2010). Efficient access to new chemical space through flow construction of drug-like macrocycles through copper-surface-catalyzed azide-alkyne cycloaddition reactions. *Chem. Eur. J.* 16: 14506–14512.

30 Tomberg, A. and Boström, J. (2020). Can easy chemistry produce complex, diverse, and novel molecules? *Drug Discovery Today* 25 (12): 2174–2181.

31 For further examples of exploitation of this platform, see (a) Czechitzky, W., Dedio, J., Desai, B. et al. (2013). Integrated synthesis and testing of substituted xanthine based DPP4 inhibitors: application to drug discovery. *ACS Med.*

https://www.twirpx.org & http://chemistry-chemists.com

Chem. Lett. 4: 768–772. (b) Pant, S.M., Mukonowshuro, A., Desai, B. et al. (2018). Design, synthesis and testing of potent, selective hepsin inhibitors via application of an automated closed-loop optimization platform. *J. Med. Chem.* 61: 4335–4347.

32 Cole, K.P., McClary Groh, J., Johnson, M.D. et al. (2017). Kilogram-scale prexasertib monolactate monohydrate synthesis under continuous-flow CGMP conditions. *Science* 356: 1144–1150.

33 See for example (a) Coley, C.W., Thomas, D.A. III, Lummiss, J.A.M. et al. (2019). A robotic platform for flow synthesis of organic compounds informed by AI planning. *Science* 365 (6453): https://doi.org/10.1126/science.aax.1566. (b) Schweidtmann, A.M., Clayton, A.D., Holmes, N. et al. (2018). Machine learning meets continuous flow chemistry: automated optimization towards the Pareto front of multiple objectives. *Chem. Eng. J.* 352: 277–282. (c) Fabry, D.C., Sugiono, E., and Rueping, M. (2016). Online monitoring and analysis for autonomous continuous flow self-optimizing reactor systems. *React. Chem. Eng.* 1: 129–133. (e) Sans, V. and Cronin, L. (2016). Towards dial-a-molecule by integrating continuous flow, analytics and self-optimisation. *Chem. Soc. Rev.* 45: 2032–2043. (f) McMullen, J.P. and Jensen, K.F. (2010). Integrated microreactors for reaction automation: new approaches to reaction development. *Annu. Rev. Anal. Chem.* 3: 19–42.

34 Movsisyan, M., Delbeke, E., I.P., Berton, J.K.E.T. et al. (2016). Taming hazardous chemistry by continuous flow technology. *Chem. Soc. Rev.* 45: 4892–4928.

35 For overviews of the development and challenges inherent to HTE, see (a) Krska, S.W., DiRocco, D.A., Dreher, S.D., and Shevlin, M. (2017). The evolution of chemical high-throughput experimentation to address challenging problems in pharmaceutical synthesis. *Acc. Chem. Res.* 50 (12): 2976–2985. (b) Shevlin, M. (2017). Practical high-throughput experimentation for chemists. *ACS Med. Chem. Lett.* 8 (6): 601–607. (c)Mennen, S.M., Alhambra, C., Allen, C.L. et al. (2019). The evolution of high-throughput experimentation in pharmaceutical development and perspectives on the future. *Org. Process Res. Dev.* 23 (6): 1213–1242. (d) Welch, C.J. (2019). High throughput analysis enables high throughput experimentation in pharmaceutical process research. *React. Chem. Eng.* 4: 1895–1911.

36 Struble, T.J., Alvarez, J.C., Brown, S.P. et al. (2020). Current and future roles of artificial intelligence in medicinal chemistry. *J. Med. Chem.* 63: 8667–8682.

https://www.twirpx.org & http://chemistry-chemists.com

5

Integrated Systems for Continuous Synthesis and Biological Screenings

Antimo Gioiello, Giada Moroni, and Bruno Cerra

University of Perugia, Laboratory of Medicinal and Advanced Synthetic Chemistry (Lab MASC), Department of Pharmaceutical Sciences, Via del Liceo 1, 06123 Perugia, Italy

5.1 Introduction: Continuous-Flow Technology to Power Medicinal Chemistry

The recent COVID-19 pandemic has highlighted the relevance of drug discovery and related basic sciences to tackle unmet medical needs and suggest therapeutic options to the healthcare system [1]. Research groups from both academia and pharmaceutical companies are facing the challenges of a new disease, a new target, and a new mechanism of action while working with time pressure and safety restrictions. Beyond COVID-19 emergency, drug discovery remains a complex, costly, and well-worn journey. The process starts with the target identification and validation prior to progression into hit identification, lead generation and optimization, and, finally, candidate selection for further development (Figure 5.1). It may take many years to identify molecules that possess suitable activity and property for entering into clinical trials. On the other hand, drug development includes additional steps such as synthetic optimization and scale-up, product formulation, toxicological and clinical studies, and hopefully regulatory approval. Although the majority of drugs fails during the development phase, the range and quality of lead generation are determining factors to reduce attrition in drug discovery [2, 3].

At the early stage of drug discovery, a crucial role is played by medicinal chemistry, a cross-disciplinary science at the interface of chemical biology, pharmacology, and medicine, whose major scope is to discover new chemical entities (NCEs) and chemical probes for understudied and druggable targets (Figure 5.1). Traditionally, medicinal chemistry relies on parallelized and compartmentalized iterative cycles constituted by molecular design, chemical synthesis, biological evaluation, and data analysis such as the structure–activity relationship (SAR), which drives the next learning run [4]. Overall, the process is time-consuming, has low throughput, and is cost ineffective with adverse issues bearing on the R&D productivity. Despite the recent important advances, breakthrough strategies pioneered in academia and developed in pharmaceutical companies are highly desired for solving current critical bottlenecks.

Flow and Microreactor Technology in Medicinal Chemistry, First Edition. Edited by Esther Alza.
© 2022 WILEY-VCH GmbH. Published 2022 by WILEY-VCH GmbH.

https://www.twirpx.org & http://chemistry-chemists.com

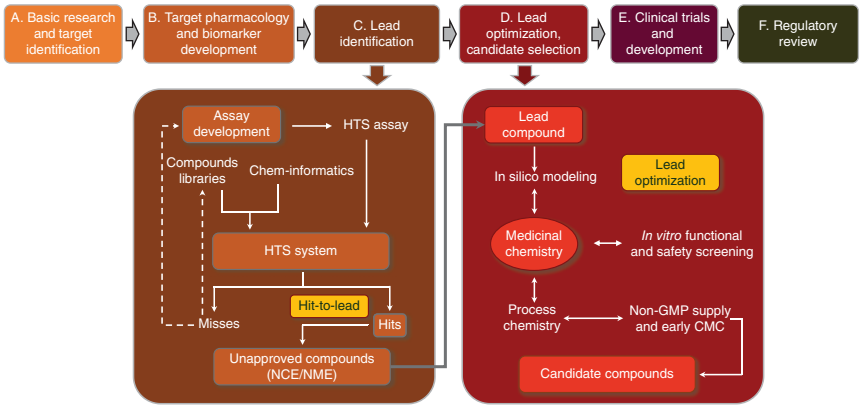

Figure 5.1 Stages of drug discovery and development with focus on activities in lead identification and optimization. NME, new molecular entity; GMP, good manufacturing practice; CMC, chemistry, manufacturing and control.

The past two decades have seen a rapid explosion in the amount of information available to drug makers that have been accompanied by the parallel rise of novel technologies designed to generate, manage, and sort incoming data. Among these, high-throughput screening (HTS) combined with automation and computational tools as artificial intelligence (AI) and learning machines (LM), have greatly extended the capability to design, test, and evaluate compounds [5, 6]. Target assays against in-house compounds collections and virtual screening campaigns are relatively low cost, rapid, and feasible for automation and have become a common practice to identify active compounds (*hits*). During hit-to-lead exploration, hit series are refined by intensive and systematic investigations around the hit core structure to generate compounds that possess desirable functional properties to examine their efficacy in *in vivo* models (*leads*). However, altering the structure of molecules to fine-tune their properties is a complicated task especially when there is the need to develop new routes of synthesis. In this case, the unavailability of versatile synthetic methodologies can limit the design and the number of compounds that medicinal chemists can synthesize. Investments in groundbreaking research toward the development of powerful strategies enabling the efficient compound throughput are therefore crucial to meet the constant demand for compounds to be tested at the different discovery stages. Today this persisting challenge can be addressed by resorting to multimodal approaches, innovative strategies, and enabling technologies that are showing a great potential in improving the process of medicinal chemistry [7–9].

In this scenario, flow chemistry has gained a growing attention and has been applied to reach chemical space and structures that were previously inaccessible, as well as to automate and parallelize chemical synthesis [7, 9, 10]. Such an approach can involve the combination of modular synthesizers with purification devices and analytical tools to facilitate the preparation of pure products ready for testing, to improve reproducibility and scalability, and to reduce costs and

https://www.twirpx.org & http://chemistry-chemists.com

operational risks if compared with manual, serial compound synthesis. In this context, machine-assisted approaches and AI for synthesis planning and reaction predictions can further accelerate target molecule synthesis. Additional benefits come from the full integration of flow synthetic systems with screening assays, robotics, computational design, and decision-making support algorithms bearing the promise to power medicinal chemistry [7, 9, 10].

In this chapter, we emphasize those studies exemplifying the efforts made in the development of flow-based systems and strategies and their impact on medicinal chemistry projects. In particular, we focus on reports that have shown the potential of these technologies for lead discovery and optimization providing streamlined approaches and a more efficient data flow. Starting from concepts and equipment, we discuss major achievements in integrating flow chemical synthesis with in-line purification and analysis of compound collections readily available for bioassays. Furthermore, latest developments in end-to-end machinery platforms coupling flow synthesis with automation, screening, computational design, and analysis as a whole discovery circuit will be also illustrated.

5.2 Equipment, Automated Systems, and Methods for Flow-Based Medicinal Chemistry

Arguably, the hit-to-lead and lead optimization are critical and rate-limiting step in drug discovery and represent a great opportunity for innovation and technological development. In this regard, two key issues are sought to be addressed in order to push current limits: streamline chemical synthesis and make medicinal chemistry learning cycles faster and efficient. Indeed, the development of a range of synthetic routes for the preparation of pure compounds is probably the major bottleneck when optimizing functional molecular properties [11], given that bench chemistry is a labor-intensive, time-consuming, and an expensive commitment. A way to strengthen the capacity of synthesis stands in the application of continuous-flow technology that is demonstrating impactful in method development and synthesis as it offers tools that provide a greater support from the discovery to the clinical development and drug manufacturing. Indeed, flow-based approaches cover the need for rapid and clean synthesis of compounds libraries with challenges for implementing robust, cost-effective process suitable for manufacture. Recent advances have further increased the amenability of flow synthesis for automation, thus reducing manual intervention, especially for repetitive experimental operations as analogs synthesis and experimental screening, while improving efficiency, safety, and environmental impact [12–14]. Thus, the coupling of flow reactors with downstream tools, software-assisted analytical devices, and feedback controls have simplified sequential operations from reagent filling to product purification and collection (Figure 5.2) [15, 16, 18]. As a breakthrough strategy, end-to-end platforms that integrate synthesis with real-time screening and computing are set to provide effective strategies to revolutionize medicinal chemistry and discovery approaches [7, 9, 10]. In order to give the reader an idea of the potential of flow chemistry

https://www.twirpx.org & http://chemistry-chemists.com

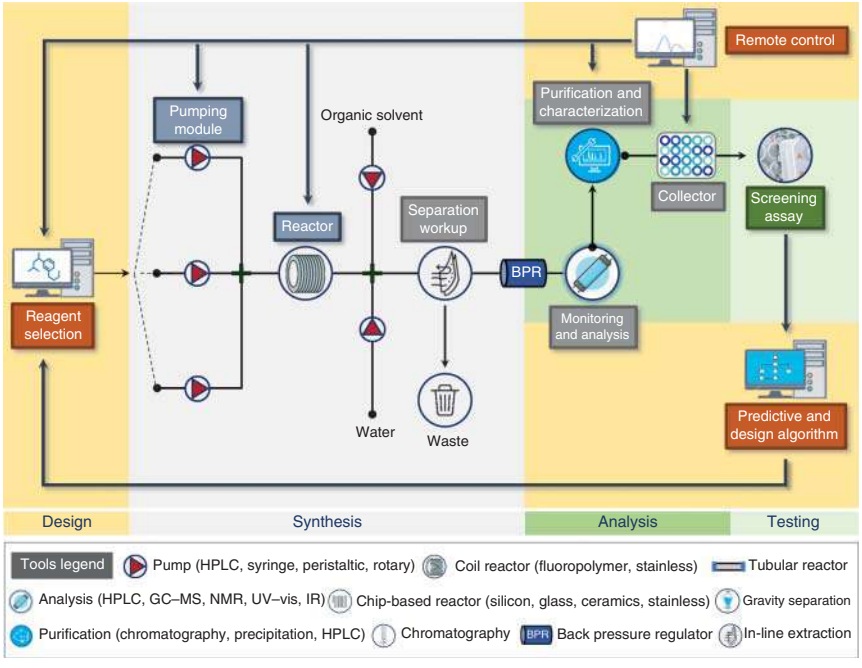

Figure 5.2 Integrated fluidic workflow for the automated molecular design–synthesis–screening–analysis–optimization for iterative medicinal chemistry discovery cycles. Source: Based on Refs. [15–17].

tools, the key features of each flow zone will be discussed with a particular focus on medicinal chemistry applications.

5.2.1 Continuous-Flow Synthesis Machines

In the last years, flow synthesizers have shown the capacity of complementing batch chemistry in multistep synthesis and innovating protocols and methods in response to current limitations and standards. The concept of flow chemistry defines chemical processes that occur in a continuous-flowing stream by reactor-based synthesizers. Pumps continuously move reagents into a reactor where reactions take place and the product is continuously collected. Benefits of adopting flow approaches derive from specific intrinsic characteristics of flow technology [17]. First of all, flow reactors allow to conduct reactions with a more precise control over the experimental conditions, thus ensuring a higher product quality, more reliable methods, and a smaller footprint in scaling-up operations. Substrates and reagents are efficiently mixed with a better heat/mass transfer that translates into improved reaction rates and productivity while enabling superheated conditions and a wider reactivity performance because of pressurization regimes. Furthermore, flow synthesizers allow the execution of hazardous chemical transformations under safety standards reducing manual handling and risks for operators, also for telescoped and multistep synthesis [19, 20].

https://www.twirpx.org & http://chemistry-chemists.com

A flow synthesizer consists of diverse interconnected and modular units, which are commercially available to meet the nature of the reaction and reactants (Figure 5.2). The modularity of flow equipment allows diverse adaptable combinations and setups by using non-wetted parts, as nuts and ferrules, that link the tubing to the respective flow zone. A typical synthesis setup includes eight basic zones: solution and reagent delivery, mixing, reactor, separator, pressure control, monitoring/analysis, purification, and collection. In the following text, we provide a brief overview on the component tools for integrated compound flow synthesis, purification, and analysis; for reviews that exhaustively cover this topic, see Plutschack et al. [17] and Ley et al. [21]:

(a) *Pumping modules*, including high-performance liquid chromatography (HPLC), syringe, peristaltic, and rotary pumps, are used to generate a continuous-flowing stream that moves reaction components fluid into the reactor under a precise control. They tightly regulate the residence time and reagent stoichiometry and can deliver homogeneous and heterogeneous solution (liquid/gas). Reagents can be eventually preloaded by sample loops.
(b) *Reactor* is the key flow unit where the reaction occurs [7, 17]. There exist diverse types such as chip-based and coil reactors whose working temperatures can be accurately regulated by thermocouples, cryogenic units, microwave irradiation, and inductive heating. Photochemical and electrochemical reactors are also available for photo- and electrochemistry. Finally, tubular, packed-bed, and tube-in-tube reactors are ideal for heterogeneous transformations that involve the use of solid catalysts, supported reagents, and gases.
(c) *Separators* employed in continuous downstream operations include camera-and-computer-based gravity separation device as well as liquid–liquid membrane-based extractor [22]. Gravity separators use a "computer-vision" approach for the dynamic flow control of the interface level between the organic and aqueous phase. On the other hand, liquid–liquid membrane separations are based on the exploitation of surface forces, a membrane wetted by one of the phases, and a pressure control element that ensures adequate operating conditions.
(d) *Analysis* of flow reactions can be carried out offline by collecting and analyzing samples manually. Automating sampling and measurement can be achieved by online analysis using HPLC, gas chromatography (GC), mass spectrometry (MS), X-ray diffraction (XRD) and in-line spectroscopy as Fourier transform infrared (FTIR), ultraviolet–visible (UV–Vis), and nuclear magnetic resonance (NMR) by means of flow-through cells. As later discussed, these last two approaches are preferred to streamline compound synthesis and characterization (see also Section 5.2.2).
(e) *Purification systems* operating in a continuous-flow modality are generally based on the use of columns or cartridges filled or packed with functionalized polymeric resins able to remove excess reagents or impurities ("scavenger" approach) or to selectively trap and then release the target product ("catch-and-release" approach) [23]. Additional purification techniques

https://www.twirpx.org & http://chemistry-chemists.com

include simulated moving-bed chromatography [24], distillation [25], and crystallization equipment [26].

(f) *Collectors* are now made available to automate compounds synthesis, analysis, and screening. The active fluidic control may be also coupled with a feedback control mechanism, for sample collection. Alternatively, after depressurization, the flow stream can be simply collected in a flask before or after downstream operations.

5.2.2 Process Analytical Technology (PAT) for Effective Integration of Synthesis and Biological Screenings in Continuous Flow

As exhaustively introduced in Chapter 2, the development of autonomous flow platforms requires the integration of process analytical technology (PAT) that enables the remote control, analysis, and structural characterization of the synthesized compounds [27, 28]. The term PAT embraces a variety of chemical, physical, microbiological, mathematical, and statistical tools and analytical measurements. In-line analysis can be performed by connecting a suitable analytical device in-series to the reactor, and the reaction mixture is analyzed right after leaving the reactor module to acquire real-time data. Although feasible in principle, compatibility between the detector and experimental reaction conditions may limit and render the actual application quite challenging. Alternatively, the analysis can be achieved by online sampling: in this case, switching valves and fluid diverting devices can be inserted within the fluidic path to split and direct aliquots of the flow stream toward the analytical equipment [29–31]. Numerous techniques, detectors, and devices are currently available for continuous-flow operations. The selection of the most appropriate PAT depends on the nature and characteristics of the flow process and on the type of information needed (Table 5.1) [40]. HPLC and GC are the most commonly used techniques as they are commercially available at low cost, easy to use, and versatile. Moreover, although more expensive, benchtop MS coupled with HPLC and NMR are preferable techniques as they permit both the quantification and structural determination of the synthesized products in a high-throughput fashion [37, 38].

5.2.3 Bioassays for In-line Compound Screening

Telescoping compound synthesis with biological evaluation using flow provides opportunity to remove spatiotemporal boundaries, long feedback timing, and delay from compound design to data analysis. Moreover, the use of small volumes of compound (from nl to pl) and the nature of flow mixing, especially under microfluidic conditions, allow to reduce waste, improve reproducibility and accurateness, and shorten time of analysis. In this section, we describe examples of bioassays development that have provided proof of concept for in-line compound testing useful for hit identification and hit-to-lead programs. Exemplifications of droplet microfluidic assays for DNA assembly, transformation/transfection, culturing, cell sorting, phenotypic assays, artificial cells, and genetic circuits were recently reviewed by Gach et al. [41].

https://www.twirpx.org & http://chemistry-chemists.com

Table 5.1 Process analytical technology in flow chemistry.

Technique	Main applications	Advantages	Limitations	References
UV–visible spectroscopy	Processes monitoring Reaction analysis Quantitative determinations	High versatility Low cost Online monitoring No sampling	Low throughput Limited structural information	[32]
Fluorescence	Immunoassays Quantitative determinations	High sensitivity Noninvasive Online monitoring	Low throughput Limited structural information Fluorophore is needed	[33]
Raman spectroscopy	Quantitative determinations Kinetic studies	Low cost Noninvasive Online monitoring No sampling	Low throughput Limited structural information	[34]
Infrared spectroscopy (IR and MIR)	Processes monitoring Reaction analysis	Low cost Noninvasive Online monitoring No sampling	Low throughput Limited structural information	[35]
High-performance liquid chromatography/gas chromatography	Quantitative determinations Qualitative analysis when coupled with MS techniques	Low cost High versatility Broad applicability	Sampling step may be required	[36]
Mass spectroscopy	Quantitative and qualitative analysis	High throughput High sensitivity High selectivity	High costs Sampling step required	[37]
Nuclear magnetic resonance	Quantitative and qualitative analysis	High throughput High selectivity	High costs Sampling step required	[38]
Reaction calorimetry	Evaluation of potential hazardous reaction mechanism and kinetic	Fast Robustness	Moderate versatility and applicability	[39]

Source: Yue et al. [32] / John Wiley & Sons.

https://www.twirpx.org & http://chemistry-chemists.com

An early example of integrated library screening was reported by Hirata et al. to measure the activity of diverse compounds against the human immunodeficiency virus (HIV) protease substrate-1 using a fluorescence resonance energy transfer (FRET) assay (Figure 5.3a) [42]. The system consisted of two pumps, two superloop devices, two coil reactors, an automated injector, and a fluorescence detector-based flow cell. The enzyme and compound solution were mixed into the first coil reactor by the carrier buffer pumped from syringe A. The superloop A introduced the protease solution into the coil reactor A, while the six-port autoinjector loaded the inhibitor solutions at diverse concentrations. The output from reactor A containing the enzyme/inhibitor mixture was then combined with the stream of the HIV protease substrate-1 to flow into the coil B. Finally, the mixture eluted to the fluorescence detector (excitation wavelength: 340 nm, emission wavelength: 490 nm) allowed to determine enzyme inhibition and dose–response curves. The continuous-flow assay was later improved with size-exclusion liquid chromatography (LC) for testing complex mixtures for protein inhibitors [43].

In 2010, Heus et al. developed a confocal fluorescence detection assay based on a nano-LC coupled to a light-emitting diode (LED) (Figure 5.3b) [44]. The system was based on a microchip reactor and a nano-LC effluent containing the potential inhibitor. The detection unit included a high intensity LED lamp, a series of excitation and emission filters, a confocal lens, a dichroic mirror, a photomultiplier tube, and a bubble cell capillary. Thus, the solution of acetylcholine binding protein (AChBP) and the fluorescent tracer ligand (DAHBA) was mixed with the nano-LC effluent within the microchip coupled to LED lamp. The light generated by the high intensity LED lamp was filtrated thought a 465 nm single bandpass filter, collimated by a confocal lens, and reflected at an angle of 90° into a bubble cell capillary through a 520 nm dichroic mirror. Finally, a photomultiplier tube detected the fluorescence variation due to the displacement of the fluorescent tracer ligand by the eluting protein ligand.

Also, electrochemical transformations have been successfully exploited to develop continuous-flow bioaffinity assay specifically applied for the identification of p38α mitogen-activated protein kinase inhibitors (Figure 5.3c) [45]. The apparatus was made by an electrochemical reaction cell, a LC, a continuous-flow bioaffinity unit equipped with a fluorescence detector, and a mass spectrometer. The solution of kinase inhibitors dissolved in the appropriate buffer was pumped through an electrochemical reactor and purified by in-line LC. After the electrochemical conversion and purification, the eluate was divided in two aliquots by a switching valve: a part was combined with the enzyme (p38 kinase α) and directed into the reaction coil A for the bioassay, while the remaining sample was analyzed by high-resolution LC–MS. A tracer molecule was added and combined into the reaction coil B, and the enzyme–tracer complex was determined by fluorescence, allowing the rapid characterization of novel p38 kinase-α inhibitors.

More recently, Patel and coworker described a microfluidic continuous-flow injection titration assay (CFITA) for monitoring the inhibition of thrombin peptidase activity (Figure 5.3d) [46]. The CFITA assay equipment was composed by a four-channels pumping system for delivering the enzyme (thrombin), its

https://www.twirpx.org & http://chemistry-chemists.com

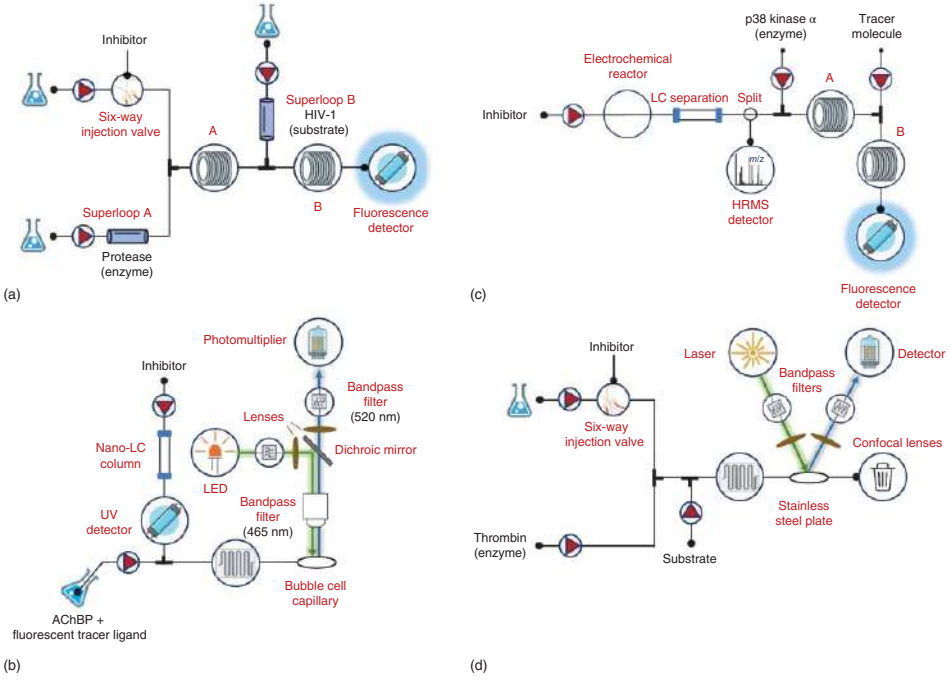

Figure 5.3 In-line screenings for continuous bioassays. (a) Continuous-flow fluorescence resonance energy transfer (FRET) assay for HIV hit discovery. (b) Microfluidic confocal fluorescence detection assay for the identification of acetylcholine binding protein inhibitors. (c) Integration of electrochemical reaction cell with a continuous-flow bioaffinity assay and LC-HRMS analysis. (d) Microfluidic continuous-flow injection titration assay (CFITA) for monitoring inhibition of thrombin peptidase activity. Source: Based on Refs. [42–46].

https://www.twirpx.org & http://chemistry-chemists.com

substrate, and enzyme inhibitors dissolved in a buffer containing Cy5 dye as the internal standard. Inhibitor titration was started by switching the six-way injection valve from "load" to "injection" position, and, at the same time, an additional pump delivered the buffer into the inhibitor channel to generate the gradient. The bioassay occurred into a stainless steel plate, while the optical equipment was made by bandpass filter, dichroic filters, a laser module for inducing the excitation, and a set of aspheric confocal lenses for baseline correction. Check valves and adapters were connected following the pumps in order to prevent backflow and for reducing tubing diameter. A digital flowmeter guaranteed the monitoring of the total system flow rate. Importantly, the CFITA assay has been recently employed and integrated into the Cyclofluidic closed-loop drug discovery flow platform [47] (see Section 5.4).

5.2.4 General Concepts for Automation, Remote Control, and Software Application to Integrated Systems

Automation bears the promise of making medicinal chemistry faster. Indeed, automation can be applied at the diverse compartments of the discovery cycle including molecular design, compound synthesis, screening, and data analysis [9]. The automation of parallelized operations is essential to ensure the continuous and expedite delivery of pure compounds readily tested to feed predictive bioactivity models and prioritize the synthesis of the subsequent round of compounds. In this context, the implementation of software is critical to fully harness the potential of automated flow-based medicinal chemistry platforms as they guarantee the orchestration and managing of the whole circuit [16, 30]. A number of tools such as the design of experiments [48], mathematical models [49], sophisticated algorithms, including evolutionary, self-optimizing, and machine learning [50–54], and cloud-based programs [12, 55] have been exploited to monitor, manage, and fine-tune integrated flow-based systems, for real-time chemical optimization, prediction, and decision-making purposes, as well as to simply collect, analyze, interpret, store, and make accessible large data set remotely [6, 14]. Also, open-source software and computer-aided technologies for automating flow systems are rapidly growing and include suites as LabVIEW [56], MATLAB® [57], LeyLab [12], OpenFlowChem [58], and ChemOS [59]. LabVIEW is a graphical programming language developed in 1986 and implemented over the last years to the current version 19.0 by National Instruments for automation control and data acquisition [56]. The graphical interface is composed by a front panel, which is an input-containing module, a block diagram that edits codes that will be graphically visualized, and a connector panel serving as connection interface. The network permits the integration and automation of systems, drivers, and benchtop applications also remotely through multiple controls and programming languages. MATLAB is an open-access multi-paradigm numerical software developed by MathWorks Inc. for matrix manipulations, functions plotting, algorithms implementation, and the creation of customizable user interfaces [57]. The software offers the possibility to communicate with other languages as LabVIEW, enabling the automation of reaction screening and optimization, library synthesis, and medicinal chemistry

https://www.twirpx.org & http://chemistry-chemists.com

learning cycle. Along this line, the software LeyLab was created on the concept of Internet of Things (IoT) to control and manage equipment located in different places [60]. The main components of LeyLab are a graphical interface accessed via Internet browser, a database for storing information and data, a communication module, and a command module containing all the code definitions and equipment commands. OpenFlowChem is an open-source platform that uses LabVIEW as the interface and MATLAB for cloud data transfer [58]. The system includes a device monitor able to handle the connected equipment, a module that provides the integration among the instruments, and an optional external safety device. Finally, ChemOS is a software package able to control robotic platforms with AI algorithms [59]. The core of the system is a learning module, which is able to autonomously and continuously propose new sets of parameters for novel experiments on the basis of previous outcomes. As LeyLab, ChemOS allows to control equipment located in different locations.

5.3 Flow Strategies for Building Bioactive Compound Libraries

Prerequisites for successful screening campaigns in drug discovery are the availability and the capability to synthesize compounds for testing. There is therefore a huge request for high-quality compound collections through the efficient building of small molecule libraries. To address this demand, chemists have developed methods and techniques that greatly increase the speed and efficiency of compound synthesis (Figure 5.4) [61]. At early-stage discovery, diversity-oriented synthesis (DOS) appears as the most effective approach as it favors the variation of drug-like basic molecular scaffolds including skeletal and stereochemical diversity. Indeed, molecular diversity is essential for specific binding events with biological targets bearing three-dimensional (3D) unique binding sites and structural diversity [62]. In this paragraph, we discuss examples from diverse groups on the challenges in the preparation of small molecule libraries and the flow methodologies employed to address them.

5.3.1 Click Chemistry

As has been already introduced in Chapter 3, click chemistry represents a powerful toolbox for preparing compound library with a high degree of structural complexity and diversity. Click reactions are stereospecific, versatile toward a wide range of substrates, simple to realize, and often highly efficient, thus not requiring further purifications [63]. Click chemistry has been successfully coupled with combinatorial chemistry, DOS, and bioorthogonal transformations especially in fragment-based approaches and bioisosteric replacement [64–66]. Recently, bioactive compounds have been synthesized by click synthesis under flow conditions, improving significantly product quality and productivity [67].

https://www.twirpx.org & http://chemistry-chemists.com

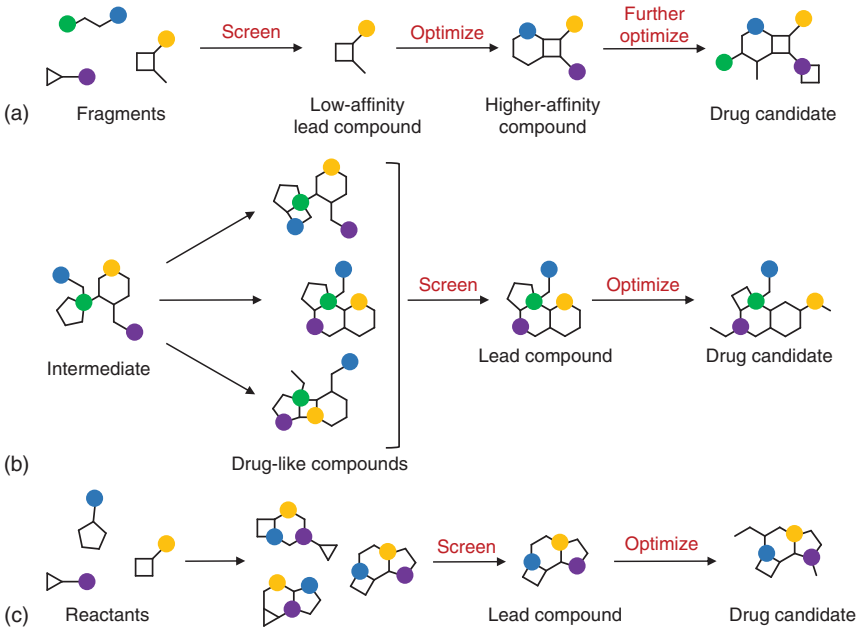

Figure 5.4 Generating compounds collections for lead and drug discovery. (a) Fragment-based screening (FBS) to identify active fragments that are submitted to systematic optimization to generate high-affinity, drug-like compounds. (b) Diversity-oriented synthesis (DOS) typically consists in using a common intermediate to prepare libraries of structurally diverse, drug-like compounds. (c) Multiple-component condensations are reactions in which three or more reactants come together in a single reaction to form a new product which contains portions of all the components. It is not necessary that all components condense in a mechanistically concerted fashion. Source: Adapted from Hajduk et al. [61].

In 2006, Wang et al. reported the automated synthesis of triazoles by Huisgen 1,3-dipolar cycloaddition between azides and acetylenic benzenesulfonamide (**1**) (Figure 5.5) [68]. In particular, the integrated microfluidic circuit was realized to synthesize and screen 32 compounds against the bovine carbonic anhydrase II (*b*CA-II). The microfluidic circuit was set up on a reaction volume of approximately 4 ml using (i) a nanoliter rotary mixer for sampling, accurate dosing, and rotary mixing of different reagents (acetylene azides with or without inhibitors); (ii) microliter chaotic mixer to guarantee an efficient mixing and homogeneous solution between the reagent solutions from the rotary mixing and *b*CA-II buffer; (iii) a microfluidic multiplexer that drove the reaction mixture into the corresponding microvessels for *in situ* click chemistry reactions. The preparation of the entire screening experiments needed approximately 30 minutes. The reaction circuit was placed in a moisture-regulated incubator at 37 °C for 40 hours until reaction competition, and the reaction mixtures were collected into the respective microvessel. LC coupled with MS was useful for the purification and identification of 10 hits out of 32 triazole analogs synthesized.

https://www.twirpx.org & http://chemistry-chemists.com

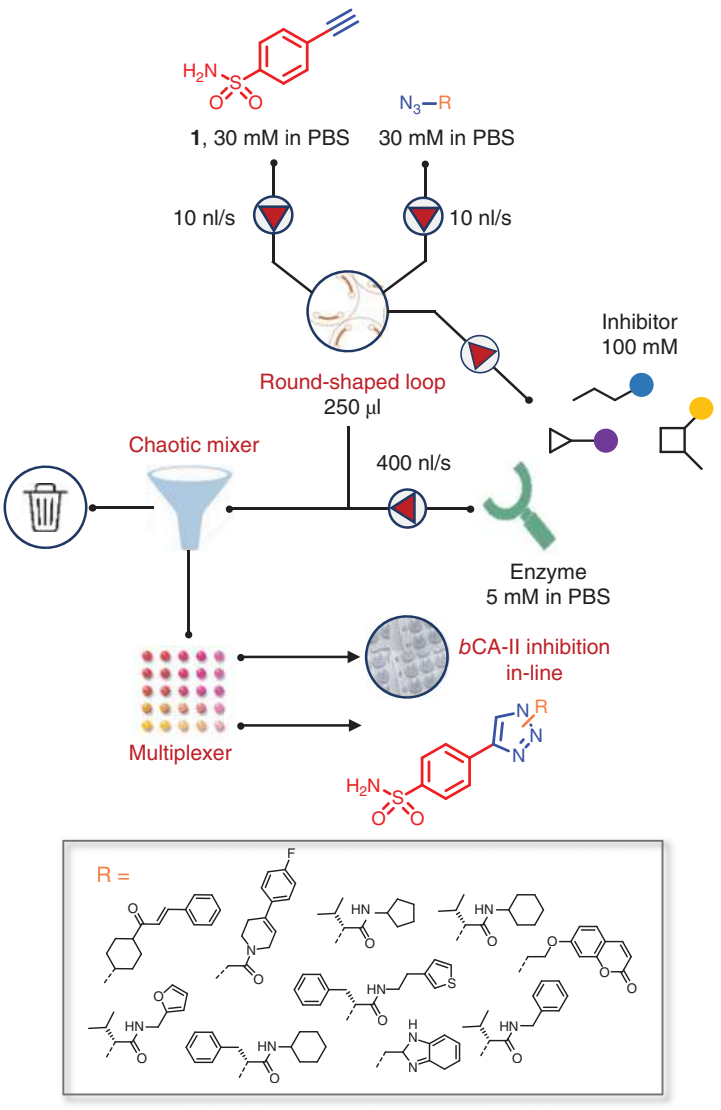

Figure 5.5 Microfluidic platform for parallel synthesis and screening of triazole-based derivatives as carbonic anhydrase II (*b*CA-II) inhibitors. Source: Based on Wang et al. [68].

In 2009, the same authors described a second-generation platform performing 1024 *in situ* click chemistry reactions reducing the volume scale (approximately 400 nl) and the screening time from 1 minute to 17 seconds per cycle [69]. In addition, the reaction circuit was coupled with a solid-phase extraction (SPE) to purify crude mixtures from polar or charged impurities, favoring a faster hit identification by direct electrospray ionization (ESI)–MS and multiple reaction monitoring (MRM) traces. The chip system was composed of a pair of microfluidic multiplexers for reagent loading, a 150 nl rotary mixing, a 250 nl serpentine channel

https://www.twirpx.org & http://chemistry-chemists.com

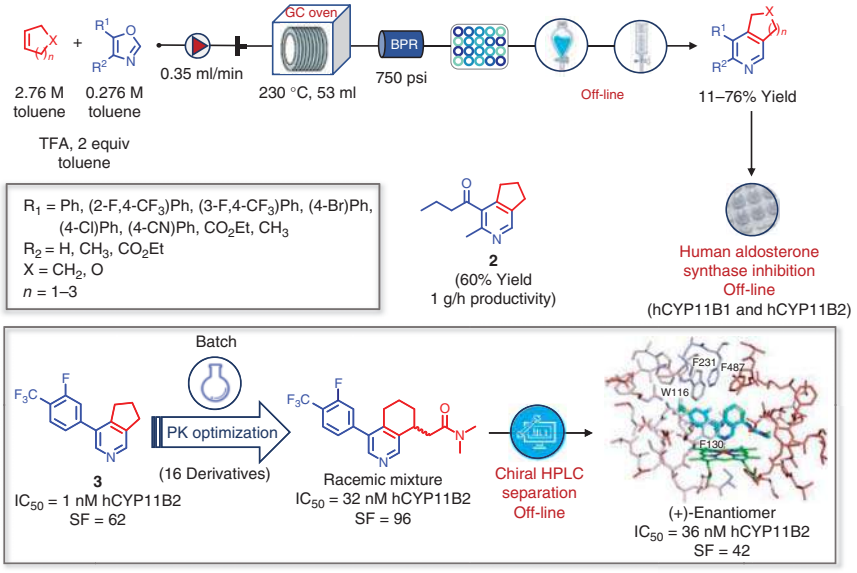

Figure 5.6 Flow synthesis of oxacycloalka- and cycloalka[*c*]pyridines as human aldosterone synthase (hCYP11B2) inhibitors by continuous-flow inverse-electron-demand Kondrat'eva. TFA, trifluoracetic acid. Source: Based on Lehmann et al. [70].

with a total volume of 400 nl, a polytetrafluoroethylen (PTFE) tube for off-chip incubation and storage of the reaction mixtures. The system operations were realized in an automated fashion using a computer-controlled interface (LabVIEW, National Instrument Inc.) able to regulate pneumatically backpressure valves and vacuum suctions. As a result, the entire procedure to screen 1024 reaction mixtures was completed in 290 minutes.

In 2013, Britton and coworkers showed the continuous-flow inverse-electron-demand Kondrat'eva preparation of oxacycloalka- and cycloalka[*c*]pyridines (Figure 5.6) [70]. The synthesis involved a [4 + 2] cycloaddition between cycloalkenes and oxazoles followed by dehydration of the cycloadduct. A model reaction was evaluated under batch microwave conditions, optimized, translated into a flow apparatus, and validated on diverse scaffolds. The customized flow instrumentation was assembled with a HPLC pump, a stainless steel reactor heated by a GC oven, and a back pressure regulator (BPR). The crude products were collected manually and quenched with Et_3N to afford the desired annulated pyridine derivatives in 11–76% isolated yield after chromatographic purification. The scalability of the process was also proved to prepare 6.9 g of ethyl-3-methyl-6,7-dihydro-5*H*-cyclopenta[*c*]pyridine-4-carboxylate (**2**) (yield: 60%; productivity: 1 g/h) (Figure 5.6). A selection of products was tested on human aldosterone synthase (hCYP11B2) to determine the relative IC_{50} values and selectivity factor (SF) over hCYP11B1 [71]. Compound **3** was identified as a potent (IC_{50} = 1 nM) and selective inhibitor (SF = 62) and underwent chemical

https://www.twirpx.org & http://chemistry-chemists.com

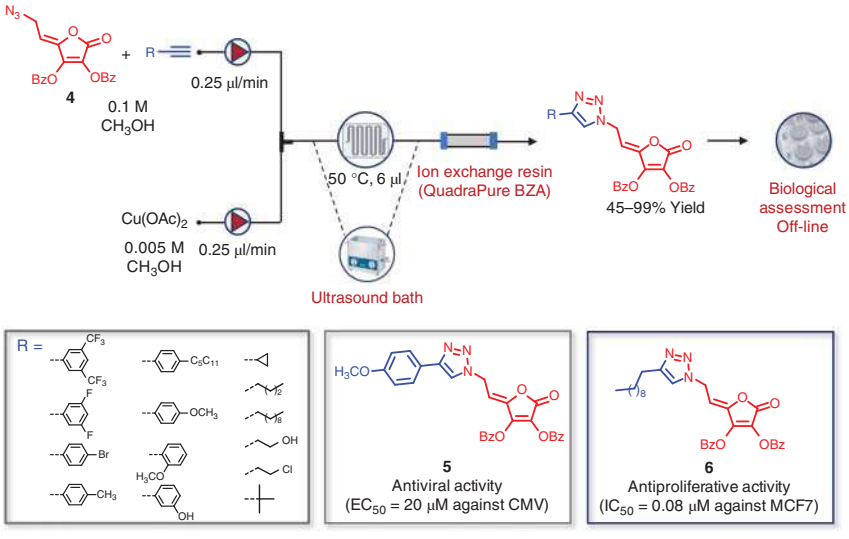

Figure 5.7 Synthesis of 1,2,3-triazolyl-4,5-didehydro-5,6-dideoxy-L-ascorbic acid derivatives by Cu(I)-catalyzed 1,3-dipolar cycloaddition under ultrasound-flow conditions. Reaction were performed by loop injection of a 0.1 M solution of azide (**4**) and alkynes (1 equiv), and a 0.005 M solution of $Cu(OAc)_2$ in MeOH at 0.5 µl/min of total flow rate (τ = 9 minutes). The microreactor was heated at 50 °C and placed into an ultrasound bath (35 kHz). Source: Based on Macan et al. [72].

optimization via batch synthesis to enhance the aqueous solubility and decrease the lipophilicity.

The flow synthesis of a library of 1,2,3-triazolyl-4,5-didehydro-5,6-dideoxy-L-ascorbic acid derivatives for SAR studies was achieved by Cu(I)-catalyzed 1,3-dipolar cycloaddition between an azido intermediate (**4**) and diversely functionalized alkynes (Figure 5.7) [72]. Reactions were performed with $Cu(OAc)_2$ combining ultrasound irradiation with microfluidic reactor to reduce reaction time, avoid side products formation, and improve product yield. Substrates and reagents were loaded into two injection loops and reacted within a microreactor at 50 °C placed into an ultrasound bath. The output was collected by a fraction collector, and the crude mixture was quenched by means of a polymer-supported benzylamine (QuadraPure BZA) scavenger resin. The reaction mixture was filtered on cotton whole and analyzed by HPLC (Figure 5.7). The pure products were evaluated as antiproliferative, antiviral, and scavenging agents with compound **5** exhibiting a good *in vitro* antiviral activity against cytomegalovirus (CMV) (EC_{50} = 20 µM). In addition, the decyl-analog **6** showed a specific antitumoral activity against female tumor cell lines, as breast adenocarcinoma and cervical carcinoma [73]. Interestingly, most of the synthesized derivatives also showed a promising antioxidant activity [74].

More recently, researchers at UCLA (Los Angeles, USA) reported the successful application of a microfluidic system for the identification of small molecule mimetics targeting protein–protein interaction in Alzheimer's disease (AD) [75]. Starting

https://www.twirpx.org & http://chemistry-chemists.com

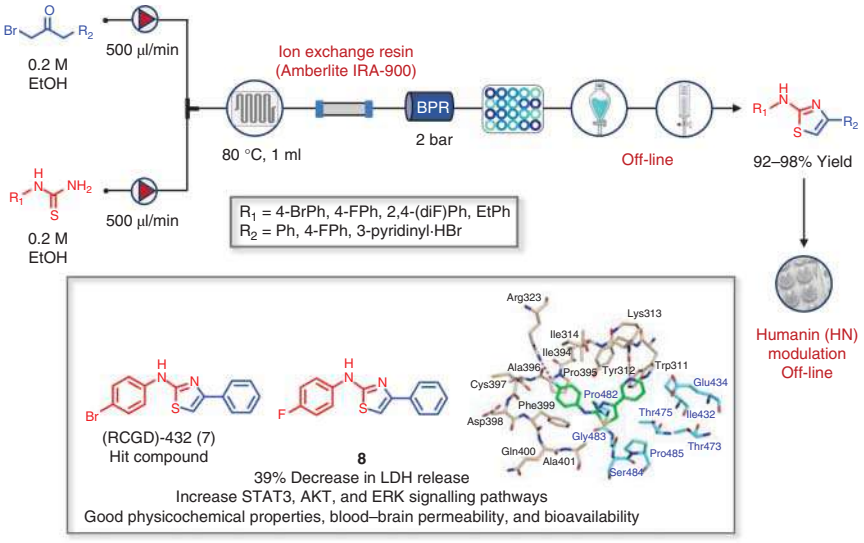

Figure 5.8 Flow synthesis and biological characterization of 2-aminothiazoles as humanin (HN) mimetics. The synthesis was achieved by Hantzsch condensation between 2-bromo-1-arylethan-1-one analogs and arylthiourea derivatives. The reaction components were premixed in 1 : 1 ratio at 0.2 M concentration in EtOH, and the mixture was pumped into a preheated microchip reactor via a syringe pump. The reactor output passed through a column packed with Amberlite IRA-900 to trap the acidic by-product.

from the hit compound (RCGD)-423 (**7**) that was identified by HTS of a UCLA internal library, the design, synthesis, and biological evaluation of a collection of seven 2-aminothiazoles was accomplished by Hantzsch condensation between 2-bromo-1-arylethan-1-ones and arylthiourea derivatives under catalyst-free conditions (Figure 5.8). The reactor output was purified using a column packed with Amberlite IRA-900 to give the desired products in excellent yield (92–98%) after chromatography. The synthesized compounds were then evaluated for NMDA-induced toxicity by measuring the activity of lactate dehydrogenase (LDH) released. Among these, compound **8** was found with an activity comparable to the direct antagonist MK801. The neuroprotective effects of **8** were also confirmed by evaluating the increase in phosphorylation of STAT3, AKT, and ERK signaling pathways in HEK293 cells, SH-SY5Y cells, and primary hippocampal neurons. Finally, the suitable *in silico* physicochemical properties (MW, total polar surface area (TPSA), calculated partition coefficient (cLogP)) and the good blood–brain permeability and bioavailability made compound **8** a promising lead candidate to be advanced in animal models of Alzheimer's disease.

5.3.2 Multicomponent Reactions (MCRs)

Multicomponent reactions (MCRs) involve the one-pot combination of three or more reactants to generate a product that incorporates most of the structural features from the starting materials [76–78]. MCRs are operationally simple yet

https://www.twirpx.org & http://chemistry-chemists.com

synthetically powerful as they offer high structural complexity and molecular diversity in a single step. Step and atom economy, stereochemistry selectivity, possibility for post-modifications, time and energy saving, and environment-friendly conditions are additional characteristics that render MCRs efficient tools for synthetic chemists. Therefore, the development of new MCRs for organic synthesis and medicinal chemistry is highly sought. In this context, the combination of MCRs with enabling technologies as flow chemistry can significantly accelerate the preparation of compound libraries readily available for biological screenings [79].

In 2014, the team of G. Schneider at ETH illustrated the Ugi three-component synthesis under microfluidic conditions coupled with computer-driven ligand–target association prediction of imidazopyridine derivatives (Figure 5.9) [80]. The flow equipment used for this application consisted of a borosilicate DeanFlow microchip, a zigzag mixer, and a solenoid valve for automating the building block filling, dilution, and dispensing. Once optimized, the method was applied for the synthesis of 12 imidazopyridines obtained in 5–53% isolated yields and high purity. The system was coupled with a Gaussian process regression model trained by means of ChEMBL database to obtain the predicted *p*Affinity against different targets. As a result, five potential targets including adenosine receptors A_1 and A_{2B}, adrenergic receptors α_{1A} and α_{1B}, and PDE10A were selected for further investigations. Nine out of twelve compounds matched the predicted outcome when tested in radioligand displacement and cell-based functional activity assays. In particular, compounds **9** and **10** exerted antagonistic activity against the α_{1B} adrenergic receptor, compounds **11** and **12** exhibited a good binding for the adenosine receptors A_1, and compound **13** showed an antagonist profile for the adrenergic α_{1A} and adenosine A_{2B} receptor (Figure 5.9). Finally, design parameters including the ligand efficiency (LE), lipophilic ligand efficiency (LLE), and size-independent ligand efficiency (SILE) were also calculated to drive hit selection toward further chemical exploration.

More recently, the development of the MCR Povarov reaction under continuous-flow mode was exploited for the rapid synthesis of tricyclic and tetracyclic compounds readily available for hit identification and hit-to-lead explorations in the field of steroid-responsive receptors [81, 82]. The synthetic approach was optimized to guarantee flowability, high yield, and productivity using a synthesis platform designed to incorporate mesoreactors, downstream operations, and automation to reduce material handling and to increase safety standards and production, therefore speeding timing from design to test (Figure 5.10).

The syntheses were performed by mixing solutions of aromatic aldehydes and HCl (10 wt%), aromatic amines, and dienophiles in a four-way connector. Reaction components were then pumped into the reactor coil with a total flow rate of 0.8 ml/min at 25 °C. The reactor output was combined with a stream of H_2O and Et_2O to facilitate by extraction the removal of salts and PEG300. The ethereal solution was concentrated and submitted to automated flash chromatography assisted by UV detector for fraction collection before being submitted to *in silico* and *in vitro* screening. Thus, a first set of 22 tricyclic tetrahydroquinolines obtained as racemic mixture in 46–89% yield and >95% purity was characterized in terms of molecular descriptors to assess drug-like criteria and tested for their activity on the G-protein coupled estrogen

https://www.twirpx.org & http://chemistry-chemists.com

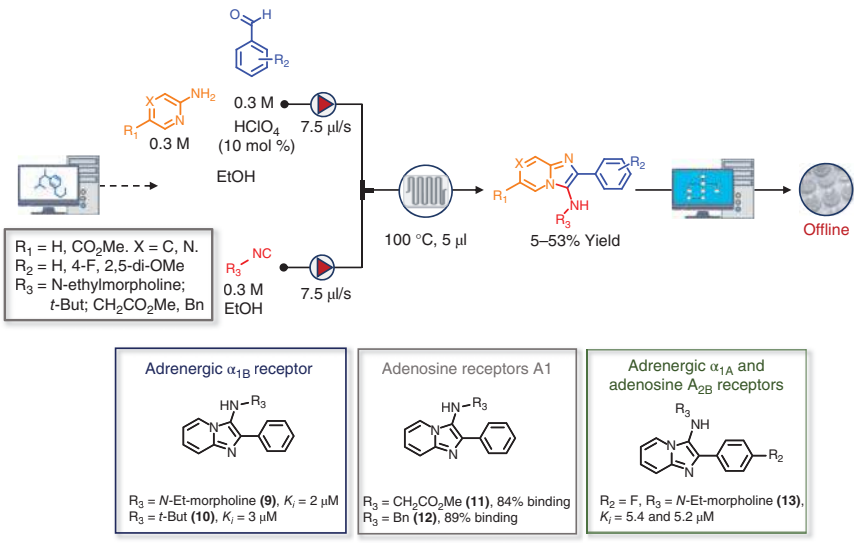

Figure 5.9 Microfluidic platform for the synthesis of imidazopyridines. Desired products were prepared by acid-catalyzed Ugi three-component reaction between amine, aldehyde, and isocyanide. Compounds were first screened by computer-based target prediction, and best compounds were then tested for receptor activity.

receptor (GPER) [81]. In particular, a selection of compounds was evaluated in a PathHunter β-arrestin G protein-coupled receptor (GPCR) assay with derivative **14** exhibiting a similar activation to the endogenous ligand 17β-estradiol. Interestingly, none of the tested compounds acted as ligands of the estrogen receptor α (ERα) both in agonist and antagonist mode when tested in AlphaScreen coactivator assays at different doses (Figure 5.10).

In 2019, the flow synthesizers were integrated with automation, analytical, and computational tools to prepare and characterize novel tetracyclic compounds as steroid-mimicking agonists of the pregnane X receptor (PXR) [82]. Initial virtual screening experiments led to the identification of UPF-2365 (**15**) as a micromolar PXR agonist in AlphaScreen assays. A collection of pure UPF-2365 analogs designed on the basis of computational studies was synthesized with a throughput of two compounds per hour in 58–85% isolated yield. The flow synthesis equipment consisted of a software-controlled automated reagent injector, two-channels syringe pumps, a mesoreactor coil, a BPR, an in-line liquid–liquid separator, four-way connectors, UV detector, and automated fraction collector (Figure 5.10). Pure diasteroisomers were then tested as racemic mixture in a single-dose (20 µM) AlphaScreen against the PXR receptor. The online HPLC analysis and electronic circular dicroism (ECD) determination assisted by quantum mechanical calculations were useful for the purification and stereochemical characterization of single enantiomers with compound **16** being identified as the most potent agonist (EC_{50} = 1.2 µM; efficacy = 119%) of the series and amenable for further optimization.

https://www.twirpx.org & http://chemistry-chemists.com

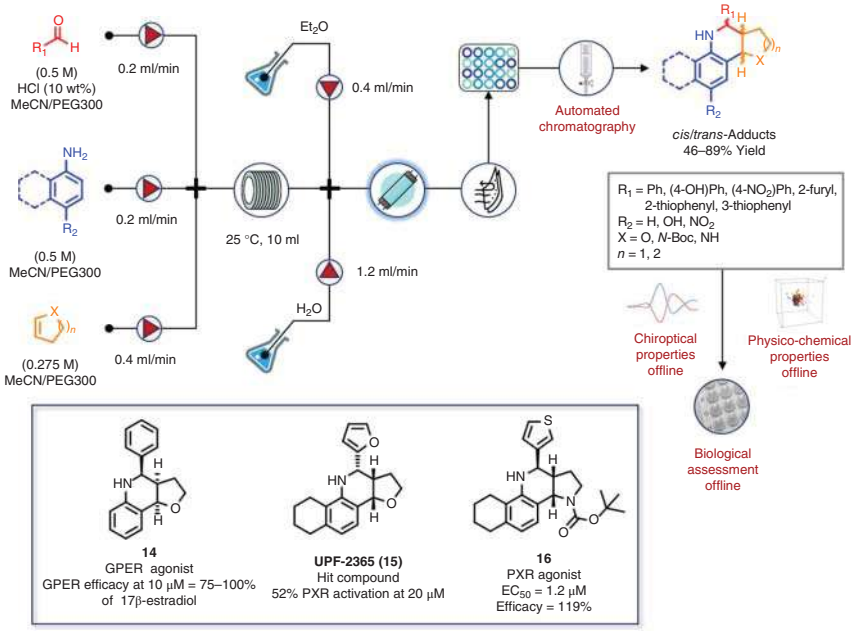

Figure 5.10 Flow setup up for the multicomponent synthesis of pure tetrahydroquinoline libraries. The synthetic unit was coupled with HPLC and CD analysis for assessing the purity and the structural determination of enantiomeric products readily evaluated for *in silico* descriptors and *in vitro* AlphaScreen assays against steroid receptors GPER and PXR.

5.3.3 Linear and Multistep Synthesis

Traditionally, linear and multistep syntheses involve batchwise and iterative step-by-step chemical manipulations in which the intermediate is isolated from the reaction mixture and purified before being used as the starting material for the next reaction sequence. Major limitations include the need for laborious and time-consuming purifications to remove any undesired components that might interfere with the subsequent transformations, especially when toxic, dangerous, or instable intermediates are formed [83, 84]. In this context, continuous-flow chemistry enables multiple reactions and downstream stages to be combined into a single continuous operation, therefore avoiding the necessity to isolate step intermediates. Furthermore, the assistance of automated reagent dosing and dispensing, process and equipment remote control, software-driven data analysis and product collection is of great interest especially for medicinal chemistry applications [18].

One of the pioneering work that showed the profitable application of multistep flow synthesis for bioactive compound library was reported by Ley research group [85]. Twenty-two imidazo[1,2-*a*]-pyridine analogs, including γ-aminobutyric acid isoform A (GABA-A) agonists Zolpidem (**17**) and Alpidem (**18**), were prepared in automation mode in four days and in 10–99% yield by a three-step sequence (Figure 5.11). The multistep sequence involved a first reaction between ethyl glyoxylate and acetophenone analogs induced by polymer-based sulfonic acid resin

https://www.twirpx.org & http://chemistry-chemists.com

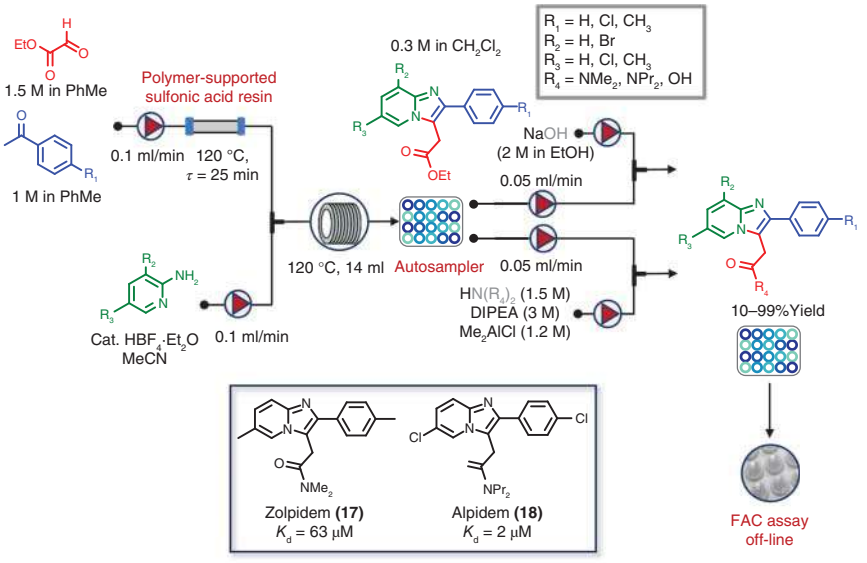

Figure 5.11 Automated flow synthesis and purification of imidazo[1,2-]-pyridine tested by frontal affinity chromatography (FAC) assay. Determination of binding constants (K_d) was performed in triplicate at 254 and 262 nm in the presence of immobilized human serum albumin (HSA).

into a tubular mesoreactor heated at 120 °C ($\tau = 25$ minutes). The reactor outcome was passed through a scavenging column packed with supported benzyl amine for removing the excess of glyoxylate. The pure ketone intermediates were dosed with an autosampler and reacted with a slight excess of diverse aminopyridines on a tubular reactor filled with a $MgSO_4$ at 50 °C to form ketimine that readily underwent 5-exo cyclization at 120 °C within a coil reactor. Crudes were purified using an acid resin for removing traces of unreacted aminopyridines. Two additional points of diversification were introduced into the imidazopyridine scaffold toward the corresponding amides and carboxylic acids analogs. The synthesized products were tested for albumin binding constants (K_d) by frontal affinity chromatography (FAC) and immobilize human serum albumin (HSA).

The same authors described a remotely controlled flow system for the preparation of novel inhibitors of the BRD9 bromodomain. In particular, the multigram scale synthesis of the key intermediate **19** was achieved by Curtius rearrangement of 3,6-dichloropyridazine-4-carboxylic acid (**20**) under continuous-flow conditions (Figure 5.12) [86]. A solution of **20**, Et_3N, *t*BuOH in toluene/acetonitrile and a solution of diphenylphosphoryl azide (DPPA) in toluene/acetonitrile were pumped at a total flow rate of 0.36 ml/min and combined in a T-mixer. The unstable acyl azide intermediate readily underwent a thermal cyclization (120 °C) in two stainless-steel reactors ($\tau = 2.3$ hours). After offline workup and chromatography, the key intermediate **19** was isolated in 39% yield. The following steps were performed in batch to give six BRD9 bromodomain inhibitors belonging to the series of triazolopyrazine sulfonamides analogs (series A). Two additional derivatives

https://www.twirpx.org & http://chemistry-chemists.com

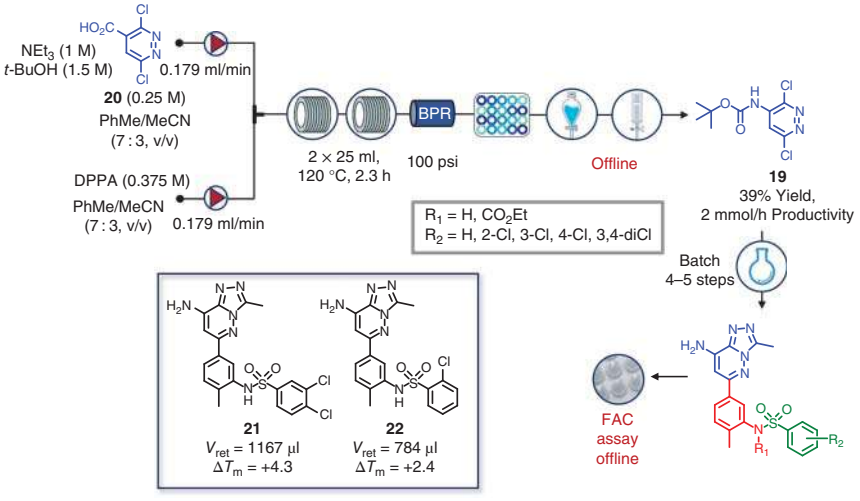

Figure 5.12 Automated flow synthesis of triazolopyrazine analogs and frontal affinity chromatography (FAC) assay against BRD9 bromodomain. Affinity constants were calculated by injecting in duplicate a solution of bromosporine in DMSO (1.9–15 µM) and detection wavelengths were 220 and 254 nm. Source: Based on Guetzoyan et al. [86].

belonging to the series of trifluoromethyl triazolopyrazine analogs were synthesized from 3,6-dichloropyrazine by three-step batch synthesis (series B). The synthesized compounds were then tested using a FAC–MS for evaluating their affinity for the BRD9 bromodomain. Thus, biotinylated BRD9 bromodomain was first overexpressed and purified, and the target protein was then immobilized on streptavidin coated beads. The customized column thus obtained was validated by injecting known BRD9 binders. The system was coupled to a MS detector and synthesized compounds were assayed by using 100 mM ammonium acetate in phosphate buffer saline (PBS). As a result, compound **21** was identified as the most potent analog of the series showing a retention time (V_{ret}) of 1167 µl in FAC–MS assay and a thermal shift (ΔT_m) of +4.3 in thermal stabilization assay against BRD9. Furthermore, albeit less potent (V_{ret} = 784 µl, ΔT_m = +2.4), compound **22** showed a better selectivity over BRD4 bromodomain.

A rapid and eco-friendly flow synthesis of a collection of 39 sulfonamide analogs was achieved by one-pot Schotten–Baumann reaction between diverse amines and sulfonyl chlorides under mild alkaline conditions [87]. Reactions were performed by loop injection of a solution of the amine and $NaHCO_3$ in H_2O/PEG400 and a solution of sulfonyl chloride in acetone. After the injection, the solutions were mixed in a T-junction, pumped with a total flow rate of 0.5 ml/min through a coil reactor set to 25 °C (τ = 15 minutes), and collected into a fraction collector assisted by UV detector (Figure 5.13). Pure primary, secondary, and tertiary sulfonamides were obtained in 60–98% yield after simple workup and evaluated for their ability to selectively inhibit tumor-associated carbonic anhydrase (CA) isoforms IX and XII [88]. The tested compounds revealed to be highly potent CA IX inhibitors in nanomolar range and to inhibit CA XII activity with different

https://www.twirpx.org & http://chemistry-chemists.com

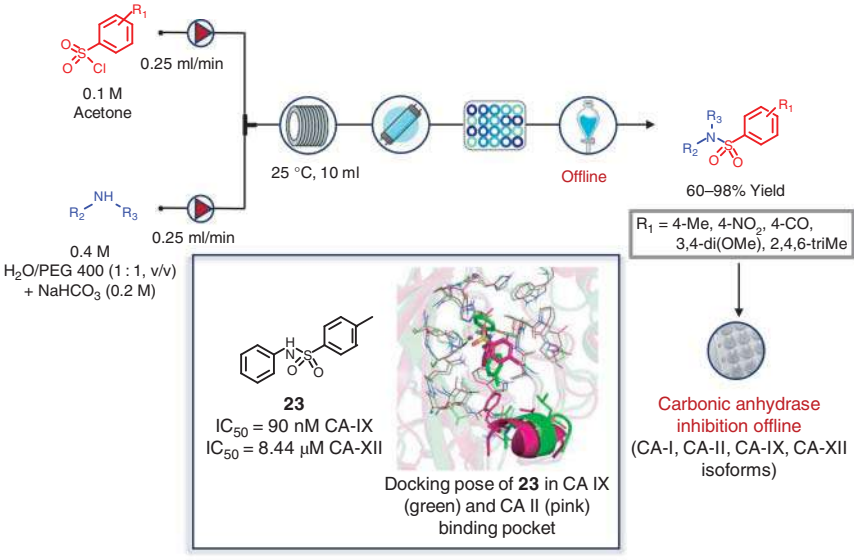

Figure 5.13 Flow synthesis and biological activity of aryl sulfonamides as selective carbonic anhydrase IX and XII inhibitors. A photophysics stopped-flow instrument was used for assaying the CA inhibition in the presence of phenol red (0.2 mM) as the indicator at 557 nm. IC_{50} values were obtained by nonlinear least-squares methods using PRISM 3.

ranks of potencies. Remarkably, 4-methyl-*N*-phenyl-benzenesulfonamide (**23**) was a selective nanomolar CA IX inhibitor with an IC_{50} of 90 nM.

An automated route for the flow synthesis of an eight-member library of 5-thiazol-2-yl3,4-dihydropyrimidin-2(1*H*)-ones (DHPMs) was developed by sequential Hantzsch and Biginelli reactions (Figure 5.14) [89]. A solution of ketal protected thioamide (**24**) and α-bromoketones in dry dimethylformamide (DMF) were pumped into the microreactor heated to 150 °C (τ = 3.75 minutes). The thus formed ketothiazoles were then mixed with a stream of 3-hydroxy benzaldehyde (**25**) and urea (**26**) and flowed through a reactor heated at 200 °C for 10 minutes. After collection, crudes were purified on a prepacked silica gel column yielding the corresponding DHPM derivatives in good overall yield (39–46%) (Figure 5.14). The synthesized compounds were evaluated as antiviral agents by measurement of the HIV replication inhibition in cell-based assays [90]. Several DHPM analogs showed sub-micromolar potency with the 4-cyanophenyl derivative (**27**) being the most potent RT inhibitor. A second round optimization allowed to identify derivative **28** as a nanomolar inhibitor of drug resistant strains of HIV with cellular potency comparable with the clinical drug nevirapine (NVP).

In 2018, the streamlined preparation of bile acids C3-glucuronides was realized by optimization of the Koenigs–Knorr reaction (Figure 5.15) [91]. The selective glucuronidation reaction was performed using a flow device equipped with a loop injection system, a pump dedicated to a reservoir of organic solvent, a tubular reactor packed with the Fetizon's reagent and fixed in a reactor heater, a BPR, and an UV detector. The reactions were carried out by injection of a toluene solution of biliary benzyl esters and the glucuronyl donor **29**. After the injection and the valve

https://www.twirpx.org & http://chemistry-chemists.com

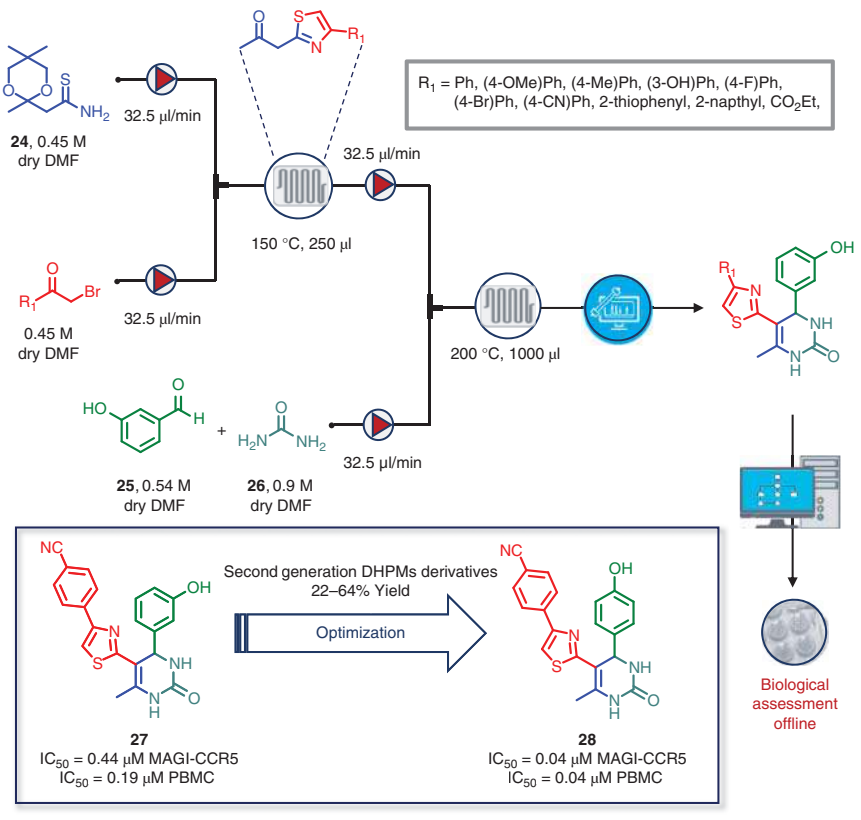

Figure 5.14 Automated sequential Hantzsch/Biginelli multicomponent flow synthesis and integrated chemical biology approach for the identification of novel HIV replication inhibitors based on 5-thiazol-2-yl3,4-dihydropyrimidin-2(1*H*)-one (DHPM) scaffold. The crude reaction mixtures were purified using reverse-phase preparative HPLC, lyophilized, and tested for anti-HIV activity (MAGI-CCR5 antiviral assay, PBMC assay, and RT biochemical assay) in triplicate (six-serial dilutions for each experiment). Furthermore, microsomal stability, plasma stability, and parallel artificial membrane permeability assay (PAMPA) *in vitro* assays were performed. Source: Based on Pagano et al. [89].

switching through the loop, the reagent solution was pumped into the reaction column packed with the Fetizon's reagent at 38 °C. After alkaline hydrolysis and reverse-phase chromatography, glucuronidated conjugates were isolated in good yield (69–95%) (Figure 5.15). The synthesized compounds were characterized in terms of physicochemical property and ability to modulate key nuclear receptors including the farnesoid X receptor (FXR) [92].

5.4 End-to-End Autonomous Discovery Platforms

The most powerful strategy to streamline medicinal chemistry and discovery cycles consists in automating and integrating in a single system compound design, synthesis, bioassays, and data analysis. To implement such approach, integrated

https://www.twirpx.org & http://chemistry-chemists.com

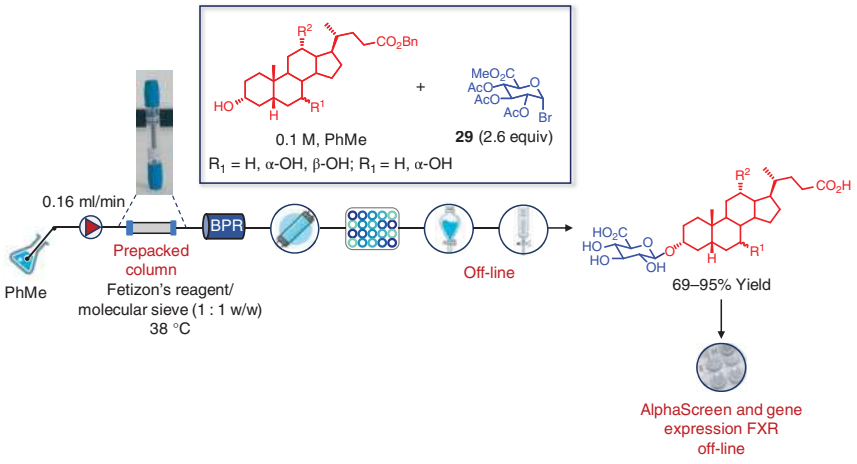

Figure 5.15 Combined flow-batch synthesis, physicochemical characterization, and biological activity of bile acids 3-glucuronides as investigative tools for studying bile acid signaling and detoxification pathways. Bile acids 3-glucuronides were prepared by solid-phase Fetizon reaction under flow conditions followed by alkaline hydrolysis and reverse-phase chromatography. Activity on FXR and other nuclear receptors was assayed by using AlphaScreen technology in a coactivator recruitment assay.

cycles need to be rapid, efficient, and based on well-designed compound libraries. At this regard, the solutions most often proposed involve chemical parallelization and miniaturization using microreactors and microfluidic devices for compound synthesis and testing. Furthermore, effective design decisions using feedback from previously tested analogs may complement the ideal platform aimed at improving the time, the cost, and the success of drug discovery.

An early proof-of-concept example of end-to-end flow-based drug discovery platform was reported by GlaxoSmithKline (GSK). The scope was to realize a microsystem technology (MST) that integrated combinatorial synthesis, online product analysis, and screening assays and enabled the high-throughput chemical synthesis and evaluation of thousands of compounds [93]. The system setup consisted of ultra high performance liquid chromatography (UHPLC) pumps, a microchip reactor, an autosampler, a dilution device, a detection system, and an LC–MS spectroscopy. Six sulfonamides were synthesized in fast serial automated mode by reacting anilines with sulfonyl chlorides in the presence of pyridine. Reaction products were purified by in-line LC, readily submitted to UV/MS detection/analysis, and tested by fluorogenic assay for their inhibitory effect on T-cell tyrosine phosphatase (TCPTP). The biological data were generated by monitoring the fluorescence of an on-chip incubation of TCPTP and 6,8-difluoro-4-methylumbelliferyl phosphate (DiFMUP). TCPTP cleaves the phosphate group from DiFMUP, generating the fluorescent species DiFMU (Figure 5.16). Despite the small set of compounds, this early utilization of microfluidics combined with MST demonstrate their disrupting potential to overcome synthesis limitations, improve the timing for synthesis–testing cycles, reduce reagents and solvents consumption, and avoid storage and supply-chain issues.

https://www.twirpx.org & http://chemistry-chemists.com

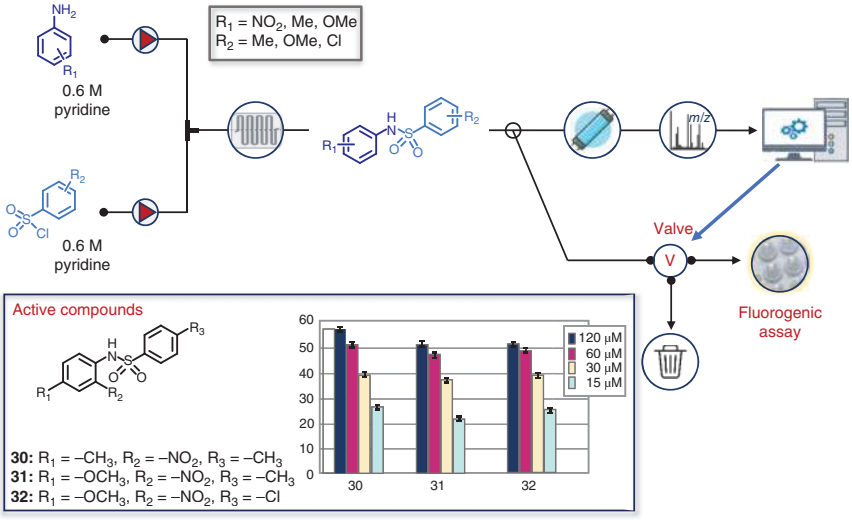

Figure 5.16 Integrated flow platform for the automated synthesis and in-line biological screening of sulfonamide as T-cell tyrosine phosphatase (TCPTP) inhibitors. The synthesized compounds were tested using Caliper's standard fluorogenic assay on Caliper 250 HTS system. The data were generated by monitoring the fluorescence of an on-chip incubation of TCPTP and 6,8-difluoro-4-methylumbelliferyl phosphate.

More recently, the collaboration between Cyclofluidic Ltd. and Sanofi-Aventis, Sandexis LLP, Accelrys Ltd. led to the development and validation of a flow technology platform that well integrated the key elements of medicinal chemistry discovery cycles. The platform called CyclOps™ made use of flow synthesis, in-line analytical techniques, biological screening, and algorithm-based drug design to accelerate hit-to-lead explorations and efficiently deliver novel lead compounds [47, 94–96]. SAR analysis on hit series was instrumental to plan the first round of analogs synthesis designed by a predictive activity model that refined itself after every iterative cycle. Therefore, products were continuously generated and purified, analyzed by in-line analytical devices, and collected. Prior to testing, products concentration was adjusted with the assay buffer using a liquid handling robot and tested at the proper concentration in a chip-based fluorescence assay. IC_{50} values thus obtained feed the algorithm-driven learning cycles. Remarkably, in all the proof-of-concept studies, authors demonstrated a close correlation between integrated platform data and data generated within the corresponding traditional medicinal chemistry approach validating the overall strategy and technology.

The platform was first applied to the identification of novel Abl kinase inhibitors (Figure 5.17) [94], as has been explained in Chapter 4. Starting from the XRD structure of Ponatinib (**33**), a known Abl kinase inhibitor, 22 compounds were initially synthesized by Sonogashira cross-coupling reaction under palladium-induced flow catalysis (5–31% yield; >95% purity) and tested in about 30 hours. For each tested inhibitor, a threefold dilution series was generated by an integrated liquid handling robot. The enzyme and the substrate solution were added to each test solution to assess the residual enzyme activity by fluorescence (excitation 360 nm,

https://www.twirpx.org & http://chemistry-chemists.com

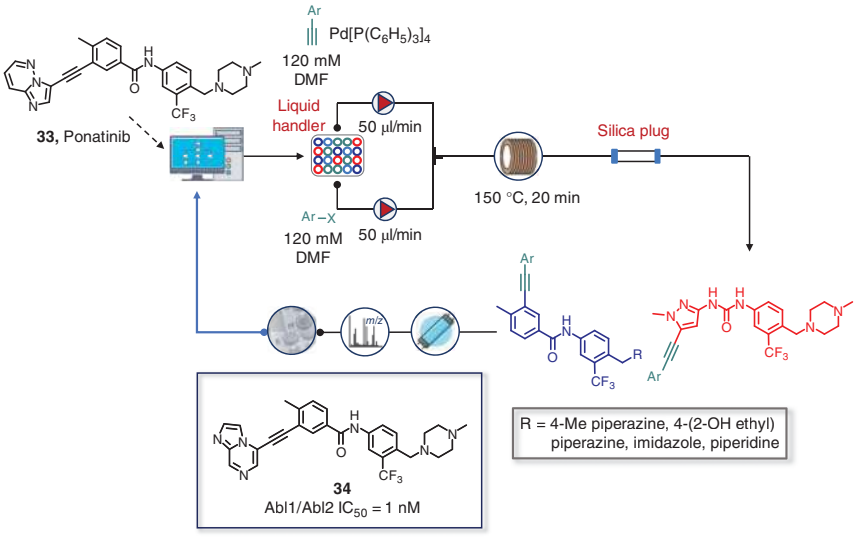

Figure 5.17 Fully integrated and fully automated CyclOps platform from Cyclofluidic Ltd. for closed-loop algorithm-guided design, synthesis, purification, and screening of Abl kinase inhibitors. Ponatinib analogs were synthesized by Sonogashira cross-coupling reaction between aryl halides and alkynes, and purified by in-line preparative HPLC before testing. Source: Based on Desai et al. [94].

emission 485 nm). After a total of 90 cycles of design–synthesis–screening, 64 new compounds were synthesized and evaluated against Abl1 and Abl2 kinase in approximately four days with an overall success synthetic rate of 71%. Within the synthesized compounds, the discovery process disclosed a novel template and hinge binding motif with $pIC_{50} > 8$ against Abl kinase in both wild-type and clinically relevant mutants. In particular, the amide derivative **34** was a nanomolar inhibitor ($IC_{50} = 1$ nM) endowed with a good membrane permeability and a suitable clearance in human liver microsomes (Figure 5.17).

In another application, Tarver and coworkers illustrated how to expedite the development of xanthine-based dipeptidyl peptidase 4 (DPP4) inhibitors by a two-steps autonomous flow synthesis (Figure 5.18) [95]. The compound library was assembled by the reaction of BOC-protected diamines and 8-bromo xanthine in *N*-methyl-pyrrolidone (NMP). The reactor outcome containing the *N*-BOC-protected xanthine derivatives was mixed with an aqueous solution of methanesulfonic acid for BOC removal. After automated reagent dosing and injection, the components were pumped at 0.1 ml/min of total flow rate into a 2 ml stainless steel coil reactor heated at 150 °C ($\tau = 20$ minutes). For deprotecting the *tert*-butyloxycarbonyl group, MsOH was pumped at 50 µl/min and the mixture reacted into a second 2 ml coil reactor heated at 90 °C ($\tau = 13$ minutes). Products were purified by in-line LC–MS system, diluted with the assay buffer, and tested in a 384-well plate for the assessment of residual enzyme activity on both porcine and human DDP4 isoforms. The enzyme (0.82 mU/ml for porcine DPP4 or 34 U/ml for human DPP4) was added and the residual enzyme activity was monitored by

https://www.twirpx.org & http://chemistry-chemists.com

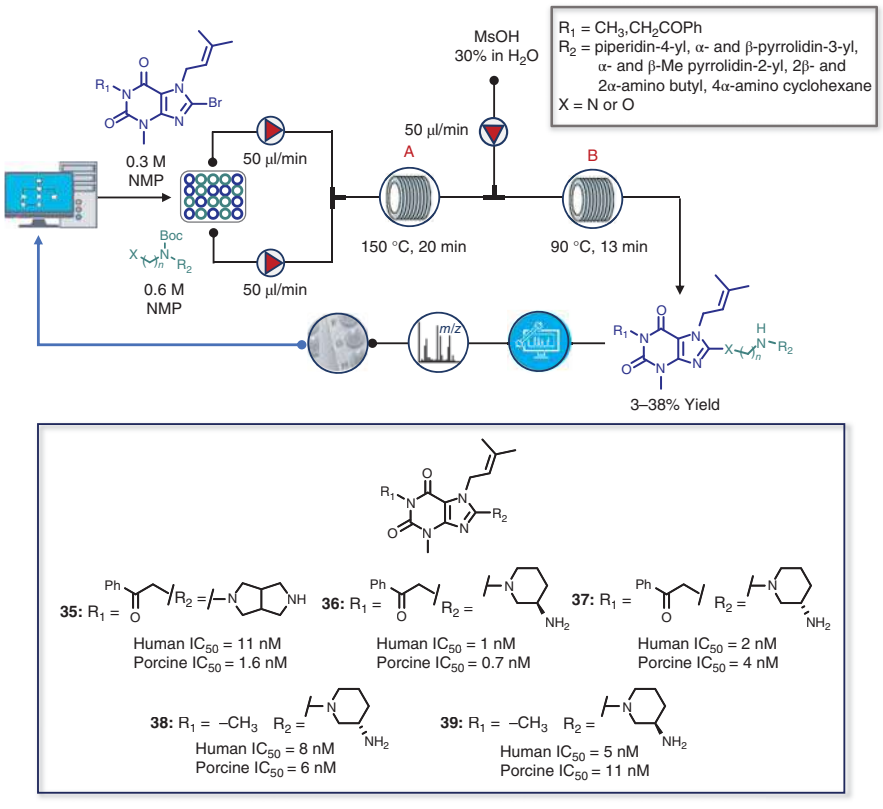

Figure 5.18 Fully integrated and fully automated CyclOps platform from Cyclofluidic Ltd. for closed-loop algorithm-guided design, synthesis, purification, and screening of dipeptidyl peptidase 4 (DPP4) inhibitors. Source: Based on Czechtizky et al. [95].

adding the substrate at a final concentration equivalent to the K_M^{app}. A total of 29 compounds was synthesized with yields ranging from 3% to 38% and tested in 24 hours. Among these, compounds **35**–**39** showed a nanomolar potency on both enzymes. The acquired SAR information was exploited to design and synthesize a new set of derivatives using amino alcohol substrates (Figure 5.18). Overall, the chemistry success rate was of 93%, demonstrating method robustness and no need of extra optimization time to achieve a generic flow synthesis with a range of reagents.

More recently, CyclOps was instrumental to streamline the discovery of hepsin inhibitors (Figure 5.19) [96]. Compound **40** was selected as the hit compound on the basis of inhibition potency (IC_{50} = 1.13 µM), selectivity for hepsin over urokinase-type plasminogen activator (uPA) (IC_{50} > 10 µM), and amenability for structural modifications. In this case, the automated discovery platform was coupled with hepsin and uPA testing and algorithms for substrate selection and potency prediction (Figure 5.19). The flow synthesis involved the reaction between protected amino acids and substituted sulfonyl chlorides, acyl chlorides, or isocyanates in the presence of diisopropylethylamine (DIPEA). Intermediates were

https://www.twirpx.org & http://chemistry-chemists.com

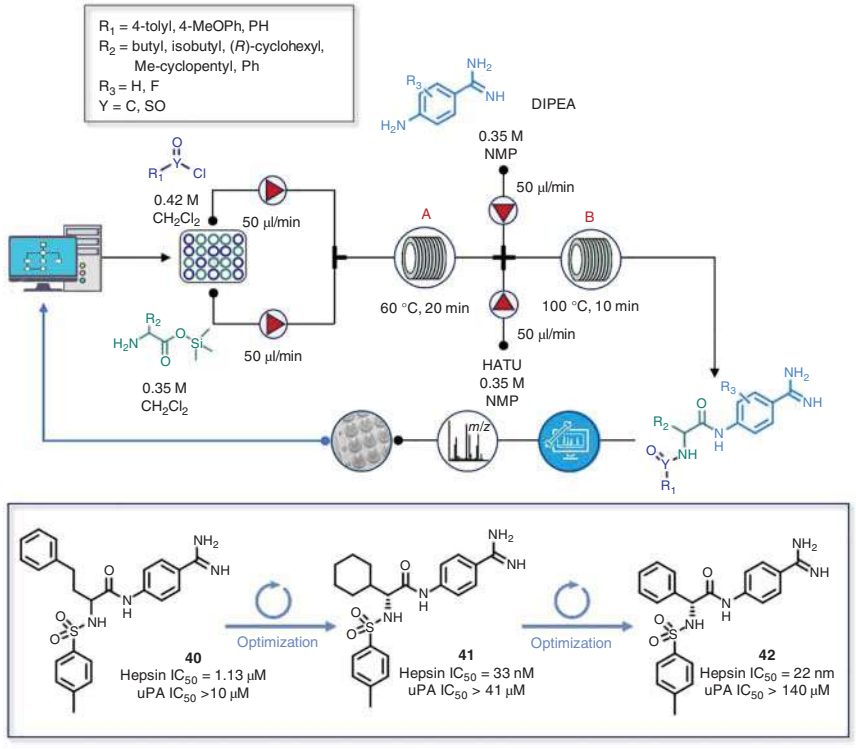

Figure 5.19 Fully integrated and fully automated CyclOps platform from Cyclofluidic Ltd. for closed-loop algorithm-guided design, synthesis, purification, and screening of hepsin inhibitors. Tested compounds were obtained by condensation between silylated amino acids and sulfonyl chlorides, acyl chlorides, or isocyanates (total flow rate = 100 µl/min, coil volume = 2 ml, $\tau = 20$ minutes, $T = 60\,°C$) followed by amidation with amidine and HATU (total flow rate = 200 µl/min, coil volume = 2 ml, $\tau = 10$ minutes, $T = 100\,°C$). Source: Based on Pant et al. [96].

reacted with a solution of amidine dihydrochloride and DIPEA and hexafluorophosphate azabenzotriazole tetramethyl uronium (HATU). A virtual chemical space of 5472 compounds was explored by means of 63 reaction components including amino acids, sulfonyl/acid chlorides/isocyanates, and aminoamidines. The first run of 24 closed-loop synthesis and screening assisted by multiparameter optimization method (best objective under-sampled [BOUS]) led to 44 active compounds. Structural refinement by applying Chase Objective tool allowed to disclose the (*R*)-cyclohexylglycine compound **41** as the most potent hepsin inhibitors with an IC_{50} of 33 nM and a high selectivity index over uPA (Figure 5.19). Twenty-one additional experiments from a restricted amino acid pool afforded the (*R*)-phenylglycine derivative **42** that showed a better potency (IC_{50} = 22 nM) and selectivity (>6000-fold). The compound proved to be selective over a panel of 10 serine proteases, endowed with good absorption, distribution, metabolism, excretion, and toxicity (ADMET) profile, and effective in oncogenic functional assays.

In 2014, scientists at Hoffmann-La Roche developed a similar automated flow-based system for the rapid generation of β-secretase (BACE1) inhibitors

https://www.twirpx.org & http://chemistry-chemists.com

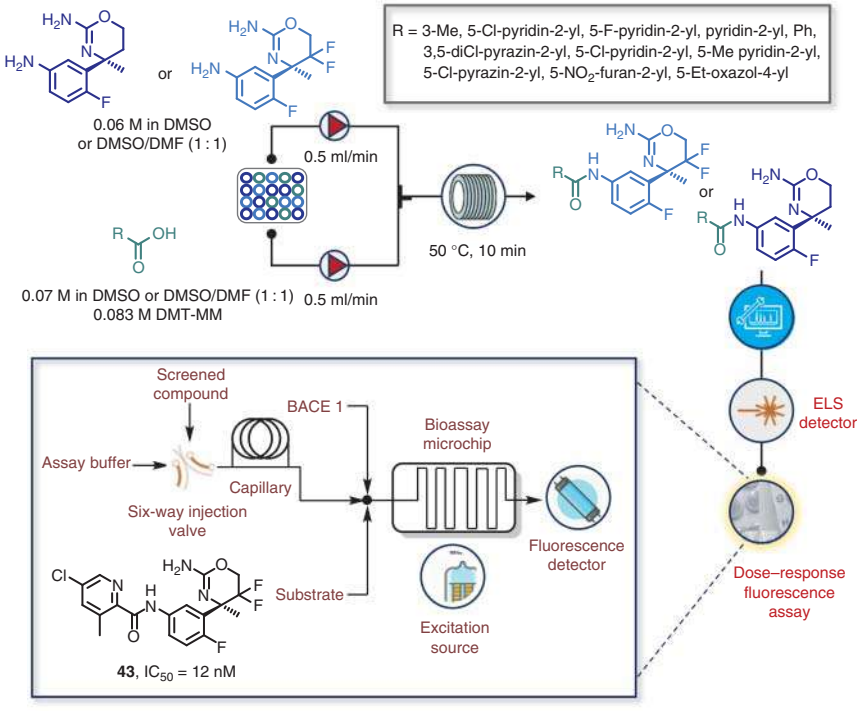

Figure 5.20 Fully integrated and automated flow platform for the discovery of BACE1 inhibitors. The bioassay chip was primed for two minutes with streams of enzyme (90 nM), substrate (0.9 μM), and assay buffer, at 0.8 ml/min for each pump. Source: Based on Werner et al. [97].

prepared by amidation of commercially available anilines and carboxylic acids (Figure 5.20) [97]. Starting from a 2×10 set of commercially available anilines and carboxylic acids, a small library of amides was quickly generated by coupling reaction under continuous-flow conditions in the presence of 4-(4,6-dimethoxy-1,3,5-triazin-2-yl)-4-methylmorpholinium tetrafluoroborate (DMT-MM) as the coupling reagent. Reactions were performed by automated dosing and injection of the two reaction components which were pumped at 1 ml/min of total flow rate and reacted into a 10 ml-reactor coil heated at 50 °C. Crudes were purified using in-line preparative HPLC and analyzed by calibrated HPLC–ELSD. Aliquots of each compound were injected by a liquid handler into the dispersion capillary to generate a compound concentration gradient and then dispersed with the buffer into the bioassay chip. The bioassay chip was primed with streams of enzyme, substrate, and assay buffer. After incubation, the enzyme activity was determined using a gradient calibration, and the resulting dose–response curve was used to extrapolate the IC_{50} values. Overall, the closed loop of synthesis and dose–response fluorescence assay required 60 minutes of total cycle time per compound. Among compounds generated, **43** was found to inhibit BACE1 activity with an IC_{50} of 12 nM (Figure 5.20).

https://www.twirpx.org & http://chemistry-chemists.com

Also DNA libraries have been achieved using autonomous flow platforms. In particular, Linshiz et al. reported a microfluidic approach for the iterative design–synthesis–screening assays of DNA-based products assisted by Isothermal Hierarchical DNA Construction (IHDC) software (Box 5.1) [98]. The miniaturized device allowed to perform transformation into different hosts (e.g. *Escherichia coli* and *Saccharomyces cerevisiae*), functional (cell growth and protein expression), and colorimetric assays, as well as image data analysis. The system consisted of a microfluidic chip, an electronic pneumatic control system, a temperature regulation system, and computational software for automation with a web-based interface (Figure 5.21A). Similarly, researchers at the Scripps Institute described a lab-on-chip microfluidic assembly for hit deconvolution by sequencing of DNA-encoded compound beads (Figure 5.21B) [99]. DNA-encoded compound beads were screened in ultra-high-throughput fashion and the photochemical cleavage from the bead was followed by assay incubation. Hit identification by laser-induced fluorescence-based binding assay for their activity as inhibitors of cathepsin D.

Box 5.1 Hierarchical DNA Constructor

DNA Constructor is a web-based applicative software for supporting the design of complex combinatorial DNA libraries. The software works through a specific scripting language and algorithms that allow to optimize and customize the hierarchical construction protocols, minimizing the formation of specific DNA fragments while reducing at the same time the number of steps required. Compared to traditional polymerase chain reaction (PCR)-based technique, hierarchical DNA construction under isothermal conditions (IHDC) offers several advantages including the minimization of reagents consumption by recycling components shared among different DNA fragments, the reduced human intervention for equipment control, the amenability for automation under microfluidic conditions, and the shorter processing time per cycle. IHDC works via recombinase polymerase amplification (RPA): primers are incorporated between the strands and then elongated by the action of a polymerase that produce ssDNA. The overlapping ssDNA molecules hybridize, priming each other for an overlap extension elongation reaction to form dsDNA, which is then amplified under isothermal condition resulting in the formation of the desired elongated dsDNA. In particular, Linshiz et al. successfully applied software-assisted IHDC under microfluidic conditions for building DNA fragment of 754 base pairs of length starting from eight synthetic oligomers. By using a microfluidic chip with 16 input/output wells, the authors performed in a fully automated fashion two hierarchical construction trees consisting of seven separate synthetic steps each. As a result, a combinatorial library of DNA molecules encode the entire red fluorescent protein (RFP) and two halves of green fluorescent protein (GFP) in less than three hours, which correspond to 15 minutes for each IHDC step. Source: Based on Linshiz et al. [98].

https://www.twirpx.org & http://chemistry-chemists.com

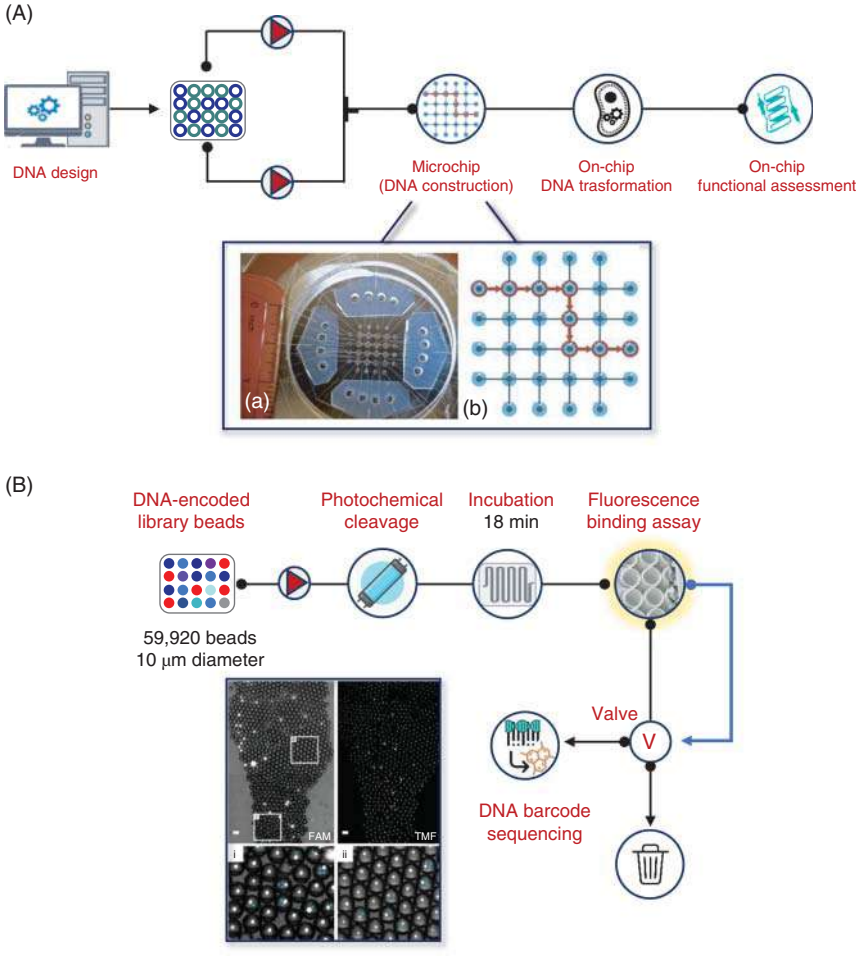

Figure 5.21 (A) Schematic representation of the first automated microfluidic platform for synthetic biology. (B) Microfluidic platform for ultra-high-throughput hit deconvolution by sequencing of DNA-encoded compound beads. DNA-encoded beads (10 μm diameter, 1920 beads, 729 encoding sequences) were mixed with negative control beads (58 000 beads, 1728 encoding sequences) and screened for cathepsin D inhibition activity in a biochemical enzymatic assay in the presence of pepstatin as the positive control. An integrated waveguide irradiates the droplet flow at 365 nm inducing the photochemical cleavage of compound from the bead into the droplet volume. Droplets dosed with compound (1–3 μM) were then incubated for 18 minutes and a confocal laser-induced detector measured the fluorescence emitted by the droplet. Source: (a) Based on Linshiz et al. [98] / with permission of Springer Nature. (b) Based on MacConnell et al. [99].

Recently, Guo and coworkers applied a modular flow platform for the identification of competitive inhibitors of bovine serum albumin (BSA) by testing a dynamic combinatorial libraries (DCLs) built by fragment-based tactic (Figure 5.22) [100]. Thus, a microscale flow synthesizer was coupled with size-exclusion chromatography (SEC)–MS solving major limitations of the conventional protein-directed

https://www.twirpx.org & http://chemistry-chemists.com

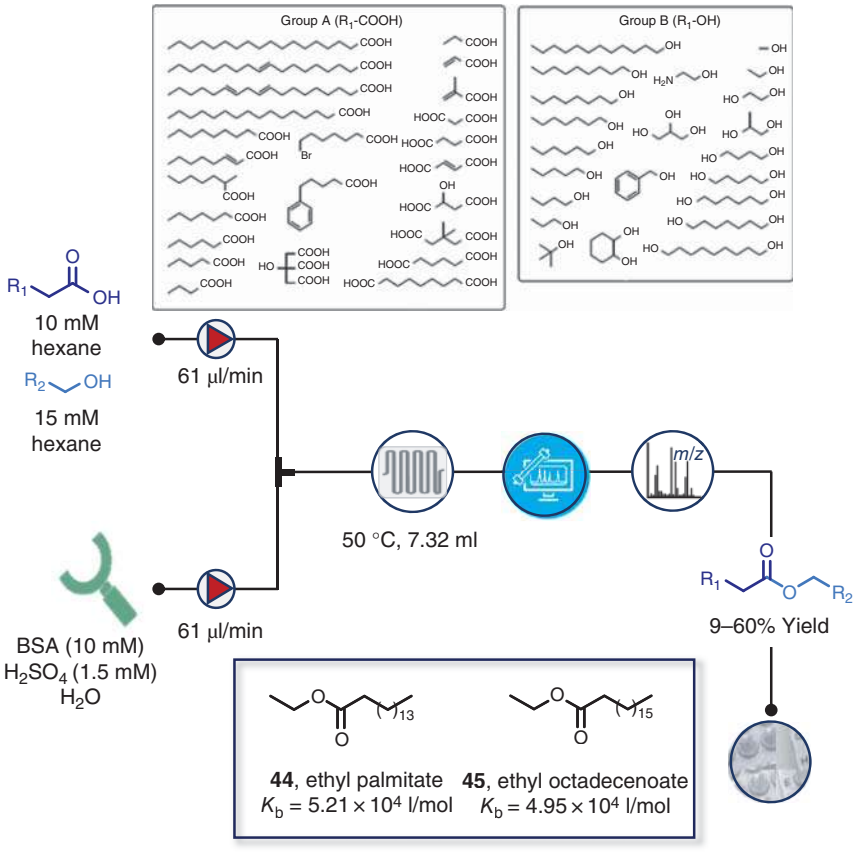

Figure 5.22 Integrated flow platform for the synthesis and identification of protein binders. Fluorescence spectra for each compound were recorded at concentration ranging from 0.4 to 2.4 nM, $T = 298$ K, pH = 7.4, and $\lambda_{emission} = 280$ nm. Source: Based on Qiu et al. [100].

dynamic combinatorial chemistry (DCC), including the poor inhibitor reactivity at low concentrations, the reduction of protein activity, or inhibitor decomposition at long equilibration times, as well as the low throughput of analytical detection methods. The setup involved the esterification of a pool of carboxylic acids (10 mM) and alcohols (15 mM) in *n*-hexane. DLC esters thus generated were mixed with a stream of H_2SO_4 (pH = 1, 1.5 mM) and BSA (10 mM) in distilled water and pumped at 122 µl/min of total flow rate into a microchip reactor ($V = 7.32$ ml, $\tau = 60$ minutes) where the incubation and equilibration took place at 50 °C. A total of 528 DCL esters were synthesized in a microchip reactor technology, purified, analyzed, and readily evaluated by concentration-dependent fluorescence assay to identify ethyl palmitate **44** and ethyl octadecanoate **45** as potent BSA binders ($K_b = 4.95$ and 5.21×10^4 l/mol, respectively).

https://www.twirpx.org & http://chemistry-chemists.com

5.5 Conclusions and Future Outlook

Drug discoverers are putting significant efforts to develop smart systems and integrated strategies through a multidisciplinary and multimodal approaches that merge the diverse knowledges, competencies, technologies, and scientific equipment. The long-term vision is to realize autonomous discovery platforms that can accelerate time frames and success in drug discovery and development. In this chapter, we have set out to highlight a range of specific solutions that have been implemented to go beyond the traditional "design–synthesis–test–analyze" cycle, which lies in the core of hit-to-lead and lead optimization processes. In particular, we discussed major achievements in continuous-flow technology as a powerful medicinal chemistry toolbox that enables the integration of chemical synthesis, purification, and analysis with screening assays and computing. There have been extraordinary and exciting proof-of-concept studies for expedited library synthesis and in-line biological screenings that lay the foundation to realize integrated compound optimization flow-based platforms that would significantly impact the time, cost, and attrition of the small molecule discovery cycle while leading to a new paradigm in early drug discovery. Even with the amazing advances, there remain considerable conceptual and technical challenges for a wider adoption in medicinal chemistry including chemical reaction flowability, conduction of complex and telescoped synthesis, compatibility between compartment units and devices, limited bioassays for in-line screening, and integration in a single self-operating circuit. Significant investments in education and technologies associated with closer collaborations between academia and pharmaceutical companies can certainly tackle these future challenges that could substantially improve the effectiveness of medicinal chemistry and drug discovery research.

References

1 World Health Organization (WHO) (2019). https://www.who.int/emergencies/diseases/novel-coronavirus-2019/global-research-on-novel-coronavirus-2019-ncov (accessed 05 January 2022).

2 Dowden, H. and Munro, J. (2019). Trends in clinical success rates and therapeutic focus. *Nat. Rev. Drug Discovery* 18: 495–496.

3 Brown, D.G. and Boström, J. (2018). Where do recent small molecule clinical development candidates come from? *J. Med. Chem.* 61: 9442–9468.

4 Holenz, J. and Brown, D.G. (2016). Modern lead generation strategies. In: *Lead Generation: Methods and Strategies* (ed. J. Holenz, R. Mannhold, H. Kubinyi and G. Folkers), 13–34. Weinheim, Germany: Wiley-VCH Verlag GmbH & Co.

5 Gromski, P.S., Henson, A.B., Granda, J.M., and Cronin, L. (2019). How to explore chemical space using algorithm and automation. *Nat. Rev. Chem.* 3: 119–128.

https://www.twirpx.org & http://chemistry-chemists.com

6 Saikin, S.K., Kreisbeck, C., Sheberla, D. et al. (2019). Closed-loop discovery platform integration is needed for artificial intelligence to make an impact in drug discovery. *Expert Opin. Drug Discovery* 14: 1–4.

7 Gioiello, A., Piccinno, A., Lozza, A.M., and Cerra, B. (2020). The medicinal chemistry in the era of machines and automation: recent advances in continuous flow technology. *J. Med. Chem.* 63 (13): 6624–6647. https://doi.org/10.1021/acs.jmedchem.9b01956.

8 Blakemore, D.C., Castro, L., Churcher, I. et al. (2018). Organic synthesis provides opportunities to transform drug discovery. *Nat. Chem.* 10: 383–394.

9 Schneider, G. (2018). Automating drug discovery. *Nat. Rev. Drug Discovery* 17: 97–113.

10 Fleming, G.S. and Beeler, A.B. (2017). Integrated drug discovery in continuous flow. *J. Flow Chem.* 7: 124–128.

11 Campos, K.R., Coleman, P.J., Alvarez, J.C. et al. (2019). The importance of synthetic chemistry in the pharmaceutical industry. *Science* 363: 244–252.

12 Fitzpatrick, D.E., Battilocchio, C., and Ley, S.V. (2016). A novel internet-based reaction monitoring, control and autonomous self-optimization platform for chemical synthesis. *Org. Process Res. Dev.* 20: 386–394.

13 Skilton, R.A., Bourne, R.A., Amara, Z. et al. (2015). Remote-controlled experiments with cloud chemistry. *Nat. Chem.* 7: 1–5.

14 Houben, C. and Lapkin, A.A. (2015). Automatic discovery and optimization of chemical processes. *Curr. Opin. Chem. Eng.* 9: 1–7.

15 Chow, S., Liver, S., and Nelson, A. (2018). Streamlining bioactive molecular discovery through integration and automation. *Nat. Rev. Chem.* 2: 174–183.

16 Sans, V. and Cronin, L. (2016). Towards dial-a-molecule by integrating continuous flow, analytics and self-optimisation. *Chem. Soc. Rev.* 45: 2032–2043.

17 Plutschack, M.B., Pieber, B., Gilmore, K., and Seeberger, P.H. (2017). The Hitchhiker's guide to flow chemistry. *Chem. Rev.* 117: 11796–11893.

18 Shukla, C.A. and Kulkarni, A.A. (2017). Automating multistep flow synthesis: approach and challenges in integrating chemistry, machines and logic. *Beilstein J. Org. Chem.* 13: 960–987.

19 Dallinger, D., Gutmann, B., and Kappe, C.O. (2020). The concept of chemical generators: on-site on-demand production of hazardous reagents in continuous flow. *Acc. Chem. Res.* https://doi.org/10.1021/acs.accounts.0c00199.

20 Movsisyan, M., Delbeke, E.I.P., Berton, J.K.E.T. et al. (2016). Taming hazardous chemistry by continuous flow technology. *Chem. Soc. Rev.* 45: 4892–4928.

21 Ley, S.V., Fitzpatrick, D.E., Ingham, R.J., and Myers, R.M. (2015). Organic synthesis: march of the machines. *Angew. Chem. Int. Ed.* 54: 3449–3464.

22 Wang, K. and Luo, G. (2017). Microflow extraction: a review of recent development. *Chem. Eng. Sci.* 169: 18–33.

23 Ley, S.V., Baxendale, I.R., Bream, R.N. et al. (2000). Multi-step organic synthesis using solid-supported reagents and scavengers: a new paradigm in chemical library generation. *J. Chem. Soc., Perkin Trans. 1* 1 (23): 3815–4195.

https://www.twirpx.org & http://chemistry-chemists.com

24 O'Brien, A.G., Horváth, Z., Lévesque, F. et al. (2012). Continuous synthesis and purification by direct coupling of a flow reactor with simulated moving-bed chromatography. *Angew. Chem. Int. Ed.* 51: 7028–7030.

25 Baumann, M. (2019). Integrating reactive distillation with continuous flow processing. *React. Chem. Eng.* 4: 368–371.

26 Mascia, S., Heider, P.L., Zhang, H. et al. (2013). End-to-end continuous manufacturing of pharmaceuticals: integrated synthesis, purification, and final dosage formation. *Angew. Chem. Int. Ed.* 52: 12359–12363.

27 Price, G.A., Mallik, D., and Organ, M.G. (2017). Process analytical tools for flow analysis: a perspective. *J. Flow Chem.* 7: 82–86.

28 Simon, L.L., Pataki, H., Marosi, G. et al. (2015). Assessment of recent process analytical technology (PAT) trends: a multiauthor review. *Org. Process Res. Dev.* 19: 3–62.

29 Kwak, J.S., Zhang, W., Tsoy, D. et al. (2017). A multiconfiguration valve for uninterrupted sampling from heterogeneous slurries: an application to flow chemistry. *Org. Process Res. Dev.* 21: 1051–1058.

30 Reizman, B.J. and Jensen, K.F. (2016). Feedback in flow for accelerated reaction development. *Acc. Chem. Res.* 49: 1786–1796.

31 McMullen, J.P. and Jensen, K.F. (2011). Rapid determination of reaction kinetics with an automated microfluidic system. *Org. Process Res. Dev.* 15: 398–407.

32 Yue, J., Falke, F.H., Schouten, J.C., and Nijhuis, T.A. (2013). Microreactors with integrated UV/Vis spectroscopic detection for online process analysis under segmented flow. *Lab Chip* 13: 4855–4863.

33 Ryu, G., Huang, J., Hofmann, O. et al. (2011). Highly sensitive fluorescence detection system for microfluidic lab-on-a-chip. *Lab Chip* 11: 1664–1670.

34 Mozharov, S., Nordon, A., Littlejohn, D. et al. (2011). Improved method for kinetic studies in microreactors using flow manipulation and noninvasive Raman spectrometry. *J. Am. Chem. Soc.* 133: 3601–3608.

35 Galaverna, R., Breitkreitz, M.C., and Pastre, J.C. (2018). Conversion of D-fructose to 5-(hydroxymethyl)furfural: evaluating batch and continuous flow conditions by design of experiments and in-line FTIR monitoring. *ACS Sustainable Chem. Eng.* 6: 4220–4230.

36 Welch, C.J., Gong, X., Cuff, J. et al. (2009). Online analysis of flowing streams using microflow HPLC. *Org. Process Res. Dev.* 13: 1022–1025.

37 Loren, B.P., Wleklinski, M., Koswara, A. et al. (2017). Mass spectrometric directed system for the continuous-flow synthesis and purification of diphenhydramine. *Chem. Sci.* 8: 4363–4370.

38 Giraudeau, P. and Felpin, F. (2018). Flow reactors integrated with in-line monitoring using benchtop NMR spectroscopy. *React. Chem. Eng.* 3: 399–413.

39 Ferretti, A.C., Mathew, J.S., and Blackmond, D.G. (2007). Reaction calorimetry as a tool for understanding reaction mechanisms: application to Pd-catalyzed reactions. *Ind. Eng. Chem. Res.* 46: 8584–8589.

40 Bakeev, K.A. (ed.) (2010). *Process Analytical Technology: Spectroscopic Tools and Implementation Strategies for the Chemical and Pharmaceutical Industries*. Chichester, GB-WSX: Wiley.

https://www.twirpx.org & http://chemistry-chemists.com

41 Gach, P.C., Iwai, K., Kim, P.W. et al. (2017). Droplet microfluidics for synthetic biology. *Lab Chip* 17: 3388–3400.

42 Hirata, J., Ariese, F., Gooijer, C., and Irth, H. (2003). Continuous-flow protease assay based on fluorescence resonance energy transfer. *Anal. Chim. Acta* 478: 1–10.

43 Hirata, J., Chung, L.P., Ariese, F. et al. (2005). Coupling of size-exclusion chromatography to a continuous assay for subtilisin using a fluorescence resonance energy transfer peptide substrate: testing of two standard inhibitors. *J. Chromatogr. A* 1081: 140–144.

44 Heus, F., Giera, M., de Kloe, G.E. et al. (2010). Development of a microfluidic confocal fluorescence detection system for the hyphenation of nano-LC to on-line biochemical assays. *Anal. Bioanal.Chem.* 398: 3023–3032.

45 Falck, D., de Vlieger, J.S.B., Giera, M. et al. (2012). On-line electrochemistry–bioaffinity screening with parallel HR-LC-MS for the generation and characterization of modified p38α kinase inhibitors. *Anal. Bioanal.Chem.* 403: 367–375.

46 Ramjee, M.K. and Patel, S. (2017). Continuous-flow injection microfluidic thrombin assays: the effect of binding kinetics on observed enzyme inhibition. *Anal. Biochem.* 528: 38–46.

47 Parry, D.M. (2019). Closing the loop: developing an integrated design, make, and test platform for discovery. *ACS Med. Chem. Lett.* 10: 848–856.

48 Gioiello, A., Mancino, V., Filipponi, P. et al. (2016). Concepts and optimization strategies of experimental design in continuous-flow processing. *J. Flow Chem.* 6: 167–180.

49 Rasmuson, A., Andersson, B., Olsson, L. et al. (ed.) (2014). *Mathematical Modeling in Chemical Engineering*. Cambridge, GB: Cambridge University Press.

50 Clayton, A.D., Schweidtmann, A.M., Clemens, G. et al. (2020). Automated self-optimisation of multi-step reaction and separation processes using machine learning. *Chem. Eng. J.* 384: 123340.

51 Henson, A.B., Gromski, P.S., and Cronin, L. (2018). Designing algorithms to aid discovery by chemical robots. *ACS Cent. Sci.* 4: 793–804.

52 Granda, J.M., Donina, L., Dragone, V. et al. (2018). Controlling an organic synthesis robot with machine learning to search for new reactivity. *Nature* 5559: 377–381.

53 Schweidtmann, A.M., Clayton, A.D., Holmes, N. et al. (2018). Machine learning meets continuous flow chemistry: automated optimization towards the Pareto front of multiple objectives. *Chem. Eng. J.* 352: 277–282.

54 Fitzpatrick, D.E., Battilocchio, C., and Ley, S.V. (2016). Enabling technologies for the future of chemical synthesis. *ACS Cent. Sci.* 2: 131–138.

55 Farahzadi, A., Shams, P., Rezazadeh, J., and Farahbakhsh, R. (2018). Middleware technologies for cloud of things: a survey. *Digital Commun. Networks* 4: 176–188.

56 Elliott, C., Vijayakumar, V., Zink, W., and Hansen, R. (2007). National instruments LabVIEW: a programming environment for laboratory automation and measurement. *JALA* 12: 17–24.

https://www.twirpx.org & http://chemistry-chemists.com

57 Matlab. https://www.mathworks.com/products/matlab.html (accessed 05 January 2022).

58 Cherkasov, N., Bai, Y., Expósito, A.J., and Rebrov, E.W. (2018). OpenFlowChem – a platform for quick, robust and flexible automation and self-optimisation of flow chemistry. *React. Chem. Eng.* 3: 769–780.

59 Roch, L.M., Häse, F., Kreisbeck, C. et al. (2018). ChemOS: orchestrating autonomous experimentation. *Sci. Rob.* 3: eaat5559.

60 Fitzpatrick, D.E., Maujean, T., Evans, A.C., and Ley, S.V. (2018). Across-the-world automated optimization and continuous-flow synthesis of pharmaceutical agents operating through a cloud-based server. *Angew. Chem. Int. Ed.* 57: 15128–15132.

61 Hajduk, P.J., Galloway, W.R.J.D., and Spring, D.R. (2011). Drug discovery: a question of library design. *Nature* 470: 42–43.

62 Kim, J., Kim, H., and Park, S.B. (2014). Privileged structures: efficient chemical "navigators" toward unexplored biologically relevant chemical spaces. *J. Am. Chem. Soc.* 136: 14629–14638.

63 Kolb, H.C., Finn, M.G., and Sharpless, K.B. (2001). Click chemistry: diverse chemical function from a few good reactions. *Angew. Chem. Int. Ed.* 40: 2004–2021.

64 Thirumurugan, P., Matosiuk, D., and Jozwiak, K. (2013). Click chemistry for drug development and diverse chemical-biology applications. *Chem. Rev.* 113: 4905–4979.

65 Jiang, X., Hao, X., Jing, L. et al. (2019). Recent applications of click chemistry in drug discovery. *Expert Opin. Drug Discovery* 14: 779–789.

66 Hou, J., Liu, X., Shen, J. et al. (2012). The impact of click chemistry in medicinal chemistry. *Expert Opin. Drug Discovery* 7: 489–501.

67 Kappe, C.O. (2010). Click chemistry under non-classical reaction conditions. *Chem. Soc. Rev.* 39: 1280–1290.

68 Wang, J., Sui, G., Mocharla, V.P. et al. (2006). Integrated microfluidics for parallel screening of an *in situ* click chemistry library. *Angew. Chem. Int. Ed.* 118: 5402–5407.

69 Wang, Y., Lin, W.-Y., Liu, K. et al. (2009). An integrated microfluidic device for large-scale *in situ* click chemistry screening. *Lab Chip* 9: 2281–2285.

70 Lehmann, J., Alzieu, T., Martin, R.E., and Britton, R. (2013). The Kondrat'eva reaction in flow: direct access to annulated pyridines. *Org. Lett.* 15: 3550–3553.

71 Martin, R.E., Lehmann, J., Alzieu, T. et al. (2016). Synthesis of annulated pyridines as inhibitors of aldosterone synthase (CYP11B2). *Org. Biomol. Chem.* 14: 5922–5927.

72 Macan, A.M., Šalić, A., Gregorić, T. et al. (2017). Continuous flow-ultrasonic synergy in click reactions for the synthesis of novel 1,2,3-triazolyl appended 4,5-unsaturated L-ascorbic acid derivatives. *RSC Adv.* 7: 791–800.

73 Macan, A.M., Harej, A., Cazin, I. et al. (2019). Antitumor and antiviral activities of 4-substituted 1,2,3-triazolyl-2,3-dibenzyl-L-ascorbic acid derivatives. *Eur. J. Med. Chem.* 184: 111739.

https://www.twirpx.org & http://chemistry-chemists.com

74 Harej, A., Macan, A.M., Stepanić, V. et al. (2019). The antioxidant and antiproliferative activities of 1,2,3-triazolyl-L-ascorbic acid derivatives. *Int. J. Mol. Sci.* 20: 4735.

75 Alam, M.P., Bilousova, T., Spilman, P. et al. (2018). A small molecule mimetic of the humanin peptide as a candidate for modulating NMDA-induced neurotoxicity. *ACS Chem. Neurosci.* 9: 462–468.

76 Herrera, R.P. and Marquès, E. (ed.) (2015). *Multicomponent Reactions: Concepts and Applications for Design and Synthesis*. Weinheim, Germany: Wiley-VCH, GmbH & Co. KGaA.

77 Dömling, A., Wei Wang, W., and Wang, K. (2012). Chemistry and biology of multicomponent reactions. *Chem. Rev.* 112: 3083–3135.

78 Zhi, S., Ma, X., and Zhang, W. (2019). Consecutive multicomponent reactions for the synthesis of complex molecules. *Org. Biomol. Chem.* 17: 7632–7650.

79 Van Mileghem, S., Veryser, C., and De Borggraeve, W.M. (2018). Flow-assisted synthesis of heterocycles via multicomponent reactions. In: *Flow Chemistry for the Synthesis of Heterocycles. Topics in Heterocyclic Chemistry* (ed. U. Sharma and E. Van der Eycken), 133–159. Cham, Switzerland AG: Springer.

80 Reutlinger, M., Rodrigues, T., Schneider, P., and Schneider, G. (2014). Combining on-chip synthesis of a focused combinatorial library with computational target prediction reveals imidazopyridine GPCR ligands. *Angew. Chem. Int. Ed.* 53: 582–585.

81 Cerra, B., Mostarda, S., Custodi, C. et al. (2016). Integrating multicomponent flow synthesis and computational approaches for the generation of a tetrahydroquinoline compound based library. *Med. Chem. Commun.* 7: 439–446.

82 Cerra, B., Carotti, A., Passeri, D. et al. (2019). Exploiting chemical toolboxes for the expedited generation of tetracyclic quinolines as a novel class of PXR agonists. *ACS Med. Chem. Lett.* 10: 677–681.

83 Damien, W. and Jamison, T.F. (2010). Continuous flow multi-step organic synthesis. *Chem. Sci.* 1: 675–680.

84 Britton, J. and Raston, C.L. (2017). Multi-step continuous-flow synthesis. *Chem. Soc. Rev.* 46: 1250–1271.

85 Guetzoyan, L., Nikbin, N., Baxendale, I.R., and Ley, S.V. (2013). Flow chemistry synthesis of zolpidem, alpidem and other $GABA_A$ agonists and their biological evaluation through the use of in-line frontal affinity chromatography. *Chem. Sci.* 4: 764–769.

86 Guetzoyan, L., Ingham, R.J., Nikbin, N. et al. (2014). Machine-assisted synthesis of modulators of the histone reader BRD9 using flow methods of chemistry and frontal affinity chromatography. *Med. Chem. Commun.* 5: 540–546.

87 Gioiello, A., Rosatelli, E., Teofrasti, M. et al. (2013). Building a sulfonamide library by eco-friendly flow synthesis. *ACS Comb. Sci.* 15: 235–239.

88 Rosatelli, E., Carotti, A., Ceruso, M. et al. (2014). Flow synthesis and biological activity of aryl sulfonamides as selective carbonic anhydrase IX and XII inhibitors. *Bioorg. Med. Chem. Lett.* 24: 3422–3425.

89 Pagano, N., Herath, A., and Cosford, N.D.P. (2011). An automated process for a sequential heterocycle/multicomponent reaction: multistep continuous flow

https://www.twirpx.org & http://chemistry-chemists.com

synthesis of 5-(thiazol-2-yl)-3,4-dihydropyrimidin-2(1*H*)-ones. *J. Flow Chem.* 1: 28–31.

90 Pagano, N., Teriete, P., Mattmann, M.E. et al. (2017). An integrated chemical biology approach reveals the mechanism of action of HIV replication inhibitors. *Bioorg. Med. Chem.* 25: 6248–6265.

91 Mostarda, S., Filipponi, P., Sardella, R. et al. (2014). Glucuronidation of bile acids under flow conditions: design of experiments and Koenigs–Knorr reaction optimization. *Org. Biomol. Chem.* 12: 9592–69600.

92 Mostarda, S., Passeri, D., Carotti, A. et al. (2018). Synthesis, physicochemical properties, and biological activity of bile acids 3-glucuronides: novel insights into bile acid signalling and detoxification. *Eur. J. Med. Chem.* 144: 349–358.

93 Wong Hawkes, S.Y.F., Chapela, M.J.V., and Montembault, M. (2005). Leveraging the advantages offered by microfluidics to enhance the drug discovery process. *QSAR Comb. Sci.* 24: 712–721.

94 Desai, B., Dixon, K., Farrant, E. et al. (2013). Rapid discovery of a novel series of Abl kinase inhibitors by application of an integrated microfluidic synthesis and screening platform. *J. Med. Chem.* 56: 3033–3047.

95 Czechtizky, W., Dedio, J., Desai, B. et al. (2013). Integrated synthesis and testing of substituted xanthine based DPP4 inhibitors: application to drug discovery. *ACS Med. Chem. Lett.* 4: 768–772.

96 Pant, S.M., Mukonoweshuro, A., Desai, B. et al. (2018). Design, synthesis, and testing of potent, selective hepsin inhibitors via application of an automated closed-loop optimization platform. *J. Med. Chem.* 61: 4335–4347.

97 Werner, M., Kuratli, C., Martin, R.E. et al. (2014). Seamless integration of dose–response screening and flow chemistry: efficient generation of structure–activity relationship data of beta-secretase (BACE1) inhibitors. *Angew. Chem. Int. Ed.* 53: 1704–1708.

98 Linshiz, G., Jensen, E., Stawski, N. et al. (2016). End-to-end automated microfluidic platform for synthetic biology: from design to functional analysis. *J. Biol. Eng.* 10: 3.

99 MacConnell, A.B., Price, A.K., and Paegel, B.M. (2017). An integrated microfluidic processor for DNA-encoded combinatorial library functional screening. *ACS Comb. Sci.* 19: 181–192.

100 Qiu, C., Fang, Z., Zhao, L. et al. (2019). Microflow-based dynamic combinatorial chemistry: a microscale synthesis and screening platform for the rapid and accurate identification of bioactive molecules. *React. Chem. Eng.* 4: 658–662.

https://www.twirpx.org & http://chemistry-chemists.com

https://www.twirpx.org & http://chemistry-chemists.com

6

Application of Continuous-Flow Processing in Multistep API and Drug Syntheses

Faith M. Akwi and Paul Watts

Nelson Mandela University, Faculty of Science, Department of Chemistry, University Way, Port Elizabeth, 6031, South Africa

6.1 Introduction

Drug shortage and access is a major global problem that is reported to cause strain on health systems of many countries [1] with mainly developing economies being hit the hardest [2]. A number of different factors play a role in fueling this problem such as unfavorable political and ethical issues, natural disasters, change in drug markets and demand, poor supply and chain management systems, the high cost of manufacturing quality products, and/or change in manufacturing processes and product formulations to mention but a few [3–6]. An analysis of the causes of drug shortages in a sample of 163 drugs between 2013 and 2017 by the US Food and Drug Administration (FDA) economists showed that about 62% of these drugs went into shortage due to disruptions in supply mainly caused by manufacturing or product quality issues [7]. This puts into perspective the importance of product quality in the manufacture of active pharmaceutical intermediates (APIs) and final product formulations. From available literature sources, it is evident that the introduction of continuous-flow processing technology in the synthesis of fine and specialty chemicals can provide a potentially feasible solution toward cost-effective flexible manufacturing of high purity APIs and drugs in high throughput and in an environmentally friendly way [8–11]. Moreover, it also has the ability to enable shorter manufacturing to market times, therefore contributing to solving the drug shortage and access problem; however, acceptance of such technologies by regulatory bodies very much determines their widespread use. In the advent of the FDA and European Medicines Agency (EMA's) support toward the use of continuous-flow processing [12–14], the pharmaceutical manufacturing industry has witnessed an increased interest in the technology. There has been an equally huge rise in research and development efforts in academia toward establishing industrially viable continuous-flow processes for the synthesis of APIs and drug candidates [15–21]. Using current examples, we detail the use of continuous-flow processing in the total multistep syntheses of APIs; some of which are featured on the World Health Organization's (WHO) 2018 list of essential

Flow and Microreactor Technology in Medicinal Chemistry, First Edition. Edited by Esther Alza.
© 2022 WILEY-VCH GmbH. Published 2022 by WILEY-VCH GmbH.

https://www.twirpx.org & http://chemistry-chemists.com

medicines [22] for the treatment of curable ailments and the management of life threatening conditions.

6.2 Antibacterial Agents

6.2.1 Ciprofloxacin

Ciprofloxacin is a 6-fluoroquinolone derivative, which is on the WHO's list of essential of medicines used for the treatment of inhalational anthrax, salmonella infections and shigellosis in children, complicated urinary tract infections, and lower respiratory tract infections [23]. Tosso et al. reported an efficient continuous-flow synthesis of ciprofloxacin **1** via a chemoselective *C*-acylation by early insertion of the cyclopropylamine moiety to yield the desired vinylogous cyclopropyl amide **2**. In this alternative route where a three-reactor platform was used (Figure 6.1), no isolation and purification of intermediates was required [24]. Using tetrahydrofuran (THF) as a reaction solvent and prior optimized batch conditions, the "one-flow" synthesis of quinolone **4** was effected via the *C*-acylation of vinylogous amide **2** and acyl chloride **3** in the presence of excess lithium bis(trimethylsilyl)amide (LiHMDS) in a 2 ml reactor coil. Quinolone **4** was generated in 95% isolated yield in a one minute residence time. To achieve a truly telescoped continuous-flow synthesis, piperazine **5** in dimethyl sulfoxide (DMSO) was preheated at 60 °C and mixed with the outlet stream from the first reactor prior to being fed into a 10 ml reactor coil kept at 140 °C (75 psi back pressure). In 2.5 minutes, 96% conversion to piperazine ester derivative **6** was achieved; **6** was thereafter flowed into the next 10 ml reactor coil in which it was hydrolyzed in the presence of NaOH at 120 °C; 90% conversion to **7** was achieved in 1.2 minutes. This was followed by an offline pH adjustment with HCl to furnish 83%

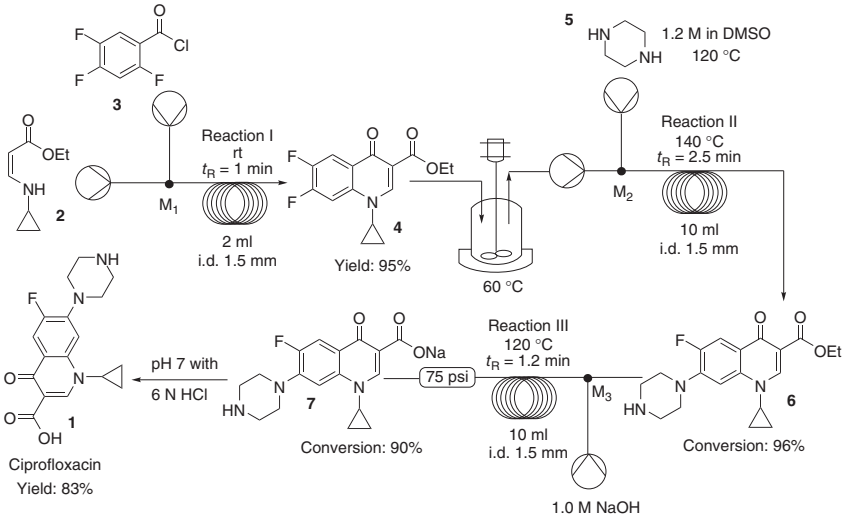

Figure 6.1 Continuous-flow synthesis of ciprofloxacin **1**. Source: Tosso et al. [24].

https://www.twirpx.org & http://chemistry-chemists.com

isolated yield of **1**. The telescoped continuous-flow process was reported to have a throughput of 15.8 g/h. A 4.7 minute end-to-end greener continuous-flow process for the synthesis of ciprofloxacin void of purification, separation, and isolation of intermediates was elegantly developed. The use of additional solvents for the isolation and purification of intermediates was also avoided.

6.2.2 Linezolid

The first ever fully continuous seven-step flow synthesis of linezolid **8**, another antibiotic on the WHO's list of essential medicines, has been reported [25]. Linezolid is used as a last line of defense treatment against multidrug resistant gram-positive bacteria [26]. The continuous-flow process successfully furnished linezolid in seven steps without any intermediate purification and solvent exchanges (Figure 6.2).

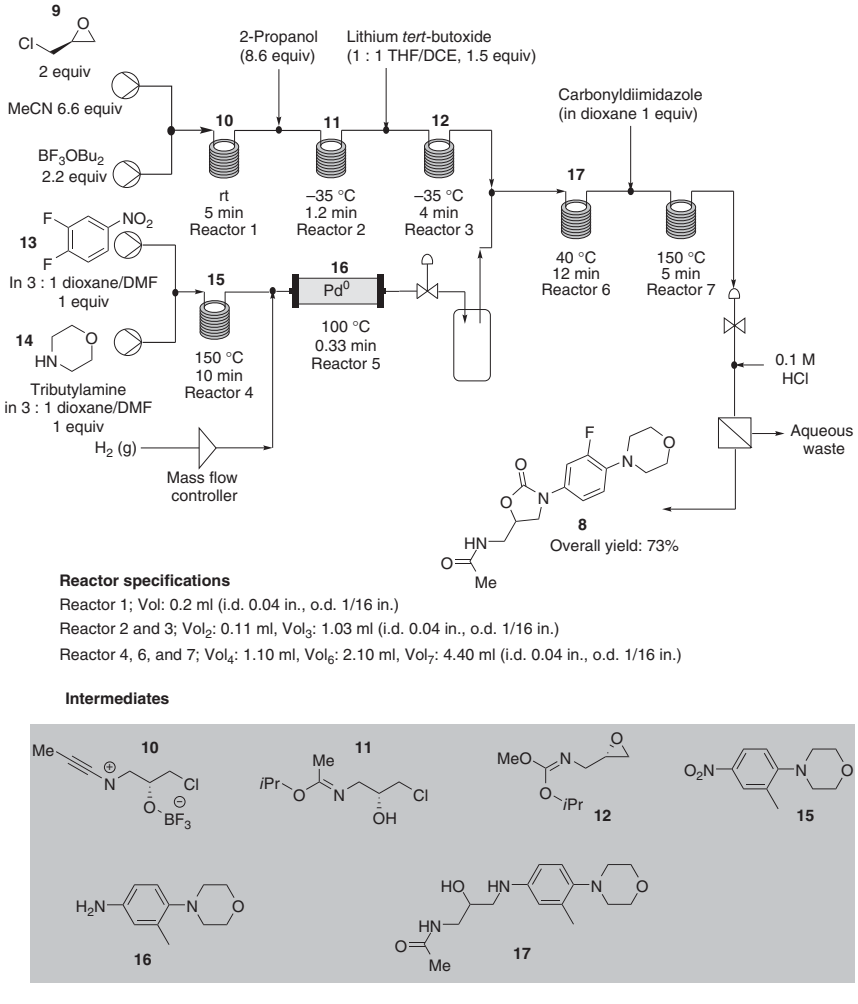

Figure 6.2 Seven-step continuous-flow synthesis of linezolid **8**.

https://www.twirpx.org & http://chemistry-chemists.com

Most importantly, the use of protecting groups was avoided, in turn rendering the process green and environment friendly. The continuous-flow synthesis of linezolid was started from a Ritter reaction between (+)-epichlorohydrin (2 equiv) **9** and acetonitrile (6.6 equiv) in the presence of BF_3OBu_2 (2.2 equiv) as a Lewis acid at room temperature to give amide **10** in 90% isolated yield in only five minutes residence time. A reactive quench of the Lewis acid using 2-propanol (8.6 equiv) at −35 °C for 1.2 minutes, which generated the soluble boronic ester by-product, was integrated into the flow system. The nitrilium ion intermediate from the Ritter reaction reacted with the 2-propanol to give imidate **11**, which was thereafter treated with lithium *tert*-butoxide (1.5 equiv) in THF:1,2-dichloroethane solvent system (1 : 1) at −35 °C for four minutes to give epoxide **12**. The use of 1,2-dichloroethane helped to keep the lithium chloride salts formed during the formation of the epoxide **12** in solution. Side product formation was also minimized in the epoxide formation due to the presence of the imidate **11** rather than the reactive amine.

Next, the authors looked into the synthesis of aniline **16,** which was generated via a nucleophilic substitution reaction between morpholine (1 equiv) **14** and 3,4-difluoronitrobenzene (1 equiv) **13** at 150 °C in a mixed solvent system of 1,4 dioxane and *N*,*N*-dimethylformamide (3 : 1) and in the presence of tributylamine. The reaction went to completion in only 10 minutes residence time to afford **15**. This was followed by reduction using Pd(0) in a packed-bed reactor in the presence of hydrogen gas at reaction 100 °C and back pressure of 100 psi. The hydrogen gas:liquid flow rate was kept at a ratio of 15 : 1, respectively. Aniline **16** was generated in 0.33 minutes. For this transformation, the group skillfully chose the 1,4 dioxane and *N*,*N*-dimethylformamide solvent system that not only enhanced the substitution reaction but also kept all reactants and by-products in solution. It should also be noted that no dehalogenation by-product was observed. The reduction went to full completion to give desired aniline **16**. Excess hydrogen was removed from the system using a gravity-sealed container, and the scrubbed reaction stream containing aniline **16** rejoined the mainstream continuous-flow system using an additional pump to react with epoxide **12** to furnish amino alcohol **17** in 12 minutes at 40 °C. The authors report that any attempts at increasing the reaction temperature and decreasing the residence time led to decreased conversion due to possible hydrolysis of the imidate to amine in the presence of water generated from the reduction step. In this process, the isolation of unstable amino alcohol **17** was not required. The continuous-flow system enabled its use, as it was generated, for the final step to obtain oxazolidinone derivative **8**, linezolid. Amino alcohol **17** was treated with *N*,*N*-carbonyldiimidazole in dioxane at 150 °C for five minutes after which HCl was added and in-line separation was performed. Linezolid was collected and purified off-line to give 73% isolated yield (816 mg/h) in a total residence time of 27 minutes. An *E*-factor of 25 was calculated for this process (Figure 6.2).

6.2.3 Cefotaxime

Cefotaxime **18** is a commercial cephalosporin antibiotic used in the treatment of joint infections, pneumonia, meningitis, urinary tract infections,

https://www.twirpx.org & http://chemistry-chemists.com

gonorrhea, pelvic inflammatory disease, cellulitis, and sepsis [27]. Pieper et al. recently developed a continuous-flow process for this broad spectrum API [28]. (*Z*)-(2-Aminothiazol-4-yl)-methoxyiminoacetic acid (34.8 mmol) **19** in dimethylacetamide was treated with 4-toluenesulfonyl chloride (31.4 mmol) in the presence of triethylamine (33.9 mmol) at −11 °C to generate intermediate **20** with toluenesulfonic acid as a by-product in a stirred tank reactor for 1.5 hours. This solution was reported to only be stable for an hour. On the other hand, a mixture of 7-aminocephalosporanic acid (27.54 mmol) **21** and triethylamine (67.44 mmol) in methanol was kept chilled at 0 °C in the second reactor tank. The two solutions were thus fed into a 10 ml tubular reactor for the amidation reaction of 7-aminocephalosporanic acid **21** with intermediate **20** in the presence of triethylamine to afford cefotaxime **18**. The excellent heat transfer in the continuous-flow system, which is attributed to the large surface area to volume ratio, facilitated an increase in the working reaction temperature of the process to a more manageable −10 °C. At a residence time of one minute, 97.2% conversion of 7-aminocephalosporanic acid (ACA) **21** was achieved to give 81% yield of cefotaxime **18**. The authors also managed to demonstrate the feasibility of using methanol, a more environmentally friendly solvent compared with dichloromethane for the amidation reaction. The continuous-flow system was reported to have the ability to deliver a space–time yield of approximately 3000 kg/m^3 h, 400 times higher than that of the batch system (6.5 m^3 reactor volume, 200 kg 7-ACA **21** input, total reaction time, and setup of six hours) with smaller holdup volumes, thus ensuring process safety (Figure 6.3).

6.2.4 Rifampicin

Li et al. demonstrate the coupling of a separation technique i.e. in-line crystallization in the microreactor synthesis of rifampicin **22** [29]. Rifampicin is an antibiotic also

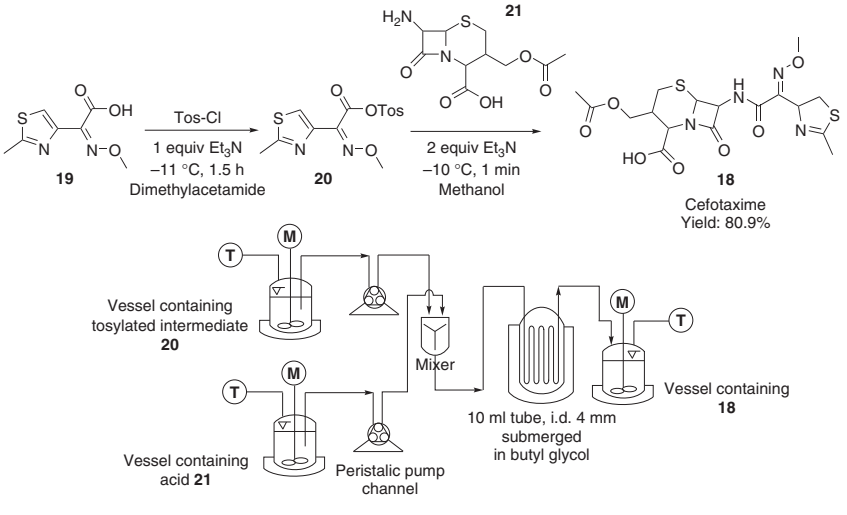

Figure 6.3 A cefotaxime **18** synthesis in a tubular flow reactor.

https://www.twirpx.org & http://chemistry-chemists.com

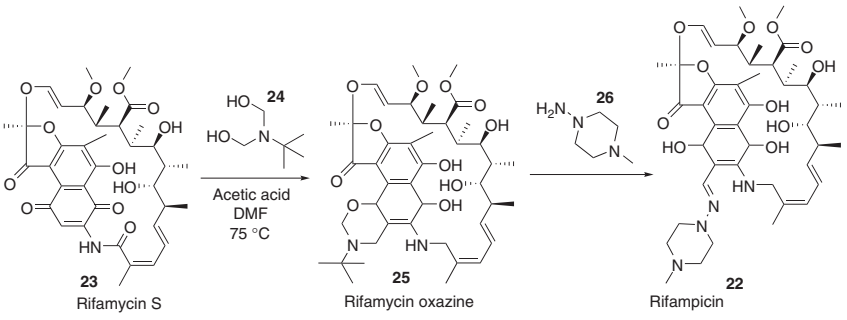

Scheme 6.1 Synthetic route toward rifampicin **22**.

on the WHO's list of essential medicines used for the treatment of tuberculosis [30], leprosy [31], and Legionnaire's disease [32]. The two-step synthesis was performed in an R-series flow chemistry microreactor system from Vapourtec. It was started off with the condensation of rifamycin S (1 equiv) **23** and *tert*-butylamine (100% w/w 1.3 equiv) **24** in the presence of acetic acid (4 equiv) to afford rifamycin oxazine **25** with a conversion of 82% in 25 minutes (Scheme 6.1). This was followed by the ring opening reaction between rifamycin oxazine **25** and 1-amino-4-methylpiperazine (1.7 equiv) **26** at 80 °C to furnish rifampicin **22** in 85% conversion in 15 minutes. Finally, precipitation of the product **22** from the dimethylformamide (DMF) reaction mixture was investigated, and water proved to be a suitable antisolvent. Additionally, in order to overcome potential reactor clogging issues, optimum reactor internal diameter and reaction stream flow rate were studied, and it was found that a microreactor internal diameter of 2 mm and a flow rate of 4 ml/min ensured a successful microflow crystallization with an optimal DMF:water ratio of 1 : 5. A 91% yield of rifampicin was recorded from the crystallization process. Careful selection of ideal solvents capable of keeping starting material rifamycin S **23** and desired product rifampicin **22** in solution coupled with ideal reactant concentrations enabled the development of a fully continuous process without the hiccups of blockages and tasking solvent exchange protocols (Figure 6.4). A 67% overall yield of rifampicin **22** was achieved in 1.5 hours compared with 51% reported in the batch synthesis.

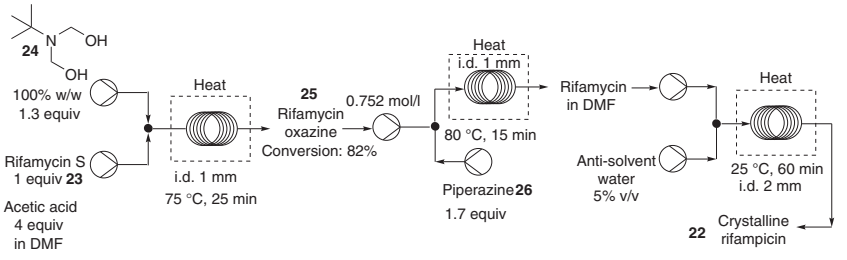

Figure 6.4 Flow synthesis of rifampicin **22**.

https://www.twirpx.org & http://chemistry-chemists.com

Furthermore, the molar ratio of piperazine **26** to rifamycin oxazine **25** required for the ring opening reaction in this process was greatly reduced by 25%.

6.3 Anticancer Agents

6.3.1 Lomustine

Jaman et al. have synthesized lomustine, an anticancer agent for the treatment of brain tumors and Hodgkin's lymphoma under continuous-flow conditions [33]. The carbamylation and nitrosation steps toward lomustine **27** were individually optimized prior to telescoping the process that did not require isolation or purification of the intermediate. In the carbamylation step, leading toward the synthesis of intermediate compound **30**, cyclohexamine **28** was reacted with 1-chloro-2-isocyanato-ethane (1.4 equiv) **29** in a Chemtrix S1 glass system fitted with a 3225 SOR reactor chip. An isolated yield of 92% **30** was reported in 60 seconds at a reaction temperature of 50 °C using tetrahydrofuran as a reaction solvent. The second step was optimized in a similar microreactor setup used in the carbamylation reaction. *tert*-Butyl nitrile (3 equiv) was used as a nitrosating agent with acetonitrile/ethanol as a reaction solvent system. At a reaction temperature of 25 °C and residence time of eight minutes, 91% of pure **27** was isolated by a simple hot filtration of the crude product from petroleum ether to remove intermediate compound **30**. This reaction step was skillfully optimized using desorption electron spray ionization mass spectrometry. It should also be pointed out that the use of $NaNO_2$ (3 equiv)/HCO_2H (neat) was also studied as an alternative nitrosating agent; however, it was found that under similar stoichiometric conditions, at a reaction temperature of 0 °C, a residence time of five minutes was required to furnish lomustine **27** in only 74% isolated yield.

To enable the telescoped synthesis of lomustine **27** shown in Figure 6.5, a Zaiput liquid–liquid extractor was employed to remove the base from the carbamylation reaction. The total synthesis was reoptimized in fluorinated ethylene propylene (FEP) tubing reactors. The carbamylation reaction was optimized at 50 °C and a residence time of one minute, while the nitrosation step required eight minutes and a reaction temperature of 25 °C. With these reaction conditions, the total continuous-flow synthesis of lomustine in the presence of 0.01 equiv of base was achieved giving 63% (110 mg/h) over all isolated yield in nine minutes, which corresponds to one dose per two hours. For an API that is administered orally every six weeks, this is a very promising approach toward its synthesis that can readily offer a feasible solution to its shortage.

6.3.2 Imatinib

Using a similar approach of skillfully manipulating flow setups and solvent mixtures, Fu and Jamison have developed a continuous-flow modular synthesis of imatinib that operates efficiently without the need of solvent switches, in-line purification, or packed-bed reactors as shown in Figure 6.6 [34]. Imatinib **31**

https://www.twirpx.org & http://chemistry-chemists.com

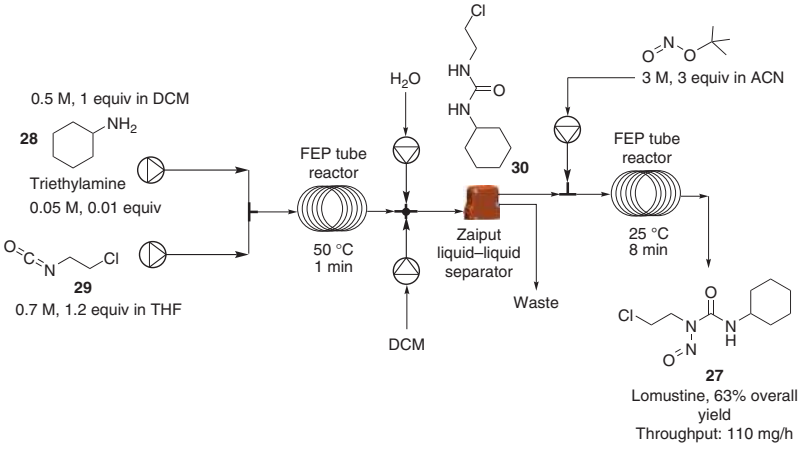

Figure 6.5 Telescoped flow synthesis of lomustine **27**.

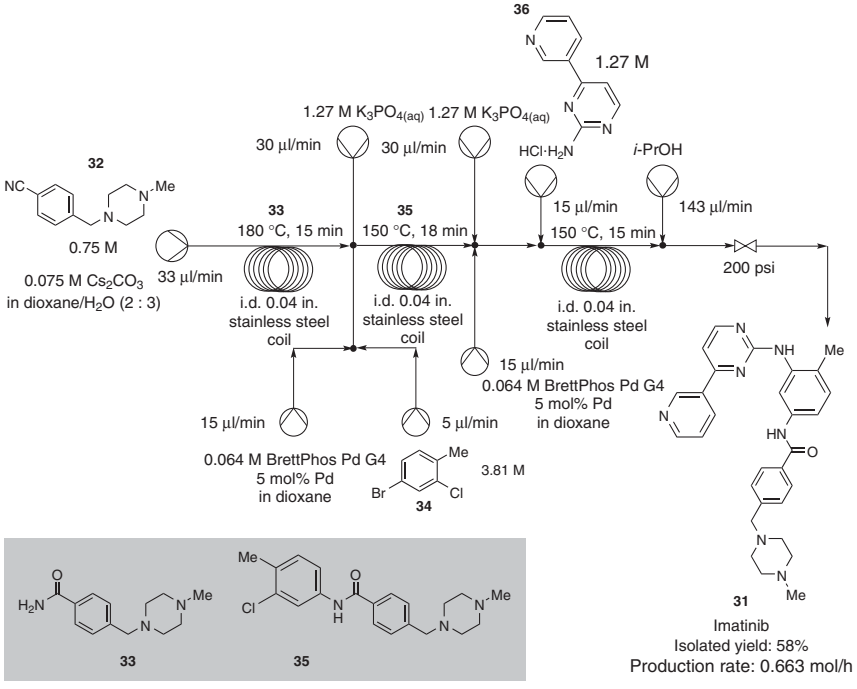

Figure 6.6 Telescoped flow synthesis of imatinib **31**. Source: Fu and Jamison [34].

https://www.twirpx.org & http://chemistry-chemists.com

is a Bcr-AbI tyrosine kinase inhibitor currently on the WHO's list of essential medicines. It is used in the treatment of leukemia and gastrointestinal stromal tumor. (The application of flow chemistry for the Imatinib case is broadly explained in Chapter 4.) The hydration of nitrile **32** (0.8 M in dioxane/water solvent system [2 : 3 v/v]) was successfully performed in a continuous-flow manner in the presence of 10 mol% Cs_2CO_3 at 180 °C (240 psi back pressure) to give desired product **33** in 91% yield after 15 minutes. This stream was fed to the next reactor for the chemoselective amidation reaction with **34** at 150 °C for 15 minutes. Amide **35** was then subjected to C–N bond formation with 2-aminopyrimidine derivative **36** in a continuous-flow process. The conjugate acid of 2-aminopyrimidine derivative **36** was dissolved in water (1 M) and mixed with BrettPhos Pd G4 catalyst (0.025 M, 5 mol% Pd in dioxane) in a T-mixer whose outlet stream was connected to another T-mixer to meet a second stream containing K_3PO_4 (3 M) and amide **35** in dioxane/water solvent system. This collective stream was thereafter fed into a stainless steel coil (i.d.: 0.04″) maintained at 150 °C (back pressure: 200 psi) to furnish imatinib in 58% isolated yield in total residence time of 48 minutes. A production rate of 0.663 mmol/h was recorded. Furthermore, two novel imatinib analogs were also synthesized in 57–66% yield with excellent chemoselectivity using this continuous-flow protocol.

6.4 Antifungal Agents

6.4.1 Fluconazole

Szeto et al. recently demonstrate how continuous-flow synthesis enabled the development of a simple streamlined multistep synthesis of fluconazole **37** that can easily be operated by non-experts in the field (Figure 6.7) [35]. Fluconazole is a first generation bis-triazole antifungal medicine used in the treatment of invasive fungal infections [36]. The API was achieved via four principal chemical transformations, i.e. Friedel–Crafts acylation, alkylation, Corey–Chaykovsky epoxidation, and epoxide opening. In a 10 ml perfluoroalkoxyalkane (PFA) reactor, the Friedel–Crafts acylation of 1,3-difluorobenzene **38** (1 equiv in nitromethane) with chloroacetyl chloride **39** (1.3 equiv, neat) in the presence of $AlCl_3$ (1.15 equiv in nitromethane) was reacted to afford α-chloroketone **40** (90% conversion) in 25 minutes at 80 °C.

To effect the insertion of the triazole moiety, 1,2,4-trizole derivative **44** (20 equiv, 10 M) and α-chloroketone **40** (0.5 M) in a *N*-methyl-pyrrolidone (NMP):H_2O solvent system (2 : 1) were reacted in a 10 ml PFA reactor at 150 °C from which a 96% conversion was obtained in 35 minutes residence time (Figure 6.8). A huge excess of the triazole **44** was however required to minimize over alkylation derivative of compound **43**. An alternative route was investigated using *N*-aminotriazole **41**. The two-step process using *N*-aminotriazole **41** toward intermediate **43** in NMP:H_2O (3 : 1) solvent system at 130 °C for 35 minutes gave 100% conversion after deamination ($NaNO_2$ in 4 M HCl).

Despite the fact that no over alkylation of compound **42** was observed, the authors report being unable to pursue this route for the development of the continuous-flow

https://www.twirpx.org & http://chemistry-chemists.com

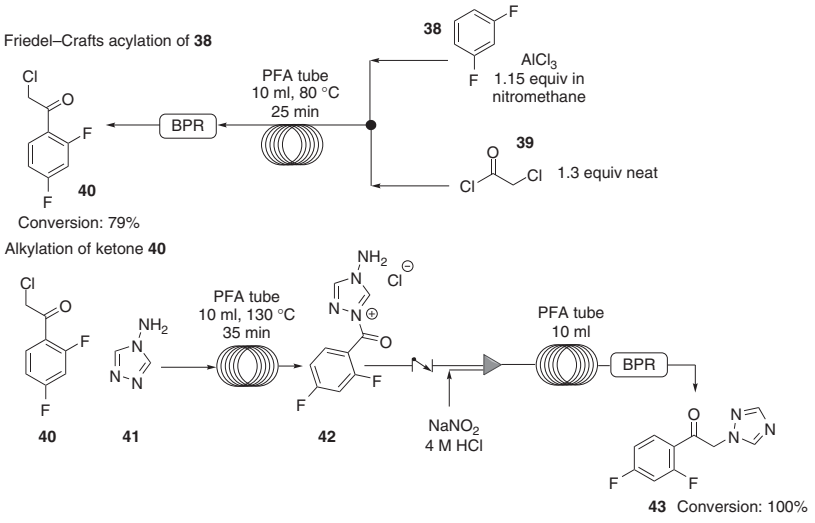

Figure 6.7 Friedel–Crafts acylation and alkylation steps in the flow synthesis of fluconazole **37**. Source: Szeto et al. [35]/Springer Nature.

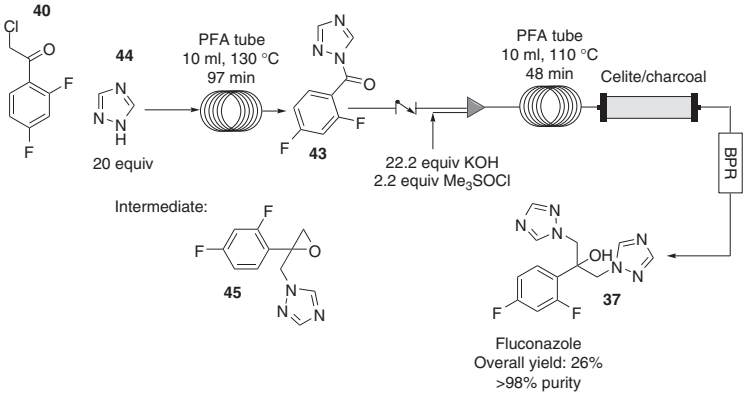

Figure 6.8 A telescoped flow synthesis of fluconazole **37**.

synthesis of fluconazole **37**. This was due to the downstream aqueous workup that would be required after the deamination step to facilitate a telescoped synthesis (Figure 6.7).

The Corey–Chaykovsky epoxidation/epoxide ring opening was performed in a similar reactor as the first two steps. Using Me_3SOI (1.2 equiv, 0.6 M), 1,2,4-triazole derivative **43** (1 equiv, 0.5 M) was treated with KOH (2.4 equiv, 1.2 M) at 80 °C in 15% H_2O:DMSO solvent system. Only 57% conversion to desired product was recorded. It was also noted that an increase in temperature led to an increase in conversion;

https://www.twirpx.org & http://chemistry-chemists.com

however, the insolubility of Me_3SOI became problematic. As a result, the authors opted for the more soluble Me_3SOCl. At similar stoichiometric conditions using NMP:H_2O (1 : 1) as a solvent system, a 96% conversion was obtained at 110 °C in 40 minutes residence time. Further investigations toward the feasibility of telescoping the alkylation, Corey–Chaykovsky epoxidation, and ring opening showed that the excess 1,2,4 triazole **44** from the alkylation of **40** was able to facilitate ring opening of epoxide **45** downstream of the flow process (Figure 6.8). Using NMP as a reaction solvent, α-chloroketone **40** and 1,2,4-triazole **44** (20 equiv) were fed into a 10 ml PFA reactor at 130 °C for 97 minutes to obtain intermediate **43,** which was further treated with Me_3SOCl (2.2 equiv) in the presence of KOH (22.2 equiv) at 110 °C for 48 minutes to furnish epoxide **45**. The excess 1,2,4 triazole **44** in the system subsequently effected ring opening to generate fluconazole **37** in 26% over all yield. A simple continuous-flow process for the synthesis of fluconazole with a celite/charcoal in-line purification column was developed (Figure 6.8).

In contrast, Korwar et al., in 2017, developed a semicontinuous-flow method toward the synthesis of fluconazole **37** where an aryl-turbo Grignard **47** was employed to obtain intermediate **49** from 1,3-dichloroacetone **48** in a telescoped synthesis to afford 87% isolated yield of intermediate **49** (total residence time: 3.5 minutes at room temperature) [37]. The last step toward fluconazole was however optimized in batch mode to give 74% conversion in 4.5 hours using MeOH:H_2O (90%) as a solvent system in the presence of Na_2CO_3 as a base (Figure 6.9). Both approaches present huge improvements toward the synthesis of fluconazole **37**; nevertheless, the continuous-flow process by Szeto et al. provides shorter processing time, which can be equated to providing a higher throughput per unit time.

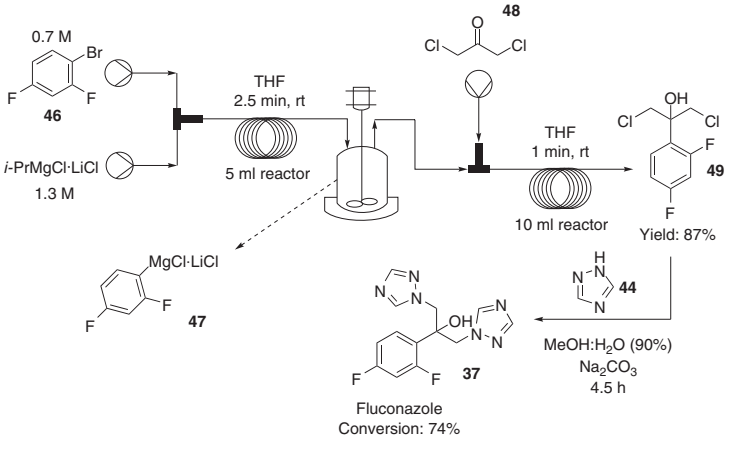

Figure 6.9 An aryl turbo Grignard-based semicontinuous-flow synthesis of fluconazole **37**.

https://www.twirpx.org & http://chemistry-chemists.com

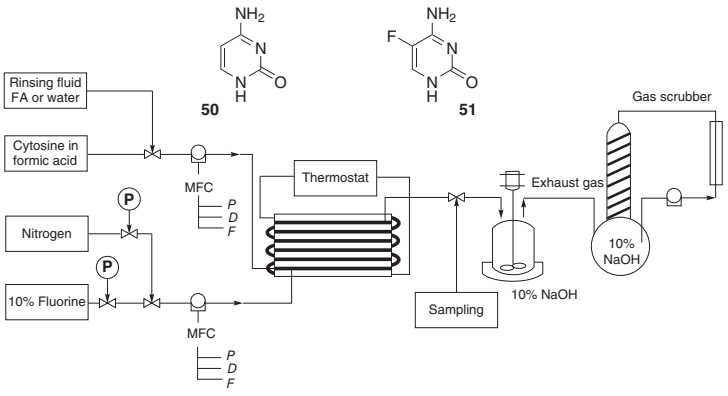

Figure 6.10 Continuous-flow synthesis of flucytosine **51** via fluorination of cytosine **50**.

6.4.2 Flucytosine

Flucytosine **50**, another antifungal drug on the WHO's list of essential medicines has been successfully synthesized in a one-step continuous-flow process shown in Figure 6.10 using fluorine gas [38]. Together with amphotericin B, flucytosine has recently been recommended for the first line treatment of cryptococcal meningitis [39]. It is also a vital intermediate in the synthesis of emtricitabine [40] and capecitabine [41] anti-HIV and anticancer drugs, respectively. The gas–liquid phase reaction was performed in a narrow-bore stainless steel tube (i.d.: 1.4 mm, length: 1 m) through which a solution of cytosine **51** in formic acid (4 mmol/h) and fluorine gas (5 mmol/h, 10% in nitrogen) was flowed. Excellent conversion (>99%) of cytosine **51** was achieved in 90 minutes with 63% isolated yield of flucytosine **50**. The synthesis was also scaled up with ease in a mesoscale Boostec flow reactor system fabricated from silicon carbide consisting of six process plates (volume: 61 ml, total channel length: 16 m). A high throughput of 59 g/h of flucytosine **50** (83% isolated yield, >99% purity) was achieved from 0.54 mol/h of cytosine **51** and 0.7 mol/h of fluorine (10% in nitrogen). Notably, the precise reaction parameter control in the continuous-flow systems, which in turn provided high selectivity and thus minimized the formation of undesired difluorinated compounds, was demonstrated compared to the batch process (38% isolated yield) in the fluorination of cytosine **51**.

6.5 Anti-HIV Agents

6.5.1 (*R*)-Propylene Carbonate: An Intermediate Toward Anti-HIV Drug, Tenofovir

Suveges et al. recently reported a continuous-flow synthesis of (*R*)-propylene carbonate **52**, a key intermediate in the synthesis of tenofovir [42]. Tenofovir is a

https://www.twirpx.org & http://chemistry-chemists.com

nucleotide adenosine 5′monophosphate derivative commercially available as a prodrug, tenofovir disoproxil fumarate used for the treatment of HIV [43] and hepatitis B virus (HBV) [44]. It is also used in combination with emtricitabine, emtricitabine, and efavirenz, and emtricitabine and rilpivirine, or elvitegravir/cobicistat [45]. The authors obtained glycidol **54** from glycerol carbonate **53** (66% conversion in seven minutes) using $NaAlO_2$ as a catalyst at 90 °C in a packed-bed flow reactor. The same reaction took 90 minutes in a batch microwave reactor at 117 °C. An attempt to obtain (*R*)-glycidol **55** from kinetic resolution of racemic glycidol **54** using porcine pancreas lipase demonstrated a lack of selectivity in glycidol **54** conversion. Both enantiomers of glycidol acetate were found to interact with the enzyme moreover with similar interaction energies (−10.935 and −10.831 kcal/mol for *R* and *S* enantiomers, respectively). Hydrogenolysis of racemic glycidol **54** was thereafter opted for from which >99% conversion of diol **55** was obtained in 17 minutes from a tube in tube and a 10% Pd/C packed-bed reactor system at room temperature. The flow system provided an excellent improvement in reaction time and output compared to the batch reaction that took 60 hours to afford 86% conversion. The successful kinetic resolution of diol **55** required prior introduction of a trityl group on the primary hydroxyl group of **55** in order to improve the chiral recognition and selection of the secondary hydroxyl by the enzyme. In a 3 ml coil reactor kept at 30 °C, the trityl group was introduced to diol **55** to provide 63% conversion of trityl ether **57** in 15 minutes. A reduction in reaction time was also observed in this flow synthesis in contrast to the batch synthesis (12 hours). This was followed by kinetic resolution of the trityl ether **57** using immobilized lipase Novozyme 435 and vinyl acetate **58** as an acyl donor at 30 °C in a packed-bed column reactor. A conversion of 47% with enantiomeric ratios >170 was obtained in a shorter reaction time of seven minutes compared with the 12 hours in the batch synthesis. This was backed up by the fact that the use of biocatalysts in continuous-flow systems often yields satisfactory reaction outputs due to the efficient mass transfer and continuous removal of product and unreacted reactants from the reaction space as compared with batch systems [46]. A space–time yield of 98 g/h was obtained from the continuous-flow process, which was demonstrated to be stable; no change in conversion and selectivity was observed when it was kept running for eight hours. A 97% conversion was obtained in 30 minutes via dual deprotection of intermediate (*R*)-**60** in a packed-bed column reactor using $NaHSO_4{\cdot}SiO_2$ at 30 °C. (*R*)-**61** was thereafter subjected to suitable flow conditions for carbonate formation; dimethyl carbonate as solvent in the presence of 1,8-diazabicyclo[5.4.0]undec-7-ene (DBU) at 120 °C in a 3 ml coil reactor gave 94% yield (*R*)-propylene carbonate **52** in one hour. The authors demonstrate how a highly selective synthesis of (*R*)-propylene carbonate **52** with tremendously short reaction time and excellent yield was enabled in continuous-flow systems (Figure 6.11).

6.5.2 Dolutegravir

Recently, Jamison and coworkers reported a seven-step flow synthesis of a second generation HIV integrase strand transfer inhibitor used for the treatment of HIV-1 infections, dolutegravir **62** [47]. The flow synthesis was adapted from a reported GlaxoSmithKline process chemistry batch route for cabotegravir. Using a one by

https://www.twirpx.org & http://chemistry-chemists.com

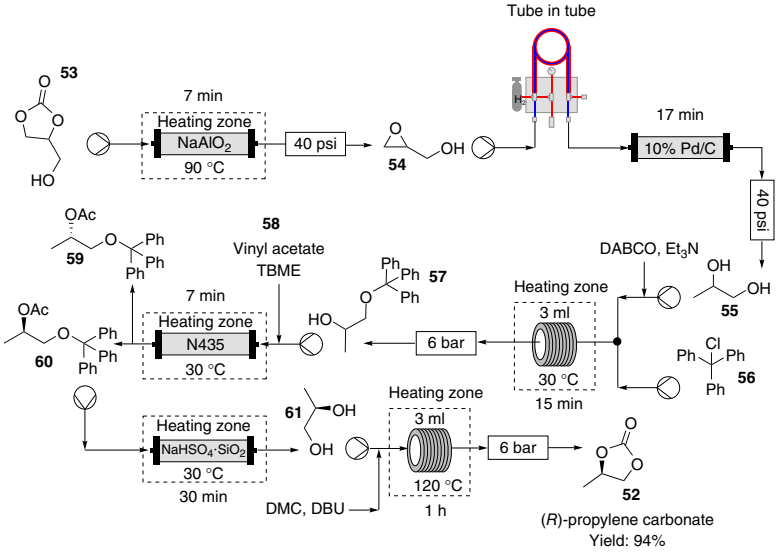

Figure 6.11 Modular flow synthesis of (*R*)-propylene carbonate **52**.

one reaction step screening and optimization approach in both batch and flow reactors, telescoped flow synthesis of dolutegravir **62** was achieved. The investigation of the flow synthesis of dolutegravir **62** was started from the condensation of methyl-4-methoxyacetoacetate **63** with DMF–dimethyl acetal (DMA) **64** to give vinylogous amide **65** in full conversion. The intermediate **67** was thereafter furnished from a two-step telescoped synthesis in 95% yield and a throughput of 43 g/h. Pyridone **69** was successfully obtained from the reaction of **67** and dimethyl oxalate **68** in an isolated yield of 56% and a throughput of 3.4 g/h from a fully continuous three-step synthesis (Figure 6.12) in a total residence time of 74 minutes.

Direct amidation of **70** under basic and acidic conditions was also investigated, from which it was found that LiOMe or NaOMe in a mixed solvent system of methanol and toluene gave optimum yield of 95% at 80 °C in 35 minutes. Unfortunately, any attempts to telescope this protocol with the previous steps were futile due to extensive clogging. The continuous-flow amidation of **70** was thus carried out under acidic conditions. This was followed by continuous-flow deprotection of acetal **72** and cyclization with (*R*)-3-aminobutan-1-ol **73** to obtain **74**, which could only be achieved via a two-step flow process. This avoided the formation of by-product **75** gotten from elimination of hemiaminal ether functionality and deprotected pyridine. **74** was furnished in a total residence time of 66 minutes at a reaction temperature of 100 °C. The deprotection of acetal **72** and cyclization with (*R*)-3-aminobutan-1-ol **73** was telescoped with the previous step, i.e. acid-catalyzed direct amidation of **70**. In 290 minutes, compound **74** was obtained in 48% yield. A three-step telescoped flow synthesis of **74** was successfully attained (Figure 6.13).

The investigation was concluded with a modular flow synthesis of **62** via demethylation of **74** using LiBr. An 89% yield of **62** was reported to have been obtained within

https://www.twirpx.org & http://chemistry-chemists.com

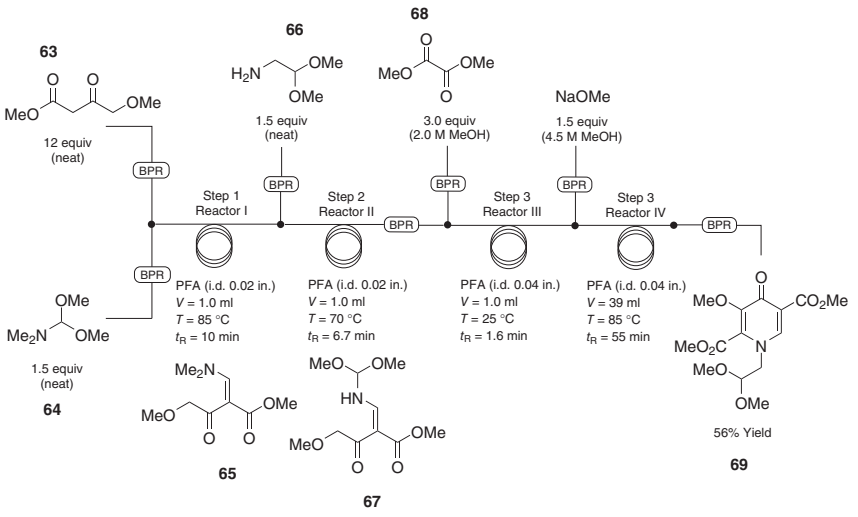

Figure 6.12 A three-step telescoped pyridone flow synthesis toward dolutegravir **62**.

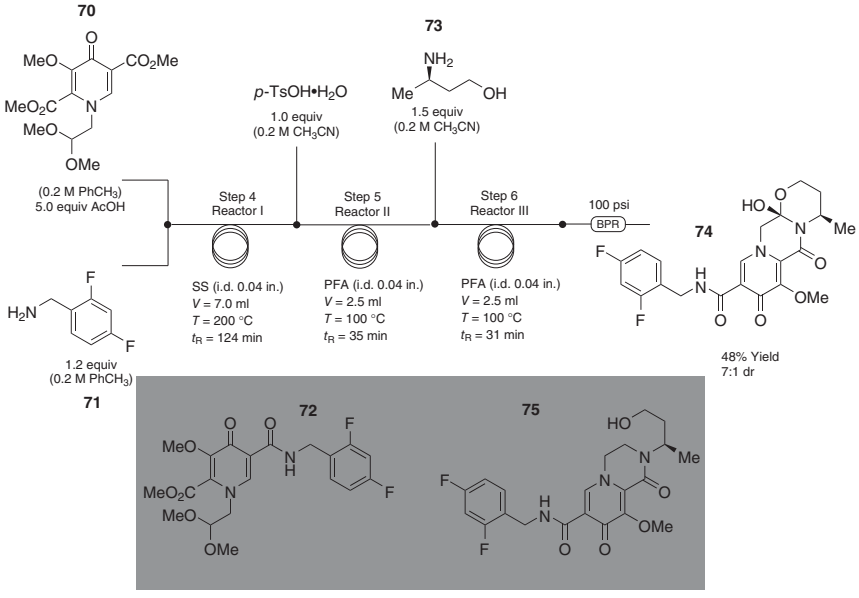

Figure 6.13 A three-step telescoped flow synthesis of amide derivative **74**.

a residence time of 31 minutes at 100 °C (Figure 6.14). Jamison and coworkers successfully translated seven batch reaction steps in the synthesis of dolutegravir **62** to a continuous-flow synthesis. In addition, short reaction times, good yield, and selectivity; benefits of continuous-flow processing, were showcased in the telescoped and stand-alone flow protocols developed. In the grand scale of things, this in turn will ultimately contribute to shortening the manufacture to market times as well as

https://www.twirpx.org & http://chemistry-chemists.com

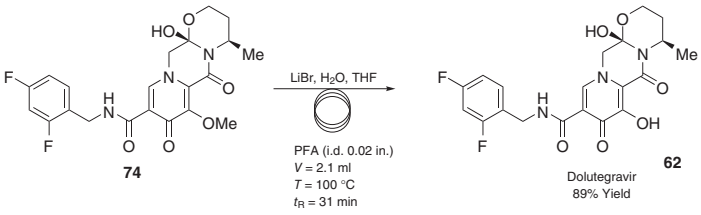

Figure 6.14 Demethylation of amide derivative **74** in the flow synthesis of dolutegravir **62**.

reducing the cost of production of dolutegravir, therefore, providing more and easy access of the drug to infected persons.

6.5.3 Lamivudine

Mandala et al. report a semicontinuous-flow synthesis of lamivudine [48] **76**, a nucleoside reverse transcriptase inhibitor sold under trade names: Epivir and Epivir-HBV with a high potency in the treatment of HIV-1 and hepatitis B virus as well as the human T-lymphotropic virus (HTLV) [49, 50]. 5-Acetoxy oxathiolane **81**, the first key intermediate, was synthesized in a two-step telescoped continuous-flow synthesis from 1,4-dithiane-2,5-diol **77** and menthyl glyoxalate **78** (Figure 6.15). The flow synthesis of intermediates **79** and **81** was first attempted individually in Little Things Factory microreactors prior to telescoping from which, 5-hydroxy oxathiolane **79** was obtained in 88% conversion in 20 minutes. In order to obtain (2*R*,5*R*)-5-acetoxyoxathiolane **82**, 5-hydroxy oxathiolane **79** was treated with acetic anhydride **80** and pyridine in acetonitrile at ambient temperature to give a 95% conversion in 9.7 minutes. A batch mode recrystallization of the crude at −20 °C gave isomer **82** in 48% yield.

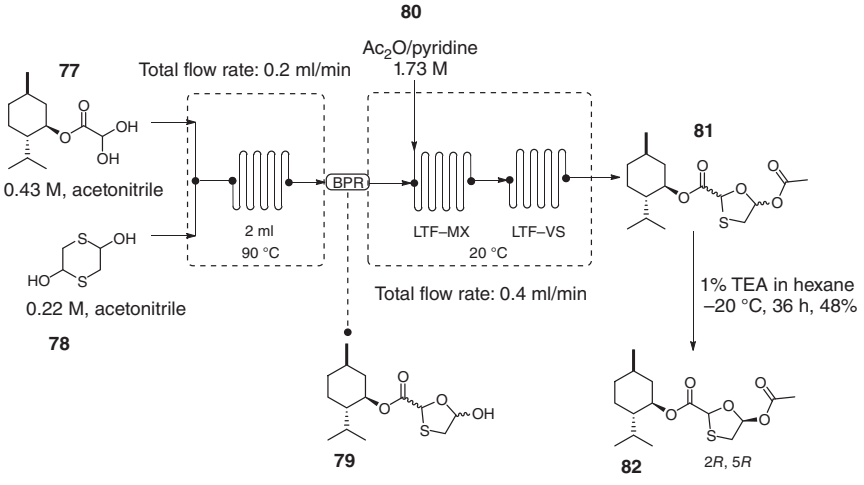

Figure 6.15 Continuous-flow synthesis of (2*R*,5*R*)-5-acetoxyoxathiolane **82**.

https://www.twirpx.org & http://chemistry-chemists.com

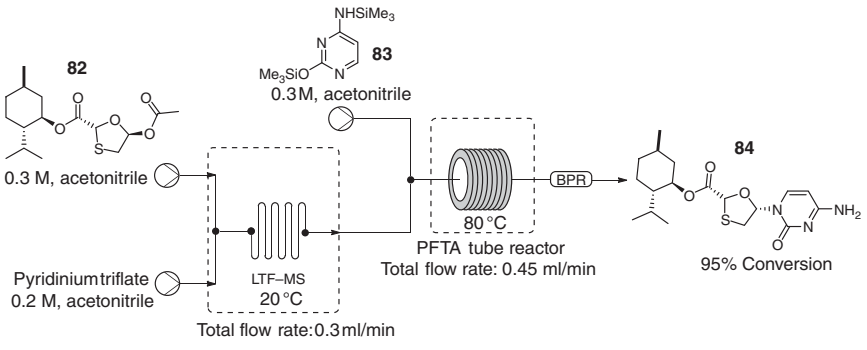

Figure 6.16 Continuous-flow N-glycosidation of compound **82**.

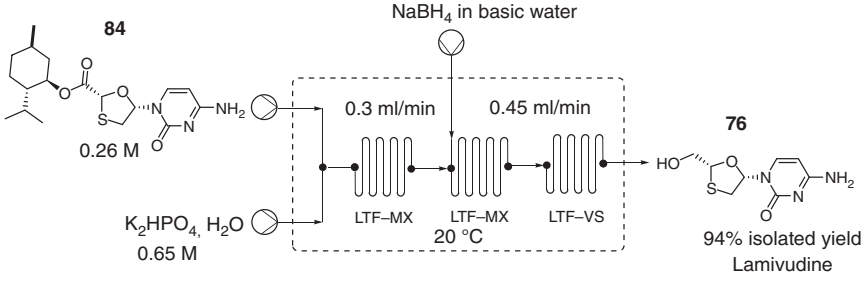

Figure 6.17 Reduction of nucleoside **84** in continuous-flow microreactors.

The N-glycosidation of isomer **82** with nucleobase **83** in the presence of pyridinium triflate posed major challenges in flow due to the poor solubility of the silylated nucleobase. An in-house built thermal controlled syringe wrapping was used to maintain the nucleobase syringe solution at 55–60 °C, thus keeping the base in solution throughout the experimentation (Figure 6.16). At 80 °C, the *N*-glycosidation product **84** was furnished in 95% yield in only 8.4 minutes. The flow synthesis also allowed for the use of a low catalyst concentration (0.2 M).

Finally, $NaBH_4$ reduction of nucleoside **84** in the presence of K_2HPO_4 in Little Things Factory microreactors gave lamivudine **76** in 94% isolated yield and >99% purity in 3.3 minutes (Figure 6.17).

6.5.4 Efavirenz

This is a non-nucleotide reverse transcriptase inhibitor administered orally as a 600 mg tablet taken once daily for the treatment of HIV infection [40]. Chada et al. recently reported a continuous-flow synthesis of an intermediate toward efavirenz **85** starting from *N*-Boc 4-chloroaniline **86** [51] in which *n*-butyllithium was used to facilitate its *ortho*-lithiation. The synthesis also comprised of an in-line reaction quench; a packed bed of anhydrous silica, which was effortlessly added to the microreactor system as shown in Figure 6.18.

https://www.twirpx.org & http://chemistry-chemists.com

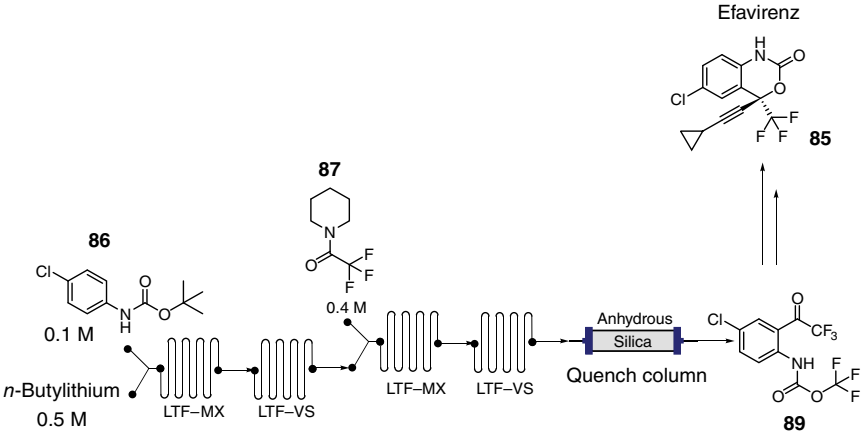

Figure 6.18 Ortho-lithiation of *N*-Boc 4-chloroaniline **86** in the synthesis of an intermediate toward efavirenz **85**.

Accurate reaction parameter control was demonstrated in this synthesis; moreover, the *ortho*-lithiation was successfully performed at temperatures higher than the norm (−78 °C). Using 0.25 M *n*-BuLi, 0.1 M of **86** at −45 °C, and a 0.2 M concentration of **87** gave 70% conversion of **86** to **89**. The flow synthesis of intermediate **89** via the *ortho*-lithiation of *N*-Boc-protected chloroaniline **86** and trifluoroacylation using **87** provided higher conversion at higher temperatures and lower equivalents of *n*-BuLi in the absence of tetramethylethylenediame (TMEDA) compared with its batch synthesis (28% at −78 °C and 5 equiv of *n*-BuLi). Additionally, the flow reactor system ensured process safety and rapid parameter optimization using small amounts of reagents.

6.6 Serotonin Modulators and Stimulators

6.6.1 Flibanserin

Bana et al. have reported a four-step continuous-flow synthesis of flibanserin **90**, an aryl piperazine-type serotonin receptor modulator drug [52] used in the treatment of female hypoactive sexual desire disorder (HSDD) [53]. The four-step synthesis involved reductive amination reactions facilitated by 10% Pd/C, benzimidazolone formation, and biphasic flow deprotection, which were elegantly integrated with an in-line purification protocol (Figure 6.19). Carbamate **91** and aldehyde **92** were hydrogenated using an H-Cube Pro™ on 10% Pd/C at 100 °C and 10 bar to provide full conversion of **93** in eight seconds. This was followed by ring closure of **93** to form benzimidazolone derivative **94** in full conversion in the presence of DBU (200 °C, 7.4 minutes). The biphasic flow deprotection of **94** to afford intermediate **95** was achieved in 6.8 minutes using aqueous HCl and isopropyl acetate at 100 °C after which the organic phase containing the aldehyde **95** was obtained using a gravitational phase separator. The aldehyde **95** was thereafter

https://www.twirpx.org & http://chemistry-chemists.com

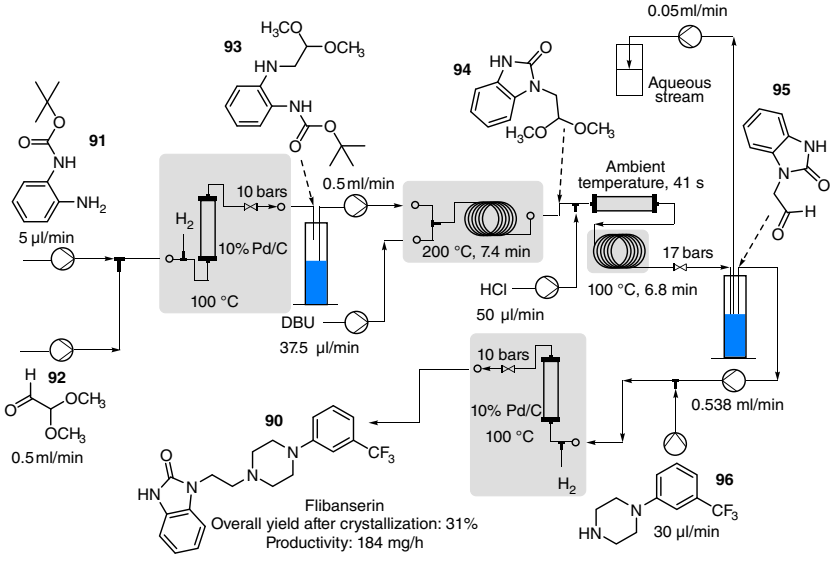

Figure 6.19 Total continuous-flow synthesis of flibanserin **90**.

used in the second reductive amination reaction with piperazine **96** to give full conversion of flibanserin **90** in 12 seconds at 100 °C and a pressure of 10 bar. The authors report that a steady-state operation was possible for more than 2.5 hours without any manual interaction. A 31% overall yield of crystalline flibanserin HCl was obtained after off-line salt formation and precipitation. Compared to the reported batch syntheses of flibanserin **90**, the reported four-step continuous-flow process is much more superior; flibanserin base was furnished in shorter reaction time with a calculated productivity of 184 mg/h equating to 44 doses of 100 mg per 24-hour operation. This demonstrates how continuous-flow processing can provide a feasible solution to the global shortage of important potent molecules such as these.

6.6.2 Vortioxetine

Similarly, Boros et al. demonstrate how flow synthesis in the final step of vortioxetine **97** involving piperazine ring formation led to the highest yield and purity ever reported for the API [54]. Vortioxetine is an antidepressant drug, which belongs to the class of bis-aryl sulfanyl amines. It is used for the treatment of depression by targeting the selective serotonin (5-HT) reuptake inhibitors, 5-HT_{1A} and $5HT_7$ [55]. The piperizine ring formation was afforded via the reaction between 2-[(2,4-dimethylphenyl)sulfanyl]aniline **98** with bis 2-(chloroethyl)amine hydrochloride **99**. This reaction in batch mode took up to 27 hours to give a 63% isolated yield (99% purity by high-performance liquid chromatography [HPLC]) of **97**; however, there was a significant amount of side products detected, which required laborious purification steps to obtain the pure L-(+)-mandelate salt of the desired compound **97**. Using a specialized reactor system consisting of three

https://www.twirpx.org & http://chemistry-chemists.com

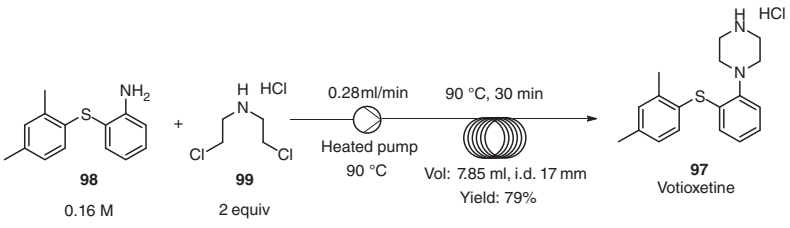

Figure 6.20 Final step continuous-flow synthesis toward votioxetine **97**.

independent thermostable modules, i.e. a heated flask, heated high pressure syringe pump (H-ION HI-PD100), and a heater module (H-ION-HI-HM250), the flow synthesis process of vortioxetine **97** was developed. A preheated solution of 2-[(2,4-dimethylphenyl)sulfanyl]aniline (0.16 M) **98** and bis 2-(chloroethyl)amine hydrochloride (2 equiv) **99** in NMP:toluene (1 : 1) solvent system at 90 °C was flowed through a tubular reactor maintained at a reaction temperature of 190 °C from which 79% yield **97** based on HPLC was recorded. Compound **97** was transformed into its L-(+)-mandelic salt in 99.6% purity (Figure 6.20).

The efficient control of reaction parameters such as residence time and reaction temperature was very crucial for this chemical transformation. Due to the excellent heat transfer in the continuous-flow reactor setup, the side products, which were observed in the batch synthesis, were minimized, and thus desired compound **97** was attained in excellent purity.

6.6.3 Melitracen HCl

This is a tricyclic API, which is part of a drug formulation taken orally for the treatment of depression and anxiety [56]. Pedersen et al. have recently disclosed a Grignard-based continuous-flow synthesis process toward melitracen HCl **100** [57]. This comprised of an energy-efficient room temperature addition of the Grignard **101** followed by hydrolysis of magnesium alkoxide intermediate **103** and dehydration of alcohol **104**. Melitracen HCl was thereafter obtained from the simple gravimetric phase separation and crystallization with HCl. The choice of solvents and careful investigation of optimum reaction conditions was essential in the development of a continuous-flow process. For example, in the Grignard addition step, THF was found to be a suitable solvent, which provided a solution to the first bottleneck, i.e. insolubility of the magnesium alkoxide intermediate **103** formed and providing satisfactory dissolution of starting material **102**.

Compared with the batch process, the flow process shown in Figure 6.21 facilitated a one-step hydrolysis of **103** and dehydration of **104**. Using 37% HCl, full conversion of **104** to dehydrated product **105** was attained in a very short time. In order to go around the inevitable solid formation, a result of the pH adjustment from acidic to basic using ammonia after generating the dehydration product **105**, 40% acetic acid was incorporated into the flow process prior to pH adjustments. This accomplished a homogeneous stream devoid of solids, which upon basification with ammonia gave rise to a biphasic stream. Melitracen HCl **100** was obtained after phase separation

https://www.twirpx.org & http://chemistry-chemists.com

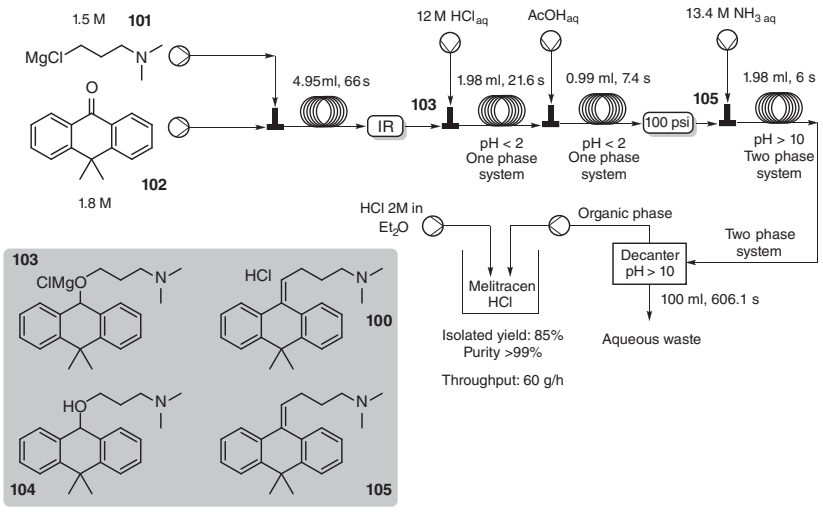

Figure 6.21 A streamlined flow process for the synthesis of melitracen HCl **100**.

and crystallization using 2 M HCl in ether. The authors successfully developed a high-yielding continuous-flow process from which 300 g of melitracen HCl was produced from a stock feed of 240 g starting material **102**. The flow process was also demonstrated to be energy efficient since all the steps were carried out at ambient temperature. Additionally, the continuous-flow approach facilitated rapid and easy streamlining of melitracen HCl synthesis into fewer reaction steps; moreover, infrared (IR) in-line monitoring and purification techniques, liquid–liquid separation, and downstream crystallization were concatenated in the process.

6.7 Cholinesterase Inhibitor

6.7.1 Donepezil

A recently reported base-catalyzed aldol condensation of aromatic ketones with aldehydes using strongly basic anion exchange resin (A26) as a catalyst in continuous flow shows the synergistic effect of employing a combination of heterogeneous catalysis and continuous-flow synthesis [58]. This protocol was adopted for a two-step flow synthesis of donepezil **106** (Figure 6.22), a cholinesterase inhibitor used in the treatment of Alzheimer's disease [59]. Using a solvent system of THF/*i*-PrOH (9 : 1) and 2% water, substrates **107** and **108** were fed into a 7 g A26 packed-bed column reactor (ϕ 10 × 100 mm SUS column) and heated at 55 °C to give intermediate **109** in 92–95% yield in three hours. A turnover frequency of 0.13 h^{-1} and space–time yield of 972 g/l d was recorded. The flow synthesis of enone **109** was thereafter telescoped with the Pd-DMSi/Al_2O_3-catalyzed hydrogenation at 25 °C to produce 7.7 g/d of donepezil **106** for more than 30 hours. Additionally, no traces of ketone reduction or debenzylation product were observed. A high throughput continuous-flow process for the synthesis of donepezil **106** was developed.

https://www.twirpx.org & http://chemistry-chemists.com

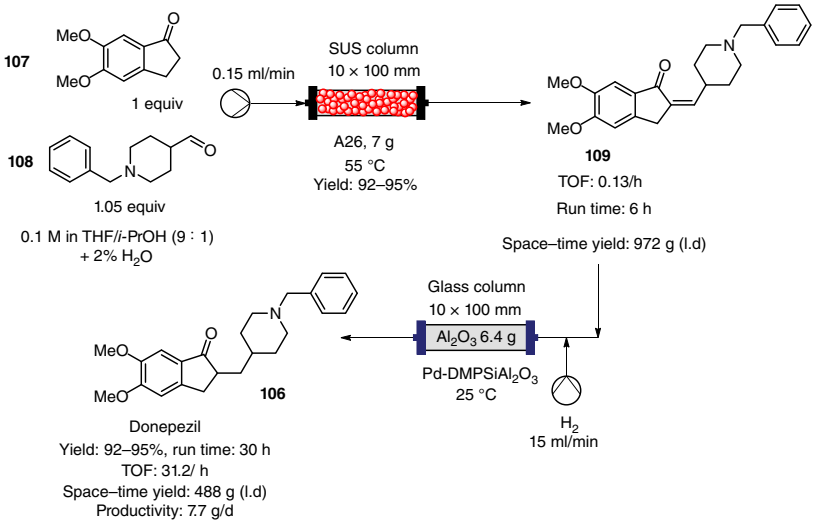

Figure 6.22 Continuous-flow synthesis of donepezil **106**.

6.8 Antimalarial Agent

6.8.1 Hydroxychloroquine

Yu et al. have reported a high-yielding multigram continuous-flow synthesis of hydroxychloroquine **110** [60], an antimalarial drug used in the treatment and prevention of malaria and dermatological disorders [61]. It is also an effective non-steroidal drug with anti-inflammatory activity used for the treatment of rheumatoid arthritis in patients with cardiovascular diseases [62, 63]. 5-Iodopentan-2-one **112** was synthesized from a 55% aqueous solution of hydroiodic acid and neat 3-acetyldihydrofuran-2(3*H*)-one **111** pumped at 1 ml/min from which an isolated yield of 89% was obtained in five minutes residence time at 80 °C. Using a Zaiput membrane separator, an in-line extraction procedure ($NaHCO_3$:hexane/methyl *tert*-butyl ether [MTBE]) was coupled to the continuous-flow system to afford pure 5-iodopentan-2-one **112,** which was subsequently reacted with 2-(ethylamino)ethan-1-ol **113** to give 5-(ethyl(2-hydroxyethyl)amino)pentan-2-one **114** in >80% yield. Oxime **115** was rapidly generated from a telescoped flow process by reaction of **114** with hydroxylamine in the presence of K_2CO_3 packed in a column cartridge. It was found that reagent concentration greatly affected the yield of **115** and as such 1 M solutions of 5-iodopentan-2-one **112**, 2-(ethylamino)ethan-1-ol **113,** and hydroxylamine gave the highest yield of oxime **115** (78% isolated yield) in 20 minutes (flow rate: 1 ml/min) at 100 °C. This was followed by reductive amination of **115**, which was performed in a continuous-flow tank reactor (CSTR) under hydrogen (10 bar) with mechanical stirring using Raney nickel catalyst at 80 °C. In four hours, 98%

https://www.twirpx.org & http://chemistry-chemists.com

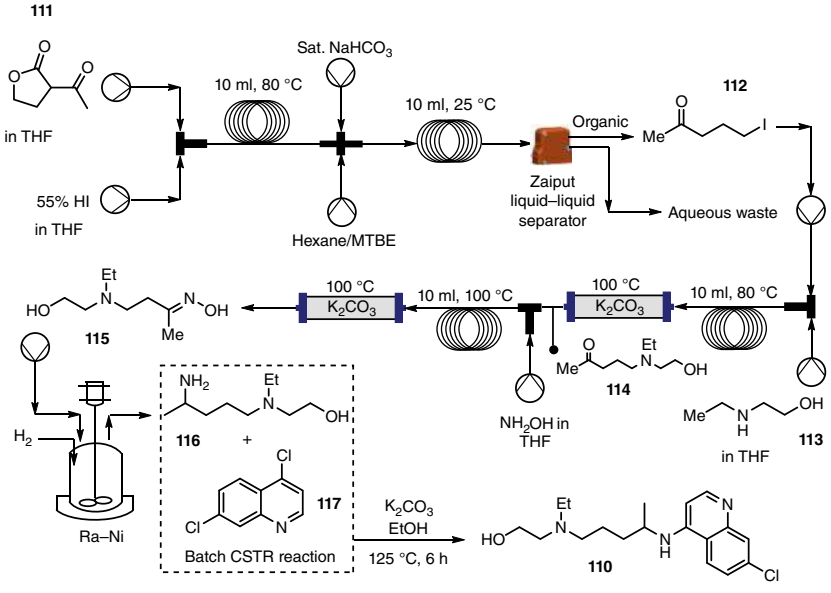

Figure 6.23 A combined flow and batch synthesis approach toward hydroxychloroquine **110**.

conversion of **115** to amine **116** was achieved from a 2 M solution of oxime **115**. The entire process was telescoped to afford key intermediate **116** in 68% overall isolated yield as shown in Figure 6.23. Hydroxychloroquine **110** was finally furnished in six hours from amine intermediate **116** and quinoline derivative **117** in the presence of K_2CO_3:Et_3N (1 : 1) using ethanol as a reaction solvent at 125 °C. Compared to the batch reaction, which takes 24–48 hours, the CSTR synthesis of hydroxychloroquine **110** from amine intermediate **116** only took six hours illustrating the potential of this process in enabling the reduction of manufacture to market times of the API (Figure 6.23). The telescoped synthesis provided an overall isolated yield of 78% hydroxychloroquine **110**.

6.9 Non-peptide Angiotensin II Receptor Blocker

6.9.1 Valsartan

Hiebler et al. have reported a multistep synthesis of valsartan precursor **118** [64]. Valsartan is a non-peptide angiotensin II receptor blocker used for the treatment of high blood pressure [65] and management of hypertension [66]. The late stage valsartan precursor was obtained in three synthetic steps, i.e. *N*-acylation, Suzuki–Miyaura cross-coupling, and methyl ester hydrolysis. In a telescoped continuous-flow system, valsartan precursor **118** was obtained in 96% overall yield in an estimated total residence time of one hour (Figure 6.24).

https://www.twirpx.org & http://chemistry-chemists.com

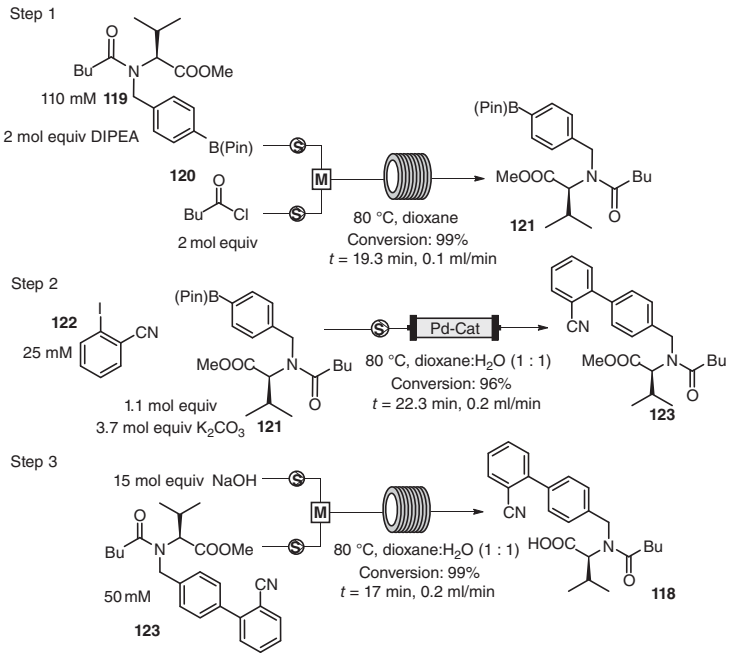

Figure 6.24 A modular flow synthesis of a valsartan precursor **118**.

At a reaction temperature of 80 °C, the *N*-acylation of boronic acid pinacol ester **119** with valeryl chloride **120**, in the presence of *N*,*N*-diisopropylethylamine (DIPEA), was performed in a polyether ether ketone (PEEK) coil using dioxane as the solvent to obtain 99% conversion of **119** in 19.3 minutes (Figure 6.24). The outlet stream from this reactor was first neutralized with aqueous K_2CO_3 (3.7 mol equiv) using a T-mixer. This dioxane/H_2O stream containing intermediate **121** was thereafter flowed through a plug and play HPLC column reactor packed with palladium-substituted cerium-tin-oxide ($Ce_{0.20}Sn_{0.79}Pd_{0.01}O_{2-\delta}$) heterogeneous catalyst. The Suzuki–Miyaura cross-coupling reaction with 2-iodobenzonitrile **122** in the presence of K_2CO_3 at 80 °C provided a 96% yield of intermediate **123** in 22.3 minutes. This reaction stream was premixed with NaOH in dioxane/H_2O in a split and recombine reactor and was subsequently flowed into another PEEK coil reactor heated at 80 °C to effect the methyl ester hydrolysis reaction and furnish the desired compound **118** in 17 minutes (Figure 6.24). The outlet stream was quenched with MeOH:H_2PO_4 (55 : 45) and analyzed by HPLC. Valsartan precursor **118** was obtained in 96% over all yield in an estimated total residence time of one hour and 73% *ee* determined by HPLC. The individual steps, performed in batch including the purification and isolation of intermediates **121** and **123,** gave only 28% overall yield of the valsartan precursor **118**.

https://www.twirpx.org & http://chemistry-chemists.com

6.10 Cystic Fibrosis Transmembrane Conductance Regulator

6.10.1 Ivacaftor

Ivacaftor **124**, a 4-quinolone-3-carboxylic acid ester used of the treatment of cystic fibrosis, has been synthesized in a continuous-flow process [67]. A one-pot quadruple reaction involving ozonolysis, enaminone formation, aza-Michael addition–elimination, and deformylation was developed for the synthesis of ivacaftor **124** (Figure 6.25). Safe ozonolysis of indole ester **125** to afford β-keto ester **126** in 100% conversion at 0 °C in two seconds was carried out in a 30 ml continuous-flow reactor with an overall throughput of 84 g/d. This route avoided the generation of hazardous and explosive ozonide intermediate. The ozonolysis reaction was then followed by cyclization of β-keto ester **126** with DMF–DMA in a continuous-flow tubular reactor from which full conversion to quinolone ester **127** was achieved in 40 minutes at room temperature. In order to achieve a telescoped continuous-flow process for the synthesis of **127**, extraction of β-keto ester **126** using ethyl acetate and its subsequent separation using a gravity-based separator had to be coupled to the flow system. In batch mode, quinolone ester **127** was hydrolyzed to generate corresponding carboxylic acid, which was coupled with amine **128** to furnish ivacaftor **124** in 46% yield. A safe, energy efficient synthesis of

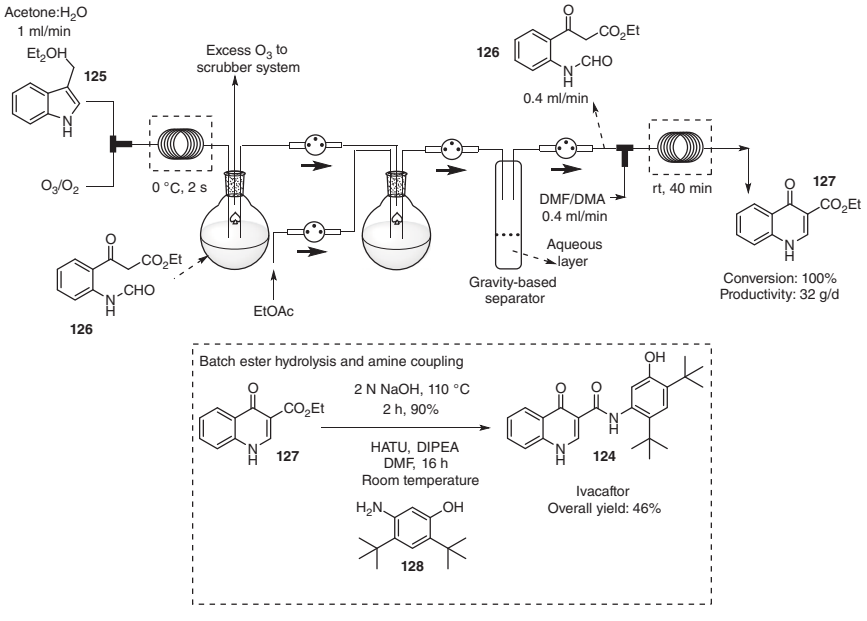

Figure 6.25 A "one-pot" quadruple reaction synthesis approach toward ivacaftor **124**.

https://www.twirpx.org & http://chemistry-chemists.com

quinolone ester **127**, a key intermediate toward the synthesis of ivacaftor **124,** was efficaciously established in a continuous-flow system. In contrast, the conventional batch synthesis of **124** according to literature requires higher temperatures and corrosive reagents [68].

6.11 Non-steroidal Anti-inflammatory Agent

6.11.1 Ibuprofen

This is a non-steroidal anti-inflammatory drug on the WHO's list of essential medicines used for pain management in medical conditions [69] such as osteoarthritis [70]. In 2015, Snead and Jamison reported a three-minute continuous-flow process for the synthesis and purification of ibuprofen [71] **129**. In comparison to prior research on the synthesis of this API, the reported route provided exceptional yields (>90%) per reaction step in very short reaction times (one minute per step). The three-step process comprised of (i) Friedel–Crafts acylation of isobutylbenzene **130** with propionyl chloride **131** in the presence of inexpensive $AlCl_3$ to give ketone **132**, (ii) oxidative 1,2-aryl migration in aryl ketone **132** effected by iodine monochloride (ICI) in the presence of trimethyl orthoformate to afford methyl ester **133**, and finally (iii) saponification of ester **133** was achieved using sodium hydroxide to give **129**.

The continuous-flow process was enabled by an integrated in-line liquid–liquid separation system fitted after an HCl quench of the first reaction step as shown in Figure 6.26. The oxidative 1,2-aryl migration reaction in flow was reported to suffer from clogging due to the formation of insoluble iodine via disproportionation of ICI in *n*-propanol; however, this was solved by using neat ICI for the reaction. A second in-line liquid–liquid separator was added to the process after the ester hydrolysis

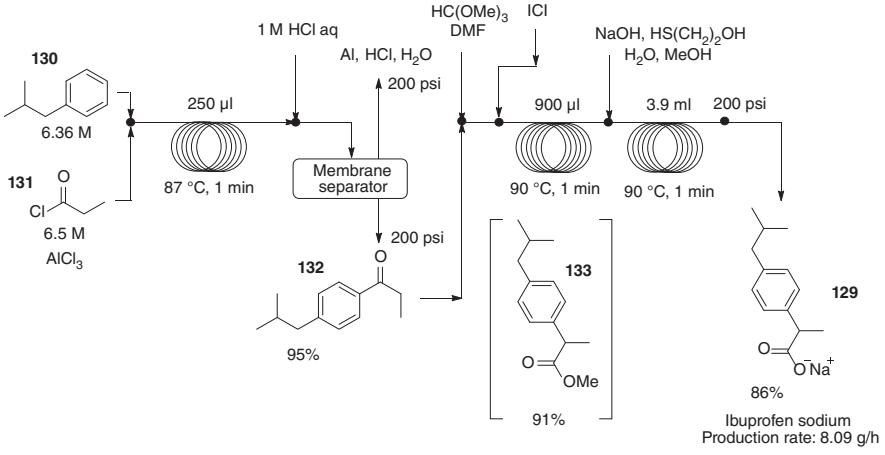

Figure 6.26 Three-step continuous-flow synthesis of ibuprofen **129**.

https://www.twirpx.org & http://chemistry-chemists.com

step to afford ibuprofen **129**. The process was successfully scaled-up and provided a production rate of 500 mg/min.

Most recently, Lee et al. prepared ibuprofen **129** from inexpensive and inactive *p*-xylene **134** [72]. Three-step C–H metalations of benzylic positions facilitated by *in situ* generation of Schlosser's base were successfully performed in flow reactors to afford ibuprofen **129**. Rapid screening of reaction parameters, which was enabled by the continuous-flow synthesis protocol, was demonstrated in the first step of the synthesis, wherein C–H metalation of *p*-xylene **134** in the presence of Schlosser's base generated from *t*-BuOK and BuLi followed by methylation using methyl triflate were both rapidly and smoothly optimized by varying over one hundred reaction conditions. A 95% yield of *p*-ethyl toluene **135** was obtained from the metalation of *p*-xylene (0.3 M in 2-MeTHF) **134** with 1.2 equiv of *t*-BuOK and *t*-BuLi each at −20 °C for 3.14 seconds followed by methylation using methyl triflate (3 equiv in ether). Only 1% 1,4-diethylbenzene, a reaction by-product was detected at these conditions. This was followed with metalation of *p*-ethyl toluene **135** and its subsequent reaction with isopropyl iodide to afford 1-ethyl-4-isobutylbenzene **136** in 93% yield at −40 °C in a total residence time of 80.9 seconds with no by-product detected. Ibuprofen **129** was finally obtained from a third C–H metalation reaction involving 1-ethyl-4-isobutylbenzene **136** and a combination of *t*-BuOK/*t*-BuLi super base. This afforded an anionic intermediate, which in the presence of CO_2 at −40 °C furnished ibuprofen **129** in 57% isolated yield, 2.3 g in 10 minutes (Figure 6.27).

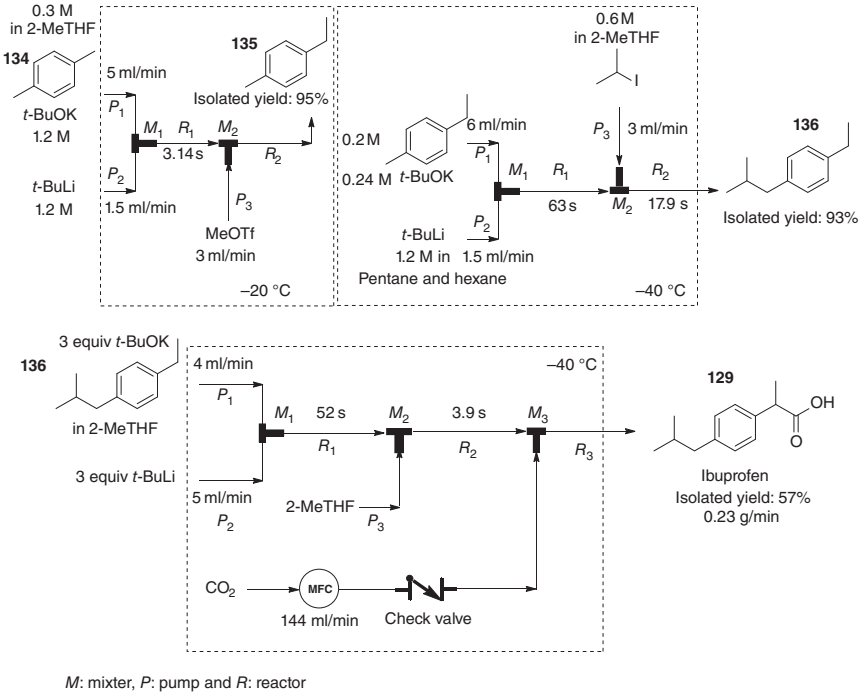

M: mixter, *P*: pump and *R*: reactor

Figure 6.27 C–H metalation in the continuous-flow synthesis of ibuprofen **129**.

https://www.twirpx.org & http://chemistry-chemists.com

In summary, two routes characterized with different and quite problematic chemistries toward the synthesis of a common target molecule **129** were successfully carried out in a continuous-flow manner.

6.12 Conclusion

The development of sustainable holistic approaches toward improving global health is very important for the survival of the human race, and as such, governments, public health policy makers, academic institutions not forgetting the pharmaceutical industry are all playing major roles in providing viable solutions toward this cause. Over the years, innovative discoveries and technologies for diagnostics, testing, and treatment of diseases, changes in policies, and expedited approval of new drug manufacturing techniques in an attempt to enable discovery and access to drugs have been witnessed. On the other hand, from a research and development perspective in the manufacture of potent APIs, it is also safe to say that there has been a rise in new techniques that can facilitate the efficient synthesis of these compounds. In this chapter, the use of continuous-flow technology has been illustrated to have the potential to provide APIs in high throughput with excellent purity and very short synthesis times, which is very crucial in reducing the already extremely long manufacture to market times, one of the driving factors of drug shortages and access. Furthermore, in a few examples discussed here, the combined use of continuous-flow and batch syntheses is shown. It should be emphasized that not all batch syntheses can be translated to or benefit from flow processing. However, more often than not, there are usually reaction steps in a synthetic route toward an API that can be translated to flow processes. This is the key point that needs to be understood in order to successfully develop efficient manufacturing processes for APIs synthesis using continuous-flow systems.

References

1 Gray, A. and Manasse, H.R. Jr., (2012). Shortages of medicines: a complex global challenge. *Bull. World Health Organ.* 90: 158–158A.
2 Pheage, T. (2016–2017). Dying from lack of medicines. Encouraging local production, right policies the way out. http://www.un.org/africarenewal/magazine/december-2016-march-2017/dying-lack-medicines (accessed 13 May 2020).
3 Acosta, A., Vanegas, E.P., Rovira, J. et al. (2019). Medicine shortages: gaps between countries and global perspectives. *Front. Pharmacol.* 10: 1–21.
4 Iyengar, S., Hedman, L., Forte, G., and Hill, S. (2016). Medicine shortages: a commentary on causes and mitigation strategies. *BMC Med.* 14 (1): 1–3.
5 ASHP (2018). Drug shortages roundtable: minimizing the impact on patient care. *Am. J. Health-Syst. Pharm.* 75 (11): 816–820.

https://www.twirpx.org & http://chemistry-chemists.com

6 Drug shortages: root causes and potential solutions. (2019).

7 Woodcock, J. (2019). To help reduce drug shortages, we need manufacturers to sell quality – not just medicine. https://www.fda.gov/news-events/fda-voices/help-reduce-drug-shortages-we-need-manufacturers-sell-quality-not-just-medicine (accessed 13 May 2020).

8 Helal, N.A., Elnoweam, O., Eassa, H.A. et al. (2019). Integrated continuous manufacturing in pharmaceutical industry: current evolutionary steps toward revolutionary future. *Pharm. Pat. Anal.* 8 (4): 139–161.

9 Zhang, P., Weeranoppanant, N., Thomas, D.A. et al. (2018). Advanced continuous flow platform for on-demand pharmaceutical manufacturing. *Chem. Eur. J.* 24: 1–10.

10 Berton, M., de Souza, J.M., Abdiaj, L. et al. (2020). Scaling continuous API synthesis from milligram to kilogram: extending the enabling benefits of micro to the plant. *J. Flow Chem.* 10: 73–92.

11 Bogdan, A.R. and Dombrowski, A.W. (2019). Emerging trends in flow chemistry and applications to the pharmaceutical industry. *J. Med. Chem.* 62 (14): 6422–6468.

12 Pharmaceutical Technology Editors (2016). FDA approves tablet production on Janssen continuous manufacturing line. http://www.pharmtech.com/fda-approves-tablet-production-janssen-continuous-manufacturing-line (accessed 13 May 2020).

13 Niamh Marriott (2017). EMA approves Janssen's Prezista continuous manufacturing line. http://www.europeanpharmaceuticalreview.com/news/62587/ema-continuous-manufacturing (accessed 13 May 2020).

14 United States Food and Drug Administration (2019). Quality considerations for continuous manufacturing guidance for industry. https://www.fda.gov/regulatory-information/search-fda-guidance-documents/quality-considerations-continuous-manufacturing.

15 de Souza, R., Aguiar, R., Leão, R.A.C. et al. (2019). Continuous-flow protocol for the synthesis of enantiomerically pure intermediates of anti epilepsy and anti tuberculosis active pharmaceutical ingredients. *Org. Biomol. Chem.* 17: 1552–1557.

16 Cole, K.P., Groh, J.M.C., Johnson, M.D. et al. (2017). Kilogram-scale prexasertib monolactate monohydrate synthesis under continuous-flow CGMP conditions. *Science* 356 (6343): 1144–1150.

17 Movsisyan, A.M., De Coen, L.M., Heugebaert, T. et al. (2019). Continuous flow synthesis of the phenothiazine antipsychotics: a feasibility study. *Eur. J. Org. Chem.* 2019 (6): 1350–1354.

18 Ötvös, S.B., Pericàs, M.A., and Kappe, C.O. (2019). Multigram-scale flow synthesis of the chiral key intermediate of (−)-paroxetine enabled by solvent-free heterogeneous organocatalysis. *Chem. Sci.* 10: 11141–11146.

19 de Oliveira Silva, R.R., Cuesta Calvo, P.V., Fernandes da Silva, M. et al. (2019). Flow synthesis of a thiazolidine drug intermediate in capillary microreactor. *Chem. Eng. Technol.* 42 (2): 465–473.

https://www.twirpx.org & http://chemistry-chemists.com

20 Lima, M.T., Finelli, F.G., de Oliveira, A.V.B. et al. (2020). Continuous-flow synthesis of dimethyl fumarate: a powerful small molecule for the treatment of psoriasis and multiple sclerosis. *RSC Adv.* 10 (5): 2490–2494.

21 de Souza, J.M., Berton, M., Snead, D.R., and Mcquade, D.T. (2020). A continuous flow sulfuryl chloride based reaction-synthesis of a key intermediate in a new route toward emtricitabine and lamivudine. *Org. Process Res. Dev.* 24 (10): 2271–2280.

22 World Health Organisation (2019). WHO model list of essential medicines – 21st list. https://www.who.int/publications/i/item/WHOMVPEMPIAU2019.06.

23 Saubern, J.B. and Bradley, J.S. (2018). Antimicrobial agents. In: *Principles and Practices of Pediatric Infectious Diseases* (ed. S.S. Long, C.G. Prober and M. Fischer), 1499–1531. Philadelphia, PA: Elsevier.

24 Tosso, N.P., Desai, B.K., de Oliveira, E. et al. (2019). A consolidated and continuous synthesis of ciprofloxacin from a vinylogous cyclopropyl amide. *J. Org. Chem.* 84 (6): 3370–3376.

25 Russell, A.M.G. and Jamison, T.F. (2019). Seven-step continuous flow synthesis of linezolid without intermediate purification. *Angew. Chem. Int. Ed.* 58 (23): 7678–7681.

26 Hashemian, S.M.R., Farhadi, T., and Ganjparvar, M. (2018). Linezolid: a review of its properties, function, and use in critical care. *Drug Des. Dev. Ther.* 12: 1759–1767.

27 Greenwood, D. (2010). B-lactam antibiotics: cephalosporins. In: *Antibiotics and Chemotherapy* (ed. R.G. Finch, S.R. Norrby, D. Greenwood and R.J. Whitley), 170–199. Philadelphia, PA: Saunders.

28 Pieper, M., Kumpert, M., König, B. et al. (2018). Process development for synthesizing the cephalosporin antibiotic cefotaxime in batch and flow mode. *Org. Process Res. Dev.* 22 (8): 947–954.

29 Li, X., Liu, Z., Qi, H. et al. (2018). Continuous preparation for rifampicin. *J. Flow Chem.* 8: 129–138.

30 Garbis, H., Tonningen, M.R., and Van Reuvers, M. (2007). Anti-infective agents. In: *Drugs During Pregnancy and Lactation* (ed. C. Schaefer, P. Peters and R.K. Miller), 123–177. Philadelphia, USA: Saunders, Elsevier.

31 Walker, S.L., Withington, S.G., and Lockwood, D.N.J. (2014). Leprosy. In: *Manson's Tropical Diseases* (ed. J. Farrar, T. Junghanss, D. Dalloo, et al.), 506–518. Saunders Ltd.

32 Varner, T.H., Bookstaver, P.B., Rudisill, C.N., and Albrecht, H. (2011). Role of rifampin-based combination therapy for severe community-acquired Legionella pneumophila pneumonia. *Ann. Pharmacother.* 45 (7–8): 967–973.

33 Jaman, Z., Sobreira, T.J.P., Mufti, A. et al. (2019). Rapid on-demand synthesis of lomustine under continuous flow conditions. *Org. Process Res. Dev.* 23 (3): 334–341.

34 Fu, W.C. and Jamison, T.F. (2019). Modular continuous flow synthesis of imatinib and analogues. *Org. Lett.* 21 (15): 6112–6116.

35 Szeto, J., Vu, V., Malerich, J.P., and Collins, N. (2019). Multi-step continuous flow synthesis of fluconazole. *J. Flow Chem.* 9: 35–42.

https://www.twirpx.org & http://chemistry-chemists.com

36 Shoham, S., Groll, A.H., Petraitis, V., and Walsh, T.J. (2017). Systemic antifungal agents. In: *Infectious Diseases* (ed. J. Cohen, S.M. Opal and W.G. Powderly), 1336–1344. Amsterdam, Netherlands: Elsevier Ltd.

37 Korwar, S., Amir, S., Tosso, P.N. et al. (2017). The application of a continuous Grignard reaction in the preparation of fluconazole. *Eur. J. Org. Chem.* 2017 (44): 6495–6498.

38 Harsanyi, A., Conte, A., Pichon, L. et al. (2017). One-step continuous flow synthesis of antifungal who essential medicine flucytosine using fluorine. *Org. Process Res. Dev.* 21 (2): 273–276.

39 World Health Organisation (2018). Guidelines for the diagnosis, prevention and management of cryptococcal disease in HIV-infected adults, adolescents and children. https://www.who.int/publications/i/item/9789241550277.

40 Eckhardt, B.J. and Gulick, R.M. (2017). Drugs for HIV infection. In: *Infectious Diseases* (ed. J. Cohen, W.G. Powderly and S.M. Opal), 1293–1308. Elsevier Ltd.

41 Reddy, V.P. (2015). Organofluorine compounds as anticancer agents. In: *Organofluorine Compounds in Biology and Medicine*, 265–300. Amsterdam, Netherlands; Oxford, UK; Waltham, USA: Elsevier.

42 Suveges, N.S., Rodriguez, A.A., Diederichs, C.C. et al. (2018). Continuous-flow synthesis of (*R*)-propylene carbonate: an important intermediate in the synthesis of tenofovir. *Eur. J. Org. Chem.* 2018 (23): 2931–2938.

43 Nelson, M.R., Katlama, C., Montaner, J.S. et al. (2007). The safety of tenofovir disoproxil fumarate for the treatment of HIV infection in adults: the first 4 years. *AIDS* 21 (10): 1273–1281.

44 Duarte-Rojo, A. and Heathcote, E.J. (2010). Efficacy and safety of tenofovir disoproxil fumarate in patients with chronic hepatitis B. *Ther. Adv. Gastroenterol.* 107–119.

45 Tsibris, A.M.N. and Hirsch, M.S. (2015). Antiretroviral therapy for human immunodeficiency virus infection. In: *Mandell, Douglas and Bennett's Principles and Practice on Infectious Diseases* (ed. J.E. Bennette, R. Dolin and M.J. Blaser), 1622–1641. Philadelphia, PA: Saunders.

46 Britton, J., Majumdar, S., and Weiss, G.A. (2018). Continuous flow biocatalysis. *Chem. Soc. Rev.* 47: 5891–5918.

47 Ziegler, R.E., Bimbisar, K., Desai, J.J. et al. (2018). 7-Step flow synthesis of the HIV integrase inhibitor Dolutegravir. *Angew. Chem. Int. Ed.* 57 (24): 7181–7185.

48 Mandala, D., Chada, S., and Watts, P. (2017). Semi-continuous multi-step synthesis of lamivudine. *Org. Biomol. Chem.* 15: 3444–3454.

49 Cihlar, T. and Ray, A.S. (2010). Nucleoside and nucleotide HIV reverse transcriptase inhibitors: 25 years after zidovudine. *Antiviral Res.* 85 (1): 39–58.

50 Ferir, G., Kaptein, S., Neyts, J., and de Clercq, E. (2008). Antiviral treatment of chronic hepatitis B virus infections: the past, the present and the future. *Rev. Med. Virol.* 18 (1): 19–34.

51 Chada, S., Mandala, D., and Watts, P. (2017). Synthesis of a key intermediate towards the preparation of efavirenz using *n*-butyllithium. *J. Flow Chem.* 7 (2): 37–40.

https://www.twirpx.org & http://chemistry-chemists.com

52 Bana, P., Szigetvári, Á., Kóti, J. et al. (2019). Flow-oriented synthetic design in the continuous preparation of the aryl piperazine drug flibanserin. *React. Chem. Eng.* 4: 652–657.

53 James, J.E. (2016). The Commercial Culture of Medicine. In: *The Health of Populations: Beyond Medicine*, 175–212. Cambridge, Massachusetts: Academic Press.

54 Boros, Z., Nagy-Győr, L., Kátai-Fadgyas, K. et al. (2019). Continuous flow production in the final step of vortioxetine synthesis. Piperazine ring formation on a flow platform with a focus on productivity and scalability. *J. Flow Chem.* 9: 101–113.

55 Garnock-Jones, K.P. (2014). Vortioxetine: a review of its use in major depressive disorder. *CNS Drugs* 28: 855–874.

56 Jiulong, C., Wei, F., Dong, R., and Wang, S. (2019). A kind of flupentixol and melitracen pharmaceutical composition and preparation method thereof. Patent No. CN105663062B. Nanjing Zhuo Kang Medical Science and Technology Co., Ltd.

57 Pedersen, M.J., Skovby, T., Mealy, M.J. et al. (2018). Redesign of a Grignard-based active pharmaceutical ingredient (API) batch synthesis to a flow process for the preparation of melitracen HCl. *Org. Process Res. Dev.* 22 (2): 228–235.

58 Laroche, B., Saito, Y., Ishitani, H., and Kobayashi, S. (2019). Basic anion-exchange resin-catalyzed aldol condensation of aromatic ketones with aldehydes in continuous flow. *Org. Process Res. Dev.* 23 (5): 961–967.

59 Fujimoto, Y. and Iwatsubo, T. (2014). Strengthening/building Alzheimer's disease global clinical trial site capabilities and capacity in and for emerging markets. Lessons learned from Japan. In: *Global Clinical Trials for Alzheimer's Disease* (ed. M. Bairu and M.W. Weiner), 289–304. San Diego, CA: Elsevier Academic Press.

60 Yu, E., Mangunuru, H.P.R., Telang, N.S. et al. (2018). High-yielding continuous-flow synthesis of antimalarial drug hydroxychloroquine. *Beilstein J. Org. Chem.* 14: 583–592.

61 Callen, J.P., Rosenbach, M., and Camisa, C. (2020). Comprehensive dermatologic drug therapy. In: *Antimalarial Agents* (ed. S.E. Walverton and J.J. Wu), 234–244. Amsterdam: Elsevier.

62 Imazio, M., Maestroni, S., Valenti, A. et al. (2017). Desirable and adverse effects of antiinflammatory agents on the heart. In: *The Heart in Rheumatic, Autoimmune and Inflammatory Diseases: Pathophysiology, Clinical Aspects and Therapeutic Approaches* (ed. U. Nussinovitch), 617–643. London, UK; San Diego, USA; Cambridge, USA; Oxford, UK: Academic Press.

63 Sharma, T.S., Joyce, E., and Wasko, M.C.M. (2016). Anti-malarials: are there benefits beyond mild disease? *Curr. Treat. Options Rheumatol.* 2 (1): 1–12.

64 Hiebler, K., Soritz, S., Gavric, K. et al. (2019). Multistep synthesis of a valsartan precursor in continuous flow. *J. Flow Chem.* 10: 283–294.

65 Selvaraj, S., Claggett, B.L., Böhm, M. et al. (2020). Systolic blood pressure in heart failure with preserved ejection fraction treated with sacubitril/valsartan. *J. Am. Coll. Cardiol.* 75 (14): 1644–1656.

https://www.twirpx.org & http://chemistry-chemists.com

66 Kario, K. (2018). The sacubitril/valsartan, a first-in-class, angiotensin receptor neprilysin inhibitor (ARNI): potential uses in hypertension, heart failure, and beyond. *Curr. Cardiol. Rep.* 20 (5).

67 Vasudevan, N., Sharma, M.K., Reddy, S.D., and Kulkarni, A.A. (2018). A multi-step continuous flow synthesis of cystic fibrosis medicine Ivacaftor. *React. Chem. Eng.* 3: 520–526.

68 Hughes, D.L. (2019). Patent review of synthetic routes and crystalline forms of the CFTR-modulator drugs ivacaftor, lumacaftor, tezacaftor and elexacaftor. *Org. Process Res. Dev.* 23 (11): 2302–2322.

69 Collins, D. (2020). Ibuprofen for acute pain relief in the emergency department. *BMJ Evidence Based Med.* .

70 Pelletier, J.P., Martel-Pelletier, J., Rannou, F., and Cooper, C. (2016). Efficacy and safety of oral NSAIDs and analgesics in the management of osteoarthritis: evidence from real-life setting trials and surveys. *Semin. Arthritis Rheum.* 45 (4): s22–s27.

71 Snead, D.R. and Jamison, T.F. (2015). A three-minute synthesis and purification of ibuprofen: pushing the limits of continuous-flow processing. *Angew. Chem. Int. Ed.* 54 (3): 983–987.

72 Lee, H.J., Kim, H., and Kim, D.P. (2019). From *p*-xylene to ibuprofen in flow: three-step synthesis by a unified sequence of chemoselective C–H metalations. *Chem. Eur. J.* 25 (50): 11641–11645.

https://www.twirpx.org & http://chemistry-chemists.com

https://www.twirpx.org & http://chemistry-chemists.com

7

Continuous-Flow Multistep Synthesis of Active Pharmaceutical Ingredients

Yuesu Chen and Jean-Christophe M. Monbaliu

University of Liège, Center for Integrated Technology and Organic Synthesis, Department of Chemistry, MolSys Research Unit, B6a Allée du Six Août, 13, B-4000 Liège (Sart Tilman), Belgium

7.1 Introduction

Active pharmaceutical ingredients (APIs) are the high value-added bioactive chemicals ultimately used in a final pharmaceutical formulation [1]. The chemical synthesis of APIs thus plays a central role in the manufacturing of APIs. Generally, APIs are constructed stepwise from structurally simpler building blocks by series of organic reactions; each reaction step enables a connection/disconnection, functional group conversion, or structural rearrangement [2]. In the past century, organic chemists have made an enormous progress in promoting the efficiency of chemical synthesis by means of new catalytic approaches, multicomponent reactions [3, 4], microwave synthesis [5, 6], and continuous-flow reactions.

In the last decade, the widespread use of continuous-flow microreactors in preparative chemistry is gradually changing the way of thinking of organic and process chemists [7]. The inherent features of microreactors, such as the intensified transport processes, the structural robustness, and the continuous-flow operation contribute to a cleaner, safer, and easy scalable synthetic process. Chemical reactions could access novel process windows (NPW) in microreactors, which enable a further enhancement of productivity, significantly reducing the time, space, and environmental footprint [8, 9].

Traditionally, the multistep synthesis in batch is carried out in an iterative fashion, which requires the isolation of intermediates between the steps (Scheme 7.1a). Large amounts of solvent and other material (quench, extraction, purification by chromatography, etc.) are consumed in these intermediate workup and purification steps. In most reported flow cases in API synthesis, microreactors are invoked to tackle the "tough" steps without significantly changing the iterative nature of the entire process (Scheme 7.1b). The continuous-flow operation of the microreactors provides a promising opportunity to perform multiple reaction steps in a network of interconnected flow reactors, avoiding the laborious isolation of the intermediates ("one-flow" synthesis, often referred to as process concatenation or telescoping) (Scheme 7.1c) [10–12].

Flow and Microreactor Technology in Medicinal Chemistry, First Edition. Edited by Esther Alza.
© 2022 WILEY-VCH GmbH. Published 2022 by WILEY-VCH GmbH.

https://www.twirpx.org & http://chemistry-chemists.com

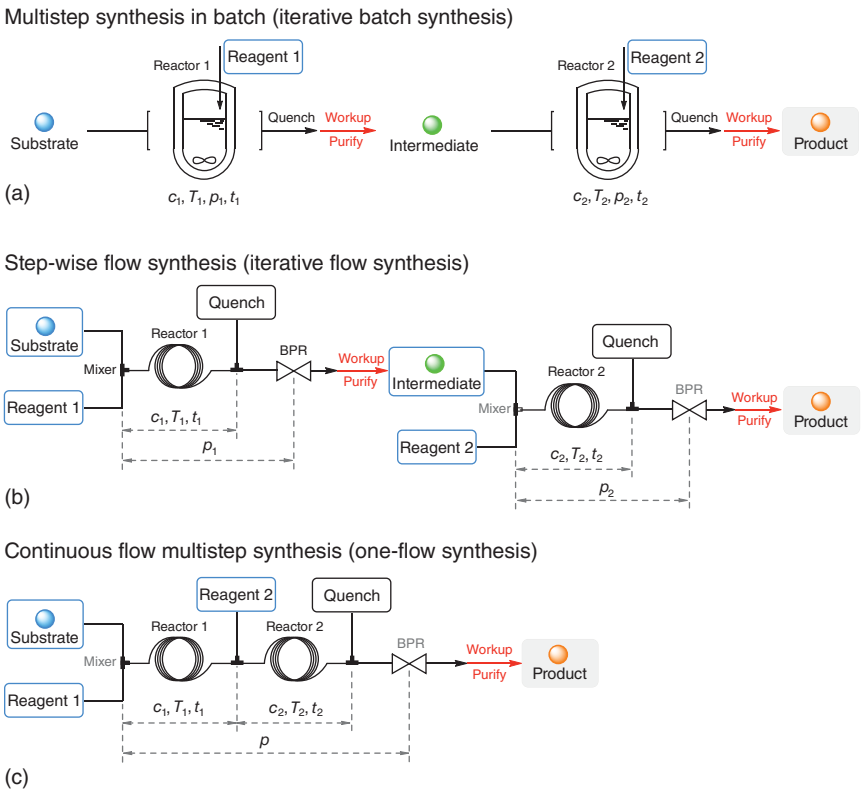

Scheme 7.1 Multistep synthesis in batch and flow. (Details of the pumping and injection units of the flow systems are denoted by round-cornered rectangle frames at the inlets). Source: Based on Pieber et al. [10], Wegner et al. [11], Webb and Jamison[12].

The objective of this chapter aims to provide the synthetic chemists with a brief overview on the application of multistep flow synthesis of APIs and drug precursors. Selected examples include processes with the concatenation of at least two reaction steps for the synthesis of APIs and related compounds. Starting from the simplest case – reagent generator – the state of the art of multistep flow synthesis is introduced through representative examples predominantly published since 2017 in an increasing gradient of complexity (number of steps). For further examples on the same topic, the reader is redirected toward recent reviews [13–15].

7.2 Generators of Small Molecule Reagents

The application of reagent generator in flow can be regarded as the simplest multistep model. Based on the single-step flow reactor (Scheme 7.2a), the reagent feed is replaced by a reagent generator (Scheme 7.2b), where the reagent is continuously generated and delivered to the downstream reactor in a required concentration and flow rate. After the incorporation of the reagent generator, the precursor(s)

https://www.twirpx.org & http://chemistry-chemists.com

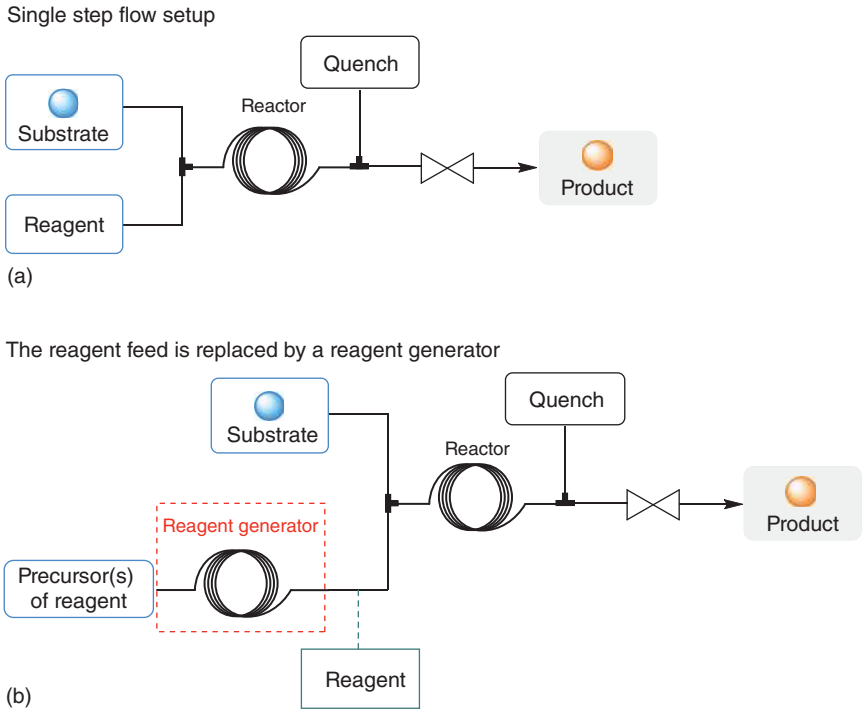

Scheme 7.2 The application of reagent generator in flow – the simplest multistep flow system.

of the reagent is injected to the flow system instead of the reagent itself; this feature is especially beneficial in dealing with gaseous, hazardous, and highly reactive reagents that are challenging to handle in large quantities [16]. In contrast to the *in situ* reagent generation (one-pot reaction), the spatial separation of the generation and consumption of the reagent in flow allows the use of different conditions and minimizes their mutual interference. Moreover, its combination with in-line separation techniques enables the change of reaction media (solvent) and the removal of by-products. These features have made microreactor systems as an enabling platform for in-line reagent generation and multistep synthesis.

The storage of reactive gas cylinders inside laboratories are considered as potential safety threats. Ideally, the "on-demand" generation of reactive gases from liquid solutions and their immediate consumption within chemical transformations should be considered as the best laboratory practice. The commercialized hydrogenator H-Cube™ by ThalesNano® is one of the earliest reactors that relied on this concept; it integrates a water electrolysis hydrogen generator and interchangeable catalyst cartridges, hence enabling high-temperature and high-pressure continuous-flow hydrogenations under safe conditions (Scheme 7.3) [17, 18]. This type of reactor was, for instance, used by de Souza and coworkers for a tandem hydrogenation/reductive amination step in the synthesis of anesthetic Mepivacaine (**1**) [19].

https://www.twirpx.org & http://chemistry-chemists.com

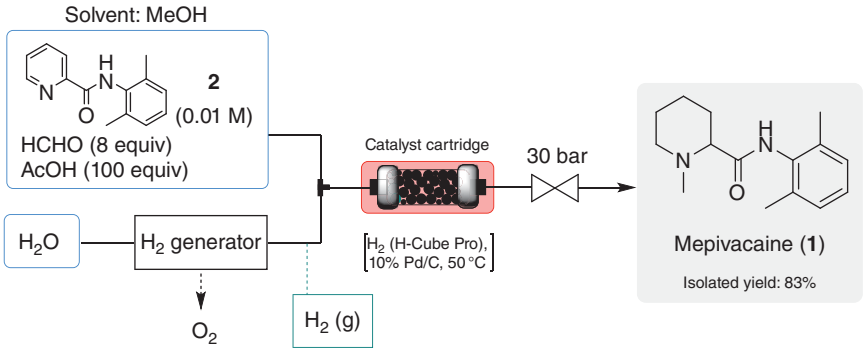

Scheme 7.3 The synthesis of Mepivacaine in ThalesNano® H-Cube™. Source: Based on Cossar et al. [17] and Irfan et al. [18].

For the generation of soluble gases, membrane technologies enable reagent transfer between immiscible solvents or chemically incompatible reaction media. For instance, Kappe and coworkers developed a chlorine generator that relied on the reaction of bleach and hydrochloric acid [20]. The generated chlorine was extracted with chloroform and separated from the aqueous phase by a membrane separator for the subsequent downstream reactions (Scheme 7.4b). Using a similar generator setup, the same research group managed to generate nitrosyl chloride (NOCl) from an aqueous reaction phase for photonitrozation applications [22]. Another example of a common, synthetically useful reactive gas is C_1-building block diazomethane (CH_2N_2). As has been already introduced in previous chapters of the present book, CH_2N_2 is notorious for its toxicity and explosiveness. Among the various continuous-flow systems [23], the tube-in-tube reactor setup (Scheme 7.4c) could safely handle the generation, separation, and reaction of anhydrous CH_2N_2. Diazomethane is typically generated in the inner layer and diffuses through a gas-permeable membrane to reach the reaction medium in the outer layer [24]. Kappe and coworkers made use of a tube-in-tube CH_2N_2 generator for the synthesis of α-chloro ketone precursors of HIV protease inhibitors such as Atazanavir (**10**) [21] (Scheme 7.5). Moreover, the tube-in-tube reactor setup is also suitable for the in-line generation of trifluoromethyl diazomethane [25], hydrogen cyanide [26], and carbon monoxide [27], as well as the in-line dosage [28] and removal [29] of the gases.

Similarly, for the liquid and dissolved solid unstable reagents, generators often rely on the configurations shown in Scheme 7.4a,b, depending on the compatibility with the downstream steps. The reagent generators provide a safe and controllable means for the synthetic application of several volatile, toxic, and highly reactive small molecules, such as bromine [30], cyanogen bromide (BrCN) [31], and Vilsmeier–Haack reagent (Me_2N^+=NHX) [32, 33].

Apart from the small molecule reagents, reactive species carrying larger building blocks like organometallic reagents [34] are also accessible in flow from their generators. More detailed examples are discussed in the next sections. Some examples of

https://www.twirpx.org & http://chemistry-chemists.com

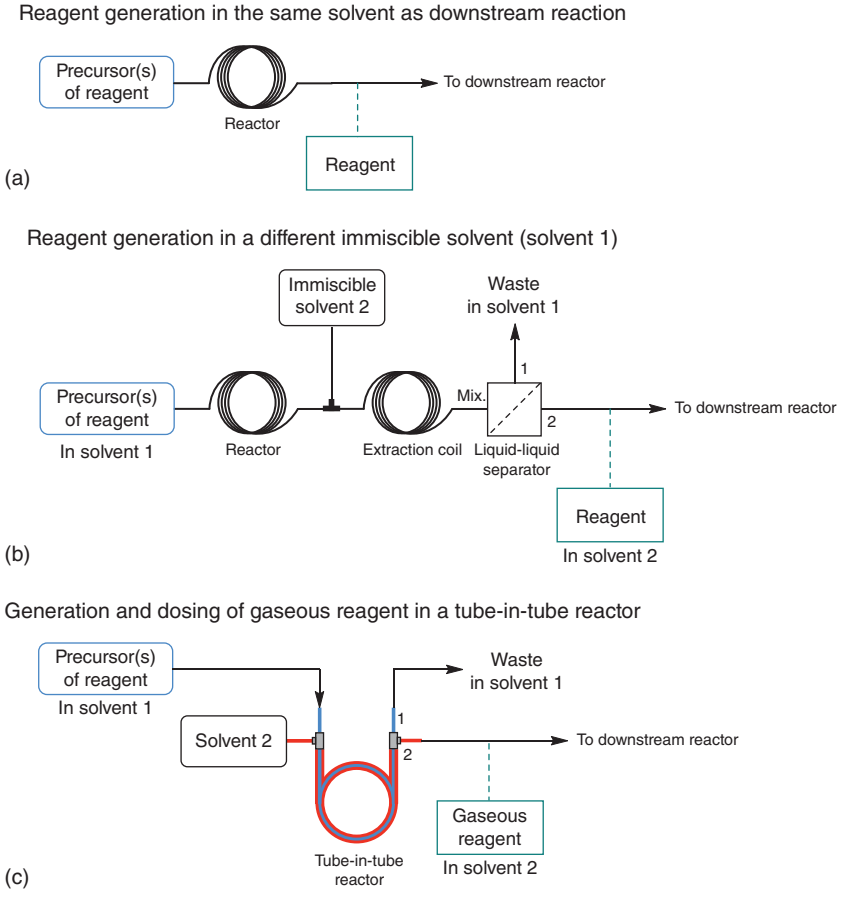

Scheme 7.4 Three representative configurations of reagent generators. Source: Pinho et al. [21]/American Chemical Society.

reagent generators are gathered in Table 7.1 in parallel with their generation reactions; some of the entries are already mentioned in the context.

7.3 Two-Step Flow Synthesis

The two-step flow synthesis and the reagent generator share exactly the same principle: the first reactor serves as the "substrate generator" for the second (compare Schemes 7.1c and 7.2b). Despite the compatibility of the reaction media (solvent, by-products), in order to achieve a high overall yield, the local concentration of the key component and the reaction time for each step (coupled with reactor volume and flow rates of the feed streams) should be taken into consideration during the process design and optimization to ensure high conversion and selectivity of each step.

In this and the following sections, the APIs denoted with "WHO essential" are essential medications for a basic healthcare system. These substances are included

https://www.twirpx.org & http://chemistry-chemists.com

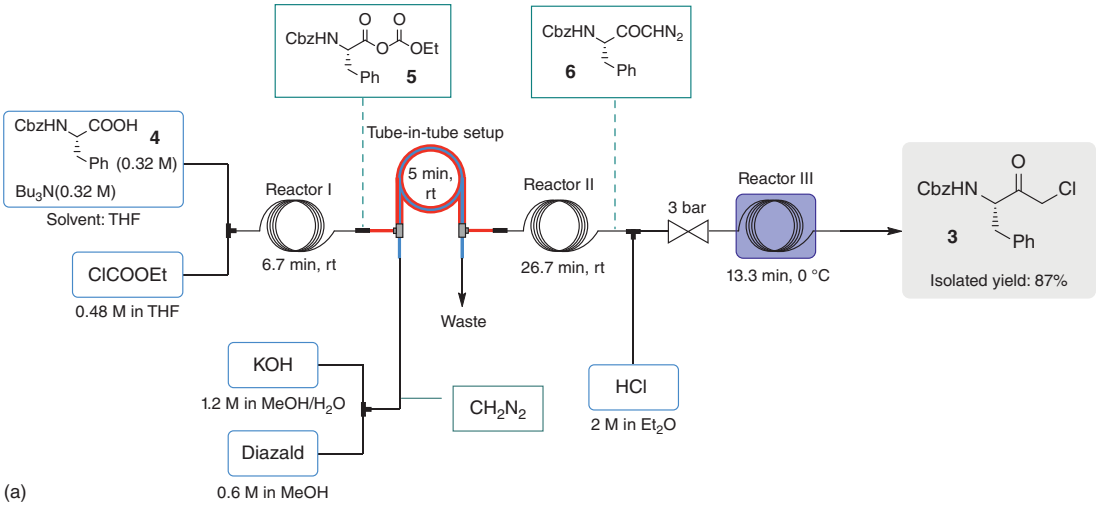

Scheme 7.5 The flow setup (a) for a three-step synthesis of an α-chloroketone precursor of HIV protease inhibitors (b) using a tube-in-tube diazomethane generator.

https://www.twirpx.org & http://chemistry-chemists.com

Table 7.1 Reagent generators and their generation reactions.

Entry	Reagent	Feature	Generation reactions	Setup[a)]	References
1	H_2	Explosive	$2H_2O \rightarrow 2H_2 + O_2$ (H-Cube)	a	[19]
2	Cl_2	Toxic, corrosive	$NaClO + 2HCl \rightarrow NaCl + Cl_2 + H_2O$	b	[20]
3	NOCl	Toxic, corrosive	$NaNO_2 + 2HCl \rightarrow NaCl + NOCl + H_2O$	b	[22]
4	CH_2N_2	Toxic, explosive	$p\text{-}TolSO_2NMeNO + KOH \rightarrow p\text{-}TolSO_3K + CH_2N_2 + H_2O$	c	[21]
			$H_2NCONMeNO + KOH \rightarrow NH_3 + CO_2 + CH_2N_2 + H_2O$	a	[35]
5	$(CF_3)CHN_2$	Toxic, explosive	$(CF_3)CH_2NH_2 + NaNO_2 + H_2SO_4 \rightarrow (CF_3)CHN_2 + NaHSO_4 + 2H_2O$	c	[25]
6	HCN	Highly toxic	$2NaCN + H_2SO_4 \rightarrow Na_2SO_4 + 2HCN$	c	[26]
7	CO	Toxic, flammable	$HCOOH \rightarrow CO + H_2O$	c	[27]
8	Br_2	Toxic, corrosive	$NaBrO_3 + 6HBr \rightarrow NaBr + 3Br_2 + 3H_2O$	a	[30]
9	BrCN	Highly toxic	$KCN + Br_2 \rightarrow KBr + BrCN$	b	[31]
10	$Me_2N^+{=}NHX$	Reactive, hygroscopic	$HCONMe_2 + POCl_3 \rightarrow [Me_2N^+{=}NHCl][Cl_2PO^-]$	a	[32]
			$CBr_4 + 2HCONMe_2 \rightarrow 2[Me_2N^+{=}NHBr]Br^- + CO_2$	a	[33]
11	$R_1R_2C{=}N_2$	Potentially explosive	$R_1R_2C{=}NNH_2 + MnO_2 \rightarrow R_1R_2C{=}N_2$	a	[36]
12	ArMgBr	Highly reactive, air sensitive	$ArBr + Mg \rightarrow ArMgBr$	a	[37]
			$RH + TMP\text{-}MgCl{\cdot}LiCl^{b)} \rightarrow RMgCl + TMP\text{-}H + LiCl$	a	[38]
13	Cl_2CHLi	Highly reactive, air sensitive	$CH_2Cl_2 + {}^n BuLi \rightarrow Cl_2CHLi + {}^n BuH$	a	[39]
14	ArLi	Highly reactive, air sensitive	$ArBr + {}^n BuLi \rightarrow ArLi + {}^n BuBr$	a	[40]
15	RZnX	Highly reactive, pyrophoric	$2RX + ZnCl_2 + 2\,Mg \rightarrow R_2Zn + MgX_2 + MgCl_2$	a	[41]
			$2RLi + ZnCl_2 \rightarrow R_2Zn + 2LiCl$	a	[42]

a) General setups refer to Scheme 7.4.
b) TMP = 2,2,6,6-tetramethylpyperidyl.

https://www.twirpx.org & http://chemistry-chemists.com

in the *Model List of Essential Medicines* by the World Health Organization (WHO) (https://www.who.int/medicines/publications/essentialmedicines/en).

7.3.1 Clausine C Derivatives

Carbazole scaffolds are commonly found in bioactive natural products [43]. Collins and coworker developed a two-step flow protocol for the synthesis of 1-substituted Clausine C (Scheme 7.6) [44]. The upstream photoreactors I and III serve as generators of 1-bromo Clausine C (**11**): the carbazole moiety was constructed via an intramolecular nitrene insertion triggered by the photo-cleavage of azide (**12**). For the preparation of 1-(hetero)aryl Clausine C (**14**) (Scheme 7.6a), the effluent containing **11** was combined with a solution of (hetero)aryl boronic acid (**13**) and a base and then underwent Suzuki cross-coupling in a column packed with heterogeneous palladium-based SiliaCat© catalyst (reactor II) to afford **14**. The reaction time of this step (21 minutes) is significantly shorter than that of its batch counterpart (14 hours), giving good yields for aryl coupling partners and moderate yields for heteroaryls. For the preparation of 1-benzyl derivative (**16**), a sequential flow photochemical process (Scheme 7.6b) was applied, in which the photoredox/nickel dual-catalyzed cross-coupling with benzyl trifluoroborate (**15**) took place in the second photoreactor (reactor IV).

7.3.2 Amino Alcohol APIs from Glycerol

Like other petroleum-based C_3 building blocks, glycerol has been produced from propylene like glycidol (**20**) and epichlorohydrin (**21**). Nowadays, glycerol (**17**) is obtained in large volumes as a by-product of the saponification/transesterification of animal and vegetable oil. Monbaliu and coworkers developed a continuous-flow protocol for the upgrading of bio-based glycerol to β-amino alcohol APIs via epichlorohydrin (Scheme 7.7) [45]. Glycerol was converted to epichlorohydrin in a two-step flow process (Scheme 7.7a). The heating with concentrated hydrochloric acid (reactor I) gave a mixture of chlorohydrins (**19**). The presence of catalyst pimelic acid (**18**) enhanced the yield and selectivity to dichlorohydrin (**19c**), which was subsequently cyclized to **21** upon treatment with NaOH (reactor II). Quantitative conversion and high yield for this highly exothermic cyclization step were achieved within one minute when performing on a Corning® Advanced-Flow™ G1 SiC reactor. The separation of **21** from water-soluble **20** was realized with in-line extraction: the effluent from reactor II was mixed with an organic solvent in a mixing column packed with glass beads and then separated with a Zaiput® membrane separator. The bio-based solvent *n*-butyl acetate (b.p. 126 °C) exhibited excellent extraction performance, but the low boiling methyl *tert*-butyl ether (MTBE, b.p. 55 °C) enabled an easier downstream solvent removal and was therefore utilized. Using the bio-based epichlorohydrin, the authors managed to synthesize two amino alcohol APIs in a one-flow process within 40 minutes total residence time (Scheme 7.7b): propranolol (**25a**) (a medication against hypertension, WHO essential) and naftopidil (**25b**) (a medication against prostatic hyperplasia).

https://www.twirpx.org & http://chemistry-chemists.com

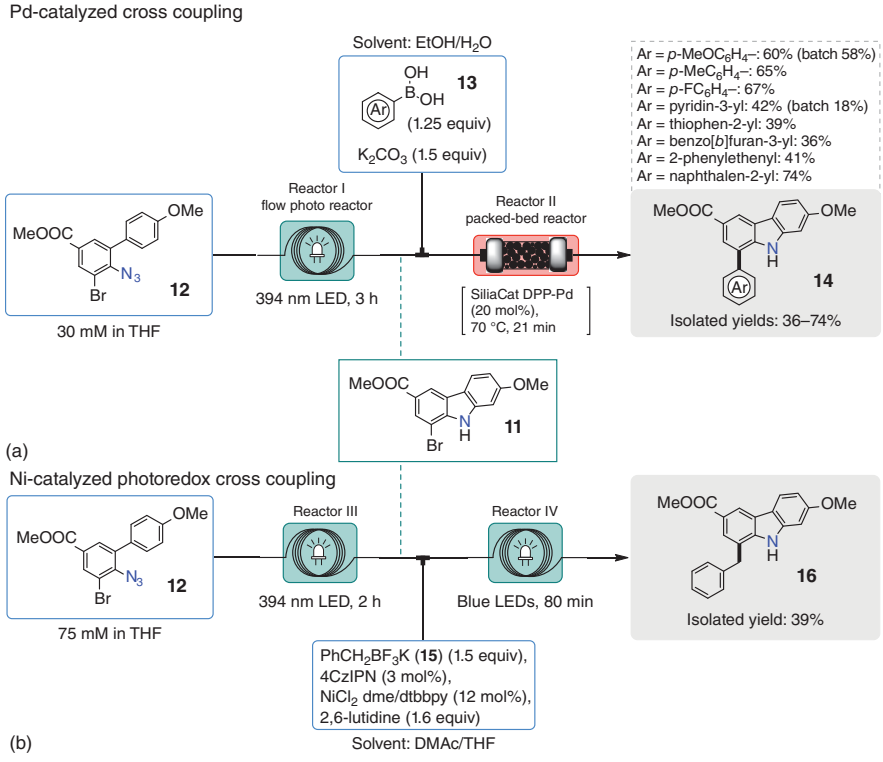

Scheme 7.6 The continuous-flow synthesis of 1-substituted Clausine C derivatives (4CzIPN = 2,4,5,6-tetra(9*H*-carbazol-9-yl)isophthalonitrile; dme = 1,2-dimethoxyethane; dtbbpy = 4,4′-di-*tert*-butyl-2,2′-dipyridyl). Source: Parisien-Collette et al. [44]/John Wiley & Sons.

https://www.twirpx.org & http://chemistry-chemists.com

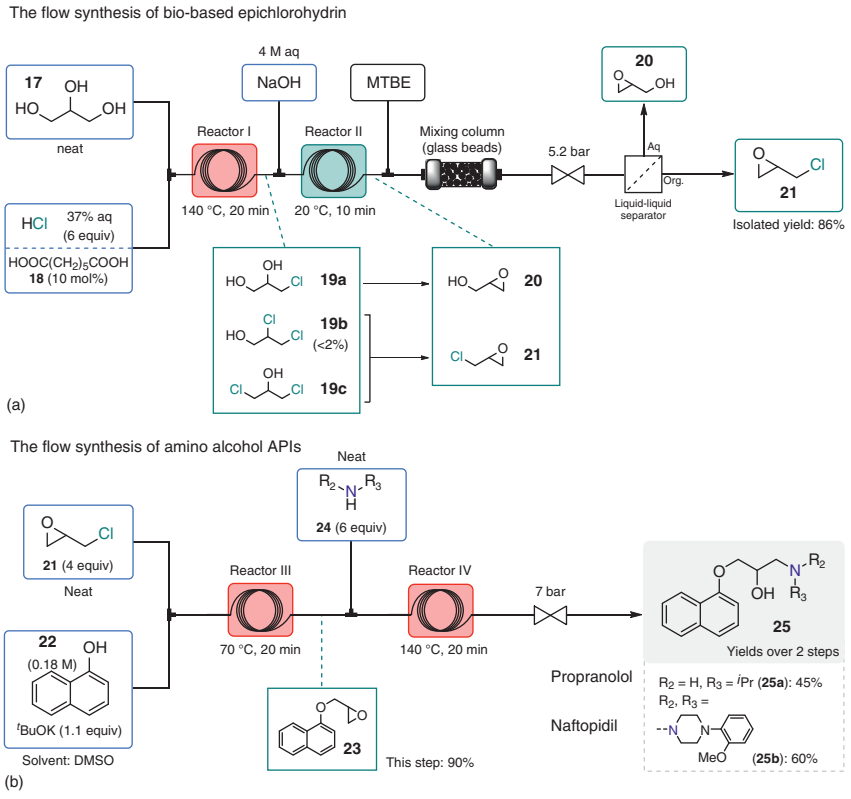

Scheme 7.7 The upgrading of glycerol to amino alcohol APIs in flow. Source: Morodo et al. [45]/Royal Society of Chemistry.

7.3.3 Oxymorphone

Oxymrophone (**26**) is an opiate analgesic synthesized from naturally occurring alkaloid oripavine (**28**). It is also an intermediate in the manufacturing of naloxone (**27**), an effective antagonist for the treatment of acute opioid overdosing (WHO essential). Kappe and coworkers developed a one-flow process for the synthesis of **26** involving an in-line solvent swapping between two miscible reaction media ($HCOOH/H_2O$ and *N*,*N*-dimethylactamide [DMAc]) (Scheme 7.7) [46]. In reactor I, oripavine (**28**) was hydroxylated by the *in situ* generated performic acid at 100 °C. The effluent containing 14-hydroxymorphinone (**29**) formate was mixed in-line with a diluted ammonia solution and dichloromethane (DCM) and then partitioned by gravity, collecting the free base **29** in the organic phase. Since the hydrogenation of **29** in DMAc was much faster than in other solvents, the DCM layer containing the free base (**29**) was subsequently mixed with DMAc (b.p. 165 °C) and warmed up to 95 °C in a heated coil, where DCM (b.p. 40 °C) was vaporized. In this manner, **29** was concentrated in DMAc (0.2 M) and collected in a heated vessel (80 °C) to prevent the condensing of DCM. The DMAc solution of **29** was then pumped into a ThalesNano

https://www.twirpx.org & http://chemistry-chemists.com

H-Cube hydrogenator (reactor II, structure; see Scheme 7.3), giving a solution of **26** after <1 minute residence time. The collected solution can be directly used for the Pd-catalyzed N-demethylation (88% assayed yield in batch). Crystalline product (**26**) was obtained in 86% yield (based on **28**) after removing the solvent. The reaction condition could be telescoped to thebaine for the synthesis of oxycodone, another commercial opiate painkiller.

7.3.4 Hydroxychloroquine

Hydroxychloroquine (HCQ, **30**) is an antimalarial drug and an effective drug for the treatment of rheumatoid arthritis (WHO essential). However, the global access to HCQ (**30**) has been hampered by its high manufacturing costs. The preparation of the key intermediate **34** has been the main cost driver because of the use of carbonyl protection group. Gupton and coworkers published a flow protocol for the synthesis of HCQ without resorting to functional group protection or precious metal (Scheme 7.8) [47]. The synthesis started with the iododecarboxylation of α-acetyl butyrolactone (**31**), giving the iodoketone (**32**) in high yield (reactor I). A large excess of HI (aq.) is necessary for the high conversion. The reaction mixture was neutralized in-line, while the iodoketone (**32**) was extracted with MTBE and separated from the aqueous waste with a membrane separator (Scheme 7.8a). The displacement of the iodine atom of **32** with amine (**33**) occurred readily to give the key intermediate (**34**) in good yield (>80%) (reactor II). From **34**, a reductive amination could in theory afford the side chain of HCQ (**36**) in one step. However, because of the limited solubility of ammonia in tetrahydrofuran (THF) and the difficulty in exchanging the miscible solvent in-line (cf. Scheme 7.9), the seemingly straightforward reductive amination became unfeasible. The authors decided to convert **34** to its oxime (**35**) and perform the hydrogenation in a continuous-flow tank reactor (CSTR). The preparation of **34** (reactor II) and its oximization (reactor III) were performed in one stream using THF as common solvent, giving the oxime in 78% yield. Columns packed with solid potassium carbonate placed between the steps to scavenge acid (I) and water (II). The final step connecting the side chain (**36**) with quinoline (**37**) was carried out in batch to afford HCQ (**30**) in 78% yield (For more details about the algorisms see Chapter 6).

7.4 Linear Multistep Flow Synthesis

Linear multistep synthesis can be treated as a succession of fluidically connected generators; i.e. one of the inlets of a downstream generator is connected to the outlet of an upstream generator and so on. An example generator of cyanogen bromide (BrCN) is shown in Scheme 7.10; it consisted of a Br_2 generator (reactor I) and a BrCN generator (reactor II) [31]. Similar to the two-step flow synthesis, same considerations should be taken when joining and operating multiple reaction steps in one stream.

https://www.twirpx.org & http://chemistry-chemists.com

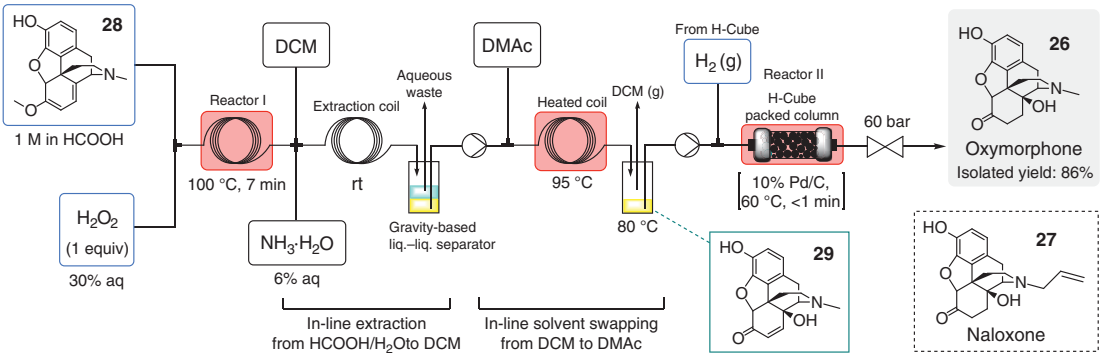

Scheme 7.8 The synthesis of hydroxychloroquine in flow.

https://www.twirpx.org & http://chemistry-chemists.com

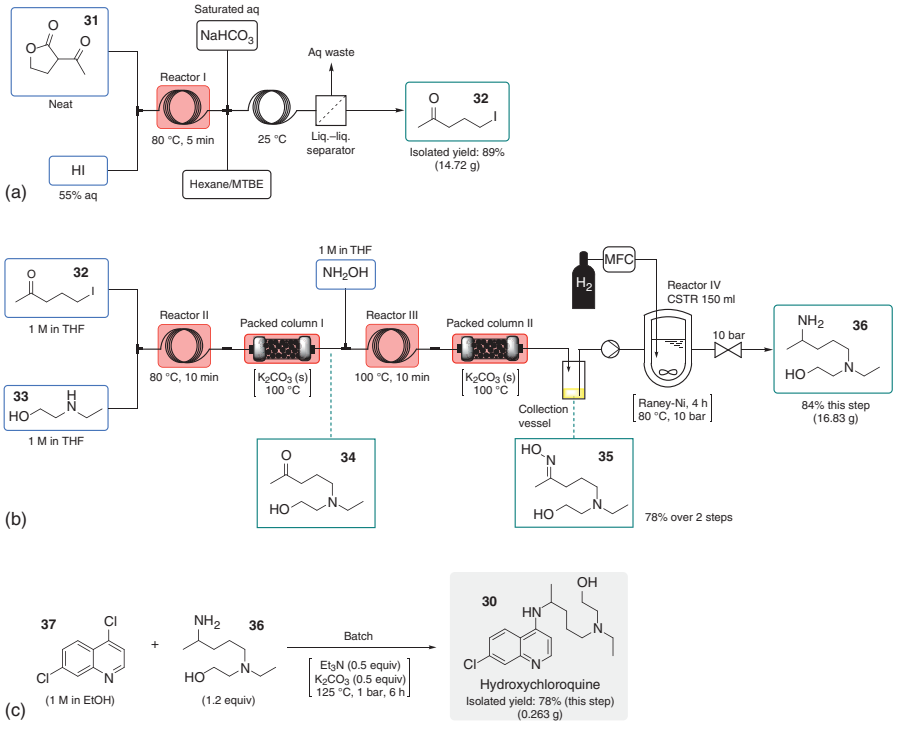

Scheme 7.9 The continuous-flow synthesis of oxymorphone. Source: Yu et al. [47]/Beilstein Institute for the Advancement of Chemical Sciences.

https://www.twirpx.org & http://chemistry-chemists.com

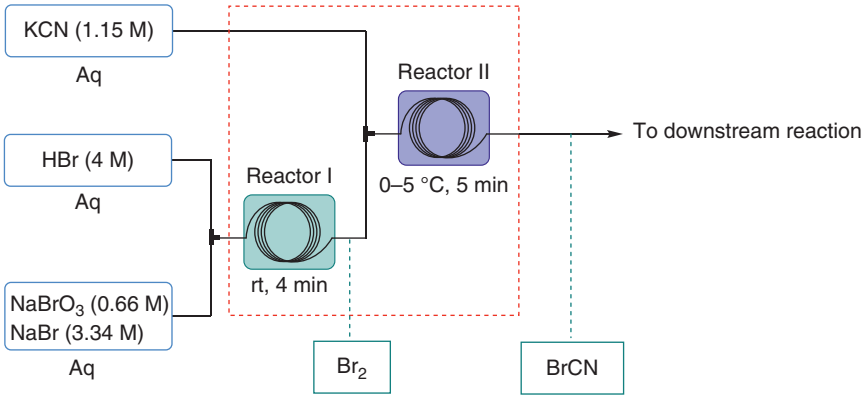

Scheme 7.10 A nested generator of cyanogen bromide.

7.4.1 Valsartan Precursor

Valsartan (**38**) (Diovan™ Novartis®) is a potent, orally active angiotensin II receptor blocker. It is widely used in the treatment of hypertension and chronic heart failure. The key step in the synthesis of **38** is the introduction of the biaryl moiety. In 1991, Ciba-Geigy patented a synthetic route starting from L-valine methyl ester and a biphenyl aldehyde (overall yield <10%). In 2019, Gruber-Woelfler and coworkers presented a one-flow synthesis of Valsartan precursor (**44**) allowing a late-stage construction of the biaryl scaffold (Scheme 7.11) [48]. Three reactions were integrated in one-stream: the N-acylation of the boronic ester substrate (**40**) (reactor I), the Suzuki–Miyaura cross-coupling with 2-halobenzonitrile (**39**) (reactor II), and the hydrolysis of the methyl ester (**43**) (reactor III). Each step was optimized in batch and flow separately. For the cross-coupling step, the palladium-substituted cerium–tin oxide ($Ce_{0.20}Sn_{0.79}Pd_{0.01}O_{2-\delta}$) was used as heterogeneous catalyst packed in a high-performance liquid chromatography (HPLC) column (reactor II); the 1 : 1 mixture of dioxane/water was chosen as solvent, since it could minimize the catalyst leaching and dissolve the aqueous base solution. The integrated process was operated for six hours, giving **44** in 96% assayed yield along with 77% enantiomeric excess, whereas the three-step batch procedure offered only 28% overall yield (For more details about the algorisms see Chapter 6).

7.4.2 Eflornithine

Eflornithine (**45**) is an API (WHO essential) used for the treatment of the second stage of the African trypanosomiasis (sleeping sickness). This compound was currently synthesized from diethyl malonate, acrylonitrile, and chlorodifluoromethane ($CHClF_2$, R-22) over five steps with <40% overall yield. However, the production of R-22 is phasing out under Montreal protocol due to its ozone depleting potential. Fluoroform (CHF_3, R-23) is a large-volume gaseous side product in the production of polytetrafluoroethylen (PTFE); its release into the environment is forbidden because of its high global warming potential. Kappe and coworkers developed a three-step flow protocol using CHF_3 as difluoromethyl source (Scheme 7.12) [49].

https://www.twirpx.org & http://chemistry-chemists.com

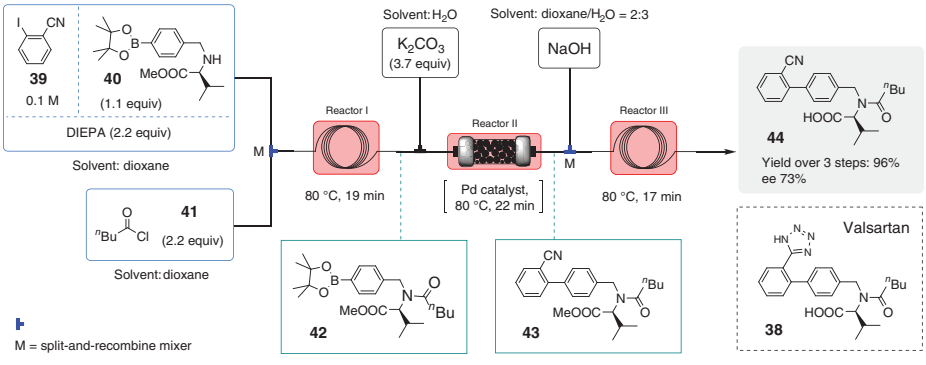

Scheme 7.11 The continuous-flow synthesis of a Valsartan precursor. Source: Heibler et al. [48]/Springer Nature.

https://www.twirpx.org & http://chemistry-chemists.com

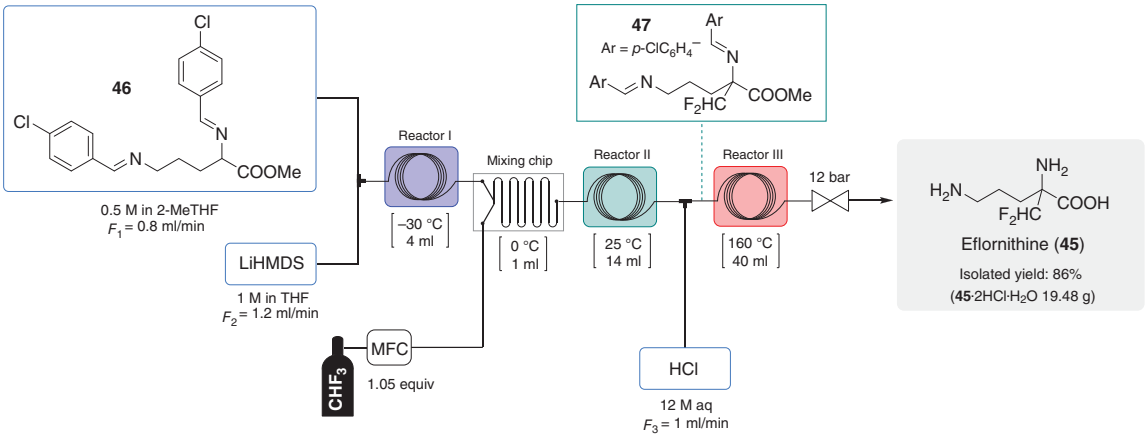

Scheme 7.12 The continuous-flow synthesis of Eflornithine. Source: Köckinger et al. [49]/American Chemical Society.

https://www.twirpx.org & http://chemistry-chemists.com

The substrate, *N*-protected ornithine methyl ester (**46**), was α-deprotonated upon mixing with two equivalent of lithium hexamethyldisilazide (LiHMDS) at low temperature (reactor I). The effluent of reactor I was mixed with CHF_3 gas in a glass mixing chip (Uniqsis®) and entered reactor II operating at room temperature, where the difluoromethylation took place; CHF_3 was deprotonated with the second mole of base and underwent an α-elimination giving difluorocarbene (CF_2); such species was captured by the carbanion of the substrate. The *N*-protected difluoromethylation product (**47**) was combined with concentrated HCl (aq) and heated at 160 °C in a perfluoroalkoxy alkanes (PFA) coil (reactor III) to afford Eflornithine dihydrochloride monohydrate (**45**·2HCl·H_2O) in 86% isolated yield (19.48 g).

During their initial optimization, deprotonations with other bases such as ^{n}BuLi, LDA, KO^{t}Bu, and LiO^{t}Bu turned out to be unsuccessful. The glass mixing chip was introduced to ensure an effective gas–liquid mixing under high flow rates. Because of the solid formation (e.g. LiF, **45**·HCl) from the reaction mixture, the pressure of the flow system was maintained by a Zaiput BPR with a small dead volume and large enough channel width to ensure a smooth flow without clogging.

7.4.3 Ketamine

Ketamine (**48**) is a general anesthetic on the WHO list of essential medicines. It has also been found to be a rapid-acting antidepressant for the treatment of major depressive disorders with imminent risk of suicide. Ketamine and its analogs have been synthesized from a commercially available ketone (**49**) through a bromination–imination–thermolysis sequence (Stevens' procedure) [50], which uses toxic solvents and reagents of low atom economy. In order to provide an environmentally favorable alternative that bypasses problematic steps or conditions, Monbaliu and coworkers developed a continuous-flow process for the synthesis of racemic ketamine, making use of an industrial flow reactor platform (Corning Advanced-Flow reactors) (Scheme 7.13) [51]. The aerobic hydroxylation of ketone **49** is highly exothermic and limited by mass transfer (hours in batch), whereas it completes cleanly within a few minutes in flow (reactor I) with green reagents, solvent, and phase transfer catalyst (PEG-400). A computational study on the side product formation assisted the optimization of this step. In the imination step (reactor II), mild condition and fast reaction were enabled by applying triethyl borate as Lewis acid catalyst. The thermal rearrangements (reactor III) were found to be unimolecular processes with rather high activation barriers, accounting for their high reaction temperature (≥180 °C) required. Montmorillonite K10 packed in the column served as heterogeneous acid catalyst, which shorten the reaction time to five minutes. The final one-flow process concatenating three steps gave ketamine hydrochloride (**48**·HCl) in 62% isolated yield and excellent purity over 20 minutes. The gradual poisoning of K10 by the bases from upstream became pronounced over longer reaction time, hence necessitating an intermediate base removal between reactors II and III for the preparation in larger scales.

https://www.twirpx.org & http://chemistry-chemists.com

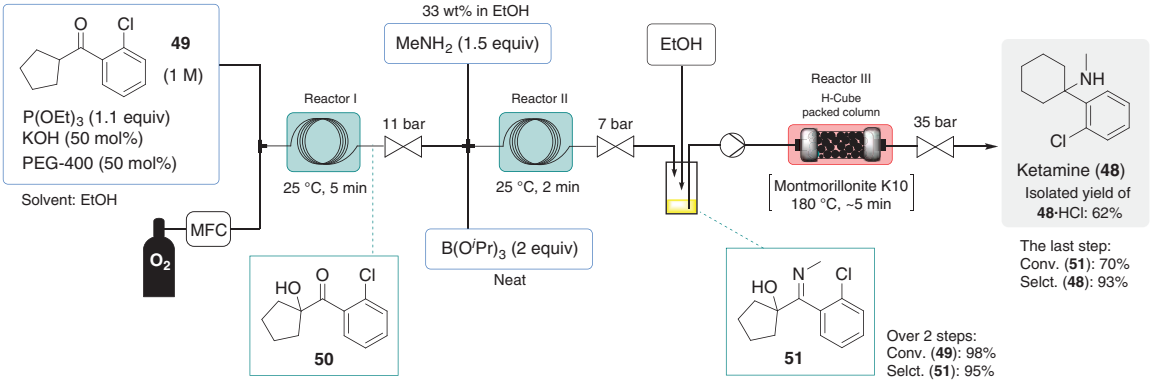

Scheme 7.13 The continuous-flow synthesis of Ketamine. Source: Kassin et al. [51]/Royal Society of Chemistry.

https://www.twirpx.org & http://chemistry-chemists.com

7.4.4 Lesinurad

Lesinurad **52** (Zurampic™, AstraZeneca) is a urate anion exchange transporter 1 (URAT1) inhibitor approved in 2015 by the US Food and Drug Administration (FDA) for treating high blood uric acid levels associated with gout. Pastre and coworkers presented a flow synthesis starting from a commercially available isothiocyanate **53** (Scheme 7.14a) [52]. The substrate underwent a three-step continuous reaction series to construct the heterocycle (reactors I and II) and the side chain (reactor III); the resultant precursor **58** was brominated (reactor IV) and hydrated (reactor V) in two separated flow steps to afford Lesinurad in 68% yield after crystallization. A total residence time of c. 2 hours was reported in flow, whereas its batch counterpart required 32 hours to give 40% overall yield.

The authors' early attempt to introduce the cyclopropyl group after the formation of the molecular skeleton (**61**) (Scheme 7.14b) turned out to be unsatisfactory, since the presence of the 1,2,4-triazole hampered the Suzuki coupling to complete, resulting in a poor overall yield of **52** (24%).

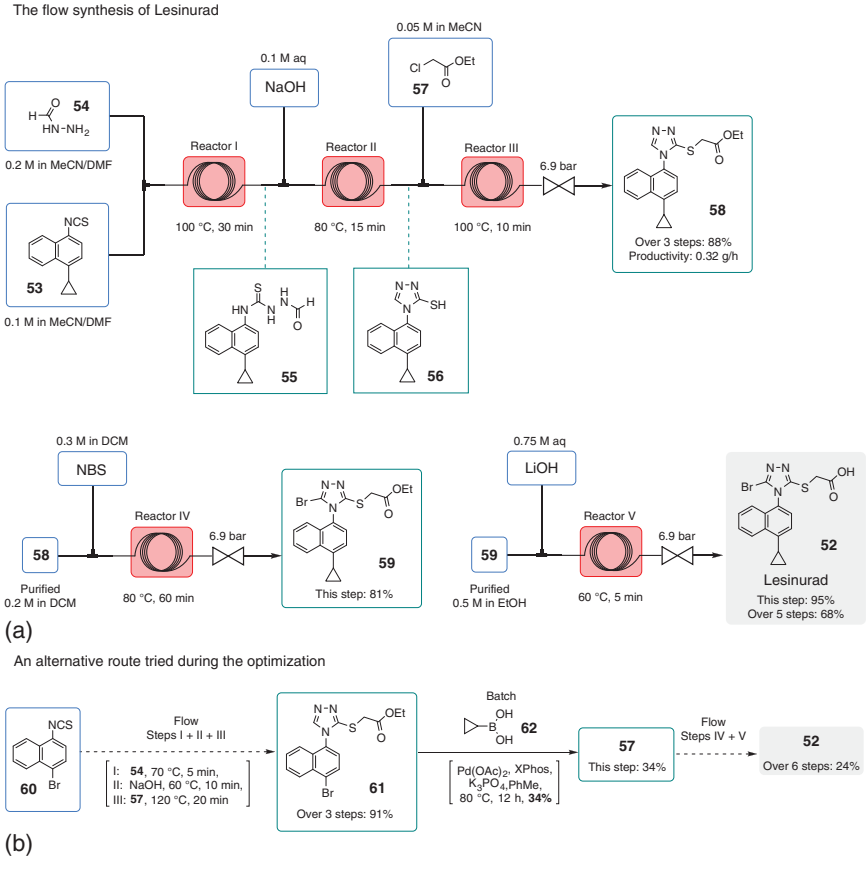

Scheme 7.14 The continuous-flow synthesis of Lesinurad. Source: Damião et al. [52]/Royal Society of Chemistry.

https://www.twirpx.org & http://chemistry-chemists.com

7.5 Convergent Multistep Flow Synthesis

In the construction of more complicated molecular structure, a convergent route is often more favorable than a single lengthy linear synthesis: smaller fragments of the target molecule (TM) are synthesized in shorter linear routes and put together by a convergent reaction close to the final step; therefore, the number of steps in the route connecting the substrate to the TM is shorter. When the convergent synthesis is transposed in flow, the reaction step joining the fragments has more than one "generator" integrated on its upstream sections. The example shown in Scheme 7.5 can be regarded as an example of convergent synthesis.

7.5.1 A Histone Deacetylase Inhibitor Precursor

Microfluidic conditions offer an ideal platform for handling highly reactive organometallic species with (sub-) second-level residence time (flash chemistry). Biaryl compounds bearing aminomethyl groups, like piperidyl methyl, are potential bioactive reagents. Nagaki and coworkers published an integrated synthesis of the precursor (**63**) of a histone deacetylase (HDAC) inhibitor (**64**), which contains such structural moiety (Scheme 7.15) [40]. The flow system integrated five reaction steps, four of which were performed within second-level residence time: the Br–Li exchange (reactor I), the borylation of the aryl lithium **66** (reactor II), the hydrolysis of the borate **67** (reactor III), and the generation of the reactive Pd catalyst (reactor IV). The Suzuki–Miyaura coupling between **68** and **69** (reactor V) completed the synthesis after heating the effluent at 50 °C for 1.5 hours in batch, affording the desired product (**63**) in quantitative yield after chromatography.

During the optimization of the lithiation and borylation steps (reactors I and II), the authors found that the channel width of the mixer is crucial to achieve a high yield for **67**. A 500 μm inner diameter for mixer M_2 is sufficient to ensure an effective mixing.

7.5.2 Linezolid

The WHO essential antibacterial drug linezolid (**70**) is a primarily used as a last line of defense treatment against multidrug-resistant gram-positive bacteria. Early routes for the synthesis of linezolid are lengthy (>7 steps) and rely on protecting groups. Jamison and coworker have developed a fully continuous sequence involving seven chemical transformations in one uninterrupted flow setup (Scheme 7.16) [53]. Two fragments of the target molecule (**78** and **74**) were constructed in two separated streams and then combined in the last two steps to complete the synthesis. The first stream started from (+)-epichlorohydrin (**71**) and acetonitrile. The Lewis acid (^{n}Bu$_2$O·BF$_3$)-catalyzed Ritter-type intermediate (**72**) (from reactor I) was quenched with isopropanol at low temperature, converting BF_3 to the soluble boronic ester (reactor II). Under the reaction condition, the formation of oxazoline side product (**80**) was largely suppressed; the nucleophilic reaction with diethyl ether (**81**) was minimized by increasing the steric hindrance of the solvent (^{n}Bu$_2$O). The resultant

https://www.twirpx.org & http://chemistry-chemists.com

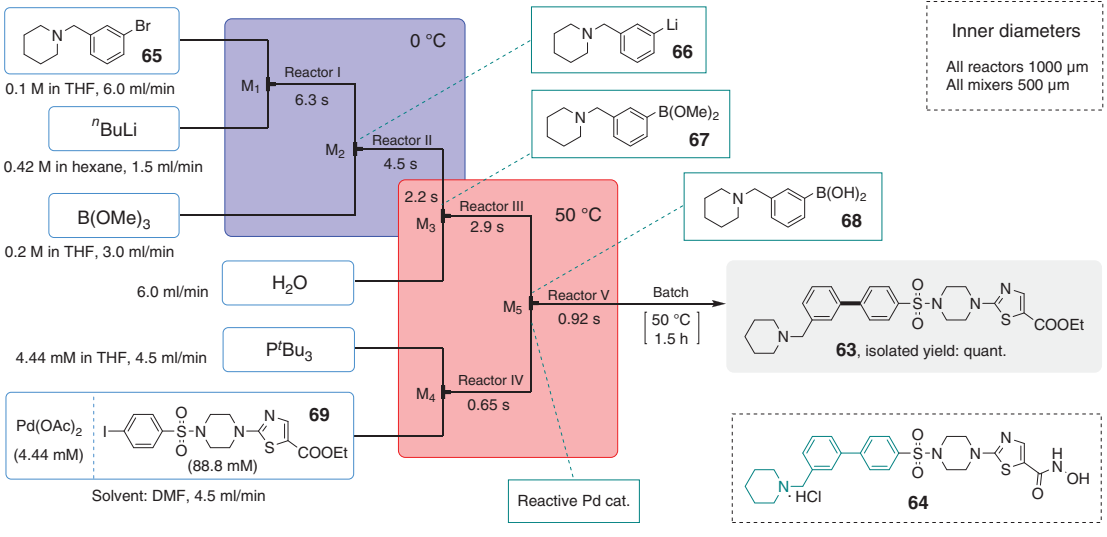

Scheme 7.15 Flash chemistry synthesis of a histone deacetylase (HDAC) inhibitor precursor. Source: Takahashi et al. [40]/John Wiley & Sons.

https://www.twirpx.org & http://chemistry-chemists.com

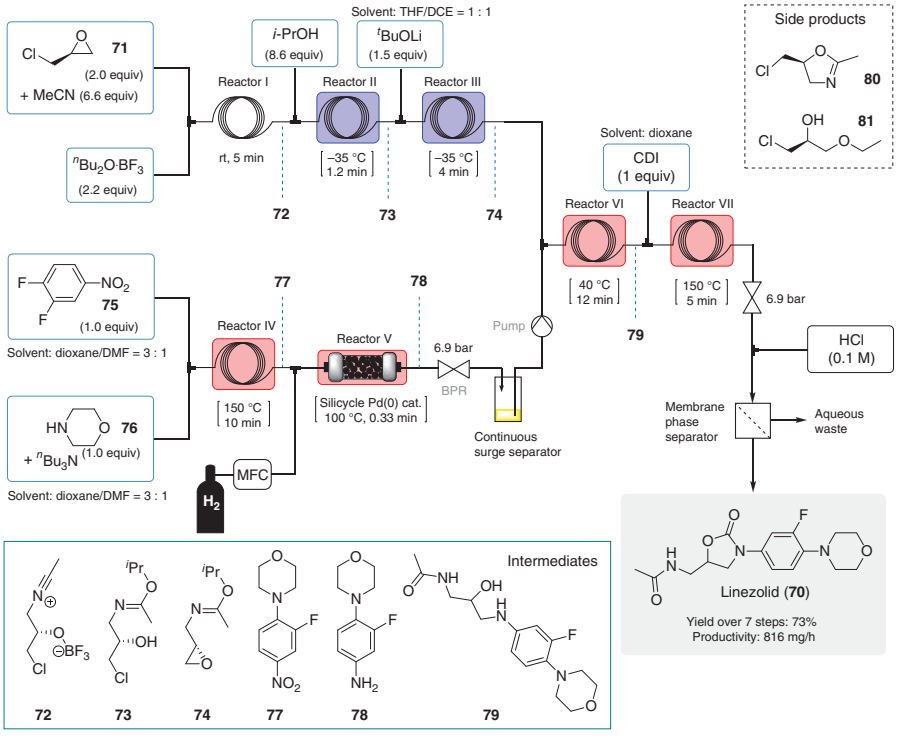

Scheme 7.16 The continuous-flow synthesis of linezolid. Source: Russell and Jamison [53]/John Wiley & Sons.

https://www.twirpx.org & http://chemistry-chemists.com

imidate chlorohydrin (**73**) was deprotonated by ^{t}BuOLi, giving epoxide **74** (reactor III). The second half of the **70** molecule were prepared via the S_NAr reaction between 3,4-dinitrofluoronitrobenzene (**75**) and morpholine (**76**) (reactor IV) followed by Pd-catalyzed hydrogenation in packed-bed reactor (reactor V). The solution of aniline **78** was separated from hydrogen gas in a sealed vessel and then reintroduced to the flow system. After the reaction with epoxide **74** (reactor VI), two fragments were joined together. Amino alcohol **79** and aniline **78** could not be isolated from the crude reaction mixtures because of their rapid oxidation. The condensation with *N*,*N*-carbonyldiimidazole (CDI) at 150 °C (reactor VII) finalized the synthesis; at the outlet of the flow system, immidiazole was removed by an in-line extraction with HCl (aq), affording linezolid (**70**) in 73% yield (over seven steps) after an offline chromatography. The total residence time of 27 minutes is much shorter than that of other existing processes (>60 hours), corresponding to a throughput of 816 mg/h.

7.6 Advanced Technologies for Multistep Flow Synthesis

In the previous paradigms, the end-to-end connection of different reaction steps has significantly improved the efficiency of multistep API synthesis, while the dependence on human labor is reduced. The customized flow setups and process parameters for the synthesis of a specific compound are widely pursued in industry to maximize the efficient access to that molecule [54]. The integration of in-line analytics and various sensors could acquire copious amounts of process data, the efficient generation and management of which are essential elements to enable better understanding, control, and intensification of the drug manufacturing process [55]. Such data can also be exploited for fully benefiting from the assets of flow for the rapid optimization of complex reaction conditions or sequences with the integration of Design of Experiment (DoE) strategies aiming at self-optimizing systems and the integration of artificial intelligence (AI) for exploring new routes.

7.6.1 Sensors and In-line Analysis

Sensors for real-time measurement of the reaction parameters are playing an important role in the acquisition of data from the flow system. The temperature, pressure, and flow rate sensors are commonly integrated with the thermostats, pumps, and mass flow controllers, enabling a visual reading of their values. These basic sensors have been integrated in some commercialized flow setups for laboratories and industry, allowing the monitoring and control of these parameters on a user's interface.

The external T/p [56], electrochemical [57], and optical sensors can be implemented to the flow systems without significantly rebuilding the setup: only a flow cell embedding the sensor is to insert. Many common spectroscopic probes can be connected to the flow system in a similar fashion for the in-line analysis of the reaction mixture [58], such as UV–Vis [22], near-infrared (NIR) [59], Raman [60, 61], and infrared (IR) [62, 63]. These techniques are fundamental to the process analytical technology (vide supra).

https://www.twirpx.org & http://chemistry-chemists.com

7.6.2 Process Analytical Technology (PAT)

Process analytical technology (PAT) is defined as "a system for designing, analyzing, and controlling manufacturing processes through timely measurement of critical process parameters (CPP) which affect critical quality attributes (CQA)" by FDA [55]. As has been showed in previous chapters of the present book, the application of PAT in flow chemistry enables the information feedback for process control, automated optimization, kinetic study, and reaction telescoping, guiding the progress of drug discovery in an efficient manner [64].

The sensor probes and instruments for in-line analysis are connected to computer software for the processing and visualization of the data. Large instruments (like nuclear magnetic resonance [NMR]) sometimes require reactants to flow through [65–67]. For the methods requiring the injection of a dilute solution, like mass spectra (MS) [68], gas chromatography (GC) [69], and HPLC [70], a local redesign of the flow path to accommodate the autosampler is sometimes necessary [71].

Utilizing a Modular Micro Reaction System (MMRS) equipped with a Lonza FlowPlate® Lab reactor, manufactured by Ehrfeld Mikrotechnik, Kappe and coworkers investigated a two-step organolithium chemistry with integrated PAT support (Scheme 7.17) [72]. The deprotonation of the substrate (**82**) was monitored using in-line ReactIR, where disappearance of the ester C=O stretching peak could be clearly quantified. Subsequently, the addition of lithium enolate (**83**) to the electrophile (**84**) was monitored by in-line NMR using the formyl and arene protons as distinct markers. The final reaction mixture was quantified by online ultra high performance liquid chromatography (UPLC), whose sampling was performed on an in-line dilution bypass. The pumps and sensors were connected to a HiTec Zang® LabManager™ unit and controlled by LabVision® software. With the support of PAT, the optimization process was significantly accelerated (17 iterations within two hours). The product **86** was isolated in 70% yield after a 70 minutes run under the optimized condition.

For the kilogram scale synthesis of prexasertib (**87**) monolactate monohydrate, a checkpoint kinase 1 (CHK1) inhibitor, Cole and coworkers monitored their automated continuous-flow system with PAT, especially in-line HPLC (Scheme 7.18) [73]. This complex automatic system involved several unit operations that are quite uncommon for sub-gram scale reactions, such as counter current extraction, rotary evaporation, in-line crystallization, and filtration. The entire system worked for a few days, producing 24 kg (c. 114 000 doses) of lactate in good yield and purity. During this long run, a disturbance was detected by HPLC; a considerable amount of **89** and **87** were observed at the outlet of reactor II. The authors separated that fraction and soon found out that the evaporative loss of the base (*N*-ethylmorpholine) from the feed solution had occurred over time, resulting in the accumulation of HCl in the reaction mixture.

7.6.3 Self-optimization

Traditionally, the optimization of process parameters was achieved manually in a trial-and-error manner, since the flow system, the analytical instruments, and

https://www.twirpx.org & http://chemistry-chemists.com

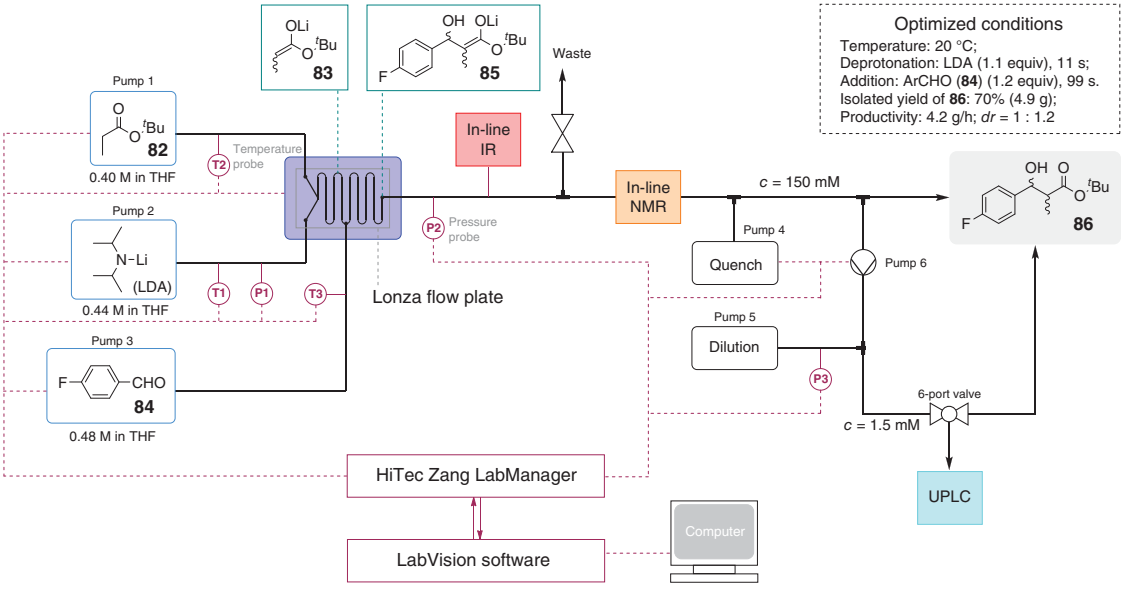

Scheme 7.17 A modular flow platform integrated with PAT tools for multistep reactions. Source: Modified from Sagmeister et al. [72].

https://www.twirpx.org & http://chemistry-chemists.com

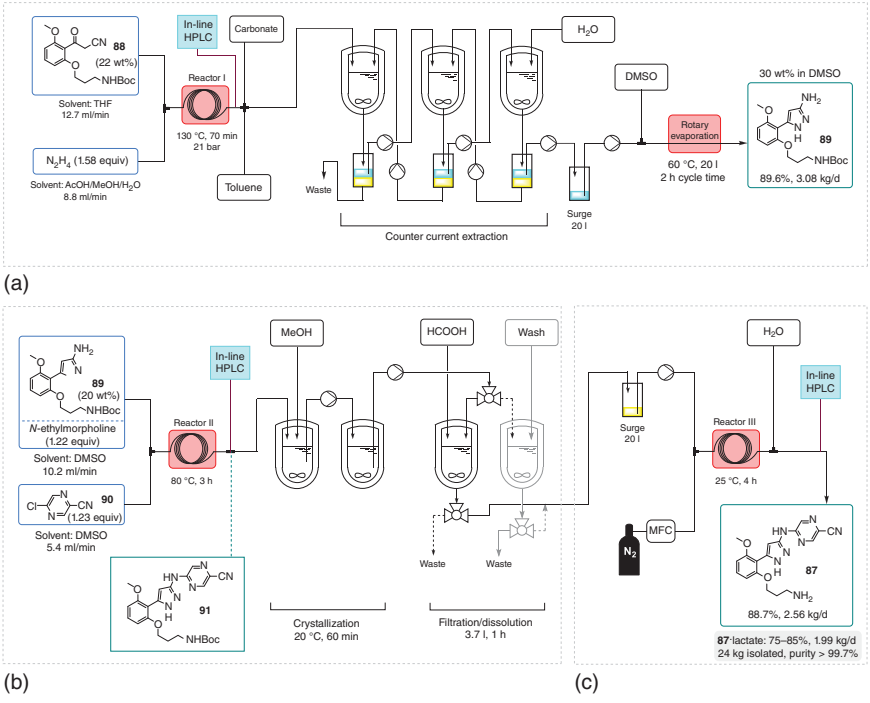

Scheme 7.18 Monitoring kilogram-scale synthesis of prexasertib monolactate monohydrate with PAT: (a) condensation with hydrazine, (b) S_NAr reaction, and (c) deprotection (simplified flowchart; the final reaction step – the formation of the lactate is not shown). Source: Modified from Cole et al. [73].

the chemists are working independently, their cooperation relies on the chemists' knowledge and a priori decision. With the assistance of PAT tools and computational software, the feedback loop for the resetting of the process parameters can be closed to enable an automatic optimization without human intervention [74].

For the optimization of the individual steps in the synthesis of natural product carpanone (**92**), Felpin and coworkers developed an autonomous system supported by MatLab® platform (Scheme 7.19) [75]. The composition of reaction mixture was analyzed by in-line HPLC or NMR. The custom-made algorithm derived from the downhill simplex (Nelder–Mead) method and golden section search method [74] was executed for the black-box optimizations that assume no a priori knowledge of the chemical reactions. Starting from the commercially available sesamol (**93**), four chemical steps (Williamson reaction, Claisen rearrangement, isomerization, and oxidative dimerization) were optimized to their best yields and efficiency over 68 experiments, giving carpanone in 67% overall yield. For the rearrangement and the isomerization steps (Scheme 7.19b,c), the optimal conditions located in the high T/p regime were found out by the software over c. 20 iterations, giving the product with high throughput. The optimized conditions for the last two steps (Scheme 7.19c,d) achieved improved selectivity and yields than that of their batch

https://www.twirpx.org & http://chemistry-chemists.com

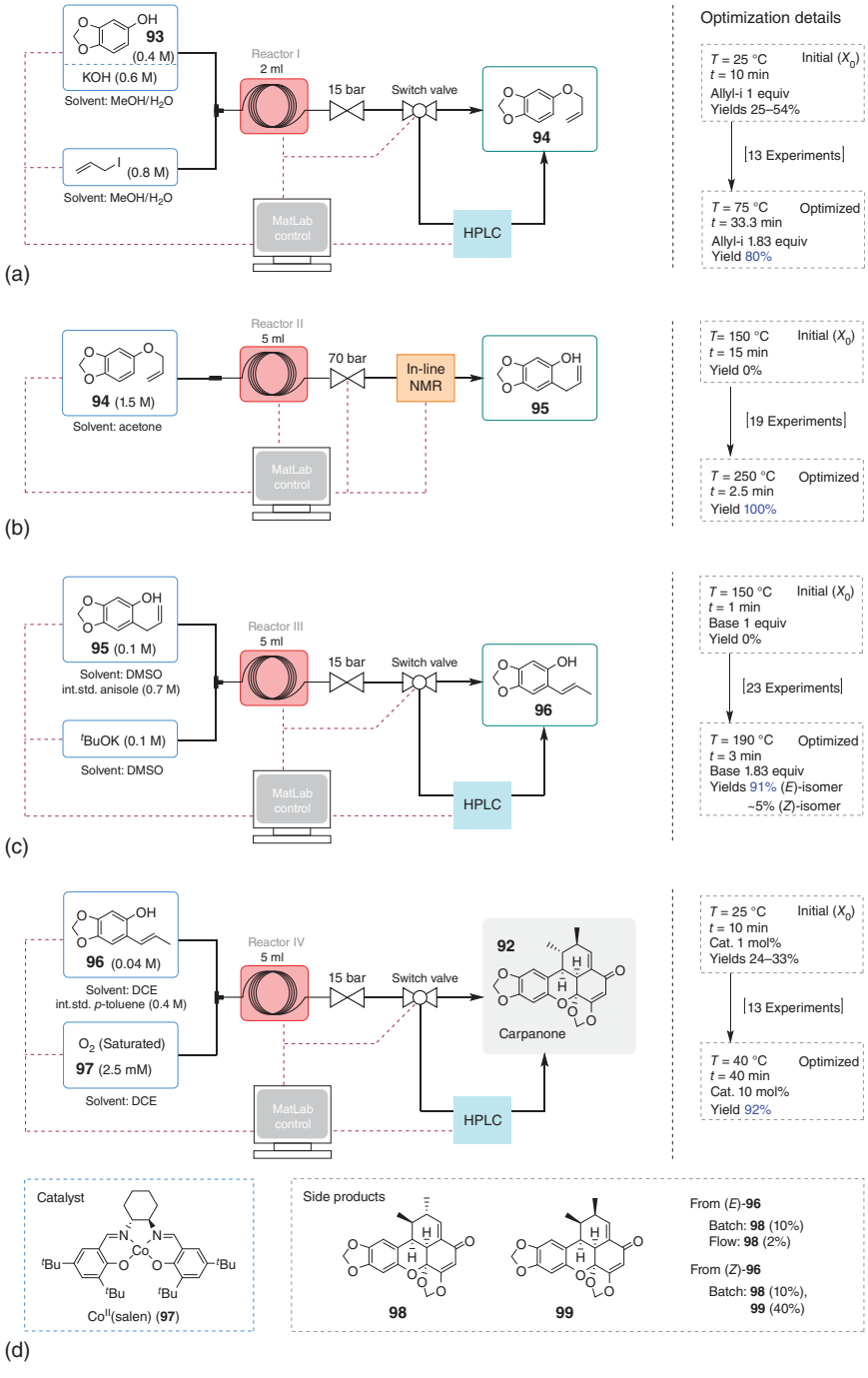

Scheme 7.19 Auto-optimization of each step in the synthesis of Carpanone. Source: Cortés-Borda et al. [75]/American Chemical Society.

https://www.twirpx.org & http://chemistry-chemists.com

counterparts. Recently, the same algorithm was applied for the self-optimization in the synthesis of pyridine–oxazoline (PyOX) ligands [70].

7.6.4 Modular Flow System

Continuous-flow systems have been considered to be less flexible, since they are normally tailored to specific chemical reactions. Some measures of redesign or re-optimization have typically to be taken before performing a varied array of reactions on the same flow setup. Nowadays, the commercially available lab-scale flow reactors could only manage one to two chemical steps on one piece of equipment with standardized modules.

In 2016, the research groups of Jamison and coworker developed a reconfigurable system for the on-demand manufacturing of pharmaceuticals for smaller targeted patient populations [76]. Modules for complex multistep synthesis, in-line purifications, post-synthesis workup and handling, crystallization, real-time monitoring, and formulation of drug products were integrated in a refrigerator-sized device. The setup has been reconfigured for the production of four APIs (diphenhydramine, lidocaine, diazepam, and fluoxetine) in high purity and throughput, also including their final liquid formulation as injectable dosages.

Two years later, the same research groups presented a compact, modular system that enables automated optimization and scale-up of multistep reactions (Scheme 7.20a) [77]. The flexibility of the flow system was featured by five universal bays that could host any standardized reaction module (Scheme 7.20b) for the particular chemistry to be performed. Raman, IR, and mass spectroscopy were integrated in the system for in-line analysis. The Stable Noisy Optimization by Branch and Fit (SNOBFIT) algorithm supported by MatLab was used for the global optimization of single- or multistep processes as has been introduced in Chapter 3. The user only needs to load the modules and reagents to get the optimization or synthesis started through a graphical interface (Scheme 7.20c). The versatility of the system was proven by the black-box optimization of C–C and C–N cross-coupling, olefination, reductive amination, nucleophilic aromatic substitution (S_NAr), photoredox catalysis, and a multistep sequence. A library of nine compounds (10 mg scale) was rapidly generated via S_NAr reaction within 20 minutes, demonstrating the potential of application in drug discovery. A two-step synthesis of cyclobutanone was optimized on this platform (Scheme 7.20d): the generation of ketene (**101**) and the [2 + 2] were handled in a concatenated setup, giving **103** in 77% yield with good stereoselectivity.

Apart from modular reactors, Cronin and coworkers made use of a chemical to computer-automated design (ChemCAD) approach that translates traditional bench-scale synthesis into a platform-independent digital code. This in turn guides the production of a 3D printed reactor that encloses the entire synthetic route for the on-demand multistep synthesis of pharmaceuticals [78].

https://www.twirpx.org & http://chemistry-chemists.com

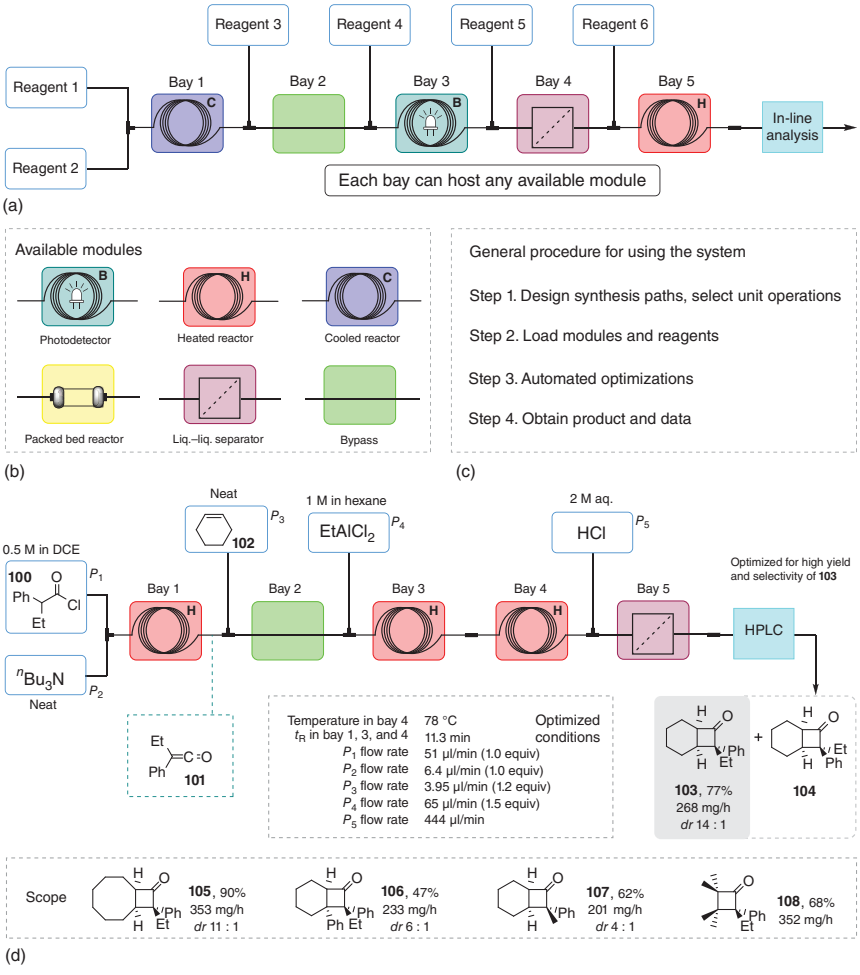

Scheme 7.20 A reconfigurable system for automated optimization of diverse chemical reactions. Source: Based on Bédard et al. [77].

7.6.5 Toward Full Automation

In the previous examples, the design of the synthetic route has been performed outside of the reactor system; i.e. the flow system requires a known route to carry out the synthesis. The chemists have to select the substrates, the catalysts, the solvents, and the modules based on a known or designed synthetic route; this is the case even for a highly integrated self-optimization platform. It would be ideal that the system could make a molecule in response to the user's input ("dial a molecule").

As has been introduced in previous chapters, the research groups of Jamison and coworkers developed a robotic platform for the multistep synthesis informed by AI

https://www.twirpx.org & http://chemistry-chemists.com

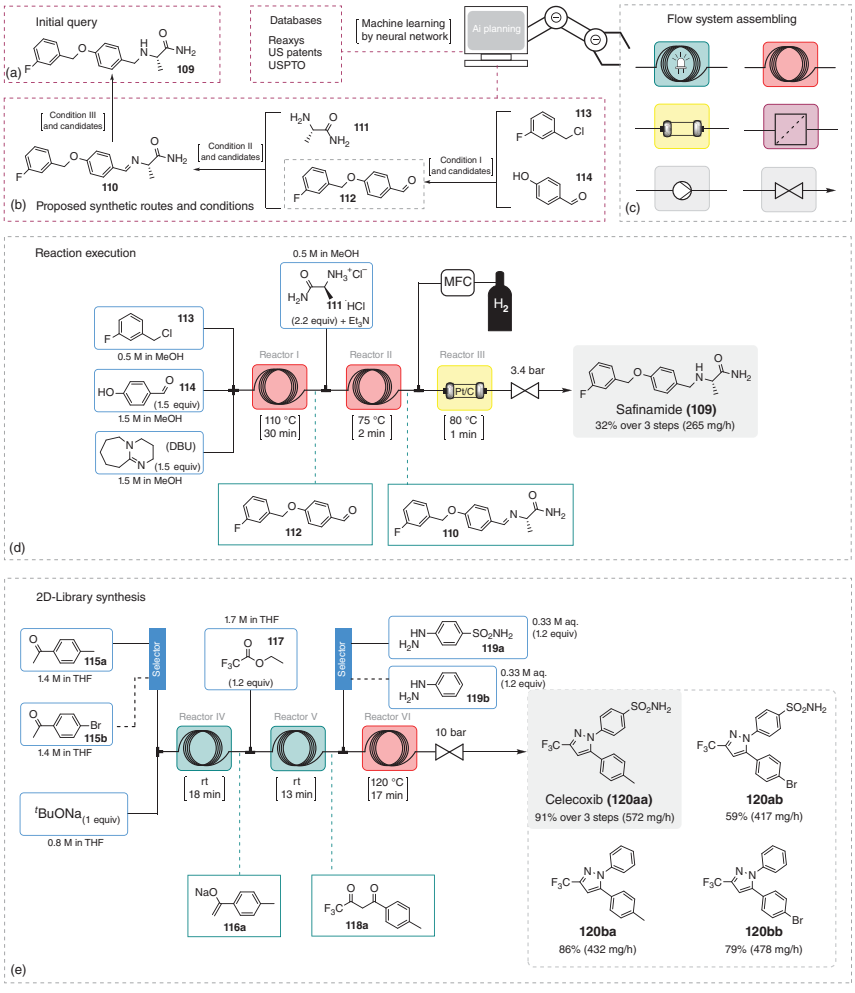

Scheme 7.21 A robotic platform for flow synthesis of organic compounds informed by AI planning. Source: Based on Coley et al. [79].

planning (Scheme 7.21) [79]. Their synthesis planning program integrates their previous efforts to generalize known chemistry to new substrates by machine learning to apply retrosynthetic transformations, to identify suitable reaction conditions, and to evaluate whether reactions are likely to be successful (Scheme 7.21b) [80]. For the synthesis of a given molecule (e.g. safinamide **109**), once the route and reaction conditions are confirmed, the robotic arm fetches the modules and the tubing from a storage rack and then connects them together to execute the reaction (Scheme 7.21c). The versatility of the system was demonstrated by the preparation of 15 APIs and drug-like compounds with varied structural complexity (e.g. Scheme 7.21d). The automatic rerouting of fluidic connections and two 24-way selector valves enable the switching among different feedstocks, which is beneficial to the library synthesis in drug discovery (Scheme 7.21e).

https://www.twirpx.org & http://chemistry-chemists.com

7.7 Conclusion

Continuous-flow technology is a versatile and promising tool for the multistep synthesis of APIs and related compounds. Despite the well-known merits for single-step reactions, like improved safety, scalability, and process intensification, the end-to-end connection of reaction steps in one flow reduces the environmental and instrumental footprints by eliminating the workup and purification of intermediates. Compared with multistep synthesis in batch, the entire chemical process could be intensified in flow in terms of higher throughput, overall yield, and product quality. The integration of flow reactors with in-line sensors, PAT tools, and computer software enables the utilization of the information generated by the chemical reactions in an efficient manner, leading to a fully automated chemical synthesis in the future.

References

1 Nusim, S. (2010). *Active Pharmaceutical Ingredients: Development, Manufacturing, and Regulation*. Bocaraton: CRC Press, Taylor & Francis Inc.

2 Warren, S. and Wyatt, P. (2008). *Organic Synthesis: The Disconnection Approach*. Chichester: Wiley.

3 Brauch, S., van Berkel, S.S., and Westermann, B. (2013). Higher-order multicomponent reactions: beyond four reactants. *Chem. Soc. Rev.* 42 (12): 4948–4962.

4 Zarganes-Tzitzikas, T., Chandgude, A.L., and Dömling, A. (2015). Multicomponent reactions, union of MCRs and beyond. *Chem. Rec.* 15 (5): 981–996.

5 Kappe, C.O. and Dallinger, D. (2009). Controlled microwave heating in modern organic synthesis: highlights from the 2004–2008 literature. *Mol. Diversity* 13 (2): 71–193.

6 De La Hoz, A., Díaz-Ortiz, Á., and Moreno, A. (2005). Microwaves in organic synthesis. Thermal and non-thermal microwave effects. *Chem. Soc. Rev.* 34 (2): 164–178.

7 Plutschack, M.B., Pieber, B., Gilmore, K., and Seeberger, P.H. (2017). The Hitchhiker's guide to flow chemistry. *Chem. Rev.* 117 (18): 11796–11893.

8 Hessel, V., Kralisch, D., and Kockmann, N. (2015). *Novel Process Windows: Innovative Gates to Intensified and Sustainable Chemical Processes*. Weinheim: Wiley-VCH.

9 Hessel, V., Kralisch, D., Kockmann, N. et al. (2013). Novel process windows for enabling, accelerating, and uplifting flow chemistry. *ChemSusChem* 6 (5): 746–789.

10 Pieber, B., Gilmore, K., and Seeberger, P.H. (2017). Integrated flow processing—challenges in continuous multistep synthesis. *J. Flow Chem.* 7 (3–4): 129–136.

11 Wegner, J., Ceylan, S., and Kirschning, A. (2012). Flow chemistry—a key enabling technology for (multistep) organic synthesis. *Adv. Synth. Catal.* 354 (1): 17–57.

https://www.twirpx.org & http://chemistry-chemists.com

12 Webb, D. and Jamison, T.F. (2010). Continuous flow multi-step organic synthesis. *Chem. Sci.* 1 (6): 675–680.

13 Gerardy, R. and Monbaliu, J.-C.M. (2018). Multistep continuous-flow processes for the preparation of heterocyclic active pharmaceutical ingredients. *Top. Heterocycl. Chem.* 56: 1–102.

14 Britton, J. and Raston, C.L. (2017). Multi-step continuous-flow synthesis. *Chem. Soc. Rev.* 46 (5): 1250–1271.

15 Hughes, D.L. (2018). Applications of flow chemistry in drug development: highlights of recent patent literature. *Org. Process Res. Dev.* 22 (1): 13–20.

16 Gutmann, B., Cantillo, D., and Kappe, C.O. (2015). Continuous-flow technology—a tool for the safe manufacturing of active pharmaceutical ingredients. *Angew. Chem. Int. Ed.* 54 (23): 6688–6728.

17 Cossar, P.J., Hizartzidis, L., Simone, M.I. et al. (2015). The expanding utility of continuous flow hydrogenation. *Org. Biomol. Chem.* 13: 7119–7130.

18 Irfan, M., Glasnov, T.N., and Kappe, C.O. (2011). Heterogeneous catalytic hydrogenation reactions in continuous-flow reactors. *ChemSusChem* 4 (3): 300–316.

19 Suveges, N.S., de Souza, R.O.M.A., Gutmann, B., and Kappe, C.O. (2017). Synthesis of mepivacaine and its analogues by a continuous-flow tandem hydrogenation/reductive amination strategy. *Eur. J. Org. Chem.* 44: 6511–6517.

20 Strauss, F.J., Cantillo, D., Guerra, J., and Kappe, C.O. (2016). A laboratory-scale continuous flow chlorine generator for organic synthesis. *React. Chem. Eng.* 1 (5): 472–476.

21 Pinho, V.D., Gutmann, B., Miranda, L.S.M. et al. (2014). Continuous flow synthesis of α-halo ketones: essential building blocks of antiretroviral agents. *J. Org. Chem.* 79 (4): 1555–1562.

22 Lebl, R., Cantillo, D., and Kappe, C.O. (2019). Continuous generation, in-line quantification and utilization of nitrosyl chloride in photonitrosation reactions. *React. Chem. Eng.* 4 (4): 738–746.

23 Yang, H., Martin, B., and Schenkel, B. (2018). On-demand generation and consumption of diazomethane in multistep continuous flow systems. *Org. Process Res. Dev.* 22 (4): 446–456.

24 Mastronardi, F., Gutmann, B., and Oliver Kappe, C. (2013). Continuous flow generation and reactions of anhydrous diazomethane using a Teflon AF-2400 tube-in-tube reactor. *Org. Lett.* 15 (21): 5590–5593.

25 Pieber, B. and Kappe, C.O. (2016). Generation and synthetic application of trifluoromethyl diazomethane utilizing continuous flow technologies. *Org. Lett.* 18 (5): 1076–1079.

26 Köckinger, M., Hone, C.A., and Kappe, C.O. (2019). HCN on tap: on-demand continuous production of anhydrous HCN for organic synthesis. *Org. Lett.* 21 (13): 5326–5330.

27 Brancour, C., Fukuyama, T., Mukai, Y. et al. (2013). Modernized low pressure carbonylation methods in batch and flow employing common acids as a CO source. *Org. Lett.* 15 (11): 2794–2797.

https://www.twirpx.org & http://chemistry-chemists.com

28 Gross, U., Koos, P., O'Brien, M. et al. (2014). A general continuous flow method for palladium catalysed carbonylation reactions using single and multiple tube-in-tube gas–liquid microreactors. *Eur. J. Org. Chem.* 2014 (29): 6418–6430.

29 Wu, J., Yang, X., He, Z. et al. (2014). Continuous flow synthesis of ketones from carbon dioxide and organolithium or Grignard reagents. *Angew. Chem. Int. Ed.* 53 (32): 8416–8420.

30 Steiner, A., Williams, J.D., Mateos, C., and Kappe, C.O. (2020). Continuous photochemical benzylic bromination using *in situ* generated Br_2: process intensification towards optimal PMI and throughput. *Green Chem.* 22 (2): 448–454.

31 Glotz, G., Lebl, R., Dallinger, D., and Kappe, C.O. (2017). Integration of bromine and cyanogen bromide generators for the continuous-flow synthesis of cyclic guanidines. *Angew. Chem. Int. Ed.* 56 (44): 13786–13789.

32 Van Den Broek, S.A.M.W., Leliveld, J.R., Becker, R. et al. (2012). Continuous flow production of thermally unstable intermediates in a microreactor with inline IR-analysis: controlled Vilsmeier–Haack formylation of electron-rich arenes. *Org. Process Res. Dev.* 16 (5): 934–938.

33 Chen, Y., Cantillo, D., and Kappe, C.O. (2019). Visible light-promoted Beckmann rearrangements: separating sequential photochemical and thermal phenomena in a continuous flow reactor. *Eur. J. Org. Chem.* 11: 2163–2171.

34 Colella, M., Nagaki, A., and Luisi, R. (2020). Flow technology for the genesis and use of (highly) reactive organometallic reagents. *Chem. Eur. J.* 26 (1): 19–32.

35 Rossi, E., Woehl, P., and Maggini, M. (2012). Scalable *in situ* diazomethane generation in continuous-flow reactors. *Org. Process Res. Dev.* 16 (5): 1146–1149.

36 Tran, D.N., Battilocchio, C., Lou, S.B. et al. (2015). Flow chemistry as a discovery tool to access sp^2–sp^3 cross-coupling reactions via diazo compounds. *Chem. Sci.* 6 (2): 1120–1125.

37 Huck, L., De La Hoz, A., Díaz-Ortiz, A., and Alcázar, J. (2017). Grignard reagents on a tab: direct magnesium insertion under flow conditions. *Org. Lett.* 19 (14): 3747–3750.

38 Petersen, T.P., Becker, M.R., and Knochel, P. (2014). Continuous flow magnesiation of functionalized heterocycles and acrylates with TMPMgCl·LiCl. *Angew. Chem. Int. Ed.* 53 (30): 7933–7937.

39 Hafner, A., Mancino, V., Meisenbach, M. et al. (2017). Dichloromethyllithium: synthesis and application in continuous flow mode. *Org. Lett.* 19 (4): 786–789.

40 Takahashi, Y., Ashikari, Y., Takumi, M. et al. (2020). Synthesis of biaryls having a piperidylmethyl group based on space integration of lithiation, borylation, and Suzuki–Miyaura coupling. *Eur. J. Org. Chem.* 2020 (5): 618–622.

41 Berton, M., Huck, L., and Alcázar, J. (2018). On-demand synthesis of organozinc halides under continuous flow conditions. *Nat. Protoc.* 13 (1): 324–334.

42 Ketels, M., Konrad, D.B., Karaghiosoff, K. et al. (2017). Selective lithiation, magnesiation, and zincation of unsymmetrical azobenzenes using continuous flow. *Org. Lett.* 19 (7): 1666–1669.

43 Knölker, H.J. (2005). Occurrence, biological activity, and convergent organometallic synthesis of carbazole alkaloids. *Top. Curr. Chem.* 244: 115–148.

https://www.twirpx.org & http://chemistry-chemists.com

44 Parisien-Collette, S. and Collins, S.K. (2018). Exploiting photochemical processes in multi-step continuous flow: derivatization of the natural product clausine C. *ChemPhotoChem* 2 (10): 855–859.

45 Morodo, R., Gérardy, R., Petit, G., and Monbaliu, J.C.M. (2019). Continuous flow upgrading of glycerol toward oxiranes and active pharmaceutical ingredients thereof. *Green Chem.* 21 (16): 4422–4433.

46 Mata, A., Cantillo, D., and Kappe, C.O. (2017). An integrated continuous-flow synthesis of a key oxazolidine intermediate to noroxymorphone from naturally occurring opioids. *Eur. J. Org. Chem.* 44: 6505–6510.

47 Yu, E., Mangunuru, H.P.R., Telang, N.S. et al. (2018). High-yielding continuous-flow synthesis of antimalarial drug hydroxychloroquine. *Beilstein J. Org. Chem.* 14: 583–592.

48 Hiebler, K., Soritz, S., Gavric, K. et al. (2020). Multistep synthesis of a valsartan precursor in continuous flow. *J. Flow Chem.* 10 (1): 283–294.

49 Köckinger, M., Hone, C.A., Gutmann, B. et al. (2018). Scalable continuous flow process for the synthesis of eflornithine using fluoroform as difluoromethyl source. *Org. Process Res. Dev.* 22 (11): 1553–1563.

50 Stevens, C.L., Elliott, R.D., and Winch, B.L. (1963). Aminoketone rearrangements. II. The rearrangement of phenyl α-aminoketones. *J. Am. Chem. Soc.* 85 (10): 1464–1470.

51 Kassin, V.E.H., Gérardy, R., Toupy, T. et al. (2019). Expedient preparation of active pharmaceutical ingredient ketamine under sustainable continuous flow conditions. *Green Chem.* 21 (11): 2952–2966.

52 Damião, M.C.F.C.B., Marçon, H.M., and Pastre, J.C. (2020). Continuous flow synthesis of the URAT1 inhibitor lesinurad. *React. Chem. Eng.* 5: 865–872. https://doi.org/10.1039/c9re00483a.

53 Russell, M.G. and Jamison, T.F. (2019). Seven-step continuous flow synthesis of linezolid without intermediate purification. *Angew. Chem. Int. Ed.* 58 (23): 7678–7681.

54 Trobe, M. and Burke, M.D. (2018). The molecular industrial revolution: automated synthesis of small molecules. *Angew. Chem. Int. Ed.* 57 (16): 4192–4214.

55 Gioiello, A., Piccinno, A., Lozza, A.M., and Cerra, B. (2020) The medicinal chemistry in the era of machines and automation: recent advances in continuous flow technology. *J. Med. Chem.*, 63(13), 6624–6647. https://doi.org/10.1021/acs.jmedchem.9b01956.

56 Znidar, D., O'Kearney-Mcmullan, A., Munday, R. et al. (2019). Scalable Wolff–Kishner reductions in extreme process windows using a silicon carbide flow reactor. *Org. Process Res. Dev.* 23 (11): 2445–2455.

57 Lebl, R., Murray, T., Adamo, A. et al. (2019). Continuous flow synthesis of methyl oximino acetoacetate: accessing greener purification methods with inline liquid-liquid extraction and membrane separation technology. *ACS Sustainable Chem. Eng.* 7 (24): 20088–20096.

58 Sans, V. and Cronin, L. (2016). Towards dial-a-molecule by integrating continuous flow, analytics and self-optimisation. *Chem. Soc. Rev.* 45 (8): 2032–2043.

https://www.twirpx.org & http://chemistry-chemists.com

59 Galaverna, R., Ribessi, R.L., Rohwedder, J.J.R., and Pastre, J.C. (2018). Coupling continuous flow microreactors to MicroNIR spectroscopy: ultracompact device for facile in-line reaction monitoring. *Org. Process Res. Dev.* 22 (7): 780–788.

60 Roberto, M.F., Dearing, T.I., Martin, S., and Marquardt, B.J. (2012). Integration of continuous flow reactors and online Raman spectroscopy for process optimization. *J. Pharm. Innovation* 7: 69–75.

61 Chaplain, G., Haswell, S.J., Fletcher, P.D.I. et al. (2013). Development and evaluation of a Raman flow cell for monitoring continuous flow reactions. *Aust. J. Chem.* 66 (2): 208–212.

62 Poscharny, K., Fabry, D.C., Heddrich, S. et al. (2018). Machine assisted reaction optimization: a self-optimizing reactor system for continuous-flow photochemical reactions. *Tetrahedron* 74 (25): 3171–3175.

63 Galaverna, R., Breitkreitz, M.C., and Pastre, J.C. (2018). Conversion of D-fructose to 5-(hydroxymethyl)furfural: evaluating batch and continuous flow conditions by design of experiments and in-line FTIR monitoring. *ACS Sustainable Chem. Eng.* 6 (3): 4220–4230.

64 Fitzpatrick, D.E. and Ley, S.V. (2018). Engineering chemistry for the future of chemical synthesis. *Tetrahedron* 74 (25): 3087–3100.

65 Emmanuel, N., Mendoza, C., Winter, M. et al. (2017). Scalable photocatalytic oxidation of methionine under continuous-flow conditions. *Org. Process Res. Dev.* 21 (9): 1435–1438.

66 Thomson, C.G., Jones, C.M.S., Rosair, G. et al. (2020). Continuous-flow synthesis and application of polymer-supported BODIPY photosensitisers for the generation of singlet oxygen; process optimised by in-line NMR spectroscopy. *J. Flow Chem.* 10 (1): 327–345.

67 Picard, B., Gouilleux, B., Lebleu, T. et al. (2017). Oxidative neutralization of mustard-gas simulants in an on-board flow device with in-line NMR monitoring. *Angew. Chem. Int. Ed.* 56 (26): 7568–7572.

68 Browne, D.L., Wright, S., Deadman, B.J. et al. (2012). Continuous flow reaction monitoring using an on-line miniature mass spectrometer. *Rapid Commun. Mass Spectrom.* 26 (17): 1999–2010.

69 Streng, E.S., Lee, D.S., George, M.W., and Poliakoff, M. (2017). Continuous N-alkylation reactions of amino alcohols using γ-Al_2O_3 and supercritical CO_2: unexpected formation of cyclic ureas and urethanes by reaction with CO_2. *Beilstein J. Org. Chem.* 13: 329–337.

70 Wimmer, E., Cortés-Borda, D., Brochard, S. et al. (2019). An autonomous self-optimizing flow machine for the synthesis of pyridine–oxazoline (PyOX) ligands. *React. Chem. Eng.* 4 (9): 1608–1615.

71 Bezerra, M.A., Lemos, V.A., de Oliveira, D.M. et al. (2020). Automation of continuous flow analysis systems – a review. *Microchem. J.* 155: 104731.

72 Sagmeister, P., Williams, J.D., Hone, C.A., and Kappe, C.O. (2019). Laboratory of the future: a modular flow platform with multiple integrated PAT tools for multistep reactions. *React. Chem. Eng.* 4 (9): 1571–1578.

https://www.twirpx.org & http://chemistry-chemists.com

73 Cole, K.P., Groh, J.M.C., Johnson, M.D. et al. (2017). Kilogram-scale prexasertib monolactate monohydrate synthesis under continuous-flow CGMP conditions. *Science* 356 (6343): 1144–1151.

74 Mateos, C., Nieves-Remacha, M.J., and Rincón, J.A. (2019). Automated platforms for reaction self-optimization in flow. *React. Chem. Eng.* 4 (9): 1536–1544.

75 Cortés-Borda, D., Wimmer, E., Gouilleux, B. et al. (2018). An autonomous self-optimizing flow reactor for the synthesis of natural product carpanone. *J. Org. Chem.* 83 (23): 14286–14289.

76 Adamo, A., Beingessner, R.L., Behnam, M. et al. (2016). On-demand continuous-flow production of pharmaceuticals in a compact, reconfigurable system. *Science* 352 (6281): 61–67.

77 Bédard, A., Adamo, A., Aroh, K.C. et al. (2018). Reconfigurable system for automated optimization of diverse chemical reactions. *Science* 361: 1220–1225.

78 Kitson, P.J., Marie, G., Francoia, J.P. et al. (2018). Digitization of multistep organic synthesis in reactionware for on-demand pharmaceuticals. *Science* 359 (6373): 314–319.

79 Coley, C.W., Thomas, D.A., Lummiss, J.A.M. et al. (2019). A robotic platform for flow synthesis of organic compounds informed by AI planning. *Science* 365 (6453): 1–9.

80 Gao, H., Struble, T.J., Coley, C.W. et al. (2018). Using machine learning to predict suitable conditions for organic reactions. *ACS Cent. Sci.* 4 (11): 1465–1476.

https://www.twirpx.org & http://chemistry-chemists.com

8

Enantioselective (Bio)Catalysis in Continuous-flow as Efficient Tool for the Synthesis of Advanced Intermediates and Active Pharmaceutical Ingredients

Laura Amenós[1], Anna M. Sobolewska[1], Esther Alza[2], and Miquel A. Pericàs[1]

[1] *Institute of Chemical Research of Catalonia (ICIQ), 16, Avda. Països Catalans, 43007 Tarragona, Spain*
[2] *Alza & Associates S.L., Sustainability Consulting, Rnda. Canigó 7-10, 08950, Barcelona, Spain*

8.1 Introduction

The development of chemical processes that uses continuous flow represents a novel area with high potential since today more efficient, environmentally friendly, and safer methodologies are required to produce fine chemicals and active pharmaceutical ingredients (APIs). These key advantages, along with higher product quality, a smaller footprint, and the ability of performing chemistries that would otherwise be impossible in batch mode, have led to this technology being increasingly adopted by pharma and biotechnology companies from drug discovery to manufacturing [1].

Despite the mentioned benefits obtained by applying continuous-flow methodologies, the pharmaceutical industry has remained committed to batch operations. However, this trend is changing due to fast-growing use of more personalized medicines and therapies involving complex compounds that renders continuous processes competitive with respect to traditional batch synthesis. Moreover, since many bioactive compounds are optically active, the main application of enantioselective catalysis is found in the pharma and fine chemicals industries, in crops protection, and in the biotechnology area [2].

The application of catalysis in continuous flow has been approached in two ways (Figure 8.1):

(a) Mixing a soluble homogeneous catalyst in the solution being pumped.
(b) Using an immobilized catalyst onto a solid support in packed-bed reactors.

Both strategies have great potential applications, but the use of a heterogeneous catalyst has additional benefits: the product is not contaminated with the catalyst, and, if this proves robust enough, the effective catalyst loading becomes a function of operation time, leading to extremely high turnover numbers (TONs) for the overall

Flow and Microreactor Technology in Medicinal Chemistry, First Edition. Edited by Esther Alza.
© 2022 WILEY-VCH GmbH. Published 2022 by WILEY-VCH GmbH.

https://www.twirpx.org & http://chemistry-chemists.com

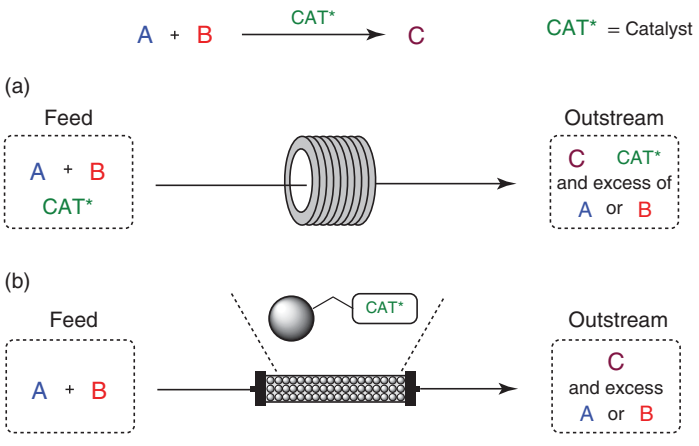

Figure 8.1 Continuous-flow catalysis with (a) homogeneous or (b) heterogeneous catalysts.

process even when the size of the reactor is small, since at any given time the substrates are exposed to (super)stoichiometric amounts of catalyst inside the reactor, and this allows high conversions in short contact times.

Moreover, asymmetric catalysis in continuous flow encompasses the important principles of green chemistry, green engineering, and emerging technology in chemistry.

In this chapter, the applications of useful enantioselective catalytic transformations in continuous flow as key step for the synthesis of chiral APIs and their advanced intermediates are reviewed. The most recent examples shown have been classified between organo-, organometallic (including homogeneous and heterogeneous division), and bio-enantioselective catalytic processes.

8.2 Homogeneous Enantioselective Catalysis in Continuous Flow

Enantioselective catalysis is frequently involved in the synthesis of bioactive compounds including APIs, agrochemicals, and many others. The synthesis of the desired stereoisomer requires the use of specifically designed catalyst that is often expensive and sensitive to some reaction parameters. In many cases the synthesis of the catalyst can be costly and time consuming. Therefore, although enantioselective batch reactions have been successfully applied in many industrial processes, the development of continuous-flow enantioselective catalytic reaction is still challenging, even when these processes include higher standards of sustainability. The continuous-flow technology offers a unique control and efficiency of the process as well as safety and environmental sustainability. Other benefits include improved atom economy, the possibility of quick modification of reaction conditions, and rapid reaction optimization. Many new methods and techniques in continuous asymmetric synthesis have been developed over the years.

https://www.twirpx.org & http://chemistry-chemists.com

8.2.1 Homogeneous Enantioselective Organocatalysis

By definition, *organocatalysis* is the acceleration of chemical reactions with a substoichiometric amount of an organic compound in the absence of a metal element [3].

Usually, organocatalysts are more robust, and not prone to decomposition during reaction, in contrast with traditional metal catalysts. Moreover, many organocatalysts have been modified to allow their immobilization onto different supports (from polymeric resins to nanoparticles or ionic liquids [ILs]), for their use as heterogeneous catalysis in flow synthesis. The immobilization of organocatalysts is long established as an approach that allows the recovery and reuse of these usually expensive molecules. The heterogeneous organocatalyst is used in continuous flow usually by placing it into a packed-bed reactor as a swellable microporous resin, as a monolithic macroporous column, covalently attached to the reactor internal walls, or even directly incorporated to the reactor as a 3D printed material [4].

Organocatalysis represents an effective methodology to perform metal-free catalytic processes avoiding the contamination of final products with potentially toxic metal specie, specially appreciated for the synthesis of active compounds. The fundamental advantages of organocatalysis are mainly related with easier experimental procedures applying mild reaction conditions. That involves low levels of chemical waste resulting in savings in time and energy and also in the overall cost of the process because usually organocatalysts are less expensive compared with organometallic species. And in the case of stereoselective reactions, the use of organocatalysts allows the achievement of high levels of enantioselectivity *in continuo* [5]. However, one of the main limitations of these processes is the tendency to deactivation of organocatalysts, a fact that reduces their efficiency for some transformations and hampers their large-scale application [6]. The identification of the mechanisms that cause deactivation is an important challenge to address in order to implement corrective measures, allowing thus a wider use of organocatalysis in pharmaceutical and fine chemicals industries.

Many research groups have focused their research in the asymmetric organocatalysis field, and all these efforts have demonstrated that organocatalytic flow processes are of practical application in the manufacturing of APIs. In this section, we have selected the most recent examples of continuous-flow enantioselective organocatalytic processes for the synthesis of molecules with pharmaceutical interest.

8.2.1.1 Enantioselective Michael Addition

The use of (*R,R*)-*trans*-1-[3,5-bis(trifluoromethyl)phenyl]-3-[2-(*N,N*-dimethylamino) cyclohexyl]thiourea as a bifunctional catalyst (**1**) for the asymmetric Michael addition of acetylacetone to β-nitrostyrene was reported by the Maggini research group in 2015 [7]. The continuous-flow system used was the Labtrix® Start standard system equipped with a 10 μl glass microreactor (Scheme 8.1). The reactants were supplied separately: one feed containing β-nitrostyrene reagent in toluene and the second one containing acetylacetone derivative and the enantioselective thiourea catalyst.

The continuous-flow process significantly accelerated the reaction providing the Michael adduct in high yield and enantioselectivity, up to 85% ee, in only

https://www.twirpx.org & http://chemistry-chemists.com

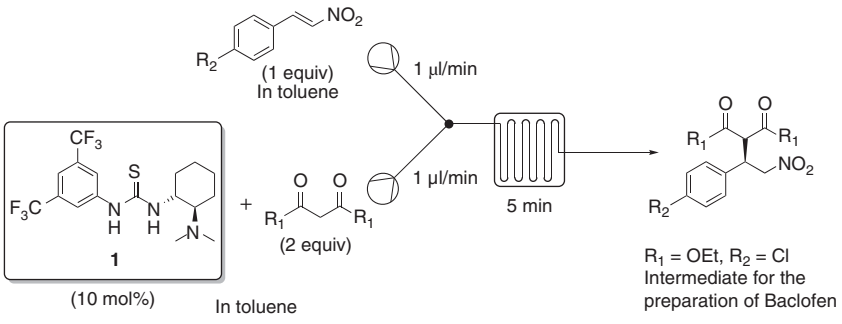

Scheme 8.1 Metal-free Michael addition of acetylacetone to β-nitrostyrene.

five minutes of residence time. The authors also reported the successful synthesis of an advanced intermediate for the preparation of the *gamma*-aminobutyric acid, or γ-aminobutyric acid ($GABA_B$) receptor agonist Baclofen applying the same methodology.

8.2.1.2 Enantioselective Aldol Reaction

The synthesis of enantiomerically pure alcohols is of great interest for pharmaceutical companies and for the synthesis of fine products, since they are key intermediates and building blocks. One powerful synthetic alternative to the traditional methodologies using organometallics is the enantioselective aldol addition. In 2019, the asymmetric organocatalytic aldol reaction in water with hydrophobic substrates was reported in continuous-flow conditions by Gröger and coworkers [8]. The continuous-flow system used was a capillary type tube reactor with two feed streams (Scheme 8.2). The optimized reaction conditions were using 3.6 mol% Singh's catalyst loading, in 2-propanol/phosphate buffer (pH 7), with a residence time of 60 minutes and room temperature. A mixture of 3-chlorobenzaldehyde, 2-propanol, and phosphate buffer was pumped at 0.1 ml/min. A second mixture solution consisting of Singh's catalyst (**2**), 2-propanol, acetone, and phosphate buffer was also pumped at the same flow rate. The outlet stream was quenched using a mixture of dichloromethane and 2.0 M aqueous hydrochloric acid solution (1 : 1 ratio) at 0 °C. The desired product, (*R*)-4-(3-chlorophenyl)-4-hydroxybutan-2-one, was obtained with 74% conversion and 89% ee.

8.2.1.3 Enantioselective Photooxygenation

Photochemistry, which uses light to promote reactions, is nonhazardous, environmentally friendly, and very efficient synthetic methodology, and its application is increasing rapidly, with broad and easy access.

The combination of photochemical reactivity with asymmetric organocatalysis resulted in a very useful tool to access to new reaction pathways and, thus, to enable the synthesis of novel compounds [9]. Furthermore, this synergistic combination has gained attention in the pharmaceutical industry for drug discovery and development [10]. Despite the great potential, there are still only few publications

https://www.twirpx.org & http://chemistry-chemists.com

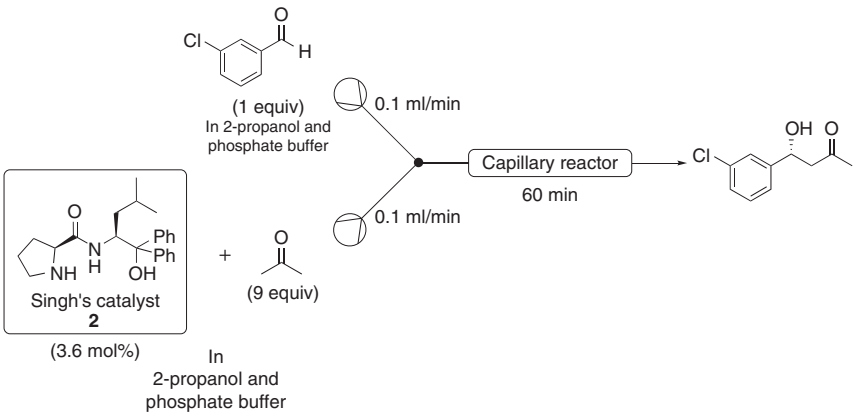

Scheme 8.2 Asymmetric organocatalytic aldol reaction promoted by Singh's catalyst (**2**).

on asymmetric photocatalysis in continuous flow using organocatalysis to control the absolute configuration of the reaction products [11].

Recently, the enantioselective photooxygenation of β-dicarbonyl compounds in continuous flow has been reported by Meng and coworkers [12]. The use of a C-2′ modified cinchonine-derived phase transfer organocatalysts reporting excellent yields (up to 97%) and high enantioselectivities (up to 90% ee). The resulting products have an α-hydroxy-β-dicarbonyl moiety, which is an important structural functionality present in a variety of natural products and pharmaceuticals. α-Hydroxy-β-dicarbonyl compounds in fact are useful synthetic building blocks for the preparation of a variety of biologically active substances, including naturally occurring heterocycles and carbocycles [13]. The authors developed a visible light-driven heterogeneous gas–liquid–liquid asymmetric aerobic oxidation reaction in continuous using a CORNING Advanced Flow Reactor flow photoreactor (Scheme 8.3). They found that the best phase transfer organocatalyst **3** could be used at 10 mol% loading adding also a 1% of phthalocyanine (Pc) as photosensitizer.

The reaction conditions used in batch were not applied since in batch low temperature is needed (−15 °C) and causes precipitation, and the strongly basic media generated upon oxidation damaged the surface of the glass reactor. For that reason, the conditions in flow were optimal. The organic phase was prepared by solubilizing the corresponding substrates, PTC **3** (10 mol%) and Pc (1 mol%) in toluene. The aqueous phase was a K_2HPO_4 solution (10%) acting as a buffer. Both solutions were pumped separately at 1.5 ml/min. Oxygen was introduced through a mass flow controller at a flow rate of 10 ml/min, with a reaction pressure of 3 atm and reaction temperature of 20 °C.

The reaction time was shortened from eight hours needed in batch to 10.92 minutes of residence time in continuous flow, with high yields and enantioselectivities being preserved. Moreover, when tetraphenylporphyrin (TPP) was used as the photosensitizer, the residence time was drastically shortened to 0.86 minutes in flow without major variations in yield or enantiomerical excess.

https://www.twirpx.org & http://chemistry-chemists.com

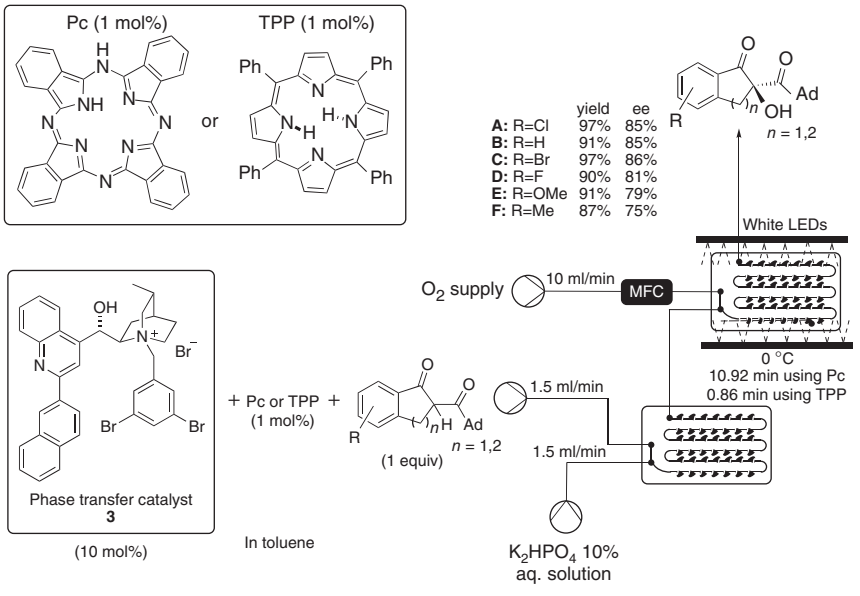

Scheme 8.3 Asymmetric photocatalytic oxidation of β-dicarbonyl substrates in continuous flow.

It could be also demonstrated that stereoselectivity was greatly decreased if the catalyst loading was reduced. However, reducing the TPP loading from 1 to 0.1 mol% was not affecting the performance of the reaction. With these results, they were able to perform a gram-scale reaction in flow to obtain 3 mmol (1.03 g) of product A, without any decrease in yield or enantioselectivity.

8.2.1.4 Enantioselective Imine Reduction

A new class of picolinamides based on chiral imidazolidinones (chiral Lewis bases, as the catalyst **4**, Scheme 8.4) for the enantioselective metal-free imine reduction, mediated by $HSiCl_3$, was reported by the group of Benaglia [14]. The high chemoselectivity to reduce C=N bonds in combination of being an extremely cheap product available in large quantities makes $HSiCl_3$ a very convenient reagent to use.

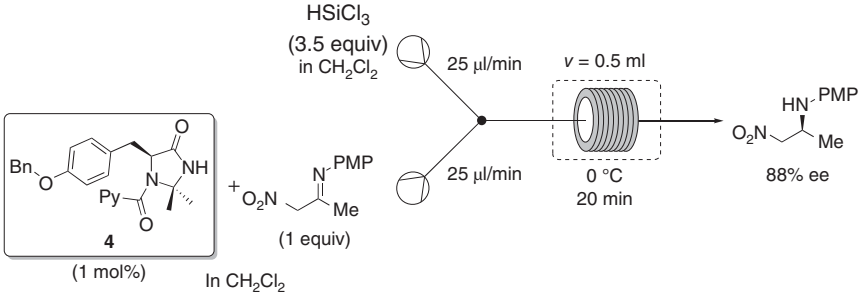

Scheme 8.4 Organocatalytic enantioselective reduction of imines in flow.

https://www.twirpx.org & http://chemistry-chemists.com

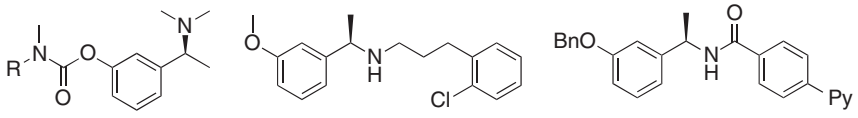

Figure 8.2 Chiral amines as valuable APIs.

After reaction optimization in batch, Benaglia and coworkers identified the active organocatalyst **4**, able to promote the reduction of a large variety of functionalized substrates with high yields and enantioselectivities (>90%) using only 0.1–1 mol% of catalyst loading. They demonstrated the synthetic potential of that approach by the preparation of advanced intermediates of important APIs. One example is the reduction of 3-alkoxy-substituted acetophenone imines, either *N*-benzyl protected or *N*-(3-phenylpropyl) substituted. This is an efficient step for the synthesis of enantiomerically pure compounds, used in the treatment of Alzheimer and Parkinson diseases, hyperparathyroidism, neuropathic pain, and neurological disorders (Figure 8.2).

The authors applied the optimized catalytic methodology in continuous flow for the synthesis of chiral α-nitroamines. These products can be easily reduced with Ni-Raney to achieve chiral 1,2-diamines in only two steps (Scheme 8.4). Chiral 1,2-diamine is a functionality displaying a broad spectrum of biological activity. This methodology is very attractive for large-scale synthesis due to the simple experimental procedure, the use of mild reaction conditions with low cost of reagents and the straightforward isolation of the products.

8.2.2 Organometallic Enantioselective Catalysis

8.2.2.1 Enantioselective Sulfoxidation

Chiral sulfoxides have increased attention as precursors and building blocks for API synthesis (e.g. esomeprazole) as well as for fragrances or as chiral auxiliaries. In 2016, the asymmetric sulfoxidation catalyzed by a biomimetic manganese complex under continuous-flow conditions was reported by Gao and coworkers (Scheme 8.5) [15]. The reaction was carried out in a coil reactor made of polytetrafluoroethylene (PTFE). Two feed solutions were used. The first contained aryl sulfide, adamantanecarboxylic acid (aca), and the catalyst, which was generated from $Mn(OTf)_2$ and a new type of porphyrin-inspired N4 ligand **5**. The second one contained 45% hydrogen peroxide in acetonitrile and isopropyl alcohol mixture. Under continuous-flow conditions the catalyst loading was reduced to 0.35 mol% with a residence time of four minutes, compared to the batch process, which required 0.5 mol% of the catalyst and two hours reaction time. A wide variety of aryl methyl sulfides were efficiently oxidized, providing the corresponding chiral sulfoxides in high yields (up to 91%) and with excellent enantioselectivity (up to 96% ee). These good yields and enantioselectivities were preserved even when extending the alkyl chain linearly from methyl to pentyl. Encouraged by these results, the authors extended the substrate scope to

https://www.twirpx.org & http://chemistry-chemists.com

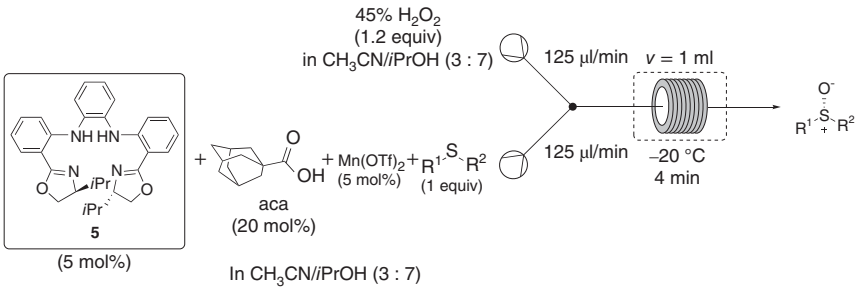

Scheme 8.5 Continuous-flow microreactor system for the asymmetric sulfoxidation. Source: Dai et al. [15]/John Wiley & Sons.

the aryl benzyl sulfides as well as a cyclic one. Also in this case high yields and excellent enantioselectivities were obtained. The screening of substrates revealed that change of substituents on the aromatic ring had no significant effect on the yield and selectivity of the reaction.

The continuous-flow system was also evaluated for the scale-up of the process. The reactor volume was increased by the reactor numbering up. The new continuous-flow system contained four reactors placed in parallel. The direct scaling of the process using aryl benzyl sulfides as substrate provided the corresponding sulfoxides in 84–86% yield and 92–98% ee in gram scale. The scope of the scale-up reaction was also extended to aryl methyl sulfides. Good yield and excellent enantioselectivity were also achieved. The process was able to be scaled up to obtain 5 g of oxidation products with 80–86% yields and 92–99% ee after 20 minutes of continuous run.

8.2.2.2 Enantioselective Epoxidation

Other important synthons widely used as precursor of APIs and pharmaceuticals are the optically active epoxides. One of the most efficient and straightforward syntheses of chiral epoxides is the catalytic asymmetric epoxidation. However, some problems observed in batch such as long reaction times, difficulties in controlling the reaction conditions, and unsafe processes dismiss the wide application of such methodologies.

The asymmetric epoxidation of electron-deficient olefins catalyzed by an iron complex under continuous-flow conditions was also reported by the Gao group (Scheme 8.6) [16]. They employed a polyether ether ketone (PEEK) coiled microreactor with a total volume of 1 ml to show the application of this organocatalytic methodology in continuous flow. A syringe pump was used to feed the microreactor with the reagents through a T-junction. The T-mixer and microreactor were cooled to −20 °C. The reaction mixture was quenched in the outstream with 10% aqueous sodium thiosulfate. The optimized reaction conditions were applied to a variety of trisubstituted cyclic enones that were successfully converted into the corresponding chiral epoxides within a short residence times ranging from two to four minutes. As a result of electronic effects, electron-withdrawing substituents at the *ortho* or *para* positions of the substrates had a negative effect on the yields, going from 42% to 70%.

https://www.twirpx.org & http://chemistry-chemists.com

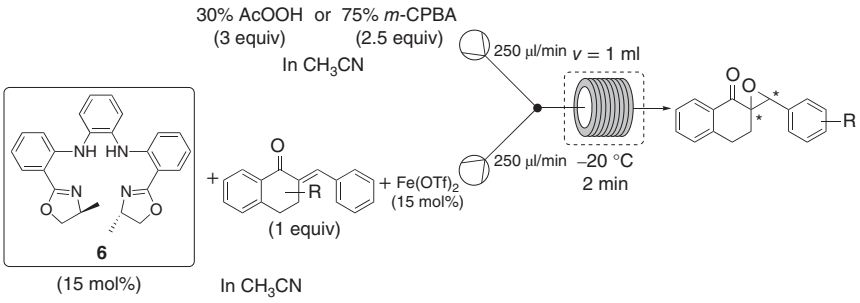

Scheme 8.6 Continuous-flow microreactor system for the enantioselective epoxidation. Source: Dai et al. [16]/Georg Thieme Verlag KG.

In these cases, the longer residence time of four minutes was needed. In general, the epoxidation of trisubstituted enones under continuous-flow conditions afforded rapidly (<4 minutes) the desired products in an average yield of 90% with an average 92% ee, providing a good alternative to batch synthesis of enantiopure epoxides.

8.2.2.3 Enantioselective Hydrogenation

As has been mentioned before, chiral alcohols are important chemical building blocks for the synthesis of new API and drugs. One of the most applied methodology for the synthesis of optically active alcohols is the asymmetric catalytic hydrogenation of carbonyl compounds.

Asymmetric transfer hydrogenation reactions are increasing their application in industry due to the avoidance of the use of hydrogen gas (H_2) and the expenses and risks associated, which can be reduced to the minimum in combination with continuous flow [17]. As example, the asymmetric transfer hydrogenation using a bifunctional oxo-tethered ruthenium catalyst (**7**) for the synthesis of ceramides (Scheme 8.7) was reported by Saito and coworkers in 2019 [18]. They developed the first example of asymmetric transfer hydrogenation using a pipes-in-series flow reactor with oxo-tethered ruthenium complex-catalyzed dynamic kinetic resolution on a production scale. In comparison with a traditional high-pressure autoclave system, the use of continuous-flow reactor was cheaper and safer. Under optimal conditions the loading of the catalyst was only 0.2% at 85 °C and six hours of residence time. The *erythro*-alcohol was obtained in 97% conversion with excellent diastereoselectivity and enantioselectivity. This asymmetric transfer hydrogenation reaction was also performed on a large scale using 100 l vertical pipes-in-series continuous-flow reactor. This process was performed without any expensive reagents and has been successfully run at 80 kg scale, affording the target product in 96% yield.

The separation and eventually reuse of homogeneous (expensive) chiral catalysts using microfluidic systems is also important in these processes. Many research efforts for the development of continuous-flow processes with online recovery of the chiral metal and metal-free catalysts are conducted, being particularly valuable for pharma and fine chemicals industries [19].

In 2015, Jensen and coworkers reported the continuous nanofiltration and recycling of the enantioselective ruthenium hydrogenation catalyst **8** (Scheme 8.8) [20].

https://www.twirpx.org & http://chemistry-chemists.com

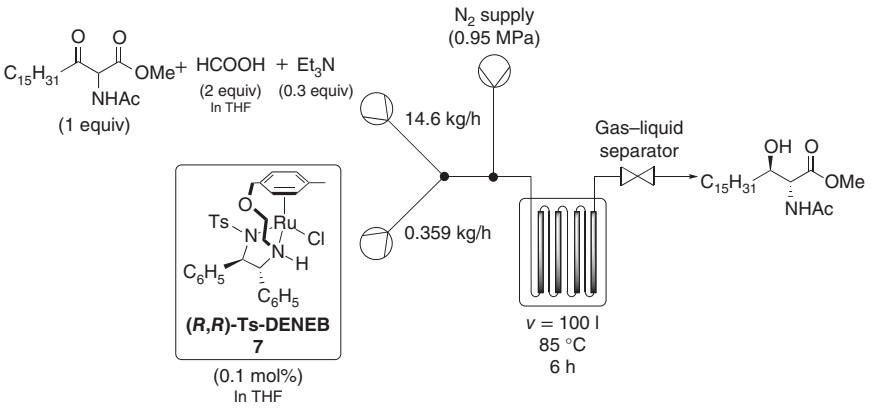

Scheme 8.7 Asymmetric transfer hydrogenation in vertical pipes-in-series reactor.

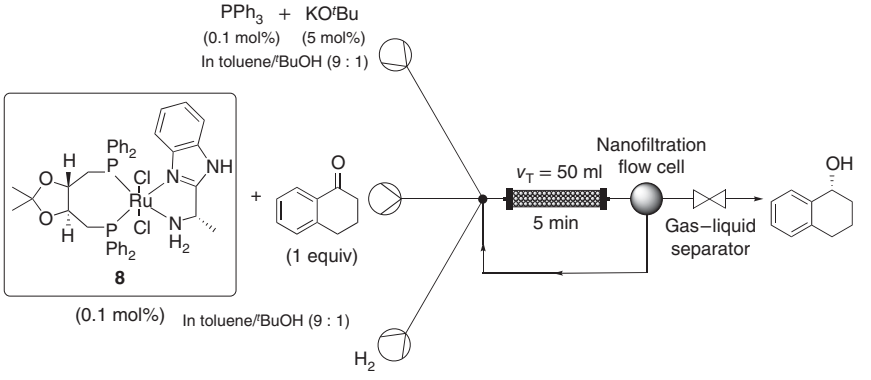

Scheme 8.8 Asymmetric hydrogenation with nanofiltration module for catalyst recycling. Source: ONeal et al. [20]/American Chemical Society.

The asymmetric hydrogenation of α-tetralone by chiral Ru diphosphine/diamine homogeneous catalyst under continuous-flow conditions with an online recovery unit, solvent-resistant nanofiltration (SRNF), of the catalyst was developed. A small-scale flow system was designed with a nanofiltration module consisting in a PEEK membrane developed by the Livingston Group at Imperial College, London. These membranes are characterized by its high compatibility with a wide range of organic solvents as well as high stability in strong basic media.

In general, the first feed solution containing the starting material was mixed with the second one containing potassium *tert*-butoxide and triphenylphosphine and the recycled stream from the SRN module, retained stream. This retained stream was prior mixed with a hydrogen gas supplied at the desired flow rate using a mass flow controller. Next, the two inlet streams and the retained stream were premixed in a four-way cross unit before entering the packed-bed reactor filled with glass beads to improve mixing. The outlet stream was directed to the SRN module where the phase separation occurred. The product stream permeated through the PEEK membrane,

https://www.twirpx.org & http://chemistry-chemists.com

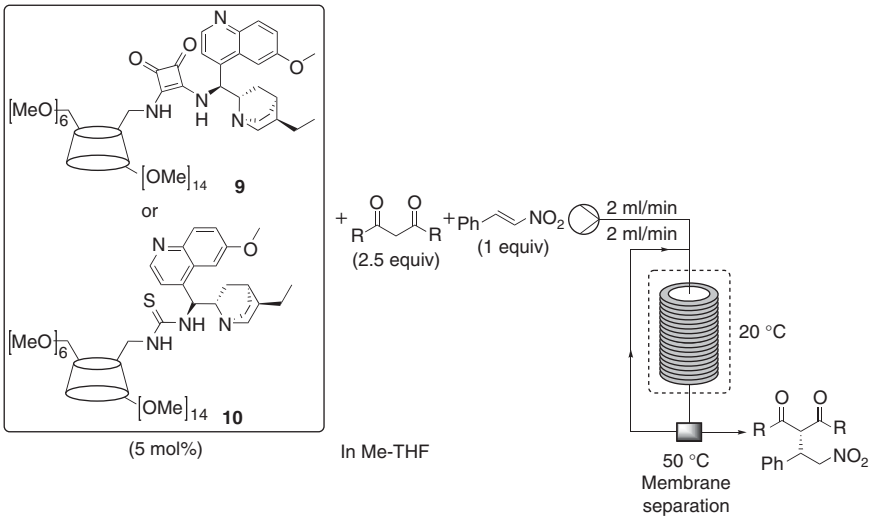

Scheme 8.9 Schematic process scheme for the continuous synthesis–separation platform.

while the catalyst was remaining in the retained stream. The concentrated catalyst solution was supplied back to the system via recirculation high-performance liquid chromatography (HPLC) pump used for the nanofiltration cell. In this way, the catalyst was continuously separated and recycled back to be used in the reactor.

The authors performed a 24-hour long experiment during which they were able to maintain high yield with a TON near 5000. During this test, the catalyst was recycled c. 60 times. The SRN membrane made of PEEK proved to be very efficient and resistant to the strong base used. The catalyst was remaining in the retained stream in c. 99.6% throughout the run. Some ruthenium was detected in the permeate stream, however, in a level lower than 200 ppb. Moreover, the enantioselectivity of the transformation suffered a minimal reduction, only from 97% to 93% ee during the long run.

8.2.2.4 Enantioselective Michael Addition

In order to facilitate the recovery and reuse of the catalysts without losing the homogeneous character of the reaction, some strategies have been developed. One recent example is the anchoring of organocatalytic species onto cyclodextrin (CD) as a methodology to facilitate the recovery of covalently bonded organocatalysts [21]. Kupai and coworkers reported the cinchona-squaramide **9** and the cinchona-thiourea **10** catalysts for the asymmetric Michael reaction of 1,3-diketones and *trans*-β-nitrostyrene in continuous flow (Scheme 8.9).

The CD moiety was found to have two key roles. First, it allows the complete recovery of the catalyst due to its size. Second, it improves the catalytic performance of the anchored cinchona-squaramide catalyst **9** due to a favorable conformation.

The continuous-flow process was performed in a coiled tube flow reactor integrated with a DM900 membrane separation unit for the catalyst separation and reuse. Under the optimal operation conditions, the resulting Michael adducts were

https://www.twirpx.org & http://chemistry-chemists.com

obtained with an 80 g/l h productivity, 98% final product purity, and up to 99% ee and 100% catalyst recovery. In addition, the separation unit was also able to recycle up to 50% of the reaction solvent.

As mentioned previously, most chiral catalysts are a valuable and often expensive class of compounds. Moreover, heavy metal residues are strictly restricted in the fine chemicals and pharmaceutical industry. The development of continuous-flow catalysis is appealing methodology because it combines the advantages of a catalytic reaction with the benefits of flow microreactors. The development of continuous-flow processes with online recovery of the chiral catalyst is improving the performance, and it would be a very powerful tool for the chemical and pharmaceutical industry. However, the use of recyclable catalysts under continuous-flow conditions represents an innovative strategy for the development of more environmentally friendly and effective synthesis. For that reason, in recent years, the number of reports paying attention to the asymmetric heterogeneous catalysis in flow has increased. The combination of chiral supported catalysts and flow chemistry promotes very sustainable way toward the synthesis of enantioenriched compounds, and it will be discussed in Section 8.3 [22].

8.3 Heterogeneous Enantioselective Catalysis in Flow

Recently, an important effort for recycling and recovering enantiomerically pure catalysts has been devoted. These are valuable and often expensive compounds that usually present challenging recovery from the crude mixture reaction due to separation issues. For instance, in some drug synthesis, metal traces are strictly forbidden, and usually additional posttreatment processes are required, increasing costs and waste. The use of heterogeneous catalyst in continuous flow allows the possibility to simplify the process, moreover in combination with continuous flow [18, 23].

There are different immobilization strategies in heterogeneous catalysis, based on the interaction between the catalyst and the solid support [24]. Covalent polymeric support is the most frequently used strategy where the immobilized catalyst is synthesized by grafting it onto a preformed support (for example, polystyrene [PS] or inorganic nanoparticle supports) or by forming an organic polymer by copolymerization of suitable monomers. Another strategy is the self-supported method. It consists in the use of self-assembled metal–organic frameworks (MOFs) using the combination of linked ligands and reactive metal centers. Adsorption method represents another easy immobilization method. In this case the heterogeneous catalyst can be obtained by simple impregnation procedure. However, due to the weak interaction between the support and the catalyst, they tend to be nonstable, and often the catalytic activity can be affected by catalyst leaching. Finally, electrostatic/ionic interaction immobilization consists on an anchoring method by catalyst adhesion, which is used to heterogenize ionic catalytic species.

In the following sections, examples of supported catalysts applied in continuous-flow chemistry to develop novel enantioselective synthetic strategies are divided in supported enantioselective catalysis and asymmetric heterogeneous organometallic catalysts.

https://www.twirpx.org & http://chemistry-chemists.com

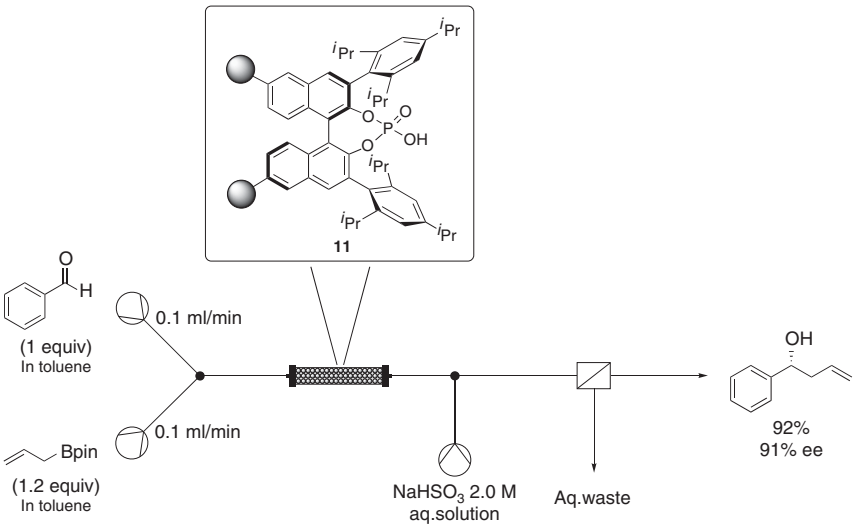

Scheme 8.10 TRIP-catalyzed enantioselective allylation of aldehydes.

8.3.1 Supported Organocatalysts

8.3.1.1 Enantioselective Allylation of Aldehydes

In 2016, the asymmetric allylboration of aldehydes was reported by Pericàs and coworkers using a new catalytic resin based on PS-supported (*R*)-3,3′-bis(2,4,6-triisopropylphenyl)-1,1′-binaphthyl-2,2′-diyl hydrogenphosphate ((*R*)-TRIP) phosphoric acid (**11**) extending the method to the enantioselective synthesis of homoallylic alcohols under continuous-flow process [25]. The immobilization on the catalyst was carried out through a copolymerization strategy.

The system consists of a packed-bed reactor containing the functional resin **11** (Scheme 8.10) and two separate solutions containing the corresponding aldehyde and the allylboronic ester, mixed just before entering into the reactor. A background reaction was observed in the collecting flask between the excess of allylboronic ester and small amounts of remaining aldehyde, which was detrimental to the enantiomeric purity of the final product. To avoid that, a downstream process was required at the end of the column, consisting in the addition of an aqueous solution of $NaHSO_3$ to scavenge any unreacted aldehyde that could be extracted in-line using a liquid–liquid separator.

(*R*)-1-phenylbut-3-en-1-ol product (Scheme 8.10) was obtained in 92% yield and 91% ee, with a TON of 282 and a productivity of 2.22 mmol/h g_{resin}, after 28 hours continuous running process. Noteworthy, no detectable decrease in the catalytic activity of the resin was observed. This flow methodology allowed the production of enantiopure homoallylic alcohol in short periods of time with highly reduced energy and material costs, under safety conditions. Remarkably, this PS-TRIP catalysts could be reactivated by acidic washings in case of deactivation.

https://www.twirpx.org & http://chemistry-chemists.com

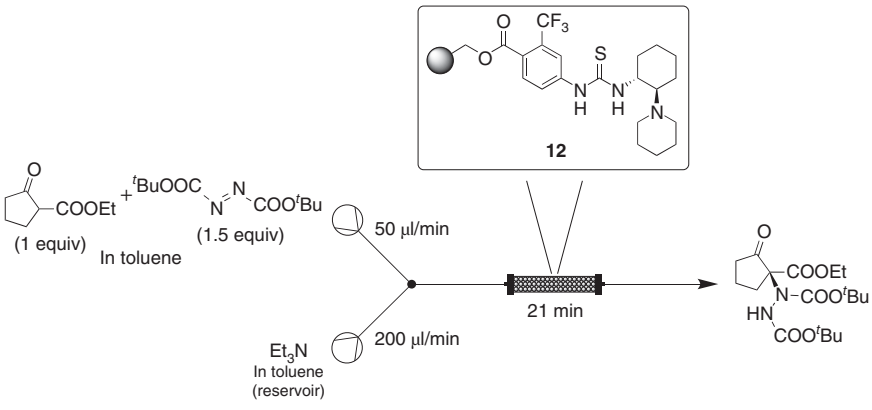

Scheme 8.11 Enantioselective α-amination of 1,3-dicarbonyl compounds. Source: Kasaplar et al. [26]/Royal Society of Chemistry.

8.3.1.2 Enantioselective α-Amination

Chiral amines are present in many bioactive molecules, and their synthesis is of great interest in pharma, agrochemicals, or fragrance industries, particularly α-amino-acids.

The Pericàs group reported in 2015 the enantioselective α-amination of 1,3-dicarbonyl compounds with azodicarboxylates catalyzed by the immobilized thiourea organocatalyst **12** (Scheme 8.11) [26]. The recyclability of the catalyst was proved in batch, and the process in continuous flow was also using a packed-bed reactor with **12**. A part from the reagents feeds, it was necessary to circulate a solution of Et_3N to wash the column periodically to preserve the catalytic activity of the resin.

The desired product containing a quaternary center was achieved in gram scale after 21 minutes at room temperature in 71% isolated yield and 93% ee with a productivity of 4.88 mmol/$mmol_{cat}$ h and a TON of 37.

8.3.1.3 Enantioselective Arylation of Aldehydes

The asymmetric arylation of aldehydes represents a good methodology for the synthesis of optically pure alcohols. In 2017, the group of Pastre reported the immobilization of several chiral amino acid-derived ligands for the enantioselective arylation of aldehydes with organozinc reagents in flow [27]. These ligands were derived from (*S*)-proline, (2*S*,4*R*)-4-hydroxyproline, (*S*)-tyrosine, and (*S*)-phenylalanine and were supported onto Merrifield resin. The best results were obtained with catalysts **13** and **14** (Scheme 8.12). The designed flow setup consisted of a glass Omnifit® column packed with the catalytic resin and fed with the stock solutions of aldehyde and the arylzinc reagent. With only 1.5 minutes of residence time, the desired products were afforded with full conversion and higher enantiomeric excess than obtained in batch (e.g. 88% ee in flow versus 76% ee in batch. Residence times depending on the substrate from 1.5 to 12 min). Moreover, the stability of the ligands was evaluated, and it was found out that **14** could be used for a longer period of time than **13**. In fact, no significant change in reaction

https://www.twirpx.org & http://chemistry-chemists.com

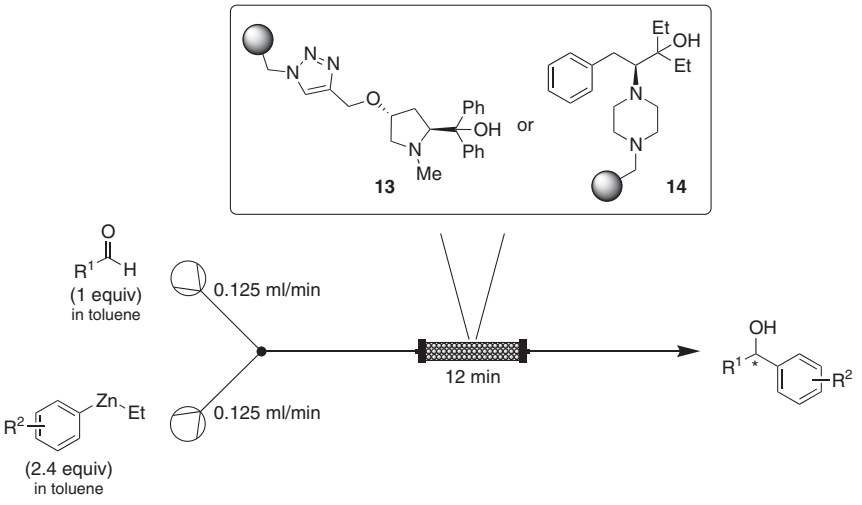

Scheme 8.12 Enantioselective organocatalyzed arylation reaction in continuous flow.

yield was observed, but the enantioselectivity slightly decreased, after a three days experiment.

8.3.1.4 Enantioselective Cyclopropanation

One of the more versatile supported organocatalysts applied for many different transformations are the diarylprolinols. Their application in the enantioselective cyclopropanation of α,β-unsaturated aldehydes in continuous flow was reported in 2016 by the Pericàs' group for the straightforward obtention of chiral cyclopropanes (Scheme 8.13) [28]. Chiral cyclopropanes are very valuable building blocks since they are key pharmacophores in bioactive compounds.

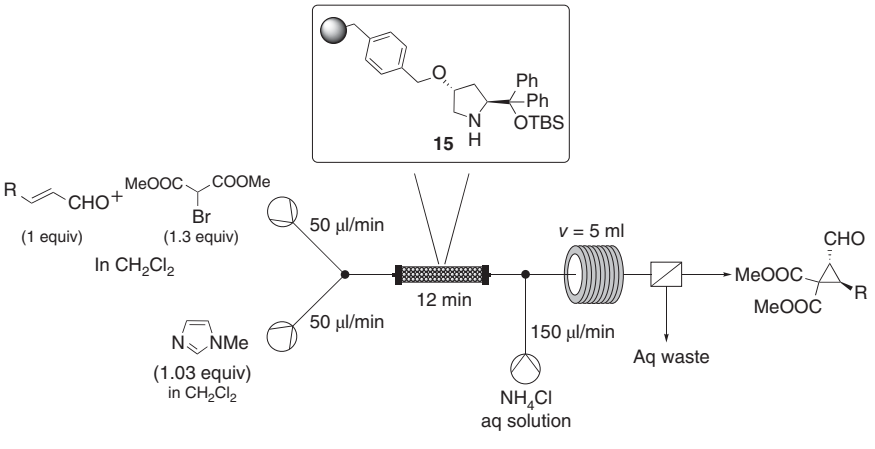

Scheme 8.13 Enantioselective cyclopropanation reaction catalyzed by supported OTBS protected diphenyl prolinol in continuous flow. Source: Lianes et al. [28]/American Chemical Society.

https://www.twirpx.org & http://chemistry-chemists.com

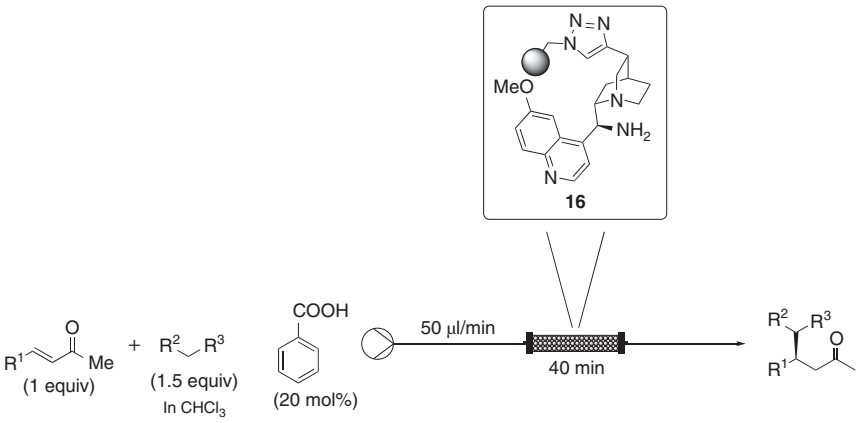

Scheme 8.14 Enantioselective Michael addition of different nucleophiles to enones. Source: Izquierdo et al. [29]/Royal Society of Chemistry.

The authors include in this work the evaluation of different solid phase (microporous versus macroporous PS) and the anchoring strategy of the catalytic resin **15** for its performance in the flow asymmetric cyclopropanation of enals with bromomalonates.

The combined flow setup includes also a glass Omnifit column packed with the catalytic resin **15**. The two reagents were mixed with the base *N*-methylimidazole, before entering the reactor. In order to prevent a secondary reaction involving ring opening of the cyclopropane, a downstream process was required. At the outstream of the packed-bed reactor, a third inlet with ammonium chloride and a liquid–liquid separator were placed to remove the base from the reaction mixture. This in-line workup allowed the isolation of the final chiral cyclopropane product after only solvent evaporation.

The catalytic resin **15** proved to be extremely robust, achieving productivities up to 2.1 mmol/h g_{resin}, with a TON of 94.0 (up to 76 hours of continuous running). Both electron-poor, electron-rich cinnamaldehydes, and heteroaromatic enals were well tolerated in this process, producing the desired cyclopropanes with high enantiomeric purity (from 89% to 96% in 12 examples).

8.3.1.5 Enantioselective Michael Reaction

Asymmetric Michael reaction is a very versatile and widely used transformation for C—C bond formation for the stereocontrolled synthesis of important building blocks. Several organocatalysts immobilized onto PS resins were proved to be highly efficient, promoting asymmetric Michael additions under batch and flow conditions. The Pericàs group has described the used of several immobilized organocatalysts for this transformation.

9-Amino(9-deoxy)epi cinchona alkaloids anchored to a PS resin was developed for the activation of enones for the addition of C-nucleophiles (Scheme 8.14) [29].

The flow process involved resin **16** packed into a simple Teflon® tube. This packed-bed reactor was heated to 30 °C to afford the desired product (3.6 g were

https://www.twirpx.org & http://chemistry-chemists.com

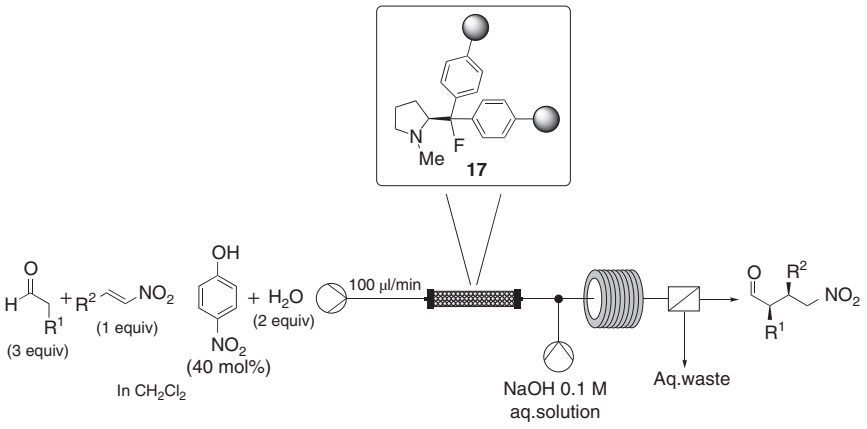

Scheme 8.15 Enantioselective Michael addition of aldehydes to nitroalkenes. Source: Sagamanova et al. [30]/American Chemical Society.

collected in 21 hours of operation, corresponding to a TON of 32, using only 0.40 mmol (450 mg) of catalytic resin **16**). Furthermore, the sequential preparation of a small library of enantiopure products in continuous was possible combining different enones with different nucleophiles using this PS-supported cinchona aminocatalyst **16** with remarkable productivity (TOF = 1.4–3.2 $mmol_{product}/mmol_{resin}$·h) and high enantioselectivities (33 examples with ee up to >99%).

In the same way, a novel polymer-supported fluorinated organocatalytic resin **17** has been developed and demonstrated great potential for the Michael addition of aldehydes to nitroalkenes (Scheme 8.15) [30]. The configuration of the flow system was also carried out by applying a packed bed reactor. In this case an additional in-line liquid–liquid workup was added to simplify the isolation of the products. In fact, the pure products were obtained only by evaporating the organic outstream with high enantioselectivity. Catalyst **17** was proven to be extremely active, being the key polymer design that did not affect the active site. The work constituted the first report of the application of this catalyst with enamine activation mode. The highly efficient continuous-flow processes designed allowed the multigram synthesis of a desired Michael adduct or the sequential generation of a library of enantiopure Michael products from different combinations of substrates (13 combinations, 94–97% ee).

The new resin **18** based on a chiral squaramide was applied in the asymmetric oxa-Miquel addition of hydroxynaphthoquinones to 2-nitro-3-arylallyl acetates for the generation in continuous flow of enantioenriched pyranonaphthoquinones, which have high potential biological value (Scheme 8.16) [31]. This transformation comprised two sequential reactions: the organocatalyzed Michael addition and the base promoted cyclization.

The outlet of the column packed with catalyst **18** was coupled with a T-junction connecting a base solution for an in-line workup. Notably, the total residence time of the process including the two reactions and the workup was only 30 minutes. Moreover, this PS-supported resin was designed to be easily synthesized and with low

https://www.twirpx.org & http://chemistry-chemists.com

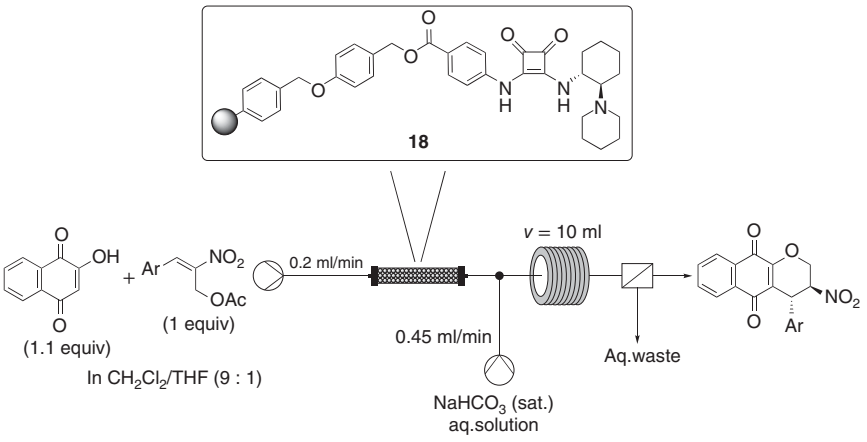

Scheme 8.16 Enantioselective oxa-Michael reaction. Source: Osorio-Planes et al. [31]/Royal Society of Chemistry.

cost and could be used for the continuous production of a library of six highly enantioenriched pyranonaphthoquinones (97–98% ee) using the same 400 mg of catalytic resin.

Finally, a new family of PS-supported *cis*-4-substituted diarylprolinols was described for the aza-Miquel reaction [32]. In particular a tandem reaction in flow consisting of an aza-Michael addition catalyzed by diarylprolinol **19** followed by hemiacetalization to afford chiral 5-hydroxyisoxazolidines (up to 83% yield, up to 99% ee) was reported (Scheme 8.17). Several α,β-unsaturated aldehydes were reacting with N-protected hydroxylamine using benzoic acid as cocatalyst. Overall, the accumulated TON in these flow processes was 134. The synthetic versatility of the enantiopure products obtained with this process was showed by a sequence consisting of their oxidation and continuous-flow hydrogenation that allowed the preparation of chiral β-amino acids, which are widely used in drug discovery and are present in a variety of natural products.

8.3.1.6 Enantioselective Tandem Michael Addition/Cyclization Reactions

The complex products obtained by the application of enantioselective tandem transformations, in particular the organocatalyzed Miquel addition followed by cyclization reactions, allow the efficient synthesis of important pharmacophores of a large number of biologically active molecules. Several examples are presented below.

The PS-supported isothiourea organocatalyst **20** based on the enantiopure benzotetramisole developed by Pericàs and co-workers showed excellent results in the domino Michael addition/cyclization reaction for the synthesis of chiral dihydropyridinones [33]. The continuous-flow process includes the sequential preactivation of the carboxylic acid (14 minutes residence time) and the organocatalytic domino transformation (7.5 minutes residence time) using a packed-bed reactor (Scheme 8.18). The integrated in-line liquid–liquid separator allowed the continuous collection of the organic phase, from which the desired chiral

https://www.twirpx.org & http://chemistry-chemists.com

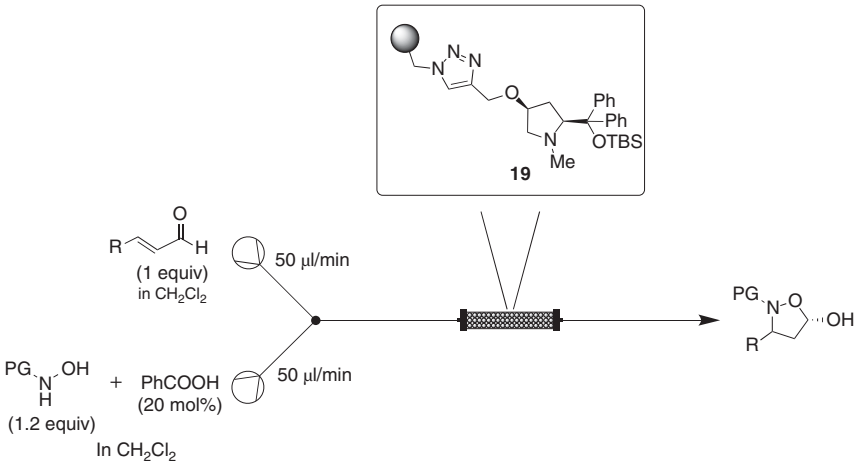

Scheme 8.17 Enantioselective aza-Michael addition reaction followed by hemiacetalization.

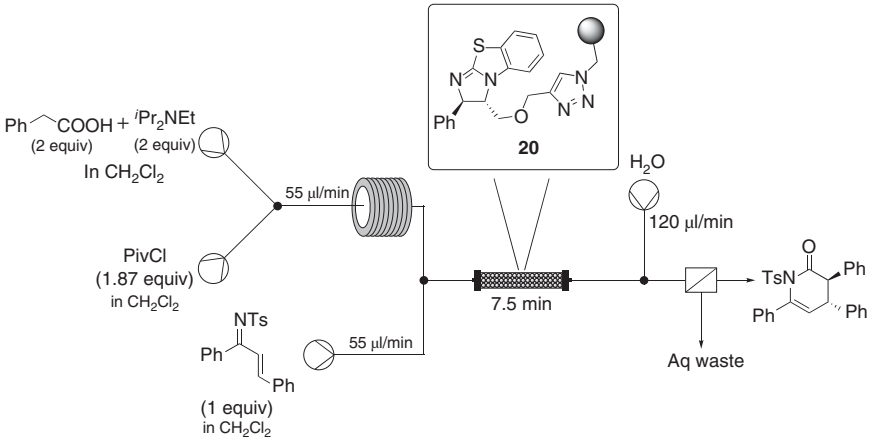

Scheme 8.18 Enantioselective domino Michael addition/cyclization.

dihydropyridinone products were obtained by simple evaporation. In particular, 4.44 g of the product (3*R*,4*R*)-3,4,6-triphenyl-1-tosyl-3,4-dihydropyridin-2(1*H*)-one (Scheme 8.18) was synthesized with >99.9% ee using a laboratory flow setup after continuous system operation during 11 hours, resulting in a TON of 22.5 (15 mol% of catalyst).

The same PS-supported isothiourea catalyst **20** mediates the enantioselective formal [4 + 2] cycloaddition reaction between unsaturated heterocycles and *in situ* activated arylacetic acids in continuous flow (Scheme 8.19) [34]. The Omnifit glass column reactor was fed with a mixture of $^{i}Pr_2NEt$ and phenylacetic acid, previously combined with pivaloyl chloride, and with a solution of alkylidene pyrazolones. 2.74 g of desired product was obtained as a single diastereoisomer (67% yield and 99% ee) during 18 hours of continuous performance and using only 600 mg of resin.

https://www.twirpx.org & http://chemistry-chemists.com

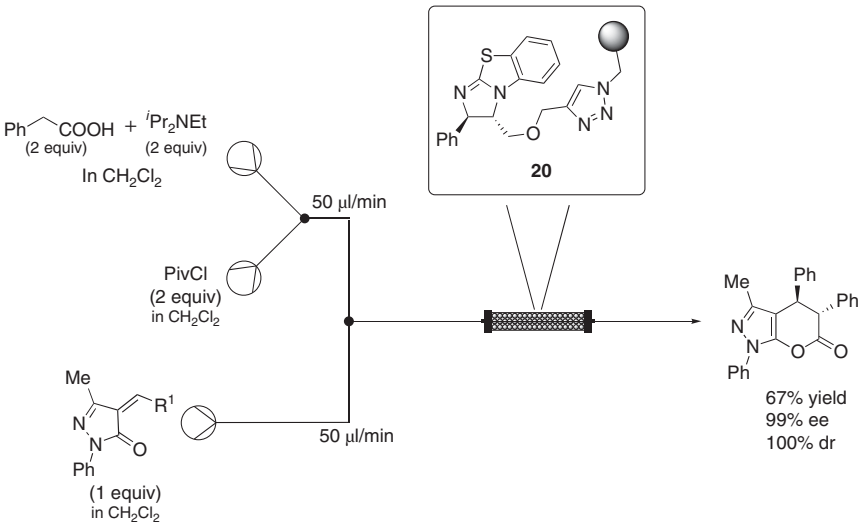

Scheme 8.19 Enantioselective [4 + 2] cycloaddition reaction. Source: Wang et al. [34]/American Chemical Society.

A particular useful enantioselective tandem reaction is the asymmetric Robinson annulation. This transformation begins with an asymmetric Michael reaction followed by an intramolecular aldol condensation to afford a six-membered ring with an α,β-unsaturated ketone. These products represent important building blocks in organic synthesis, such are the Wieland–Miescher ketone or the Hajos–Parrish ketone. The heterogenization of an organocatalyst based on Luo's diamine was developed for a fast and broad-scope enantioselective Robinson annulation process in continuous flow [35]. The PS-supported chiral vicinal diamine **21** (Scheme 8.20) was placed in a jacketed glass column (heated at 60 °C), and a preformed solution of the Michael adduct combined with *m*-nitrobenzoic acid, used as cocatalyst (5 mol%), was pumped through the column. In this way, the Wieland–Miescher ketone ($R^1 = CH_3$, $R^2 = H$) was obtained in high enantiomeric purity (91% ee) with a productivity of 0.5 g/h and TON of 117, after 24 hours operation of the flow system.

As has been showed with different examples, the catalytic asymmetric flow processes based on immobilized catalysts are very useful for preparing libraries of compounds, since different reactions can be performed in a sequential manner. Due to the versatility of the supported catalyst **21**, a diverse library of enantioenriched Robinson annulation products was sequentially prepared using the designed flow set up. The diversity-oriented continuous-flow process allowed the synthesis of a library with good enantioselectivities (89–94% ee) and very high productivities (TOF = 6.7–9.3 $mmol_{prod}/mmol_{resin}$ h).

8.3.1.7 Enantioselective Reduction of Imines

In Section 8.2.1.4 the benefit of enantioselective reduction of imines applying organocatalysis and how the group of Benaglia demonstrated the synthetic potential of that approach for the synthesis of advanced intermediates of important APIs has been shown. The same group developed a variety of immobilized chiral

https://www.twirpx.org & http://chemistry-chemists.com

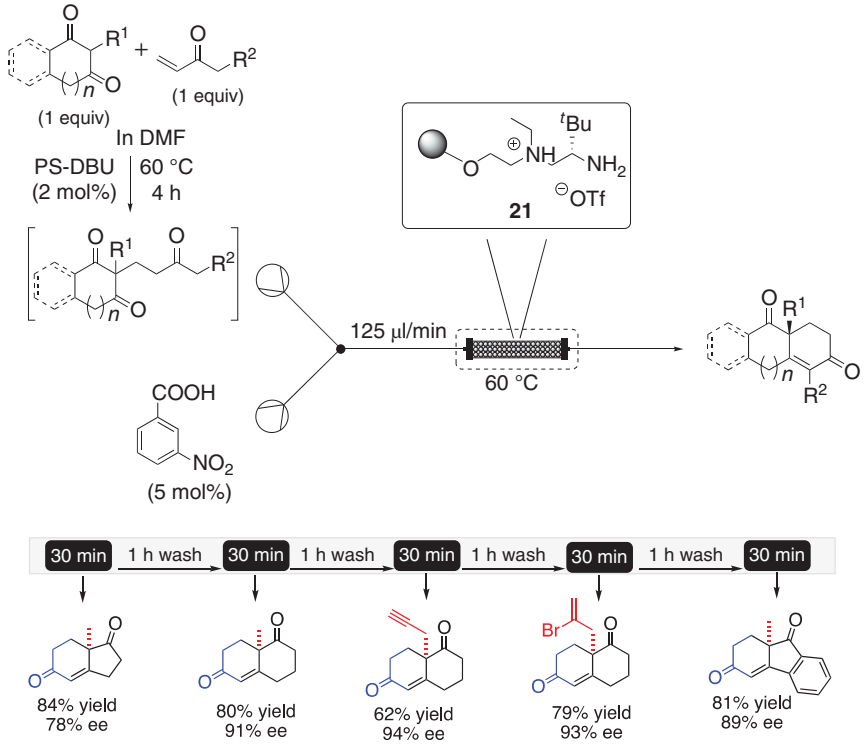

Scheme 8.20 Enantioselective Robinson annulation.

picolinamides, derived from cinchona alkaloid primary amines, supported on silica and PS [36] and solid-supported chiral imidazolidinones organocatalysts [37] for the catalytic reduction of imines with trichlorosilane. The picolinamide catalyst **22** (Scheme 8.21) and the immobilized imidazolidinone **23** (Scheme 8.22) were used in continuous flow. The process with catalyst **22** in a glass packed-bed reactor was run for three hours, and the corresponding chiral amine was continuously obtained in very high yield. However, the enantioselectivity of the process was quite low, and it dropped over time, possibly due to the presence of organic residues coming from the catalyst degradation.

The PS-supported catalyst **23** was packed into a stainless steel HPLC column and fed with a solution of the imine and the trichlorosilane. In this case the flow process was stable for seven hours, producing the corresponding chiral amine in excellent yield and good enantiomeric excess, although the stereoselectivity of the process slightly decreased over time, probably due also to the degradation of the imidazolidinone ring of the catalyst.

8.3.2 Supported Organometallic Catalysts

8.3.2.1 Enantioselective Hydrogenation

Catalytic methods are very appreciated in industry for the development of effective, good atom economy, scalable, and environmentally friendly processes, and these

https://www.twirpx.org & http://chemistry-chemists.com

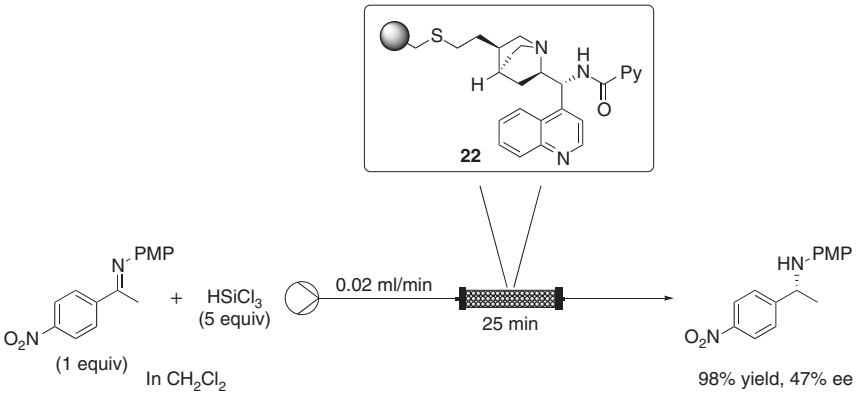

Scheme 8.21 Stereoselective reduction of imines catalyzed by supported chiral picolinamides.

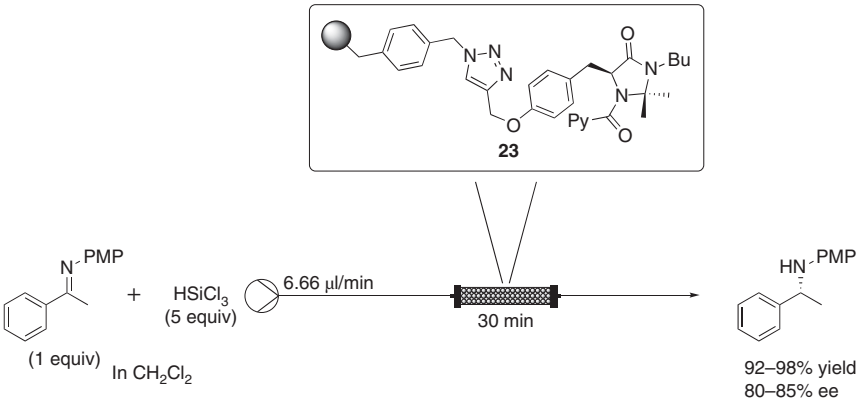

Scheme 8.22 Asymmetric reduction of imines catalyzed by supported chiral imidazolidinones.

processes are being applied for the synthesis of many API. Asymmetric hydrogenation of alkenes is probably one of the most powerful synthetic tool used in the synthesis of chiral drugs or precursors. In particular chiral rhodium catalyst complexes are the most typical species used for this process (together with ruthenium and iridium ones).

The Leitner group developed a continuous-flow process for asymmetric hydrogenation using the same commercially available catalyst (Rh/(*S,S*)-EthylDuphos) **24** used in the batch process via a straightforward and effective immobilization method [38]. They reported the use of a noncovalent immobilization strategy named Augustine approach. It consists on the use of heteropolyacids, which are dispersed on a metal oxide surface and serve as anchors for cationic organometallic complexes (Scheme 8.23). A commercially available composite of phospho tungstic acid (PTA) and aluminum oxide (Alox) was selected as the support in this case. The continuous-flow process for the synthesis

https://www.twirpx.org & http://chemistry-chemists.com

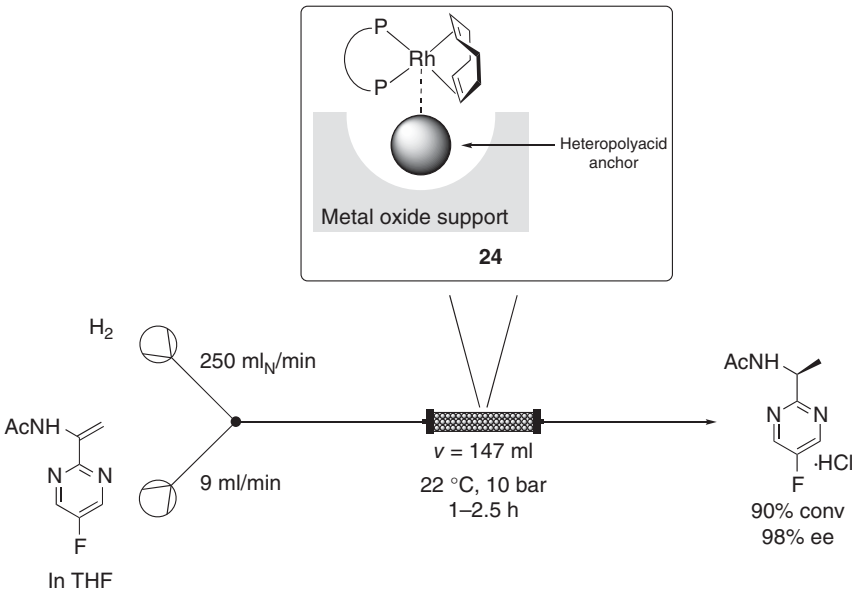

Scheme 8.23 Enantioselective rhodium-catalyzed hydrogenation in large scale.

of (*S*)-*N*-(1-(5-fluoropyrimidin-2-yl)ethyl)acetamide (key intermediate for an AstraZeneca API) was optimized, and the designed system gave an overall TON of c. 5000 within seven hours on stream with almost full conversion and high enantioselectivity. Moreover, excellent catalyst stability and retention was demonstrated at 1 kg scale, displaying results well above the predefined product specification limits (90% conversion, 98% ee, and Rh contamination <10 ppm).

The asymmetric hydrogenation of enamides in continuous flow using supported ionic liquid phase (SILP) catalyst was also described by the same group [39]. Rhodium catalyst **25** was immobilized via the SILP approach using fluorous reverse-phase silica as highly hydrophobic supporting material, in which the catalyst was dissolved. Continuous-flow systems using SILP catalysts were previously restricted to gaseous or volatile substrates, or substrates soluble in *sc*CO_2. However, using toluene as a modifier, they were able to expand the scope to highly functionalized substrates with poor solubility in *sc*CO_2. The flow system consisted of a stainless steel tube, containing the SILP catalyst **25**, used as the reactor (Scheme 8.24). Under optimal conditions, excellent stability with full conversion and high enantioselectivity was achieved (quantitative single-pass conversion, ee > 99%) over 90 hours on stream, resulting in a TON of 10 300. The metal leaching in the product solutions was below the detection limit (1 ppm), indicating effective catalyst retention and satisfying the requirements of the pharmaceutical industry for the manufacture of APIs.

8.3.2.2 Enantioselective Hydroformylation

Enantioselective hydroformylation is an important and very useful process widely applied for the synthesis of pharmaceutical and fine chemicals. The generation of

https://www.twirpx.org & http://chemistry-chemists.com

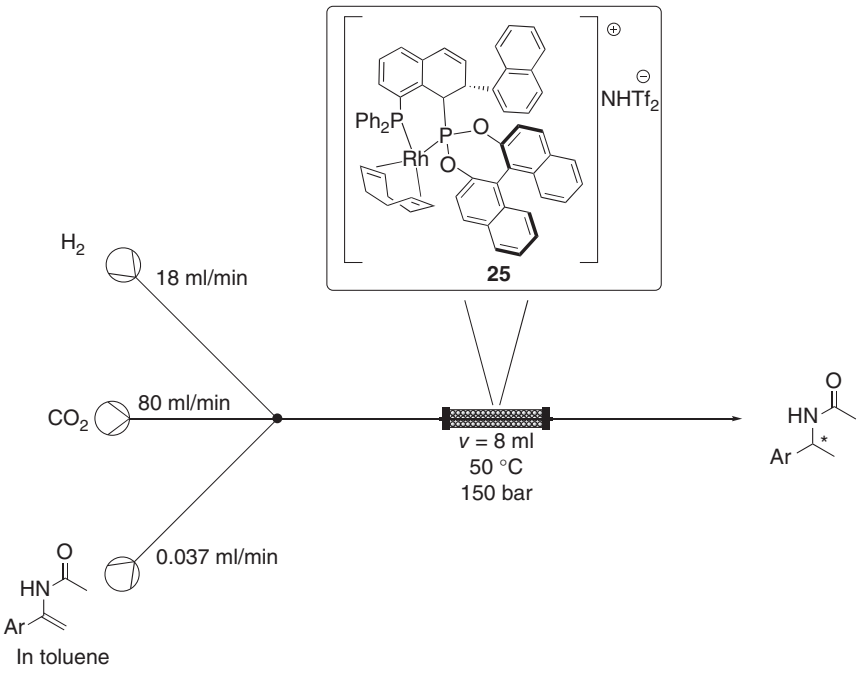

Scheme 8.24 Enantioselective rhodium-catalyzed hydrogenation of enamides.

chiral aldehydes led to key intermediates that can be then further transformed in chiral alcohols, amines, or others. Usually, the common reaction conditions involve the use of H_2 and CO with alkenes in the presence of catalytic metal complexes with chiral ligands and pressure, adding potential risk factors to the process. The advantages of continuous flow minimize those risks.

A highly enantioselective hydroformylation under continuous-flow conditions was reported by Stout and coworkers [40]. They used a vertical pipes-in-series plug flow reactor (PFR) for good gas–liquid mixing as well as scalability from small volume research to production scale. The process of interest, high pressure asymmetric hydroformylation of 2-vinyl-6-methoxynaphthalene catalyzed by Rh-BDP complex, was investigated using the research scale pipes-in-series PFR.

The use of continuous-flow techniques and vertical-bubble-flow-pipes-in-series reactor gave high vapor–liquid mass transfer rates by achieving very small liquid segments flowing through the small diameter tubing. After screening of reaction parameters such as reaction solvents, ligands, pressure, and understanding of reaction kinetics performed in a batch reactor, the process was investigated under continuous-flow conditions. The optimal reaction conditions were found to be eight hours residence time at 70 °C to provide the desired product in 98% conversion and good enantioselectivity (92% ee) while maintaining high regioselectivity (27 : 1). Moreover, oxidation of the resulting aldehyde to the carboxylic acid provides an attractive synthetic route to naproxen. The continuous-flow system was run for a total of 130 hours and continuously for 100 hours over six transitions and five

https://www.twirpx.org & http://chemistry-chemists.com

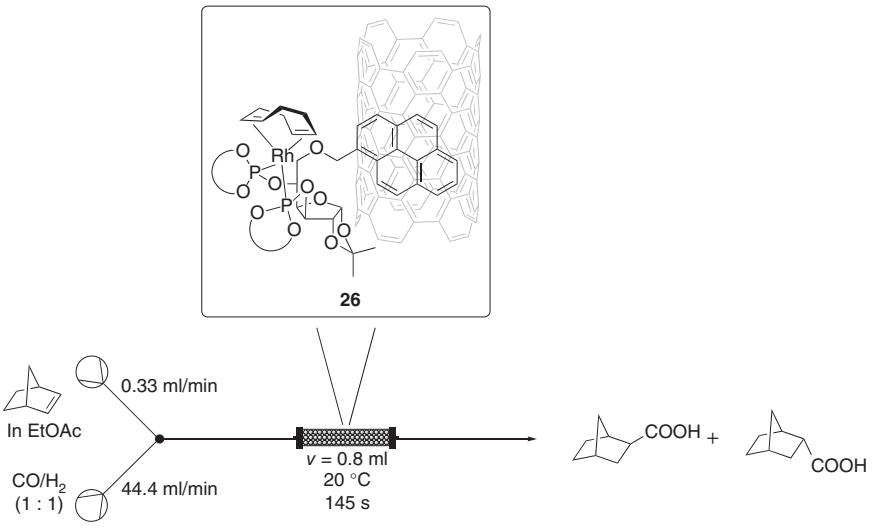

Scheme 8.25 Asymmetric hydroformylation of norbornene.

steady states. The results obtained in batch and continuous-flow mode were comparable. However, this study demonstrates that application of enantioselective hydroformylation, a high-pressure reaction with toxic and flammable reagents, can clearly benefit from continuous-flow processing and be performed safely and effectively in a pharmaceutical industry.

On the other hand, the Rh-catalyzed asymmetric hydroformylation of norbornene was also described [41]. The group of Godard developed different C1-symmetrical diphosphite ligands that displayed high activity and enantioselectivity. Encouraged by these promising results, the ligands were modified with a pyrene moiety to accomplish their immobilization onto multiwalled carbon nanotubes (MWCNT), reduced graphene oxide (rGO), and carbon beads (CBs). The recyclability of the new heterogenized catalysts was investigated, and it was found to be unsuccessful in batch due to catalyst leaching. However, under continuous-flow mode using MWCNT, the catalyst **26** revealed to be robust and to provide high ee with fast residence times, probably due to an improved gas–liquid mass transfer (Scheme 8.25).

8.3.2.3 Enantioselective 1,4-Addition to Enone

One efficient way to form a new stereogenic center and a C—C bond is the enantioselective 1,4 additions of carbon nucleophiles to α,β-unsaturated compounds. In 2018, the group of Uozumi reported the enantioselective 1,4-addition of arylboronic acids to enones catalyzed by an amphiphilic resin-supported chiral diene rhodium complex [42]. They developed a novel rhodium–chiral diene complex immobilized on amphiphilic polystyrene-poly(ethylene glycol) (PS-PEG) **27**. Encouraged by the results obtained in batch and the recyclability of the catalyst, a continuous-flow system was designed for the synthesis of enantioselective corresponding β-arylated carbonyl compounds. A packed-bed reactor containing the immobilized rhodium–chiral diene complex was fed by a solution of the enone,

https://www.twirpx.org & http://chemistry-chemists.com

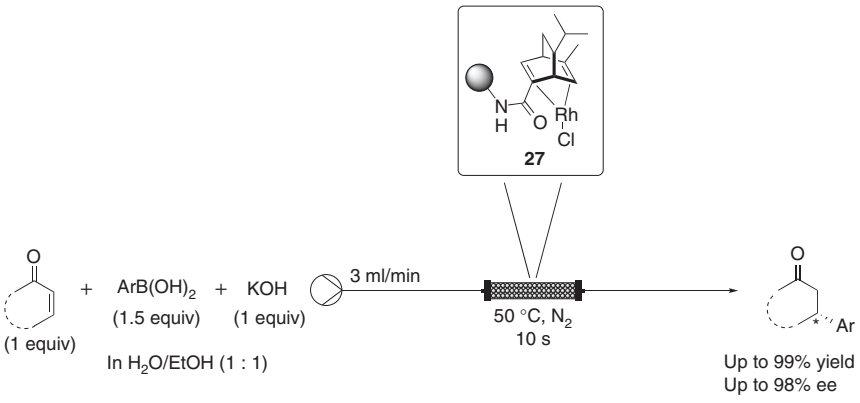

Scheme 8.26 Asymmetric 1,4-addition of arylboronic acids to enone.

the arylboronic acid, and potassium hydroxide in a 1 : 1 mixture of H_2O and EtOH (Scheme 8.26). The asymmetric 1,4-addition was completed in 10 seconds at 50 °C with high enantioselectivity. Long-term experiment allowed the 10-gram-scale synthesis of the desired adduct with high enantioselectivity, within 12 hours.

8.3.2.4 Enantioselective Nitroaldol Reaction

Another powerful transformation for a new stereogenic C—C bond formation is the catalyzed enantioselective nitroaldol (Henry) reaction between nitroalkanes and aldehydes or ketones. Shibasaki and coworkers described the synthetic utility of an MWNT-confined Nd/Na heterogeneous catalyst for the *anti*-selective catalytic asymmetric nitroaldol reaction [43]. The MWNT-confined Nd/Na heterogeneous catalyst **28** was prepared by conducting the self-assembling process in the presence of MWNT. The heterogeneous catalyst was transferred onto a stainless steel column with dried Celite® and connected to syringe pumps for the aldehyde and nitroethane (Scheme 8.27). The use of MS 3 Å and $NaHCO_3$ columns allowed to remove tiny amounts of water and acidic impurities from the aldehyde before it reached the catalyst column. The flow reaction was operated for 20 days, and the stereoselectivity was consistently high, although gradual loss in conversion was observed. The desired product was obtained in 81% yield, with >20/1 *anti*/*syn* ratio and 95% ee (*anti*), which corresponded to TON of 1661.

The same group also developed the *anti*-selective catalytic asymmetric nitroaldol reaction of α-keto esters [44]. A continuous-flow system was designed with a stainless steel column charged with MWNT-confined Nd/Na heterobimetallic catalyst **28** and fed by the substrates mixture (Scheme 8.28). This process was successfully executed by taking advantage of the heterogeneity of the Nd/Na heterobimetallic catalyst. The desired product was obtained after straight evaporation of the crude mixture, in 92% yield and with high stereoselectivity (up to *anti:syn* > 98 : 2 and 99% ee), isolating 1.52 g after 92 hours (TON of 265) when R = Me.

https://www.twirpx.org & http://chemistry-chemists.com

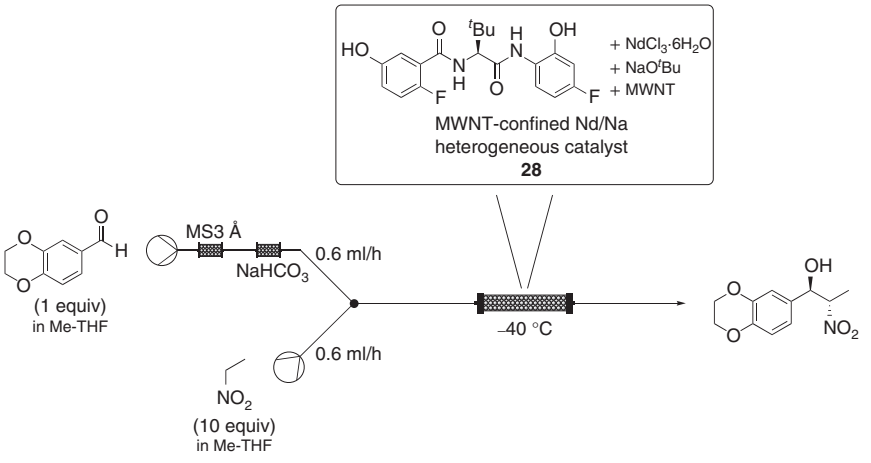

Scheme 8.27 Enantioselective nitroaldol reaction of aldehydes.

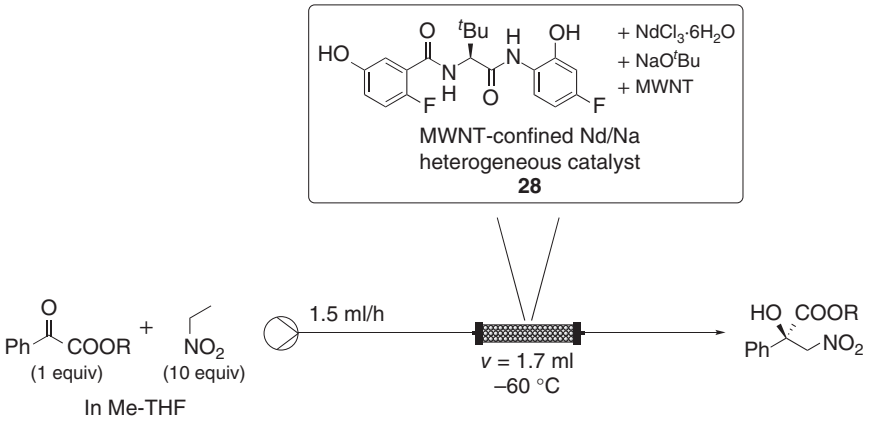

Scheme 8.28 Enantioselective nitroaldol reaction of α-keto esters.

8.4 Enantioselective Biocatalysis in Flow

The field of biocatalysis has been growing up over the past few years, representing a sustainable alternative to conventional synthetic methods. In combination with the advantages of continuous flow, the biosynthesis of complex molecules overcomes typical limitations of enzymatic classic reactions in batch [45]. Enzyme-driven asymmetric catalysis has been applied to a number of industrial processes as an efficient method for the synthesis of chiral products. However, mentioned difficulties such as enzymatic inhibition, difficulty of finding the appropriate reaction parameters for different enzymes, and difficult scale-up are the reason why there are still only few examples of biocatalytic approaches in continuous flow to achieve chiral compounds.

https://www.twirpx.org & http://chemistry-chemists.com

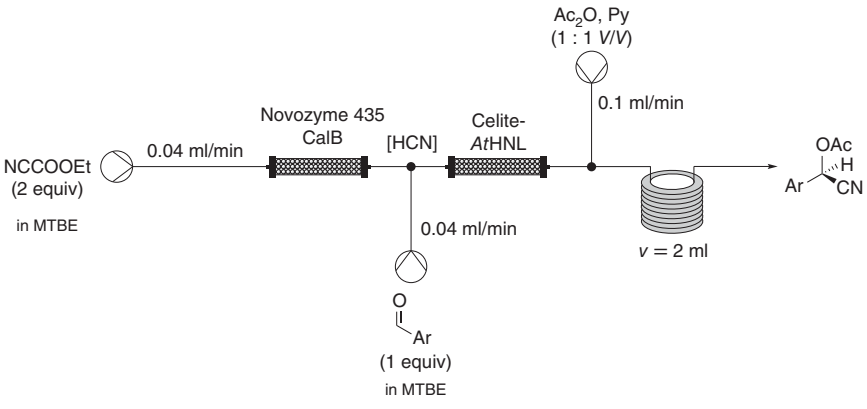

Scheme 8.29 Enantioselective biocatalyzed synthesis of *O*-acetylcyanohydrins. Source: Brahma et al. [46]/Georg Thieme Verlag KG.

The Ley group accomplished the enantioselective preparation of *O*-acetylcyanohydrins by a three-step telescoped continuous process (Scheme 8.29) [46]. This novel orthogonal biocatalytic approach consisted of an *in situ* generation of HCN employing CalB immobilized on acrylic resin (Novozyme 435) and the use of *Arabidopsis thaliana* (*At*HNL) onto Celite for the enantioselective hydrocyanation reaction. These two sequential biotransformations were controlled by safe handling of an *in situ* generated hazardous gas HCN and the in-line stabilization of the products by subsequent acetylation. High stereocontrol was obtained from the enzyme-catalyzed addition of HCN to aldehydes, giving access to a range of *O*-acetylcyanohydrins with very good conversions (75–99%) and ee values (40–96%) over three steps. Continuous-flow processes allow the use of hazardous reagent for reactions that usually present safety concerns. Moreover, this method improved the batch protocols reducing the reaction time (40 versus 345 minutes) and simplifying the operation mode.

An IL-based flow strategy for the enzymatic (lipase CALB) enantioselective transesterification of alcohols and amidation reactions has been also developed (Scheme 8.30) [47]. This system was based on the use of particle-stabilized IL droplets in oil as microreactors to build a continuous-flow system in a column reactor. A "bottom-up" fashion was a key element for this strategy. The continuous influx of reactants into the droplet microreactors and the continuous release of products from the droplet microreactors made this system a very productive strategy. In fact, after 4000 hours on stream, the enantioselective transesterification efficiency showed no significant decrease. The idea of the use of IL droplets for bigger scale implies to have a huge number of microreactors all working together in parallel, resulting in a macroscale continuous-flow reaction for the efficient enzymatic enantioselective transesterification or amidation.

A versatile synthesis of alcohols from amines was reported by Paradisi and coworker through a self-sustaining closed-loop multienzymatic platform [48]. The biocatalytic synthesis of a wide range of noncommercially available products in

https://www.twirpx.org & http://chemistry-chemists.com

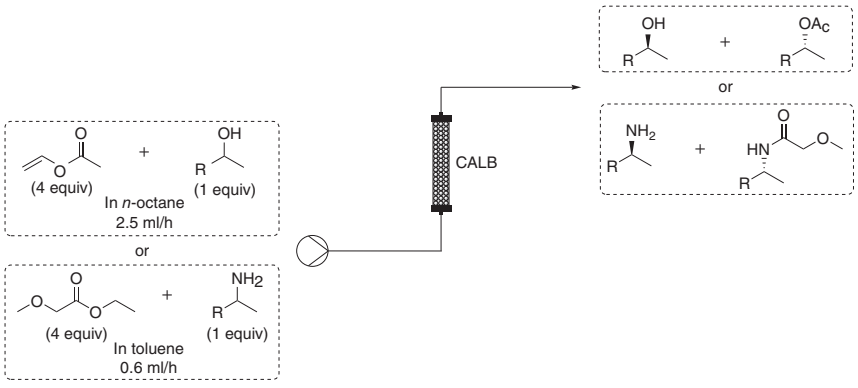

Scheme 8.30 IL droplet-based flow system for enantioselective transesterification or amidation. Source: Zhang et al. [47]/American Chemical Society.

continuous flow was successfully achieved, affording the desired secondary alcohols with excellent yields (80% to >99%) and optical purity (>99% ee) (Scheme 8.31). The process consisted of a multienzymatic cascade reaction that combines a ω-transaminase from *Halomonas elongate* (HEWT) with oxidoreductases, such as horse liver alcohol dehydrogenase (HLADH) or a ketoreductase from *Pichia glucozyma* (KRED1-Pglu), for the preparation of aromatic alcohols from the corresponding amines in continuous flow. This strategy led to an ultraefficient zero-waste process with cofactor recycling, in-line recovery of benign by-products, and recirculation of the aqueous media that contains the recycled cofactors in catalytic amounts. This closed-loop process increased the efficiency of the system and enabled the automation of the process. A simple trapping column, as downstream of the process, allowed the separation of the pure products and by-products. The conversion of amines into the corresponding alcohols was significantly enhanced with this strategy, due to the elimination of the amine/aldehyde condensations that, in

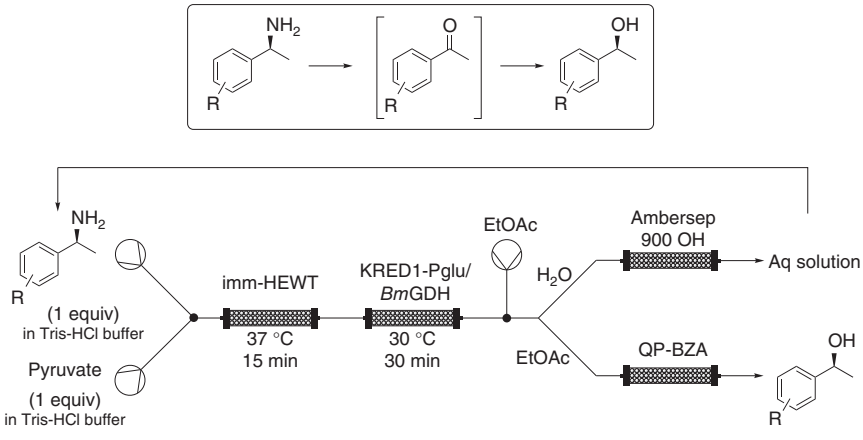

Scheme 8.31 Synthesis of secondary alcohols from aromatic amines.

https://www.twirpx.org & http://chemistry-chemists.com

batch, presents several limitations. Moreover, the synthesis of alcohols from amine starting materials is an excellent strategy for the preparation of pharmaceuticals and polymers.

The same group also developed the enantioselective hydrolysis of naproxen esters [49]. They developed the hydrolytic enantioselective cleavage of different racemic non-steroidal anti-inflammatory drugs (NSAIDs) ester derivatives. *Bacillus subtilis* (BS2m) was chosen as enzymes for the enantioselective hydrolysis of naproxen esters in continuous flow, based on batch results. Immobilization of a fusion BS2m with the T4 lysozyme (BS2mT4L1) on an epoxy-derivatized methacrylate support (EC-403) yielded the biocatalyst that was utilized in a packed-bed reactor (Scheme 8.32). The high degree of insolubility of the naproxen butyl ester resulted in a slurry, which made the reaction in flow difficult. However, the addition of Triton® X-100 to the substrate allows to perform the hydrolysis, yielding (*R*)-naproxen in 24% molar conversion and 80% ee with six minutes residence time.

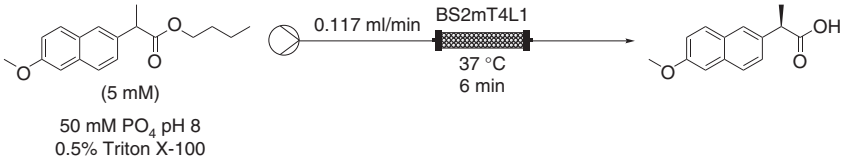

Scheme 8.32 Enantioselective hydrolysis of naproxen butyl ester.

Other two types of enzymatic reductions of a hydrophobic ketone in the presence of an alcohol dehydrogenase (ADH) for the synthesis of chiral alcohols have been reported [50]. Due to their excellent enantioselectivity and successful utilization in the synthesis of APIs, ADH was chosen as the enzyme class to use. A simple flow setup was designed, being capable to minimize some workup limitations. A segmented flow system based on a biphasic methyl *tert*-butyl ether (MTBE)/buffer mixture was successfully applied for enzymatic reduction (Scheme 8.33). Two different types of biotransformation were investigated based on the use of two different ADHs. ADH from *Lactobacillus brevis* was utilized for the reduction of acetophenone and ADH from *Ogataea minuta* for 2,2,2-trifluoroacetophenone. Although the conversion was comparable with the results from the process in batch, they were able to significantly simplify and minimize workup efforts for this biphasic system.

8.5 Asymmetric Total Synthesis in Continuous Flow

The advantages of asymmetric catalysis performed under continuous flow have been demonstrated. However, the complete synthesis of complex chiral molecules by continuous multistep processes is challenging.

In 2015, a very nice example on the use of chiral catalysis in a multistep flow synthesis was reported by Kobayashi and coworkers [51]. They developed a multistep continuous-flow synthesis of (*R*)- and (*S*)-Rolipram. The system used in this study

https://www.twirpx.org & http://chemistry-chemists.com

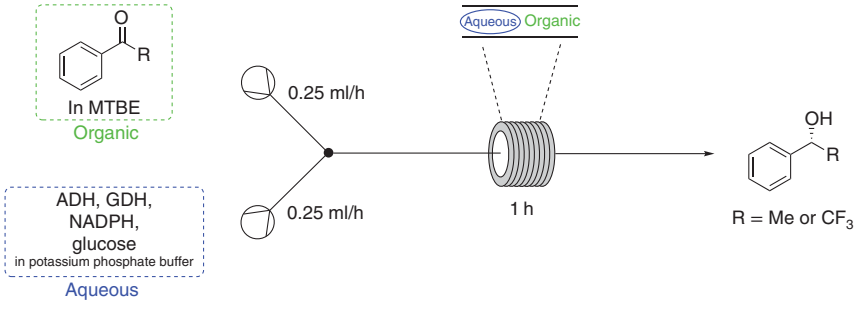

Scheme 8.33 Enzymatic segmented flow approach for the reduction of ketones.

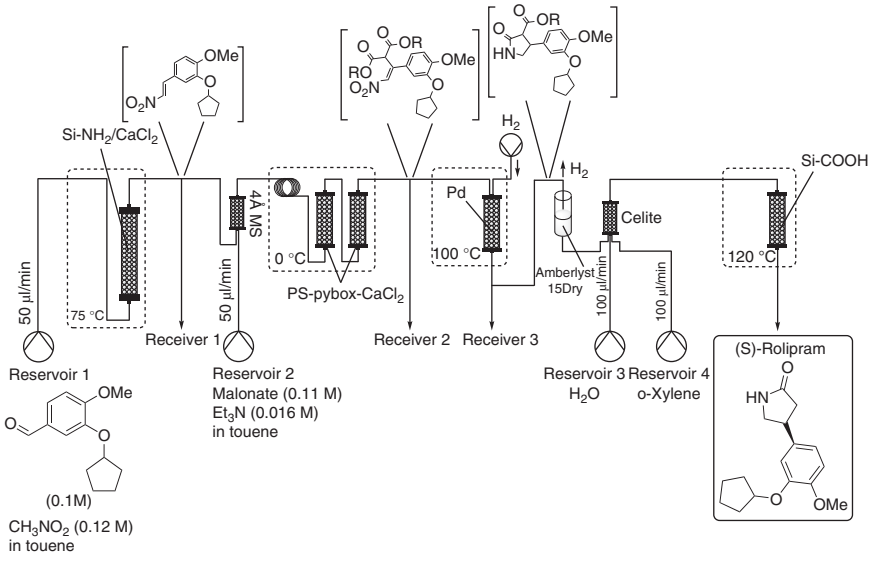

Scheme 8.34 Multistep synthesis of (*R*)- and (*S*)-rolipram applying enantioselective catalysis.

is presented in Scheme 8.34. Commercially available starting materials, aldehyde and nitromethane, were successively passed through the packed-bed reactors containing heterogeneous achiral and chiral catalysts to produce the drug directly with high enantioselectivity.

The first step of the synthesis involved a Henry-type reaction of benzaldehyde derivative with nitromethane. The outflow of the first reactor containing nitroalkene was fed into the second packed-bed reactor. The second step of the synthesis, an asymmetric addition, was the enantio-determining step of the whole process. The reaction was catalyzed either by a supported PS–(*S*)-pybox–calcium chloride catalyst or by the opposite enantiomer, PS–(*R*)-pybox–calcium chloride. In this step, two packed-bed reactors were used at 0 °C. The γ-nitro ester was obtained in 84% yield and with 94% ee. Next steps involved Pd-catalyzed hydrogenation and a decarboxylation reaction. In the third step, the desired product was obtained in

https://www.twirpx.org & http://chemistry-chemists.com

74% yield and 94% ee by using a polysilane-supported palladium/carbon catalyst (Pd/DMPSi-C). At this stage, two columns containing Amberlyst 15Dry and Celite were placed to remove any residue from the outlet stream. Next, the stream was fed into the fourth one filled with the silica-supported carboxylic acid to provide the desired product, (S)-Rolipram or its opposite enantiomer. (*S*)-Rolipram was successfully synthesized in 50% yield and 96% ee. Direct recrystallization of the crude product from water/methanol afforded optically pure (*S*)-Rolipram in 99% ee. This continuous-flow multistep system was found to be stable for at least one week. Moreover, no leaching of the palladium was observed; the level of the palladium in the solution was as low as possible, below 0.01 ppm, indicating that the product does not contain any metal.

The synthesis of (*S*)-Rolipram reported by Kobayashi and coworkers via heterogeneous catalysis under continuous-flow conditions clearly demonstrates the potential of microreactor technology and flow chemistry in sustainable synthesis. This multistep process did not require isolation of any intermediates, separation of the catalyst, or other type of workup procedures, which makes it very attractive and sustainable.

(*S*)-Pregabalin is a widely administered anticonvulsant and antiepileptic drug. The synthesis of this drug in multigram scale of an (*S*)-Pregabalin precursor in continuous flow with high enantioselectivity and with a very simple experimental procedure has been also described (Scheme 8.35) [52]. The authors used the chiral thiourea organocatalyst **1** to perform the stereoselective nucleophilic addition of diethyl malonate to the appropriate nitroalkene obtaining a key chiral intermediate that, after reduction of the nitro moiety, is followed by hydrolysis and decarboxylation. Under the best reaction flow conditions (60 °C, two minutes residence time), 1 g of desired intermediate was produced with 81% ee in only one hour using a very simple laboratory size flow set up.

Another recent example that shows the potential of asymmetric catalysis in flow chemistry for sustainable pharmaceutical manufacturing has been recently reported

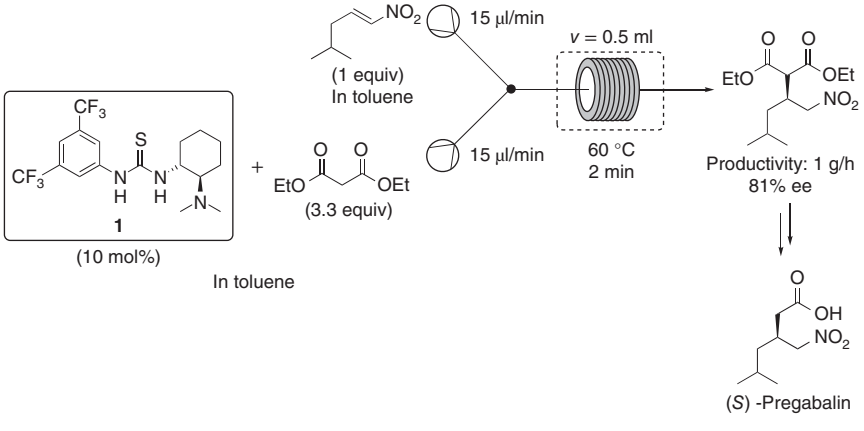

Scheme 8.35 Asymmetric organocatalytic mediated synthesis of (*S*)-pregabalin key intermediate. Source: Porta et al. [52]/MDPI.

https://www.twirpx.org & http://chemistry-chemists.com

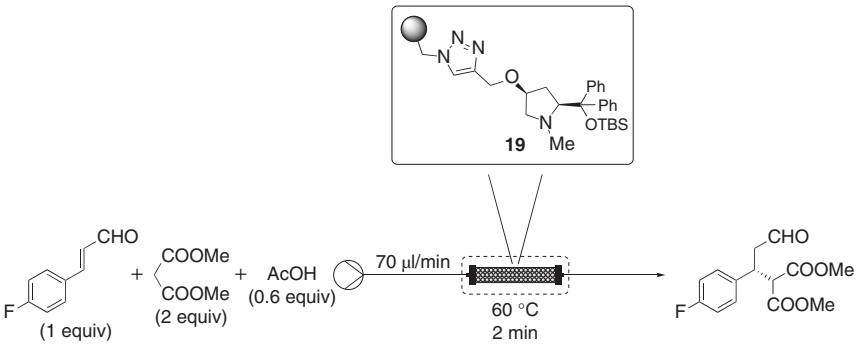

Scheme 8.36 Asymmetric Michael reaction under continuous-flow conditions.

by Kappe and coworkers where they present a multistep continuous-flow process for the synthesis of the key intermediate of (−)-Paroxetine. Paroxetine is an antidepressant drug (selective serotonin reuptake inhibitor) widely used to treat depression and other psychiatric disorders [53].

Within the multistep synthetical methodology, the key chiral aldehyde (Scheme 8.36) was obtained via organocatalytic asymmetric Michael reaction of *p*-fluorocinnamaldehyde and dimethyl malonate using the PS-supported *cis*-4-hydroxydiphenylprolinol catalyst **19** [31].

The optimal flow conditions developed were 20 minutes residence time at 60 °C and solvent-free. The desired aldehyde was obtained with 93% conversion, complete chemoselectivity, and 98.5% enantioselectivity.

The system was stable running continuously during seven hours, leading to a productivity of 2.47 g/h and achieving 17.26 g of pure product (84% isolated yield, 97% ee). It should be emphasized that the catalyst was proved to be very robust. Essentially constant selectivity (95–98% ee and 100% chemoselectivity) and very small decrease in catalytic activity (from 93% to 85% conversion) was achieved. The data generated resulted in an effective catalyst loading of 0.6 mol%, TON of 132, STY of 1.76 kg/l h, and very low waste formation confirmed by an *E*-factor of only 0.7.

This key aldehyde was then used for the multistep synthesis process of (−)-Paroxetine intermediate (Scheme 8.37). This process consisted in a sequence of a reductive amination/lactamization/amide-ester reduction to achieve the chiral key intermediate, ((3,4*R*)-4-(4-fluorophenyl)piperidin-3-yl)methanol, of (−)-Paroxetine. The telescoped process proved stable and afforded the desired product in 83% isolated yield and 96% ee with a productivity of 2.97 g/h.

An analogous diphenylprolinol catalyst supported onto a Wang resin (**29**) was also used by the group of Mlynarski in the continuous-flow organocatalytic Michael reaction to prepare a key chiral intermediate for the total asymmetric synthesis of (+)-Paroxetine (Scheme 8.38) and (+)-Femoxetine [54]. In this case, complete conversion to the desired product with *syn*/*anti* ratio of 3.2 : 1 was achieved. However, more than 16 hours were required to pump 5 ml of the starting material since the optimal required flow rate was very slow (0.005 ml/min). Unfortunately,

https://www.twirpx.org & http://chemistry-chemists.com

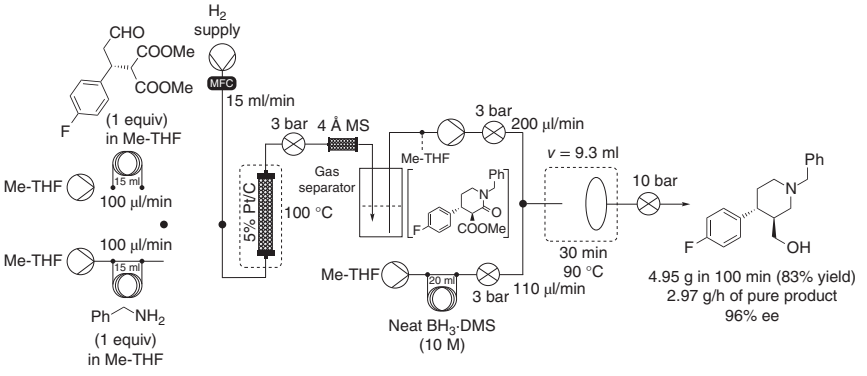

Scheme 8.37 Multistep continuous-flow synthesis of the intermediate of (–)-paroxetine.

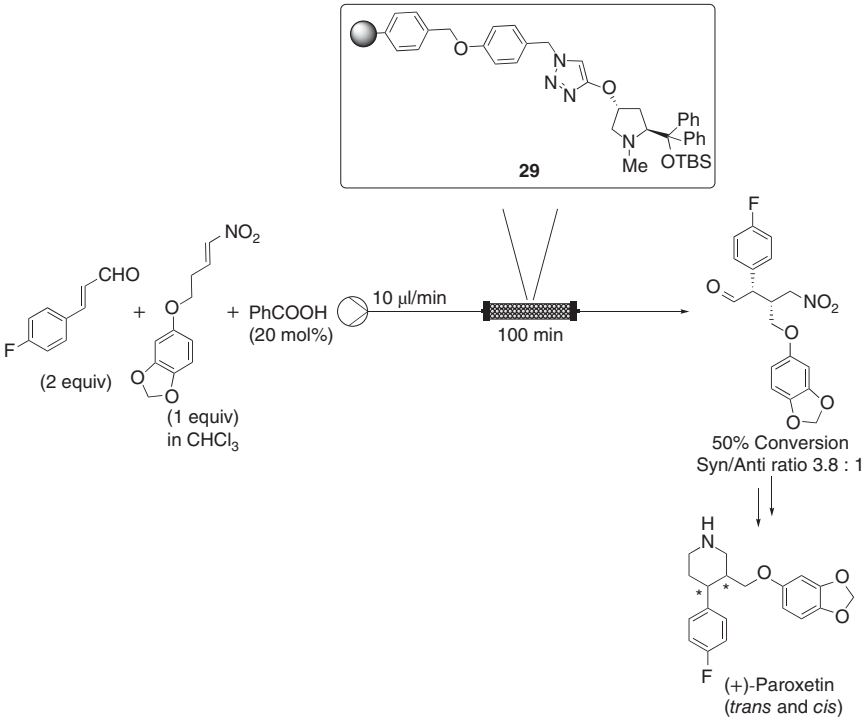

Scheme 8.38 Asymmetric Michael reaction for the synthesis of (+)-paroxetine key intermediate.

when a faster flow rate was applied (0.5 ml/min), the conversion dropped to 17% (although the *syn*/*anti* ratio observed was higher [4.5 : 1]). The authors decided to apply a compromise between residence time and productivity, so the flow rate was set to 0.01 ml/min to achieve a maximum conversion of 50% with a residence time of 100 minutes.

https://www.twirpx.org & http://chemistry-chemists.com

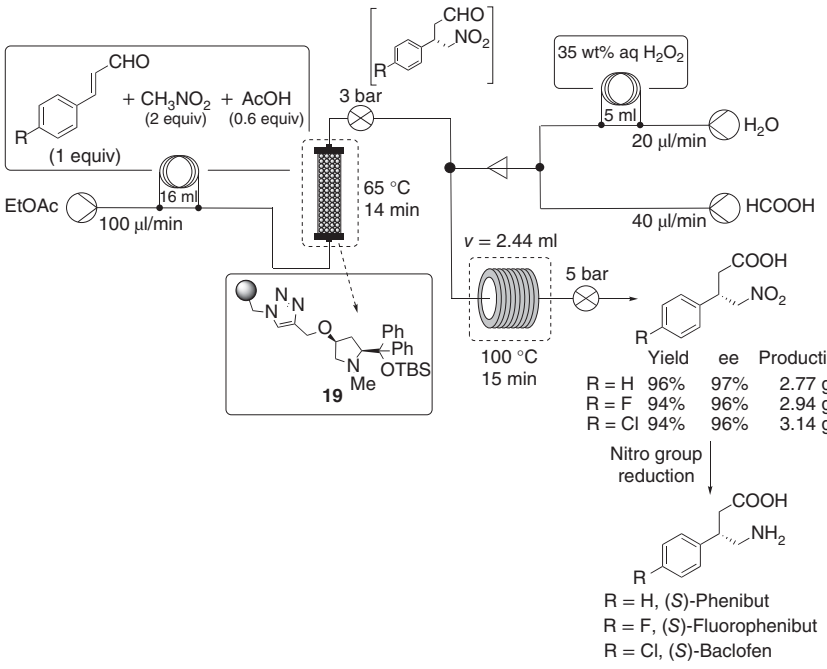

Scheme 8.39 Telescoped organocatalytic conjugate addition–aldehyde oxidation sequence for the synthesis in continuous flow of chiral GABA intermediates.

The versatility of catalyst **19** was further showed in a continuous process involving two-step asymmetric synthesis in flow of chiral γ-nitrobutyricacids as key intermediates of the GABA analogs Baclofen (antispastic drug applied as a muscle relaxant), Phenibut (anxiolytic used to treat anxiety and insomnia), and Fluorophenibut (also an anxiolytic drug) on a multigram scale [55]. The telescoped process includes an enantioselective organocatalyzed Michael addition of nitromethane to α,β-unsaturated aldehydes to obtain γ-nitro-aldehydes as key intermediate neat conditions followed by their oxidation with *in situ*-generated performic acid, leading to the desired GABA analogs (Scheme 8.39). The flow system allows the pass of reactants through a column heated at 65 °C and filled with catalyst **19**. Then neat formic acid and an aqueous H_2O_2 solution are introduced at flow rates corresponding to one equiv of H_2O_2 and five equiv of formic acid with respect to the aldehyde. The reaction mixture coming out from the packed-bed reactor and containing the γ-nitroaldehyde is mixed with the combined formic acid/H_2O_2 stream, and the resulting mixture solution is passed through a coil reactor at 100 °C where performic acid generation and aldehyde oxidation take simultaneously place.

The γ-nitrobutyric acids were obtained in high yields and excellent enantioselectivities (96–97% ee), and the processes have a remarkably high productivity. Notably, no chromatography purification is required, and the products are obtained easily at the multigram scale.

https://www.twirpx.org & http://chemistry-chemists.com

8.6 Conclusions

Important enantioselective catalytic processes in continuous flow have been presented as useful synthesis tool for the formation of important chiral APIs and advanced intermediates. The development of catalysts and processes that enable the synthesis of enantiopure products is key for many different industries. In combination with the continuous-flow technology advantages, it allows higher productivities and reproducibility in shorter times, as well as easy scalability, representing an excellent approach toward a more sustainable and smart production of complex molecules. Moreover, as the technology evolves, the future of chemical synthesis also progresses toward being more automatized, including process analytical technology (PAT)-enabled process monitoring and multistep processes, making the application of asymmetric catalysis in flow ideal for the efficient and fast synthesis of chiral chemical libraries.

References

1 (a) Baumann, M., Moody, T.S., Smyth, M., and Wharry, S. (2020). A perspective on continuous flow chemistry in the pharmaceutical industry. *Org. Process Res. Dev.* 24: 1802–1813. (b) Luis, S.V. and Garcia-Verdugo, E. (ed.) (2019). *Flow Chemistry: Integrated Approaches for Practical Applications*. Cambridge: The Royal Society of Chemistry. (c) May, S.A. (2017). Flow chemistry, continuous processing, and continuous manufacturing: a pharmaceutical perspective. *J. Flow Chem.* 7 (3–4): 137–145. (d) Gutmann, B., Cantillo, D., and Kappe, O.C. (2015). Continuous-flow technology—a tool for the safe manufacturing of active pharmaceutical ingredients. *Angew. Chem. Int. Ed.* 54: 6688–6728. (e) Darvas, F., Hessel, V., and Dorman, G. (ed.) (2014). *Flow Chemistry*. Berlin: De Gruyter. (f) Reschetilowski, W. (ed.) (2013). *Microreactors in Preparative Chemistry*. Weinheim: Wiley-VCH.

2 (a) Han, B., He, X.-H., Liu, Y.-Q. et al. (2021). Asymmetric organocatalysis: an enabling technology for medicinal chemistry. *Chem. Soc. Rev.* 50: 1522–1586. (b) Krištofíková, D., Modrocká, V., Mečiarová, M., and Šebesta, R. (2020). Green asymmetric organocatalysis. *ChemSusChem* 13: 2828–2858. (c)Hayler, J.D., Leahy, D.K., and Simmons, E.M. (2019). A pharmaceutical industry perspective on sustainable metal catalysis. *Organometallics* 38: 36–46.

3 Dalko, P.I. and Moisan, L. (2004). In the golden age of organocatalysis. *Angew. Chem. Int. Ed.* 43: 5138–5175.

4 (a) Tanimu, A., Jaenicke, S., and Alhooshani, K. (2017). Heterogeneous catalysis in continuous flow microreactors: a review of methods and applications. *Chem. Eng. J.* 327: 792–821. (b) Colella, M., Carlucci, C., and Luisi, R. (2018). Supported catalysts for continuous flow synthesis. *Top. Curr. Chem.* 376: 46. (c) de Oliveira, P.H.R., da S. Santos, B.M., Leão, R.A.C. et al. (2019). From immobilization to catalyst use: a complete continuous-flow approach towards the use of immobilized organocatalysts. *ChemCatChem* 11: 5553–5561.

https://www.twirpx.org & http://chemistry-chemists.com

5 (a) Rodríguez-Escrich, C. and Pericàs, M.A. (2015). Organocatalysis on tap: enantioselective continuous flow processes mediated by solid-supported chiral organocatalysts. *Eur. J. Org. Chem.* (6): 1173–1188. (b) Atodiresei, I., Vila, C., and Rueping, M. (2015). Asymmetric organocatalysis in continuous flow: opportunities for impacting industrial catalysis. *ACS Catal.* 5: 1972–1985. (c)Finelli, F.G., Miranda, L.S.M., and de Souza, R.O.M.A. (2015). Expanding the toolbox of asymmetric organocatalysis by continuous-flow process. *Chem. Commun.* 51: 3708–3722. (d) De Risi, C., Bortolini, O., Brandolese, A. et al. (2020). Recent advances in continuous-flow organocatalysis for process intensification. *React. Chem. Eng.* 5: 1017–1052.

6 (a) Maity, C., Trausel, F., and Eelkema, R. (2018). Selective activation of organocatalysts by specific signals. *Chem. Sci.* 9: 5999–6005. (b) Burès, J., Armstrong, A., and Blackmond, D.G. (2014). Rationalization of an unusual solvent-induced inversion of enantiomeric excess in organocatalytic selenylation of aldehydes. *Angew. Chem. Int. Ed.* 53: 8700–8704. (c) Burès, J., Armstrong, A., and Blackmond, D.G. (2013). The interplay of thermodynamics and kinetics in dictating organocatalytic reactivity and selectivity. *Pure Appl. Chem.* 85: 1919–1934.

7 Rossi, S., Benaglia, M., Puglisi, A. et al. (2015). Continuous-flow stereoselective synthesis in microreactors: nucleophilic additions to nitrostyrenes organocatalyzed by a chiral bifunctional catalyst. *J. Flow Chem.* 5 (1): 17–21.

8 Schober, L., Ratnam, S., Yamashita, Y. et al. (2019). An asymmetric organocatalytic aldol reaction of a hydrophobic aldehyde in aqueous medium running in flow mode. *Synthesis* 51 (5): 1178–1184.

9 Silvi, M. and Melchiorre, P. (2018). Enhancing the potential of enantioselective organocatalysis with light. *Nature* 554 (7690): 41–49.

10 (a) Blakemore, D.C., Castro, L., Churcher, I. et al. (2018). Organic synthesis provides opportunities to transform drug discovery. *Nat. Chem.* 10 (4): 383–394. (b) Bogdos, M.K., Pinard, E., and Murphy, J.A. (2018). Applications of organocatalysed visible-light photoredox reactions for medicinal chemistry. *Beilstein J. Org. Chem.* 14: 2035–2064.

11 (a) Sakeda, K., Wakabayashi, K., Matsushita, Y. et al. (2007). Asymmetric photosensitized addition of methanol to (*R*)-(+)-(*Z*)-limonene in a microreactor. *J. Photochem. Photobiol., A* 192 (2–3): 166–171. (b) Neumann, M. and Zeitler, K. (2012). Application of microflow conditions to visible light photoredox catalysis. *Org. Lett.* 14 (11): 2658–2661.

12 Tang, X.-F., Zhao, J.-N., Wu, Y.-F. et al. (2019). Enantioselective Photooxygenation of β-dicarbonyl compounds in batch and flow photomicroreactors. *Org. Biomol. Chem.* 17 (34): 7938–7942.

13 (a) Christoffers, J., Baro, A., and Werner, T. (2004). α-Hydroxylation of β-dicarbonyl compounds. *Adv. Synth. Catal.* 346 (2–3): 143–151. (b) Reddy, D.S., Shibata, N., Nagai, J. et al. (2009). A dynamic kinetic asymmetric transformation in the α-hydroxylation of racemic malonates and its application to biologically active molecules. *Angew. Chem. Int. Ed.* 48 (4): 803–806.

https://www.twirpx.org & http://chemistry-chemists.com

14 Brenna, D., Porta, R., Massolo, E. et al. (2017). A new class of low-loading catalysts for a highly enantioselective, metal-free imine reduction of wide general applicability. *ChemCatChem* 9 (6): 941–945.

15 Dai, W., Mi, Y., Lv, Y. et al. (2016). Development of a continuous-flow microreactor for asymmetric sulfoxidation using a biomimetic manganese catalyst. *Adv. Synth. Catal.* 358 (4): 667–671.

16 Dai, W., Mi, Y., Lv, Y. et al. (2016). Development of a continuous-flow microreactor for asymmetric epoxidation of electron-deficient olefins. *Synthesis* 48 (16): 2653–2658.

17 (a) Liao, J., Zhang, S., Wang, Z. et al. (2020). Transition-metal catalyzed asymmetric reactions under continuous flow from 2015 to early 2020. *Green Synth. Catal.* 1: 121–133. (b) Yu, T., Jiao, J., Song, P. et al. (2020). Recent progress in continuous-flow hydrogenation. *ChemSusChem* 13: 2876–2893.

18 Touge, T., Kuwana, M., Komatsuki, Y. et al. (2019). Development of asymmetric transfer hydrogenation with a bifunctional oxo-tethered ruthenium catalyst in flow for the synthesis of a ceramide (D-*erythro*-CER[NDS]). *Org. Process Res. Dev.* 23 (4): 452–461.

19 Yu, T., Ding, Z., Nie, W. et al. (2020). Recent advances in continuous-flow enantioselective catalysis. *Chem. Eur. J.* 26 (26): 5729–5747.

20 ONeal, E.J., Lee, C.H., Brathwaite, J., and Jensen, K.F. (2015). Continuous nanofiltration and recycle of an asymmetric ketone hydrogenation catalyst. *ACS Catal.* 5 (4): 2615–2622.

21 Kisszekelyi, P., Alammar, A., Kupai, J. et al. (2019). Asymmetric synthesis with cinchona-decorated cyclodextrin in a continuous-flow membrane reactor. *J. Catal.* 371: 255–261.

22 (a) Rodríguez-Escrich, C. and Pericàs, M.A. (2015). Organocatalysis on tap: enantioselective continuous flow processes mediated by solid-supported chiral organocatalysts. *Eur. J. Org. Chem.* 2015 (6): 1173–1188. (b) Atodiresei, I., Vila, C., and Rueping, M. (2015). Asymmetric organocatalysis in continuous flow: opportunities for impacting industrial catalysis. *ACS Catal.* 5 (3): 1972–1985. (c) Rodríguez-Escrich, C. and Pericàs, M.A. (2019). Catalytic enantioselective flow processes with solid-supported chiral catalysts. *Chem. Rec.* 19 (9): 1872–1890.

23 Munawwer, R., Elmore, S.C., and Wirth, T. (2011). Asymmetric reactions in flow reactors. In: *Catalytic Methods in Asymmetric Synthesis: Advanced Materials, Techniques, and Applications* (ed. M. Gruttadauria and F. Giacalone), 345–372. Palermo: Wiley.

24 Zhao, D. and Ding, K. (2013). Recent advances in asymmetric catalysis in flow. *ACS Catal.* 3 (5): 928–944.

25 Clot-Almenara, L., Rodríguez-Escrich, C., Osorio-Planes, L., and Pericàs, M.A. (2016). Polystyrene-supported TRIP: a highly recyclable catalyst for batch and flow enantioselective allylation of aldehydes. *ACS Catal.* 6 (11): 7647–7651.

26 Kasaplar, P., Ozkal, E., Rodríguez-Escrich, C., and Pericàs, M.A. (2015). Enantioselective α-amination of 1,3-dicarbonyl compounds in batch and flow with immobilized thiourea organocatalysts. *Green Chem.* 17 (5): 3122–3129.

https://www.twirpx.org & http://chemistry-chemists.com

27 Forni, J.A., Novaes, L.F.T., Galaverna, R., and Pastre, J.C. (2018). Novel polystyrene-immobilized chiral amino alcohols as heterogeneous ligands for the enantioselective arylation of aldehydes in batch and continuous flow regime. *Catal. Today* 308: 86.

28 Llanes, P., Rodríguez-Escrich, C., Sayalero, S., and Pericàs, M.A. (2016). Organocatalytic enantioselective continuous-flow cyclopropanation. *Org. Lett.* 18 (24): 6292–6295.

29 Izquierdo, J., Ayats, C., Henseler, A.H., and Pericàs, M.A. (2015). A polystyrene-supported 9-amino(9-deoxy)*epi* quinine derivative for continuous flow asymmetric Michael reactions. *Org. Biomol. Chem.* 13 (14): 4204–4209.

30 Sagamanova, I., Rodríguez-Escrich, C., Molnár, I.G. et al. (2015). Translating the enantioselective Michael reaction to a continuous flow paradigm with an immobilized fluorinated organocatalyst. *ACS Catal.* 5 (11): 6241–6248.

31 Osorio-Planes, L., Rodríguez-Escrich, C., and Pericàs, M.A. (2016). Removing the superfluous: a supported squaramide catalyst with a minimalistic linker applied to the enantioselective flow synthesis of pyranonaphthoquinones. *Cat. Sci. Technol.* 6: 4686–4689.

32 Lai, J., Sayalero, S., Ferrali, A. et al. (2018). Immobilization of *cis*-4-hydroxydiphenylprolinol silyl ethers onto polystyrene. Application in the catalytic enantioselective synthesis of 5-hydroxyisoxazolidines in batch and flow. *Adv. Synth. Catal.* 360 (15): 2914–2924.

33 Izquierdo, J. and Pericàs, M.A. (2016). A recyclable, immobilized analogue of benzotetramisole for catalytic enantioselective domino Michael addition/cyclization reactions in batch and flow. *ACS Catal.* 6 (1): 348–356.

34 Wang, S., Izquierdo, J., Rodríguez-Escrich, C., and Pericàs, M.A. (2017). Asymmetric [4 + 2] annulation reactions catalyzed by a robust immobilized isothiourea. *ACS Catal.* 7 (4): 2780–2785.

35 Cañellas, S., Ayats, C., Henseler, A.H., and Pericàs, M.A. (2017). A highly active polymer-supported catalyst for asymmetric Robinson annulations in continuous flow. *ACS Catal.* 7 (2): 1383–1391.

36 Fernandes, S.D., Porta, R., Barrulas, P.C. et al. (2016). Stereoselective reduction of imines with trichlorosilane using solid-supported chiral picolinamides. *Molecules* 21 (9): 1182–1190.

37 Porta, R., Benaglia, M., Annunziata, R. et al. (2017). Solid supported chiral *N*-picolylimidazolidinones: recyclable catalysts for the enantioselective, metal- and H_2-free reduction of imines in batch and in flow mode. *Adv. Synth. Catal.* 359 (14): 2375–2382.

38 Amara, Z., Poliakoff, M., Duque, R. et al. (2016). Enabling the scale-up of a key asymmetric hydrogenation step in the synthesis of an API using continuous flow solid-supported catalysis. *Org. Process Res. Dev.* 20 (7): 1321–1327.

39 Geier, D., Schmitz, P., Walkowiak, J. et al. (2018). Continuous flow asymmetric hydrogenation with supported ionic liquid phase catalysts using modified CO_2 as the mobile phase: from model substrate to an active pharmaceutical ingredient. *ACS Catal.* 8 (4): 3297–3303.

https://www.twirpx.org & http://chemistry-chemists.com

40 Abrams, M.L., Buser, J.Y., Calvin, J.R. et al. (2016). Continuous liquid vapor reactions part 2: asymmetric hydroformylation with rhodium-bisdiazaphos catalysts in a vertical pipes-in-series reactor. *Org. Process. Res. Dev.* 20 (5): 901–910.

41 Cunillera, A., Blanco, C., Gual, A. et al. (2019). Highly efficient Rh-catalysts immobilised by π–π stacking for the asymmetric hydroformylation of norbornene under continuous flow conditions. *ChemCatChem* 11 (8): 2195–2205.

42 Shen, G., Osako, T., Nagaosa, M., and Uozumi, Y. (2018). Aqueous asymmetric 1,4-addition of arylboronic acids to enones catalyzed by an amphiphilic resin-supported chiral diene rhodium complex under batch and continuous-flow conditions. *J. Org. Chem.* 83 (14): 7380–7387.

43 Nonoyama, A., Kumagai, N., and Shibasaki, M. (2017). Asymmetric flow catalysis: mix-and-go solid-phase Nd/Na catalyst for expeditious enantioselective access to a key intermediate of AZD7594. *Tetrahedron* 73 (11): 1517–1521.

44 Karasawa, T., Oriez, R., Kumagai, N., and Shibasaki, M. (2018). *Anti*-selective catalytic asymmetric nitroaldol reaction of α-keto esters: intriguing solvent effect, flow reaction, and synthesis of active pharmaceutical ingredients. *J. Am. Chem. Soc.* 140 (38): 12290–12295.

45 (a) Britton, J., Majumdar, S., and Weiss, G.A. (2018). Continuous flow biocatalysis. *Chem. Soc. Rev.* 47: 5891–5918. (b) Santi, M., Sancineto, L., Nascimento, V. et al. (2021). Flow biocatalysis: a challenging alternative for the synthesis of APIs and natural compounds. *Int. J. Mol. Sci.* 22: 990–1022. (c) Benítez-Mateos, A.I., Contente, M.L., Padrosa, D.R., and Paradisi, F. (2021). Flow biocatalysis 101: design, development and applications. *React. Chem. Eng.* 6: 599–611.

46 Brahma, A., Musio, B., Ismayilova, U. et al. (2016). An orthogonal biocatalytic approach for the safe generation and use of HCN in a multistep continuous preparation of chiral *O*-acetylcyanohydrins. *Synlett* 27 (2): 262–266.

47 Zhang, M., Ettelaie, R., Yan, T. et al. (2017). Ionic liquid droplet microreactor for catalysis reactions not at equilibrium. *J. Am. Chem. Soc.* 139 (48): 17387–17396.

48 Contente, M.L. and Paradisi, F. (2018). Self-sustaining closed-loop multienzyme-mediated conversion of amines into alcohols in continuous reactions. *Nat. Catal.* 1 (6): 452–459.

49 Roura Padrosa, D., De Vitis, V., Contente, M.L. et al. (2019). Overcoming water insolubility in flow: enantioselective hydrolysis of naproxen ester. *Catalysts* 9 (3): 232–241.

50 Adebar, N., Choi, J.E., Schober, L. et al. (2019). Overcoming work-up limitations of biphasic biocatalytic reaction mixtures through liquid-liquid segmented flow processes. *ChemCatChem* 11 (23): 5788–5793.

51 Tsubogo, T., Oyamada, H., and Kobayashi, S. (2015). Multistep continuous-flow synthesis of (*R*)- and (*S*)-rolipram using heterogeneous catalysts. *Nature* 520 (7547): 329–332.

52 Porta, R., Benaglia, M., Coccia, F. et al. (2015). Enantioselective organocatalysis in microreactors: continuous flow synthesis of a (*S*)-pregabalin precursor and (*S*)-warfarin. *Symmetry* 7 (3): 1395–1409.

https://www.twirpx.org & http://chemistry-chemists.com

53 Ötvös, S.B., Pericàs, M.A., and Kappe, C.O. (2019). Multigram-scale flow synthesis of the chiral key intermediate of (−)-paroxetine enabled by solvent-free heterogeneous organocatalysis. *Chem. Sci.* 10 (48): 11141–11146.

54 Szcześniak, P., Buda, S., Lefevre, L. et al. (2019). Total asymmetric synthesis of (+)-paroxetine and (+)-femoxetine. *Eur. J. Org. Chem.* 41: 6973–6982.

55 Ötvös, S.B., Llanes, P., Pericàs, M.A., and Kappe, C.O. (2020). Telescoped continuous flow synthesis of optically active γ-nitrobutyric acids as key intermediates of Baclofen, Phenibut, and Fluorophenibut. *Org. Lett.* 22 (20): 8122.

https://www.twirpx.org & http://chemistry-chemists.com

https://www.twirpx.org & http://chemistry-chemists.com

9

Innovative Process Development of Pharmaceutical Intermediates Under Continuous-Flow System

Koji Machida and Hiroaki Yasukouchi

Pharma & Supplemental Nutrition Solutions Vehicle, Kaneka Corporation, Pharma Business Division Research Group, 1-8 Miyamae-cho, Takasago-cho, Takasago, Hyogo 676-8688, Japan

9.1 Introduction

Flow reactor has unique features, such as efficient mixing, excellent heat and mass transfer, and precise control of reaction time, resulting in the improvement of both reaction yield and product quality. These features enable us to implement various chemical transformations, including highly exothermic and hazardous reactions, which have posed challenges in the conventional batch mode [1, 2]. Additionally, the process of utilizing flow reactors provides safe and efficient access to the scale-up process [3]. This emerging technology has recently been gaining considerable attention with a growing literature base [4, 5]. In the pharmaceutical industry, rapid and stable supply of high-quality drugs to the market is essential; hence, the researchers engaged in this field are highly expected to establish safe and robust manufacturing processes under strict quality controls. Continuous-flow processing, including flow reactions, can provide optimal methodologies for process intensification to meet these requirements [6]. The emerging flow technologies also provide cost advantages for pharmaceutical industries because innovative and cost-effective active pharmaceutical ingredient (API) synthetic pathway can be established while shortening the research and development period, owing to seamless scale-up from the laboratory to the manufacturing plant. Furthermore, continuous-flow processing offers advanced quality control systems by incorporating in-line/online monitoring devices (i.e. process analytical technology [PAT]) while assuring the consistency of drug quality. Therefore, regulatory agencies, such as Food and Drug Administration (FDA), European Medicines Agency (EMA), and Pharmaceuticals and Medical Devices Agency (PMDA), have been encouraging the adoption of continuous-flow processing into pharmaceutical industries to supply high-quality drugs to the market within a short delivery time [7, 8].

In this chapter, we introduced scalable flow processes for hazardous and catalytic reactions and stated that these systems apply to the synthesis of high-value API intermediates [9, 10]. In addition, we described that the flow reactor systems

Flow and Microreactor Technology in Medicinal Chemistry, First Edition. Edited by Esther Alza.
© 2022 WILEY-VCH GmbH. Published 2022 by WILEY-VCH GmbH.

https://www.twirpx.org & http://chemistry-chemists.com

installed in our sites were uniquely designed as multipurpose facilities, and commercial production was accomplished under Good Manufacturing Practice (GMP) conditions.

9.2 Plug Flow Reactor System for Phosgenation Reaction

9.2.1 Introduction

The highly reactive phosgene is a useful and versatile reagent in organic synthesis, and it can be used to quickly prepare a wide variety of carbonyl compounds, which are well known for being valuable building blocks [11–15]. The adoption of chemical reactions with inexpensive phosgene is often beneficial to the development of the cost-effective synthetic route for pharmaceuticals, agrochemicals, and other fine chemicals. However, the handling of toxic and volatile phosgene under the batch system poses safety issues, whereby special safety measures are required to prevent the leakage of hazardous chemicals in large-scale production, as it was introduced in Chapter 1. Thus, minimizing reaction volume is highly desirable to enhance manufacturing safety. Although heat management of exothermic phosgenation reaction is crucial for process safety and product quality, it is hard to control the reaction heat in batch mode, especially in large-sized reactors, due to poor heat transfer. Thus, there is a safety risk on industrial production with hazardous materials under batchwise conditions. Continuous-flow system provides a small reaction volume and equipment size, which allows the minimization of hazardous chemicals in a reactor and facilitates equipment segregation. Moreover, heat control for exothermic reactions is readily achievable, owing to excellent heat removal efficiency. Hence, the process safety of hazardous reactions is expected to be dramatically enhanced against that of the conventional batch mode. Although gaseous phosgene can be used to perform phosgenation reactions, the utilization of a phosgene surrogate as the less toxic material is desirable to mitigate the safety risk [16–18]. To enhance the process safety, we chose less toxic solid triphosgene that can be transformed into phosgene with amines.

In this study, we used triphosgene and amine to establish safe and scalable flow reactor system for phosgene reactions (Figure 9.1). In this flow system, the starting material and phosgene derived from triphosgene react in a coiling tube while continuously yielding a controlling reaction temperature using water bath and an emerging solution containing the desired product. This flow system allows the *in situ* generation and consumption of poisonous phosgene within a piece of closed and compact equipment. Furthermore, the residual phosgene in the eluting stream can be easily decomposed by quenching it in acid solution with stirring. We assume that the triphosgene-mediated flow system is an ideal approach to minimize the operators' exposure to hazardous materials in a manufacturing plant. Accordingly, we started our investigations to establish and develop a safety process for phosgenation reactions using continuous-flow system.

https://www.twirpx.org & http://chemistry-chemists.com

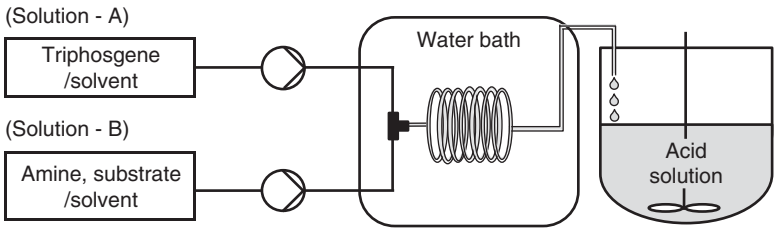

Figure 9.1 Illustration of the flow system for phosgenation reaction.

9.2.2 Feasibility Study

We initially performed the chloroformate reaction as a model phosgene reaction in flow mode. The suitable amine for the phosgene flow system was examined to prevent the precipitation of amine HCl salt before performing the continuous-flow experiments. The results of the solubility test of several amine HCl salts revealed that no solid formation was encountered by tributylamine in most of the versatile and green solvents. Therefore, we concluded that tributylamine could be suitable for a chloroformate reaction under continuous-flow condition.

First, chloroformate compounds were synthesized using the flow equipment (Table 9.1). In this system, the T-piece mixer and the coiling reaction tube were immersed in a temperature-controlled water bath. Then, triphosgene in toluene (Solution A) and the mixture of substrate/tributylamine in toluene (Solution B) were transferred to the mixer before passing into the coiling tube by feeding pumps. The resulting solution containing the desired product was continuously quenched in the acid solution while stirring at 0 °C. In the case of **1b** synthesis, the flow reaction successfully proceeded, and an excellent reaction yield was accomplished in a short residence time without clogging issue. A decrease in reaction yield was observed in the comparative batch mode because the decomposition of **1b** occurred due to long reaction time. It was also revealed that chloroformate compound **2b** was successfully prepared in excellent yield under milder condition. These experiments demonstrated that our flow system is compatible with the phosgenation reaction and that flow reaction has an advantage in reaction yield over the conventional bath reaction.

Second, several pharmaceutical intermediates were prepared using the same flow reactor system to expand the range of applications. *N*-Carboxyanhydride **3b** and urea compound **4b**, which are known as advanced intermediates of imidapril (angiotensin-converting enzyme [ACE] inhibitor) [19] and relebactam (β-lactamase inhibitor) [20], were chosen as target products. In this study, flow reactions were performed using **3a** and **4a** as the starting materials to obtain the corresponding compounds. The investigation results suggested that the desired API intermediates were successfully synthesized in satisfactory yields within a short residence time while preventing the precipitation issue (Table 9.2).

Our investigations demonstrated that our flow reactor system using triphosgene/tributylamine applies to a wide variety of phosgenation reactions, including the preparation of pharmaceutical intermediates.

https://www.twirpx.org & http://chemistry-chemists.com

Table 9.1 The preparation of chloroformate compounds under continuous-flow methodology.[a)]

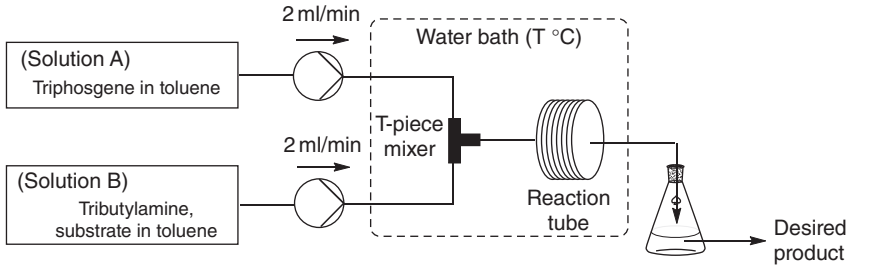

Substrate	Desired product	System	*T* (°C)	Residence time	Yield (%)[b)]
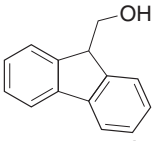 **1a**	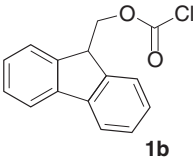 **1b**	Flow	0	1 min	90
		Flow	0	4 min	98
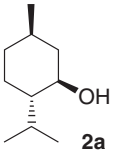 **2a**	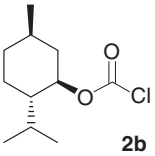 **2b**	Batch	−5	3 h[c)]	60
		Flow	30	1 min	99

a) I.d. = 2 mm.
b) Determined by HPLC analysis.
c) Reaction time.

9.2.3 Establishment and Development of Continuous-Flow Process for API Synthesis

Encouraged by the promising results of the feasibility study, we used our phosgene flow technology to establish and develop a cost-effective synthetic process for API. In this study, we focused on solifenacin (M3 muscarinic receptor antagonist) [21] as a target API. The synthetic pathway of solifenacin, which comprises four steps in batch, was already established in our research group. This synthetic process, however, had a technical issue in that a considerable amount of epimer impurity was generated during the reaction, whereby the sacrifice of crystallization yield and the recrystallization step of API was required to remove epimer impurity. This synthetic

https://www.twirpx.org & http://chemistry-chemists.com

Table 9.2 Synthesis of pharmaceutical intermediates in continuous-flow mode.[a)]

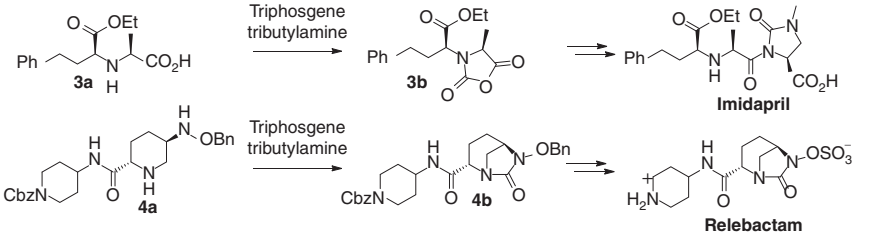

Substrate	Desired product	Solvent	Reaction temperature (°C)	Residence time (min)	Yield (%)[b)]
3a	**3b**	Toluene/THF[c)]	60	3	76
4a	**4b**	THF	0	2	85

a) I.d. = 2 mm.
b) Determined by HPLC analysis.
c) Triphosgene was dissolved in toluene. Tributylamine and **3a** were dissolved in THF.

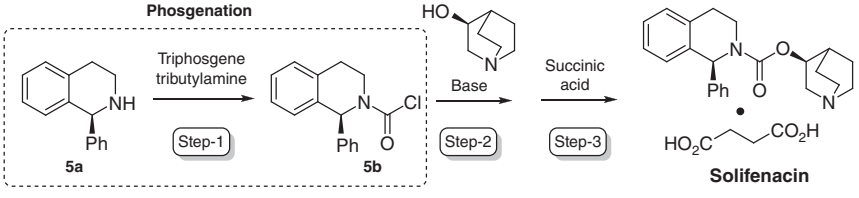

Scheme 9.1 New synthetic route for Solifenacin.

route resulted in a high production cost. Hence a new synthetic pathway was established in our laboratory to address this issue (Scheme 9.1). The new process yields a decrease in step number (4 → 3 steps), with no epimerization during the reaction.

Furthermore, an increase in crystallization yield was observed, and no recrystallization was required mainly because epimer impurity control was achieved during the reaction. It was expected that the new API process would have cost advantages over the previous one because the total yield can be improved by about 30%. The newly established pathway, however, posed a safety issue in large-scale production since the phosgenation reaction was contained at Step-1. Thus, we adopted the continuous-flow process at Step-1 in order to establish the safety scale-up process.

First, the preparation of **5b** in flow mode was carried out using the same laboratory equipment depicted in Table 9.3 (Method A). As indicated by the results, although starting material **5a** was completely consumed, the low reaction yield (45%) was provided due to a large amount of by-product (**5c**) generation. Unfortunately, no improvement was observed despite all our efforts for optimization studies in this flow system. We anticipated that the preparation of a sufficient amount of phosgene before the main reaction was essential to solve the problem since an undesired

https://www.twirpx.org & http://chemistry-chemists.com

Table 9.3 Synthesis of pharmaceutical intermediate **5b** in continuous-flow mode.

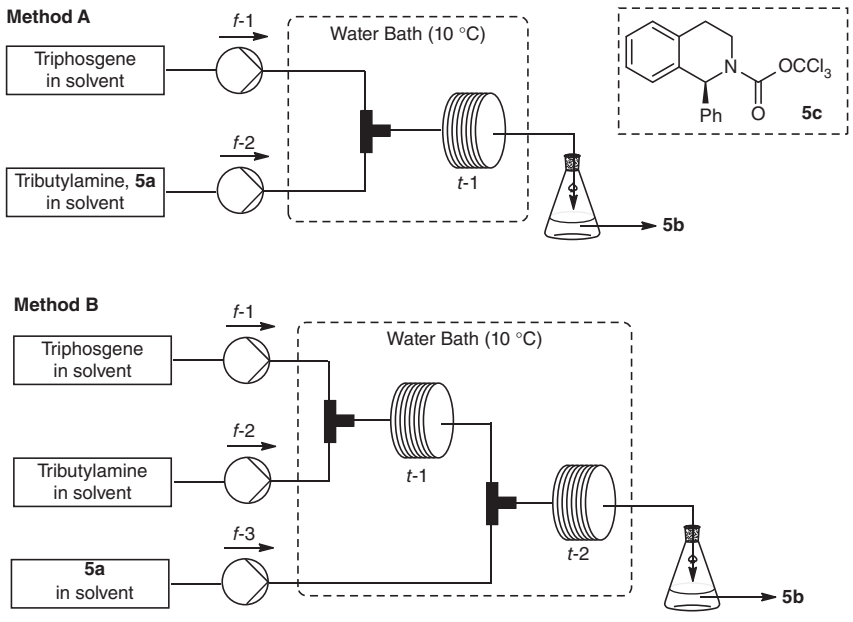

Method	Residence time		Flow rate (ml/min)			I.d. (mm)	Yield (%)[a)]	Generation of impurity 5c
	t-1	*t*-2	*f*-1	*f*-2	*f*-3			
A	2 min	—	2.0	2.0	—	2.0	45	Yes
B	4 min	2 min	1.0	1.0	2.0	2.0	90	No
B	5 s	10 s	1.0	1.0	2.0	0.5	96	No
B	5 s	10 s	39.5	39.5	79	3.0	98	No

a) Determined by HPLC analysis.

by-product seems to be generated by a reaction between **5a** and triphosgene. Second, the new laboratory equipment, presented as Method B in Table 9.3, was assembled in order to perform this approach. In this setup, phosgene was prepared in the first reaction tube by mixing triphosgene and tributylamine. The resulting solution was then combined with **5a** at the second reaction tube. When residence times *t*-1 and *t*-2 were set at four and two minutes, the reaction yield dramatically increased to 90% with undetectable amount of **5c**. Next, both residence times were investigated to determine the optimal condition. The results of the optimization studies revealed that a residence time of only 5–10 seconds was sufficient to provide a high reaction yield.

Finally, a scale-up study was conducted by increasing the flow rate and inner diameter (the total flow rate increased from 4.0 to 158 ml/min; inner diameter increased from 0.5 to 3.0 mm). The results revealed that the desired product was obtained in a

https://www.twirpx.org & http://chemistry-chemists.com

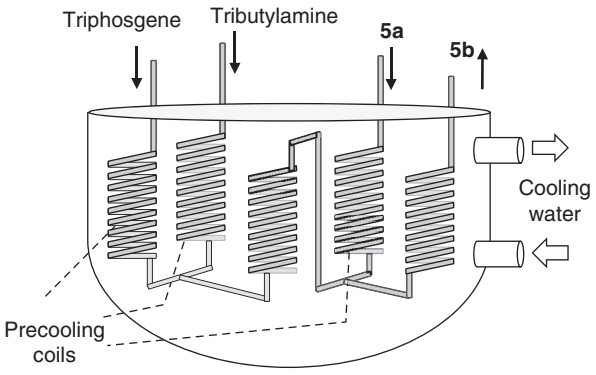

Figure 9.2 The image of the pilot flow reactor for preparation of **5b**.

comparable yield to the small-scale experiments, and around 64 g of **5b** was successfully produced over only 4.5 minutes of operation. Our investigations revealed that the key intermediate of solifenacin can be successfully prepared through the phosgene flow reaction system (see Method B in Table 9.3) and that the flow system with triphosgene/tributylamine is amenable to the scale-up process.

As the final step, we manufactured a few hundred kilograms of solifenacin under GMP condition via the new synthetic route containing phosgene flow reaction that we had established. Phosgenation in flow mode, a key step of the new synthetic pathway, was conducted by a pilot flow reactor facility installed in Osaka Synthetic Chemical Laboratories, Inc. (Japan, Kaneka's 100% subsidiary; see Figure 9.2 for the image of our pilot facility). Compact coils were submerged in the circulating cooling water during the reaction, and the precooling coils were integrated before each reaction tube to accurately control the reaction temperature (see Section 9.4.1 for more details about the concept of our flow reactor system). Around 100 kg (three lots) of desired intermediate **5b** were successfully manufactured with the pilot flow reactor as process validation (PV) production by scaling out the process while achieving satisfactory productivity (1.9 kg/h) without sacrificing reaction yield. In addition, the desired API (i.e. solifenacin) was prepared on a large scale through our newly established process. We used the scalable flow technology to establish a cost-effective synthetic route for solifenacin while increasing the process safety. Furthermore, a large-scale API production with the pilot flow reactor was accomplished under GMP condition.

9.3 Simple and Practical Packed-Bed Reactor System for Catalytic Reactions

9.3.1 Introduction

Since the flow processes using packed-bed reactor systems have several advantages over the traditional batch processes, such as enhanced reaction efficiency, owing to the high exposure of the substrate to the catalyst and its excellent reusability, many

https://www.twirpx.org & http://chemistry-chemists.com

research groups have shown their interest in the enabling system and its usefulness [22–25]. We herein introduce two types of packed-bed reactor systems utilizing anion-exchange resin and immobilized cells (IMCs) as catalysts.

9.3.2 Deacylation Reaction with Anion-Exchange Resin

Hydroxy compounds are common class of substances among pharmaceuticals, agrochemicals, and other fine chemicals. Hydroxy groups are generally required to be protected or deprotected in the course of the synthetic route toward the target compound because of their high reactivity. Acyl substituents are among the most useful protecting groups mainly because the corresponding esters are relatively stable under a wide range of conditions, such as weak basic, oxidative, and reductive circumstances [26–28]. It has been reported that acyl groups are readily deprotected by hydrolysis or alcoholysis with acid, base, or enzyme catalysts [29–31]. These examples in batch mode, however, often involve tedious work-ups, such as extraction and filtration, to remove the remaining catalyst before proceeding to the next step. Furthermore, a certain amount of product might be lost in the aqueous phase during extraction when the desired product, the hydroxyl compound, is highly soluble in water. Thus, process improvement in the deacylation process, especially for an industrial scale, is desirable to increase productivity. We herein describe an efficient and practical deacylation process using a continuous packed-bed flow reactor system with an inexpensive anion-exchange resin as a catalyst (Figure 9.3). The anion-exchange resin was activated by replacing chloride ion with methoxide ion before the feeding of substrate **6**. In this system, it is expected that the desired hydroxy compounds **8** can be easily obtained in high purity by passing acyl compounds **6** through the column, which is filled with the catalyst. Then, both by-product **7** and methanol are readily removed by concentration without time-consuming work-ups, such as extraction and filtration. Consequently, the productivity of the deacylation process can be considerably enhanced compared with the conventional batch process. Therefore, we addressed the development of efficient and practical deacylation reaction using the packed-bed reactor system.

9.3.2.1 Feasibility Study

The deacylation reactions using a packed-bed reactor system were initially investigated using several model substrates to assess the feasibility of the process (see Table 9.4). In this system, a commercially available anion-exchange resin (DIAION PA 308 from Mitsubishi Chemical Co., Ltd.) was used as a catalyst and pretreated according to the following procedures before the main reaction. At first, the counter anion of the resin was changed from chloride to methoxide by passing sodium methoxide in methanol through the column. Then, methanol was flushed into the column to remove the remaining sodium methoxide. After the activation of the resin, each substrate in methanol was pumped through the column at the space velocity (SV) of $4\,h^{-1}$, and the reaction solution was subsequently collected from the outlet. When benzyl acetate **9** was used as a model substrate, the flow reaction proceeded successfully to produce the product in excellent yield while offering

https://www.twirpx.org & http://chemistry-chemists.com

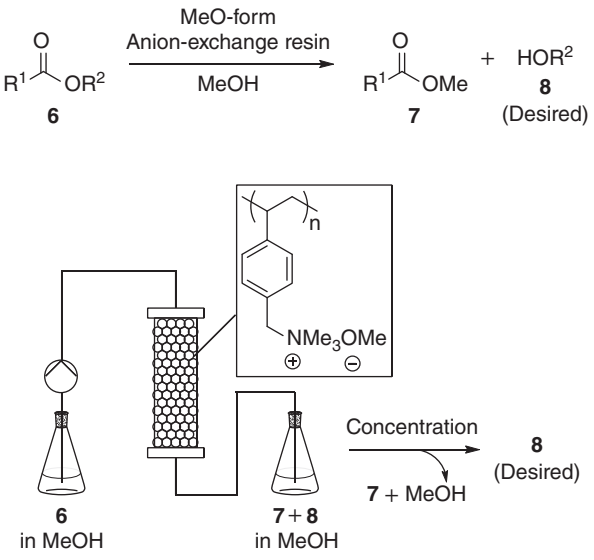

Figure 9.3 Illustration of the packed-bed reactor system for deacylation reaction.

several advantages over the comparative batch reaction. The reaction time was drastically shortened due to the high exposure of the substrate to the catalyst.

Moreover, poor filterability of the resin, which is caused by fine particles generated during the agitation in batch mode, could be circumvented in the flow mode. By adjusting the reaction temperature, the same protocol could be applied to the other compounds protected by the acyl group (**10** and **11**). It should be noted that the by-product, methyl ester, was readily removed by simple concentration after the flow reaction in all the experiments. We demonstrated that our packed-bed reactor system with anion-exchange resin applies to deacylation reactions and that reaction efficiency can be improved over the batch system.

9.3.2.2 Application for Pharmaceutical Intermediates and Scale-up

As the next step, we focused on the synthesis of pharmaceutical intermediates to demonstrate the practicability of our packed-bed reactor system. The chiral compounds **12b** and **13b** have been reported to be the key intermediates of API (i.e. efinaconazole and atorvastatin) (see Scheme 9.2) [32–35]. We assumed that these intermediates would be obtained from the corresponding precursors **12a** and **13a** containing pivaloyl and acetyl groups.

First, the screening of anion-exchange resins was conducted using the intermediate **12a** as a starting material (Table 9.5). A wide variety of anion-exchange resins with different physical properties were examined for this investigation. It was revealed that the resins with lower cross-linking density tend to provide better reaction yield in this flow system. They are also likely to offer a larger reaction space for the substrate to interact with methoxide, leading to higher reactivity. Although the highest yield was obtained using DOWEX 1X2 (100–200 mesh), the unit price of the resin was found to be higher in bulk scale compared with other resins that we screened.

https://www.twirpx.org & http://chemistry-chemists.com

Table 9.4 Deacylation reaction with an anion-exchange resin in a packed-bed reactor.

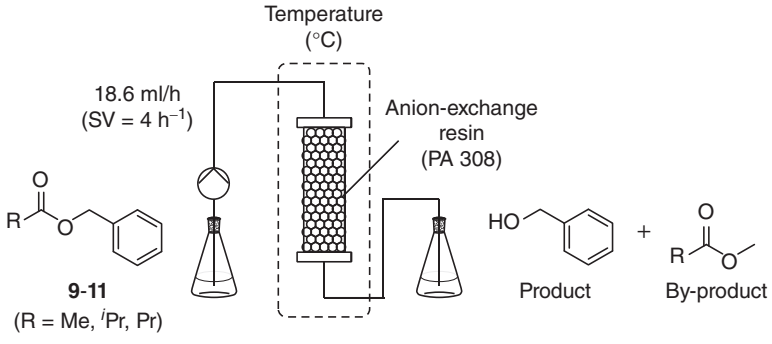

Run	Substrate	Reaction mode	Residence time (min)	Temperature (°C)	Conversion (%)	Yield (%)[a]
1	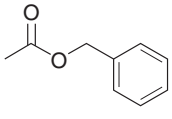 **9**	Flow	<15[b]	25	98	98
2		Batch	120[c]	25	98 (65)[d]	98
3	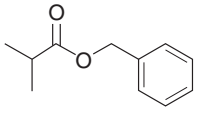 **10**	Flow	<15[b]	50	88	90
4	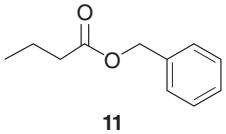 **11**	Flow	<15[b]	50	95	93

a) Determined by HPLC analysis.
b) The residence time was determined as the resin volume in the column (in ml) divided by the flow rate (in ml/h).
c) Reaction time.
d) The result for a reaction time of 15 min is indicated in parentheses.

https://www.twirpx.org & http://chemistry-chemists.com

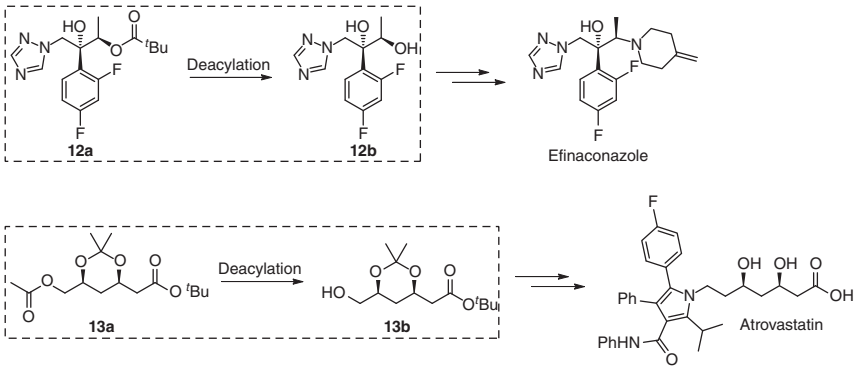

Scheme 9.2 Application examples of the packed-bed reactor system for pharmaceutical intermediates. Source: Based on Tamura et al. [32], Cheng et al. [33], Beck et al. [34] and Fan et al. [35].

Accordingly, from the economic and availability perspectives, we decided to use DIAION PA306s as a catalyst, although the yield was slightly lower than the yield using DOWEX 1X2 (100–200 mesh). Next, the reaction conditions, such as the reaction temperature and the SV value, were further examined in the flow mode using DIAION PA 306s to improve the reaction yield of **12b**. The investigation results revealed that an excellent reaction yield was obtained at a higher temperature and a lower SV value (see Run 4 in Table 9.6). The same system was used to prepare **13b** to expand the substrate scope. The results revealed that **13b** was successfully synthesized in an excellent reaction yield (Run 7 in Table 9.6).

It is worth noting that the acetyl group was selectively deacylated in Runs 6 and 7, with *tert*-butyl ester moiety remaining intact. Toward the industrial production, a large-scale experiment was subsequently conducted with the larger inner diameter of the column at the higher flow rate to ensure the scalability of the system (Run 5 in Table 9.6). The result indicated that the reaction yield was comparable with that of the small-scale experiment, and high throughput (flow rate: 198 ml/h; productivity: c. 72 mmol/h) was attained while preventing deterioration in quality and high-pressure drop. Thus, we demonstrated that our packed-bed reactor system, which utilizes an anion-exchange resin as a catalyst, is compatible with the preparation of various API intermediates and amenable to scale-up.

Finally, to ensure the practicability of our flow system, we evaluated the durability and recyclability of the catalyst according to the following procedures. The methanol solution of **12a** was continuously supplied into the column filled with DIAION PA 306s at 50 °C and SV = 1 h^{-1} for seven days, whereas the reaction conversion was monitored through an offline high-performance liquid chromatography (HPLC) analysis during the operation. The high conversion was maintained for 94 hours, representing the superior durability of the catalyst. Subsequently, the deactivation of the resin was observed with a rapid decrease in the conversion (see first trial in Figure 9.4).

As noted earlier, the deactivated resin was then subjected to the same procedure for activation, and its durability was reevaluated. Consequently, similar to the result

https://www.twirpx.org & http://chemistry-chemists.com

Table 9.5 Screening of anion-exchange resins for the deacylation reaction.

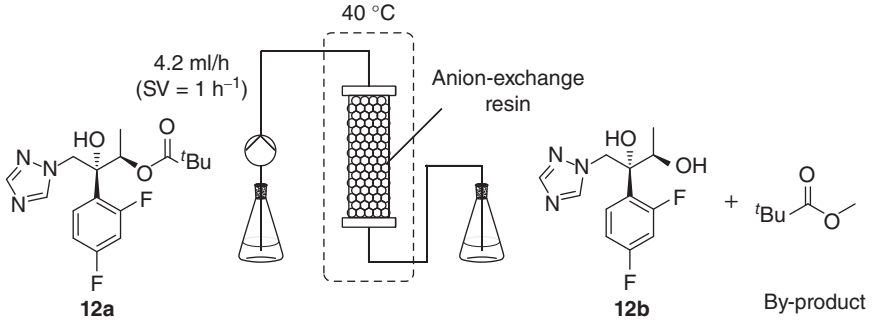

	Anion-exchange resin				
Run	**Name**	**Type**	**Ion-exchange capacity (equiv/l)**	**Cross-linking density (%)**	**Yield (%)[a)]**
1	DOWEX 1X2 (100–200 mesh)	Gel	0.6	2	92
2	DIAION PA306s	Porous	≥0.8	3	87
3	DIAION PA308	Porous	≥1.0	4	74
4	DIAION HPA25L	Highly porous	≥0.5	25	49
5	AMBERLITE IRA900J	MR	≥1.0	No data	58

a) Determined by HPLC analysis.

of the first trial, the reaction conversion was fully recovered to 99.9% and maintained for 93 hours, illustrating that the catalyst was completely regenerated (see second trial in Figure 9.4). The plausible mechanism for deactivation of the resin is shown in Figure 9.5. Methyl pivalate, which is generated as a by-product in the main reaction, is hydrolyzed by minute amounts of water in the solvent, followed by replacement of methoxide by the resulting pivalate. These experiments demonstrate that our flow system is compatible with the preparation of general hydroxy compounds, including pharmaceutical intermediates, and is amenable for large-scale production, owing to the high durability of the catalyst.

9.3.3 Reductive Amination with Biocatalyst

Stereoselective/chemoselective reactions utilizing biocatalysts have been recognized as powerful methodologies for the manufacturing of APIs along with their intermediates. Our research group specializes in both organic synthesis and biotransformation and has established many competitive synthetic routes for API intermediates, such as chiral alcohols, amines, and nonnatural amino acids in batch mode [33–41]. Additionally, these compounds were successfully manufactured using industrially

https://www.twirpx.org & http://chemistry-chemists.com

Table 9.6 Optimization of reaction conditions for pharmaceutical intermediates.[a)]

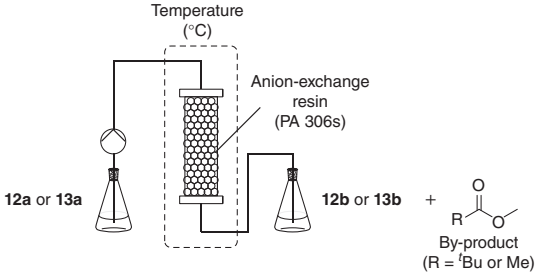

Run	Substrate	Product	Column diameter (mm)	Resin volume (ml)	Temperature (°C)	SV (h^{-1})	Yield (%)[b)]
1	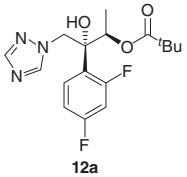 **12a**	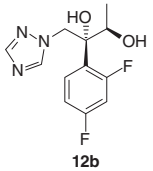 **12b**	0.9	3.9	25	5	8

https://www.twirpx.org & http://chemistry-chemists.com

Table 9.6 (Continued)

Run	Substrate	Product	Column diameter (mm)	Resin volume (ml)	Temperature (°C)	SV (h^{-1})	Yield (%)[b]
2			0.9	3.9	40	4	76
3[a]			0.9	4.2	40	1	87
4			0.9	3.9	50	1	98
5			2.2	198	50	1	99
6	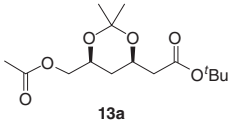 **13a**	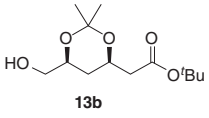 **13b**	0.9	4.7	25	25	78
7			0.9	4.7	25	5	98

a) The result of Run 2 in Table 9.5.
b) Determined by HPLC analysis.

https://www.twirpx.org & http://chemistry-chemists.com

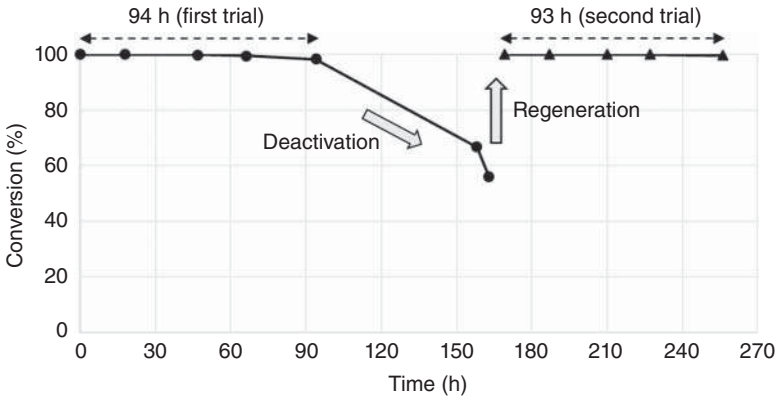

Figure 9.4 Evaluation of the catalytic activity of anion-exchange resin.

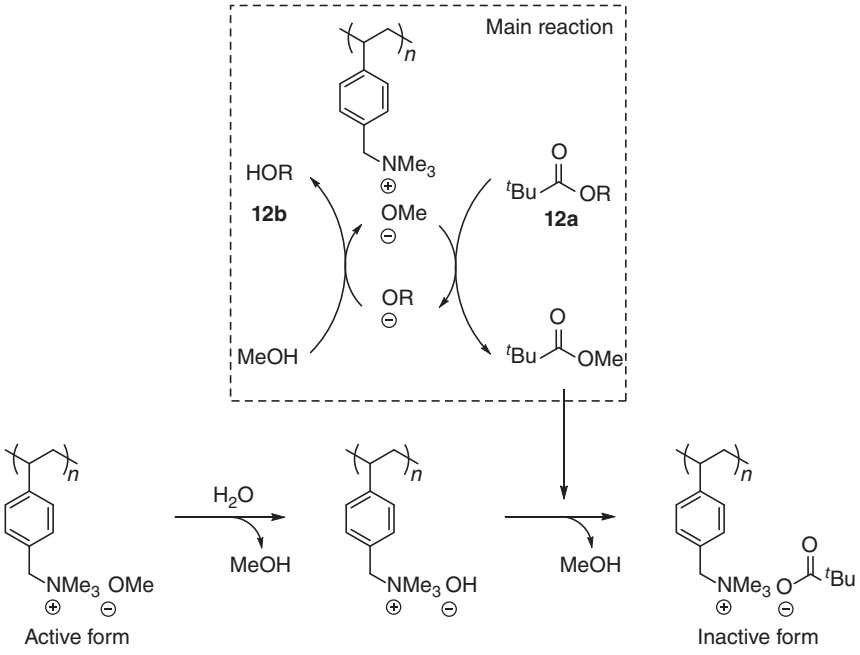

Figure 9.5 A plausible mechanism for the deactivation of resin.

applicable biocatalyst under GMP conditions. We then turned our attention to biotransformation, utilizing IMCs as a catalyst to expand the application of our flow system. We herein describe the reductive amination of α-ketoacid **14a** in flow mode with an IMC as a catalyst to afford L-*tert*-leucine **14b**, which is known as a pharmaceutical intermediate of atazanavir (HIV protease inhibitor) (Figure 9.6) [42]. α-Ketoacid **14a** in potassium phosphate buffer was passed through the column loaded with an IMC along with a catalytic amount of NAD^+ and ammonium formate.

https://www.twirpx.org & http://chemistry-chemists.com

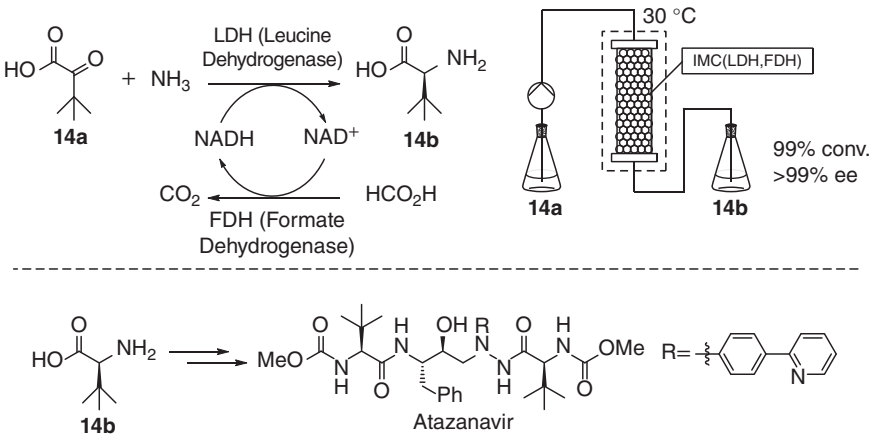

Figure 9.6 Illustration of the packed-bed reactor system for reductive amination. Source: Based on Gong et al. [42].

The results reveal that **14b** was continuously obtained with both high conversion and high optical purity. In addition, the activity of the cell persisted for 70 hours, illustrating the high durability of the biocatalyst and practicability of our flow system. We believe that this application qualifies as an excellent example to showcase the effective combination of biotransformation and flow chemistry. Further optimization studies and expansion of applications with biocatalyst in our flow system are currently under development in our research group.

9.4 Flow Reactor Facility for Large-Scale Production

9.4.1 Concept of Our Flow Reactor System

Commercial-scale flow reactor facility installed in Kaneka Singapore Co. (Pte) Ltd., Kaneka's 100% subsidiary, is illustrated in Figure 9.7.

Two reagents in the solution are transferred and combined at the T-shaped mixer. The resulting solution is then pumped in a spiral tube placed in a jacketed tank. The reaction temperature can be controlled by the circulating cooling water and monitored by the temperature sensor devices inserted in the coiling tube. Additionally, a small agitator installed in the tank increases the heat exchange efficiency under exothermic reaction in flow. It is noteworthy that a coiling tube can be replaced and customized to meet features of the target reaction. The customization examples of the reactor are shown in Figure 9.8. The number of the line and the length of the reaction tube are changeable, and the coil can be changed to the columns for the packed-bed reactor system.

In addition, a wide type of materials, such as stainless steel, Hastelloy, and Teflon®, can be used based on chemical compatibility and the type of chemistry. Furthermore, a coiling tube can be utilized for dedicated or single use to prevent

https://www.twirpx.org & http://chemistry-chemists.com

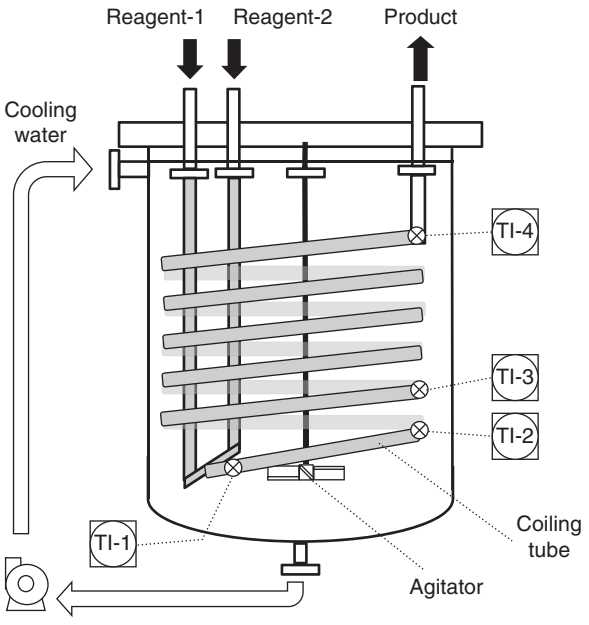

Figure 9.7 The image of commercial flow reactor in Kaneka Singapore Co. (Pte) Ltd. Source: Based on Kaneka Singapore Co. (Pte) Ltd.

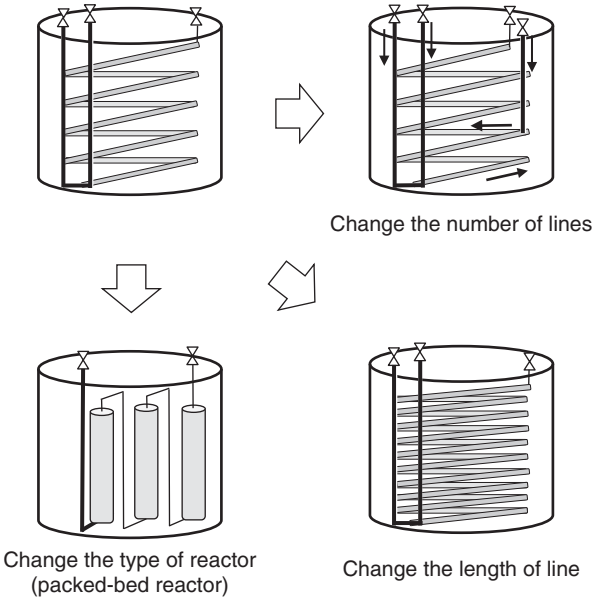

Figure 9.8 Customization examples of the flow reactor.

https://www.twirpx.org & http://chemistry-chemists.com

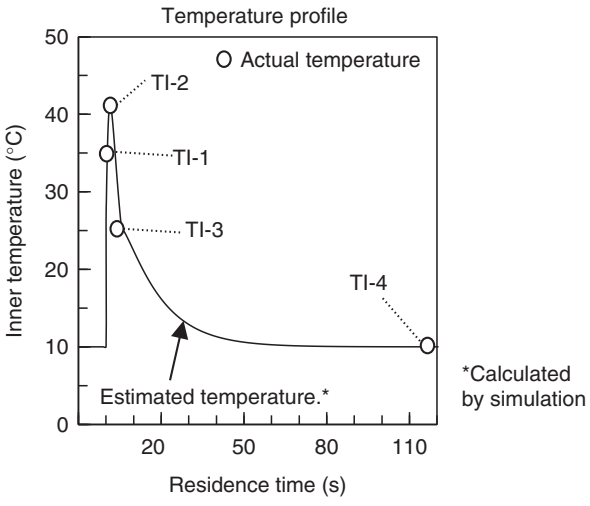

Figure 9.9 The temperature profile of phosgenation reaction in flow mode.

cross-contamination, whereby no cleaning validation for a coiling tube is required. This flow reactor can be a multipurpose facility by adopting these concepts.

9.4.2 Commercial Production

A commercial-scale flow reactor facility was used to perform large-scale production for a phosgenation reaction [43]. The reaction coil of the commercial facility in Singapore is larger than the one of the pilot plants described in Figure 9.2. Scale-up studies, including mixing effects, were conducted in combination with chemical (engineering) approaches [44]. In addition, the temperature profile of the target phosgene reaction on a large scale was simulated by the kinetic theory approach. The reaction rate constant and the overall heat transfer coefficient were carefully examined in our laboratory to design the reaction coil for manufacturing. Figure 9.9 presents the temperature profile of the flow reaction. The estimated data by simulation and actual temperature values measured by thermocouples in large-scale production yielded comparable results.

After the completion of PV production, commercial production in flow mode was launched, and metric ton of API intermediates was successfully manufactured under cGMP condition using this flow facility while achieving high productivity (throughput of the desired product: c. 11 kg/h).

9.5 Conclusions

We established a safe and efficient continuous-flow reactor system using triphosgene and tributylamine for phosgenation reactions, resulting in a homogeneous reaction that prevents clogging issues. This system is amenable to the diverse array of phosgene reactions, including the preparation of pharmaceutical intermediates. Moreover, using our flow technology, we developed a cost-effective synthetic route

https://www.twirpx.org & http://chemistry-chemists.com

for solifenacin and accomplished a few hundred kilograms of production in our pilot plant while increasing the process safety. Subsequently, we established a simple and practical packed-bed reactor system with a catalyst for the deacylation of esters. Several API intermediates with the hydroxyl group were effectively prepared by the deacylation reaction in flow without time-consuming purifications, such as reextraction and filtration. This system also demonstrated to be compatible with the scale-up process and that the catalyst provides excellent durability and regenerability for the deacylation reaction. In addition, the application example of the effective combination of biotransformation and flow chemistry using the packed-bed reactor with immobilized biocatalyst was described. Finally, we introduced our commercial flow reactor that is equipped with a removable and customizable reaction tube. Large-scale productions up to metric ton scale in flow mode were accomplished under cGMP condition in our Singapore plant. Our research group is currently studying and developing new chemical transformations, such as organometallic reactions and photoreactions, from gram to kilogram scale to expand the range of our flow application examples.

References

1 Yoshida, J. (2009). *Flash Chemistry: Fast Organic Synthesis in Microsystems*. New York: Wiley.

2 Plutschack, M.B., Pieber, B., Gilmore, K., and Seeberger, P.H. (2017). The Hitchhiker's guide to flow chemistry. *Chem. Rev.* 117: 11796–11893.

3 Chen, Y., Hone, C.A., Gutmann, B., and Kappe, C.O. (2017). Continuous flow synthesis of carbonylated heterocycles via Pd-catalyzed oxidative carbonylation using CO and O_2 at elevated temperatures and pressures. *Org. Process Res. Dev.* 21: 1080–1087.

4 Bogdan, A.R. and Dombrowski, A.W. (2019). Emerging trends in flow chemistry and applications to the pharmaceutical industry. *J. Med. Chem.* 62: 6422–6468.

5 Cambie, D., Bottecchia, C., Straathof, N.J.W. et al. (2016). Applications of continuous-flow photochemistry in organic synthesis, material science, and water treatment. *Chem. Rev.* 116: 10276–10341.

6 Kleinebudde, P., Khinast, J., and Rantanen, J. (2017). *Continuous Manufacturing of Pharmaceuticals*. New York: Wiley.

7 Lee, S.L., O'Connor, T.F., Yang, X. et al. (2015). Modernizing pharmaceutical manufacturing: from batch to continuous production. *J. Pharm. Innov.* 10: 191–199.

8 McWilliams, J.C., Allian, A.D., Opalka, S.M. et al. (2018). The evolving state of continuous processing in pharmaceutical API manufacturing: a survey of pharmaceutical companies and contract manufacturing organizations. *Org. Process Res. Dev.* 22: 1143–1166.

9 Yasukouchi, H., Nishiyama, A., and Mitsuda, M. (2018). Safe and efficient phosgenation reactions in a continuous flow reactor. *Org. Process Res. Dev.* 22: 247–251.

https://www.twirpx.org & http://chemistry-chemists.com

10 Yasukouchi, H., Machida, K., Nishiyama, A., and Mitsuda, M. (2019). Efficient and practical deacylation reaction system in a continuous packed-bed reactor. *Org. Process Res. Dev.* 23: 654–659.

11 Babad, H. and Zeiler, A.G. (1973). The chemistry of phosgene. *Chem. Rev.* 73: 75–91.

12 Eckert, H. (2011). Phosgenation reactions with phosgene from triphosgene. *Chim. Oggi* 29: 1–6.

13 Matzner, M., Kurkjy, R.P., and Cotter, R.J. (1964). The chemistry of chloroformates. *Chem. Rev.* 64: 645–687.

14 Dąbrowa, D., Niedbała, P., and Jurczak, J. (2016). Recognizing the limited applicability of job plots in studying host–guest interactions in supramolecular chemistry. *J. Org. Chem.* 81: 3576–3584.

15 Kim, E.J., Bhuniya, S., Lee, H. et al. (2014). An activatable prodrug for the treatment of metastatic tumors. *J. Am. Chem. Soc.* 136: 13888–13894.

16 Pasquato, L., Modena, G., Cotarca, L. et al. (2000). Conversion of bis(trichloromethyl) carbonate to phosgene and reactivity of triphosgene, diphosgene, and phosgene with methanol. *J. Org. Chem.* 65: 8224–8228.

17 Kavala, V., Naik, S., and Patel, B.K. (2005). A new recyclable ditribromide reagent for efficient bromination under solvent free condition. *J. Org. Chem.* 70: 4267–4271.

18 Fuse, S., Tanabe, N., and Takahashi, T. (2011). Continuous *in situ* generation and reaction of phosgene in a microflow system. *Chem. Commun.* 47: 12661–12663.

19 Ohishi, T., Hirai, Y., Kawasaki, H., et al. (2011). Method for producing optically active N-substituted aminoacyl cyclic urea derivative. Jpn. Tokkyo Koho. JP 4799085 B2 20111019.

20 Mangion, I.K., Ruck, R.T., Rivera, N. et al. (2011). Concise synthesis of a β-lactamase inhibitor. *Org. Lett.* 13: 5480.

21 Zegrockastendel, O., and Zagrodzka, J. (2009). Process for preparation of solifenacin and/or the pharmaceutically acceptable salts thereof high pharmaceutical purity. WO2009/142522 A1 20091126.

22 Tsubogo, T., Ishiwata, T., and Kobayashi, S. (2013). Asymmetric carbon-carbon bond formation under continuous-flow conditions with chiral heterogeneous catalysts. *Angew. Chem. Int. Ed.* 52: 6590–6604.

23 Zaborenko, N., Linder, R.J., Braden, T.M. et al. (2015). Development of pilot-scale continuous production of an LY2886721 starting material by packed-bed hydrogenolysis. *Org. Process Res. Dev.* 19: 1231–1243.

24 Constantinou, A., Wu, G., Corredera, A. et al. (2015). Continuous heterogeneously catalyzed oxidation of benzyl alcohol in a ceramic membrane packed-bed reactor. *Org. Process Res. Dev.* 19: 1973–1979.

25 Seayad, A.M., Ramalingam, B., Chai, C.L.L. et al. (2012). Self-supported chiral titanium cluster (SCTC) as a robust catalyst for the asymmetric cyanation of imines under batch and continuous flow at room temperature. *Chem. Eur. J.* 18: 5693–5700.

https://www.twirpx.org & http://chemistry-chemists.com

26 Ishihara, K., Kurihara, H., and Yamamoto, H. (1993). An extremely simple, convenient, and selective method for acetylating primary alcohols in the presence of secondary alcohols. *J. Org. Chem.* 58: 3791–3793.

27 Spivey, A.C. and Arseniyadis, S. (2004). Nucleophilic catalysis by 4-(dialkylamino)pyridines revisited—the search for optimal reactivity and selectivity. *Angew. Chem. Int. Ed.* 43: 5436–5441.

28 Robins, M.J., Hawrelak, S.D., Kanai, T. et al. (1979). Transformations of adenosine to the first 2′,3′-aziridine-fused nucleosides, 9-(2,3-epimino-2,3-dideoxy-β-D-ribofuranosyl)adenine and 9-(2,3-epimino-2,3-dideoxy-β-D-lyxofuranosyl)adenine. *J. Org. Chem.* 44: 1317–1322.

29 Wuts, P.G.M. and Greene, T.W. (2006). Protection for the hydroxyl group, including 1,2- and 1,3-diols. In: *Greene's Protective Groups in Organic Synthesis*, 4e (ed. P.G.M. Wuts), 230–232. Wiley.

30 Matos, M.C. and Murphy, P.V. (2007). Synthesis of macrolide-saccharide hybrids by ring-closing metathesis of precursors derived from glycitols and benzoic acids. *J. Org. Chem.* 72: 1803–1806.

31 Yokoyama, H., Otaya, K., Kobayashi, H. et al. (2000). Palladium(II)-catalyzed cyclization of urethanes and total synthesis of 1-deoxymannojirimycin. *Org. Lett.* 2: 2427–2429.

32 Tamura, K., Kumagai, N., and Shibasaki, M. (2014). An enantioselective synthesis of the key intermediate for triazole antifungal agents; application to the catalytic asymmetric synthesis of efinaconazole (Jublia). *J. Org. Chem.* 79: 3272–3278.

33 Cheng, W., Li, Y., Xue, J. et al. (2010). Preparation method of atorvastatin calcium. CN101805279, 18 August 2010.

34 Beck, G., Jendralla, H., and Kesseler, K. (1995). Practical large scale synthesis of *tert*-butyl (3R,5S)-6-hydroxy-3,5-*O*-isopropylidene-3,5-dihydroxyhexanoate: essential building block for HMG-CoA reductase inhibitors. *Synthesis* 1014–1018.

35 Fan, W., Li, W., Ma, X. et al. (2011). Ru-catalyzed asymmetric hydrogenation of γ-heteroatom substituted β-keto esters. *J. Org. Chem.* 76: 9444–9451.

36 Blaser, H.U. and Federsel, H.J. (2010). *Asymmetric Catalysis on Industrial Scale*. New York: Wiley.

37 Iwasaki, A., Washida, M., Taoka, N. et al. (2006). Process for producing optically active secondary alcohol. WO2006090814, 31 August 2006.

38 Ito, N., Kawano, S., and Yasohara, Y. (2012). Modified aminotransferase, gene thereof, and method for producing optically active amino compound using same. WO2012124639, 20 September 2012.

39 Nojiri, M., Taoka, N., and Yasohara, Y. (2014). Characterization of an enantioselective amidase from Cupriavidus sp. KNK-J915 (FERM BP-10739) useful for enzymatic resolution of racemic 3-piperidinecarboxamide. *J. Mol. Catal. B Enzyme* 109: 136–142.

40 Nojiri, M., Yoshida, F., Hirai, Y. et al. (2015). A practical chemoenzymatic synthesis of (*R*)-isovaline based on the asymmetric hydrolysis of 2-ethyl-2-methyl-malonamide. *Tetrahedron Asymmetry* 26: 1–5.

https://www.twirpx.org & http://chemistry-chemists.com

41 Nojiri, M., Yoshida, S., Kanamaru, H., and Yasohara, Y. (2016). Improved efficiency of asymmetric hydrolysis of 3-substituted glutaric acid diamides with an engineered amidase. *J. Appl. Microbiol.* 120: 1542–1551.

42 Gong, Y.F., Robinson, B.S., Rose, R.E. et al. (2000). In vitro resistance profile of the human immunodeficiency virus type 1 protease inhibitor BMS-232632. *Antimicrob. Agents Chemother.* 44: 2319–2326.

43 Commercial production utilizing flow chemistry to begin June 2018 at Kaneka Singapore. www.kaneka.co.jp/en/service/news/nr201807241 (accessed 4 October 2019).

44 Toyoda, T., Ozasa, S., and Ohishi, T. (2019). Design of a flow reactor system for safe handling of phosgenation reactions: scale-up study of T-shaped mixers for industrial chemical production. *J. Chem. Eng. Jpn.* 52: 773–777.

https://www.twirpx.org & http://chemistry-chemists.com

Index

Flow and Microreactor Technology in Medicinal Chemistry, First Edition. Edited by Esther Alza.
© 2022 WILEY-VCH GmbH. Published 2022 by WILEY-VCH GmbH.

https://www.twirpx.org & http://chemistry-chemists.com

b

https://www.twirpx.org & http://chemistry-chemists.com

https://www.twirpx.org & http://chemistry-chemists.com

d

https://www.twirpx.org & http://chemistry-chemists.com

e

f

https://www.twirpx.org & http://chemistry-chemists.com

g

h

https://www.twirpx.org & http://chemistry-chemists.com

https://www.twirpx.org & http://chemistry-chemists.com

k

l

m

https://www.twirpx.org & http://chemistry-chemists.com

n

o

p

https://www.twirpx.org & http://chemistry-chemists.com

https://www.twirpx.org & http://chemistry-chemists.com

t

u

https://www.twirpx.org & http://chemistry-chemists.com

https://www.twirpx.org & http://chemistry-chemists.com